Hawaii Ocean Time-series
Data Report 8: 1996

November 1997

Luis Tupas
Fernando Santiago-Mandujano
Dale Hebel
Craig Nosse
Lance Fujieki
Eric Firing
Roger Lukas
David Karl

with contribution by
Christopher Winn
Robert Bidigare
Michael Landry
Mai Lopez

University of Hawaii
School of Ocean and Earth Science and Technology
1000 Pope Road
Honolulu, Hawaii 96822
U. S.A.

PREFACE

Scientists working on the Hawaii Ocean Time-series (HOT) program have been making repeated observations of the hydrography, chemistry and biology of the water column at a station north of Oahu, Hawaii since October 1988. The objective of this research is to provide a comprehensive description of the ocean at a site representative of the North Pacific subtropical gyre. Cruises are made approximately once a month to the HOT deep-water station (22^{o} 45'N, 158^{o} 00'W) located about 100 km north of Oahu, Hawaii. Measurements of the thermohaline structure, water column chemistry, currents, primary production and particle sedimentation rates are made on each cruise.

This document reports the data collected in 1996. However, we have included some data from 1988-1995 to place the 1996 measurements within the context of our ongoing time-series observations. The data reported here are a screened subset of the complete data set. Summary plots are given for CTD, biogeochemical, optical, meteorological, thermosalinograph, inverted echo sounder and ADCP observations.

In order to provide easy computer access to our data, CTD data at National Oceanographic Data Center (NODC) standard pressures for temperature, potential temperature, salinity, oxygen and potential density are provided in ASCII files on the enclosed diskette. Chemical measurements are also summarized in a set of ASCII flat files on the enclosed diskette. The complete data set resides on a Sun workstation at the University of Hawaii. These data are in ASCII format, and can easily be accessed using anonymous file transfer protocol (ftp) via Internet or the World Wide Web (WWW). Instructions for using the Lotus files and for obtaining the data from the network are presented in Chapter 8. The entire data set is available at NODC.

ACKNOWLEDGMENTS

Many people participated in the 1996 cruises sponsored by the HOT program. They are listed in Tables 1.6 and 1.7. We gratefully acknowledge their contributions and support. Thanks are due to Albert Colman, Terrence Houlihan, Mai Lopez, Molly Lucas, Daniel Sadler, Fernando Santiago-Mandujano and Jefrey Snyder for participating in most of the 1996 cruises and for the tremendous amount of time and effort they have put into the program. Special thanks are given to Lisa Lum for her excellent administrative support of the program, to Sharon DeCarlo for programming and data management, Carolyn Leong and Tay Peng Chen for CTD processing and to June Firing and Kalpana Kalianpur for ADCP processing. Ursula Magaard performed many of the core chemical analyses. Ted Walsh, Terrence Houlihan and Georgia Tien performed the nutrient analyses, Molly Lucas performed the salinity measurements and Tuan Huynh and Man Kit Tsoi provided additional technical support. We gratefully acknowledge the support from Nordeen Larson and Ken Lawson of Sea-Bird for helping us to maintain the quality of the CTD data throughout the HOT program. We also would like to thank the captain and crew members of the R/V *Moana Wave* and the UH Marine Center staff for their efforts. Without the assistance of these and the many technicians, students and ancillary investigators, the data presented in this report could not have been collected, processed, analyzed and reported.

This data set was acquired with funding from the National Science Foundation (NSF) and State of Hawaii general funds. The specific grants which have supported this work are NSF grants OCE-9303094 (WOCE; Lukas and Firing) and OCE-9301368 (JGOFS; Karl, Hebel and Tupas) and the JGOFS sub-components of Christopher Winn (OCE-9315392), Michael Landry (OCE-9218152) and Robert Bidigare (OCE-9315311).

Weather buoy data used in this report were obtained by the NOAA National Data Buoy Center (NDBC) and were provided to us by the National Oceanographic Data Center (NODC). We thank Pat Caldwell for his assistance.

1.0. INTRODUCTION

The role of the oceans in climate variability is primarily in the sequestration and transportation of heat and carbon (Barnett 1978). Both can be introduced into the ocean in one place, only to return to the atmosphere, at a subsequent time, possibly at a distant location. While both heat and carbon can be exchanged with the atmosphere only carbon is lost to the seafloor through sedimentation. The oceans are known to play a central role in regulating the global concentration of CO_2 in the atmosphere (Sarmiento and Toggweiler 1984; Dymond and Lyle 1985). It is generally believed that the world ocean has removed a significant portion of anthropogenic CO_2 added to the atmosphere, although the precise partitioning between the ocean and terrestrial spheres is not well constrained (Tans et al. 1990; Quay et al. 1992; Keeling and Shertz 1992; Takahashi et al. 1997).

The cycling of carbon within the ocean is controlled by a set of reversible, reduction-oxidation reactions involving dissolved inorganic carbon (DIC) and dissolved organic carbon (DOC) with marine biota serving as the critical catalysts. Detailed information on the rates and mechanisms of removal of DIC from the surface ocean by biological processes, the export of biogenic carbon (both as organic and carbonate particles) to the ocean's interior, and the sites of remineralization and burial are all of considerable importance in the carbon cycle. The continuous downward flux of biogenic materials, termed the "biological pump" (Volk and Hoffert 1985; Longhurst and Harrison 1989), is a central component of all contemporary studies of biogeochemical cycling in the ocean and, therefore, of all studies of global environmental change.

Systematic, long-term time-series studies of selected aquatic and terrestrial habitats have yielded significant contributions to earth and ocean sciences through the characterization of climate trends. Important examples include the recognition of acid rain (Hubbard Brook long-term ecological study, Vermont; Likens et al. 1977), the documentation of increasing carbon dioxide (CO_2) in the earth's atmosphere (Mauna Loa Observatory, Hawaii; Keeling et al. 1976) and the description of large scale ocean-atmosphere climate interactions in the equatorial Pacific Ocean (Southern Oscillation Index; Troup 1965).

Long time-series observations of climate-relevant variables in the ocean are extremely important, yet they are rare. Repeated oceanographic measurements are required to gain an understanding of natural processes or phenomena that exhibit slow or irregular change, as well as rapid event-driven variations that are impossible to document reliably from a single field expedition. Time-series studies are also ideally suited for the documentation of complex natural phenomena that are under the combined influence of physical, chemical and biological controls. Examination of data derived from the few long-term oceanic time-series that do exist provides ample incentive and scientific justification to establish additional study sites (Wiebe et al. 1987).

During the embryonic phase of ocean exploration more than a century ago (Thomson 1877), it was realized that a comprehensive understanding of the oceanic habitat and its biota would require a multidisciplinary experimental approach and extensive field observations. Progress toward this goal has been limited by natural habitat variability, both in space and time, and by logistical constraints of ship-based sampling. Consequently, our current view of many complex oceanographic processes is likely biased (e.g., Dickey 1991; Wiggert et al. 1994). The synoptic and repeat perspective that is now available from research satellites is expected to improve our understanding of oceanic variability, despite certain limitations.

1.1. Oceanic Time-series Measurements in the North Pacific Ocean

A deep-ocean weather station network was established in the post-World War II period as a ship-based observation program designed to improve global weather prediction capabilities. One of the sites, Station November, was located in the eastern sector of the North Pacific Ocean gyre at 30° N, 140° W and was occupied during 121 cruises between July 1966 and May 1974. The intercruise frequency ranged from a few days to a few weeks with a typical cruise duration of 2-3 weeks, including transits. Water samples were collected from approximately 12-14 depths in the range of 0-1500 m using bottles equipped with deep-sea reversing thermometers. Salinity and, on occasion, dissolved oxygen concentrations were measured from the discrete water samples.

During the 1970s, most of the US weather ship stations were phased out of operation and were eventually replaced with more cost-effective, unattended ocean buoys. These buoys measure standard meteorological parameters as well as basic wave characteristics (e.g., significant wave direction, height, period and spectrum) but few, if any, hydrographic variables.

Physical and biogeochemical time-series investigations of the North Pacific subtropical region are sparse (Figure 1.1) and consist of a series of unrelated research programs including CLIMAX, GOLLUM, NORPAX, VERTEX, ADIOS and most recently HOT. CLIMAX I occupied a series of stations near 28° N, 155° W during August-September 1968 and CLIMAX II reoccupied the site during September of the following year. Since that time, scientists from the Scripps Institution of Oceanography have revisited the "CLIMAX region" (26.5° to 31° N, 150.5° to 158° W) on 18 cruises between 1971 and 1985 (Hayward 1987). It is important to emphasize that the temporal coverage in this time-series is biased with respect to season because approximately 70% of the cruises occurred in summer (June-Sept) and 35% were in August alone. These observations are also aliased by the annual cycle because no cruises were conducted in 1970, 1975, 1978-79, 1981 or 1984. Nevertheless, observations made during this extensive series of cruises, especially the measurements of plankton distributions, nutrient concentrations and rates of primary production, provided an unprecedented view of the oligotrophic North Pacific ecosystem structure and dynamics.

From January 1969 to June 1970, a deep ocean hydrostation (Station GOLLUM; Figure 1.1) was established by scientists at the University of Hawaii at a location 47 km north of Oahu (22°10'N, 158° W; Gordon 1970). The water depth was 4760 m and the location was selected to be beyond the biogeochemical influences of the Hawaiian Ridge (Doty and Oguri 1956). On approximately monthly intervals, 13 two-day research cruises were conducted to observe and interpret variations in particulate organic matter distributions in the water column and other parameters (Gordon 1970).

A major advance in our understanding of biogeochemical processes in the sea was made during the NSF International Decade for Ocean Exploration (IDOE)-sponsored Geochemical Ocean Sections Study (GEOSECS) Pacific Ocean expedition (August 1973 - June 1974). Although repeated ocean observations were not made during GEOSECS, the high-precision data, including numerous radioactive and stable isotopic tracers, that were collected from selected stations in the central North Pacific Ocean can be used as the basis for assessing "change," especially for the concentration and ^{13}C isotopic composition of the total dissolved carbon dioxide pool (Quay et al. 1992). In particular, GEOSECS stations #202 (33° 06' N, 139° 34' W), #204 (31° 22' N, 150° 02' W), #212 (30° N, 159° 50' W) and #235 (16° 45' N, 161° 19' W) are the most relevant to our current biogeochemical investigations at Station ALOHA (Figure 1.1).

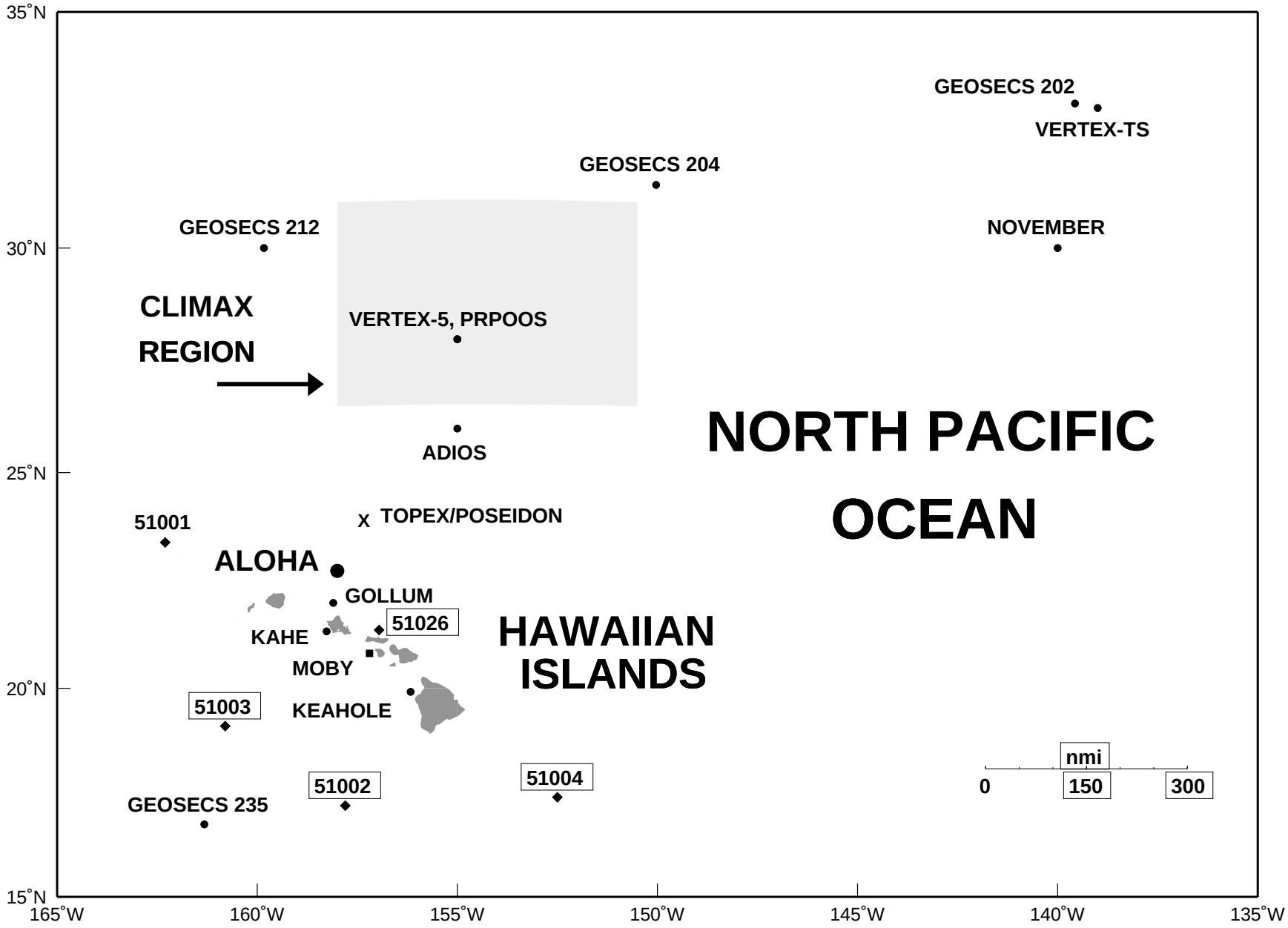

Figure 1.1: Map of the Central North Pacific Ocean showing the location of various time-series stations, including HOT.

In the early 1970's the North Pacific experiment (NORPAX) was initiated as an additional component of the NSF-IDOE. Research was focused on large scale interactions between the ocean and the atmosphere (e.g., El Niño), and the application of this knowledge to long-range climate forecasting. The Anomaly Dynamics Study was one component of NORPAX aimed at understanding interannual variability of the mid-latitude, North Pacific upper ocean thermal structure. Long-term ocean observation programs were fundamental to the success of NORPAX and, accordingly, the Trans-Pac XBT program and the Pacific Sea Level Network were established. Furthermore, the extensive 15 cruise Hawaii-to-Tahiti Shuttle time-series experiment (January 1979 - June 1980) was conducted to obtain direct measurements of the temporal variations in thermal structure of the equatorial Pacific region. These cruises also supported extensive ancillary research programs on chemical and biological oceanography, and provided a rich data set including measurements of DIC and primary productivity (Wyrtki et al. 1981).

With the abandonment of the central North Pacific Ocean weather ship stations and time-series programs such as Station GOLLUM, there remained very few sites where comprehensive serial measurements of internal variability of the ocean were continuing. The Intergovernmental Oceanographic Commission (IOC) and World Climate Research Program (WCRP) Committee on Climate Change in the Ocean (CCCO) recognized this deficiency, and in 1981 endorsed the initiation of new ocean observation programs. Reactivation of Station GOLLUM was an explicit recommendation (JSC/CCCO 1981).

In 1986, a biogeochemical time-series station was established in the northeast Pacific Ocean (33° N, 139° W) as one component of the NSF-sponsored Vertical Transport and Exchange (VERTEX) research program (Figure 1.1). A major objective of the VERTEX time-series project was to investigate seasonality in carbon export from the euphotic zone in relation to contemporaneous primary production. During an 18-month period (October 1986 - May 1988), the station was occupied for seven 1-week periods on approximately 3-month intervals. In addition to standard hydrographic surveys, samples were also collected for the measurement of dissolved inorganic and organic nutrients, particulate matter elemental analysis, primary production, nitrogen assimilation rates, microbial biomass and particle flux (Knauer et al. 1990; Harrison et al. 1992). Significant variability was observed in rates of primary production and particle flux and no clear relationship was found between new production and primary production. Despite the comprehensive scope and intensity of this research project, the sampling frequency was clearly inadequate to resolve much of the natural variability in this oligotrophic oceanic ecosystem.

In response to the growing awareness of the ocean's role in climate and global environmental change, and the need for additional and more comprehensive oceanic time-series measurements, the Board on Ocean Science and Policy (BOSP) of the National Research Council (NRC) sponsored a workshop on "Global Observations and Understanding of the General Circulation of the Oceans" in August 1983. The proceedings of this workshop (National Research Council 1984a) served as a prospectus for the development of the US component of the World Ocean Circulation Experiment (U.S.-WOCE). U.S.-WOCE has the following objectives:

- To understand the general circulation of the global ocean, to model with confidence its present state and predict its evolution in relation to long-term changes in the atmosphere and

- To provide the scientific background for designing an observation system for long-term measurement of the large-scale circulation of the ocean.

In a parallel effort, a separate research program termed Global Ocean Flux Study (GOFS) focused on the ocean's carbon cycle and associated air-sea fluxes of carbon dioxide. In September 1984, NRC-BOSP sponsored a workshop on "Global Ocean Flux Study" which served as an eventual blueprint for the GOFS program (National Research Council 1984b). In 1986, the International Council of Scientific Unions (ICSU) established the International Geosphere-Biosphere Program: A Study of Global Change (IGBP), and the following year JGOFS (Joint GOFS) was designed as a Core Project of IGBP. U.S.-JGOFS research efforts focus on the oceanic carbon cycle, its sensitivity to change and the regulation of the atmosphere-ocean CO_2 balance (Brewer et al. 1986). The broad objectives of U.S.-JGOFS are:

- To determine and understand on a global scale the time-varying fluxes of carbon and associated biogenic elements in the ocean and
- To evaluate the related exchanges of these elements with the atmosphere, the sea floor and the continental boundaries (SCOR 1990, JGOFS Rep. #5).

In order to achieve these goals, four separate program elements were defined:

- Process studies to capture key regular events,
- Long-term time-series observations at strategic sites,
- A global survey of relevant oceanic properties (e.g., CO_2) and
- A vigorous data interpretation and modeling effort to disseminate knowledge and to generate testable hypotheses.

In 1987, two separate proposals were submitted to the US-WOCE and US-JGOFS program committees by scientists at the University of Hawaii at Manoa to establish a multi-disciplinary, deep water hydrostation in Hawaiian waters. In July 1988, these proposals were funded by the National Science Foundation and Station ALOHA was officially on the map (Karl and Lukas 1996; Figure 1.1). A sister station in the western North Atlantic Ocean, near the historical Panulirus Station, was likewise funded by the US-JGOFS program and is operated by scientists at the Bermuda Biological Station for Research, Inc. (Michaels and Knap 1996).

The primary research objectives of these ocean measurement programs are to establish and maintain deep-water hydrostations for observing and interpreting physical and biogeochemical variability. The initial design called for repeat measurements of a suite of core parameters at approximately monthly intervals, compilation of the data and rapid distribution to the scientific community.

1.2. Hawaii Ocean Time-series Program

The Hawaii Ocean Time-series (HOT) Program consists of several research components lead by scientist at the University of Hawaii at Manoa (Table 1.1). The hydrographic (WOCE) and biogeochemical (JGOFS) components are fully integrated operationally and are both involved in all aspects of planning and execution of HOT Program objectives.

Table 1.1: HOT Research Components

Principal Investigators	Project Title
Robert R. Bidigare	Phytoplankton community structure
David M. Karl, Dale V. Hebel, Luis M. Tupas	JGOFS Core Component
Michael R. Landry	Zooplankton community structure
Christopher D. Winn	Inorganic Carbon System
Roger B. Lukas, Eric Firing	WOCE Core Component

1.2.1. Scientific objectives for HOT

The primary objective of HOT is to obtain a long time-series of physical and biochemical observations in the North Pacific subtropical gyre that will address the goals of the US Global Change Research Program. The objectives specific to the WOCE program are to:

- document and understand seasonal and interannual variability of water masses
- relate water mass variations to gyre fluctuations
- determine the need and methods for monitoring currents at Station ALOHA
- develop a climatology of short-term physical variability

In addition to these general primary objectives, the physical oceanographic component of HOT provides CTD/rosette sampling support for the JGOFS time-series sampling program, and supports development of new instrumentation for hydrographic observations. To date, HOT has supported research on lowered acoustic profiler measurements of currents (Firing and Gordon 1990), and on dissolved oxygen sensor technology (Atkinson et al. 1995), to name a few examples, in support of WOCE objectives.

The objectives of HOT specific to the JGOFS program are to:

- document and understand seasonal and interannual variability in the rates of primary production, new production and particle export from the surface ocean
- determine the mechanisms and rates of nutrient input and recycling, especially for N and P in the upper 200 m of the water column
- measure the time-varying concentrations of DIC in the upper water column and estimate the annual air-to-sea CO_2 flux

In addition to these general primary objectives, the JGOFS component provides logistical support for numerous complementary research programs (Table 1.2).

Table 1.2: Ancillary Projects Supported by HOT

Principal Investigator(s)	Institution	Agency	Duration	Project Title
Marlin Atkinson	Univ. of Hawaii	NSF	12/88-12/95	Calibration Stability of Two New O2 Sensors for CTDs
Lisa Campbell	Univ. of Hawaii	NSF	3/91-2/94	Phytoplankton Population Dynamics at the Hawaii Ocean Time-series Station
Lisa Campbell, Giacomo DiTullio	Univ. of Texas College of Charleston	NSF	11/94-10/97	Effects of Light and Nitrogen source on *Prochlorococcus* Growth
James Cowen	Univ. of Hawaii	NSF	8/92-12/94	Studies on the Dynamics of Marine Snow and Particle Aggregation in the North Pacific Central Gyre
Steven Emerson	Univ. of Washington	NSF	10/93-9/96	Ocean Oxygen Fluxes
Mark Huntley	Univ. of California Scripps Inst. Oceanography.	ONR	2/95-present	Particle Size Distribution at Stn. ALOHA Measured with an Optical Plankton Counter
David Karl, Renate Scharek	Univ. of Hawaii	NSF	1/95-5/96	Diatom Population Dynamics
David Karl	Univ. of Hawaii	NSF	2/96-present	LTER Cross-site Comparison Microbial Loop Dynamics
Charles Keeling	Univ. of California Scripps Inst. Oceanography.	NSF	12/88-present	A Study of the Abundance and $^{13}C/^{12}C$ Ratio of Atmosphere Carbon Dioxide and Oceanic Carbon in Relation to the Global Carbon Cycle
George W. Luther III	Univ. of Delaware	NSF	2/93- 1/96	Iodine Speciation as a Primary Productivity Indicator
Christopher Measures	Univ. of Hawaii	ONR	4/93-12/95	Temporal Variation of Dissolved Trace Element Concentrations in Response to Asian Dust Inputs
Brian Popp, David Karl	Univ. of Hawaii	NSF	6/91-5/94	Isotopic Analyses of DOC and Cell Concentrates
Paul Quay	Univ. of Washington	NOAA	6/93-present	$^{13}C/^{12}C$ of Dissolved Inorganic Carbon in the Ocean
Sansone, Francis	Univ. of Hawaii	ONR	1/96-present	Upper Ocean Methane Dynamics
Hans Thierstein	Geo. Inst. Switzerland	Swiss FIT	1/93-10/96	Calcareous Phytoplankton Dynamics
Jon Zehr	Rensselaer Polytech	NSF	1/96-present	Nitrogen Fixation Genes

1.2.2. HOT Study Site

There are both scientific and logistical considerations involved with the establishment of any long-term, time-series measurement program. Foremost among these is site selection, choice of variables to be measured and general sampling design, including sampling frequency. Equally important design considerations are those dealing with the choice of analytical methods for a given candidate variable, especially an assessment of the desired accuracy and precision, and availability of suitable reference materials, the hierarchy of sampling replication and, for data collected at a fixed geographical location, mesoscale horizontal variability.

We evaluated several major criteria prior to selection of the site for the HOT oligotrophic ocean benchmark hydrostation. First, the station must be located in deep water (>4000 m), upwind (north-northeast) of the main Hawaiian islands and of sufficient distance from land to be free from coastal ocean dynamics and biogeochemical influences. On the other hand, the station should be close enough to the port of Honolulu to make relatively short duration (<5 d) monthly cruises logistically and financially feasible. A desirable, but less stringent criterion would locate the station at, or near, previously studied regions of the central North Pacific Ocean, in particular Station GOLLUM.

After consideration of these criteria, we established our primary sampling site at 22° 45' N, 158° W at a location approximately 100 km north of the island of Oahu (Figure 1.2 and Table 1.3), and generally restrict our monthly sampling activities to a circle with a 6 nautical mile radius around this nominal site. Station ALOHA is in deep water (4750 m) and is more than one Rossby radius (50 km) away from steep topography associated with the Hawaiian Ridge. We also established a coastal station W-SW of the island of Oahu, approximately 10 km off Kahe Point (21° 20.6' N, 158° 16.4' W) in 1500 m of water. Station Kahe serves as a coastal analogue to our deep-water site and the data collected there provide a near-shore time-series for comparison to our primary open ocean site. Station Kahe is also used to test our equipment each month before departing for Station ALOHA, and to train new personnel at the beginning of each cruise.

Table 1.3: Location of HOT Stations

Station	Coordinates	Depth (m)	Comments
1 (Kahe)	21° 20.6' N, 158° 16.4' W	1,500	HOT Program coastal station
2 (ALOHA)	22° 45.0' N, 158° 00' W	4,800	HOT Program open ocean station
3	23° 25.0' N, 158° 00' W	4,800	Established in 1993
4	21° 57.8' N, 158° 00' W	4,000	Established and ended in 1993
5	21° 46.6' N, 158° 00' W	450	Established and ended in 1993
6 (Kaena)	21° 50.8' N, 158° 21.8' W	2,500	Established in 1993, ended in 1995
7 (Kauai Basin)	22° 30.8' N, 158° 10.0' W	4,800	Established in 1996

The HOT program was initially conceived as being a deep-ocean, ship- and mooring-based observation experiment that would have an approximately 20-year lifetime. Consequently, we selected a core suite of environmental variables that might be expected to display detectable change on time scales of several days to one decade. Except for the availability of existing

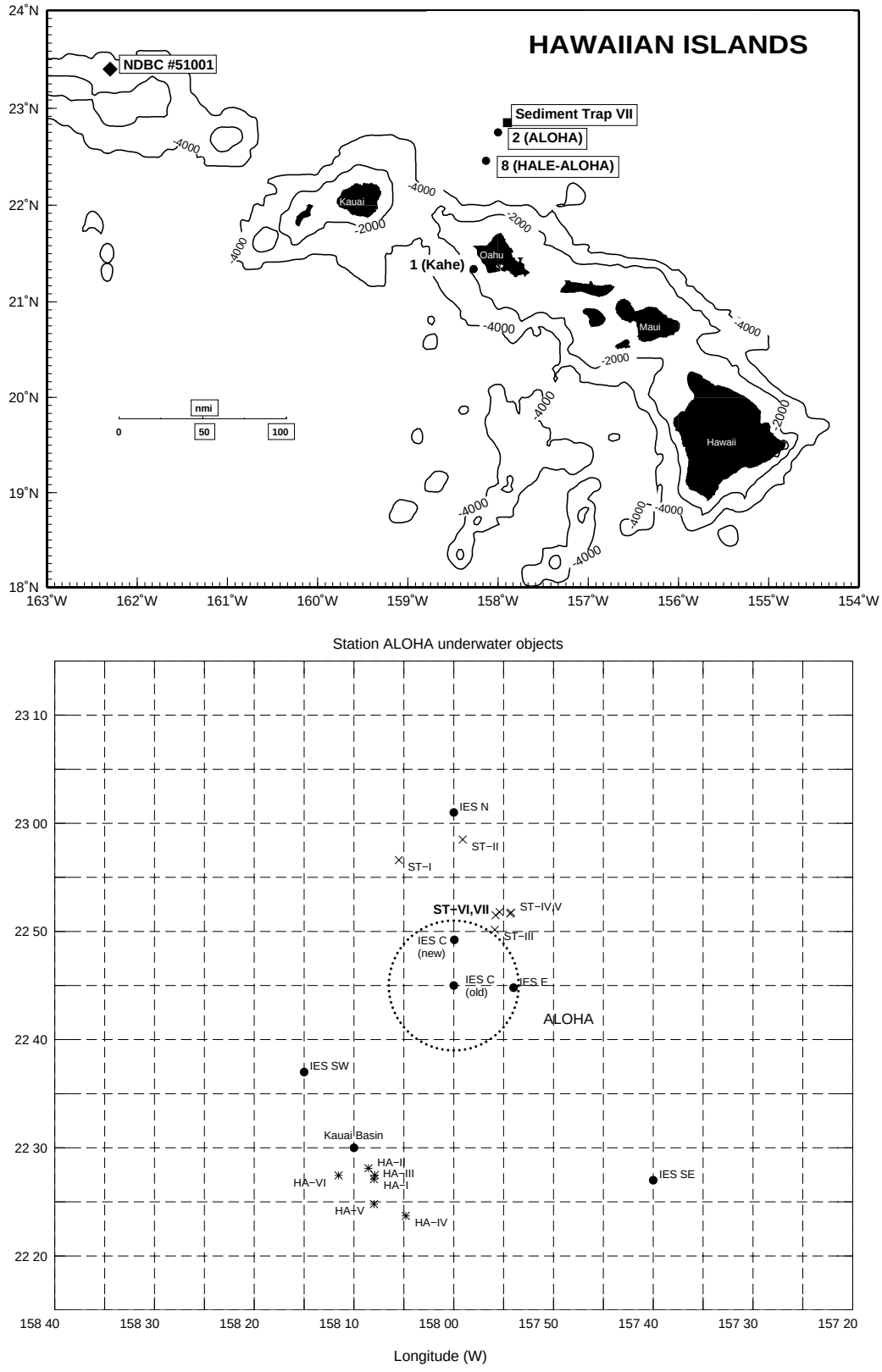

Figure 1.2: [Upper panel] Map of the Hawaiian islands showing the locations of the HOT stations and the NOAA NDBC weather buoys. [Lower panel] Station ALOHA showing its center and 6 nautical-mile radius and the location of the inverted echo sounders (IES), moored sediment traps (ST) and the HALE ALOHA mooring (HA).

satellite and ocean buoy sea surface data, the initial phase of the HOT program (Oct 1988 - Feb 1991) was entirely supported by research vessels. In February 1991, an array of five inverted echo sounders (IES) was deployed in an approximately 150 km^2 network around Station ALOHA (Chiswell 1996) and in June 1992, a sequencing sediment trap mooring was deployed a few km north of Station ALOHA (Karl et al. 1996a; Figure 1.2). In 1993, the IES network was replaced with two strategically-positioned instruments: one at Station ALOHA and the other at Station Kaena (Figure 1.2). The IES at Station Kaena was permanently retrieved in October 1995. Beginning in 1994, a single IES has been positioned and annually replaced at the center of Station ALOHA. Except for brief service intervals, both the Station ALOHA IES transducer and ALOHA sediment trap mooring have been collecting data since their respective initial deployments.

1.2.3. Field Sampling Strategy

HOT program cruises are conducted at approximately monthly intervals; the exact timing dictated by the availability of research vessels. To date, our field observations have not been severely aliased by month, season or year, except perhaps for a slight under representation of data in November and slight over representation in October (Figure 1.3). From HOT-1 (October 1988) to HOT-65 (August 1995), with the exception of HOT-42 and HOT-43 (November and December 1992), each cruise was 5 days in duration (port to port). Beginning with HOT-66 (September 1995) the standard HOT cruise was reduced by 20 % to 4 days (port to port) in order to accommodate the additional mooring-based HOT field programs.

From HOT-1 (October 1988) to HOT-32 (December 1991), underway expendable bathythermograph (XBT; Sippican T-7 probes) surveys were conducted at 7 nautical mile spacing on the outbound transect from Station Kahe to Station ALOHA. These surveys were later discontinued because the space-time correlation of the energetic, internal semi-diurnal tides made it difficult to interpret these data. In February 1995 we added an instrumented, 1.5 m Endeco towfish package (Sea-Bird CTD, optical plankton counter, fluorometer) to our sampling program (see section 2.12). Upper water column currents are measured both underway and on station using a hull-mounted Acoustic Doppler Current Profiler (ADCP), when available (Firing 1996). The majority of our sampling effort, approximately 60-72 hours per standard HOT cruise, is spent at Station ALOHA. Underway near-surface measurement of a variety of physical, chemical and biological properties is made possible by sampling seawater through a pumped intake system positioned in the hull of the R/V *Moana Wave*. In May 1995, a thermosalinograph was installed in line to the ships seawater intake system (see section 2.11). In July 1996, the existing system was replaced with a non-contaminating PVC/ stainless steel system. Several new sensors such as an underway surface pCO2 measuring system and a flow through fluorometer were installed (see section 2.2.2.3 and 2.2.6.1).

High vertical resolution environmental data are collected with a Sea-Bird CTD having external temperature (T), conductivity (C), dissolved oxygen (DO), fluorescence and light transmission sensors, and an internal pressure (P) sensor. A Sea-Bird 24-place carousel and an aluminum rosette that is capable of supporting 24 12-l PVC bottles are used to obtain water samples from desired depths. The CTD and rosette are deployed on a 3-conductor cable allowing for real-time display of data and for tripping the bottles at specific depths of interest.

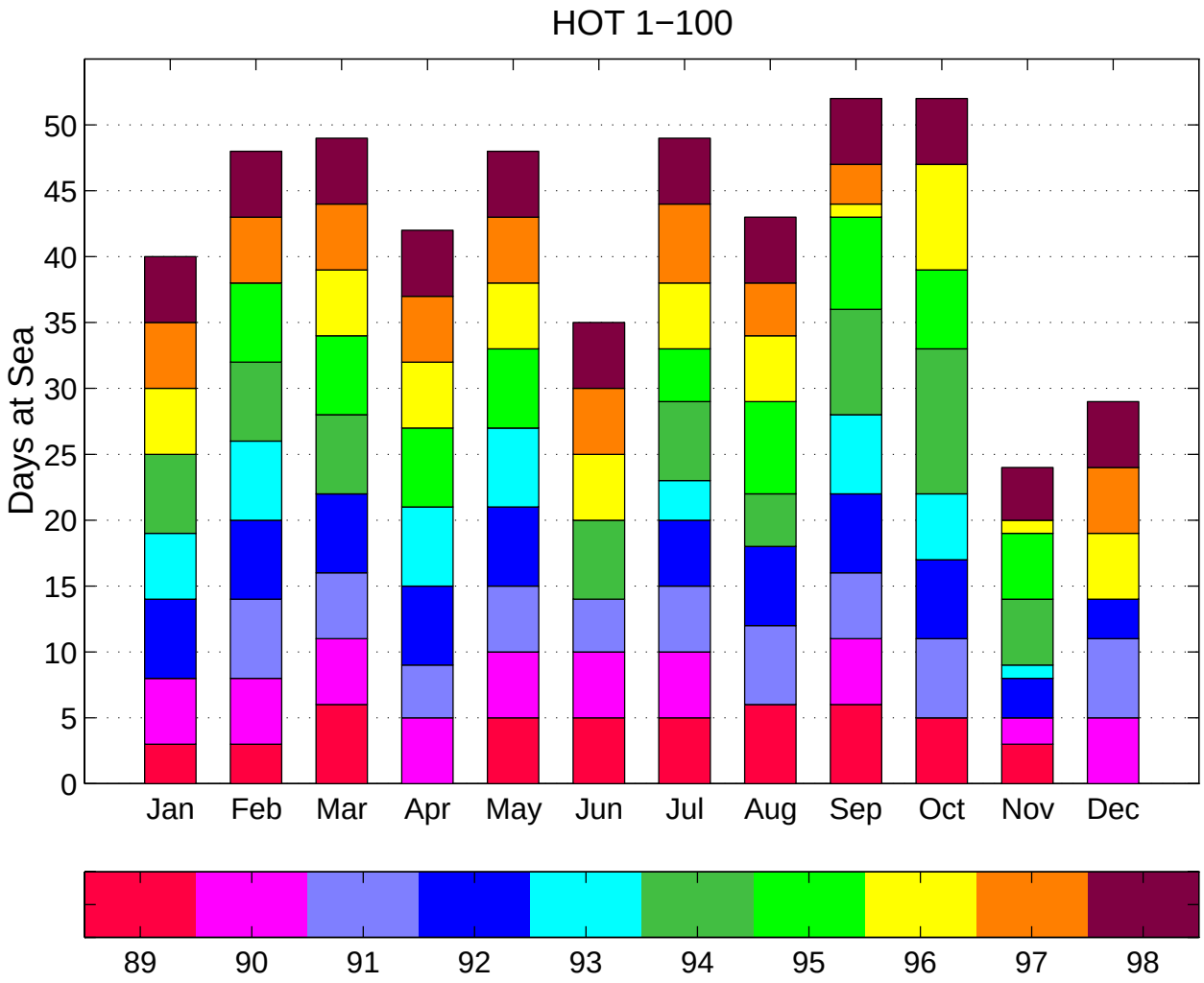

Figure 1.3: Cumulative number of days at sea per month for all HOT cruises from October 1988 to December 1998(HOT-1 to100).

The CTD system takes 24 samples sec^{-1} and the raw data are stored both on the computer and, for redundancy, on VHS-format video tapes. We also routinely collect "clean" water samples for biological rate measurements using General Oceanics Go-Flo bottles, Kevlar cable, metal-free sheave, Teflon messengers and a stainless steel bottom weight. A free-drifting sediment trap array, identical in design to the VERTEX particle interceptor trap (PIT) mooring (Knauer et al. 1979), is deployed at Station ALOHA for an approximately 2.5 day period to collect sinking particles for chemical and microbiological analyses.

Sampling at Station ALOHA typically begins with sediment trap deployment followed by a deep (> 4700 m) CTD cast and a "burst series" of at least 13 consecutive casts, on 3-hr intervals, to 1000 m to span the local inertial period (~31 hr) and three semidiurnal tidal cycles. The drift tracks of the sediment trap arrays and the location of the CTD casts for each cruise are shown in Figure 1.4.

The repeated CTD casts enable us to calculate an average density profile from which variability on tidal and near-inertial time scales has been removed. These average density profiles are useful for the comparison of dynamic height and for the comparison of the depth distribution of chemical parameters from different casts and at monthly intervals. For example, by fitting the distribution of inorganic nutrients to this average density structure, the depth of the nutricline can be defined each month, independent from the short time scale changes in the density structure of the upper water column (Dore and Karl 1996). This sampling strategy is designed to assess variability on time scales of a few hours to a few years. Very high frequency variability (< 6 hr) and variability on time scales of between 3-60 days are not adequately sampled at the present time. Initial results from the IES network suggest that these frequencies might be important at Station ALOHA (Chiswell 1996). However, no field sampling program, regardless of its intensity, can adequately resolve the entire spectrum of variability that theoretically exists in the ocean (Tabata 1965). The HOT program is no exception.

Water samples for a variety of chemical and biological measurements are routinely collected from the surface to within 5 m of the seafloor. To the extent possible, we collect samples for complementary biogeochemical measurements from the same or from contiguous casts to minimize aliasing caused by time-dependent changes in the density field. This is especially important for samples collected in the upper 300 m of the water column. Furthermore, we attempt to sample from common depths and specific density horizons each month to facilitate comparisons between cruises. Water samples for salinity determinations are collected from every water bottle to identify sampling errors. Approximately 20 % of the water samples are collected and analyzed in duplicate or triplicate to assess and track our analytical precision in sample analysis.

1.2.4. Core Measurements, Experiments and Protocols

The suite of core measurements provides a data base to validate existing biogeochemical models and to develop improved ones. Our list of core measurements has evolved since the inception of the HOT program in 1988, and now includes both continuous and discrete physical, biological and chemical ship-based measurements, *in situ* biological rate experiments, and observations and sample collections from bottom-moored instruments and buoys (Table 1.4). Continuity in the measurement parameters and their quality, rather than continuity in the methods employed, is of greatest interest. Detailed analytical methods are expected to change over time

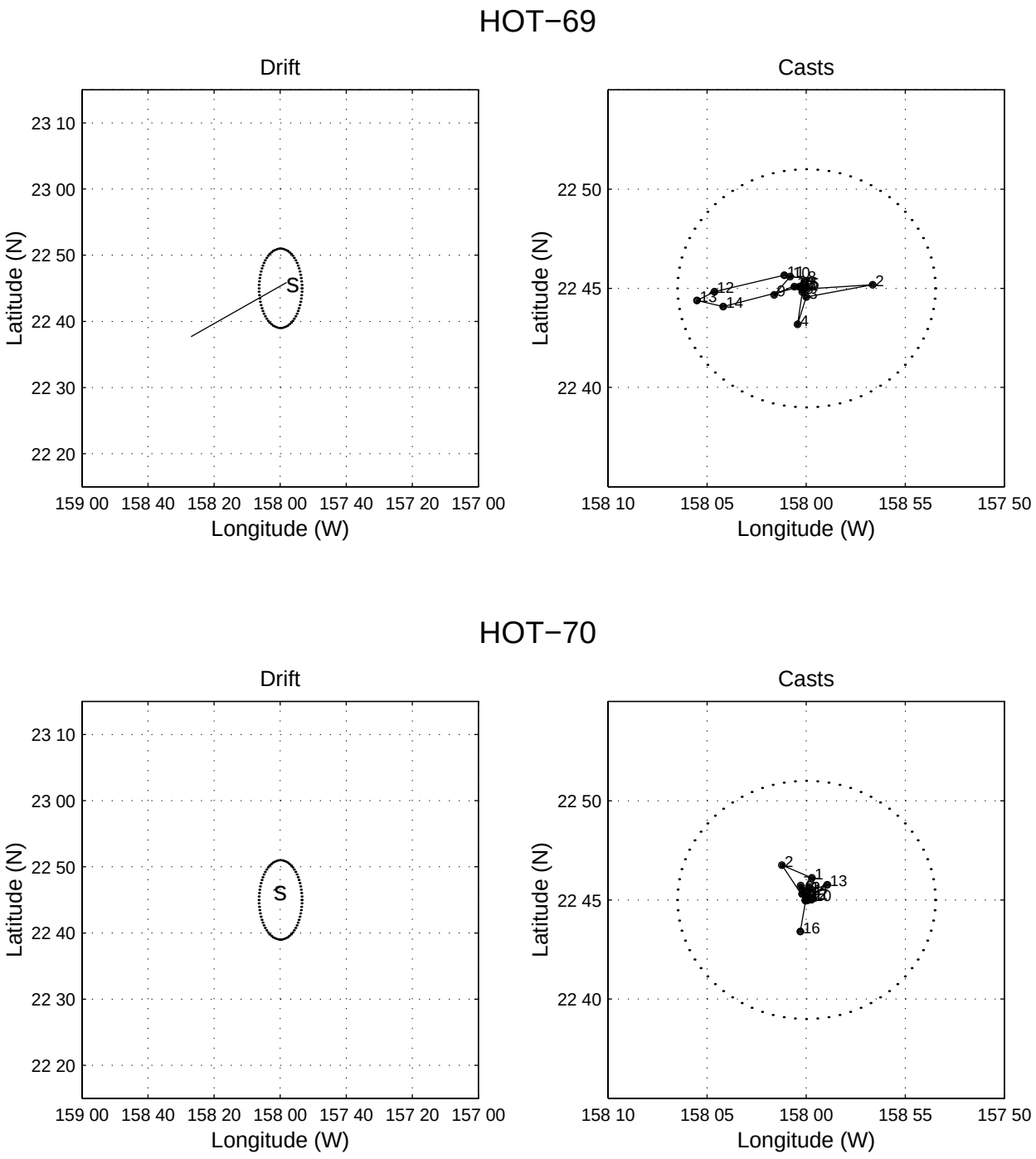

Figure 1.4: [Left panels] Drift track of the sediment trap array during each HOT cruise. Starting point indicated by S. [Right panels] CTD locations during each HOT cruise in 1996. Solid line indicates cast taken in sequence and numbers show the location of each cast. Dashed line shows the 6 nautical-mile radius of the station.

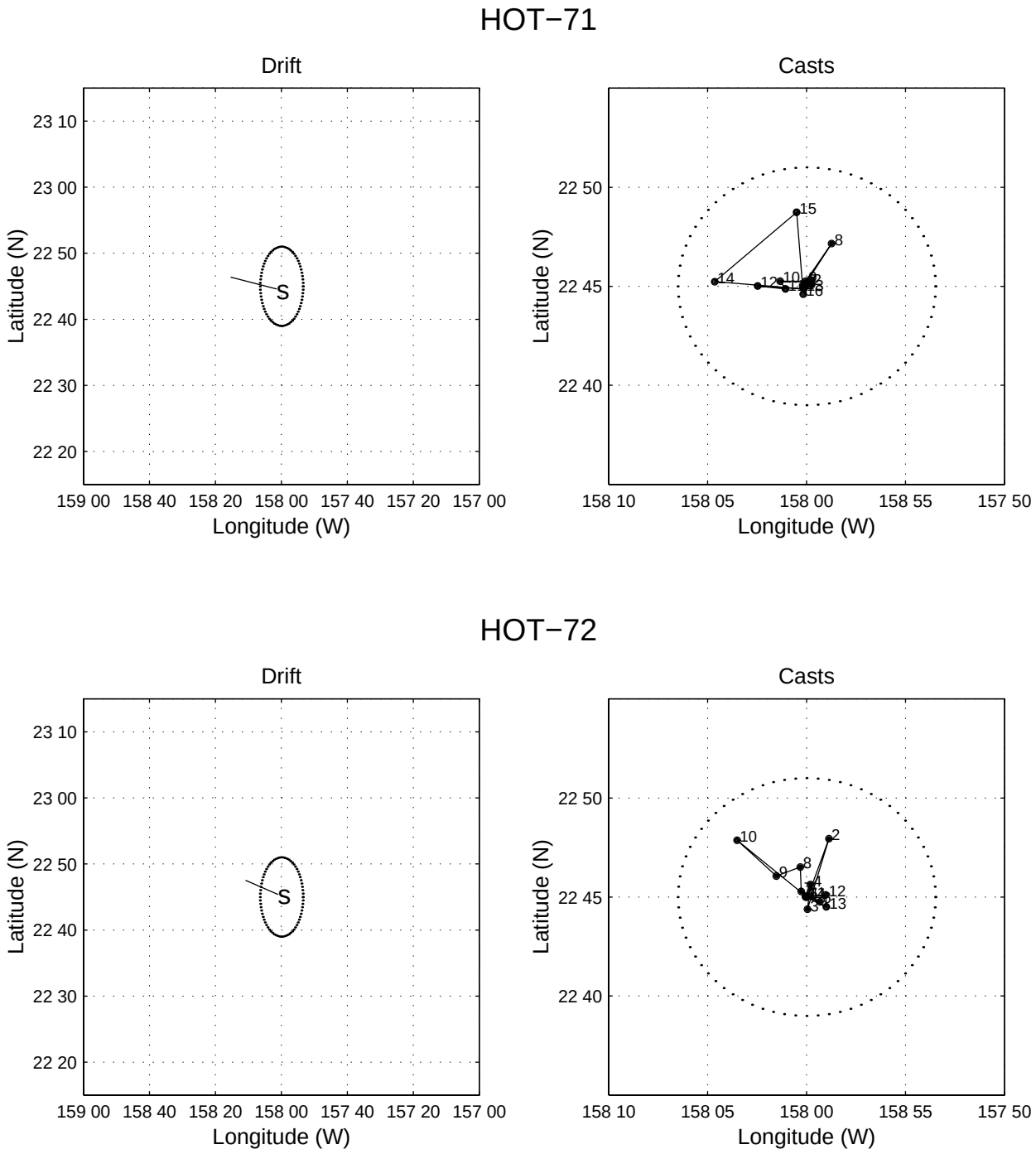

Figure 1.4: continued

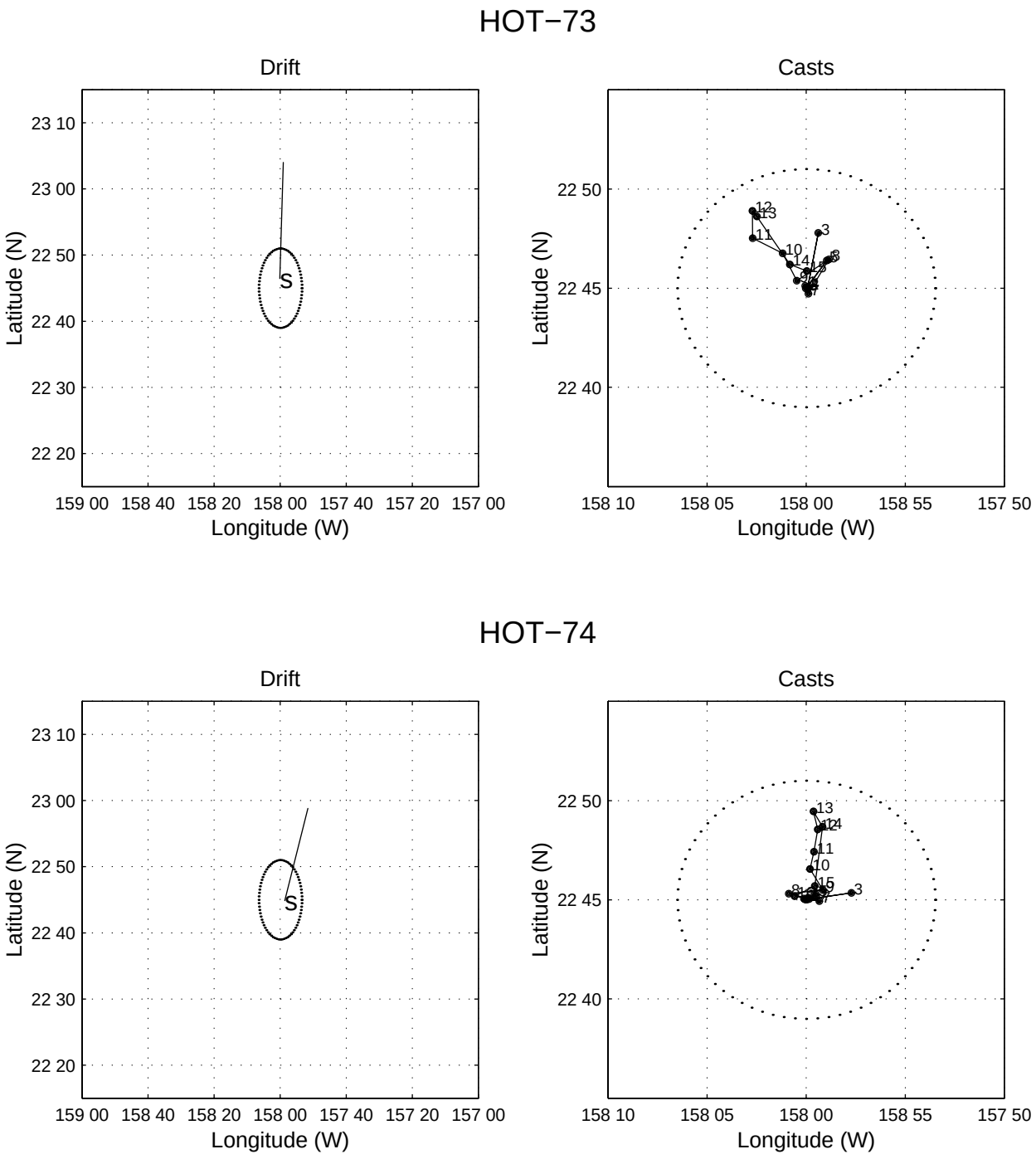

Figure 1.4: continued

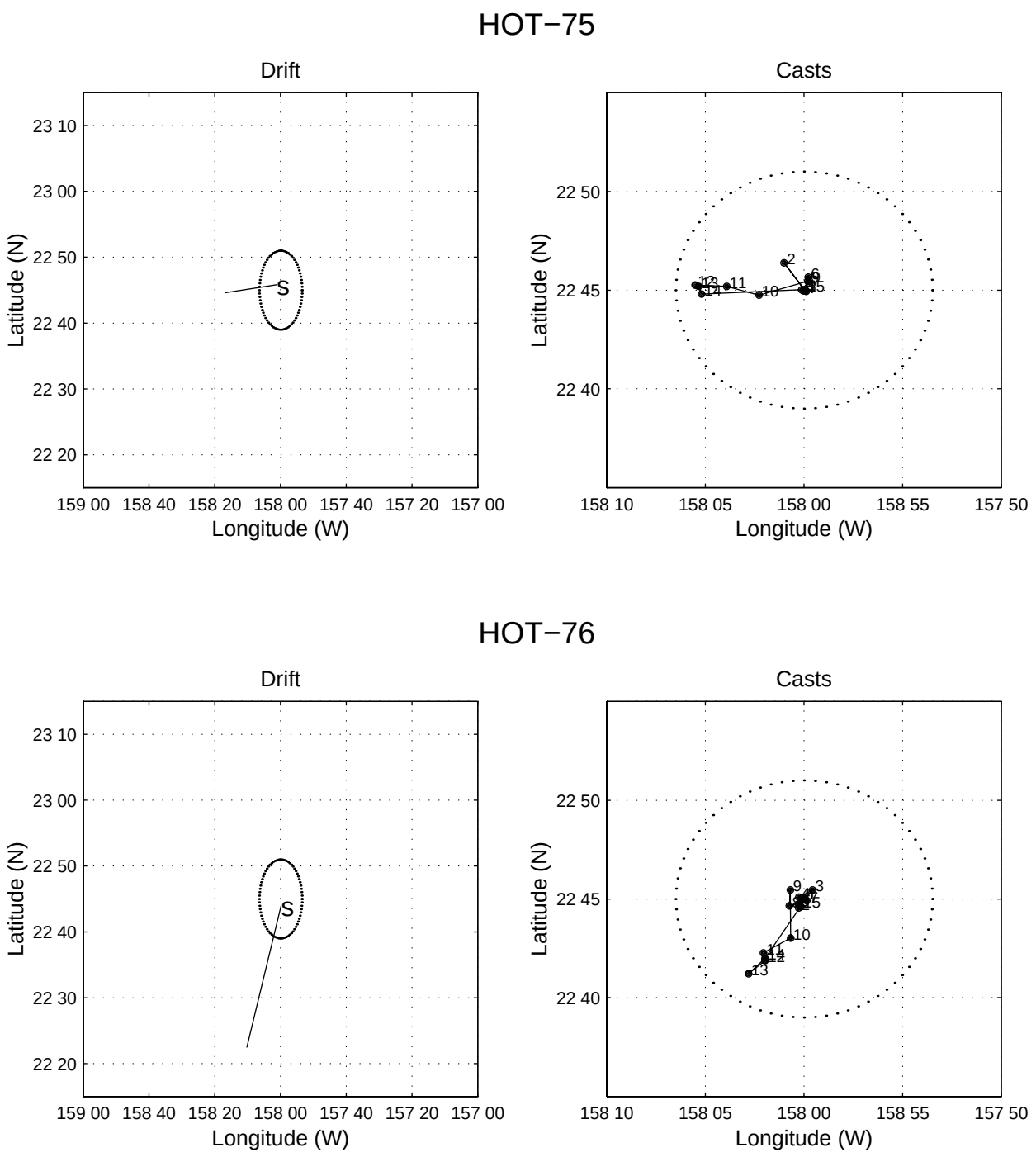

Figure 1.4: continued

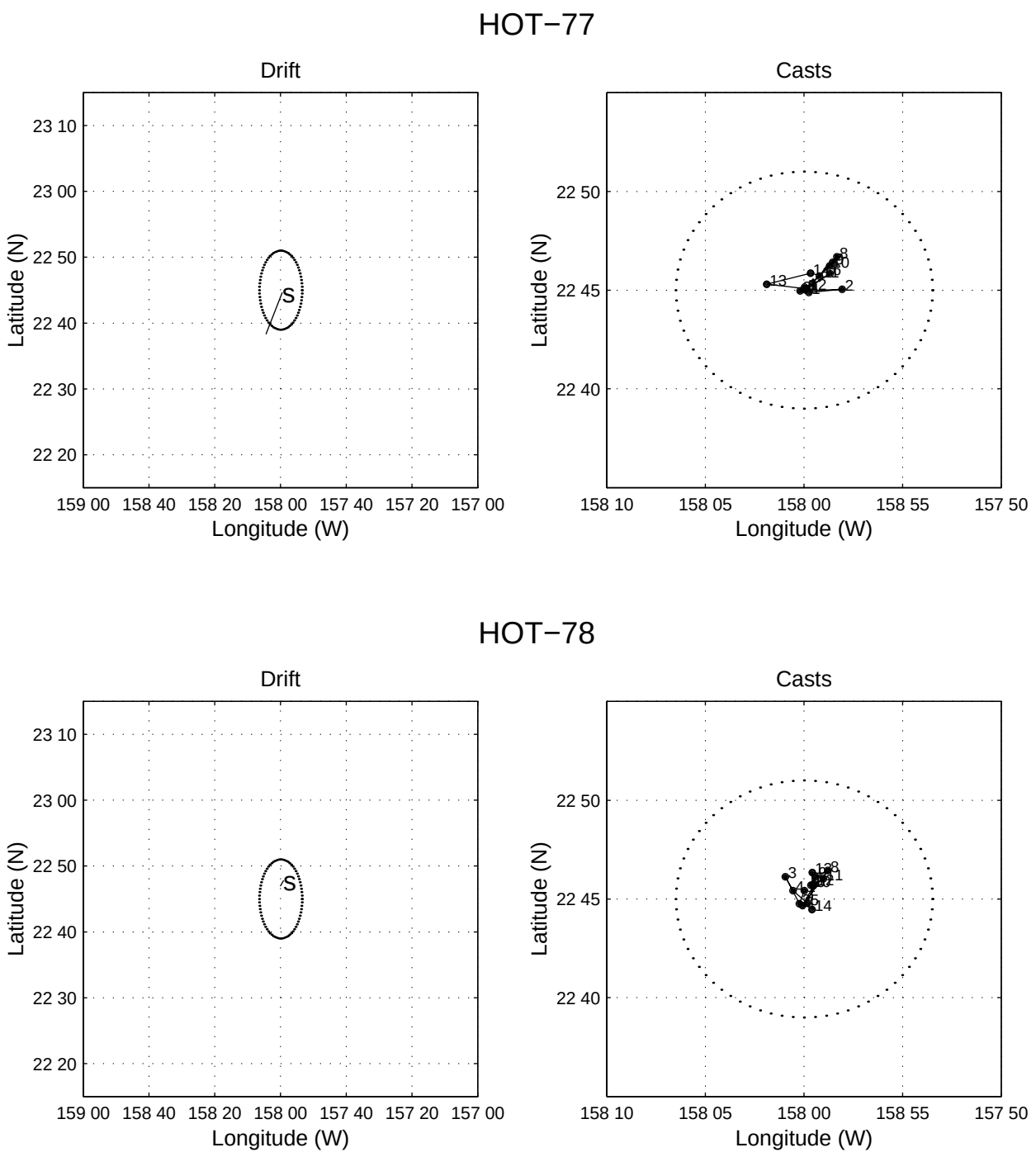

Figure 1.4: continued

through technical improvements. In addition to the core data, specialized measurements and process-oriented experiments have also been conducted at Station ALOHA (Table 1.4).

Table 1.4: Parameters Measured at Station ALOHA

Parameter	Depth Range (m)	Analytical Procedure
I. CTD Measurements		
Pressure (Depth)	0-4800	Pressure transducer on Sea-Bird CTD-rosette package
Temperature	0-4800	Thermistor on Sea-Bird CTD package with frequent calibration
Conductivity (Salinity)	0-4800	Conductivity sensor on Sea-Bird CTD package, standardization with Guildline AutoSal #8400A against Wormley standard seawater
Oxygen	0-4800	YSI sensor on Sea-Bird CTD package with Winkler standardization
Fluorescence	0-1000	Sea-Tech flash fluorometer
Beam Transmission	0-1000	Sea-Tech 25 cm path beam transmissometer, (discontinued)
II. Water Column Chemical Measurements		
Oxygen	0-4750	Winkler titration
Dissolved Inorganic Carbon	0-4750	Coulometry
Titration Alkalinity	0-4750	Automated Gran titration
PH	0-4750	Spectrophotometric
Nitrate Plus Nitrite	0-4750	Autoanalyzer
Soluble Reactive Phosphorus (SRP)	0-4750	Autoanalyzer
Silicate	0-4750	Autoanalyzer
Low Level Nitrate Plus Nitrite	0-200	Chemiluminescence
Low Level SRP	0-200	Magnesium-induced coprecipitation
Dissolved Organic Carbon	0-1000	High temperature catalytic oxidation
Dissolved Organic Nitrogen	0-1000	UV oxidation of total nitrogen
Dissolved Organic Phosphorus	0-1000	UV oxidation of total phosphorus
Particulate Carbon	0-1000	High temperature combustion
Particulate Nitrogen	0-1000	High temperature combustion
Particulate Phosphorus	0-1000	High temperature combustion
III. Biomass Measurements		
Chlorophyll *a* and Phaeopigments	0-200	Fluorometric analysis
Pigments	0-200	HPLC
Adenosine 5'-Triphosphate	0-1000	Firefly bioluminescence
Bacteria and Cyanobacteria	0-200	Flow cytometry
Meso and Microzooplankton	0-200	Net tows, elemental analysis

Table 1.4: continued

Parameter	Depth Range (m)	Analytical Procedure
IV. Carbon Assimilation and Particle Flux		
Primary Production	5-175	"Clean" ^{14}C incubations
Carbon, Nitrogen, Phosphorus	150	Free-floating particle interceptor traps
V. Currents		
Acoustic Doppler Current Profiler	0-300	Hull mounted, RDI #VM-150
Acoustic Doppler Current Profiler	0-4750	Lowered ADCP
VI. Instrumented Towfish		
Pressure (Depth)	45	Sensor on Sea-Bird package
Temperature	45	Thermistor on Sea-Bird package
Conductivity (Salinity)	45	Sensor on Sea-Bird package
Zooplankton	45	Optical Plankton Counter
Fluorescence	45	WetLabs SeaStar fluorometer on CTD package
VII. Bow Intake System		
Temperature	3	Sea-Bird remote temperature sensor in sea chest in bow of the ship with annual calibration
Conductivity (Salinity)	3	Sea-Bird temperature and conductivity sensors inside the thermosalinograph package, with similar standardization as for CTD salinity (section I)
pCO2	3	Gas equilibration, infrared detection
Fluorometry	3	Turner Designs 10-AU
VIII. Optical Measurements		
Incident Irradiance	Surface	LI-COR and Biospherical collector
Upwelling and downwelling irradiance	Surface-175	Biospherical Profiling Reflectance Refractometer PRR-600
IX. Moored Instruments		
Inverted Echo Sounder Network		Acoustic telemetry, CTD calibration
Sequencing Sediment Traps	4000	Parflux MK7-21

This report presents selected core data collected during the eighth year of the HOT Program (January-December 1996; Table 1.5). During this period, 10 regular HOT cruises were conducted using the University of Hawaii research vessel R/V *Moana Wave*. In addition, a separate R/V *Moana Wave* cruise (ST5) was conducted for the purpose of annual servicing of the bottom-moored sediment trap array and a trawl cruise to try and recover a sediment trap array that remains at the bottom of the study site. An 8-day cruise was also made to the historic Climax station to assess spatial variability and was called ALOHA-Climax 1 (AC-1). University of Hawaii shipboard technical assistance personnel (Table 1.6) assisted a total field scientific crew of 51 HOT staff, students and visiting scientists (Table 1.7) in our 1996 field work.

These selected measurements are part of a much larger HOT program data set on physical and biogeochemical variability at Station ALOHA that has been collected since October 1988. The complete data set is available to the community by several methods that are described in a subsequent section of this report (see Chapter 8).

Table 1.5: Chronology of 1996 HOT Cruises

Cruise	Ship	Depart	Return
69	R/V *Moana Wave*	15 January 1996	19 January 1996
70	R/V *Moana Wave*	25 March 1996	29 March 1996
71	R/V *Moana Wave*	22 April 1996	26 April 1996
72	R/V *Moana Wave*	20 May 1996	24 May 1996
Trawl	R/V *Moana Wave*	3 June 1996	5 June 1996
73	R/V *Moana Wave*	24 June 1996	28 June 1996
AC-1	R/V *Moana Wave*	8 July 1996	16 July 1996
74	R/V *Moana Wave*	25 July 1996	29 July 1996
75	R/V *Moana Wave*	19 August 1996	23 August 1996
76	R/V *Moana Wave*	30 September 1996	4 October 1996
ST5	R/V *Moana Wave*	7 October 1996	10 October 1996
77	R/V *Moana Wave*	28 October 1996	1 November 1996
78	R/V *Moana Wave*	9 December 1996	13 December 1996

Table 1.6: UH Shipboard Technical Assistance Group (shaded area = cruise participant)

Cruise Participant	**69**	**70**	**71**	**72**	**Trawl**	**73**	**AC-1**	**74**	**75**	**76**	**ST-5**	**77**	**78**
Dave Gravett													
Will Hervig													
Steve Poulos													
Pierlugi Pozzi													
Sharon Stahl													
	69	**70**	**71**	**72**	**Trawl**	**73**	**AC-1**	**74**	**75**	**76**	**ST-5**	**77**	**78**

Table 1.7: 1996 Cruise Personnel (shaded area = cruise participant)

Cruise Participants	69	70	71	72	Trawl	73	AC-1	74	75	76	ST-5	77	78
Al-Mutairi, Hussain													
Bishop, Craig													
Björkman, Karin													
Campbell, Lisa													
Christensen, Stephanie													
Cochran, Matthew													
Colman, Albert													
Cottrell, Bill													
Driscoll, Patrick													
Donachie, Stuart													
Donachie, Tracey													
Dumoulin, Caroline													
Dunne, John													
Foley, David													
Fujieki, Lance													
Guidry, Michael													
Hanson, Kristi													
Hebel, Dale													
Holmes, Elizabeth													
Houlihan Terrence													
Johnson, Dave													
Johnston, Shaun													
Jones, Dave													
Karl, David													
Landry, Michael													
Letelier, Ricardo													
Liu, Hong Bin													
Lopez, Mai													
Lucas, Molly													
McDonough, Kendra													
Messer, Andrea													
Monger, Bruce													
Nolla, Hector													
Nosse, Craig													
Nunnery, Scott													
Ondrusek, Michael													
Pinca, Sylvia													
	69	**70**	**71**	**72**	**Trawl**	**73**	**AC-1**	**74**	**75**	**76**	**ST-5**	**77**	**78**

Table 1.7: continued

Cruise Participants	69	70	71	72	Trawl	73	AC-1	74	75	76	ST-5	77	78
Rooney, John													
Sadler, Daniel													
Santiago-Mandujano, Fernando													
Schottle, Rolf													
Schulman, Deborah													
Selph, Karen													
Shackelford, Rachel													
Snyder, Jefrey													
Svensson, Erik													
Thomson-Bulldis, Angie													
Tupas, Luis													
Uehara, Tomoe													
West, Kristi													
Winn, Christopher													
Wright, Don													
	69	70	71	72	Trawl	73	AC-1	74	75	76	ST-5	77	78

2.0. SAMPLING PROCEDURES AND ANALYTICAL METHODS

A comprehensive summary of all sampling and analytical methods currently used in the HOT program along with information on measurement accuracy and precision can be found in the "Hawaii Ocean Time-series Program Field and Laboratory Protocols" manual. This document is available on the World Wide Web (http://hahana.soest.hawaii.edu) or can be obtained in hard copy by contacting David M. Karl [phone: (808) 956-8964; facsimile: (808) 956-5059; electronic mail: dkarl@soest.hawaii.edu]. Brief summaries of methods as well as calibration specifications and quality control / quality assurance information for CY 1996 are presented in this report. Hydrographic sampling methods are included in "WOCE Hydrographic Sampling Procedure. A primer for ship-board operations at the Hawaii Ocean Time-series Station," and is also available on the web (http://www.soest.hawaii.edu/HOT_WOCE).

2.1. Conductivity, Temperature, Depth and Dissolved Oxygen Profiling

Continuous measurements of conductivity, temperature, pressure, and dissolved oxygen content are made with a Sea-Bird SBE-911 Plus CTD package with a single pressure sensor, dual temperature and salinity sensors, and dual YSI oxygen sensors as described in Tupas et al. (1995). CTD casts are made at Stations Kahe and ALOHA during each cruise. A CTD cast to 1000 m is made at Station Kahe. At Station ALOHA a burst of consecutive CTD casts to 1000 m is made over 36 hours to span the local inertial period and three semi-diurnal tidal cycles. One WOCE standard cast within 10 m of the bottom is made during each cruise. During seven cruises in 1996 a second deep cast was obtained at station ALOHA to observe short time-space scale changes in the deep and bottom water (Lukas and Santiago-Mandujano 1996). In addition, Station 3 (north of ALOHA) was occupied during HOT-73, and Station 7 at the deepest point of the Kauai Basin (22° 30' N, 158° 10' W) was occupied during HOT-76.

2.1.1. Data Acquisition and Processing

CTD data were acquired at a rate of 24 samples per second. Digital data were stored on an IBM-compatible PC and, for redundancy, the analog signal was recorded on VHS video tapes. Backups of CTD data were made onto Bernoulli disks and later onto DAT tapes. The raw CTD data were quality controlled and screened for spikes as described in Winn et al. (1993). Data alignment, averaging, correction and reporting were done as described in Tupas et al. (1993). Conductivity spike rejection parameters were modified for some cruises in 1996. Spikes occur when the CTD samples the disturbed water of its wake. Therefore, samples from the downcast were rejected when the CTD was moving upward or when its acceleration exceeded 0.5 m s^{-2} in magnitude. Cruises 69, 70, 71, 73 and 78 were conducted under rough sea conditions, with heavy ship rolling during some of the casts, causing large vertical velocity fluctuations of the CTD package. The acceleration cutoff value had to be increased to between 0.55 and 0.65 m s^{-2} to have points available to average in each 2-dbar bin.

The data were additionally screened by comparing the sensor pairs. These differences permitted identification of problems in the sensors. Data from one pair of T-C sensors and one oxygen sensor, whichever is deemed mot reliable, is reported here.

Temperature is reported in the ITS-90 scale. Salinity and all derived units were calculated using the UNESCO (1981) routines; salinity is reported in the practical salinity scale (PSS-78). Oxygen is reported in μmol kg^{-1}.

2.1.2. Sensor Corrections and Calibrations

2.1.2.1. Pressure

The pressure calibration strategy employed a quartz pressure transducer as a transfer standard. Periodic recalibrations of this lab standard were performed with a primary pressure standard. Russka precision dead-weight pressure testers with weights meeting National Institute of Standards and Technology specifications, operated under environmentally-controlled conditions, were used as primary standards. The transfer standard was used to check the CTD pressure transducers at six-month intervals. The 1996 results of these tests showed a bias of less than 1.4 dbar in the 0 to 4500 dbar range between the CTD and transfer standard pressures. Therefore, the only correction applied to the CTD pressures was a constant offset determined at the time the CTD first enters the water on each cast.

2.1.2.1.1. Transfer Standard Calibration

The transfer standard was a Paroscientific Model 760 pressure gauge equipped with a 10,000 PSI transducer. This instrument was purchased in March 1988, and the original calibration coefficients were obtained from a calibration at Paroscientific against a primary standard. Subsequent recalibrations by the Oceanographic Data Facility at Scripps Institution of Oceanography, and by the Northwest Regional Calibration Center yielded a correction to the transfer standard (Karl et al. 1996b).

2.1.2.1.2. CTD Pressure Transducer Bench Tests

CTD pressure transducer bench tests were done using a dead-weight pressure tester and a manifold to apply pressure simultaneously to the CTD pressure transducer and to the transfer standard. All these tests had points at 6 pressure levels between 0 and 4500 dbar, increasing and decreasing pressures.

CTD pressure transducers are the same type as the transfer standard. Pressure transducer #26448 was used during all cruises in 1996. Bench tests against the calibration corrected transfer standard from August 1995 through June 1997 are given in Table 2.1. The 16 August 1995 offset at 0 dbar was used for the cruises in 1996 (Note that this offset was only used for real-time data acquisition, as a more accurate offset was later determined for the time that the CTD first enters the water on each cast). Our backup pressure transducer #51412 was also calibrated against the pressure standard.

Table 2.1: CTD Pressure Calibrations (decibars)

Calibration Date	Offset @ 0 dbar	0-4500 dbar offset	Hysteresis
Sea-Bird SBE-911 Plus #91361 / Pressure Transducer #26448			
16 August 1995	-5.9	1.4	0.2
9 January 1996	-6.3	1.2	not available
30 August 1996	-5.35	1.4	0.2
31 January 1997	-5.4	1.35	0.2
12 June 1997	-6.7	1.4	0.2
Sea-Bird SBE-911 Plus #92859 / Pressure Transducer #51412			
21 August 1995	-0.25	1.0	0.1
5 December 1995	-0.1	1.2	0.1
30 August 1996	-0.35	1.1	0.2
31 January 1997	0.0	1.25	0.2
12 June 1997	-0.7	1.5	0.2

The results in Table 2.1 indicate a variation of more than 1 dbar in the 0 dbar offset for sensor #26448 during the period of the calibrations. However, this variation is not reflected by the surface pressures recorded during cruises. CTD pressures before and after every cast are regularly recorded by the CTD operator when the CTD is on deck, and Figure 2.1 shows the median of these observations for every cruise. The variability observed in this record spanning the calibration period is only about ± 0.1 dbar (probably due to atmospheric pressure variability), and does not correspond to the 1 dbar variability observed in the bench tests. The cause of the variability in our bench tests is currently under investigation. The pressure offset between 0 and 4500 dbar from the bench tests has been nearly constant, but we are also trying to determine if the problem observed in the 0 dbar offset has affected our 0-4500 dbar offset estimates. The bench test hysteresis results for this sensor is about 0.2 dbar. The difference between before and after cast pressures from Figure 2.1 is smaller than the bench test hysteresis because most of the cruise casts only reach 1020 dbar, while the bench tests reach 4500 dbar. Table 2.1 shows less variability in the pressure offset for sensor #51412 than for sensor #26448. The 0-4500 dbar offset has been nearly constant for this sensor, with a slight increase in June 1997.

2.1.2.2. Temperature

Four Sea-Bird SBE-3-02/F temperature sensors, #741, #1416, #1591 and #886, were used in 1996 and were calibrated at Sea-Bird after every cruise (Tupas et al. 1995). The history of the sensors, as well as the procedures followed to obtain the sensor drift from the Sea-Bird calibrations are well-documented in Tupas et al. (1993, 1994b, 1995) and Karl et al. (1996b). Calibration coefficients obtained at Sea-Bird and used in the drift estimates are presented in Table 2.2. These coefficients were used in the following formula that gives the temperature (in °C) as a function of the frequency signal (f):

$$\text{temperature} = 1/\{a+b[\ln(f_0/f)]+c[\ln^2(f_0/f)]+d[\ln^3(f_0/f)]\}-273.15$$

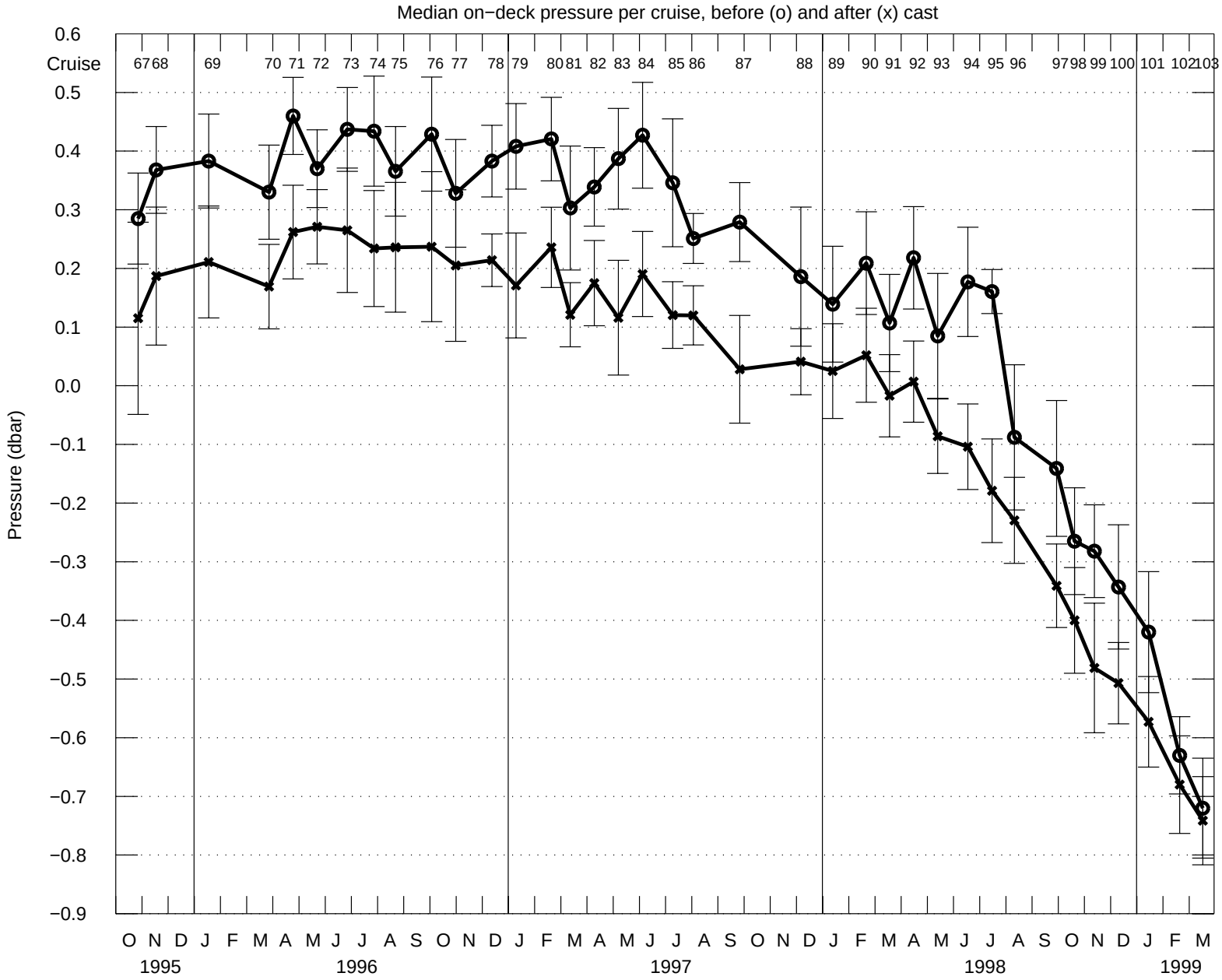

Figure 2.1: Median value of pressure on the ship's deck measured by the CTD pressure sensor before (circles) and after (crosses) each cast for HOT cruises 67-86. Error bars are 1 standard deviation from the mean. Cruise numbers are shown below the upper x-axis.

Table 2.2: Calibration Coefficients for Sea-Bird Temperature Sensors. RMS Residuals from Calibration Give an Indication of Quality of the Calibration

SN	YYMMDD	f_0	a	b	c	d	RMS (m°C)
741	970123	5937.30	3.68159674e-03	6.01976013e-04	1.55601695e-05	2.08726120e-06	0.04
741	961224	5937.17	3.68160825e-03	6.01978089e-04	1.55790423e-05	2.10423390e-06	0.03
741	961121	5937.28	3.68160521e-03	6.01997228e-04	1.56234377e-05	2.14328075e-06	0.03
741	961016	5936.94	3.68162909e-03	6.01984578e-04	1.55892487e-05	2.11334193e-06	0.04
741	960907	5936.95	3.68162831e-03	6.01983389e-04	1.55861044e-05	2.11156385e-06	0.03
741	960803	5937.04	3.68162330e-03	6.01978956e-04	1.55745177e-05	2.10206246e-06	0.03
741	960604	5937.15	3.68161245e-03	6.01969734e-04	1.55638273e-05	2.09876378e-06	0.03
741	960511	5936.98	3.68163137e-03	6.01975935e-04	1.55740862e-05	2.10619190e-06	0.02
741	960409	5937.12	3.68162119e-03	6.01960817e-04	1.55230920e-05	2.06760945e-06	0.05
741	960130	5936.98	3.68162931e-03	6.01962577e-04	1.55584608e-05	2.09468187e-06	0.03
741	951221	5936.84	3.68164814e-03	6.01972939e-04	1.55640449e-05	2.09602180e-06	0.04
741	951130	5936.76	3.68165657e-03	6.01974876e-04	1.55675430e-05	2.09609068e-06	0.03
741	951109	5936.75	3.68165818e-03	6.01978038e-04	1.55720771e-05	2.10144369e-06	0.04
741	951010	5936.79	3.68165301e-03	6.01972584e-04	1.55610823e-05	2.09136837e-06	0.03
741	951005	5936.73	3.68166104e-03	6.01980832e-04	1.55690345e-05	2.09403037e-06	0.03
741	950909	5936.70	3.68166527e-03	6.01982205e-04	1.55748402e-05	2.10165805e-06	0.03
1591	970123	6256.10	3.68159382e-03	6.03665542e-04	1.48094210e-05	1.76783952e-06	0.27
1591	961224	6255.99	3.68160535e-03	6.03673174e-04	1.48453596e-05	1.79943519e-06	0.27
1591	961121	6256.09	3.68160231e-03	6.03694156e-04	1.48708643e-05	1.81153943e-06	0.26
1591	961016	6255.76	3.68162604e-03	6.03670380e-04	1.48363905e-05	1.79473557e-06	0.26
1591	960907	6255.78	3.68162550e-03	6.03672072e-04	1.48430393e-05	1.80083873e-06	0.26
1591	960803	6255.82	3.68162056e-03	6.03658566e-04	1.48253692e-05	1.78983895e-06	0.25
1591	960709	6256.18	3.68158699e-03	6.03660525e-04	1.48363049e-05	1.79824977e-06	0.27
1591	960604	6255.94	3.68160959e-03	6.03648813e-04	1.48118821e-05	1.78108767e-06	0.27
1591	960511	6255.80	3.68162870e-03	6.03672267e-04	1.48578892e-05	1.81250639e-06	0.26
1591	960409	6255.90	3.68161809e-03	6.03654056e-04	1.48084674e-05	1.77203057e-06	0.26
1591	960130	6255.87	3.68162648e-03	6.03661297e-04	1.48071743e-05	1.76793444e-06	0.27
1591	951221	6255.73	3.68164531e-03	6.03673400e-04	1.48253529e-05	1.77803186e-06	0.27
1591	951128	6255.76	3.68164121e-03	6.03665605e-04	1.48116946e-05	1.76870354e-06	0.27
1591	951107	6255.77	3.68164219e-03	6.03670342e-04	1.48212416e-05	1.77715650e-06	0.28
1591	951010	6255.70	3.68165008e-03	6.03668926e-04	1.48159116e-05	1.77153493e-06	0.27
1591	951005	6255.65	3.68165808e-03	6.03677708e-04	1.48286716e-05	1.78045375e-06	0.28
1591	950909	6255.60	3.68166237e-03	6.03681962e-04	1.48436806e-05	1.79226317e-06	0.27
1591	950808	6255.54	3.68166578e-03	6.03669874e-04	1.48268255e-05	1.78327845e-06	0.28
1591	950629	6269.82	3.68029613e-03	6.03617050e-04	1.48534105e-05	1.81423355e-06	0.27
1591	950426	6269.62	3.68031886e-03	6.03633012e-04	1.48719170e-05	1.82098432e-06	0.28
1591	950323	6255.13	3.68171247e-03	6.03691208e-04	1.48607314e-05	1.80847897e-06	0.28
1591	950216	6255.41	3.68169061e-03	6.03693580e-04	1.48590071e-05	1.79916622e-06	0.28
2045	960730	2446.40	3.64679706e-03	5.89561321e-04	7.89409057e-06	-2.98132357e-06	0.07
2045	951011	2333.97	3.67453326e-03	5.90351814e-04	8.29452366e-06	-1.97021281e-06	0.51
2078	961217	2772.55	3.68022581e-03	5.92832713e-04	1.62002729e-05	1.77796339e-06	0.03
2078	951019	2772.32	3.68029270e-03	5.92819697e-04	1.61663533e-05	1.75679211e-06	0.03

Table 2.2: continued

SN	YYMMDD	f_0	a	b	c	d	RMS (m°C)
1416	970123	6230.98	3.68159846e-03	6.01858312e-04	1.51837195e-05	2.27180519e-06	0.16
1416	961224	6230.88	3.68160976e-03	6.01816996e-04	1.50392461e-05	2.14219483e-06	0.18
1416	961121	6230.92	3.68160594e-03	6.01799370e-04	1.49774932e-05	2.08956931e-06	0.18
1416	961016	6230.64	3.68163057e-03	6.01825030e-04	1.50579381e-05	2.15885092e-06	0.17
1416	960907	6230.68	3.68163004e-03	6.01845292e-04	1.51322492e-05	2.22208158e-06	0.17
1416	960803	6230.74	3.68162483e-03	6.01843946e-04	1.51556537e-05	2.25677588e-06	0.14
1416	960709	6231.07	3.68159136e-03	6.01825172e-04	1.51173387e-05	2.22430594e-06	0.15
1416	960604	6230.86	3.68161411e-03	6.01833092e-04	1.51365466e-05	2.23954346e-06	0.14
1416	960511	6230.72	3.68163329e-03	6.01860751e-04	1.52088782e-05	2.29691843e-06	0.15
1416	960409	6230.81	3.68162241e-03	6.01855548e-04	1.52212389e-05	2.31455094e-06	0.15
1416	960201	6230.71	3.68164082e-03	6.01867370e-04	1.52188168e-05	2.30343179e-06	0.13
1416	951221	6230.66	3.68164969e-03	6.01864683e-04	1.52037079e-05	2.29087490e-06	0.13
1416	951128	6230.71	3.68164555e-03	6.01838091e-04	1.51229297e-05	2.22774169e-06	0.11
1416	951107	6230.72	3.68164747e-03	6.01868566e-04	1.52209156e-05	2.30775457e-06	0.13
1416	951010	6230.71	3.68165430e-03	6.01862471e-04	1.51919005e-05	2.28088302e-06	0.12
1416	951005	6230.65	3.68166225e-03	6.01868789e-04	1.52001653e-05	2.28815621e-06	0.10
1416	950909	6230.66	3.68166627e-03	6.01850522e-04	1.51385467e-05	2.23880325e-06	0.07
1416	950808	6230.60	3.68166972e-03	6.01826839e-04	1.50854479e-05	2.20135113e-06	0.06
1416	950629	6244.88	3.68029900e-03	6.01782528e-04	1.51291120e-05	2.24419184e-06	0.04
1416	950426	6244.66	3.68032097e-03	6.01723202e-04	1.49695983e-05	2.12976704e-06	0.05
1416	950323	6230.19	3.68171386e-03	6.01747188e-04	1.48356092e-05	2.00273790e-06	0.11
1416	950216	6230.51	3.68169292e-03	6.01746979e-04	1.47979567e-05	1.95138530e-06	0.10
1416	950215	6244.15	3.68037741e-03	6.01762536e-04	1.50487658e-05	2.17350592e-06	0.04
1416	950126	6244.52	3.68034429e-03	6.01762980e-04	1.50565351e-05	2.17979832e-06	0.07
1416	950121	6604.29	3.64668597e-03	6.00127980e-04	1.47845402e-05	2.26485999e-06	0.05
1416	941222	6243.96	3.68039767e-03	6.01763025e-04	1.50286299e-05	2.14854816e-06	0.07
1416	941215	6243.91	3.68040347e-03	6.01766822e-04	1.50357450e-05	2.15120592e-06	0.07
1416	941208	6243.93	3.68040318e-03	6.01760183e-04	1.50137803e-05	2.13377720e-06	0.07
1416	941203	6230.42	3.68171174e-03	6.01831351e-04	1.50357279e-05	2.13826316e-06	0.03
1416	941111	6243.62	3.68042712e-03	6.01685406e-04	1.48250606e-05	1.99520905e-06	0.12
1416	941108	6243.61	3.68042771e-03	6.01682891e-04	1.48103792e-05	1.97962260e-06	0.12
886	961224	5903.14	3.68160859e-03	5.95962873e-04	1.45624901e-05	2.11836559e-06	0.04
886	961121	5903.26	3.68160535e-03	5.95988932e-04	1.46199173e-05	2.16055658e-06	0.03
886	961016	5902.98	3.68162929e-03	5.95965830e-04	1.45778207e-05	2.13574822e-06	0.03
886	960907	5902.90	3.68162856e-03	5.95974392e-04	1.45877050e-05	2.13885172e-06	0.03
886	960803	5902.94	3.68162352e-03	5.95972569e-04	1.45945154e-05	2.14581900e-06	0.03
886	960604	5903.10	3.68161286e-03	5.95951516e-04	1.45504328e-05	2.11802398e-06	0.04
886	960511	5902.95	3.68163190e-03	5.95953876e-04	1.45559001e-05	2.12377599e-06	0.04
886	960409	5903.00	3.68162079e-03	5.95960515e-04	1.46208651e-05	2.19582467e-06	0.02
886	960130	5903.00	3.68162955e-03	5.95970347e-04	1.45935940e-05	2.15057168e-06	0.03
886	951221	5902.81	3.68164858e-03	5.95964335e-04	1.45501245e-05	2.11098553e-06	0.04
1496	960118	5946.31	3.68167257e-03	5.89965822e-04	1.47447188e-05	2.95734250e-06	0.21
1496	931102	5952.17	3.68121200e-03	5.89938744e-04	1.49486143e-05	3.09294466e-06	0.22
1392	951013	2458.52	3.67466724e-03	5.87218944e-04	9.15090348e-06	-1.97663220e-06	0.28
1392	940929	2458.32	3.67487069e-03	5.87155511e-04	9.27931149e-06	-1.74690868e-06	0.89

An error in the Sea-Bird temperature calibration bath affected the calibrations between 23 April and 19 November 1996. The error was zero on 23 April and increased linearly to 0.55 x 10^{-3} °C on 19 November. All calibrations during this period were corrected.

For each sensor, the final calibration consists of two parts: first, a single "baseline" calibration is chosen from among the ensemble of calibrations during the year; second, for each cruise a temperature-independent offset is applied to remove the temporal trend due to sensor drift (Table 2.3). The offset, a linear function of time, is calculated by least squares fit to the 0-30 °C average of each calibration during the year. The maximum drift correction in 1996 was less than 2.5 x 10^{-3} °C. The baseline calibration is selected as the one for which the trend-corrected average from 0-5 °C is nearest to the ensemble mean of these averages.

Table 2.3: Temperature (T) and Conductivity (C) sensor corrections including the Thermal Inertia (α) parameter (see text). Dual temperature and conductivity sensors were used in all cruises. The last column shows the sensor pairs whose data are reported.

Cruise	T Sensor #	T Correction (°C)	C Sensor #	α	Data Reported
69	741	0.0001	1336	0.028	
	1416	-0.0006	679	0.028	All casts
70	741	0.0001	1336	0.028	
	1416	-0.0011	679	0.028	All casts
71	741	0.0000	1336	0.020	
	1416	-0.0012	679	0.028	All casts
72	741	0.0000	1336	0.020	All casts
	1591	-0.0005	679	0.020	
73	1416	-0.0016	1336	0.028	All casts
	1591	-0.0006	679	0.028	
AC-1	741	-0.00008	1336	0.020	All casts
	886	0.00012	679	0.020	
74	1416	-0.0018	1336	0.028	
	1591	-0.0007	679	0.028	All casts
75	1416	-0.0020	1336	0.028	
	1591	-0.0008	679	0.028	All casts
76	1416	-0.0022	1336	0.020	
	1591	-0.0009	679	0.020	All casts
77	741	-0.0002	1336	0.028	All casts
	1416	-0.0024	679	0.028	
78	741	-0.0003	1336	0.020	All casts
	1591	-0.0012	679	0.020	

A small residual pressure effect on the temperature sensors that affected all our measurements was identified at Sea-Bird (N. Larson, personal communication, June 1996). This effect is due to residual stress transmitted to the thermistor bead through the pressure protective metal sheath. Pressure tests conducted at Sea-Bird yielded correction factors (k) for this effect for each of our sensors (Table 2.4). The corrected temperature (Tc) was calculated from the sensor temperature (T) and the pressure (P) as: $Tc = T - kP$. The maximum correction to our 1996 temperatures due to this effect was less than 1.45×10^{-3} °C in the deeper portion of the near-bottom casts. For the majority of the casts, which only reached 1020 dbar this correction had a maximum value of 0.3×10^{-3} °C. Casts obtained in cruises before 1996 will require a correction of the same order of magnitude. This correction which is insignificant at levels other than the bottom water is being currently implemented.

Table 2.4: Correction factor for residual pressure effect on temperature

Sensor #	Pressure coefficient (k)
741	-0.28×10^{-3} °C/5000 dbar
886	-0.11×10^{-3} °C/5000 dbar
1416	1.17×10^{-3} °C/5000 dbar
1591	1.44×10^{-3} °C/5000 dbar

Another correction to our temperature measurements was due to viscous heating of the sensor tip due to the water flow (Larson and Pederson 1996). The viscous heating is a function of the water velocity past the temperature sensor (U), the kinematic viscosity of the water, and the shape of the T-C duct that conducts the water through the temperature sensor. For the 1996 cruises the temperature increase due to viscous heating was given by $T_{vh} = 0.466\ \nu^{1/2}\ U^2$ (N. Larson, personal communication, 1996). The water flow through our CTD plumbing systems was measured in the lab. A mean flow of 25.69 ml s^{-1} (with 0.30 ml s^{-1} standard deviation from 7 measurements) was obtained for the first sensor set, and 25.67 ml s^{-1} (with 0.31 ml s^{-1} standard deviation from 7 measurements) for the second set. The T-C duct has a cross section area of 0.29172 cm^2, which resulted in a water velocity of U = 0.88 m s^{-1} for both sensor sets. The kinematic viscosity was calculated as a function of temperature and density interpolating through discrete values from a table from Sverdrup et al. (1946, p. 69). T_{vh} was calculated and subtracted from all the temperatures during the 1996 cruises. The maximum viscous heating correction was 0.5×10^{-3} °C. Casts from cruises before 1996 will require a similar correction due to viscous heating.

Dual sensors were used in all the 1996 cruises. The temperature differences between sensor pairs were calculated for each cast to evaluate the quality of the data, and to identify possible problems with the sensors. Means and standard deviations of the differences in 2-dbar bins were calculated from the ensemble of all casts at station ALOHA for each cruise. Both sensors performed correctly during the 1996 cruises, showing temperature differences within expected values. The mean temperature difference as a function of pressure was typically less than 1×10^{-3} °C, with a standard deviation of less than 0.5×10^{-3} °C below 500 dbar. The largest variability was observed in the thermocline, with standard deviation values of up to 5×10^{-3} °C.

Sensor #741

This sensor was used as part of the dual-sensor configuration during cruises HOT-69 through 72, HOT-77, 78 and during cruise AC-1. The sensor suffered an offset in its calibration level in August 1995. The cause of this offset was not identified but it also affected the sensor drift rate (Karl et al. 1996b). Only calibrations obtained after this date were used in this analysis.

The calibrations between 9 September 1995 and 23 January 1997 were used to calculate the sensor drift and the drift corrections. A linear fit to the 0-30 °C average offset from each calibration (Table 2.2) relative to 9 September 1995 gave an intercept of -1.65×10^{-6} °C with a slope of 1.229×10^{-6} °C day^{-1}. The RMS deviation of the offsets from this fit was 1.07×10^{-4} °C. For comparison, the drift rate before the sensor suffered an offset in its calibration level was 6.699×10^{-7} °C day^{-1}.

The 11 May 1996 calibration was used as a baseline for the cruises. When corrected for linear drift to 1 July 1996 (the midpoint of the cruise dates), this calibration gave the smallest deviation in the 0-5 °C temperature range from the set of all calibrations used to determine the drift (also corrected for linear drift to 1 July 1996). The mean deviation was -1.5×10^{-5} °C with a range of variation of less than 2×10^{-5} °C. The set of all calibrations had deviations in the range of $\pm 5 \times 10^{-4}$ °C. Because of the small drift of this sensor, the resulting drift corrections for each cruise were very small and inconsequential (Table 2.3).

Sensor #1416

This sensor was used during cruises HOT-69 through 71 and HOT-73 through 77. On 4 November 1994 the sensor's turret joint was resoldered as recommended by Sea-Bird to prevent sensor drift due to possible micro-cracks in the solder. The calibrations after this date were used to determine a drift of 6.12×10^{-6} °C day^{-1} with a -4.30×10^{-5} °C intercept and 2.6×10^{-4} °C RMS residual. The 5 October 1995 calibration was used as baseline for the cruises. This calibration yielded the smallest 0-5 °C mean deviation from the others, all drift-corrected to 1 June 1996 (midpoint date between the cruises). The deviation was -2.34×10^{-5} °C with less than 1×10^{-4} °C range of variation. The set of all calibrations had deviations in the range $\pm 5 \times 10^{-4}$ °C.

Sensor #1591

This sensor was used during cruises HOT-72 through 76, and HOT-78. The sensor suffered an change in its drift rate starting on 26 January 1995, but the reason could not be identified. Calibrations after this date yielded a drift of 3.08×10^{-6} °C day^{-1} with a 5.73×10^{-5} °C intercept and 9.5×10^{-5} °C RMS residual. The 28 November 1995 calibration was used as baseline for the cruises. This calibration yielded the smallest 0-5 °C mean deviation from the others, all drift-corrected to 15 September 1996 (midpoint date between the cruises). The deviation was 2.66×10^{-5} °C with less than 3×10^{-5} °C range of variation. The set of all calibrations had deviations in the range $\pm 5 \times 10^{-4}$ °C.

Sensor #886

This sensor was used during the AC-1 cruise. The sensor was opened on 29 November 1995 for an evaluation at Sea-Bird and this produced an offset in its calibration level. Only calibrations after this date were included in this analysis. A drift of 7.2 x 10^{-7} °C day^{-1} was calculated, with a -3.3 x 10^{-6} °C intercept and 3.1 x 10^{-4} °C RMS residual. The 24 December 1996 calibration was used as baseline for the cruise. This calibration yielded the smallest 0-5 °C mean deviation from the others, all drift-corrected to 12 July 1996 (midpoint date of the cruise). The deviation was -7.4 x 10^{-6} °C with less than 1 x 10^{-5} °C range of variation. The set of all calibrations had deviations in the range ± 5 x 10^{-4} °C.

2.1.2.3. Conductivity

Two sensors were used during the 1996 cruises #1336 and #679. The history of the sensors is well-documented in Tupas et al. (1993, 1994b, 1995) and Karl et al. (1996b). The dual sensor configurations are shown in Table 2.3. As mentioned earlier, only the data from the most reliable sensor (and its corresponding temperature sensor pair, as shown in Table 2.3) are reported here.

The sensors were calibrated at Sea-Bird on 20 December 1995 and 19 November 1996. Sea-Bird advised us to use the November 1996 calibration as the base set of coefficients for all cruises during 1996 after they discovered an error in the December 1995 calibration performed in artificial seawater. The source of the error has been solved by conducting all subsequent Sea-Bird calibrations in natural seawater.

A small residual pressure effect on some conductivity sensors was identified at Sea-Bird (N. Larson, personal communication, July 1996). This effect is due to epoxy jackets that are not sufficiently elastic. Structural rigidity in the epoxy prevents full ocean pressure from being transmitted to the glass cell. A new epoxy composition and curing procedure used in conductivity sensors with serial numbers after 1000 produced unexpected strength and rigidity in the epoxy jacket. The residual pressure effect is stable and linear in pressure. Sensor #1336 has been affected by this pressure effect and was corrected following a procedure recommended by Sea-Bird. A compression coefficient for the sensor was calculated by comparing the sensor conductivities against bottle data below 1000 dbar from the deep casts of cruises HOT-73 through -79 and applied to all 1996 cruises. The maximum correction to the deeper portion of the deep casts was 2.8 x 10^{-4} Siemens m^{-1}, and for the majority of the casts which only reached 1020 dbar this correction was smaller than 0.06 x 10^{-4} Siemens m^{-1}.

Conductivity sensor calibrations that were being performed at the North West Regional Calibration Center (NRCC) have been transferred to Sea-Bird since August 1995. The calibration procedures are basically the same as those described in Winn et al. (1991) with some changes (N. Larson, personal communication, 1997). Sea-Bird now uses a new calibration equation which makes an explicit temperature correction for the cell geometry, in addition the residual temperature sensitivity of the circuit has been reduced. These changes allow calibration in a single salinity bath (34.7 nominal value) at six temperatures. NRCC used to calibrate at salinities of 35 and 15 at four temperatures. Sea-Bird also conducts occasional checks by calibrating at a second salinity. Sea-Bird has also discovered that artificial seawater is not adequate for high accuracy salinity calibrations (better than 0.010), and since August 1996 they use real seawater that is carefully collected, stored, UV irradiated and filtered.

The nominal calibrations were used for data acquisition. Final calibration was determined empirically from salinities of discrete water samples acquired during each cast. Prior to empirical

calibration, conductivity was corrected for thermal inertia (α) of the glass conductivity cell as described in Chiswell et al. (1990). Table 2.3 lists the value of (α) used for each cruise.

Preliminary screening of bottle samples and empirical calibration of the conductivity cell are described in Tupas et al. (1993, 1994b). For cruises HOT-69 through 78, the standard deviation cutoff values for screening of bottle samples against the calibrated CTD salinities were: 0.0036 (0-150 dbar), 0.0050 (151-500 dbar), 0.0022 (501 - 1050 dbar) and 0.0012 (1051-5000 dbar).

The conductivity calibration coefficients (b_0, b_1, b_2) resulting from the least squares fit ($\Delta C = b_0 + b_1 C + b_2 C^2$) to the CTD minus bottle conductivities (ΔC) as a function of conductivity (C) are given in Table 2.5. The quality of the CTD calibration is illustrated in Figure 2.2, which shows the differences between the corrected CTD salinities and the bottle salinities as a function of pressure for each cruise. The calibrations are best below 500 dbar because the weaker vertical salinity gradients at depth lead to less error when the bottle and CTD pressures are slightly mismatched.

The final step of conductivity calibration was a cast-dependent bias correction as described in Tupas et al. (1993) to allow for drift during each cruise or for sudden offsets due to fouling (Table 2.6). Note that a change of 1×10^{-4} Siemens m^{-1} in conductivity was approximately equivalent to 0.001 in salinity. Table 2.7 gives the mean and standard deviations for the final calibrated CTD minus water sample values.

Conductivity differences between sensor pairs were calculated the same way as for the temperature sensors (section 2.1.2.2). The range of variability as a function of pressure was about $\pm 1 \times 10^{-4}$ Siemens m^{-1}, with a standard deviation of less than 0.5×10^{-4} Siemens m^{-1} below 500 dbar, from the ensemble of all the cruise casts. The largest variability was in the halocline, with standard deviations reaching up to 5×10^{-4} Siemens m^{-1} between 50 and 300 dbar.

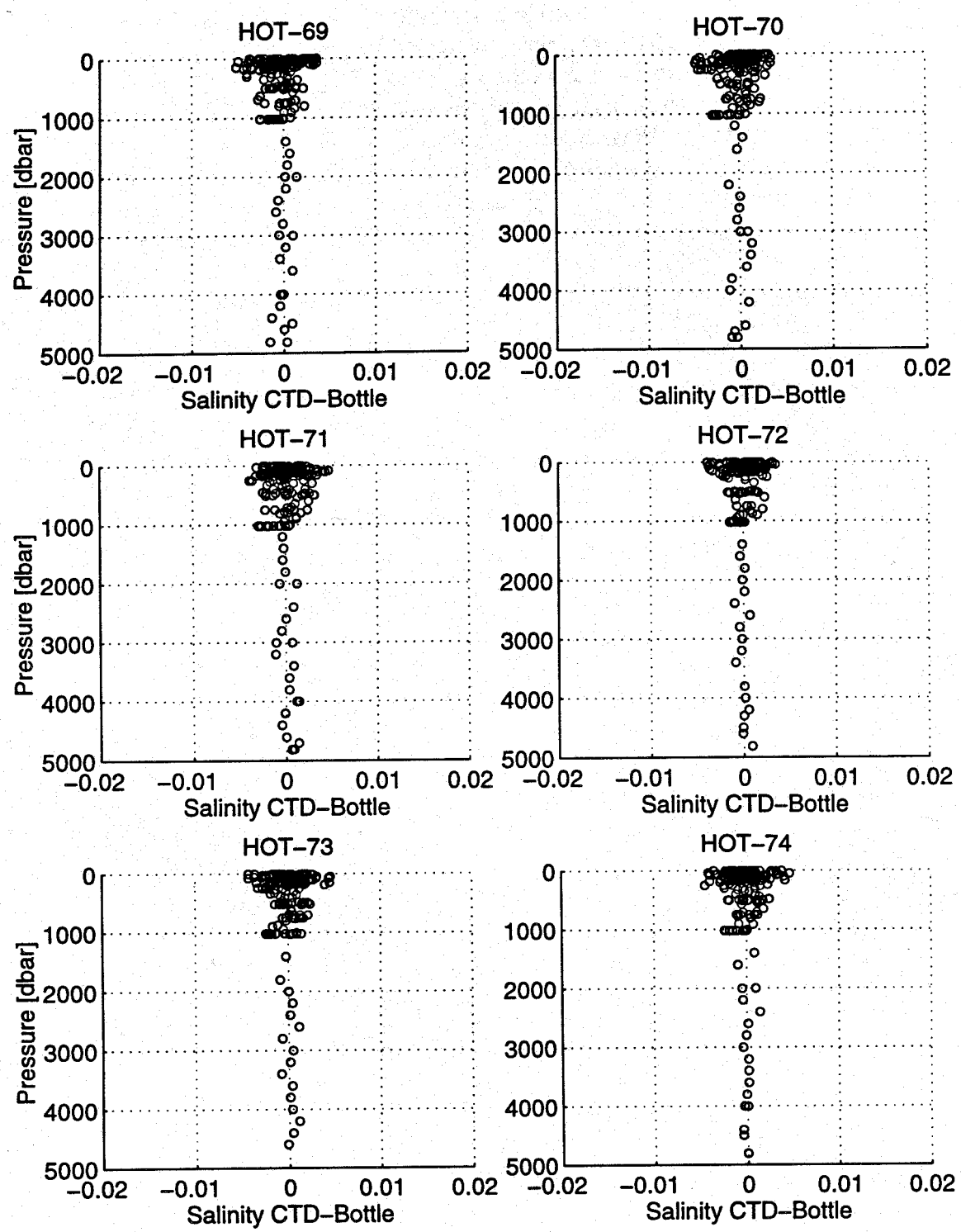

Figure 2.2: Difference between calibrated CTD salinities and bottle salinities for each cruise and all casts at Station ALOHA in 1996.

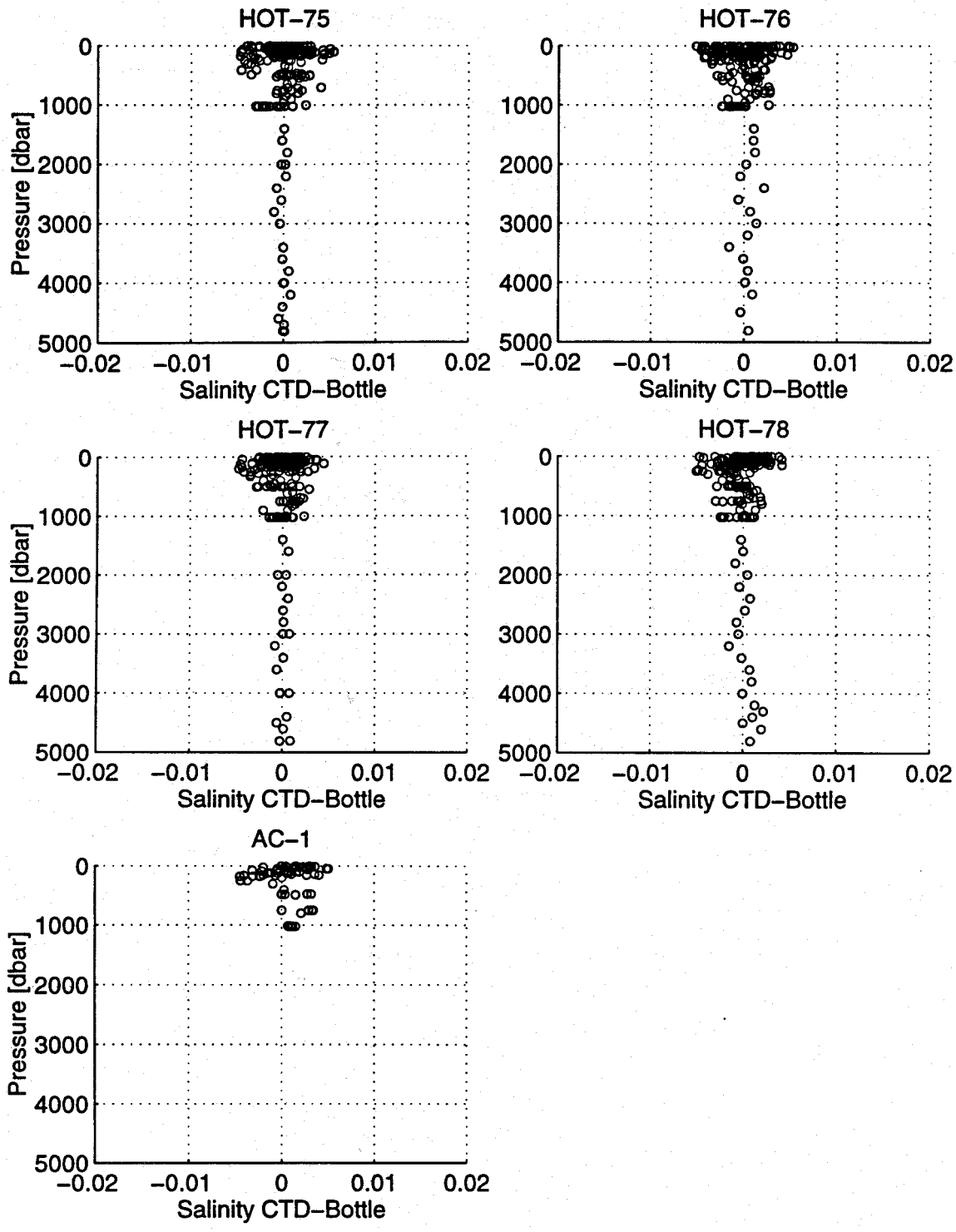

Figure 2.2: continued

Table 2.5: Conductivity Calibration Coefficients

Cruise	Sensor #	b_0	b_1	b_2
69	679	0.001377	-0.000309	0
	1336	0.000970	-0.000216	0
70	679	0.001201	-0.000253	0
	1336	0.000823	-0.000168	0
71	679	0.001291	-0.000285	0
	1336	0.000799	-0.000178	0
72	679	0.001081	-0.000256	0
	1336	0.000781	-0.000169	0
73	679	0.003776	-0.001607	0.000151
	1336	0.004814	-0.002145	0.000220
AC-1	679	-0.000975	-0.000028	0
	1336	0.000622	-0.000213	0
74	679	0.001499	-0.000495	0
	1336	0.001211	-0.000379	0
75	679	0.001365	-0.000462	0
	1336	0.001231	-0.000420	0
76	679	0.001478	-0.000460	0
	1336	0.003176	-0.001332	0.000106
77	679	0.001511	-0.000483	0
	1336	0.001003	-0.000344	0
78	679	0.000906	-0.000320	0
	1336	0.007155	-0.003308	0.000342

Table 2.6: Individual Cast Conductivity Corrections (units are Siemens m^{-1})

Cruise	Station	Cast	C correction
69	2	1	0.00010376
69	2	16	0.00006250
70	2	1	0.00014825
70	2	11	-0.00012544
70	2	13	-0.00019562
70	2	16	0.00000197
71	2	1	0.00010690
71	2	4	-0.00018602
71	2	5	-0.00010331
71	2	6	-0.00004117
71	2	10	-0.00035498
72	2	2	-0.00001088
72	2	13	-0.00007747
74	2	1	0.00002869
74	2	7	-0.00020316
75	2	1	0.00003807
75	2	14	-0.00009547
75	2	15	-0.00014273
76	2	15	-0.00014276
78	2	1	0.00012210

Table 2.7: CTD-Bottle Salinity Comparison for Each Cruise

		0 to 4700 db		500 to 4700 db	
Cruise	**Sensor #**	**Mean**	**SD**	**Mean**	**SD**
69	1336	0.0004	0.0017	-0.0001	0.0010
	679	-0.0001	0.0017	-0.0002	0.0011
70	1336	0.0005	0.0017	0.0001	0.0010
	679	0.0000	0.0016	-0.0002	0.0011
71	1336	0.0002	0.0016	0.0002	0.0013
	679	0.0002	0.0017	0.0001	0.0014
72	1336	0.0001	0.0014	0.0000	0.0009
	679	0.0000	0.0017	0.0000	0.0010
73	1336	0.0000	0.0016	0.0000	0.0011
	679	0.0000	0.0017	0.0001	0.0012
AC-1	1336	0.0000	0.0020	0.0008	0.0013
	679	0.0000	0.0022	0.0006	0.0014
74	1336	-0.0001	0.0017	-0.0001	0.0011
	679	0.0000	0.0017	0.0000	0.0010
75	1336	0.0000	0.0019	0.0000	0.0011
	679	0.0001	0.0020	0.0001	0.0013
76	1336	0.0000	0.0020	0.0000	0.0014
	679	0.0000	0.0021	0.0001	0.0013
77	1336	0.0000	0.0016	0.0003	0.0012
	679	0.0000	0.0018	0.0001	0.0011
78	1336	-0.0001	0.0016	0.0000	0.0013
	679	0.0000	0.0017	0.0000	0.0010

2.1.2.4. Oxygen

Two YSI Inc. probes (#13341 and #13251) were used in a dual-sensor configuration during the 1996 cruises. The history of the sensors is documented in Tupas et al. (1995) and Karl et al. (1996b). A new procedure was implemented in late 1995 to check for possible sensor problems. The data from the sensor pair are plotted after each cast for evaluation. In addition, before each cruise the sensor's membrane is inspected closely for wrinkles or tears, and for air bubbles in the electrolyte reservoir. Also lab checks of atmospheric oxygen level recommended by Sea-Bird are performed before every cruise. Sensor #13251 was calibrated and its membrane and electrolyte were replaced at Sea-Bird on 15 December 1995, in addition replacement of the membrane and electrolyte were performed in our lab on sensor #13251 before cruise HOT-70 and replacement of electrolyte on both sensors before cruise HOT-76. These measures have resulted in oxygen traces with less drift throughout cruises than in previous years.

Only the data from sensor #13251 are reported here for all cruises, the other sensor (#13341) showed a slight drift during some of the cruises.

Water bottle oxygen data were screened and the sensors were empirically calibrated following procedures described previously (Winn et al. 1991; Tupas et al. 1993). Analysis of water bottle samples is described in section 2.2.1. The calibration procedure follows Owens and

Millard (1985), and consists of fitting a non-linear equation to the CTD oxygen current and oxygen temperature. The bottle values of dissolved oxygen and the downcast CTD observations at the potential density of each bottle trip were grouped together for each cruise to find the best set of parameters with a non-linear least squares algorithm. Two sets of parameters were usually obtained per cruise, corresponding to the casts at Stations 1 and 2. During HOT-70 there was a slight drift in the CTD oxygen sensor throughout Station 2 casts. This cruise required two set of calibration parameters at Station 2. Cruise AC-1 required five sets of calibration coefficients. Each set of coefficients was obtained from stations grouped in adjacent geographical locations as follows: station 1; stations 2 and 9; stations 3, 7 and 8; stations 4 and 6; and station 5 (Refer to Figure 2.13, AC-1 cruise track).

Table 2.8 gives the means and standard deviations for the final calibrated CTD oxygen values minus the water sample values for the regular HOT cruises and Table 2.9 for the ALOHA-Climax cruise.

Table 2.8: CTD-Bottle Dissolved Oxygen per Cruise (µmol kg^{-1})

		Station 1, Kahe Point		Station 2, ALOHA			
		0 to 1500 dbar		0 to 4700 dbar		500 to 4700 dbar	
Cruise	Sensor #	Mean	SD	Mean	SD	Mean	SD
69	13251	0.01	1.12	0.01	1.98	0.16	0.97
70	13251	0.01	0.80	-0.02	1.51	-0.07	1.27
71	13251	0.01	1.26	0.30	1.88	0.65	1.41
72	13251	0.00	1.00	0.16	1.32	0.43	0.85
73	13251	-0.01	1.79	0.07	1.19	0.19	0.72
74	13251	0.00	1.37	0.12	1.64	0.28	0.91
75	13251	0.34	1.80	0.12	1.46	0.25	1.18
76	13251	0.01	2.13	0.16	1.43	0.15	0.99
77	13251	0.01	1.60	0.18	1.18	0.20	0.84
78	13251	0.02	1.46	0.08	1.04	0.07	0.80

Table 2.9: CTD-Bottle Dissolved Oxygen during AC-1 (µmol kg^{-1})

AC-1		0-1500 dbars	
Stations	Sensor #	Mean	SD
1	13251	0.00	1.08
2, 9	13251	-0.01	1.71
3, 7, 8	13251	0.02	2.29
4, 6	13251	0.04	2.42
5	13251	-0.01	1.13

2.1.3. Salinity

Salinity samples were collected, stored and analyzed as described in Tupas et al. (1993). Samples from a large batch of "secondary standard" seawater were measured after every 24 to 36 bottle samples to detect drift in the salinometer. The typical standard deviation of the secondary standard measurements was near ± 0.001 (Table 2.10). Most of the cases with standard deviation greater than 0.001 were due to a drift in the salinometer. For these cruises, a salinometer drift was determined using the secondary standard seawater as a reference, and a correction to the samples was applied. Typical corrections ranged from 0.001 to 0.0025. HOT-70 was the only cruise which showed a standard deviation greater than 0.001 that was unexplainable in terms of salinometer drift.

Secondary standard seawater batches are usually made from 60 liters of seawater taken from a depth of 1000 m from Station ALOHA. Secondary standard Batch #11 was prepared in November 1995 and had a lower salinity than other batches because 10 of the 60 liters used to make the batch came from 500 m water instead of 1000 m. Batch #12 was made in May 1996 and Batch #13 was prepared in October 1996.

Table 2.10: Precision of Salinity Measurements Using Lab Standards

Cruise	Mean Salinity ± SD	# Samples*	Substandard Batch #	IAPSO Batch #
69	34.42245 ± 0.00040	14	11	p123, p128
70	34.42096 ± 0.00101	17	11	p128
71	34.42020 ± 0.00111	17	11	p128
72	34.47980 ± 0.00052	14	12	p128
73	34.48029 ± 0.00088	14	12	p128
AC-1	34.48053 ± 0.00105	18	12	p128
74	34.48078 ± 0.00129	21	12	p128
75	34.48094 ± 0.00141	20	12	p128
76	34.44772 ± 0.00144	16	13	p128
77	34.44783 ± 0.00106	17	13	p128
78	34.44625 ± 0.00100	24	13	p128

*Number of secondary standard salinity samples measured during each run.

2.2. Biogeochemical Measurements

At Stations Kahe and ALOHA, water samples for chemical analyses were collected from discrete depths using 12-liter PVC bottles with teflon coated internal springs as closing mechanisms. Sampling strategies and procedures are well documented in the previous data reports and in the HOT Program Field and Laboratory Protocols manual. This report contains only a subset of the total data base which can be extracted from the accompanying diskette or electronically over the Internet (see Chapter 8). To assist in the interpretation of these data and to save users the time to estimate the precision of individual chemical analysis, we have summarized precision estimates from replicate determinations for each constituent on each HOT cruise in 1996.

2.2.1. Dissolved Oxygen

Dissolved oxygen samples were collected and analyzed using a computer-controlled potentiometric end-point titration procedure as described in Tupas et al. (1993). As in previous years we measured, using a calibrated digital thermistor, the temperature of the seawater sample at the time the iodine flask was filled. This was done to evaluate the magnitude of sample temperature error which affects the calculation of oxygen concentrations in units of µmol kg^{-1}. Figure 2.3 (upper panel) shows a plot of the difference between sample temperature and potential temperature computed from the *in situ* temperature measured at the time of bottle trip, versus pressure. The lower panel of the same figure shows a plot of the difference between oxygen concentration using on-deck and potential temperatures versus pressure. The depth dependent variability in Δ oxygen is a result of the absolute magnitude of the oxygen concentration and the standard procedures we employ for sampling the water column.

The mean precision of our oxygen analyses in 1996 was 0.16 %. Oxygen concentrations measured over the 8 years of the program are plotted at three constant potential density horizons in the deep ocean along with their mean and 95% confidence intervals (Figure 2.4). The deviations ranged (maximum - minimum values) from a low of 2.00 µmol kg^{-1} at σ_θ = 22.782 to 4.61 µmol kg^{-1} at σ_θ = 27.675. These results indicate that analytical consistency has been maintained over the past 8 years of the HOT program.

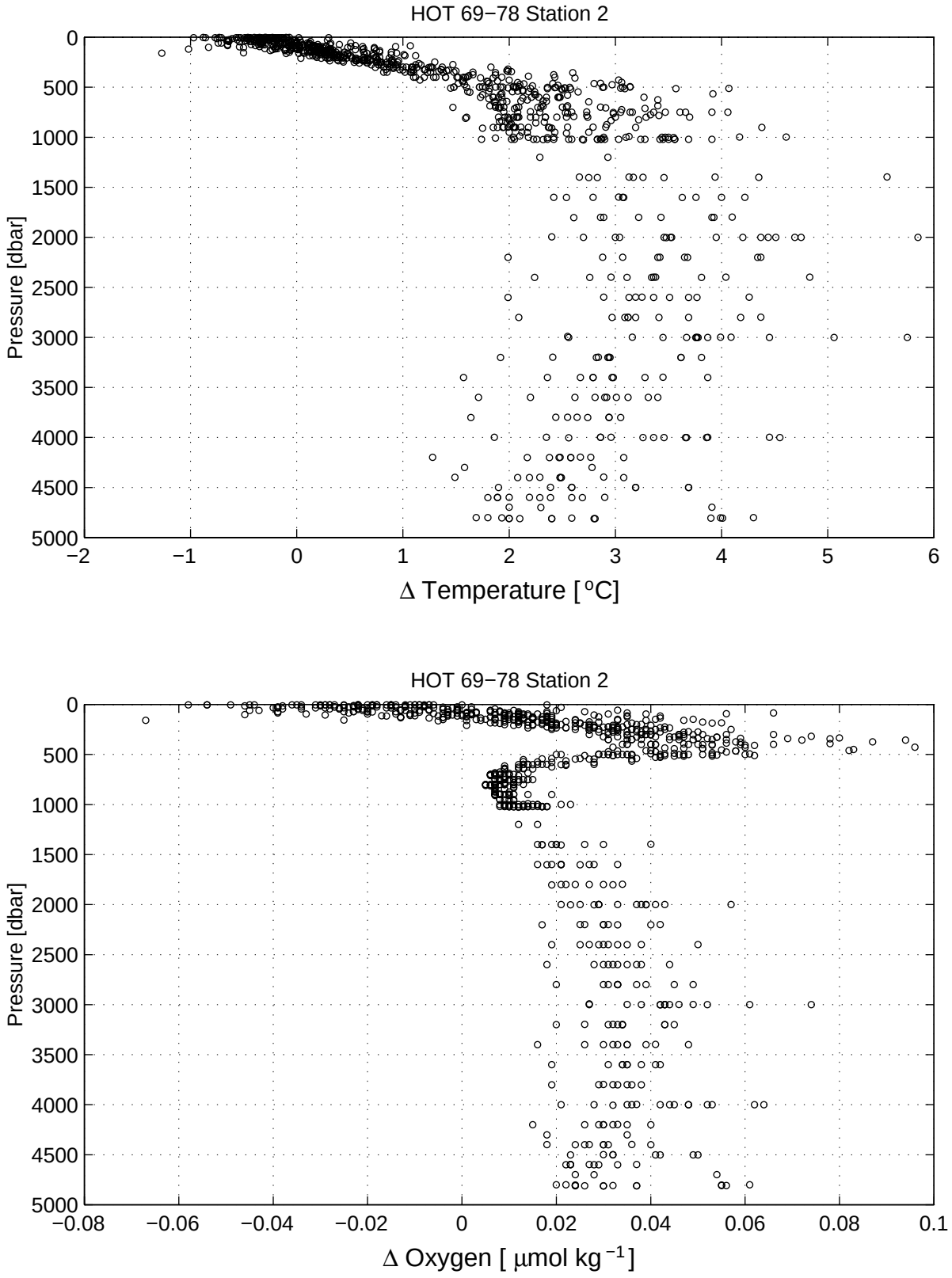

Figure 2.3: [Upper panel] Difference between sample temperature at the time of sample collection and potential temperature calculated from in situ temperature at the time of bottle trip. [Lower panel] Difference in oxygen concentration corrected for temperatures measured at the time of sample collection and potential temperature calculated from in situ temperature.

Figure 2.4: Oxygen concentrations at three potential density horizons over time at Station ALOHA. [Upper panel] Oxygen concentrations at potential densities of 27.782, 27.758 and 27.675 during 1996. [Lower panel] Oxygen concentrations at these same horizons from 1988-1996.

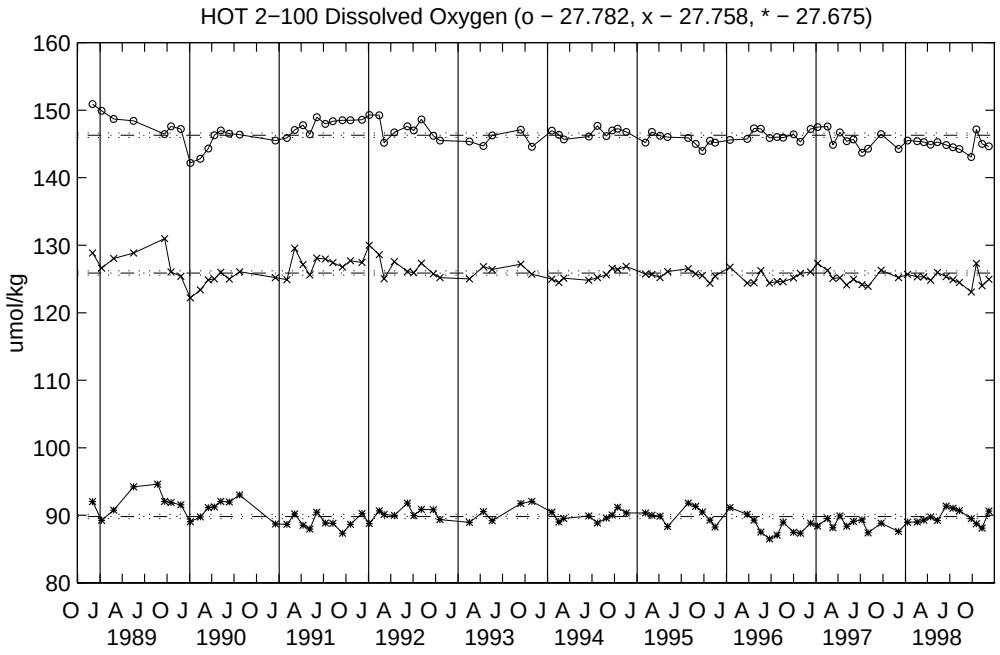

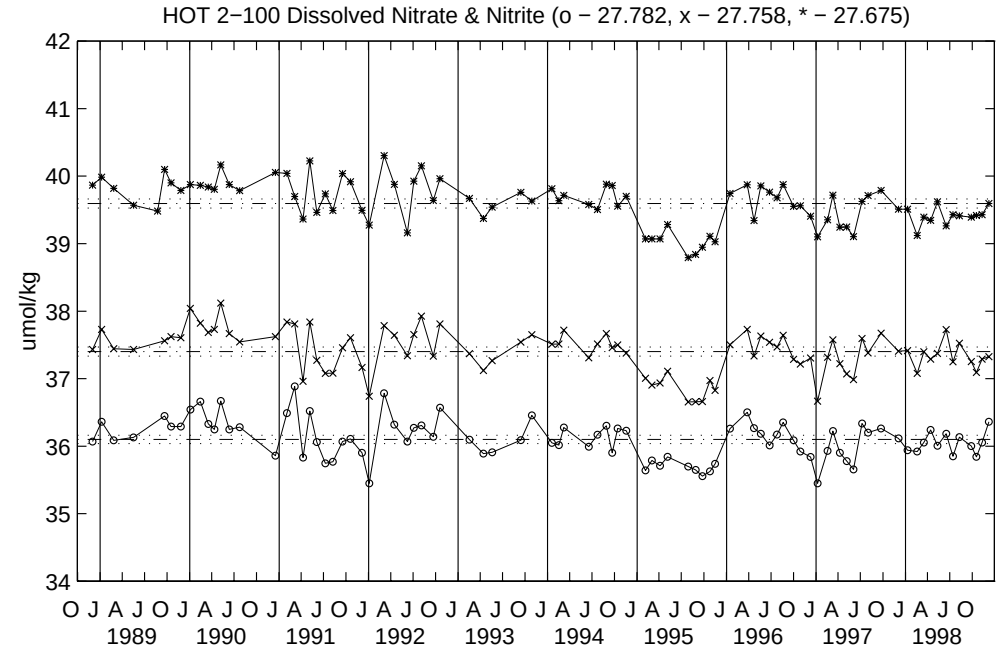

Figure 2.5: [Nitrate +Nitrite] concentrations at three potential density horizons over time at Station ALOHA. [Upper panel] [Nitrate + Nitrite] concentrations at potential densities of 27.782, 27.758 and 27.675 during 1996. [Lower panel] [Nitrate + Nitrite] concentrations at these same horizons from 1988-1996.

Table 2.10: Precision of Winkler Titration Method

HOT	CV (%)	SD (µmol l^{-1})	n
69	0.08	0.16	12
70	0.28	0.44	13
71	0.08	0.14	12
72	0.07	0.13	13
73	0.13	0.26	15
AC-1	0.19	0.40	42
74	0.12	0.21	14
75	0.14	0.24	17
76	0.23	0.41	11
77	0.25	0.54	16
78	0.13	0.23	10

2.2.2. Inorganic Carbon Parameters

2.2.2.1. Dissolved Inorganic Carbon and Titration Alkalinity

Samples for dissolved inorganic carbon (DIC) were measured using a Single Operator Multi-parameter Metabolic Analyzer (SOMMA) which was manufactured at the University of Rhode Island and standardized at the Brookhaven National Laboratory. Analyses of primary DIC standards (Tupas et al. 1993) indicated that the precision of replicate samples is approximately 1 µmol kg^{-1}. Titration alkalinity was determined using the Gran titration method as described in Tupas et al. (1993). The precision of the titration procedure was approximately 5 µequiv kg^{-1}. Accuracy was established with certified reference standards obtained from Andrew Dickson at Scripps Institution of Oceanography and compared to analyses by Charles D. Keeling also at Scripps Institution of Oceanography for DIC and Andrew Dickson for alkalinity. A summary of the control data is shown in Table 2.11

Table 2.11. Control Data for 1996 HOT DIC and alkalinity measurements (µmol kg^{-1})

			HOT		Keeling	
Measurement	CRM #	n	Mean	Std. Dev.	Mean	Std. Dev.
DIC	32	4	1998.03	0.92	1997.01	0.93
	34	16	2060.41	1.16	2061.52	1.62
	35	23	2111.18	1.54	2111.62	0.82
	36	22	2051.30	3.09	2050.21	0.72
					Dickson	
Alkalinity	35	99	2351.92	2.28	2354.05	0.05
	36	13	2283.01	1.89	2283.83	0.77

2.2.2.2. pH

Beginning in 1992, pH was determined spectrophotometrically using the indicator m-cresol purple following the methods described in Tupas et al. (1993). The absorbance of the mixture was measured at wavelengths of 578 and 434 nm on a Perkin Elmer Model 3 dual-beam spectrophotometer and converted to pH on the seawater scale according to Clayton and Byrne (1993). The mean and standard deviation of the difference of sets of duplicate pH measurements was 0.0009 and 0.00077 respectively.

2.2.2.3. pCO_2

In October 1996 (HOT-76) an automated, semi-continuous system for measuring the partial pressure of carbon dioxide in seawater was installed in-line with the ship's clean-seawater intake system to measure underway surface seawater pCO_2. The system is calibrated using three standard gases of known CO_2 concentrations covering the range of 200-400 ppm (Scott Specialty Gases calibrated at SIO). A separate reference gas calibrated at 349.0 ppm is measured for quality assurance. Calibration and standardization are done at system startup and approximately every 2.5 hours. The present system consists of a shower head equilibrator operating at a flow rate of approximately 8 l min^{-1}. Equilibrated gas and bow air are both sampled every 10 minutes. The gases pass through a napthyon tube drier and a magnesium perchlorate scrubber into a LICOR 6250 infrared detector. The reference chamber is purged with reference gas after every 3 cycles of bow/equilibrator measurements. Gas flow rates into the detector are at approximately 0.5 l min^{-1}. The system output gives the CO_2 concentration of the bow-intake air and the surface seawater in ppm. The system begins operating when the ships is in clean open water and is fully operational at Station Kahe. The system is turned off after departing the last station.

2.2.3. Inorganic Nutrients

2.2.3.1. Standard Methods

Samples for the determination of dissolved inorganic nutrient concentrations (soluble reactive phosphorus, [nitrate+nitrite] and silicate) were collected as described in Tupas et al. (1993). Analyses were conducted at room temperature on a four-channel Technicon Autoanalyzer II continuous flow system at the University of Hawaii Analytical Facility by Mr. Ted Walsh. A summary of the precision of analyses for 1996 is shown in Table 2.12. Figures 2.5-2.7 show the mean and 95% confidence limits of nutrient concentrations measured at three potential density horizons for the 8 years of the program. In addition to standard automated nutrient analyses, specialized chemical methods (section 2.2.3.2) are used to determine concentration of nutrients that are normally below the detection limits of autoanalyzer methods.

2.2.3.2. High Precision, High Sensitivity Methods

The chemiluminescent method of Cox (1980) as modified for seawater by Garside (1982) was used to determine the [nitrate+nitrite] content of near surface (0-200 m interval) water samples (Tupas et al. 1993). The limit of detection for [nitrate+nitrite] was approximately 2 nM with a precision and accuracy of ±1 nM (Dore et al. 1996).

Low level soluble reactive phosphorus (SRP) concentrations in the euphotic zone were determined according to the magnesium induced coprecipitation (MAGIC) method of Karl and Tien (1992). Typical precision estimates for triplicate determinations of SRP are from 1-3 % with a detection limit of 10 nmol l^{-1}. This latter measurement is also corrected for arsenate interference of the molybdenum blue colorimeteric procedure (Johnson 1971), and thus provides a more accurate estimate of SRP.

Table 2.12: Precision of Dissolved Inorganic Nutrient Analyses

	Soluble Reactive Phosphorus				[Nitrate+Nitrite]				Silicate			
	Analytical*		Field**		Analytical		Field		Analytical		Field	
HOT	mean CV (%)	mean SD (µM)	mean CV (%)	mean SD (µM)	mean CV (%)	mean SD (µM)	mean CV (%)	mean SD (µM)	mean CV (%)	mean SD (µM)	mean CV (%)	mean SD (µM)
69	0.5	0.008	0.6	0.008	0.4	0.084	0.4	0.140	0.4	0.22	0.4	0.53
70	0.5	0.019	0.3	0.006	0.4	0.091	0.1	0.025	0.2	0.17	0.2	0.10
71	0.7	0.011	0.3	0.006	0.4	0.108	0.3	0.067	0.2	0.16	0.3	0.21
72	0.8	0.010	0.8	0.016	0.4	0.063	0.4	0.078	0.4	0.28	1.3	0.51
73	0.8	0.013	0.2	0.005	0.6	0.144	0.1	0.025	0.3	0.20	0.9	0.44
AC-1	0.2	0.006	0.5	0.012	0.3	0.120	0.6	0.176	0.2	0.24	0.8	0.27
74	1.0	0.019	0.4	0.005	0.4	0.126	0.2	0.053	0.4	0.38	1.1	0.92
75	0.8	0.011	0.7	0.011	0.4	0.088	0.2	0.035	1.3	0.28	2.0	0.55
76	0.4	0.008	0.6	0.013	0.5	0.121	0.3	0.078	0.2	0.22	1.9	0.38
77	0.5	0.010	0.1	0.004	0.4	0.097	0.3	0.107	0.2	0.15	0.4	0.27
78	0.7	0.008	0.3	0.005	0.4	0.070	0.2	0.033	0.2	0.16	0.6	0.36
Mean	0.6	0.010	0.4	0.008	0.4	0.101	0.3	0.074	0.4	0.22	0.9	0.41
SD	0.2	0.004	0.2	0.004	0.1	0.025	0.2	0.049	0.3	0.07	0.6	0.22

*Average coefficient of variation (i.e. standard deviation as a percentage of the mean) for analytical replicates (i.e. replicate analysis of a single sample) for SRP concentrations ≥ 0.4 µM, nitrate + nitrite ≥ 0.2 µM and silicate concentrations ≥ 2.0 µM.

**Average coefficient of variation for field replicates (i.e. analysis of replicate samples from the same Niskin bottle) for the above concentration ranges per nutrient.

Figure 2.6: Soluble reactive phosphorus concentrations at three potential density horizons over time at Station ALOHA. [Upper panel] Soluble reactive phosphorus concentrations at potential densities of 27.782, 27.758 and 27.675 during 1996. [Lower panel] Soluble reactive phosphorus concentrations at these same horizons from 1988-1996.

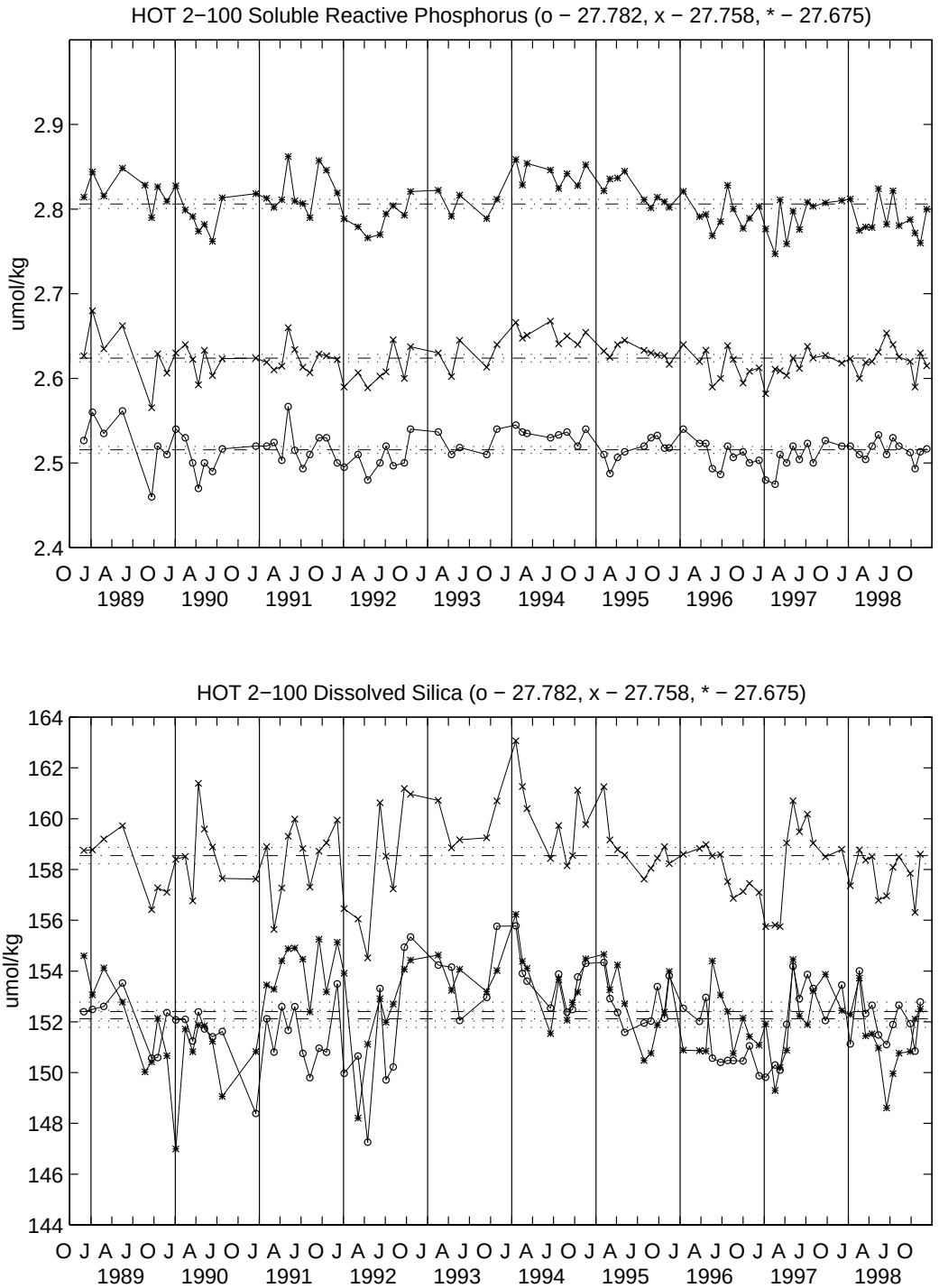

Figure 2.7: Silicate concentrations at three potential density horizons over time at Station ALOHA. [Upper panel] Silicate concentrations at potential densities of 27.782, 27.758 and 27.675 during 1996. [Lower panel] Silicate concentrations at these same horizons from 1988-1996.

2.2.4. Organic Nutrients

Dissolved organic carbon (DOC) was determined by the high temperature catalytic oxidation method (Tupas et al. 1994a) using an automated DOC analyzer (Qian and Mopper 1996). Dissolved organic nitrogen (DON) was calculated as the difference between total dissolved fixed nitrogen (TDN) and [nitrate+nitrite] concentrations. Dissolved organic phosphorus (DOP) was calculated as the difference between total dissolved phosphorus (TDP) and SRP concentrations. Dissolved "organic" phosphorus concentrations using this method will include inorganic polyphosphates. TDN and TDP were determined by the UV oxidation method as described in Tupas et al. (1993). A summary of the precision of these analyses is given in Table 2.13. DOC, DON and DOP concentrations over the 8 years of the program at the 500 and 1000 dbar horizons are plotted with their mean and 95% confidence intervals (Figures 2.8-2.10).

Table 2.13: Precision of Dissolved Organic Nutrient Analyses

	DON		DOP		DOC	
Cruise	mean CV (%)	mean SD (µmol kg^{-1})	mean CV (%)	mean SD (µmol kg^{-1})	mean CV (%)	mean SD (µmol kg^{-1})
69	7.6	0.24	4.6	0.007	2.2	1.20
70	7.0	0.32	8.5	0.016	1.1	1.01
71	8.8	0.36	6.3	0.012	1.8	1.47
72	2.1	0.09	5.9	0.009	1.3	1.06
73	2.9	0.17	21.9	0.027	3.8	2.70
AC-1	8.2	0.31	8.1	0.009	ND	ND
74	6.2	0.19	6.4	0.011	1.9	1.17
75	3.5	0.11	6.5	0.012	2.1	1.33
76	10.4	0.32	22.4	0.031	1.5	1.15
77	3.9	0.11	14.2	0.028	2.8	1.81
78	5.0	0.24	3.9	0.007	2.9	2.02

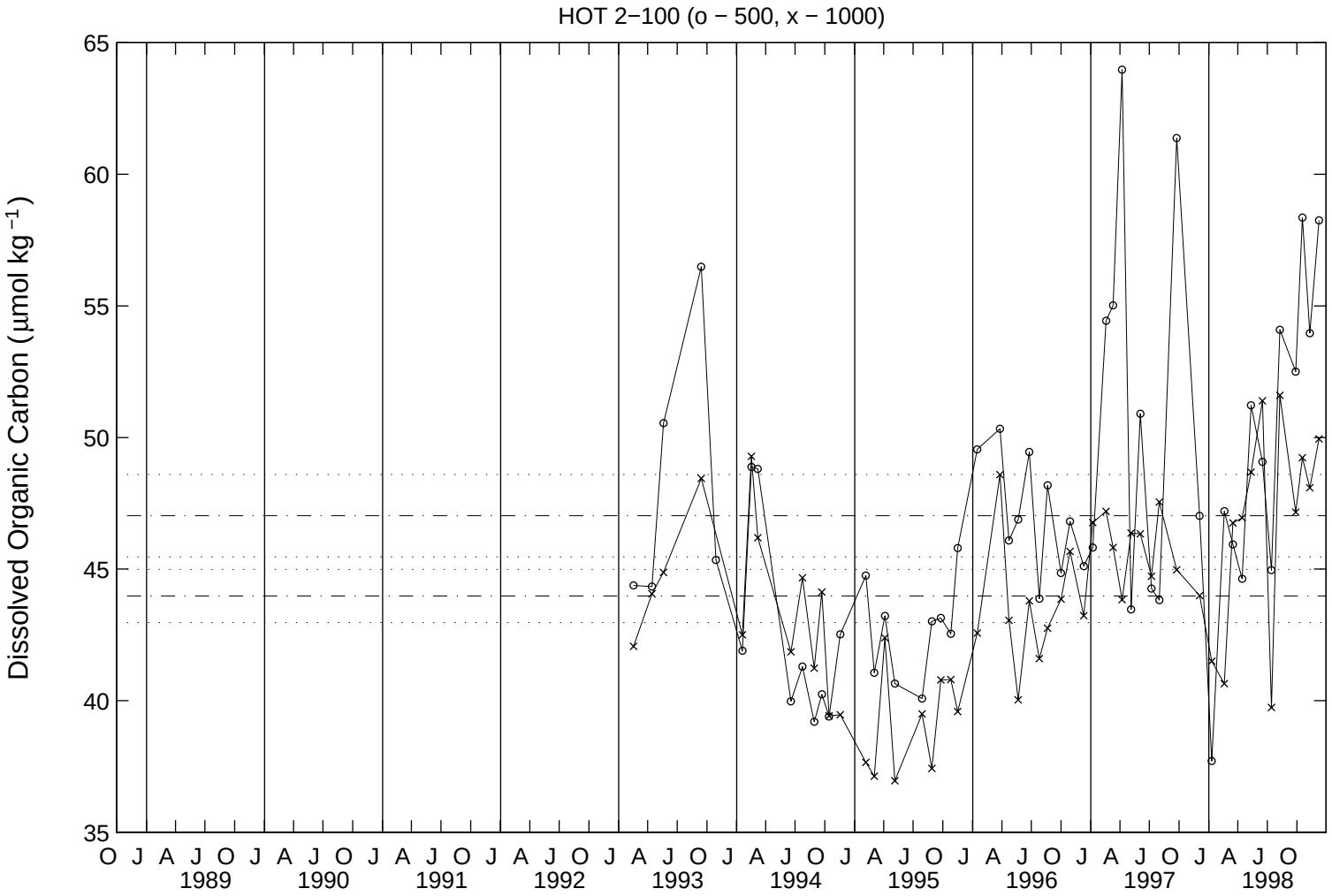

Figure 2.8: Dissolved organic carbon (DOC) concentrations at 500 and 1000 dbar horizons over time at Station ALOHA. [Upper panel] DOC concentrations at these horizons in 1996. [Lower panel] DOC concentrations at these same horizons from 1993-1996.

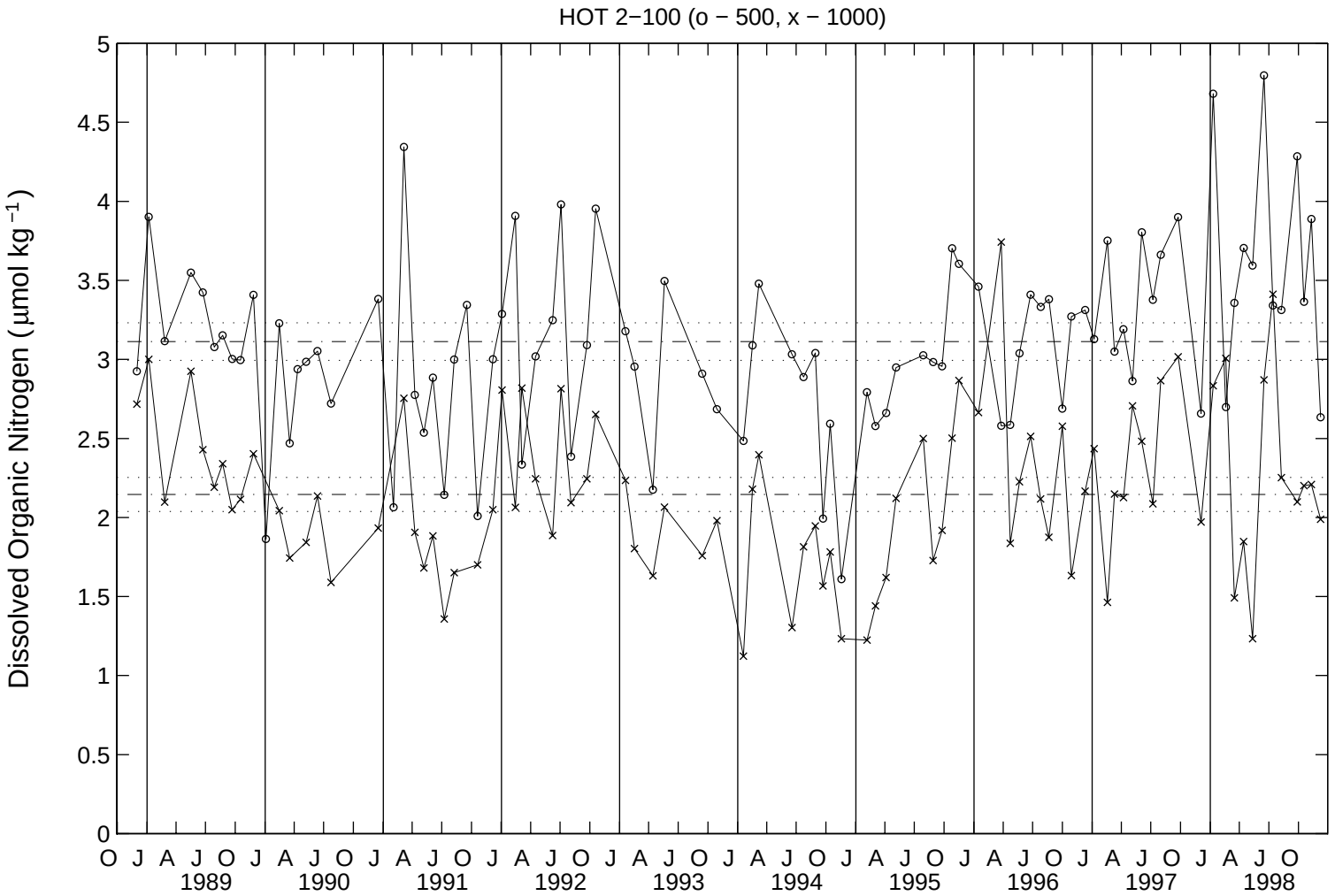

Figure 2.9: Dissolved organic nitrogen (DON) concentrations at 500 and 1000 dbar horizons over time at Station ALOHA. [Upper panel] DON concentrations at these horizons in 1996. [Lower panel] DON concentrations at these same horizons from 1988-1996.

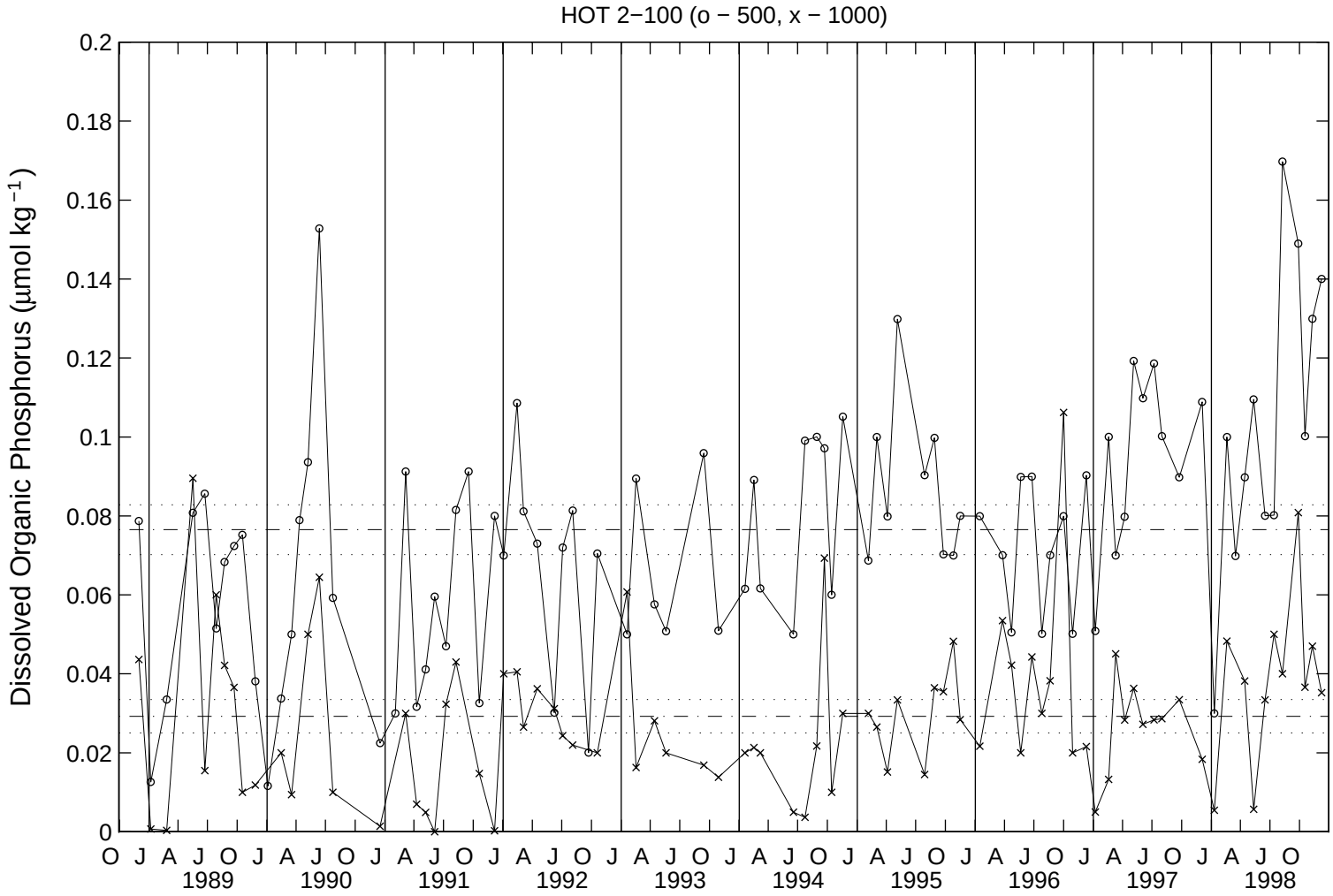

Figure 2.10: Dissolved organic phosphorus (DOP) concentrations at 500 and 1000 dbar horizons over time at Station ALOHA. [Upper panel] DOP concentrations at these horizons in 1996. [Lower panel] DOP concentrations at these same horizons from 1988-1996.

2.2.5. Particulate Matter

Samples for analysis of particulate matter were prefiltered through 202 µm Nitex mesh to remove large zooplankton and collected onto combusted GF/F glass fiber filters (acid washed for particulate phosphorus). Particulate carbon (PC) and nitrogen (PN) on the filters were analyzed using a Europa automated nitrogen and carbon analyzer. Particulate phosphorus (PP) was analyzed by converting the material to orthophosphate by high temperature ashing followed by acid hydrolysis and determining the orthophosphate content by colorimetry. Precision of particulate matter analysis is presented in Table 2.14.

Table 2.14: Precision of Particulate Matter Analyses

	Particulate Carbon		Particulate Nitrogen		Particulate Phosphorus	
Cruise	mean CV (%)	mean SD (µmol kg^{-1})	mean CV (%)	mean SD (µmol kg^{-1})	mean CV (%)	mean SD (nmol kg^{-1})
69	2.3	0.4	1.7	0.07	6.5	0.026
70	49.3	8.5	63.5	2.36	14.0	0.053
71	1.9	0.4	8.8	0.46	4.9	0.021
72	9.5	2.2	8.6	0.32	55.4	0.152
73	9.4	2.2	6.4	0.32	12.5	0.060
AC-1	ND*	ND	ND	ND	7.4	0.032
74	4.7	1.1	1.7	0.07	12.6	0.053
75	3.3	0.8	2.1	0.07	24.6	0.113
76	4.3	0.1	4.5	0.14	0.4	0.002
77	9.8	2.3	6.6	0.28	13.1	0.064
78	1.1	0.3	8.0	0.21	10.2	0.042

*Not determined, no replicate samples taken

2.2.6. Pigments

2.2.6.1. Standard Fluorometric Method

Chlorophyll a (chl *a*) and phaeopigments were measured fluorometrically on a Turner Designs Model 10-AU fluorometer using 100 % acetone as the extractant and standard techniques (Strickland and Parsons 1972). Analytical precision for this analysis is presented in Table 2.15. Integrated values for pigment concentrations were calculated using the trapezoid rule.

2.2.6.2. High Performance Liquid Chromatography

Chlorophyll *a* and accessory photosynthetic pigments were also measured (Table 2.16) by high performance liquid chromatography (HPLC) according to Bidigare et al. (1990). A new HPLC method following SCOR recommendation was adopted in 1994. This method is a modification of the method developed by Wright et al. (1991). The new method allows for a better separation of lutein and zeaxanthin as well as monovinyl and divinyl chlorophyll *a*. Figure

2.11 shows the relationship between chlorophyll *a* measured by fluorometry and chlorophyll *a* measured by HPLC for 1996. A summary of response factors for all HPLC pigment analyses from 1988 to 1996 are shown in Table 2.17.

Table 2.15: Precision of Fluorometric Chlorophyll *a* and Phaeopigment Analyses

	Chl *a*		Phaeopigment	
Cruise	Mean CV (%)	SD ($\mu g\ l^{-1}$)	Mean CV (%)	SD ($\mu g\ l^{-1}$)
69	4.2	0.006	7.1	0.013
70	4.8	0.007	4.8	0.010
71	4.7	0.006	5.9	0.012
72	4.9	0.006	6.0	0.009
73	5.8	0.008	5.3	0.010
AC-1	8.2	0.012	6.9	0.029
74	5.3	0.005	6.0	0.024
75	9.6	0.013	4.3	0.013
76	3.4	0.005	4.7	0.015
77	2.2	0.004	3.7	0.009
78	2.8	0.004	5.0	0.010

Table 2.16: 1996 HPLC Pigment Analysis Response Factors

Pigment	RF*	RF**
Chlorophyll c & Mg 3,8D***	0.257	
Peridinin	0.520	0.440
19'-Butanoyloxyfucoxanthin	0.408	0.470
Fucoxanthin	0.406	0.504
19'-Hexanoyloxyfucoxanthin	0.401	0.541
Violaxanthin	0.400	0.620
Diadinoxanthin	0.265	0.697
Zeaxanthin	0.311	0.834
MV Chlorophyll *b*	0.960	0.945
MV Chlorophyll *a*	0.716	1.000
DV Chlorophyll *a*	0.515	1.000
α-carotene	0.301	1.154
β-carotene	0.311	1.161

* RF - Response Factor ($ng\ l^{-1}$ unit-absorbance peak-$area^{-1}$) at 436 nm
** RT - Retention Time relative to chlorophyll a
*** Chlorophyll c = c1 + c2 + c3; Mg 3,8D = Mg 3,8 divinyl phaeoporphyrin a5 monomethyl ester

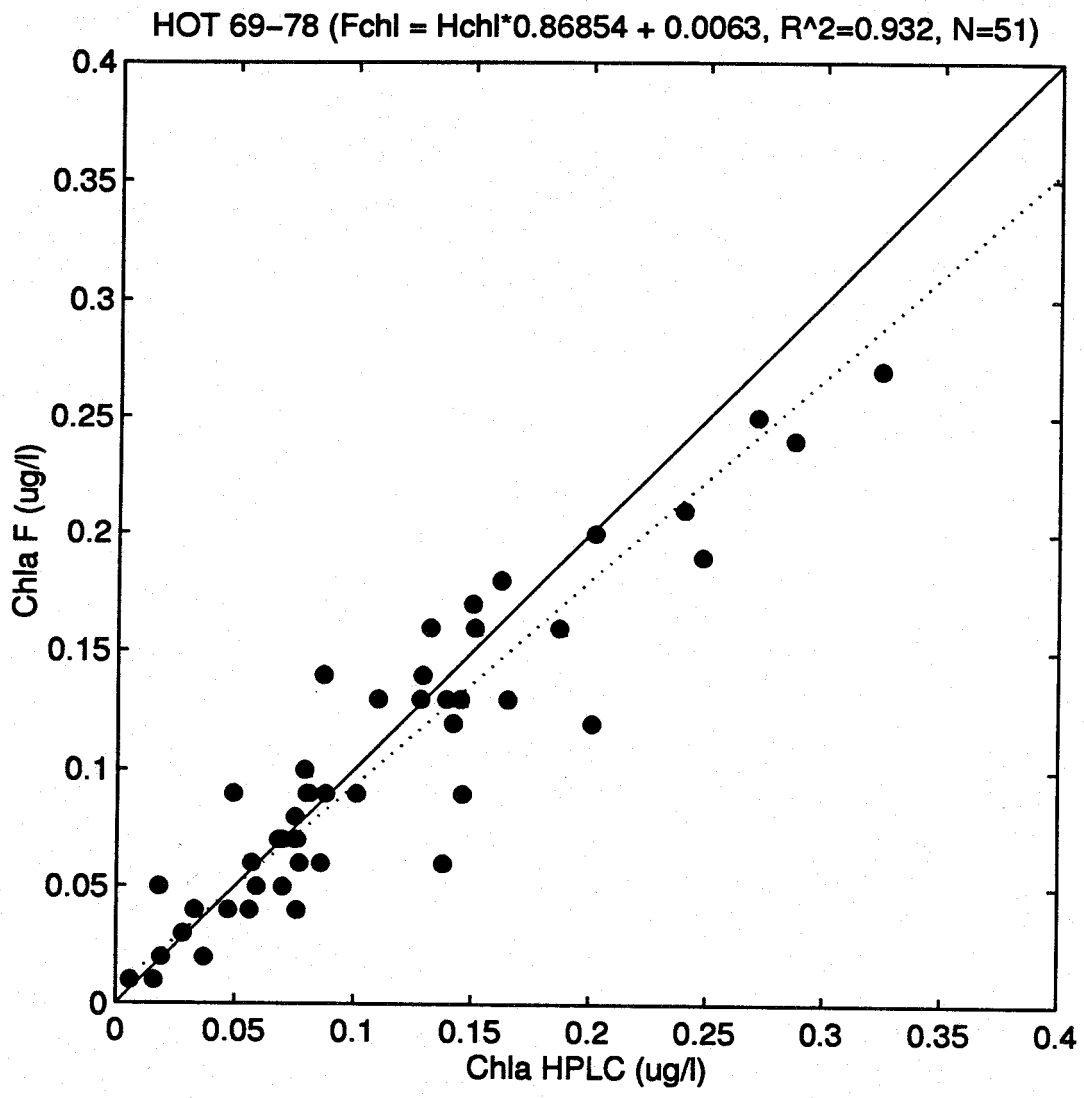

Figure 2.11: Chlorophyll a measured by fluorometry (Chla F) versus chlorophyll a measured by HPLC (Chla HPLC) for all data collected in 1996. The solid line shows the 1:1 x-y relationship while the dashed line is a model II regression analysis of the data set. The regression equation is at the tops of the figure.

Table 2.17: Summary of HPLC Pigment Analysis Response Factors

HOT cruise Sample Loop Method	1-50 500 µl Bidigare*	51-59 200 µl Wright**	60-69 200 µl Wright**	70-78 200 µl Wright**
Chlorophyll c	0.455	0.236	0.241	0.257
Chlorophyll c_1 + c_2	0.455	0.236	0.241	0.257
Peridinin	0.587	0.498	0.488	0.520
19'-Butanoyloxyfucoxanthin	0.421	0.375	0.383	0.408
Fucoxanthin	0.454	0.372	0.381	0.406
19'-Hexanoyloxyfucoxanthin	0.401	0.364	0.376	0.401
Prasinoxanthin	0.434	0.364	0.375	0.400
Violaxanthin	N/A***		0.375	0.400
Diadinoxanthin	0.261	0.251	0.249	0.265
Alloxanthin	N/A***	0.268	0.271	0.289
Lutein	N/A***	0.344	0.352	0.376
Zeaxanthin	0.305	0.273	0.292	0.311
MV Chlorophyll *b*	1.423	0.932	0.901	0.960
Total Chlorophyll *a*	0.729	N/A****	N/A****	N/A****
MV Chlorophyll *a*	N/A***	0.697	0.671	0.716
DV Chlorophyll *a*	N/A***	0.436	0.483	0.515
Total carotenes	0.264	N/A****	N/A****	N/A****
α-carotene	N/A***	0.276	0.282	0.301
β-carotene	N/A***	0.285	0.292	0.311

* Bidigare et al. 1990; units are ng $area^{-1}$
** Wright et al. 1991; units are ng l^{-1} $area^{-1}$
*** not detected in Bidigare method
****not detected in Wright method

2.2.6.3. Underway Surface Fluorometry

Beginning with HOT-76 (September 1996), a Turner Designs Model 10-AU fluorometer was installed on the R/V *Moana Wave* to measure continuous *in vivo* chlorophyll (fluorescence) from surface seawater sampled by the ship's seawater intake system. The underway measurements are calibrated by taking discrete samples from the outflow of the fluorometer and extracting the pigments according to standard methods (2.2.6.1).

2.2.7. Adenosine 5'-Triphosphate

Water column adenosine 5'-triphosphate (ATP) concentrations were determined using the firefly bioluminesence technique as described by Karl and Holm-Hansen (1978). The precision of ATP determinations in 1996 are given in Table 2.18.

Table 2.18: Precision of ATP Analyses

Cruise	Mean CV (%)	Mean SD (μg m^{-3})
69	11.2	1.711
70	9.0	1.331
71	18.6	2.355
72	9.9	0.844
73	16.3	1.686
AC-1	16.7	1.682
74	9.9	1.880
75	6.9	0.919
76	18.2	1.840
77	14.2	1.322
78	18.9	2.036

2.3. Biogeochemical Rate Measurements

2.3.1. Primary Production

Photosynthetic production of organic matter was measured by a trace-metal clean, ^{14}C method. Incubations were conducted *in situ* at eight depths for at least 12 hours using a free-drifting array as described by Winn et al. (1991). Integrated carbon assimilation rates were calculated using the trapezoid rule with the shallowest value extended to 0 m and the deepest extrapolated to a value of zero at 200 m.

2.3.2. Particle Flux

Particle flux was measured at a standard reference depth of 150 m, with an additional depth at 200 m during HOT-69 and 70, using sediment traps deployed on a free-floating array for approximately 2.5 days during each cruise. Sediment trap design and collection methods are described in Winn et al. (1991). Samples were analyzed for particulate C, N and P using methods described in section 2.2.5.

2.4. Microbial Community Structure

Analysis of bacterial number was made at the University of Hawaii, Department of Oceanography's Flow Cytometer Facility by Mr. Hector Nolla using an EPICS 753 flow cytometer (Coulter Electronics Corporation, Hialeah, FL, USA) which has been upgraded with a Cicero Data Acquisition System (Cytomation Inc., Boulder, Colorado). A consistent delivery of sample volume and sample flow rate (100 μl at 50 μl min^{-1} and 50 μl at 50 μl min^{-1} was regularly achieved using a Microsample Delivery System (MSDS, Coulter Electronics Corporation, Hialeah, FL, USA). Prior to analysis by flow cytometry, samples were prepared using standard protocols (Campbell et al. 1994). Hoechst 33342 was added to each sample at a final concentration of 1 μg ml^{-1} (Monger & Landry 1993). Samples were also amended with 0.57 and

0.98 μm microspheres (visible excitation, Fluoresbrite Polysciences) as well as 0.46 μm, UV-only excitable beads. Samples were illuminated simultaneously with 1 Watt of the 488 nm line, and 225 mW UV line, originating from a dual platform equipped with 5 Watt Argon lasers (90-5, Coherent Laser Products, Palo Alto CA). Fluorescence was detected using band pass interference filters for orange fluorescence (575 nm), red fluorescence (680 nm) and blue fluorescence (450 nm). Measurements from these parameters, as well as forward angle light scatter (FALS) and 90 degree light scatter (LS), were amplified into a 3-decade logarithmic scale and stored in a list mode file. Analysis of these files, using CYTOPC (Vaulot 1989), permitted the identification and enumeration of the various populations in the microbial community. The enumeration output from this analysis was corrected for volume (cells ml^{-1}). In addition, an enumeration efficiency factor, based on flow cytometer sample counting rates, was derived using 0.98 μm beads.

2.5. Zooplankton Community Structure

2.5.1. Mesozooplankton Collection

Samples for the assessment of mesozooplankton have been routinely collected on HOT cruises since 1994 using a 1 m^2 plankton net with a 202 μm Nitex mesh. The square net frame has a bottom depressor to make it dive steeply and smoothly through the depth range of the tow, and the bridle system does not cross the net mouth thereby minimizing animal avoidance. A Brancker time-depth-temperature recorder is attached to the frame to determine the depth of tow and confirm even collection at each depth. A General Oceanics flow meter is centered at the net mouth to estimate the volume of water filtered. The net is towed obliquely at a speed of 1.0-1.5 knots while deploying and retrieving the tow line at a constant speed (about 20 meters min^{-1}; total line out = 200 meters; 20 minute tow duration; average depth of tow ≈ 175 meters). Three midnight (between 2200-0200 local time) and three mid-day (between 1000-1400 local time) are conducted on each cruise.

2.5.2. Sample Processing

Contents of the net cod ends are immediately anesthetized with carbonated water to prevent gut evacuation. The net samples are then divided using a Folsom splitter with one-half preserved in 4 % buffered formaldehyde with 2 mg l^{-1} strontium sulfate to prevent acantharians from dissolving, and approximately one-fourth (depending on sample density) size fractionated through nested screens of 5, 2, 1, 0.5 and 0.2 mm Nitex mesh. The remaining one-fourth sample is prepared for live silhouette photography (Ortner et al. 1979) which provides a permanent record of delicate gelatinous forms. Each size fraction is concentrated on a preweighed Nitex screen, rinsed with isotonic ammonium formate to remove salts, sucked dry under low vacuum and flash frozen in liquid nitrogen.

2.5.3. Biomass Determinations

Frozen samples are defrosted in the dark at room temperature, weighed wet (moist) on an analytical balance before (total weight wet) and after (fraction removed) drying. Random subsamples of the zooplankton mass are set aside for enumeration and pigment analysis. The remaining sample is dried at 60 °C, reweighed [total sample dry weight = measured dry weight/fraction of total wet weight dried] and analyzed for carbon and nitrogen biomass (Perkin Elmer Model 2400 CHN Elemental Analyzer).

2.5.4. Gut Pigment Analysis

Subsamples for pigment analysis are homogenized with a tissue grinder in 90% acetone. Chlorophyll *a* and phaeopigments concentration are determined fluorometrically on a Turner Model 10-AU fluorometer.

2.6. ADCP Measurements

Upper ocean currents were measured on all ten HOT cruises and the ALOHA-Climax cruise, using the ADCP mounted on the R/V *Moana Wave* (RD Instruments model VM-150). There were no significant data gaps. GPS navigation was available throughout all cruises; differential GPS was used on all cruises beginning with HOT-72, with the exceptions of HOT-72 Leg 2 and a 2.5 hour interval on HOT-74.

ADCP velocities were corrected for gyro compass errors as measured by the Ashtec 3DF GPS attitude sensor on the R/V *Moana Wave*. Gaps of up to 3 hours in Ashtec data occurred on all cruises except HOT-75, and 1-2 hours gaps were common. These short gaps were filled by linearly interpolating the gyro error estimates. On HOT-72, Leg 1, 3DF were available only for the first 8 hours, so an approximate formula was used to estimate the gyro corrections for the remainder of the cruise:

$$\theta = b1 + b2(V) + b3\ (\cos H) + b4\ (\sin H)$$

where V is the northward component of ship's velocity, H is gyro heading, and coefficient b1 to b4 were determined by least-squares fit to the 3DF data at all points, so the same formula was used with the coefficients estimated from 3 prior HOT cruises (67, 68 Leg 1, 68 Leg 2). Coefficients b3 and b4 were set to zero because they were inconsistent from cruise to cruise. Coefficient b1 and b2 were calculated from each of the 3 prior cruises using only underway data, an then averaged before generating the corrections for HOT-69.

2.7. Optical Measurements

2.7.1. Solar Irradiance

Incident irradiance at the sea surface was measured on each HOT cruise with a LI-COR LI-200 data logger and cosine collector. The instrument recorded data from the time the ship departed Snug Harbor and until its return.

2.7.2. Downwelling Irradiance and Upwelling Radiance

Vertical profiles of upwelling and downwelling irradiance were made using a Biospherical Profiling Reflectance Refractometer (PRR-600). This instrument measures downwelling irradiance (Ed) and upwelling radiance (Lu) as well as surface irradiance from a deck unit on 7 channels (Table 2.19). The radiance channels comply with the SeaWIFS optical parameters. The instrument is lowered by hand and depending on the subsurface currents, is deployed to a depth between 120 and 150 meters.

Table 2.19: Channels and Wavelengths Measured by PRR

Channel	Downwelling	Upwelling	Surface
1	412	412	412
2	443	443	443
3	490	490	490
4	510	510	510
5	555	555	555
6	665	665	665
7	PAR	683	PAR

2.7.3. Flash Fluorescence

Flash fluorescence was measured with a Sea Tech Model ST0250 flash fluorometer and the data collected with the Sea-Bird CTD system. Flash fluorescence traces were collected on as many casts as possible. Because an absolute radiometric standard is not available for flash fluorometers, instrument drift was corrected by checking the relative response of the instrument between cruises using fluorescent plastic sheeting as described in Tupas et al. (1993). A linear relationship of the form, $Vn = b\ Vo + a$, was used to convert all fluorescence data to a common voltage scale, where Vn is the normalized voltage, Vo is the output voltage and a and b are constants derived from the two deep water intervals. The constants used in 1996 were $a = 1.6669$ and $b = 0.6503$.

2.7.4. Beam Transmission

On HOT-69 only, beam transmission was measured with a Sea Tech 25 cm path length transmissometer. Transmission data were collected using the Sea-Bird CTD system in a fashion analogous to that described for flash fluorescence. The data collected on this cruise showed that the instrument was not operating properly and was considered unreliable. No beam transmission data are available for 1996.

2.8. Meteorology

2.8.1. Shipboard Observations

Wind speed and direction, atmospheric pressure, wet- and dry-bulb air temperature, sea surface temperature (SST), cloud cover and sea state were recorded at four-hour intervals while on station ALOHA by the science personnel. Meteorological observations were also obtained every 4 hours by the ship's officers on the bridge of the R/V *Moana Wave* throughout each cruise. The time series of shipboard observations obtained by the science group was plotted and obvious outliers were identified and flagged. The SST-dry air temperature and wet-dry air temperature plots also helped to identify outliers. Bad data points were often replaced with the ship's data. Outliers in the shipboard wind observations were detected by comparison with the buoy winds.

2.8.2. Buoy Observations

Two National Data Buoy Center (NDBC) meteorological buoys are located in the vicinity of the ALOHA Station (Figure 1.1). Buoy #51001 is 400 km west of Station ALOHA at 23.4 °N, 162.3 °W, and buoy #51026 is located north of Molokai at 21.4 °N, 156.96 °W. These buoys collect hourly observations of air temperature, sea surface temperature, atmospheric pressure, wind speed and direction and significant wave height. In 1996, hourly wind speed and direction were obtained from NDBC buoy #51001. This buoy was not operational during cruises HOT-70, 71 and 72. Buoy #51026, whose data has been used in previous data reports, failed to record wind velocity since December 1995, and the buoy was decommissioned in November 1996.

2.9. Inverted Echo Sounder

One inverted echo sounder (IES, #127) located in the center of the ALOHA station (C) recorded data during 1996. The IES was deployed on 28 October 1995 and recovered on 28 October 1996. Another IES (#126) was deployed at ALOHA station on 28 October 1996. The history of the IESs in the HOT site is well documented in Tupas et al. (1994b, 1995) and Karl et al. (1996b). A summary is presented in Table 2.20.

Table 2.20: Summary of IES Deployments and Recoveries

Name	Location	Water depth	Schedule
6 (Kaena)	21° 50.8'N 158° 21.8'W	2,500 meters	May 1993-Jun 1994, Jun 1994-Oct 1995
N	23° 00.7'N 157° 59.9'W	4,800 meters	Feb 1991-Feb 1992, Jun 1992-May 1993
C	22° 44.9'N 157° 59.9'W	4,800 meters	Feb 1991-Feb 1992, Jun 1992-May 1993 May 1993-Jun 1994, Jun 1994-Oct 1995, Oct 1995-Oct 1996, Oct 1996-Jul 1997,
SW	22° 37.0'N 158° 14.7'W	4,800 meters	Feb 1991-Feb 1992, Jun 1992- May 1993
SE	22° 30.0'N 157° 45.2'W	4,800 meters	Feb 1991-Feb 1992, Jun 1992- May 1993
E	22° 44.8'N 157° 54.0'W	4,800 meters	Feb 1991- Feb 1992

2.10. Moored Sediment Traps

A bottom-moored sediment trap experiment has been in place since June 1992 at a site near Station ALOHA (Figure 1.2). Schedule of deployments and retrievals is shown in Table 2.21. The ALOHA-V mooring was deployed in October 1996 and is currently on the seafloor. The present experiment consists of 1 Parflux MK7-21 sequencing sediment collectors located at 4000 m. A separate sampling cup is rotated into the collector position on an approximately 15-20 day cycle, depending on the deployment period. Samples from each cup are initially divided into four 60-ml volumes (also referred to as splits). Each split is further divided into the volumes required for the various analyses (Table 2.22).

Table 2.21: Schedule of Deployments and Recoveries of Moored Sediment Trap

Designation	Location	Depth	Schedule
ALOHA-I	22° 57.3' N, 158° 06.2' W	4,800	Jun 1992- Sept 1993
ALOHA-II	23° 06.7' N, 157° 55.8' W	4,800	Sept 1993 - Oct 1994
ALOHA-III	22° 50.2' N, 157° 55.9' W	4,800	May 1995 - Oct 1995
ALOHA-IV	22° 51.7' N, 157° 54.3' W	4,800	Nov 1995 - Oct 1996
ALOHA-V	22° 51.7' N, 157° 54.3' W	4,800	Oct 1996 - Dec 1997

Table 2.22: Distribution of Sample Materials From Bottom-Moored Sediment Traps

Investigators	Analyses
D. Karl, L. Tupas, D. Hebel. U. Magaard, T. Houlihan, D. Sadler, H. Nolla (University of Hawaii)	Total mass, dissolved N, P, Si, total and biogenic particulate C, N, P, Si, fluorometric chlorophyll a, phaeopigments, stable isotopes, bacterial abundance
R. Bidigare, S. Christensen (University of Hawaii)	Pigments by HPLC, diatom abundance and composition
D. Bird (University of Quebec at Montreal)	Virus abundance
S. Honjo, S. Manganini (Woods Hole Oceanographic Institution)	Lithogenic analysis
L. Sautter (College of Charleston)	Foraminiferan abundance
F. Prahl (Oregon State University)	Alkenone concentrations
J. Dymond (Oregon State University)	Barite

2.11 Thermosalinograph

2.11.1 Data acquisition

An SBE-21 Seacat thermosalinograph was used for the HOT-70 through 78 cruises and during the AC-1 cruise. HOT-70 to 73 and AC-1 used Seacat thermosalinograph sensor #2045 while HOT-74 through 78 used Seacat thermosalinograph sensor #1392. Thermosalinograph data are not available for HOT-69 as the instrument was not operational during that cruise.

The thermosalinograph was installed in a pumped intake line in the hull of the R/V *Moana Wave*. A SeaBird remote temperature sensor, installed in a sea chest in the bow of the ship, recorded temperature data from about 3 m depth. This location allows for relatively undisturbed water to enter the thermosalinograph. Beginning with HOT-76 (September 1996), the newly installed clean seawater intake system was used and the thermosalinograph was attached to its system. HOT-70 through 77, as well as AC-1, used SeaBird remote temperature sensor #2078 while HOT-78 used remote temperature sensor #1496.

The SBE-21 Seacat thermosalinograph calculates salinity using an internal temperature and conductivity sensor. Data were obtained every 10 seconds. In order to calibrate the conductivity sensor, bottle salinity samples were periodically taken from the thermosalinograph intake line. To calculate salinity, a pressure of 20 dbar was assumed to compensate for the pressure caused by the pump for the intake line (30 psi). Approximately 5 hours of data were affected by a malfunctioning pump and pump seal during the beginning of HOT-70. A pump problem also occurred during HOT-72 which, along with an electronics problem, affected all 5 days of data. A computer logging problem caused the loss of 15 hours of thermosalinograph data during HOT-74. Another computer logging problem caused the loss of 3 hours of data during HOT-77.

2.11.2. Data processing and sensor calibration

2.11.2.1. Nominal Calibration

2.11.2.1.1. Temperature

The internal temperature sensors (#1392 and #2045) and external temperature sensors (#1496 and #2078) were calibrated at Sea-Bird. The calibration coefficients obtained at Sea-Bird are given in Table 2.2. These sensors are the same type as that used for the CTD measurements so the same procedure for drift estimation was followed.

Sensor #1392

For sensor #1392, a drift rate of -3.8×10^{-6} °C day^{-1} was determined using the 29 September 1994 and 13 October 1995 calibrations. The 29 September 1994 calibration was performed after the sensor's electronics had been reworked. This sort of work usually causes a change in the drift of a sensor so the calibrations prior to this date were not used for drift calculation purposes. All the cruises which used internal temperature sensor #1392 (HOT-74 through 78) calculated temperatures using the 13 October 1995 baseline calibration. For HOT-74 through 78 drift corrections of -1.1×10^{-3} °C, -1.2×10^{-3} °C, -1.3×10^{-3} °C, -1.4×10^{-3} °C and -1.6×10^{-3} °C were applied respectively.

Sensor #1496

A drift rate of 1.5×10^{-5} °C day^{-1} was determined using the 2 November 1993 and 19 January 1996 calibrations for remote temperature sensor #1496. Temperatures were calculated with the 13 October 1995 baseline calibration. A drift correction of 4.9×10^{-3} °C was applied to the temperatures from the only cruise which used sensor #1496, HOT-78.

Sensor #2045

For internal temperature sensor #2045, a drift rate of 3.3×10^{-6} °C day^{-1} was determined using the 11 October 1995 and 30 July 1996 calibrations. Temperatures were calculated with the 11 October 1995 baseline calibration. Six cruises used internal temperature sensor #2045: HOT-70 to 74 and AC-1. Drift corrections of 0.6×10^{-3} °C, 0.6×10^{-3} °C, 0.7×10^{-3} °C, 0.9×10^{-3} °C and 0.9×10^{-3} °C were computed for those cruises respectively. However, these drifts were considered inconsequential as they are smaller than the accuracy of the temperature sensor and hence were not applied to the temperature data collected from sensor #2045.

Sensor #2078

Using the 19 October 1995 and 17 December 1996 calibrations, a drift rate of 3.6×10^{-6} °C day^{-1} was determined for remote temperature sensor #2078. For HOT-70 through HOT-73, drift corrections of 0.6×10^{-3} °C, 0.7×10^{-3} °C, 0.8×10^{-3} and 0.9×10^{-3} °C were computed for those cruises respectively. These drifts were not applied as they are smaller than the accuracy of the temperature sensor. A drift correction of 0.9×10^{-3} °C was computed for AC-1 and it also was not applied. Drift corrections of 1.0×10^{-3} °C, 1.1×10^{-3} °C, 1.3×10^{-3} °C and 1.4×10^{-3} °C were computed and applied to the HOT-74 through 77 cruises respectively.

2.11.2.1.2. Conductivity

Sea-Bird conductivity sensor #2045 was used to collect thermosalinograph conductivity data for HOT-70 through 73 as well as AC-1. Conductivity sensor #1392 was used to collect thermosalinograph conductivity data for HOT-74 through HOT-78. For sensor #2045, all conductivity data were nominally calibrated with coefficients obtained at Sea-Bird on 13 October 1995. For sensor #1392, all conductivity data were nominally calibrated with coefficients which were also obtained at Sea-Bird on 11 October 1995. However, the final salinity data reported here were calibrated against bottle data as explained in Section 2.11.2.3.

2.11.2.2 Processing

The thermosalinograph data were screened for gross errors, setting upper and lower bounds of 35 °C and 18 °C for temperature and 6 Siemens m^{-1} and 3 Siemens m^{-1} for conductivity. One gross external temperature error was detected for HOT-72 and the value was replaced with a 5-point median value. For HOT-74, there were 11268 gross temperature errors as the external temperature sensor was recording values over 135 °C for approximately 24 hours. These temperature points were flagged as bad. A new quality control system was established beginning with the HOT-72 thermosalinograph data. Starting with HOT-72, and for every subsequent cruise, each temperature and salinity point is given a flag to determine whether the data are good, suspect or bad.

A 5-point running median filter was used to detect temperature and conductivity spikes in the thermosalinograph data. Glitches in temperature and conductivity detected by the 5-point median filter were immediately replaced by the median. Threshold values of 0.3 °C for temperature and 0.1 Siemens m^{-1} for conductivity were used for the median filter. Only a few or zero points were replaced after running the median filter for each cruise. A 3-point triangular running mean filter was used to smooth the temperature and conductivity data from all the cruises after they had gone through spike detection.

2.11.2.3 Empirical Calibration

The thermosalinograph salinity was calibrated empirically by comparing it to bottle salinity samples drawn from the plumbing near the thermosalinograph (Figure 2.12). Bottle salinity samples were analyzed as described in Section 2.1.3.

The time delay between the water passing through the thermosalinograph and it reaching the bottle sampling area was determined to be about 50 seconds using autocorrelation between bottle and thermosalinograph samples. The thermosalinograph data were extracted within ± 90 seconds around the sample time minus the 50 second delay for the comparison with the bottle data.

A cubic spline was fit to the time-series of the differences between the bottle conductivity and the thermosalinograph conductivity separately for all the 1996 HOT and AC cruises. The correction of the thermosalinograph conductivities was obtained from the cubic spline fit. Salinity was calculated using these corrected conductivities, thermosalinograph temperatures and pressure of 20 dbar. The mean values for the salinity bottle minus final calibrated thermosalinograph were less than 1×10^{-4} for each cruise. Table 2.23 gives the standard deviations for the salinity bottle minus final calibrated thermosalinograph values. HOT-72 shows a very large standard deviation compared to the other cruises. As mentioned in Section 2.9.1, a pump as well as an electronics problem occurred which affected all the salinity data for HOT-72. Hence, all HOT-72 salinity data have been flagged as either suspect or bad.

Table 2.23: Bottle-Thermosalinograph Salinity Comparison

Cruise	Sensor #	Standard Deviation
70	2045	0.0017
71	2045	0.0027
72	2045	0.0061
73	2045	0.0034
AC-1	2045	0.0020
74	1392	0.0014
75	1392	0.0009
76	1392	0.0017
77	1392	0.0013
78	1392	0.0009

2.11.2.4 Comparison with CTD Data

The corrected thermosalinograph salinity data were compared with the downcast CTD salinity at 4 dbar for the purpose of checking the calibration (Figure 2.12).

The thermosalinograph data were averaged using data sampled one minute after the acquisition time of the CTD sample. The linear fit of the time-series of CTD-thermosalinograph salinity differences showed that the CTD salinity was higher than the thermosalinograph salinity for four of the cruises (Figure 2.12).

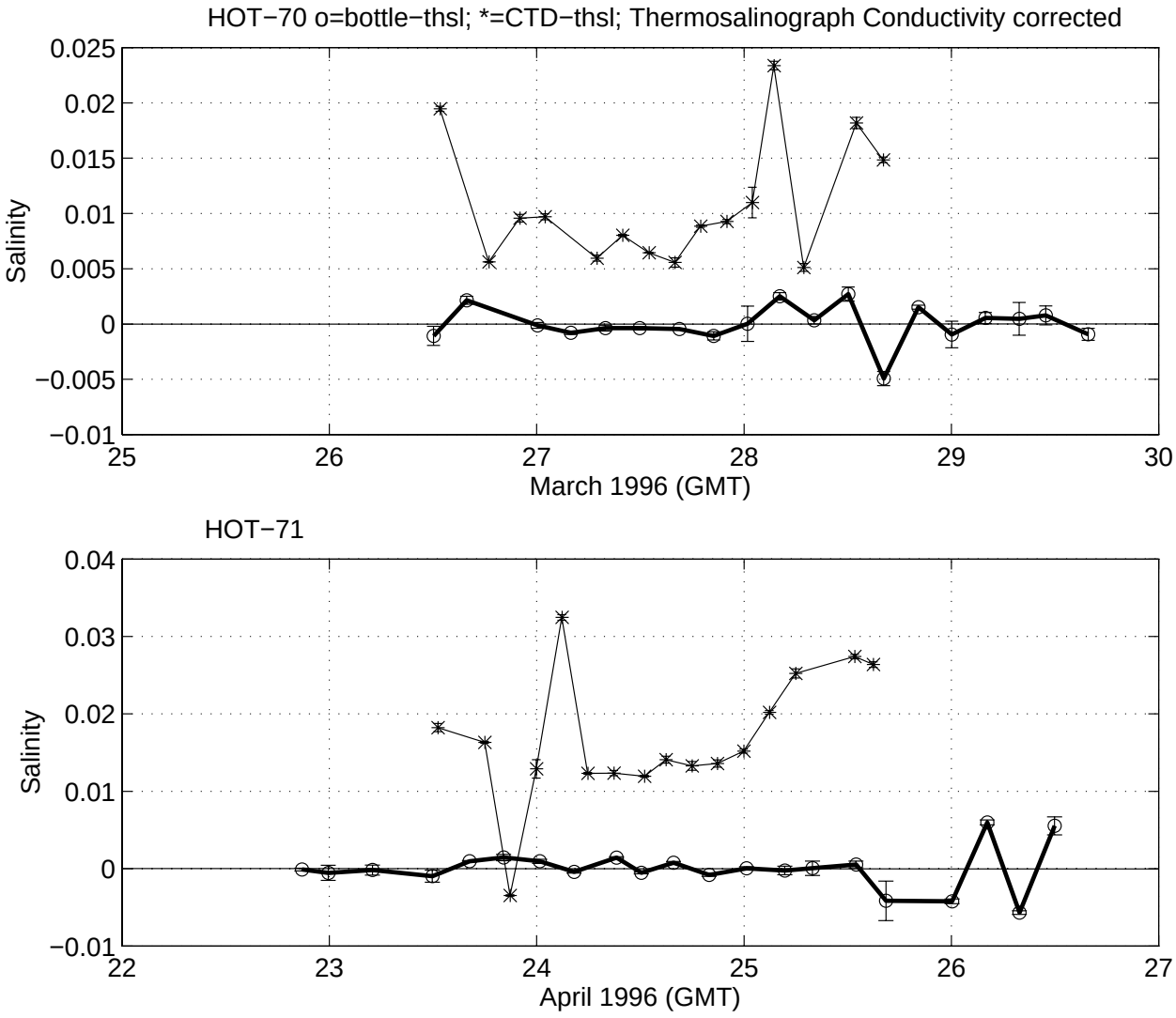

Figure 2.12: Differences between bottle salinities and thermosalinograph salinities (thick line) and differences between CTD salinities and thermosalinograph salinities (thin line) for all HOT cruises in 1996 and AC-1. A thin straight line shows a linear fit for the bottle and thermosalinograph salinity differences. Circles indicate average values around the bottle sampling time and asterisks indicate average values around the acquisition of the CTD data. The bars indicate the standard deviation. See text for the details of the averaging process.

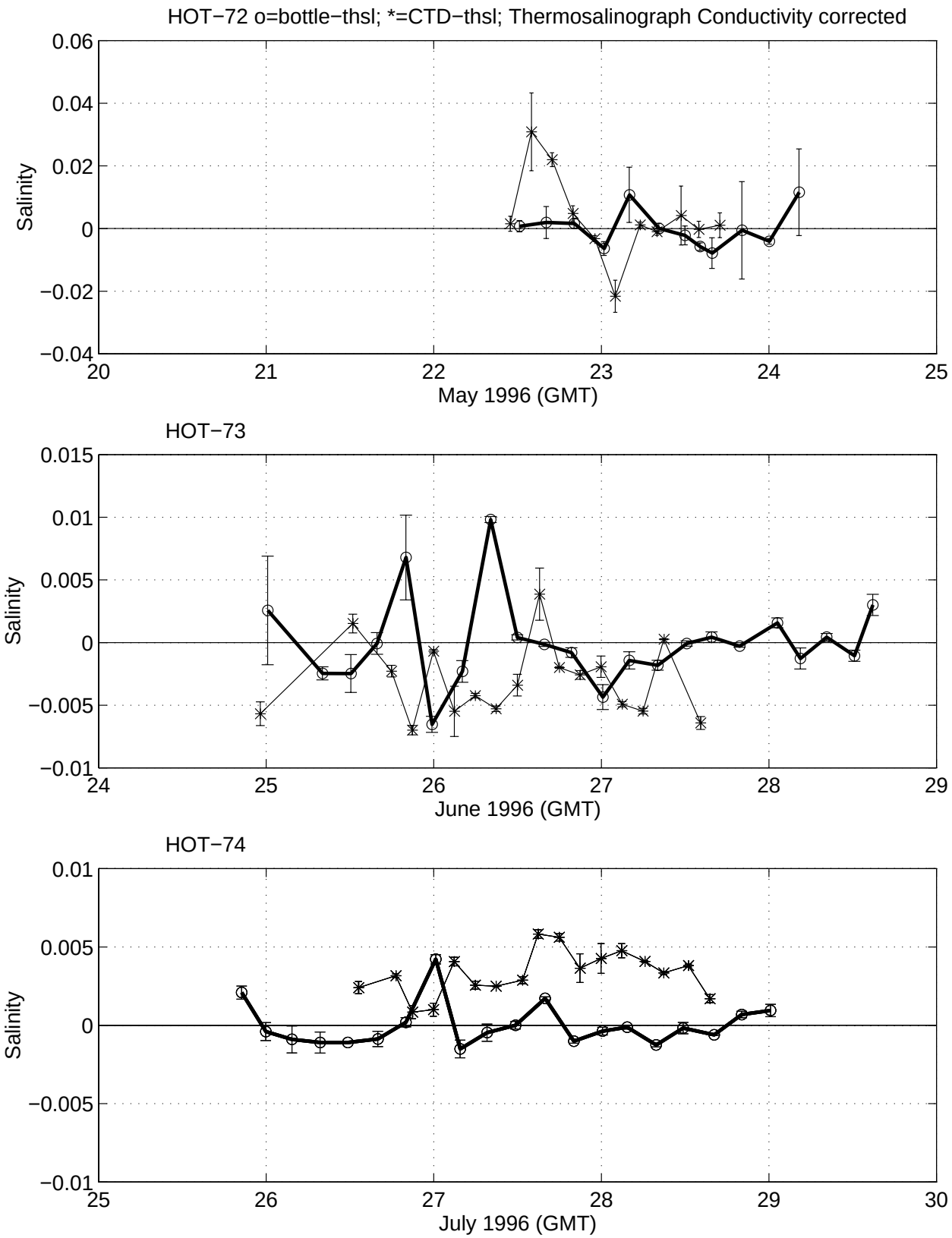

Figure 2.12: continued

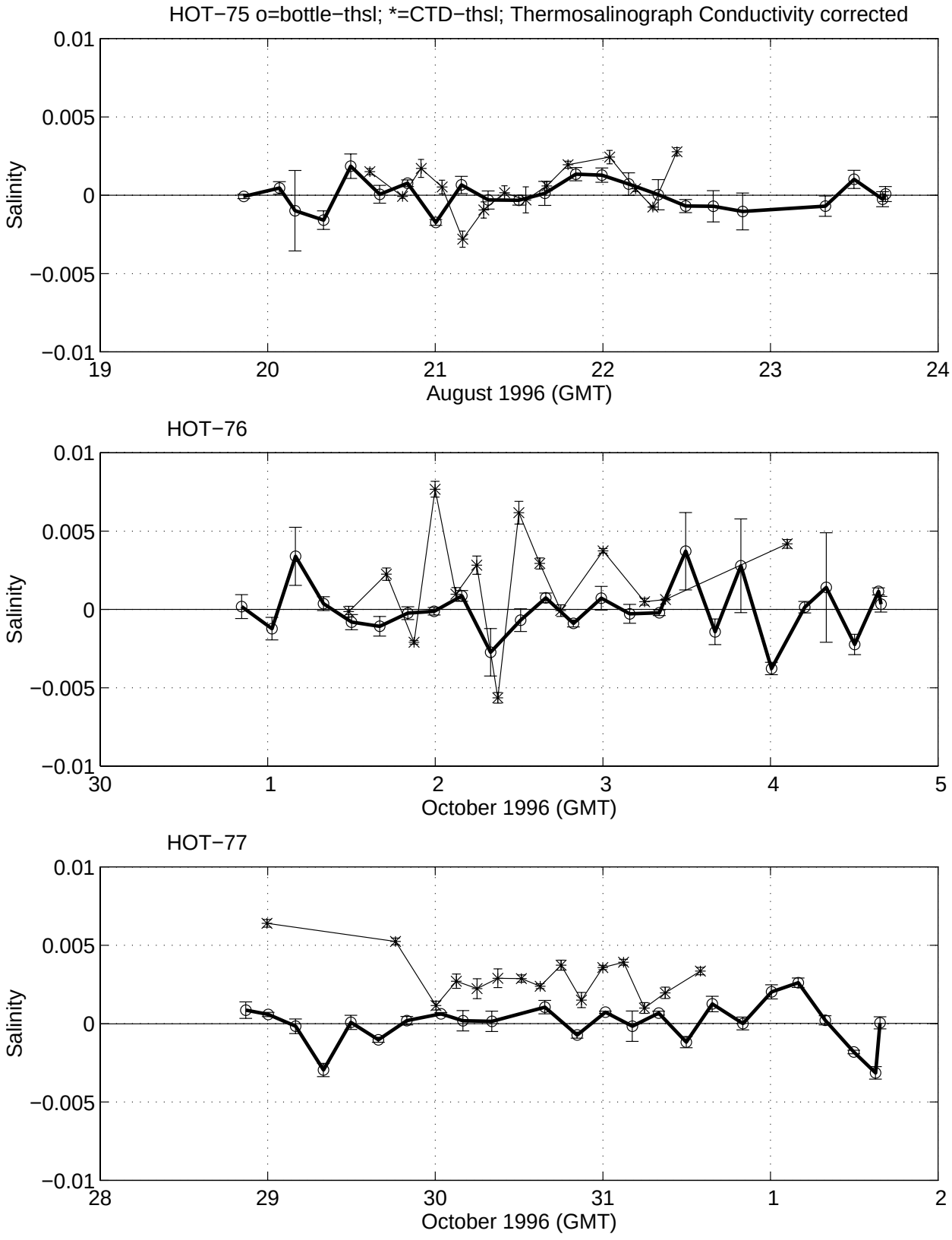

Figure 2.12: continued

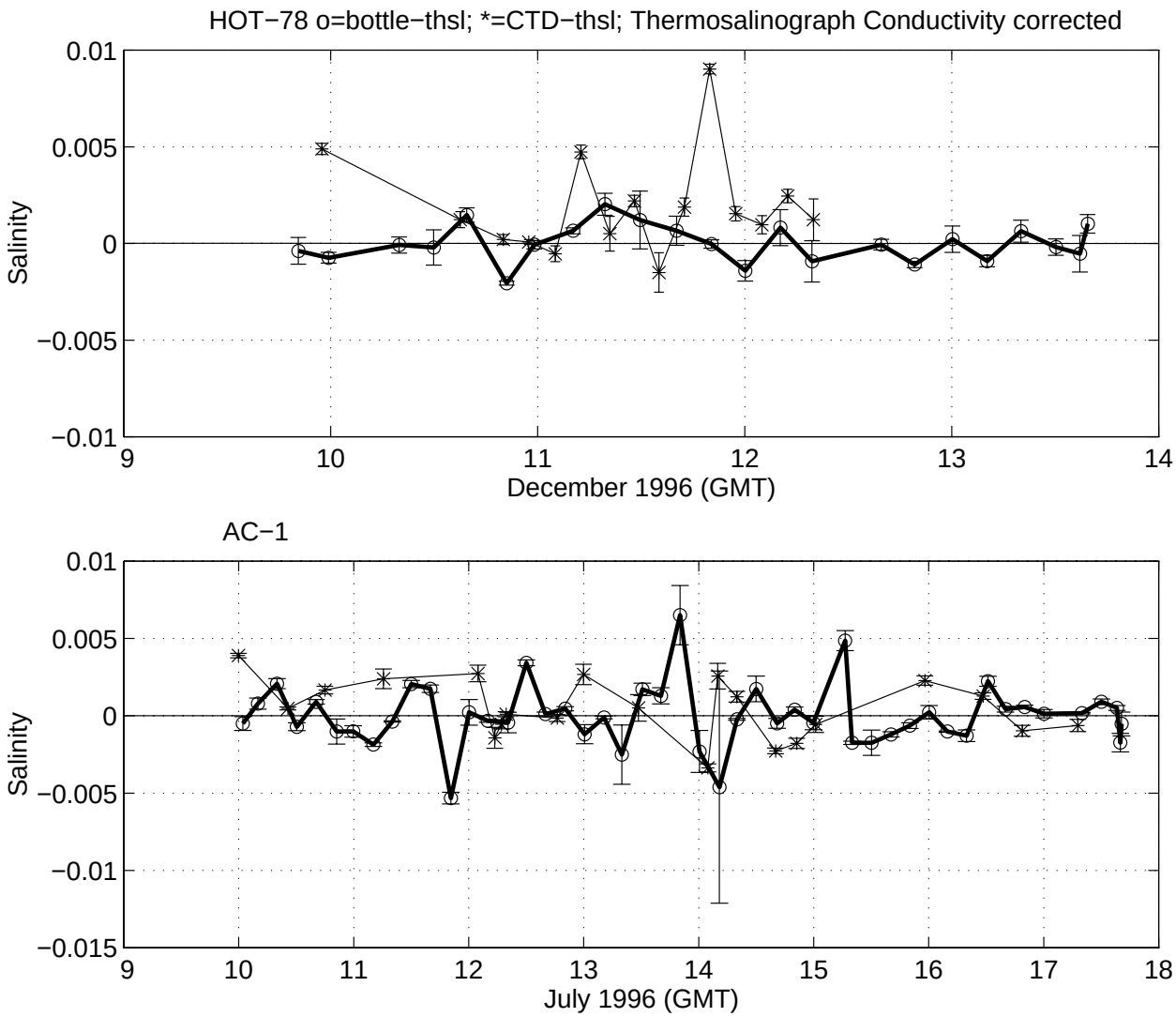

Figure 2.12: continued

The pump problem mentioned in Section 2.11.1 for HOT-72 fouled the first three days of conductivity data for HOT-72 causing an incomplete thermosalinograph salinity analysis. The analysis for HOT-74 ends prematurely due to a computer logging problem which is also noted in Section 2.11.1.

2.12. Towed Instrumentation

Before the return transit to Honolulu, a series of transects are made within the 6 nautical mile radius of Station ALOHA to obtain data from a towed instrument package consisting of an Endeco Instruments 1.5 m fin, a Sea-Bird (SBE-19) CTD and a Focal Instruments Optical Plankton Counter (OPC). This is a joint project between the HOT-JGOFS core component and scientists from Scripps Institution of Oceanography (Mark Huntley, P.I.) which started with HOT-60 (February 1995). A WetLabs SeaStar fluorometer was added to the package for HOT-64 (July 1995). The package is deployed on a 3-conductor cable and towed at a constant depth at a speed of 8 knots. The package collects data on physical (temperature and conductivity) and biological (zooplankton biomass and size spectrum, chlorophyll *a*) variability in the mixed-layer of the water column. The sampling pattern typically consists of zigzags within a square extending from 22.65° N to 22.85° N, 157.9° W to 158.1° W, and a transect along the regular ship track into Honolulu. In 1996 the target towing depth was 45 m, with variations of approximately ± 5 m due to changes in ship speed and heading.

2.13. Regional Study

In July of 1996 a transect study was conducted to evaluate regional variability in hydrographic and biogeochemical parameters between Station ALOHA and the historical Climax study area. The cruise was made from July 8-16, 1996 on the R/V *Moana Wave* and covered a cruise track that overlaid the Topex-Poseidon satellite track (Figure 2.13).

The primary purpose of the cruise was to:

1) Determine the regional variability and gradients in selected biogeochemical and physical properties of the upper water column from Station ALOHA to the Climax Program study site.
2) Assess upper water column characteristics at Climax using modern techniques for comparison to the historical data set.
3) Compare depth specific phytoplankton and mesozooplankton communities with near synoptic resolution at ALOHA and Climax.
4) Determine regional variability in phosphorus pool inventories and dynamics.
5) Determine along-track variability in particle concentration, pCO_2, chlorophyll a, and hydrographic parameters.

Station coordinates are given in Table 2.24. Stations 1 to 5 were the originally planned, however, Stations 6 to 9 were added to document the development and extent of an algal bloom encountered during this cruise.

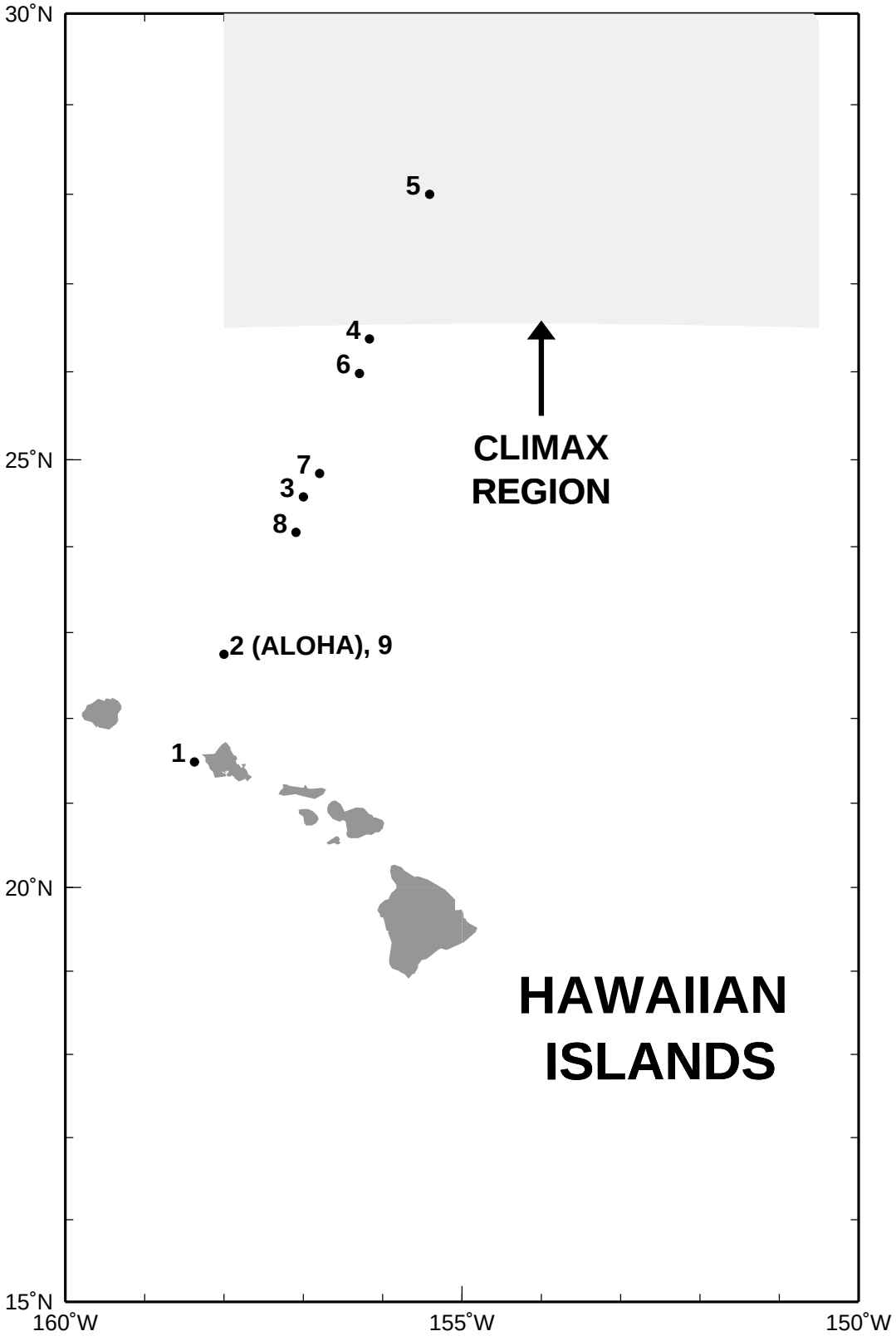

Figure 2.13: Station locations during ALOHA-Climax 1 cruise. Stations 2 and 9 are Station ALOHA and Station 5 was designated as Station Climax.

Parameters studied during this cruise are presented in Table 2.25. Protocols were obtained from Climax investigators (e.g., Hayward 1987) to be used in comparison to HOT methods.

Table 2.24: Location of station for ALOHA-Climax 1 cruise

Station	Location	Date	Comments
1	21° 29.04’ N, 158° 22.44’ W	8 July 1997	
2	22° 45.00’ N, 158° 00.00’ W	9 July 1997	Station ALOHA
3	24° 34.20’ N, 157° 00.00’ W	10 July 1997	
4	26° 22.50’ N, 156° 10.02’ W	11 July 1997	
5	28° 00.00’ N, 155° 24.60’ W	12 July 1997	Station Climax
6	25° 58.91’ N, 156° 17.62’ W	14 July 1997	
7	24° 50.22’ N, 156° 47.66’ W	15 July 1997	
8	24° 09.90’ N, 157° 05.45’ W	15 July 1997	
9	22° 45.00’ N, 158° 00.00’ W	15 July 1997	Station ALOHA

Table 2.25: Parameters measured during ALOHA-Climax 1 cruise (shaded section means sample was taken)

Station	1	2	3	4	5	6	7	8	9
Water column									
Hydrography	■	■	■	■	■	■	■	■	■
Salinity	■	■	■	■	■	■	■	■	■
Dissolved Oxygen	■	■	■	■	■	■	■	■	■
Dissolved inorganic carbon	■	■	■	■	■				
Alkalinity	■	■	■	■	■				
Nitrate + Nitrite	■	■	■	■	■				
Soluble Reactive Phosphorus (SRP)	■	■	■	■	■				
Silicate	■	■	■	■	■				
Dissolved Organic Carbon	■	■	■	■	■				
Dissolved Organic Nitrogen	■	■	■	■	■				
Dissolved Organic Phosphorus	■	■	■	■	■				
Particulate Carbon		■	■		■				
Particulate Nitrogen		■	■		■				
Particulate Phosphorus		■	■		■				
Particulate Silica					■				
Low-level Nitrogen	■	■	■	■	■				
Low-level SRP	■	■	■	■	■		■		
Chlorophyll a	■	■	■	■	■		■		
Phaeopigments	■	■	■	■	■		■		
HPLC Pigments		■			■				
Heterotrophic Bacteria	■	■	■	■	■				
Photosynthetic Bacteria	■	■	■	■	■				
Adenosine 5’ Triphosphate		■			■				
Bacterial Lipopolysacharride	■	■	■	■	■				
Primary Production Experiment									
Salinity		■			■				
Chlorophyll a		■			■				
Phaeopigments		■			■				
Light incubations		■			■				
Dark Incubations		■			■				
Heterotrophic Bacteria		■			■				
Photosynthetic Bacteria		■			■				
Protocol Comparison									
Primary production		■			■				
Chlorophyll a		■			■				
Phaeopigments		■			■				

3.0. CRUISE SUMMARIES

The cruise summaries presented here give an overview of the activities conducted during the 1996 HOT cruises. A more thorough Chief Scientist's report can be found on the web page See Section 8.3.

3.1. HOT-69: Luis Tupas, Chief Scientist

The R/V *Moana Wave* departed Snug Harbor at 0900 HST on 15 January 1996 with 15 scientists on-board. All objectives of the JGOFS and WOCE programs were accomplished. Stations Kahe and ALOHA were occupied. All core samples were taken within the 36-hour CTD burst sampling period. All samples for ancillary projects were taken. Floating sediment trap and primary production arrays were successfully deployed and recovered. Zooplankton tows were conducted mid-day and mid-night while at Station ALOHA. A second deep cast was conducted on the last day on station. The optical plankton counter (OPC) was towed within Station ALOHA without any problem. OPC transect was terminated to allow ample transit time to Honolulu. ADCP were running throughout the cruise. The ship arrived at Snug Harbor at 0800 on 19 January 1996.

3.2. HOT-70: Luis Tupas, Chief Scientist

The R/V *Moana Wave* departed Snug Harbor at 0830 HST on 25 March 1996 with 16 scientists on-board. All objectives of the JGOFS and WOCE programs were accomplished. Stations Kahe and ALOHA were occupied. All core samples were taken within the 36-hour CTD burst sampling period. All samples for ancillary projects were taken. Floating sediment trap and primary production arrays were successfully deployed and recovered. A separate array which held an upside-down, Parflux MK7-21 sediment trap was successfully deployed and retrieved. Zooplankton tows were conducted mid-day and mid-night while at Station ALOHA. The optical plankton counter was towed within Station ALOHA without any problem. The pump of the continuous water sampler, however, did not function when tested with the OPC. OPC transect was terminated to allow ample transit time to Honolulu. ADCP and thermosalinograph were running throughout the cruise. The ship arrived at Snug Harbor at 0800 on 29 March 1996.

3.3. HOT-71: Dale Hebel, Chief Scientist

The R/V *Moana Wave* departed Snug Harbor at 0900 HST on 22 April 1996 with 13 scientists on-board. All objectives of the JGOFS and WOCE programs were accomplished. Stations Kahe and ALOHA were occupied. All core samples were taken within the 36-hour CTD burst sampling period. All samples for ancillary projects were taken. Floating sediment trap and primary production arrays were successfully deployed and recovered. Zooplankton tows were conducted mid-day and mid-night while at Station ALOHA. After the last CTD cast, the ship steamed to the location of the moored sediment trap array that was unsuccessfully deployed

during HOT-60. The acoustic release was successfully interrogated. Its precise location was determined by acoustic triangulation. After triangulation procedures, the ship returned to Station ALOHA for the OPC transect. The optical plankton counter was towed within Station ALOHA without any problem. OPC transect was terminated to allow ample transit time to Honolulu. ADCP and thermosalinograph were running throughout the cruise. The ship arrived at Snug Harbor at 0740 on 26 April 1996.

3.4. HOT-72: Fernando Santiago-Mandujano, Chief Scientist

The R/V *Moana Wave* departed Snug Harbor at 0900 HST on 20 May 1996 with 17 scientists on-board. Stations Kahe and ALOHA were occupied. All objectives of the JGOFS and WOCE programs were accomplished despite a loss of station time to perform a medical evacuation. After arrival at Station ALOHA, one of the science party was injured which required immediate medical attention. The captain and chief scientist decided to evacuate the injured scientist by transporting him to Kaneohe Bay (Heeia Kea small boat harbor) where he was transported to a medical facility. The ship left Station ALOHA just after midnight, completed the round trip and returned to Station ALOHA by 1430 on 21 May. Sediment trap deployment began immediately and the first CTD cast was conducted at 1600. All core samples were taken within the 36-hour CTD burst sampling period. All samples for ancillary projects were taken. Floating sediment trap and primary production arrays were successfully deployed and recovered. Zooplankton tows were conducted mid-day and mid-night while at Station ALOHA. The optical plankton counter was towed within Station ALOHA without any problem. OPC transect was terminated to allow ample transit time to Honolulu. ADCP and thermosalinograph were running throughout the cruise. The ship arrived at Snug Harbor at 0800 on 24 May 1996.

3.5. Trawl: Terrence Houlihan, Chief Scientist

The R/V *Moana Wave* departed Snug Harbor at 0800 HST on 2 June 1996 with 5 scientists on-board. The objective of this cruise was to recover the moored sediment trap which was unsuccessfully deployed in February 1995 (HOT-60). Although both acoustic releases confirmed their release configuration, the array did not lift from the bottom. The grappling array was deployed for approximately 20 hours without success. The ship departed the site at 2000 on 4 June and arrived at Snug Harbor at 0800 on 5 June.

3.6. HOT-73: Luis Tupas, Chief Scientist

The R/V *Moana Wave* departed Snug Harbor at 0900 HST on 24 June 1996 with 15 scientists on-board. All objectives of the JGOFS and WOCE programs were accomplished. Stations Kahe, ALOHA and Station 3 were occupied. All core samples were taken within the 36-hour CTD burst sampling period. All samples for ancillary projects were taken. Floating sediment trap and primary production arrays were successfully deployed and recovered. Zooplankton tows were conducted mid-day and mid-night while at Station ALOHA. After the

last CTD cast, the ship steamed to Station 3 to conduct a deep cast. After the CTD cast, the ship returned to Station ALOHA for the OPC transect. The optical plankton counter was towed within Station ALOHA without any problem. OPC transect was terminated to allow ample transit time to Honolulu. ADCP and thermosalinograph were running throughout the cruise. The ship arrived at Snug Harbor at 0730 on 28 June 1996.

3.7. ALOHA-Climax 1: Dale Hebel, Chief Scientist

The R/V *Moana Wave* departed Snug Harbor at 0900 HST on 8 July 1996 with 15 scientists aboard. Dale Hebel substituted as chief scientist for Dave Karl who suffered an injury prior to the cruise. Five stations were planned along the cruise track from Oahu to Station Climax (see Section 2.13, Regional Study). Four additional stations were made during the cruise At each station a minimum of one CTD cast was made to 1000 meters. Additional water samples were taken with Go-Flo bottles at selected stations. Extensive water sampling and experiments were conducted at Station ALOHA and Station Climax. Optical measurements, zooplankton net tows were also conducted. A moored sediment trap was deployed at Station Climax to be retrieved the following year. The OPC was towed between Stations Climax and ALOHA on the return transect. ADCP and thermosalinograph were running throughout the cruise. The ship arrived at Snug Harbor at 0950 on 16 July 1996.

3.8. HOT-74: Fernando Santiago-Mandujano, Chief Scientist

.

The R/V *Moana Wave* departed Snug Harbor at 0900 HST on 25 July 1996 with 15 scientists on-board. All objectives of the JGOFS and WOCE programs were accomplished. Stations Kahe and ALOHA were occupied. All core samples were taken within the 36-hour CTD burst sampling period. All samples for ancillary projects were taken. Floating sediment trap and primary production arrays were successfully deployed and recovered. Malfunctions in the Go-Flo bottles necessitated the use of CTD water samples for half of the depths for the primary production experiment. Zooplankton net tows were conducted mid-day and mid-night while at Station ALOHA. A second deep cast was conducted at Station ALOHA. After the CTD cast, the optical plankton counter was towed within Station ALOHA without any problem. The OPC transect was terminated earlier than scheduled because of ship's engine problems which required more transit time to Honolulu. ADCP and thermosalinograph were running throughout the cruise. The ship arrived at Snug Harbor at 0730 on 29 July 1996.

3.9. HOT-75: Dale Hebel, Chief Scientist

The R/V *Moana Wave* departed Snug Harbor at 0900 HST on 19 August 1996 with 13 scientists on-board. All objectives of the JGOFS and WOCE programs were accomplished. Stations Kahe and ALOHA were occupied. All core samples were taken within the 36-hour CTD burst sampling period. All samples for ancillary projects were taken. The OPC was towed for a short period between Stations Kahe and ALOHA. Floating sediment trap and primary production arrays were successfully deployed and recovered. All Go-Flo bottles were repaired after the previous cruise and functioned properly during this cruise. Zooplankton tows were conducted mid-day and mid-night while at Station ALOHA. After the last CTD cast, the optical plankton counter was towed within Station ALOHA without any problem. After completing the transect, the ship steamed towards Honolulu. ADCP and thermosalinograph were running throughout the cruise. The ship arrived at Snug Harbor at 0730 on 23 August 1996.

3.10. HOT-76: Luis Tupas, Chief Scientist

The R/V *Moana Wave* departed Snug Harbor at 0900 HST on 30 September 1996 with 15 scientists on-board. All objectives of the JGOFS and WOCE programs were accomplished. Stations Kahe, ALOHA and Kauai Basin (Station 7) were occupied. All core samples were taken within the 36-hour CTD burst sampling period. All samples for ancillary projects were taken. Floating sediment trap and primary production arrays were successfully deployed and recovered. Zooplankton tows were conducted mid-day and mid-night while at Station ALOHA. After the last CTD cast, the optical plankton counter (OPC) was towed within Station ALOHA without any problem. After completing the transect, the ship steamed towards the deepest point of the Kauai Basin where a deep cast was conducted. After the cast the ship began its transit to Honolulu. The newly installed clean-seawater intake system was operated on this cruise. The thermosalinograph was transferred to this line and a pCO_2 system and flow through fluorometer were installed using feed water from this line for underway analysis. All underway systems, including ADCP were running throughout the cruise. The ship arrived at Snug Harbor at 0630 on 4 October 1996.

3.11. Sediment Trap-5: David Karl, Chief Scientist

The R/V *Moana Wave* departed Snug Harbor at 0800 HST on 7 October 1996 with 2 scientists aboard. The cruise objective was to recover the bottom moored sediment trap that was deployed on ST-4 (12 November 1995). All objectives of the cruise were accomplished. The ship arrived at Snug Harbor on 10 October 1996 at 0730.

3.12. HOT-77: Luis Tupas, Chief Scientist

The R/V *Moana Wave* departed Snug Harbor at 0930 HST on 28 October 1996 with 13 scientists aboard. All objectives of the JGOFS and WOCE programs were accomplished. Stations Kahe and ALOHA were occupied. All core samples were taken within the 36-hour CTD burst sampling period. All samples for ancillary projects were taken. Floating sediment trap and primary production arrays were successfully deployed and recovered. Zooplankton tows were conducted mid-day and mid-night while at Station ALOHA. An inverted echo sounder was retrieved and a new one was deployed at the center of Station ALOHA. A second deep cast was conducted at Station ALOHA. After the last CTD cast, the optical plankton counter was towed within Station ALOHA without any problem. After the transect, the ship began its transit to Honolulu. ADCP, thermosalinograph, pCO_2 and fluorometer were running throughout the cruise. The ship arrived at Snug Harbor at 0700 on 1 November 1996.

3.13. HOT-78: Dale Hebel, Chief Scientist

The R/V *Moana Wave* departed Snug Harbor at 0930 HST on 9 December 1996 with 16 scientists on-board. All objectives of the JGOFS and WOCE programs were accomplished. Stations Kahe and ALOHA were occupied. All core samples were taken within the 36-hour CTD burst sampling period. All samples for ancillary projects were taken. Floating sediment trap and primary production arrays were successfully deployed and recovered. Zooplankton tows were conducted mid-day and mid-night while at Station ALOHA. A bathymetric survey was made over the proposed site of the HALE ALOHA physical-biogeochemical mooring after the last CTD cast. After the survey, the optical plankton counter was towed within Station ALOHA without any problem. After the transect, the ship began its transit to Honolulu. ADCP, thermosalinograph, pCO_2 system and fluorometer were running throughout the cruise. The ship arrived at Snug Harbor at 0700 on 13 December 1996.

4.0. RESULTS

4.1. Hydrography

Hydrographic variability at Station ALOHA 1996 was somewhat similar to that during 1995. Very low salinities were observed in the upper 100 dbar for about 5 months centered in the middle of the year (Figures 6.1.9 to 12). Similar low values were also observed early in 1995 and during 1989. Associated with the 1996 low salinities were high temperatures (Figure 6.1.7) causing extreme low densities (Figure 6.1.8) not seen in any previous year of the program. At about 300 dbar, an oxygen minimum developed early in 1996 and lasted about 5 months, this minimum seemed to be accompanied by a decrease in salinity and an increase in the nutrient concentrations (Figures 6.1.15 to 22). Similar features had been observed previously in 1990, 1992, and 1995. In the bottom water, a cold water anomaly of up to 0.025 °C started developing in a 200-m layer above the bottom by the end of 1996, reaching extreme values during HOT-78. This anomaly was accompanied by an increase in salinity and oxygen concentrations. Similar cold events were also observed in 1991, 1993 and 1995.

4.1.1. 1996 CTD Profiling Data

Profiles of temperature, salinity, oxygen and potential density (σ_θ) were collected at both Station Kahe and Station ALOHA. The profiles from Station ALOHA during 1996 are presented in Figure 6.1.1. The results of bottle determinations of oxygen, salinity and inorganic nutrients are also shown. In addition, stack plots of CTD temperature and salinity profiles for all 1000 m casts conducted at Station ALOHA are presented (Figure 6.1.2). The data collected for Station Kahe during 1996 are presented in Figures 6.1.3. The temperature, salinity and oxygen profiles obtained from the deep casts at Station ALOHA during 1996 are presented in Figures 6.1.4-6. The development of a cold water anomaly near the bottom at the end of the year is apparent in the potential temperature profiles of Figure 6.1.4. The lowest temperatures (as low as 1.074 °C) were observed during HOT-78.

4.1.2. Time-series Hydrography, 1988-1996

The hydrographic data collected during the past eight years of HOT are presented in a series of contour plots (Figures 6.1.7-22). These figures show the data collected in 1996 within the context of the longer time-series database. The CTD data used in these plots are obtained by averaging the data collected during the 36-hour period of burst sampling. Therefore, much of the variability which would otherwise be introduced by internal tides in the upper ocean has been removed. Figures 6.1.7 and 6.1.8 show the contoured time-series record for potential temperature and density in the upper 1000 dbar for all HOT cruises through 1996. Seasonal variation in temperature for the upper ocean is apparent in the maximum of near-surface temperature of about 26 °C and the minimum of approximately 23 °C. Oscillations in the depth of the 5 °C isotherm below 500 dbar appear to be relatively large with displacements up to 100 dbar. The main pycnocline is observed between 100 and 600 dbar, with a seasonal pycnocline developing between June and December in the 50-100 dbar range (Figure 6.1.8). The cruise-to-cruise changes in the upper pycnocline illustrate that variability in density is not always resolved by our quasi-monthly sampling.

Figures 6.1.9-12 show the contoured time-series record for salinity in the upper 1000 dbar for all HOT cruises through 1996. The plots show both the CTD and bottle results plotted against pressure and potential density. Most of the differences between the contoured sections of bottle salinity and CTD salinity are due to the coarse distribution of bottle data in the vertical as compared to the CTD observations. Some of the bottles in Figure 6.1.12 are plotted at density values lower than the indicated sea surface density. This is due to surface density changing from cast to cast within each cruise, and even between the downcast and the upcast during a single cast.

Surface salinity is variable from cruise-to-cruise, with no obvious seasonal cycle and some substantial interannual variability. The surface salinity is low in late 1989, increases to a maximum in late 1990, decreases again during 1991 and 1992, rises to an extreme high in late 1993 and decreases again in 1994. For about five months in early 1995 it reaches extreme low values only comparable to those in 1989. It increases in late 1995 and decreases again to extreme values for about five months in mid 1996. The salinity maximum is generally found between 50 and 150 dbar, and within the potential density range 24-25 kg m^{-3}. A salinity maximum region extends to the sea surface in the later part of 1990 and 1993, as indicated by the 35.2 contour reaching the surface. This contour nearly reaches the surface late in 1988 and 1989. The maximum shows salinities smaller than normal in early 1995 and 1996, and throughout these two years the values are below 35.2. The maximum value of salinity in this feature is subject to short-term variations of about 0.1 which is probably due to the proximity of Station ALOHA to the region where this water is formed at the sea surface (Tsuchiya 1968). The variability of this feature is itself variable. Throughout 1989 there were extreme variations of a couple of months duration with 0.2 amplitude. The variability was much smaller and slower thereafter, except for a few months of rapid variation in earlier 1992. The salinity minimum is found between 400 and 600 dbar (26.35-26.85 kg m^{-3}). There is no obvious seasonal variation in this feature, but there are distinct periods of higher than normal minimum salinity in early 1989, in the fall of 1990, in early 1992 and in the summer of 1996. These variations are related to the episodic appearance at Station ALOHA of energetic fine structure and submesoscale water mass anomalies (Lukas and Chiswell 1991; Kennan and Lukas 1995). Exceptionally intense anomalies were present during HOT-cruise 71. Large salinity variations were observed near the salinity minimum accompanied by large variations in dissolved oxygen (Figure 6.1.1c, lower right panel).

Figures 6.1.13 and 6.1.14 show contoured time-series data for oxygen in the upper 1000 dbar at Station ALOHA. The oxygen data show a strong oxycline between 400 and 625 dbar (26.25-27.0 kg m^{-3}), and an oxygen minimum centered near 800 dbar (27.2 kg m^{-3}). During 1989, there was a persistent oxygen maximum near 300 dbar (25.75 kg m-3), which appeared again during 1991 and shortly in early 1993 and mid 1994. At the same level, an oxygen minimum developed in early 1990 and late 1991, mid 1992, late 1994 and early 1996. This minimum was accompanied by an increase in the concentration of nutrients (see below), and a decrease in salinity. The oxygen minimum exhibited some interannual variability as well, with values less than 30 μmol kg^{-1} appearing in the last half of 1989 and the first half of 1990, reappearing, less intensely, in 1991 and 1992, again strongly in 1993 and 1994, weakening in 1995 and reappearing strongly in 1996. A time series of mean oxygen obtained from bottle data in a layer spanning the oxygen minimum (27-27.8 kg m^{-3}, Figure 6.1.23a) also shows this variability. Superimposed to this variability is a general trend towards lower values of dissolved oxygen in the intermediate waters. The surface layer shows a seasonality in oxygen concentrations, with highest values in the winter. This roughly corresponds to the minimum in surface layer temperature (Figure 6.1.7). An oxygen maximum at about 100 m appears in the latter half of

1991 and persists through 1992, reappears again in 1993 and persists through 1994, it reappears again in the latter half of 1995 and 1996.

Figures 6.1.15-22 show [nitrate+nitrite], soluble reactive phosphorus and silica at Station ALOHA plotted against both pressure and potential density. The nitricline is located between about 200 and 600 dbar (25.75-27 kg m^{-3}; Figures 6.1.15 and 16). Most of the variations seen in these data are associated with vertical displacements of the density structure, and when [nitrate+nitrite] is plotted versus potential density, most of the contours are level. An increase in [nitrate+nitrite] can be seen in the beginning of 1996 between 25-26.25 kg m^{-3} (Figure 6.1.16). This increase appears similar to events seen in March-April 1990, January 1992, February 1993 and February-March 1995. These events can likely be attributed to mesoscale features such as eddies. It is possible for eddies to transport water with different biogeochemical characteristics from distant sources into the region of Station ALOHA. As in the previous events, the increase of [nitrate+nitrite] in March 1996 is accompanied by a decrease in the oxygen concentration apparent between 25-26.25 kg m^{-3} (Figure 6.1.14). The 1996 soluble reactive phosphorus record is similar to the [nitrate+nitrite] in the upper water column (Figure 6.1.19).

During 1996, the intermediate waters between 27.0-27.8 kg m^{-3} recovered from anomalously low [nitrate+nitrite] which was observed during 1995 (Figure 6.1.17). This anomaly is apparent in a time series of mean [nitrate+nitrite] obtained from bottle data between 27.0-27.8 kg m^{-3} (Figure 6.1.23b). A decrease in [nitrate+nitrite] between 27.0-27.8 kg m^{-3} began in late 1994, with a comparable increase from mid-1995 through early 1996. The maximum decrease appears to be about 1 µmol kg^{-1} below 27.5 kg m^{-3} where nitrate concentrations are about 40 µmol kg^{-1}. This decrease appears to be real as it does have coherence over time. A precision estimate of 0.3 % has been made for [nitrate+nitrite] measurements involving the high concentration samples associated with intermediate water (Dore and Karl 1996). This translates to a precision of roughly 0.12 µmol kg^{-1} for samples with a concentration of 40 µmol kg^{-1}. Hence, the 1 µmol kg^{-1} decrease seen during 1995 is well within the precision level for the concentrations observed. However, the amount of the decrease could be approaching the accuracy limits of [nitrate+nitrite] measurements. The absolute value of these limits are currently being researched. Further research is in progress to determine the validity of the 1995 low [nitrate+nitrite] episode. This work includes analysis of the standards used when measuring [nitrate+nitrite], consistency checks with other variables, as well as comparisons with independent data sources. The low [nitrate+nitrite] episode observed in 1995 (Figure 6.1.23b) is accompanied by an increase in oxygen concentration (Figure 6.1.23a) in the intermediate waters between 27.0-27.8 kg m^{-3}.

Intermediate water soluble reactive phosphorus (between 27.0-27.8 kg m^{-3}) continues to decrease throughout 1996 with a trend established in early 1994 (Figure 6.1.20). A time series of mean soluble reactive phosphorus in this layer shows this trend clearly (Figure 6.1.23c). A preliminary look at the 1997 soluble reactive phosphorus data suggests that the decrease appears to end in March 1997. Decreases in soluble reactive phosphorus in the deeper waters could persist for long periods of time as the oceanic ecosystem associated with Station ALOHA has been hypothesized to be phosphorus limited in recent years (Karl et al. 1995; Karl and Tien 1997; Karl et al. 1997). Oxygen concentrations between 27.0-27.8 kg m^{-3} (Figure 6.1.23a) vary during the decrease of soluble reactive phosphorus from early 1994 through 1996 (Figure 6.1.23c) without any apparent correlation.

4.2. Biogeochemistry

4.2.1. Dissolved oxygen

A contour plot of dissolved oxygen in the upper 200 m of the water column from 1988-1996 analyzed from water samples collected at discrete depths is shown in Figure 6.2.1. Dissolved oxygen shows a maximum between 20 and 120 m depth and is fairly mixed in that layer. Gradients begin to form below 100 meters. The development of this maximum appears to occur during the spring and summer months and becomes mixed down in the winter.

4.2.2. Inorganic carbon

4.2.2.1. Dissolved inorganic carbon and titration alkalinity

Dissolved inorganic carbon (DIC) and titration alkalinity measured in the upper 200 dbar of the water column over the past 8 years of the time-series program are presented in Figures 6.2.2 and 6.2.3. Time-series of titration alkalinity and DIC in the mixed layer are presented in Figure 6.2.4. Titration alkalinity normalized to 35 ppt salinity averages approximately 2305 µequiv kg^{-1} and, within the precision of the analysis, appears to remain relatively constant at Station ALOHA. This observation is consistent with the results of Weiss et al. (1982) who concluded that titration alkalinity normalized to salinity remains constant in both the North and South Pacific subtropical gyres. In contrast to titration alkalinity, the concentration of DIC varies annually. DIC in the mixed layer is highest in winter and lowest in summer. This oscillation is consistent with an exchange of carbon dioxide across the air-sea interface driven by temperature dependent changes in mixed layer pCO_2.

Titration alkalinity shows considerable time-dependent variability around the shallow salinity maximum, centered at about 125 dbar, and the salinity minimum, centered at about 400 dbar. These variations are largely associated with variability in salinity at these depths and disappear when alkalinity is normalized to 35 ppt. Titration alkalinity normalized to 35 ppt salinity is elevated in surface waters in spring of 1990 and winter of 1994.

DIC data is unavailable for HOT cruise 70 and 71 (March and April 1996). DIC calculated from pH and alkalinity data since HOT-55 have been plotted in Figure 6.2.4. There is excellent correspondence between calculated and measured DIC.

4.2.2.2 pH

Measurements for pH using the spectrophotometric method were started in 1992. The structure of pH (Figure 6.2.5) in the upper water column closely resembles that of dissolved inorganic carbon (Figure 6.2.2). There appears to be a slight increase in pH during the winter months and gradually decreases after that. This is directly related the drawdown of inorganic carbon in the water column during the spring and summer periods.

4.2.2.3. pCO2

Underway measurements of surface pCO2 concentrations started in HOT-76 (September 1996) and the system underwent various modifications to adapt it for continuous and uninterrupted use. Data are unavailable at present but the 1996 data will be included in the 1997 data report.

4.2.3. Inorganic nutrients

Euphotic zone nutrient concentrations at Station ALOHA are at or well below the detection limits of the autoanalyzer methods (Figures 6.1.15 to 20). Other analytical techniques and instrumentation are used to measure the nanomolar levels of [nitrate + nitrite] and SRP in the upper water column. Figures 6.2.6 and 6.2.7 show the profiles obtained from our low level nutrient analyses in 1996 and their respective contour plots in Figures 6.2.8 and 6.2.9. The upper 100 m is generally depleted in [nitrate + nitrite] with a few intrusions during the winter periods. At depths shallower than 100 dbar, SRP is typically less than 150 nmol kg^{-1} and on occasion, as low as 15 nmol kg^{-1}. SRP concentrations appear to vary by at least 3-fold in this region. Concentrations of [nitrate + nitrite] at depths less than 100 m are always less than 10 nmol kg^{-1} and are often less the 5 nmol kg^{-1}. Figures 6.2.10 and 6.2.11 show integrated upper water column (0-100 m) inventories for [nitrate+nitrite] and SRP. The trends observed are very different for these two important macronutrients. The [nitrate + nitrite] plot shows evidence of the, generally, late winter (February) nutrient injections into the euphotic zone that were discussed previously. SRP on the other hand displays a systematic and sustained decrease from about 10 mmol SRP m^{-2} in 1989 to less than 5 mmol SRP m^{-2} in 1995 (Karl and Tien 1996). We believe that this draw down in SRP is a result of bacterial nitrogen fixation, and a shift from a N-controlled to a P-controlled ecosystem (Karl et al. 1995, 1997). The reasons for this shift are not known for sure but an experimental investigation of several mechanisms is currently under investigation.

4.2.4. Organic nutrients

Contour plots of dissolved organic carbon (DOC), nitrogen (DON) and phosphorus (DOP) are presented in Figures 6.2.12 to 14. DOC concentrations are about 100 µmol kg^{-1} at the surface and decrease rapidly to about 60 µmol kg^{-1} at about 300 m. DON is about 6 µmol kg^{-1} at the surface and gradually decreases to about 2 µmol kg^{-1} about 800 meters. DOP is about 0.3 µmol kg^{-1} at the surface and gradually decrease to about 0.1 µmol kg^{-1} at about 300 m.

4.2.5. Particulate matter

Particulate carbon (PC), nitrogen (PN) and phosphorus (PP) concentrations in the surface ocean over the eight years of the program are shown in Figures 6.2.15 to 17. PC varies between 1.3-3.3 µmol kg^{-1}, PN between 0.08-0.65 µmol kg^{-1} and PP between 8-35 nmol kg^{-1} in the upper 100 m of the water column. PC and PN show a clear annual cycle with the greatest particulate concentrations in summer/fall and lowest in winter. A significantly larger PN concentration was observed in the late fall of 1993 with only a slight increase in PC and a decrease in PP. The temporal distributions and magnitude of PC, PN, and PP in 1996 were similar to previous years.

4.2.6. Pigments

A contour plot of chlorophyll *a* concentrations measured using standard fluorometric techniques from 0 to 200 dbar over the eight years of the program is shown in Figure 6.2.18. As expected a chlorophyll maximum with concentrations up to 300 µg m^{-3} is observed at approximately 100 dbar. The chlorophyll *a* concentrations at depths shallower than 50 m display a clear annual cycle increasing in the fall and winter and decreasing through spring and summer which is approximately 4-6 months out of phase with the annual oscillation at the base of the euphotic zone (Winn et al. 1995).

4.2.7. Adenosine 5' Triphosphate

The concentration of particulate ATP closely resembles that of particulate matter with a maximum concentration at the surface and decreasing with depth (Figure 6.2.19). An annual cycle is evident at about 100 meters where the chlorophyll maximum also occurs. There appears to be coherence in the dynamics of chlorophyll and ATP at this depth (Winn et al. 1995).

4.3. Biogeochemical Rates

4.3.1. Primary Productivity

The results of the ^{14}C incubations and pigment determinations for samples collected from Go-Flo casts in 1996 are presented in Tables 4.1 and 4.2. Table 4.1 presents the primary production and fluorometric pigment measurements made at individual depths on all 1996 cruises. Table 4.2 presents integrated values for irradiance, pigment concentration and primary production rates. The pigment concentrations and ^{14}C incorporation rates reported are the average of triplicate determinations. Integrated primary production rates measured over all 8 years of the program are shown in Figure 4.1 in order to place the 1996 results within the context of the time-series data set.

Rates of primary production, integrated over the euphotic zone during the eight years of the time-series program, show a seasonal cycle. Measured rates ranged from less than 200 to greater than 800 mg C m^{-2} d^{-1} with the highest rate being observed in May 1995. This variability,

Table 4.1: Primary Production and Pigment Summary

Cruise	Depth (m)	Mean Chl *a* (mg m^{-3})	Std. Dev. Chl *a* (mg m^{-3})	Mean Phaeo (mg m^{-3})	Std. Dev. Phaeo (mg m^{-3})	Light (mg C m^{-3}) Rep #1	Light (mg C m^{-3}) Rep #2	Light (mg C m^{-3}) Rep #3	Dark (mg C m^{-3}) Rep #1	Dark (mg C m^{-3}) Rep #2	Dark (mg C m^{-3}) Rep #3
69	5	0.060	0.005	0.024	0.000	4.30	5.23	5.75	0.15	0.16	0.14
69	25	0.065	0.002	0.061	0.070	4.84	4.47	4.87	0.18	0.18	0.19
69	45	0.063	single	0.031	single	3.10	3.69	3.15	0.16	no sample	0.18
69	75	0.124	0.002	0.077	0.006	no sample	0.94	0.75	0.13	0.13	0.12
69	100	0.153	0.006	0.236	0.015	0.65	0.77	0.83	0.10	0.11	0.11
69	125	0.052	0.003	0.096	0.006	0.15	0.17	0.19	0.03	0.04	0.03
69	150	0.026	0.000	0.061	0.000	no sample	0.05	0.05	0.04	0.05	0.04
69	175	0.120	0.005	0.186	0.005	0.08	0.06	0.07	0.05	0.06	0.07
70	5	0.053	single	0.057	single	no sample	7.81	6.60	0.18	0.17	0.14
70	25	0.056	single	0.062	single	6.66	5.55	7.81	0.17	0.17	0.16
70	45	0.053	single	0.050	single	6.39	6.28	6.44	0.58	0.55	0.25
70	75	0.092	single	0.087	single	1.36	no sample	1.83	0.14	0.14	0.13
70	100	0.088	single	0.165	single	1.20	1.22	1.09	0.10	0.11	0.09
70	125	0.137	single	0.393	single	0.84	0.93	0.89	0.05	0.05	0.05
70	150	0.030	single	0.076	single	0.10	0.10	0.10	0.05	0.05	0.06
70	175	0.038	single	0.064	single	0.07	0.08	0.06	0.08	0.08	0.09
71	5	0.044	0.005	0.041	0.002	6.52	7.27	6.31	0.29	0.33	0.27
71	25	0.039	0.002	0.039	0.006	6.13	7.24	7.11	0.23	0.26	0.25
71	45	0.039	0.002	0.045	0.001	5.45	5.16	5.18	0.36	0.54	0.31
71	75	0.064	0.003	0.096	0.007	0.19	0.21	0.18	0.20	0.29	0.46
71	100	0.109	0.001	0.169	0.008	1.61	1.70	1.58	0.28	0.28	0.27
71	125	0.167	0.016	0.467	0.043	1.11	1.29	1.06	0.12	0.14	0.13
71	150	no sample	no sample	no sample	no sample	no sample	no sample	no sample	no sample	no sample	no sample
71	175	0.059	0.002	0.115	0.006	0.13	0.14	0.13	0.18	0.20	0.23
72	5	0.042	0.002	0.046	0.004	8.68	8.73	9.15	0.10	0.22	0.21
72	25	0.042	0.004	0.050	0.005	6.99	8.19	7.92	0.25	0.19	0.24
72	45	0.054	0.007	0.075	0.012	5.77	5.17	5.94	0.22	0.35	0.22
72	75	0.091	0.002	0.135	0.005	2.19	1.92	2.13	0.22	0.23	0.23
72	100	0.128	0.002	0.296	0.022	1.88	2.15	2.40	0.15	0.17	0.12
72	125	0.096	0.003	0.297	0.004	0.68	0.76	0.67	0.14	0.17	0.14
72	150	0.065	0.009	0.176	0.009	0.23	0.25	0.28	0.14	0.15	0.21
72	175	no sample	no sample	no sample	no sample	no sample	no sample	no sample	no sample	no sample	no sample

Table 4.1: (continued)

Cruise	Depth (m)	Mean Chl *a* (mg m^{-3})	Std. Dev. Chl *a* (mg m^{-3})	Mean Phaeo (mg m^{-3})	Std. Dev. Phaeo (mg m^{-3})	Light (mg C m^{-3}) Rep #1	Light (mg C m^{-3}) Rep #2	Light (mg C m^{-3}) Rep #3	Dark (mg C m^{-3}) Rep #1	Dark (mg C m^{-3}) Rep #2	Dark (mg C m^{-3}) Rep #3
73	5	0.045	0.004	0.032	0.001	9.20	7.42	8.79	0.23	0.20	0.17
73	25	0.047	0.000	0.031	0.011	6.20	8.02	8.27	0.21	0.32	0.21
73	45	0.071	0.013	0.070	0.015	4.69	6.53	7.33	0.22	0.33	0.26
73	75	0.107	0.007	0.143	0.002	0.86	0.64	0.85	0.13	0.13	0.14
73	100	0.163	0.014	0.278	0.007	2.10	1.98	2.10	0.13	0.15	0.14
73	125	0.144	0.132	0.599	0.336	0.58	0.71	0.66	0.08	0.06	0.07
73	150	0.101	0.013	0.375	0.035	0.27	0.28	0.28	0.20	0.16	0.10
73	175	0.042	0.000	0.050	0.015	0.17	0.15	0.17	0.15	0.15	0.14
74	5	0.058	0.000	0.100	0.001	9.19	9.86	7.76	0.21	0.22	0.14
74	25	0.061	0.011	0.106	0.024	7.24	8.11	7.60	0.21	0.23	0.21
74	45	0.062	0.005	0.102	0.002	4.65	5.08	5.09	0.38	0.29	0.27
74	75	0.099	0.002	0.169	0.025	1.71	1.99	1.88	0.16	0.15	0.14
74	100	0.185	0.020	0.327	0.034	0.92	0.92	0.91	0.08	0.08	0.08
74	125	0.187	0.024	0.535	0.085	0.34	0.37	0.37	0.05	0.06	0.04
74	150	0.066	0.000	0.298	0.043	0.11	0.09	0.10	0.11	0.08	0.06
74	175	0.028	0.002	0.144	0.008	0.05	0.07	0.05	0.07	0.08	0.07
75	5	0.050	0.001	0.074	0.007	10.13	11.52	8.72	0.22	0.22	0.15
75	25	0.071	0.032	0.112	0.042	7.26	7.44	12.72	0.19	0.21	0.20
75	45	0.079	0.015	0.124	0.003	9.15	8.37	8.60	0.31	0.37	0.25
75	75	0.122	0.001	0.226	0.004	0.35	0.42	0.63	0.16	0.21	0.17
75	100	0.186	0.003	0.488	0.043	1.94	1.73	1.72	0.11	0.10	0.10
75	125	0.172	0.022	0.601	0.003	0.59	0.68	0.66	0.04	0.06	0.06
75	150	0.041	0.002	0.144	0.003	0.09	0.08	0.09	0.11	0.09	0.06
75	175	0.026	0.002	0.087	0.019	0.04	0.04	0.04	0.05	0.11	0.18
76	5	0.079	0.002	0.082	0.004	11.37	9.41	10.78	0.27	0.25	0.28
76	25	0.100	0.009	0.102	0.010	9.09	9.59	9.49	0.21	0.20	0.19
76	45	0.152	0.004	0.163	0.013	4.80	5.36	5.55	0.54	0.30	0.16
76	75	0.261	0.012	0.300	0.003	3.86	3.74	2.79	0.08	0.10	0.11
76	100	0.093	0.003	0.115	0.008	0.64	0.70	0.69	0.47	0.39	0.43
76	125	0.066	0.002	0.234	0.006	0.28	0.28	0.26	0.07	0.07	0.07
76	150	0.027	0.000	0.097	0.005	0.08	0.07	0.07	0.13	0.09	0.08
76	175	0.173	0.000	0.231	0.005	0.10	0.11	0.14	0.13	0.12	0.12

Table 4.1: (continued)

Cruise	Depth (m)	Mean Chl *a* (mg m^{-3})	Std. Dev. Chl *a* (mg m^{-3})	Mean Phaeo (mg m^{-3})	Std. Dev. Phaeo (mg m^{-3})	Light (mg C m^{-3}) Rep #1	Light (mg C m^{-3}) Rep #2	Light (mg C m^{-3}) Rep #3	Dark (mg C m^{-3}) Rep #1	Dark (mg C m^{-3}) Rep #2	Dark (mg C m^{-3}) Rep #3
77	5	0.068	0.000	0.057	0.010	6.15	5.85	5.56	0.26	0.21	0.20
77	25	0.068	0.003	0.053	0.008	3.56	3.69	4.13	0.24	0.27	0.14
77	45	0.070	0.003	0.056	0.003	1.56	1.04	1.92	0.24	0.20	0.19
77	75	0.223	0.010	0.244	0.032	2.60	2.96	no sample	0.10	0.09	0.10
77	100	0.200	0.011	0.490	0.037	0.78	0.85	0.99	0.08	0.05	0.06
77	125	0.093	0.001	0.279	0.021	0.18	0.19	0.19	0.06	0.06	0.06
77	150	0.051	0.003	0.126	0.013	0.07	0.04	0.04	0.07	0.05	0.04
77	175	0.015	0.002	0.036	0.003	0.04	0.04	0.04	no sample	no sample	no sample
78	5	0.141	0.000	0.120	0.011	3.56	4.60	5.75	0.18	0.14	0.17
78	25	0.149	0.000	0.118	0.000	6.64	5.23	6.75	0.18	0.16	0.15
78	45	0.142	0.001	0.115	0.012	2.93	3.73	4.67	0.29	0.21	0.22
78	75	0.135	0.002	0.110	0.012	0.86	0.97	1.17	0.12	0.13	0.14
78	100	0.233	0.006	0.349	0.026	0.80	1.05	0.97	0.07	0.06	0.10
78	125	0.124	0.009	0.325	0.009	0.26	0.26	0.29	0.07	0.07	0.10
78	150	0.055	0.001	0.107	0.014	0.11	0.09	0.11	0.12	0.11	0.10
78	175	0.132	0.007	0.148	0.005	0.09	0.11	0.11	0.11	0.12	0.12

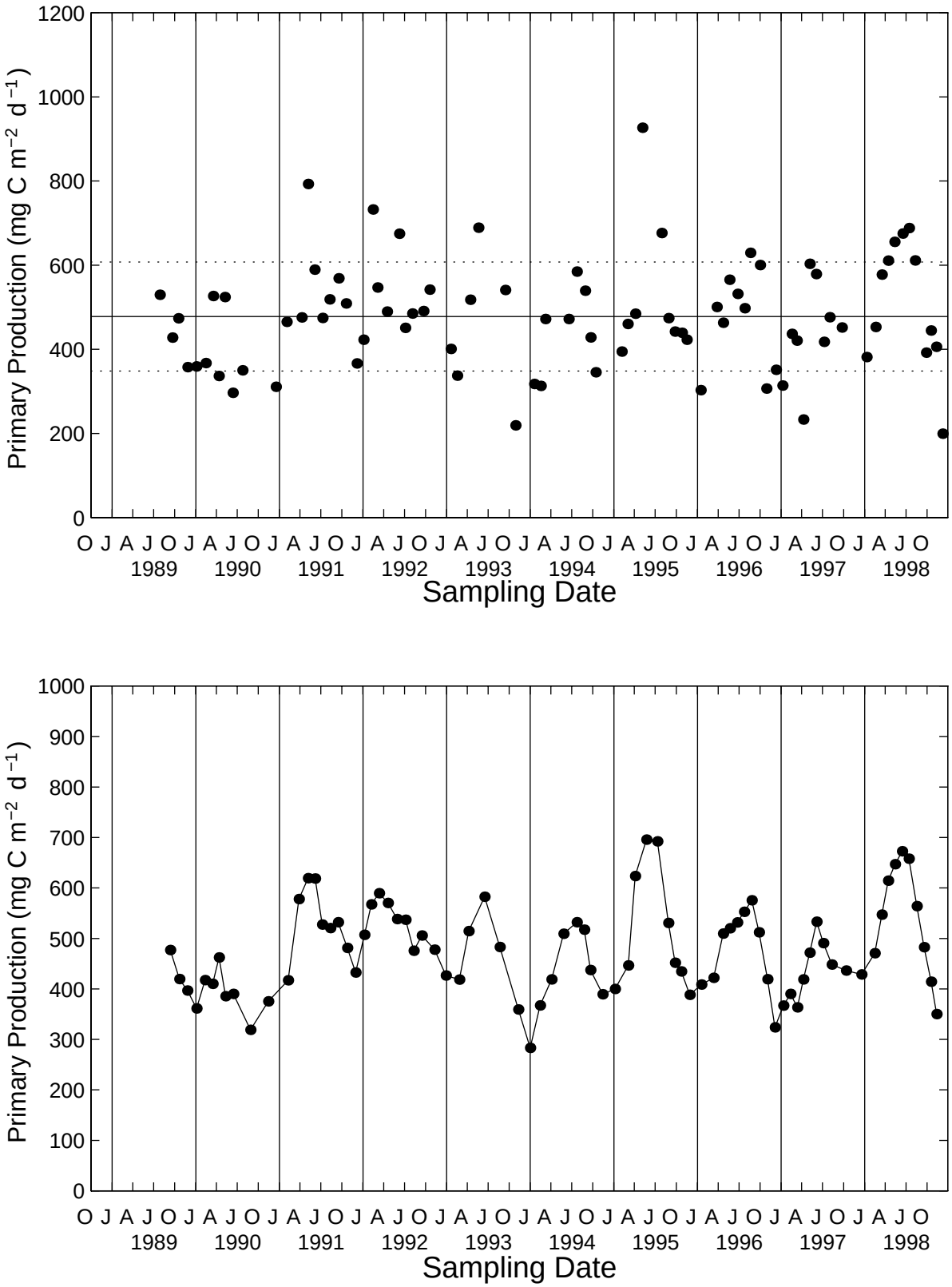

Figure 4.1: [Upper panel] Integrated (0-200 m) primary production rates from 1988-1996. Solid line represents the average production (477 mg C m^{-2} d^{-1}), dashed line is one standard deviation (122 mg C m^{-2} d^{-1}). [Lower panel] 3-point running mean of integrated primary production rates.

with a range of a factor of 4, is surprisingly large. However, the majority of the primary production estimates were between 250 and 600 mg C m^{-2} d^{-1}, and the average rate of primary production was approximately 477 mg C m^{-2} d^{-1}. Although this value is higher than historical measurements for the central ocean basins (Ryther 1969), it is consistent with more recent measurements using modern methodology (Martin et al. 1987; Laws et al. 1989; Knauer et al. 1990).

Table 4.2: Primary Production and Pigment Summary Integrated Values (0-200 m)

Cruise	Incident Irradiance* (E m^{-2} d^{-1})	Pigments (mg m^{-2})				Incubation Duration (hrs)	Assimilation Rates (mg C m^{-2} d^{-1})			
		Chl a		Phaeo			light		dark	
		Mean	SE	Mean	SE		Mean	SE	Mean	SE
69	33.2	15.1	0.12	17.5	1.35	12.0	302	6	19	0.2
70	55.4	12.6	**	22.4	**	13.5	500	12	27	1.9
71	48.1	14.6	0.32	29.8	0.87	15.0	461	6	45	2.0
72	55.6	11.7	0.14	24.3	0.34	14.0	559	8	30	1.0
73	53.7	17.1	1.68	38.7	4.23	14.0	529	18	29	1.0
74	no data	17.7	0.41	41.6	1.33	15.0	496	8	25	0.7
75	no data	17.8	0.47	44.6	0.71	15.5	629	27	27	0.9
76	52.1	21.0	0.20	29.6	0.25	14.5	599	10	35	2.1
77	38.4	19.1	0.21	32.9	0.72	14.5	306	6	19	0.7
78	28.7	24.3	0.15	31.4	0.46	12.0	350	13	23	0.6

* cosine collector

** no calculation because only a single sample was taken

4.3.2. Particle Flux

Particulate carbon (PC), nitrogen (PN), phosphorus (PP) fluxes at 150 m are presented in Table 4.3 and Figures 4.2 to 4.4 for the eight years of the program. Carbon flux displays a clear annual cycle with peaks in both the early spring and in the late summer months. The magnitude of particle flux varies by a factor of approximately three. With the exception of anomalous PP fluxes measured on the first two HOT cruises, temporal variability in PN, PP and mass flux show similar temporal trends, and also vary between cruises by about a factor of three. Elemental ratios of carbon-to-nitrogen (atom:atom) at 150 m are typically between 6-10 and show no obvious temporal pattern. These particle flux measurements and elemental ratios are consistent with those measured in the central North Pacific Ocean by the VERTEX program (Martin et al., 1987; Knauer et al. 1990). Nitrogen flux at 150 m, as a percent of photosynthetic nitrogen assimilation (calculated from ^{14}C primary production values assuming a C:N ratio [atom:atom] of 6.6) ranges between 2-10%. The average value (approximately 6.5%) is consistent with the estimate of new production for the oligotrophic central gyres made by Eppley and Peterson (1979) and with field data from the VERTEX program (Knauer et al. 1990).

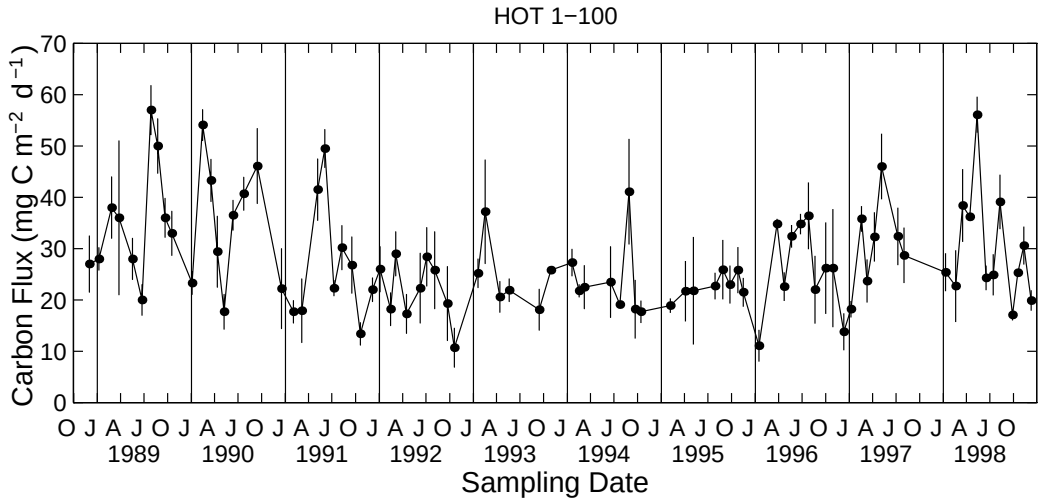

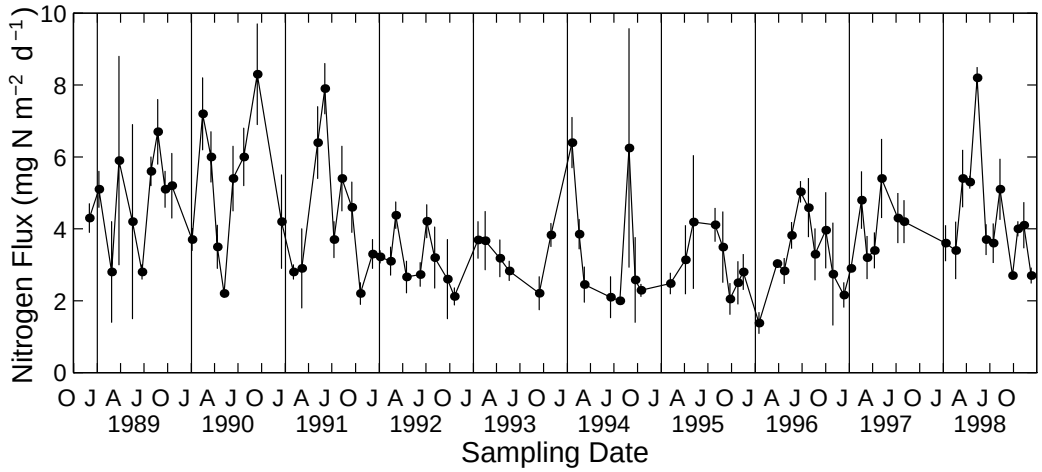

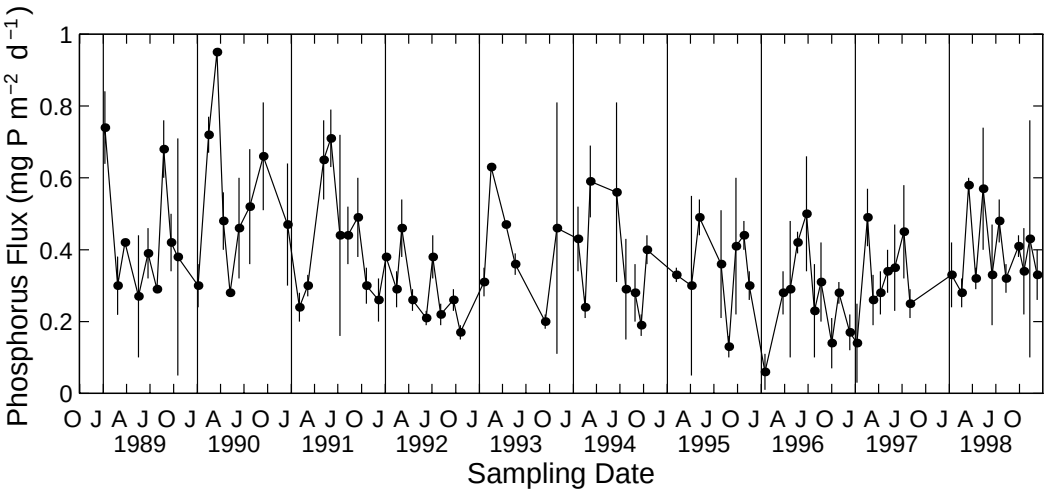

Figure 4.2: Carbon flux at 150 m measured on all HOT cruises from 1988-1996. Error bars represent the standard deviation of replicate determinations.

Figure 4.3: Nitrogen flux at 150 m measured on all HOT cruises from 1988-1996. Error bars represent the standard deviation of replicate determinations.

Figure 4.4: Phosphorus flux at 150 m measured on all HOT cruises from 1988-1996. Error bars represent the standard deviation of replicate determinations.

Table 4.3: Station ALOHA Sediment Trap Flux Data

Cruise	Depth (m)	Carbon Flux (mg m^{-2} d^{-1}) mean	SD	n	Nitrogen Flux (mg m^{-2} d^{-1}) mean	SD	n	Phosphorus Flux (mg m^{-2} d^{-1}) mean	SD	n
69	150	11.1	3.1	3	1.4	0.3	3	0.06	0.05	3
69	200	19.1	2.7	3	1.8	0.2	3	0.12	0.05	3
70	150	34.8	1.0	3	3.0	0.1	3	0.28	0.06	3
70	200	18.7	2.1	3	1.8	0.2	3	0.18	0.07	3
71	150	22.6	2.8	3	2.8	0.4	3	0.29	0.19	3 3
72	150	32.4	2.2	3	3.8	0.4	3	0.42	0.03	3
73	150	34.8	2.0	3	5.0	0.3	3	0.5	0.16	3
74	150	36.4	6.5	3	4.6	0.8	3	0.23	0.13	3
75	150	22.0	6.6	3	3.3	0.7	3	0.31	0.11	3
76	150	26.2	8.9	3	4.0	1.1	3	0.14	0.07	3
77	150	16.2	11.5	3	2.7	1.4	3	0.28	0.03	3
78	150	13.8	3.6	3	2.2	0.4	3	0.17	0.05	3

4.4. Microbial Community Structure

Depth profiles of counts of heterotrophic and photosynthetic bacteria for each cruise are presented in Figure 4.5. At the surface, heterotrophic bacterial number range from 4 to 6 x 10^5 counts ml^{-1}. In some cases bacterial number decrease with depth although there are some profiles such as HOT-73 and 78 where the numbers remain fairly constant with depth. In HOT-71, 72 and 75, a small subsurface maximum in heterotrophic bacterial number was observed. Photosynthetic bacterial number represent the counts of *Prochlorococcus* in the water column. Their concentration is about 2 x 10^5 counts ml^{-1} at the surface and usually decrease with depth but with a subsurface maximum between 50 and 100 m.

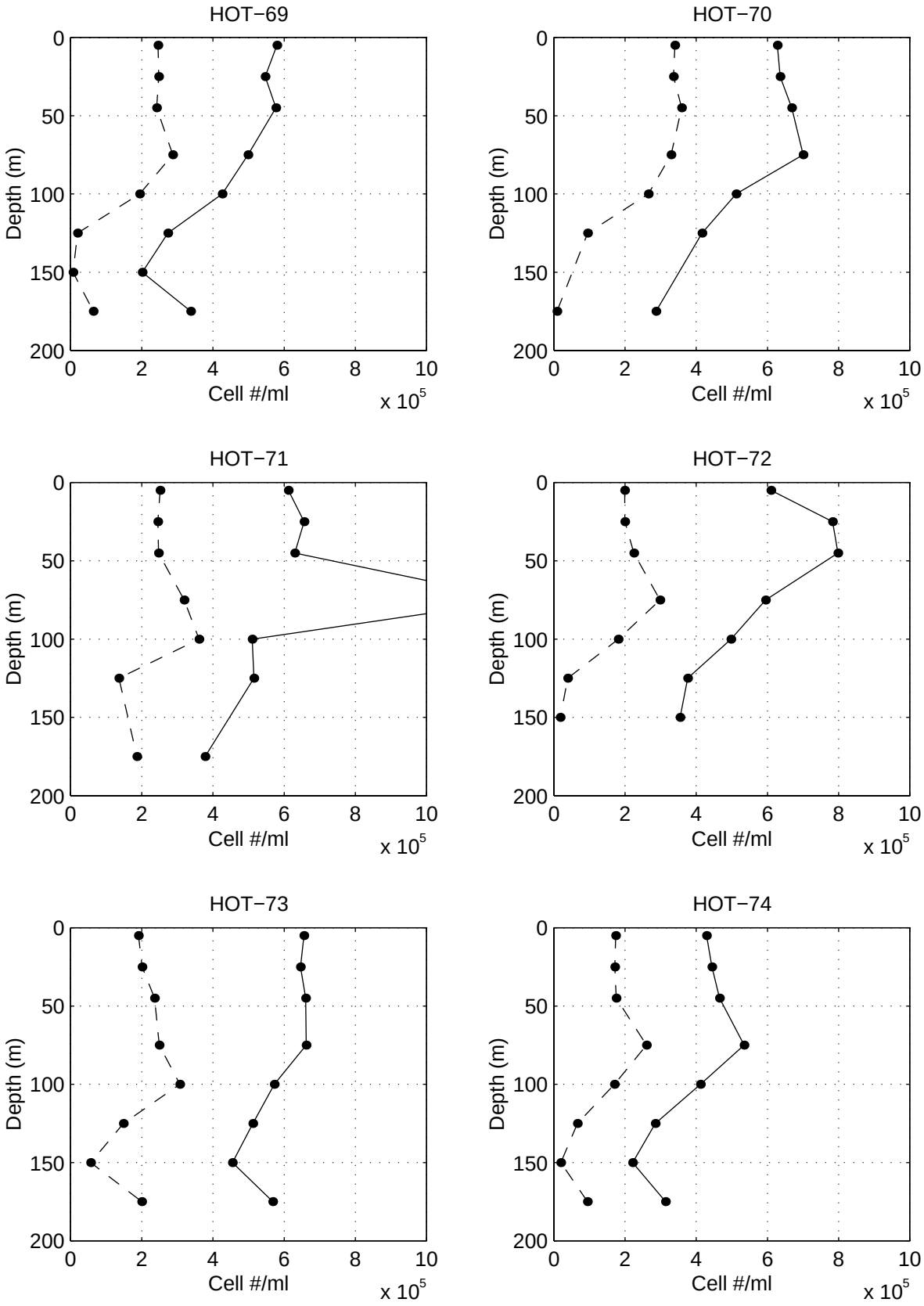

Figure 4.5: Heterotrophic bacterial numbers measured by flow cytometry at Station ALOHA.

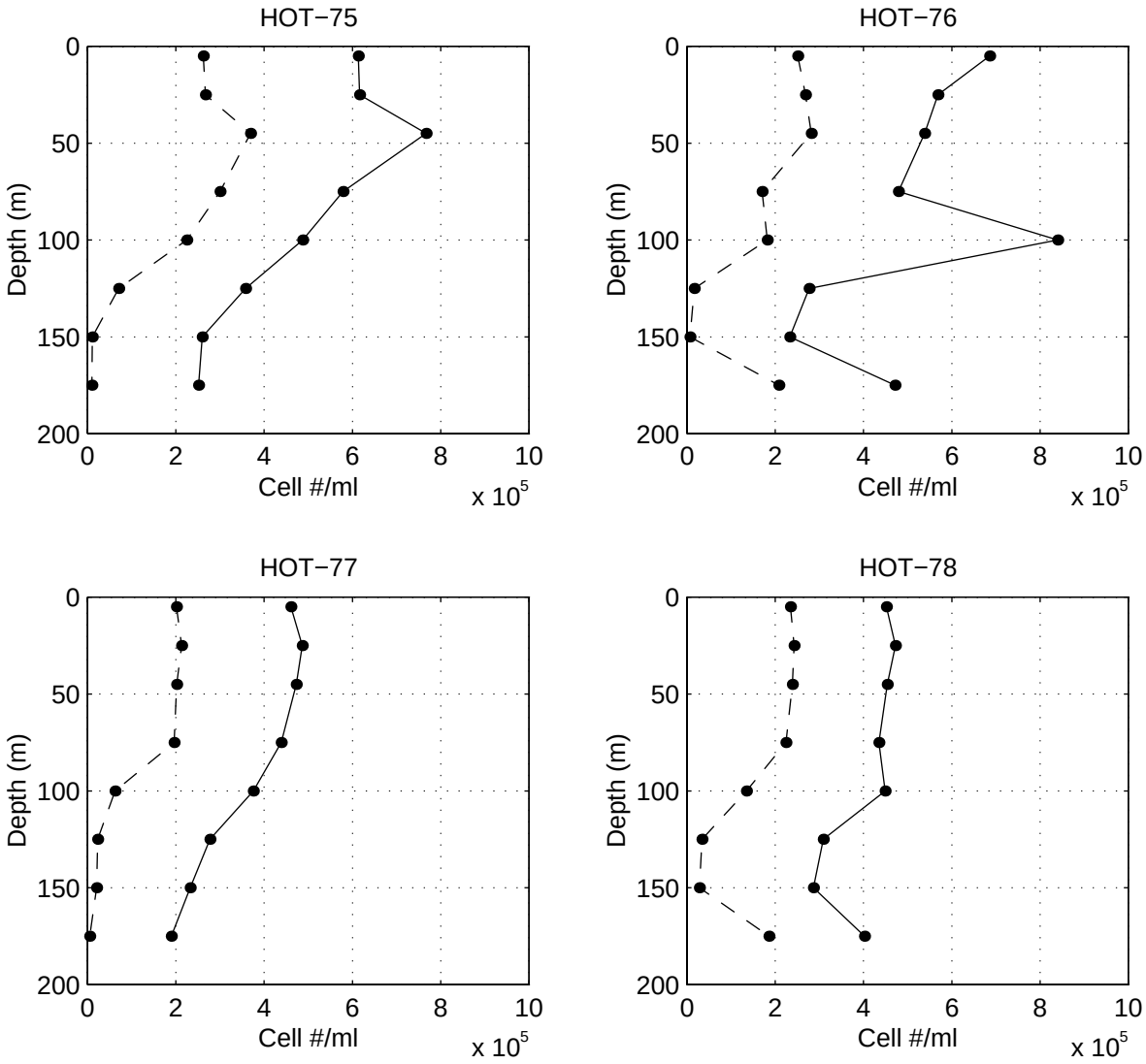

Figure 4.5: continued

4.5. Zooplankton Community Structure

Carbon biomass estimates for the mesozooplankton community at Station ALOHA are presented for 1994-1996 HOT cruises in Figures 4.6 and 4.7. Mean depth-integrated zooplankton carbon in the euphotic zone varies annually over a large range of 2-4 times with the highest values (300-600 mg C m^{-2}) typically in the late spring or summer month and lowest values (<100-200 mg C m^{-2}) in the winter. No one size category dominates the biomass distribution consistently, but larger animals (>500 μm) appear to contribute disproportionately relative to smaller forms (200-500 μm) in 1996 than in the previous tow years (Figure 4.6). Standing stocks of zooplankton are generally higher in the euphotic zone in night-time tows due to diel migrations of animals which position themselves at deeper depth during the day (Figure 4.7). These day-night differences in standing stocks, which is composed mostly of animals in the larger size fractions (> 500 μm), averages approximately a factor of two and as much as a factor of 3 or 4, within a given cruise. In contrast to the typical migration pattern of previous years and late 1996, the early months of 1996 appear to represent a period of consistently low diel variation in zooplankton standing stock.

4.6. ADCP Measurements

An overview of the shipboard ADCP data is given by the plots of velocity as a function of time and depth while on station (Figures 6.3.1a to l) and velocity as a function of latitude and depth during transit to and from Station ALOHA and Station 3, combined (Figures 6.3.2a to m). As in previous years, currents were highly variable from cruise to cruise and within each cruise.

4.7. Optical Measurements

Integrated irradiance measurements made with the on-deck cosine collector on days that primary production experiments were conducted are presented in Table 4.2.

Stack plots of the flash fluorescence from each HOT cruise in 1996 are presented in Figures 6.4.1a to 6.4.1j. *In situ* flash fluorescence profiles show the fluorescence maximum at about 110 m, characteristic of the North Pacific subtropical gyre. Percent transmission profiles consistently show increased attenuation due to increased particle load at depths shallower than 100 dbar. Fluorescence profiles show the influence of internal waves when plotted against pressure, but remain relatively constant within a cruise when plotted in density space. There is, however, substantial cruise-to-cruise variability in these properties.

Representative fluorescence profiles for a period of 8 years is shown in Figures 6.4.2 and 6.4.3. In order to facilitate comparison, only night-time profiles are presented after normalization to the average density profile obtained from the CTD burst sampling for each cruise. Month-to-month variability in the average depth of the fluorescence maximum is apparent. This is particularly evident in year 3 where the depth of the fluorescence maximum appears to increase in mid to late summer and in year 4 from summer to winter. The depth of the fluorescence maximum decreased significantly from spring to fall in 1993

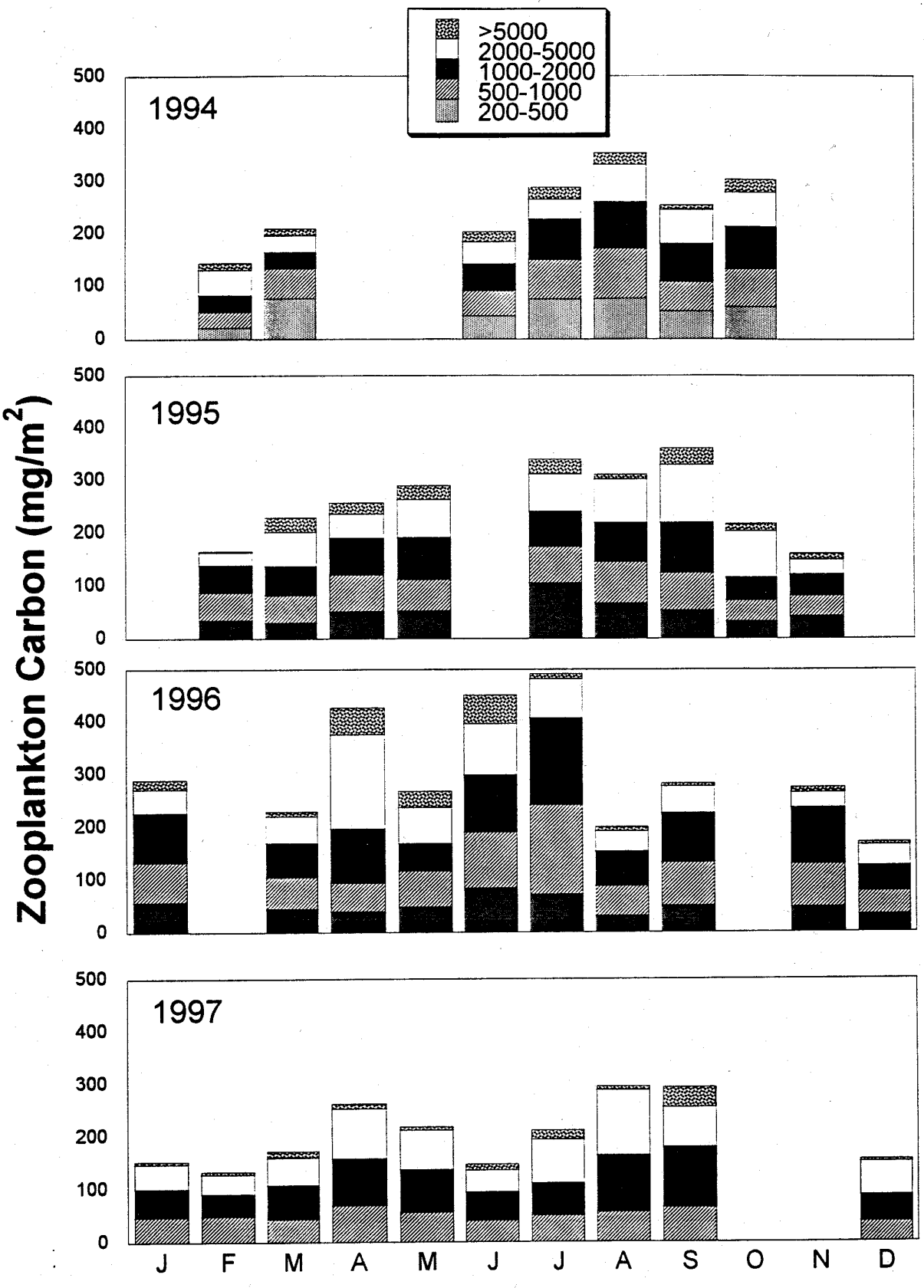

Figure 4.6: Carbon biomass estimates of mesozooplankton divided by size class for samples collected on HOT cruises from 1994-1996.

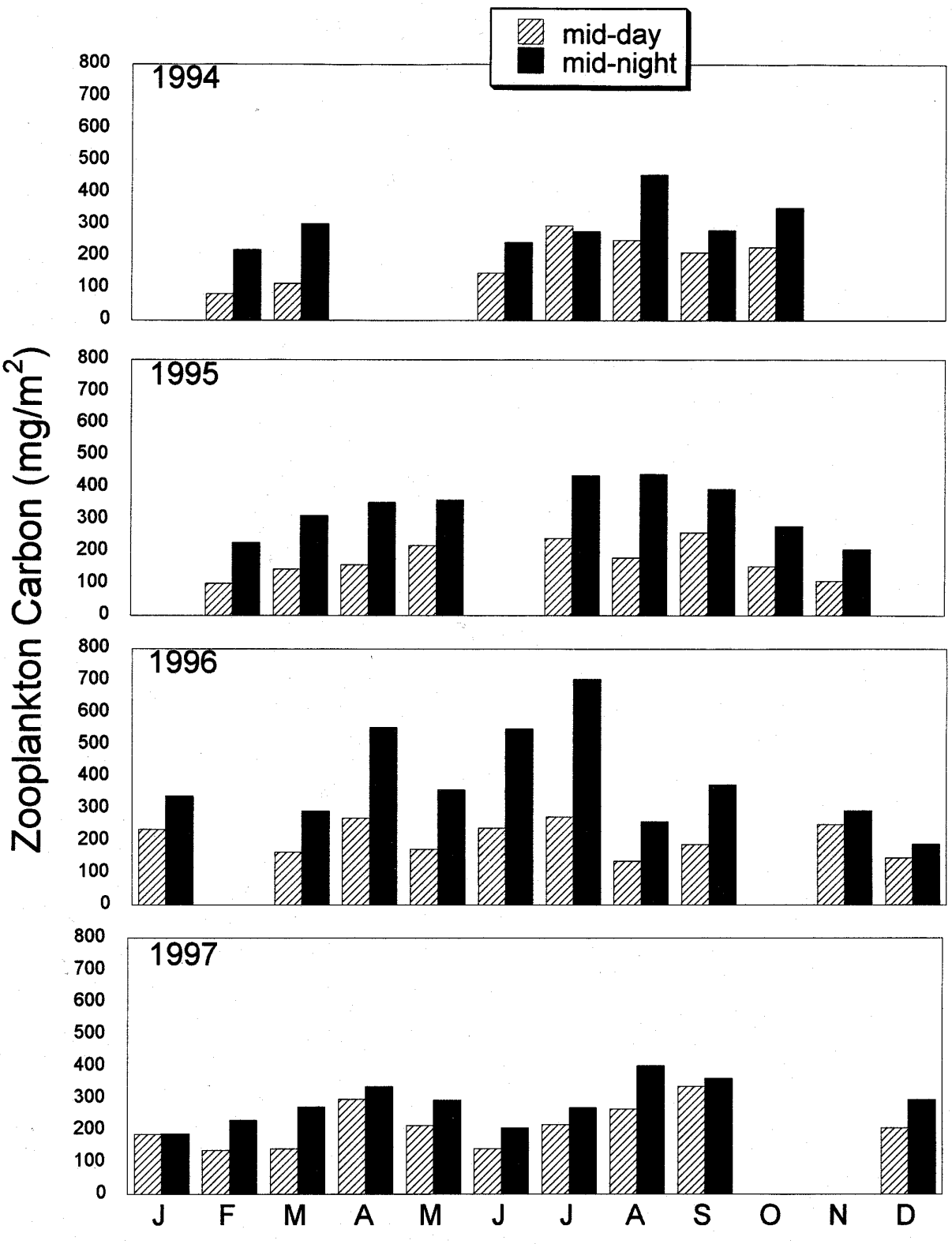

Figure 4.7: Carbon biomass estimates of mesozooplankton from mid-day and mid-night samples collected on HOT cruises from 1994-1996.

4.8. Meteorology

4.8.1. Shipboard Observations

The meteorological data collected by HOT program scientists include atmospheric pressure, sea-surface temperature and wet and dry bulb air temperature. These data are presented in Figures 6.5.1 to 6.5.3. As described by Winn et al. (1991), parameters show evidence of annual cycles, although the daily and weekly ranges are nearly as high as the annual range for some variables. In particular, during HOT-70 the dry bulb air temperature plot shows three points with temperatures higher than the rest of the cruise data (Figure 6.5.2), these data were taken near noon time and the values were confirmed by the observations collected by the ship's officers on the bridge. These high temperatures produced the low values seen in the SST-dry air temperature plot, and the high values in the dry-wet air temperature plot for this cruise (Figure 6.5.3). Wind speed and direction are also collected on HOT cruises. These data are presented in Figures 6.5.4 to 6.5.13.

4.8.2. Buoy Observations

The coherence of the data from Buoy #51001 with the data collected on HOT cruises was examined and reported in Tupas et al. (1993). We concluded from these analyses, that the data from this buoy can be used to get useful estimates of air temperature, sea-surface temperature and atmospheric pressure at Station ALOHA when the station is not occupied.

The wind vectors from buoy #51001 are plotted together with the ship observations in Figures 6.5.4-13 and 6.5.14g. As explained earlier (Section 2.8.2), data from this buoy were not available during cruises HOT-70 through 72, and wind data from buoy #51026 was not available during 1996.

4.9. Inverted Echo Sounder

Plots of dynamic height from the inverted echo sounders are presented in Figure 4.8. Only the IES at Station ALOHA provided data during 1996, the IES at Station Kaena was retrieved in October 1995 (see Section 2.9). The IES records prior to 1994 were examined and reported in Tupas et al. (1994b). It was concluded that large events with time-scales from weeks to months dominate dynamic height to such an extent that there is no clearly defined annual cycle, for instance, the highest and lowest dynamic height in 1991 occurred within the space of about a month. These events are not well sampled with the monthly spacing of the HOT cruises.

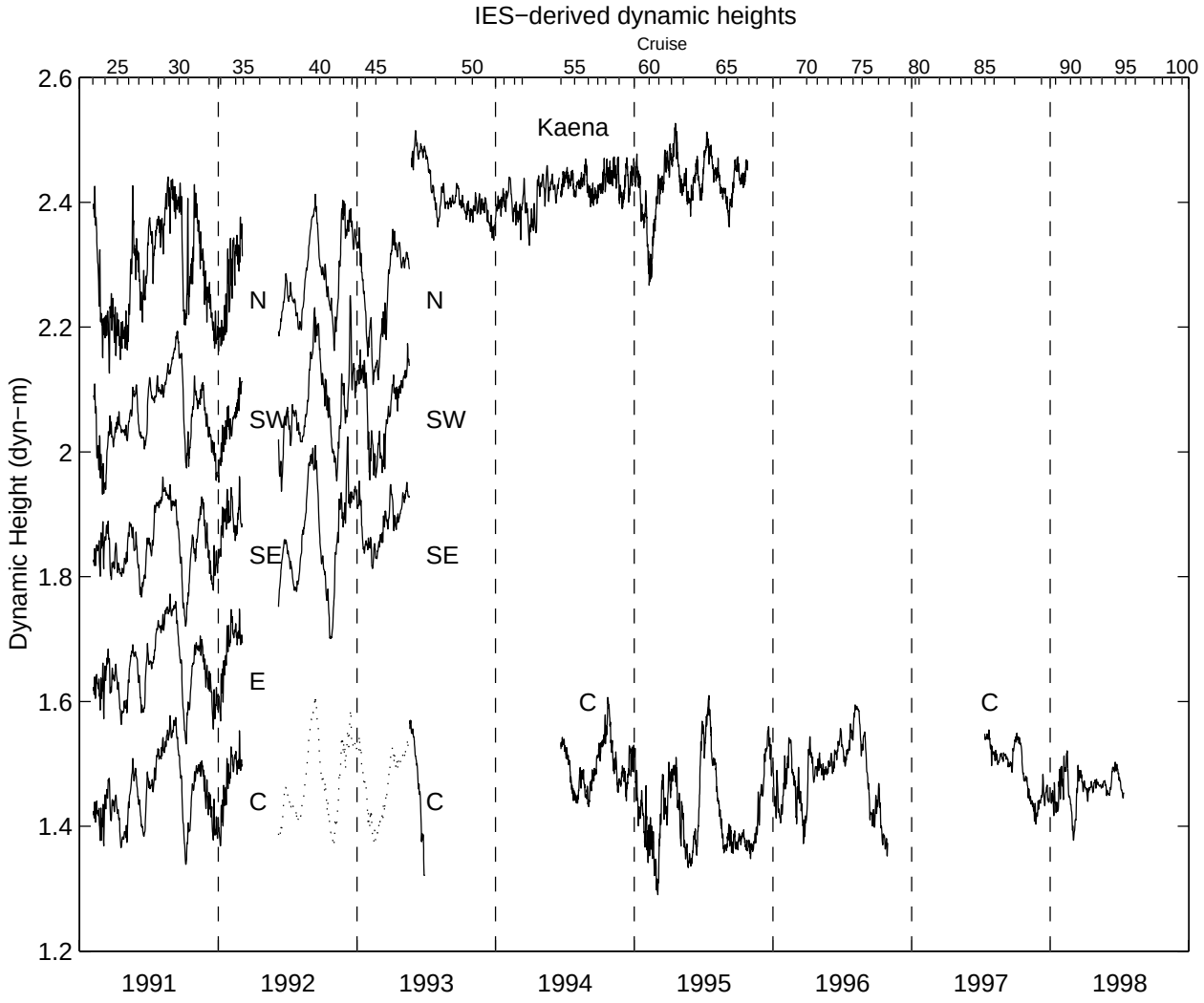

Figure 4.8: Dynamic height from the inverted echo sounders (IESs) after the removal of the semi-diurnal and diurnal tides and variability with time scales less than a day. The plots are staggered at 0.2 dyn-m intervals with the plot of the central IES (C) positioned at the correct y-scale. The dotted line on the C- record is an average of the N, SW and SE records between June 1992 and May 1993. All IES records have been calibrated from CTD casts at Station ALOHA. HOT cruise numbers are located at the upper x-axis.

4.10. Moored Sediment Traps

Particulate carbon flux measurements from the ALOHA-I and II sediment traps is shown in Figure 4.9. Particulate carbon, as well as particulate nitrogen, phosphorus and mass, showed a major export pulse during the summer periods when the upper water column was well stratified. A second export pulse was also observed in late winter-early spring but this feature appears to be different than the summer peak. The major particulate matter export was recorded in the same collector cups regardless of depth suggesting a sinking rate of about 200 m d-1. Analysis of chlorophyll a by fluorometry and HPLC pigment analyses reveal that the peak export event coincides with the removal of pigmented cells. The summer export material contains the full spectrum of major and accessory pigments. Microscopic analysis showed the dominance of diatoms during the summer export. A discussion of some of the findings has been presented in Karl et al. (1996a and 1997). Samples from ALOHA-III and IV are under analysis.

4.11 Thermosalinograph time-series

Time-series of near surface temperature (NST) and near surface salinity (NSS) measured by the thermosalinograph as well as potential density, navigation and ship speed during HOT-70 through HOT-78 are presented in Figures 6.6a to i. Thermosalinograph data from AC-1 is presented in Figure 6.7.1.

4.11.1 HOT-70

Time-series of NST and NSS measured by the thermosalinograph during this cruise are shown in Figure 6.6a. As mentioned in Section 2.11.1, a malfunctioning pump and pump seal kept the thermosalinograph off-line for the first 5 hours of this cruise. Temperatures for HOT-70 ranged from 23 to 24.4 °C and salinities ranged from 34.4 to 34.9. A large change in temperature and salinity can be seen as the ship returns to Honolulu from Station ALOHA.

4.11.2 HOT-71

Figure 6.6b shows the time-series of NST and NSS during HOT-71. Temperatures for HOT-71 ranged from 24 to 26.5 °C and salinities ranged from 34.2 to 34.8.

4.11.3 HOT-72

Figure 6.6c shows the time-series of NST during HOT-72. NSS is not available for this cruise as all salinity data from the thermosalinograph are considered suspect or bad due to a pump and electronics problem mentioned in Section 2.9.1. The electronics problem also affected the temperature data at the beginning of the cruise and those data had to be flagged bad as well.

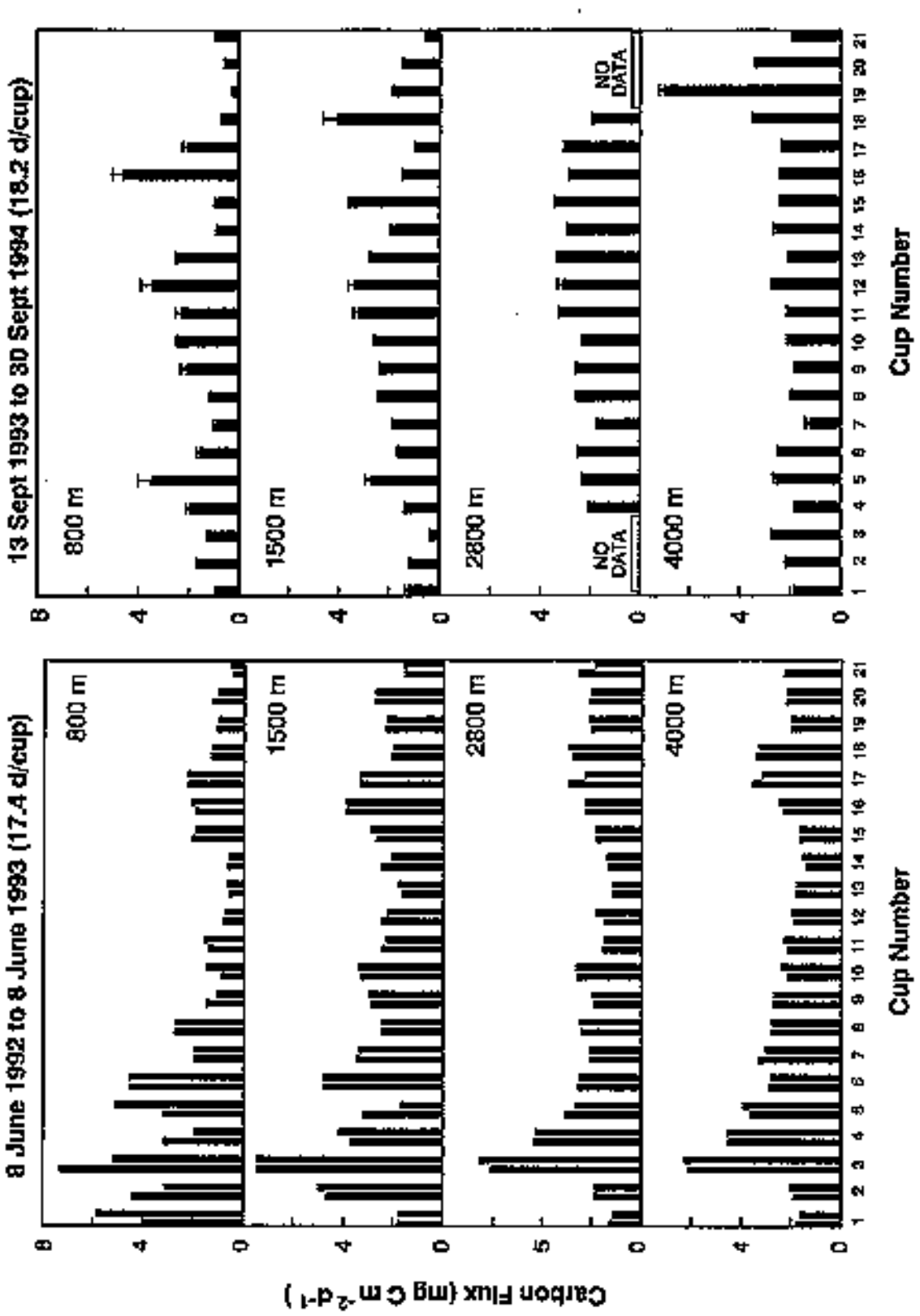

Figure 4.9:Time series record of total carbon flux as a function of time at Station ALOHA-I(left) and ALOHA-II(right) traps at the reference depths indicated.

4.11.4 HOT-73

Figure 6.6d shows the time-series of NST and NSS during HOT-73. Temperatures for HOT-73 ranged from 26 to 27.5 °C and salinities ranged from 34.4 to 34.7.

4.11.5 HOT-74

Figure 6.6e shows the time-series of NST and NSS during HOT-74. NST is plotted as a dotted line at the beginning of the cruise as the remote temperature sensor was recording values out of range (see Section 2.11.2.2). These values were replaced by using the internal temperature sensor and subtracting a mean offset (determined by finding the mean difference between the remote temperature sensor and internal temperature sensor, when the remote temperature sensor was functioning properly during this cruise) and are plotted with a dotted line. The potential density values computed during this time are also plotted with a dotted line. Temperature and salinity data end approximately 15 hours prematurely due to a computer logging problem noted in Section 2.11.1.

4.11.6 HOT-75

Figure 6.6f shows the time-series of NST and NSS during HOT-75. Temperatures for HOT-75 ranged from 26.6 to 28.6 °C and salinities ranged from 34.6 to 35.1. Some instances of small-scale variability in both temperature and salinity can be seen at times near and after local noon, possibly due to solar heating.

4.11.7 HOT-76

Figure 6.6g shows the time-series of NST and NSS during HOT-76. Temperatures for HOT-76 ranged from 27 to 28.5 °C and salinities ranged from 34.65 to 35.05. It appears the ship encountered some strong gradient features during its transit towards the end of the cruise.

4.11.8 HOT-77

As mentioned in Section 2.11.1, HOT-77 lost approximately 3 hours of thermosalinograph data due to a computer logging problem. The data loss is apparent in the time-series of NST and NSS during HOT-77 (Figure 6.6h). Temperatures for HOT-77 ranged from 26.4 to 28.2 °C and salinities ranged from 34.6 to 35.1.

4.11.9 HOT-78

Figure 6.6i shows the time-series of NST and NSS during HOT-78. Temperatures for HOT-78 ranged from 24.1 to 25.7 °C and salinities ranged from 34.8 to 35.0.

4.12. Towed instrumentation

A 3-dimensional plot of particle counts at 45 m dand grouped in size classes for 1996 is shown in Figure 4.10. A similar plot of particle volume relative to size class is shown in Figure 4.11. This figure shows that although most of the particles are in the smaller size range, mid-size particles dominate the spectrum on a per volume basis

4.13. Regional study (ALOHA-Climax 1)

4.13.1 Thermosalinograph

Time-series of NST and NSS measured by the thermosalinograph during AC-1 are shown in Figure 6.8.1. Large temperature and salinity gradients were encountered during this cruise which covered a long transect (see Figure 2.13). Overall, temperatures range from 24.5 to 27.4 °C and salinities range from 34.4 to 35.3.

4.13.2. Chlorophyll *a* Concentrations

Profiles of chlorophyll *a* are shown in Figure 6.7.2. From these profiles, it appears that Station ALOHA and Climax are quite similar. The stations in between them, however, appear different, showing a subsurface maximum at Station 3 and a subsurface minimum at Station.

4.13.3. Underway Surface Fluorescence

Underway fluorescence data at 45 meters from the towed instrument is shown in Figure 6.7.3. This data shows large spatial variability along the cruise track.

4.13.4 Primary Production

Depth profiles of primary production at Station ALOHA and Climax are shown in Figures 6.7.4 to 7. Figure 6.7.4 shows a comparison of primary production vales using the standard HOT protocol and the Climax protocol, referred to as the Hayward protocol. A significant difference is evident from water samples collected at 100 meters. Figures 6.7.6 and 6.7.7 show the profiles at Station Climax. Again HOT and Hayward protocols appear to produce different results with the exception of the 5 m water samples. Using various types of filters with the Hayward protocol, it appears that Millipore filters produce higher values than GF/F or than Nuclepore filters.

4.13.5 Meteorological Observations

Meteorological data collected during are presented as time series in Figure 6.7.8.

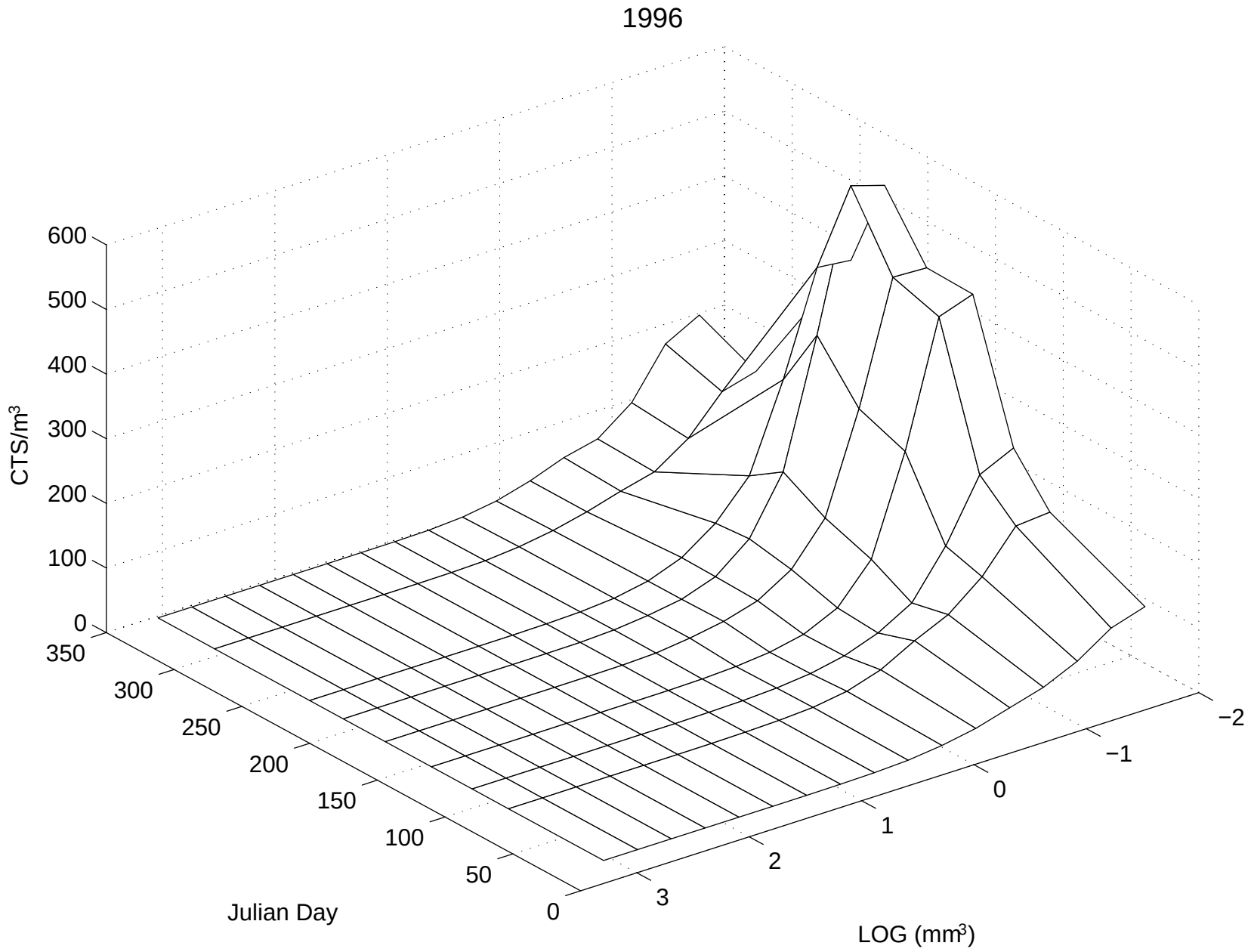

Figure 4.10:Three-dimensional plot of particle counts for different size classes over time for 1996

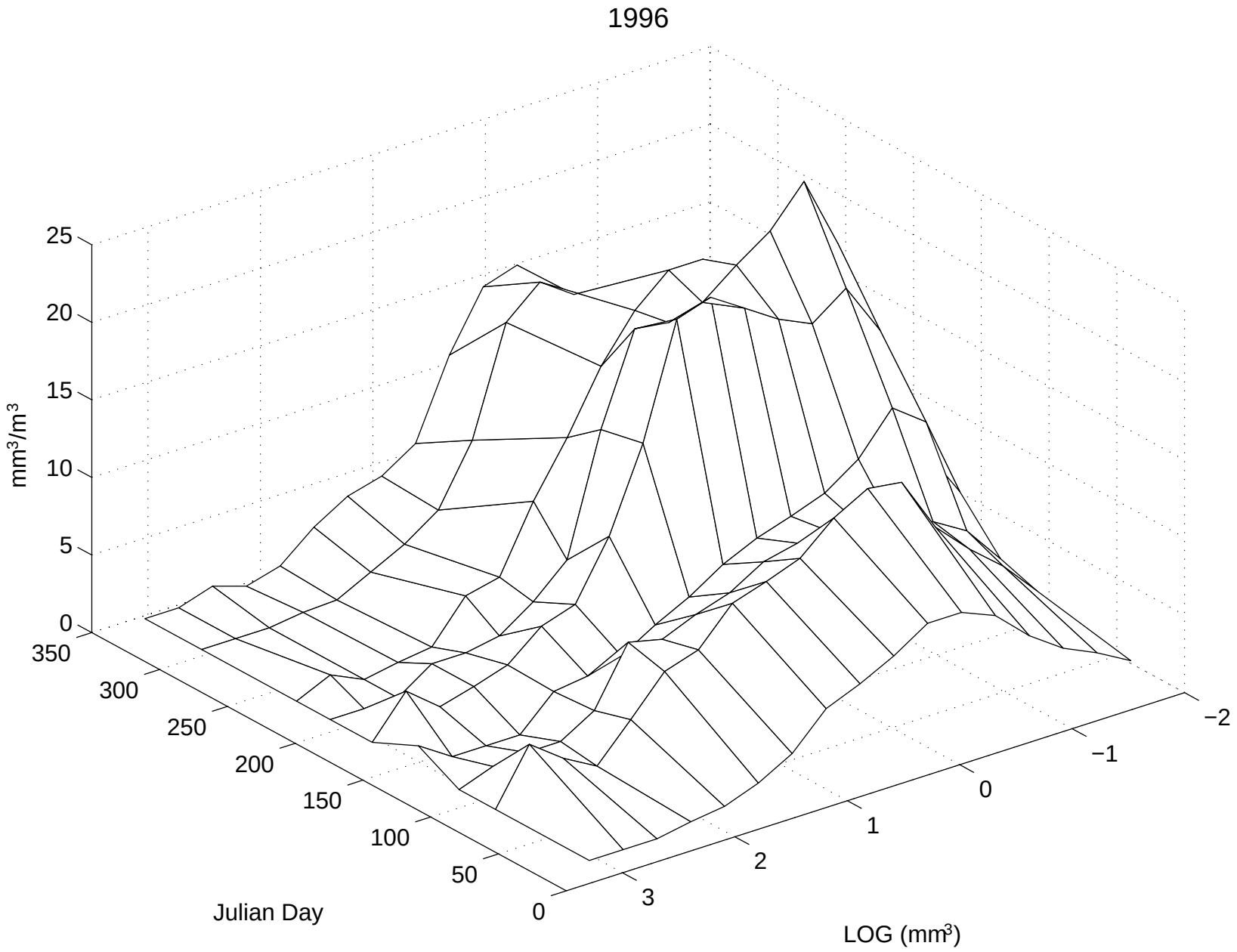

Figure 4.11:Three-dimensional plot of particle volume for different size classes over time for 1996

5.0. REFERENCES

Atkinson, M.J., F.I.M. Thomas, N. Larson, E. Terrill, K. Morita and C.C. Liu. 1995. A micro-hole potentiostatic oxygen sensor for oceanic CTDs. *Deep-Sea Research*, 42, 761-771.

Barnett, T.P. 1978. The role of the oceans in the global climate system. In: *Climatic Change*, J. Gribben, editor, Cambridge University Press, pp. 157-179.

Bidigare, R.R., J. Marra, T.J. Dickey, R. Iturriaga, K.S. Baker, R.C. Smith and H. Pak. 1990. Evidence for phytoplankton succession and chromatic adaptation in the Sargasso Sea during Spring 1985. *Marine Ecology Progress Series*, 60, 113-122.

Brewer, P.G., K.W. Bruland, R.W. Eppley and J.J. McCarthy. 1986. The Global Ocean Flux Study (GOFS): Status of the US-GOFS program. *Eos, Transactions of the American Geophysical Union*, 67, 827-832.

Campbell, L., H. Nolla and D. Vaulot. 1994. The importance of *Prochlorococcus* to community structure in the central North Pacific Ocean. *Limnology and Oceanography*, 39, 954-961.

Chiswell, S.M. 1996. Intra-annual oscillations at Station ALOHA, north of Oahu, Hawaii. *Deep-Sea Research II*, 43, 305-319.

Chiswell, S.M., E. Firing, D. Karl, R. Lukas, C. Winn. 1990. *Hawaii Ocean Time-series Program Data Report 1, 1988-1989*. School of Ocean and Earth Science and Technology, University of Hawaii, SOEST 90-1, 269 pp.

Clayton, T.D. and R.H. Byrne. 1993. Spectrophotometric seawater pH measurements: total hydrogen ion concentration scale calibration of m-cresol purple and at-sea results. *Deep-Sea Research*, 40, 2115-2129.

Cox, R.D. 1980. Determination of nitrate at the parts per billion level by chemiluminescence. *Analytical Chemistry*, 52, 332-335.

Dickey, T. 1991. The emergence of concurrent high-resolution physical and bio-optical measurements in the upper ocean and their applications. *Reviews of Geophysics*, 29, 383-413.

Dore, J.E. and D.M. Karl. 1996. Nitrite distributions and dynamics at Station ALOHA. *Deep-Sea Research*, 43, 385-402.

Dore, J.E., T. Houlihan, D.V. Hebel, G. Tien, L.M. Tupas and D.M. Karl. 1996. Freezing as a method of seawater preservation for the analysis of dissolved inorganic nutrients. *Marine Chemistry*, 53, 173-185.

Doty, M.S. and M. Oguri. 1956. The island mass effect. *Journal du Conseil pour l'Internationale Exploration de la Mer*, 22, 33-37.

Dymond, J.D. and M. Lyle. 1985. Flux comparisons between sediments and sediment traps in the eastern tropical Pacific: implication for atmospheric CO_2 variations during the pleistocene. *Limnology and Oceanography*, 30, 699-712.

Eppley, R.W. and B.J. Peterson. 1979. Particulate organic matter flux and planktonic new production in the deep ocean. *Nature*, 282, 677-680.

Firing, E. 1996. Currents observed north of Oahu during the first 5 years of HOT. *Deep-Sea Research*, 43, 281-303.

Firing, E. and R.L. Gordon. 1990. Deep ocean acoustic Doppler current profiling. In: *Proceedings of the Fourth IEEE Working Conference on Current Measurements*, G.F. Appell and T.B. Curtin, editors, IEEE, New York, pp. 192-201.

Garside, C. 1982. A chemiluminescent technique for the determination of nanomolar concentrations of nitrate and nitrite in seawater. *Marine Chemistry*, 11, 159-167.

Gordon, D.C., Jr. 1970. Chemical and biological observations at station Gollum, an oceanic station near Hawaii, January 1969 to June 1970. *Hawaii Institute of Geophysics Report*, HIG-70-22, 44 pages + 2 appendices.

Harrison, W.G., L.R. Harris, D.M. Karl, G.A. Knauer and D.G. Redalje. 1992. Nitrogen dynamics at the VERTEX time-series site. *Deep-Sea Research*, 39, 1535-1552.

Hayward, T.L. 1987. The nutrient distribution and primary production in the central North Pacific. *Deep-Sea Research*, 34, 1593-1627.

JSC/CCCO. 1981. *JSC/CCCO Meeting on Time Series of Ocean Measurements (Tokyo, May 11-15, 1981)*. World Climate Research Program, Geneva, Switzerland.

Johnson, D.L. 1971. Simultaneous determination of arsenate and phosphate in natural waters. *Environmental Science and Technology*, 5, 411-414.

Karl, D.M., J.R. Christian, J.E. Dore, D.V. Hebel, R.M Letelier, L.M. Tupas and C.D. Winn. 1996a. Seasonal and interannual variability in primary production and particle flux at Station ALOHA. *Deep-Sea Research*, 43, 539-568.

Karl, D.M. and O. Holm-Hansen. 1978. Methodology and measurement of adenylate energy charge ratios in environmental samples. *Marine Biology*, 48, 185-197.

Karl, D.M., R. Letelier, D.V. Hebel, D.F. Bird and C.D. Winn. 1992. *Trichodesmium* blooms and new nitrogen in the North Pacific gyre. In: *Marine Pelagic Cyanobacteria: Trichodesmium and Other Diazotrophs*, E.J. Carpenter et al., editors, Kluwer Academic Publishers, Netherlands, pp. 219-237.

Karl, D.M., R. Letelier, D. Hebel, L. Tupas, J. Dore, J. Christian and C. Winn. 1995 Ecosystem changes in the North Pacific subtropical gyre attributed to the 1991-92 El Niño. *Nature*, 373, 230-234.

Karl, D.M., R. Letelier, L. Tupas, J. Dore, J. Christian and D. Hebel. 1997. The role of nitrogen fixation in biogeochemical cycling in the subtropical North Pacific Ocean. *Nature*, 388, 533-538.

Karl, D.M. and R. Lukas. 1996. The Hawaii Ocean Time-series (HOT) program: Background, rationale and field implementation. *Deep-Sea Research*, 43, 129-156.

Karl, D.M. and G. Tien. 1992. MAGIC: A sensitive and precise method for measuring dissolved phosphorus in aquatic environments. *Limnology and Oceanography*, 37, 105-116.

Karl, D.M. and G. Tien. 1996. Temporal variability in dissolved phosphorus concentrations at Station ALOHA (22°45'N, 158°W). *Marine Chemistry*, 56, 77-96.

Karl, D., L. Tupas, F. Santiago-Mandujano, C. Nosse, D. Hebel, E. Firing and R. Lukas, 1996b. *Hawaii Ocean Time-series Program Data Report 7, 1995*. School of Ocean and Earth Science and Technology, University of Hawaii, SOEST 96-09, 228 pp.

Keeling, C.D., R.B. Bacastow, A.E. Bainbridge, C.A. Ekdahl, Jr., P.R. Guenther, L.S. Waterman and J.F.S. Chin. 1976. Atmospheric carbon dioxide variations at Mauna Loa Observatory, Hawaii. *Tellus*, 28, 538-551.

Keeling, R.F. and S.R. Shertz. 1992. Seasonal and interannual variations in atmospheric oxygen and implications for the global carbon cycle. *Nature*, 358, 723-727.

Kennan, S.C. and R. Lukas. 1995. Saline intrusions in the intermediate waters north of Oahu, Hawaii. *Deep-Sea Research*, 43, 215-241.

Knauer, G.A., J.H. Martin and K.W. Bruland. 1979. Fluxes of particulate carbon, nitrogen and phosphorus in the upper water column of the northeast Pacific. *Deep-Sea Research*, 26, 97-108.

Knauer, G.A., D.G. Redalje, W.G. Harrison and D.M. Karl. 1990. New production at the VERTEX time-series site. *Deep-Sea Research*, 37, 1121-1134.

Larson , N. and A.M. Pederson. 1996. Temperature measurements in flowing water: Viscous heating of sensor tips. 1st International Group for Hydraulic Efficiency Measurements (IGHEM) Meeting, Montreal, Canada, June 1996.

Laws, E.A., G.R. DiTullio, P.R. Betzer, D.M. Karl and R.L. Carder. 1989. Autotrophic production and elemental fluxes at 26° N, 155° W in the North Pacific subtropical gyre. *Deep-Sea Research*, 36, 103-120.

Likens, G.E., F.H. Bormann, R.S. Pierce, J.S. Eaton and N.M. Johnson. 1977. *Biogeochemistry of a Forested Ecosystem*. Springer-Verlag, New York.

Longhurst, A.R. and W.G. Harrison. 1989. The biological pump: Profiles of plankton production and consumption in the upper ocean. *Progress in Oceanography*, 22, 47-123.

Lukas, R. and S. Chiswell. 1991. Submesoscale water mass variations in the salinity minimum of the north Pacific near Hawaii. *WOCE Notes*, 3(1), 6-8.

Lukas, R. and F. Santiago-Mandujano. 1996. Interannual variability of Pacific deep- and bottom-waters observed in the Hawaii Ocean Time-series. *Deep-Sea Research*, 43, 243-255.

Martin, J.H., G.A. Knauer, D.M. Karl and W.W. Broenkow. 1987. VERTEX: Carbon cycling in the northeast Pacific. *Deep-Sea Research*, 34, 267-285.

Michaels, A. and A. Knap. 1996. Overview of the U.S.-JGOFS Bermuda Atlantic Time-series Study and Hydrostation S program. *Deep-Sea Research*, 43, 157-198.

Monger, B,C, and M.R. Landry. 1993. Flow cytometry analysis of marine Bacteria with H Hoechst 3342. *Applied and Environmental Microbiology*, 59, 905-911.

National Research Council. 1984a. *Global Observations and Understanding of the General Circulation of the Oceans: Proceedings of a Workshop*, National Academy Press, Washington, DC, 418 pp.

National Research Council. 1984b. *Global Ocean Flux Study: Proceedings of a Workshop*, National Academy Press, Washington, DC, 360 pp.

Ortner, P.B. E.M. Hulbert and P.H. Wiebe. 1979. Gulf Stream rings, phytohydrography and herbivore habitat contrasts. *Journal of Experimental Marine Biology and Ecology*, 39, 101-124.

Owens, W.B. and R.C. Millard. 1985. A new algorithm for CTD oxygen calibration. *Journal of Physical Oceanography*, 15, 621-631.

Qian, J. and K. Mopper. 1996. Automated high-performance, high-temperature combustion total organic carbon analyzer. *Analytical Chemistry*, 68, 3090-3097.

Quay, P.D., B. Tilbrook and C.S. Wong. 1992. Oceanic uptake of fossil fuel CO_2: Carbon-13 evidence. *Science*, 256, 74-79.

Ryther, J.H. 1969. Photosynthesis and fish production in the sea. The production of organic matter and its conversion to higher forms of life vary throughout the world ocean. *Science*, 166, 72-76.

Sarmiento, J.L. and J.R. Toggweiler. 1984. New model for the role of the oceans in determining atmospheric pCO_2. *Nature*, 308, 621-624.

Scientific Committee on Oceanic Research. 1990. *The Joint Global Ocean Flux Study (JGOFS) Science Plan.* JGOFS Report No. 5. International Council of Scientific Unions, 61 pp.

Strickland, J.D.H. and T.R. Parsons. 1972. *A Practical Handbook of Seawater Analysis*. Fisheries Research Board of Canada, 167 pp.

Sverdrup, H.U., M.W. Johnson and R.H. Fleming. 1946. *The Oceans: Their physics, chemistry and general biology*. Prentice-Hall, New York. 1087 pp.

Tabata, S. 1965. Variability of oceanographic conditions at ocean station "P" in the Northeast Pacific Ocean. *Transactions of the Royal Society of Canada*, 3, 367-418.

Takahashi, T., R.A. Feely, R.F. Weiss, R.H. Wanninkhof, D.W. Chipman, S.C. Sutherland and T.T. Takahashi. 1997. Global air-sea flux of CO_2: an estimate based on measurements of sea-air pCO_2 difference. *Proceedings of the National Academy of Sciences, USA*, 92, 8292-8299.

Tans, P.P., I.Y. Fung and T. Takahashi. 1990. Observational constraints on the global atmospheric carbon budget. *Science*, 247, 1431-1438.

Thomson, C.W. 1877. *The Atlantic, a Preliminary Account of the General Results of the Exploring Voyage of H.M.W. "Challenger,"* vol. 2, Macmillan and Company, London, p. 291.

Troup, A.J. 1965. The "southern oscillation." *Quarterly Journal of the Royal Meteorological Society*, 91, 490-506.

Tsuchiya, M. 1968. *Upper Waters of the Intertropical Pacific Ocean*. Johns Hopkins Oceanographic Studies, 4, 49 pp.

Tupas, L.M., B.N. Popp and D.M. Karl. 1994a. Dissolved organic carbon in oligotrophic waters: experiments on sample preservation, storage and analysis. *Marine Chemistry*, 48, 207-216.

Tupas, L., F. Santiago-Mandujano, D. Hebel, E. Firing, F. Bingham, R. Lukas and D. Karl. 1994b. *Hawaii Ocean Time-series Program Data Report 5, 1993.* School of Ocean and Earth Science and Technology, University of Hawaii, SOEST 94-05, 156 pp.

Tupas, L., F. Santiago-Mandujano, D. Hebel, E. Firing, R. Lukas and D. Karl. 1995. *Hawaii Ocean Time-series Data Report 6: 1994.* School of Ocean and Earth Science and Technology, University of Hawaii, SOEST 95-06, 199 pp.

Tupas, L., F. Santiago-Mandujano, D. Hebel, R. Lukas, D. Karl and E. Firing. 1993. *Hawaii Ocean Time-series Program Data Report 4, 1992.* School of Ocean and Earth Science and Technology, University of Hawaii, SOEST 93-14, 248 pp.

UNESCO. 1981. *Tenth Report of the Joint Panel on Oceanographic Tables and Standards*. UNESCO Technical Papers in Marine Science, No. 36., UNESCO, Paris.

Vaulot, D. 1989. CYTOPC: Processing software for flow cytometric data. *Signal and Noise,* 2, 8.

Volk, T. and M.I. Hoffert. 1985. Ocean carbon pumps: Analysis of relative strengths and efficiencies in ocean-driven atmospheric CO_2 changes. In: *The Carbon Cycle and Atmospheric CO_2: Natural Variations Archean to Present*, E.T. Sundquist and W.S. Broecker, editors, American Geophysical Union, Washington, D.C., pp. 99-110.

Weiss, R.F., R.A. Jahnke and C.D. Keeling. 1982. Seasonal effects of temperature and salinity on the partial pressure of CO_2 in seawater. *Nature*, 300, 511-513.

Wiebe, P.H., C.B. Miller, J.A. McGowan and R.A. Knox. 1987. Long time series study of oceanic ecosystems. *EOS, Transactions of the American Geophysical Union*, 68, 1178-1190.

Wiggert, J., T. Dickey and T. Granata. 1994. The effect of temporal undersampling on primary production estimates. *Journal of Geophysical Research*, 99, 3361-3371.

Winn, C.D., L. Campbell, J.R. Christian, R.M. Letelier, D.V. Hebel, J.E. Dore, L. Fujieki and D.M. Karl. 1995. Seasonal variability in the phytoplankton community of the North Pacific subtropical gyre. *Global Biogeochemical Cycles*, 9, 605-620.

Winn, C., S.M. Chiswell, E. Firing, D. Karl, R. Lukas. 1991. *Hawaii Ocean Time-series Program Data Report 2, 1990*. School of Ocean and Earth Science and Technology, University of Hawaii, SOEST 92-01, 175 pp.

Winn, C., R. Lukas, D. Karl, E. Firing. 1993. *Hawaii Ocean Time-series Program Data Report 3, 1991*. School of Ocean and Earth Science and Technology, University of Hawaii, SOEST 93-3, 228 pp.

Wright, S.W., S.W. Jeffrey, R.F.C. Mantoura, C.A. Llewellyn, T. Bjornland, D. Repeta and N. Welschmeyer. 1991. Improved HPLC method for the analysis of chlorophylls and carotenoids from marine phytoplankton. *Marine Ecology Progress Series*, 77, 183-196.

Wyrtki, K., E. Firing, D. Halpern, R. Knox, G.J. McNally, W.C. Patzert, E.D. Stroup, B.A. Taft and R. Williams. 1981. The Hawaii to Tahiti shuttle experiment. *Science*, 211, 22-28.

6.0 FIGURES

6.1. Hydrography

Figure 6.1.1a to j: [Upper left panel] Temperature, salinity, oxygen and potential density (σ_θ) as a function of pressure for the WOCE deep cast at Station ALOHA for each HOT cruise. [Upper right panel] Plot of [nitrate + nitrite], soluble reactive phosphate, silicate, and bottle dissolved oxygen as a function of potential temperature for all water samples. [Lower left panel] CTD temperature and salinity plotted as a function of pressure to 1000 dbar. [Lower right panel] Salinity and oxygen from CTD and water samples plotted as a function of potential temperature. Only the CTD oxygen traces in which bottle oxygen's were sampled are included.

Figure 6.1.2a to j: [Upper panel] Stack plots of temperature versus pressure to 100 dbar at Station ALOHA. Offset is 2 °C. [Lower panel] Stack plots of salinity versus pressure to 1000 dbar at Station ALOHA. Offset is 0.1.

Figure 6.1.3a to j: [Upper left panel] Temperature, salinity, oxygen and potential density (σ_θ) as a function of pressure for the cast at Station Kahe for each HOT cruise. [Upper right panel] Plot of [nitrate + nitrite], soluble reactive phosphate, silicate, and bottle dissolved oxygen as a function of potential temperature for all water samples. [Lower right panel] Plot of bottle salinity and bottle oxygen as a function of potential temperature.

Figure 6.1.4: [Upper panel] Potential temperature versus pressure for all deep casts in 1996. [Lower panel]: Potential temperature for all deep casts in 1996 from 2500 dbar.

Figure 6.1.5: [Upper panel] Salinity versus potential temperature for all deep casts in 1996. [Lower panel]: Salinity versus potential temperature for all deep casts in 1996 in the 1-5 °C range.

Figure 6.1.6: [Upper panel] Oxygen concentrations from calibrated oxygen sensor data versus potential temperature for all deep casts in 1996. [Lower panel] Oxygen versus potential temperature for all deep casts in 1996 in the 1-5 °C range.

Figure 6.1.7: Contour plot of CTD potential temperature versus pressure for HOT cruises 1-78.

Figure 6.1.8: Contour plot of potential density (σ_θ), calculated from CTD pressure, temperature and salinity, versus pressure for HOT cruises 1-78.

Figure 6.1.9: Contour plot of CTD salinity versus pressure for HOT cruises 1-78.

Figure 6.1.10: Contour plot of CTD salinity versus potential density (σ_θ) to 27.5 kg m^{-3} for HOT cruises 1-78. The average density of the sea surface is connected by the heavy line.

Figure 6.1.11: Contour plot of bottle salinity versus pressure for HOT cruises 1-78. Location of samples in the water column are indicated by the solid circles.

Figure 6.1.12: Contour plot of bottle salinity versus potential density (σ_θ)to 27.5 kg m^{-3} for HOT cruises 1-78. The average density of the sea surface is connected by the heavy line.

Figure 6.1.13: Contour plot of bottle oxygen versus pressure for HOT cruises 1-78. Location of samples in the water column are indicated by the solid circles.

Figure 6.1.14: Contour plot of bottle oxygen versus potential density (σ_θ) to 27.5 kg m^{-3} for HOT cruises 1-78. The average density of the sea surface is connected by the heavy line.

Figure 6.1.15: Contour plot of [nitrate + nitrite] versus pressure for HOT cruises 1-78. Location of samples in the water column are indicated by the solid circles.

Figure 6.1.16: Contour plot of [nitrate + nitrite] versus potential density (σ_θ) to 27.5 kg m^{-3} for HOT cruises 1-78. The average density of the sea surface is connected by the heavy line.

Figure 6.1.17: Contour plot of [nitrate + nitrite] versus potential density (σ_θ) from 27.0 to 27.8 kg m^{-3} for HOT cruises 1-78.

Figure 6.1.18: Contour plot of soluble reactive phosphate versus pressure for HOT cruises 1-78. Location of samples in the water column are indicated by the solid circles.

Figure 6.1.19: Contour plot of soluble reactive phosphate versus potential density (σ_θ) to 27.5 kg m^{-3} for HOT cruises 1-78. The average density of the sea surface is connected by the heavy line.

Figure 6.1.20: Contour plot of soluble reactive phosphate versus potential density (σ_θ) from 27.0 to 27.8 kg m^{-3} for HOT cruises 1-78.

Figure 6.1.21: Contour plot of silicate versus pressure for HOT cruises 1-78. Location of samples in the water column are indicated by the solid circles.

Figure 6.1.22: Contour plot of silicate versus potential density (σ_θ) to 27.5 kg m^{-3} for HOT cruises 1-78. The average density of the sea surface is connected by the heavy line.

Figure 6.1.23: Time series of mean bottle dissolved oxygen (A), [nitrate + nitrite] (B) and soluble reactive phosphate (C) between 27.0 and 27.8 kg m^{-3} isopycnals. The smooth line is the spline fit to the data. The asterisks in the middle of each year is the annual mean.

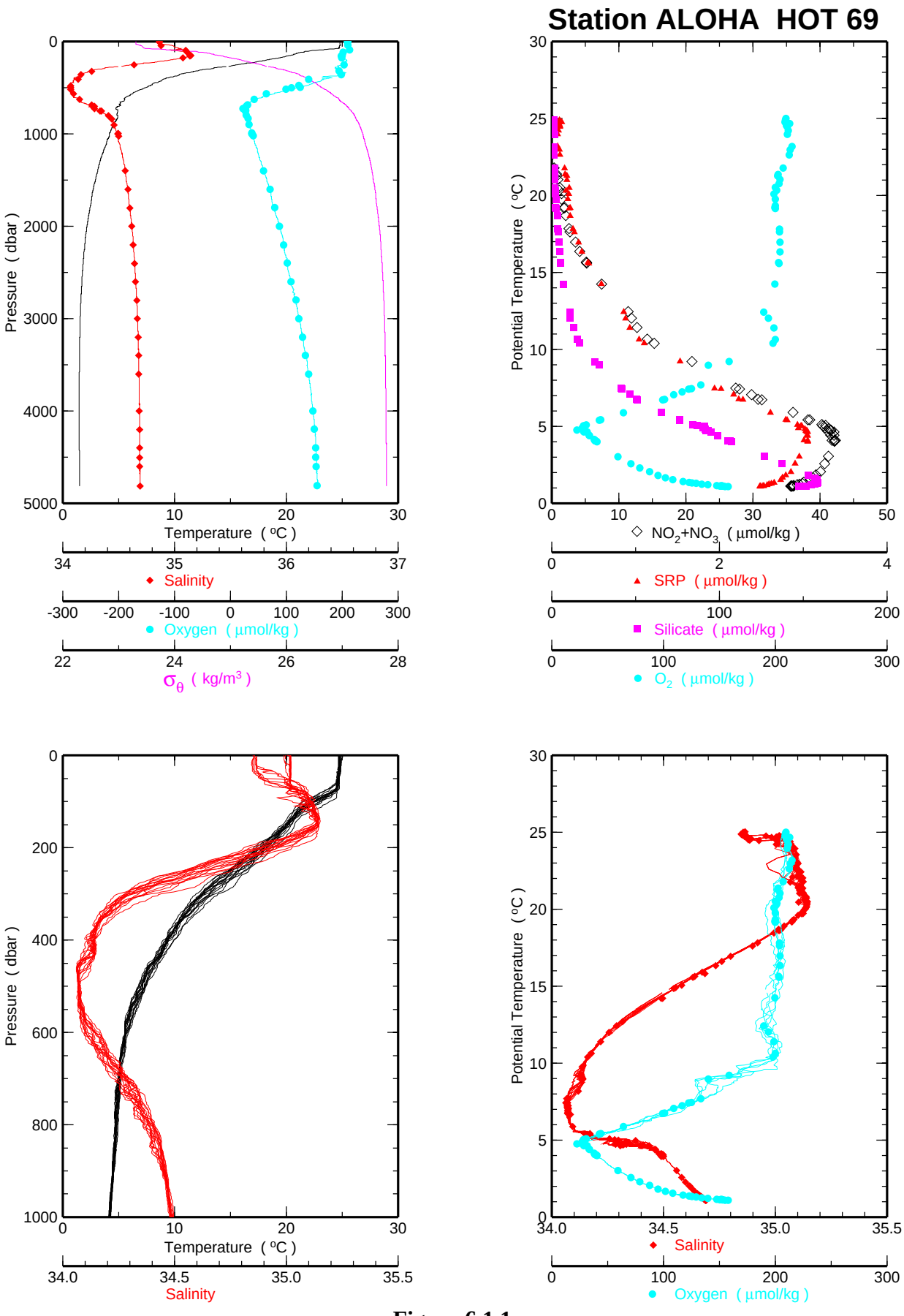
Station ALOHA HOT 69
Pressure (dbar)
Temperature (ºC)
Salinity
Oxygen (µmol/kg)
σθ (kg/m³)
Potential Temperature (ºC)
NO2+NO3 (µmol/kg)
SRP (µmol/kg)
Silicate (µmol/kg)
O2 (µmol/kg)

Figure 6.1.1a

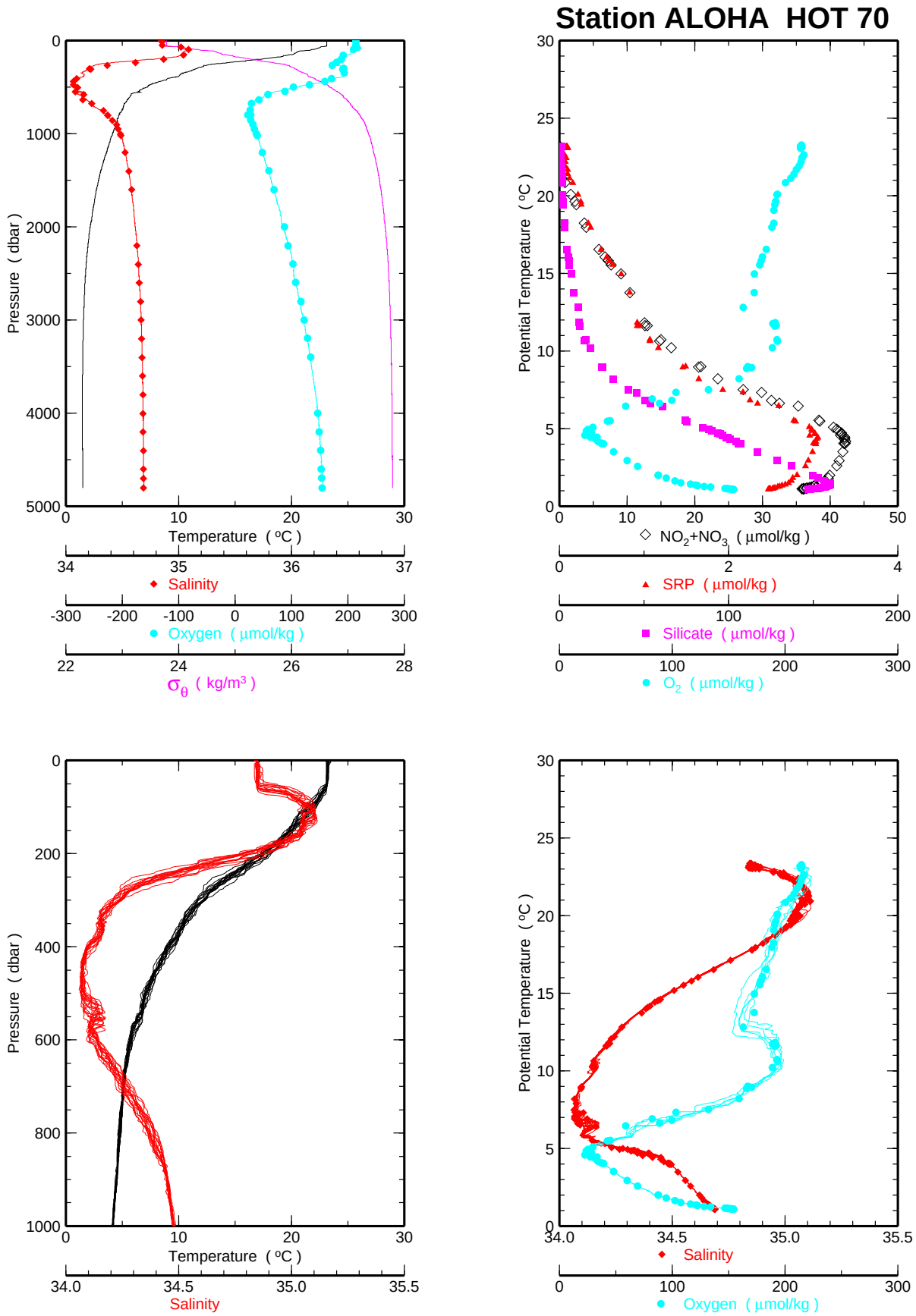
Station ALOHA HOT 70
Pressure (dbar)
Temperature (ºC)
Salinity
Oxygen (µmol/kg)
σθ (kg/m3)
Potential Temperature (ºC)
NO2+NO3 (µmol/kg)
SRP (µmol/kg)
Silicate (µmol/kg)
O2 (µmol/kg)

Figure 6.1.1b

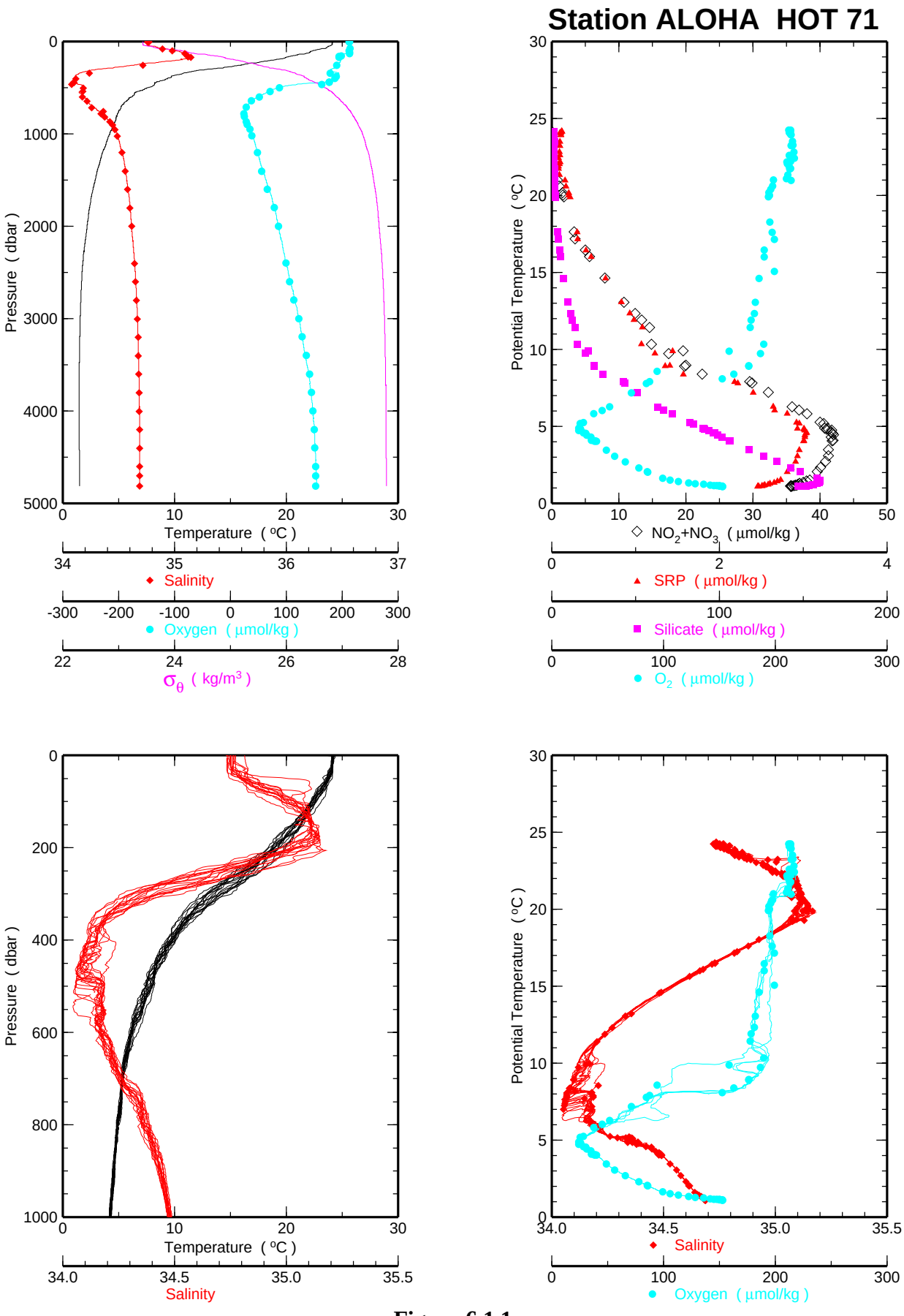
Station ALOHA HOT 71
Pressure (dbar)
Temperature (ºC)
Salinity
Oxygen (µmol/kg)
σθ (kg/m3)
Potential Temperature (ºC)
NO2+NO3 (µmol/kg)
SRP (µmol/kg)
Silicate (µmol/kg)
O2 (µmol/kg)

Figure 6.1.1c

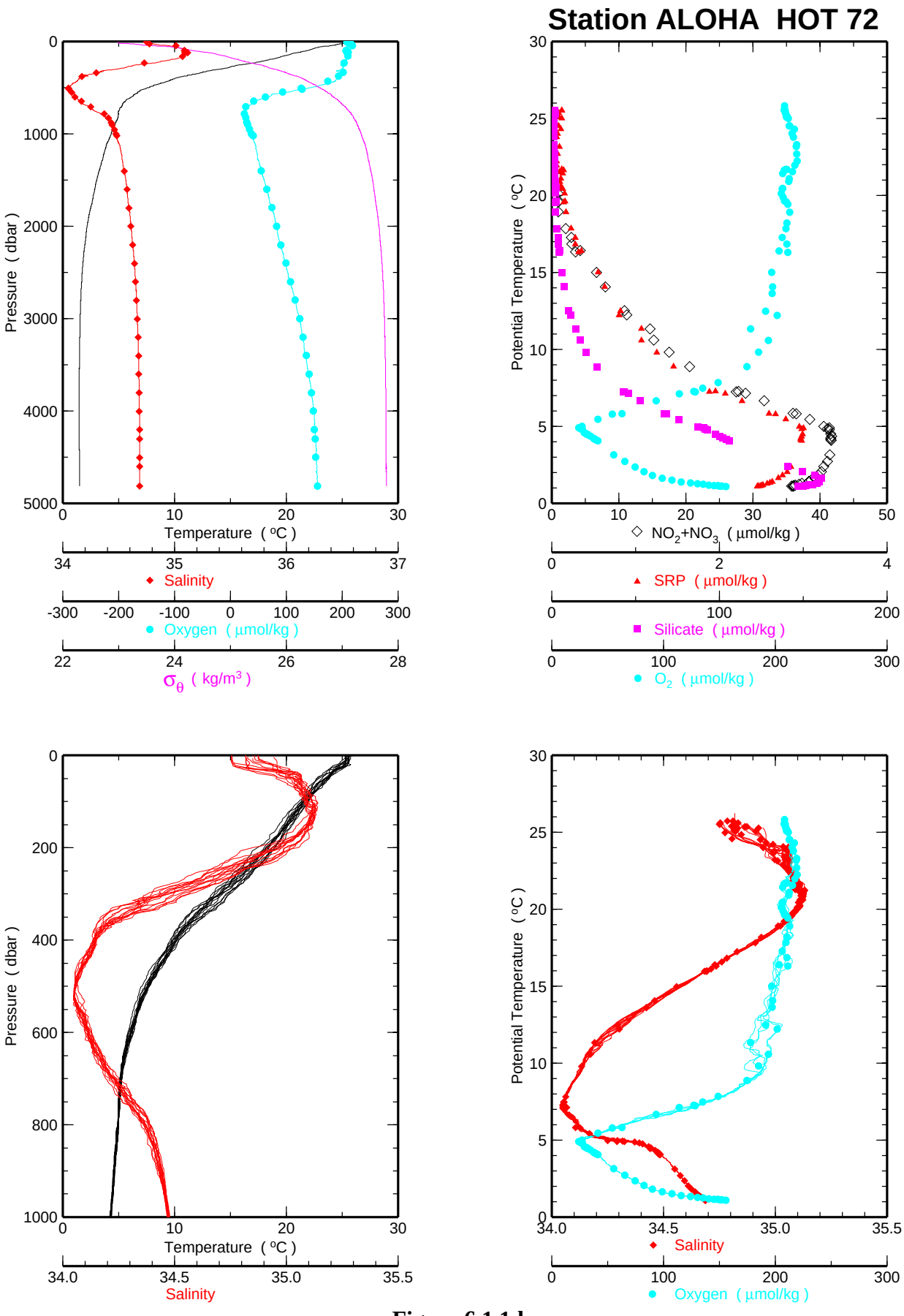
Station ALOHA HOT 72
Pressure (dbar)
Temperature (ºC)
Salinity
Oxygen (µmol/kg)
σθ (kg/m³)
Potential Temperature (ºC)
NO2+NO3 (µmol/kg)
SRP (µmol/kg)
Silicate (µmol/kg)
O2 (µmol/kg)

Figure 6.1.1d

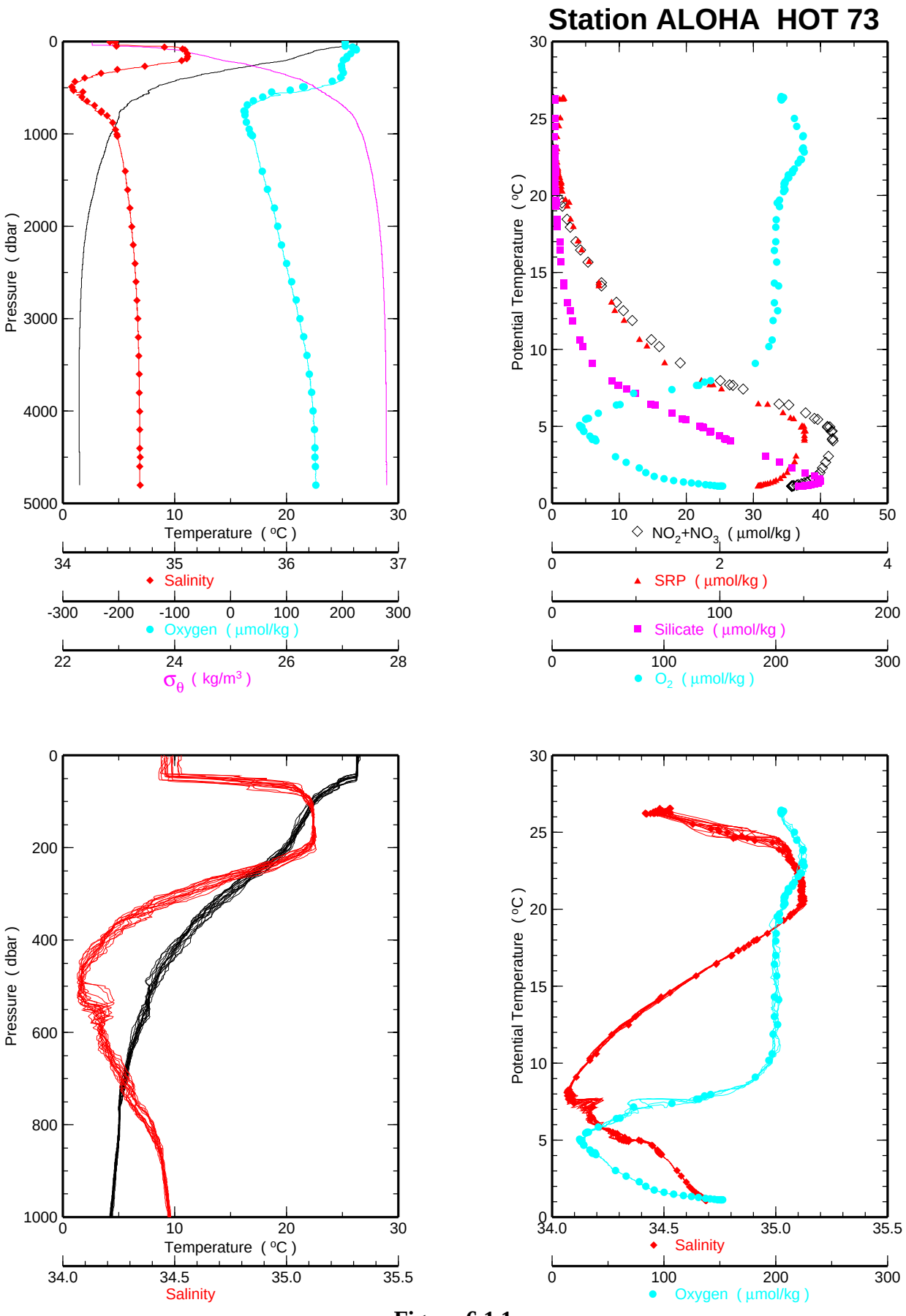
Station ALOHA HOT 73
Pressure (dbar)
Temperature (ºC)
Salinity
Oxygen (µmol/kg)
σθ (kg/m³)
Potential Temperature (ºC)
NO2+NO3 (µmol/kg)
SRP (µmol/kg)
Silicate (µmol/kg)
O2 (µmol/kg)

Figure 6.1.1e

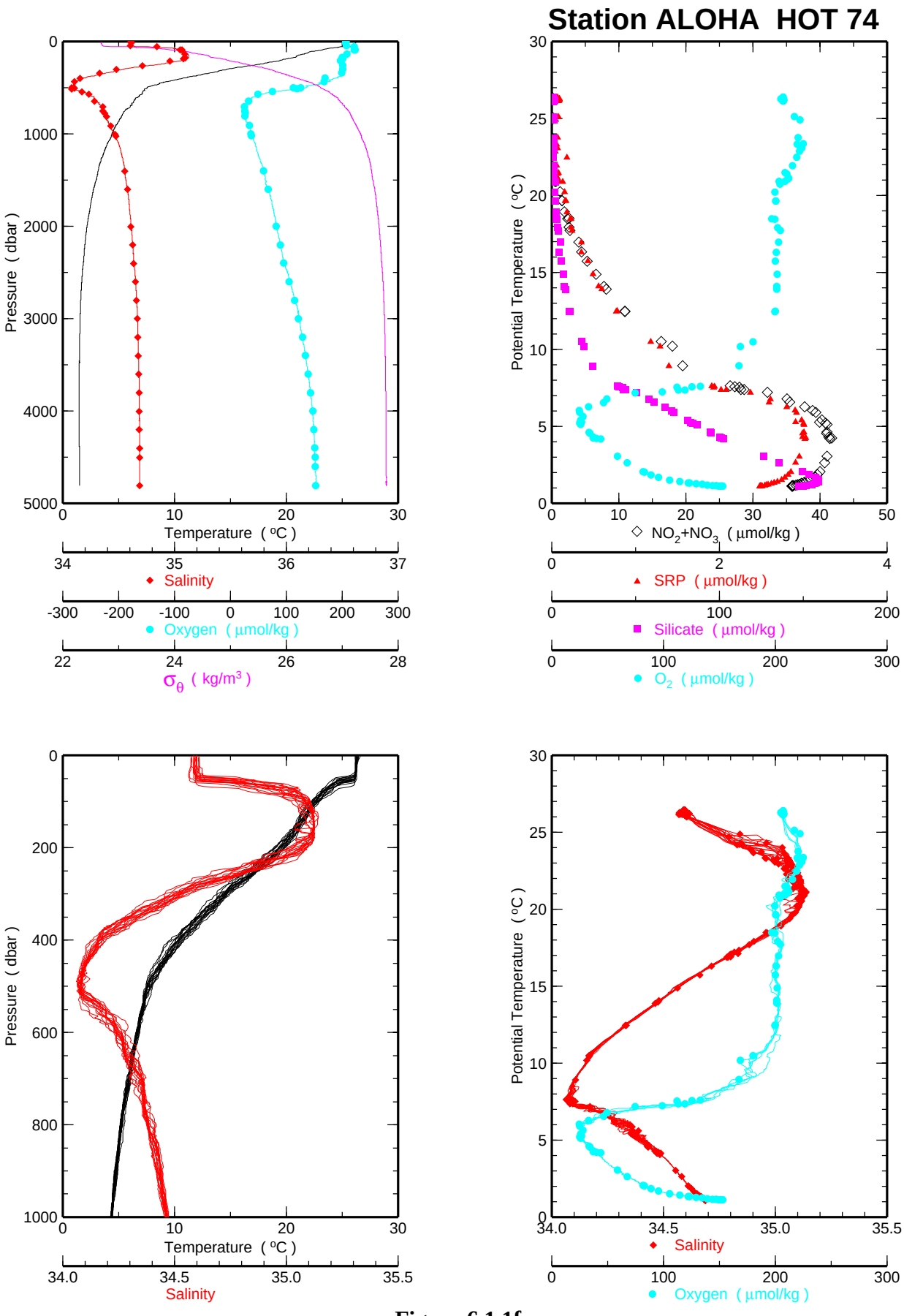
Station ALOHA HOT 74
Pressure (dbar)
Temperature (ºC)
Salinity
Oxygen (µmol/kg)
σθ (kg/m³)
Potential Temperature (ºC)
NO2+NO3 (µmol/kg)
SRP (µmol/kg)
Silicate (µmol/kg)
O2 (µmol/kg)

Figure 6.1.1f

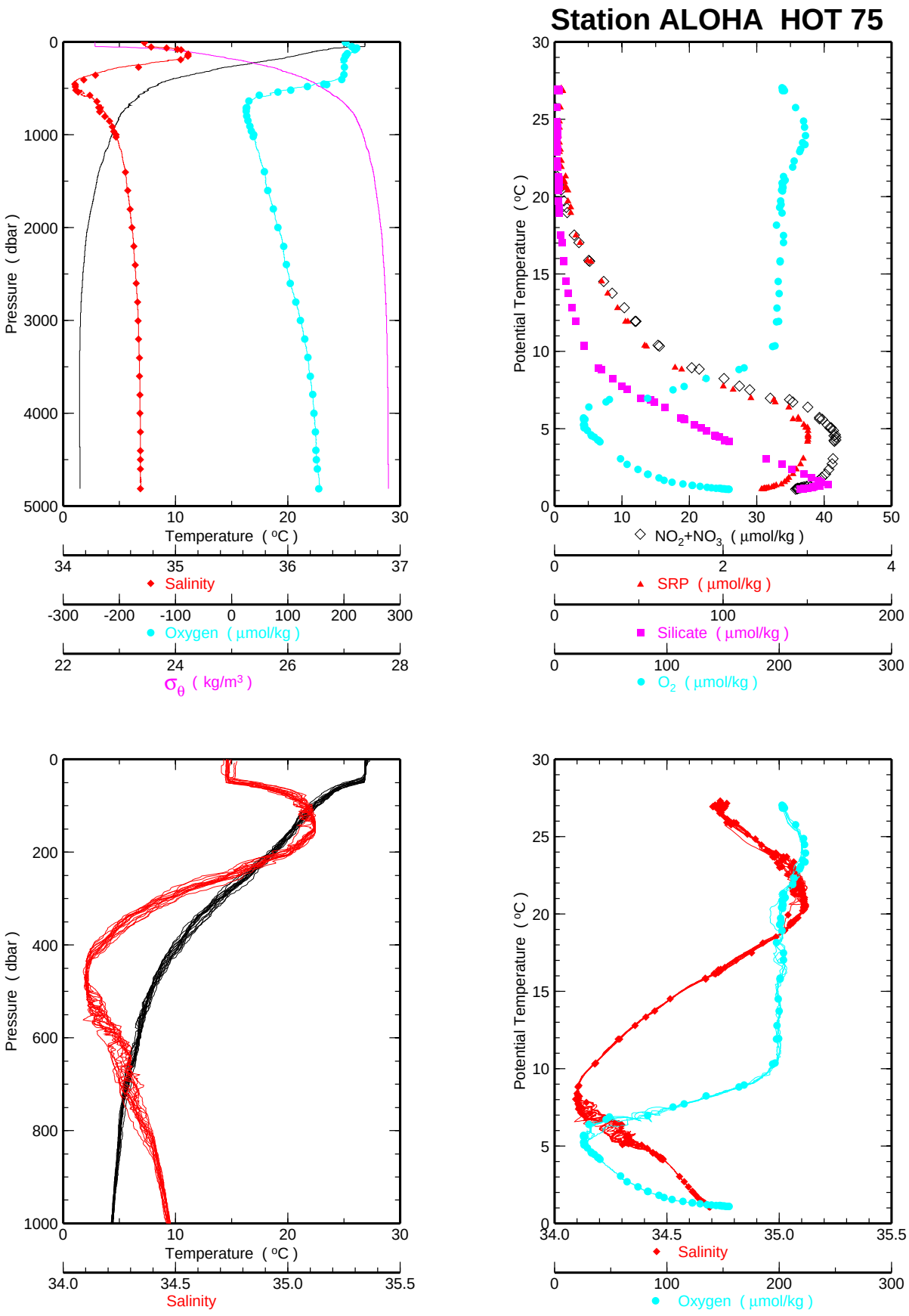
Station ALOHA HOT 75
Pressure (dbar)
Temperature (°C)
Salinity
Oxygen (µmol/kg)
σθ (kg/m³)
Potential Temperature (°C)
NO2+NO3 (µmol/kg)
SRP (µmol/kg)
Silicate (µmol/kg)
O2 (µmol/kg)

Figure 6.1.1g

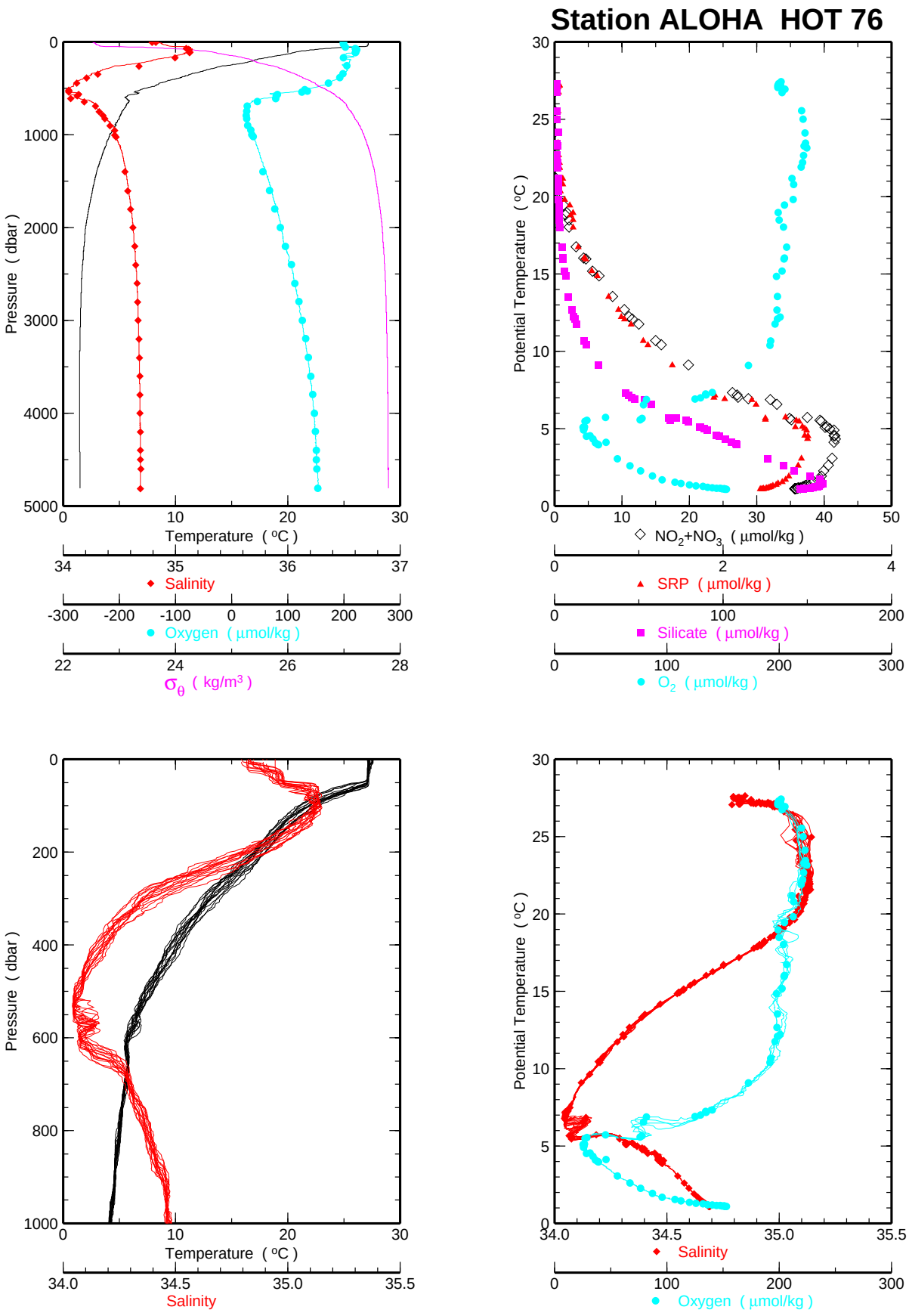
Station ALOHA HOT 76
Pressure (dbar)
Temperature (°C)
Salinity
Oxygen (µmol/kg)
σθ (kg/m3)
Potential Temperature (°C)
NO2+NO3 (µmol/kg)
SRP (µmol/kg)
Silicate (µmol/kg)
O2 (µmol/kg)

Figure 6.1.1h

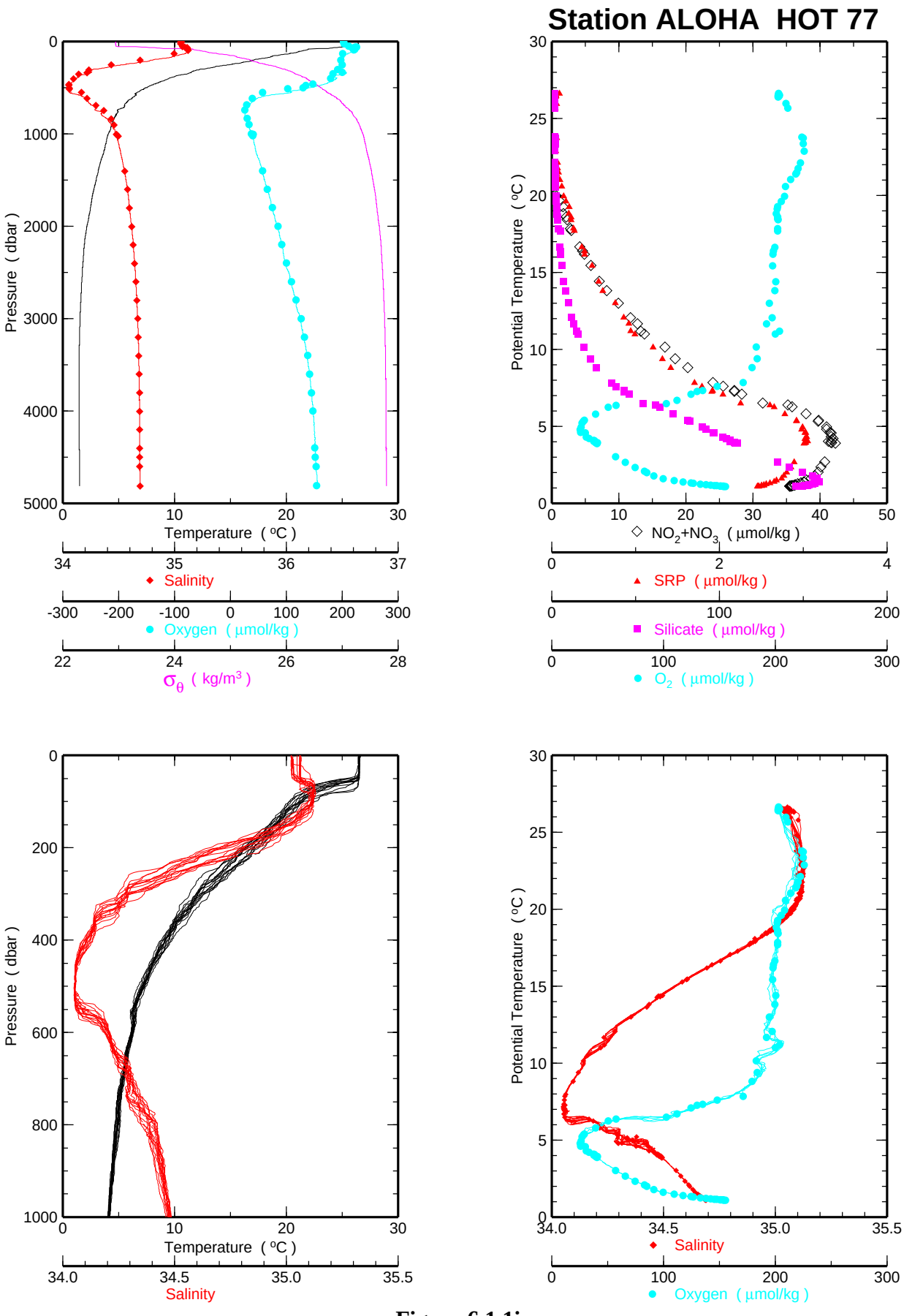
Station ALOHA HOT 77
Pressure (dbar)
Temperature (ºC)
Salinity
Oxygen (µmol/kg)
σθ (kg/m³)
Potential Temperature (ºC)
NO2+NO3 (µmol/kg)
SRP (µmol/kg)
Silicate (µmol/kg)
O2 (µmol/kg)

Figure 6.1.1i

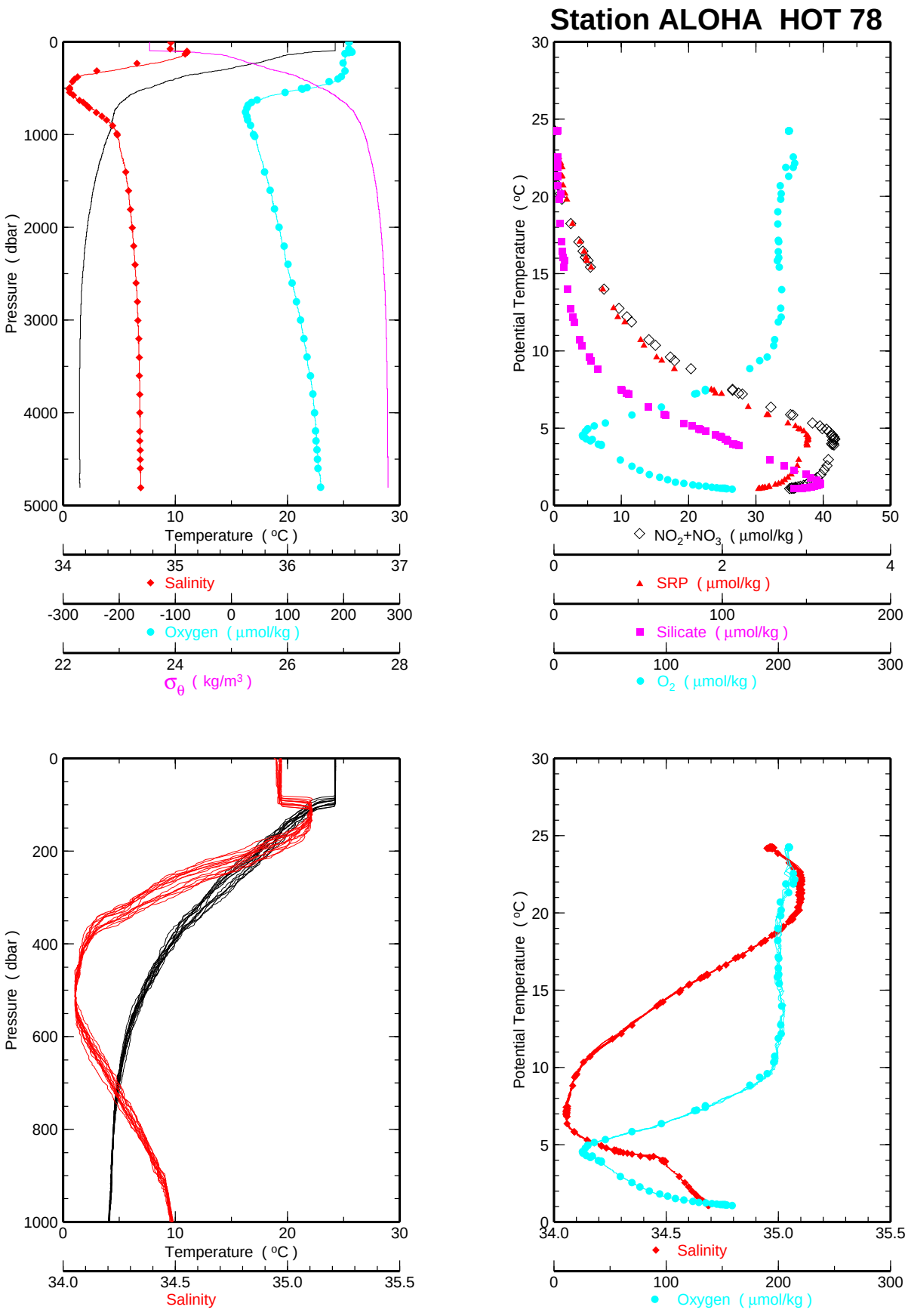
Station ALOHA HOT 78
Pressure (dbar)
Temperature (°C)
Salinity
Oxygen (µmol/kg)
σθ (kg/m³)
Potential Temperature (°C)
NO2+NO3 (µmol/kg)
SRP (µmol/kg)
Silicate (µmol/kg)
O2 (µmol/kg)

Figure 6.1.1j

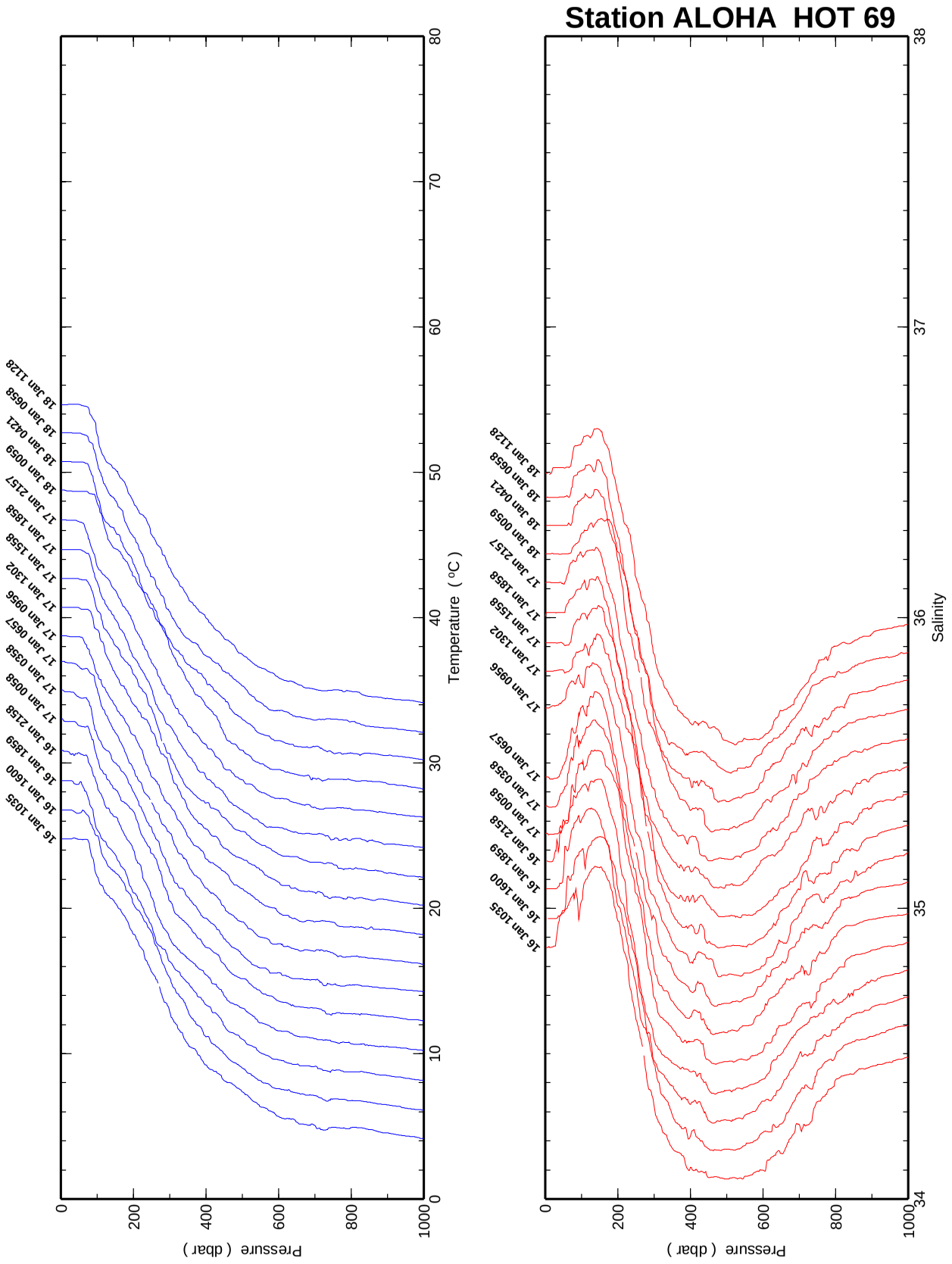
Station ALOHA HOT 69
Temperature (°C)
Salinity
Pressure (dbar)
Pressure (dbar)
18 Jan 1128
18 Jan 0658
18 Jan 0421
18 Jan 0059
17 Jan 2157
17 Jan 1858
17 Jan 1558
17 Jan 1302
17 Jan 0956
17 Jan 0657
17 Jan 0358
17 Jan 0058
16 Jan 2158
16 Jan 1859
16 Jan 1600
16 Jan 1035

Figure 6.1.2a

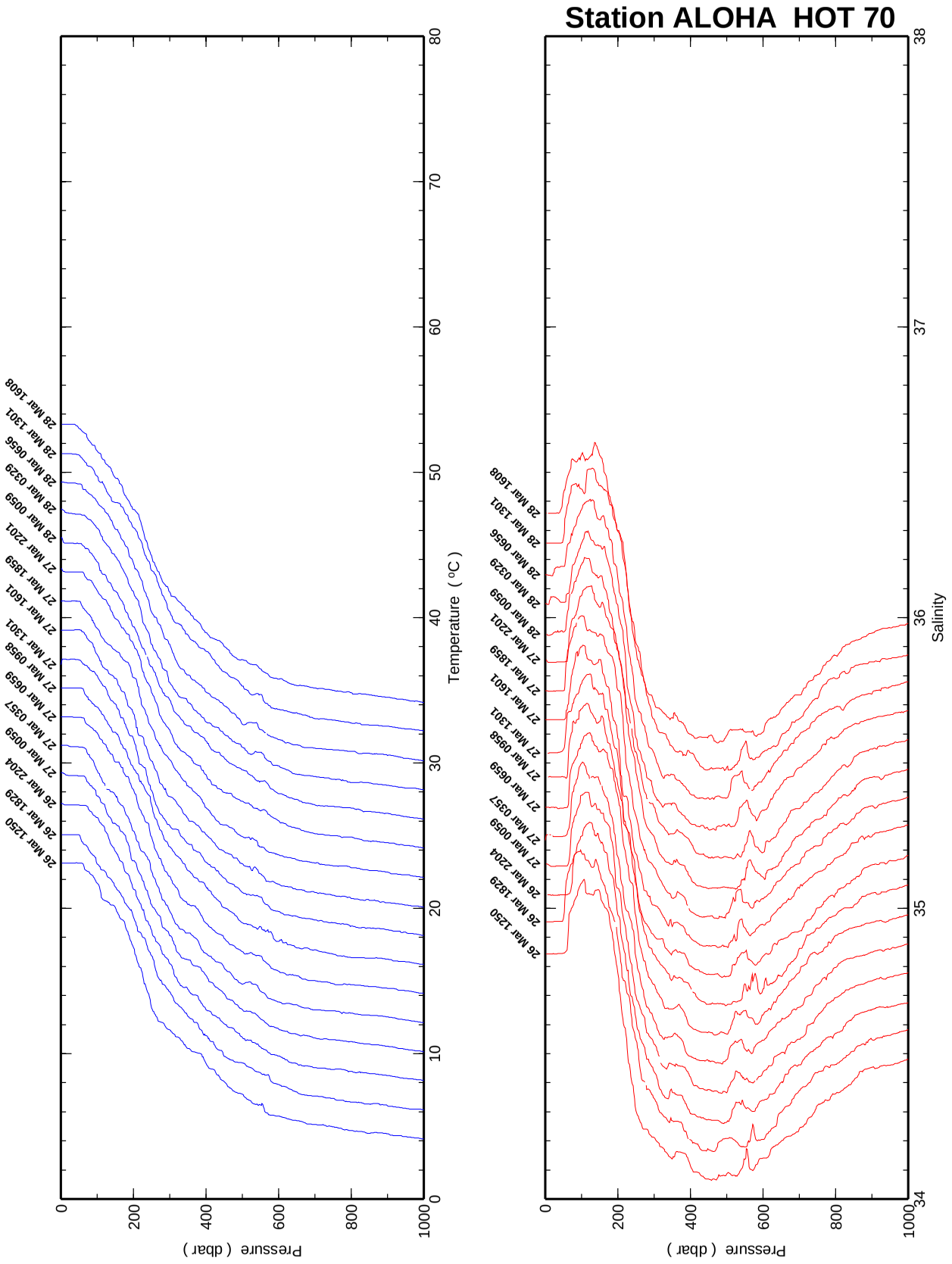
Station ALOHA HOT 70
Temperature (°C)
Salinity
Pressure (dbar)
Pressure (dbar)
28 Mar 1608
28 Mar 1301
28 Mar 0656
28 Mar 0329
28 Mar 0059
27 Mar 2201
27 Mar 1859
27 Mar 1601
27 Mar 1301
27 Mar 0958
27 Mar 0659
27 Mar 0357
27 Mar 0059
26 Mar 2204
26 Mar 1829
26 Mar 1250

Figure 6.1.2b

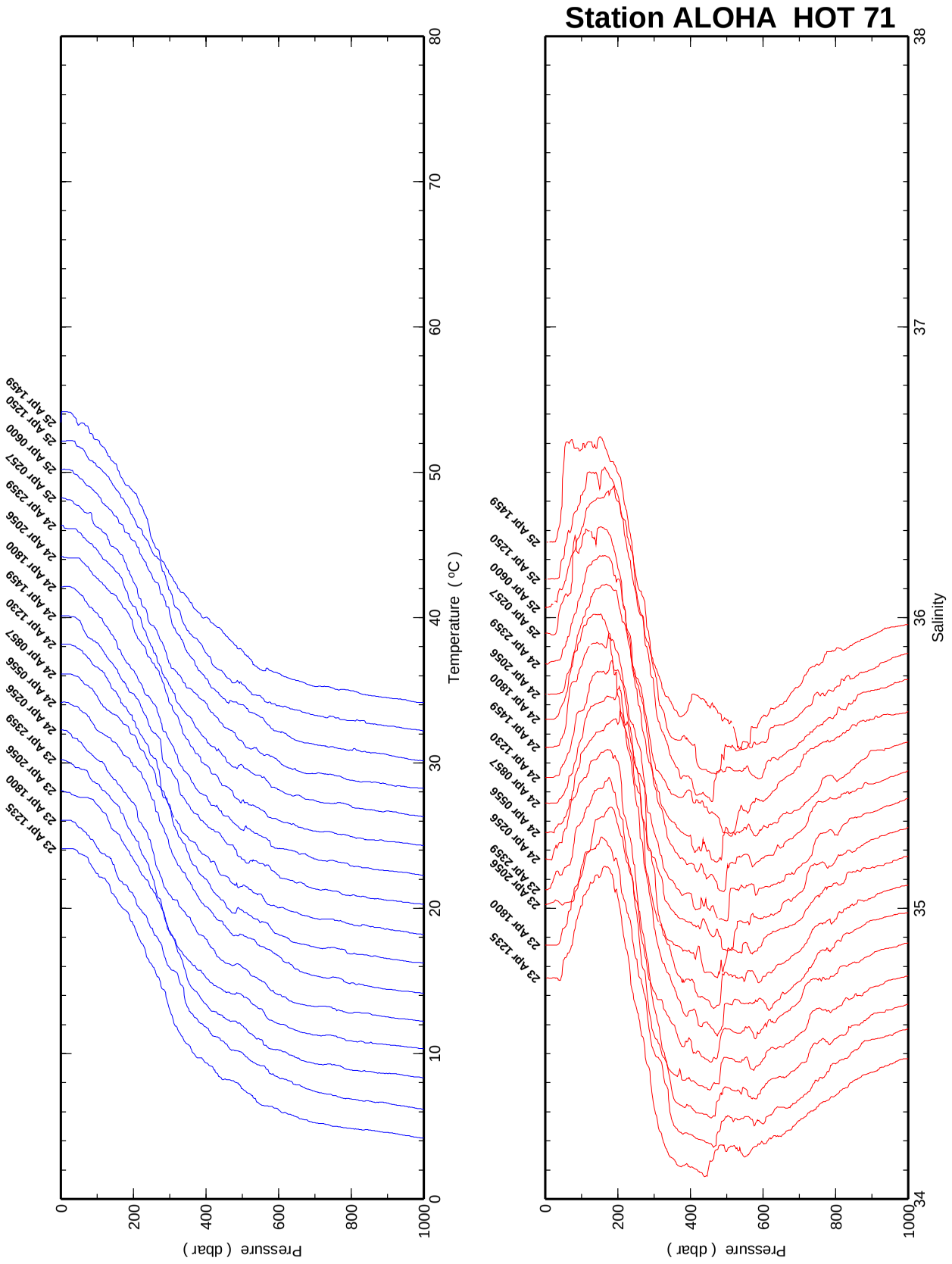
Station ALOHA HOT 71
Temperature (°C)
Salinity
Pressure (dbar)
Pressure (dbar)
25 Apr 1459
25 Apr 1250
25 Apr 0600
25 Apr 0257
25 Apr 2359
24 Apr 2056
24 Apr 1800
24 Apr 1459
24 Apr 1230
24 Apr 0857
24 Apr 0556
24 Apr 0256
24 Apr 2359
23 Apr 2056
23 Apr 1800
23 Apr 1235

Figure 6.1.2c

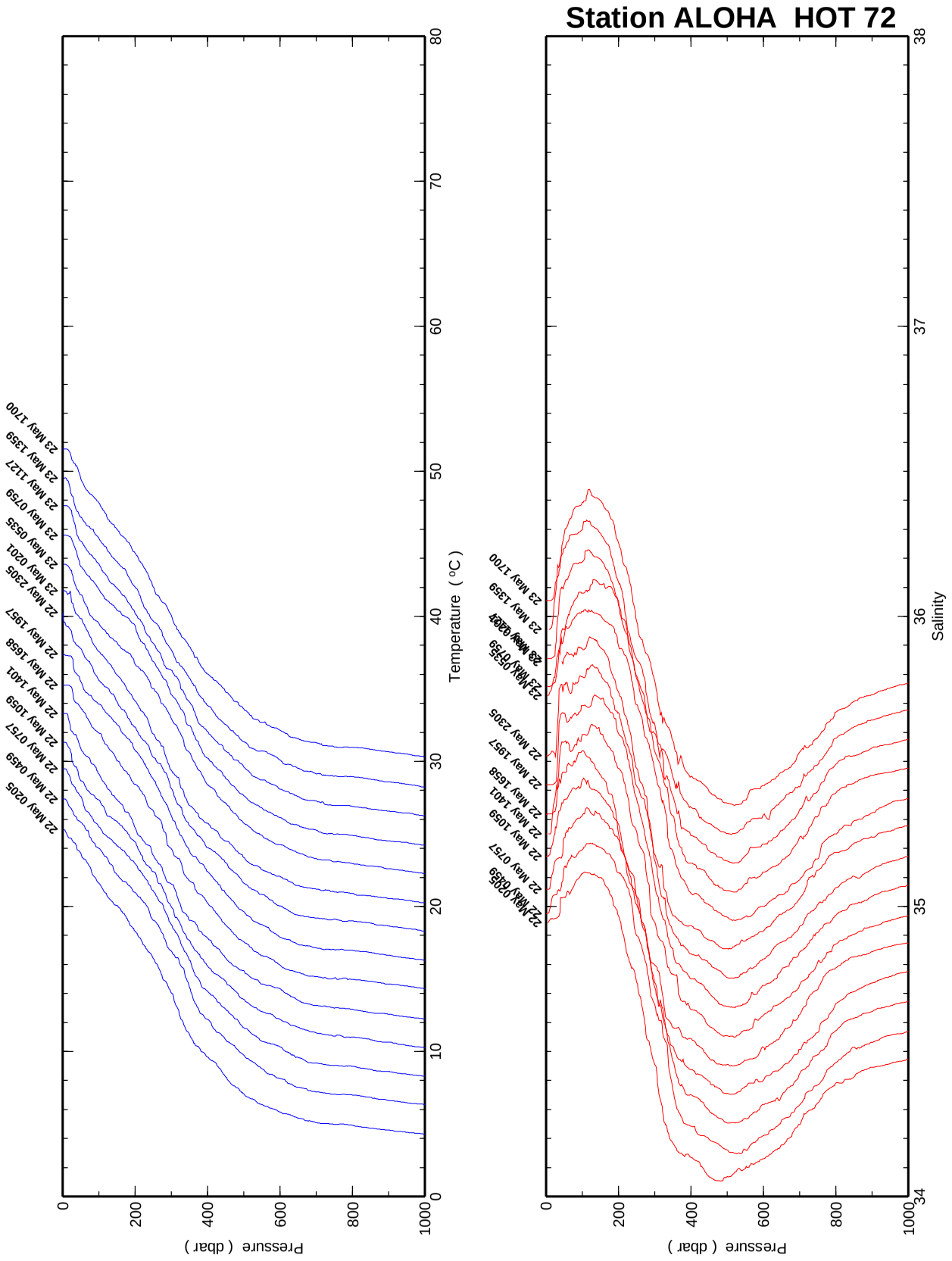
Station ALOHA HOT 72
Pressure (dbar)
Temperature (°C)
Salinity
0
200
400
600
800
1000
0
10
20
30
40
50
60
70
80
34
35
36
37
38
22 May 0205
22 May 0459
22 May 0757
22 May 1059
22 May 1401
22 May 1658
22 May 1957
22 May 2305
23 May 0201
23 May 0535
23 May 0759
23 May 1127
23 May 1359
23 May 1700

Figure 6.1.2d

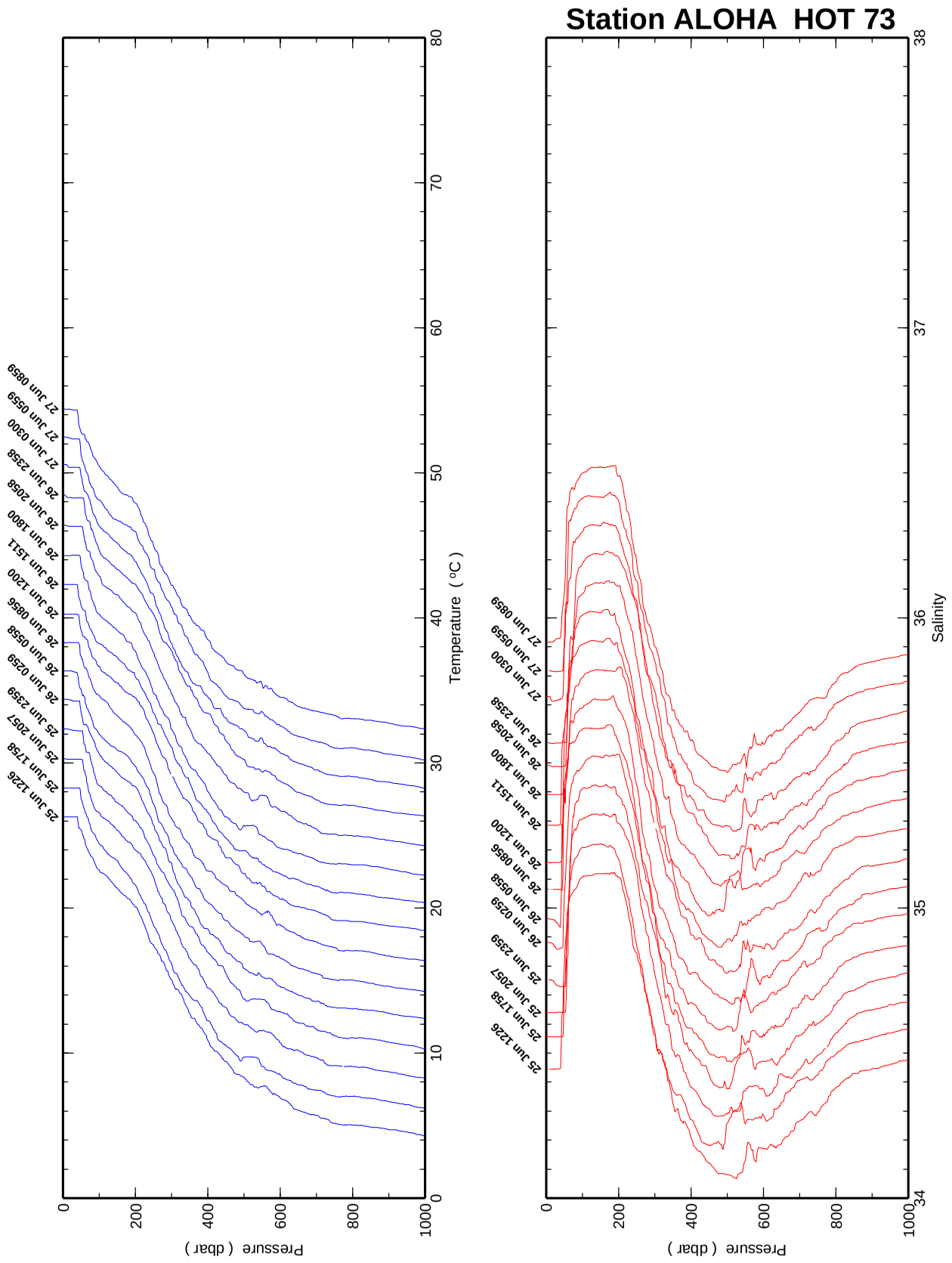
Station ALOHA HOT 73
Temperature (°C)
Salinity
Pressure (dbar)
Pressure (dbar)
27 Jun 0859
27 Jun 0559
27 Jun 0300
26 Jun 2358
26 Jun 2058
26 Jun 1800
26 Jun 1512
26 Jun 1200
26 Jun 0856
26 Jun 0558
26 Jun 0259
25 Jun 2359
25 Jun 2057
25 Jun 1758
25 Jun 1226

Figure 6.1.2e

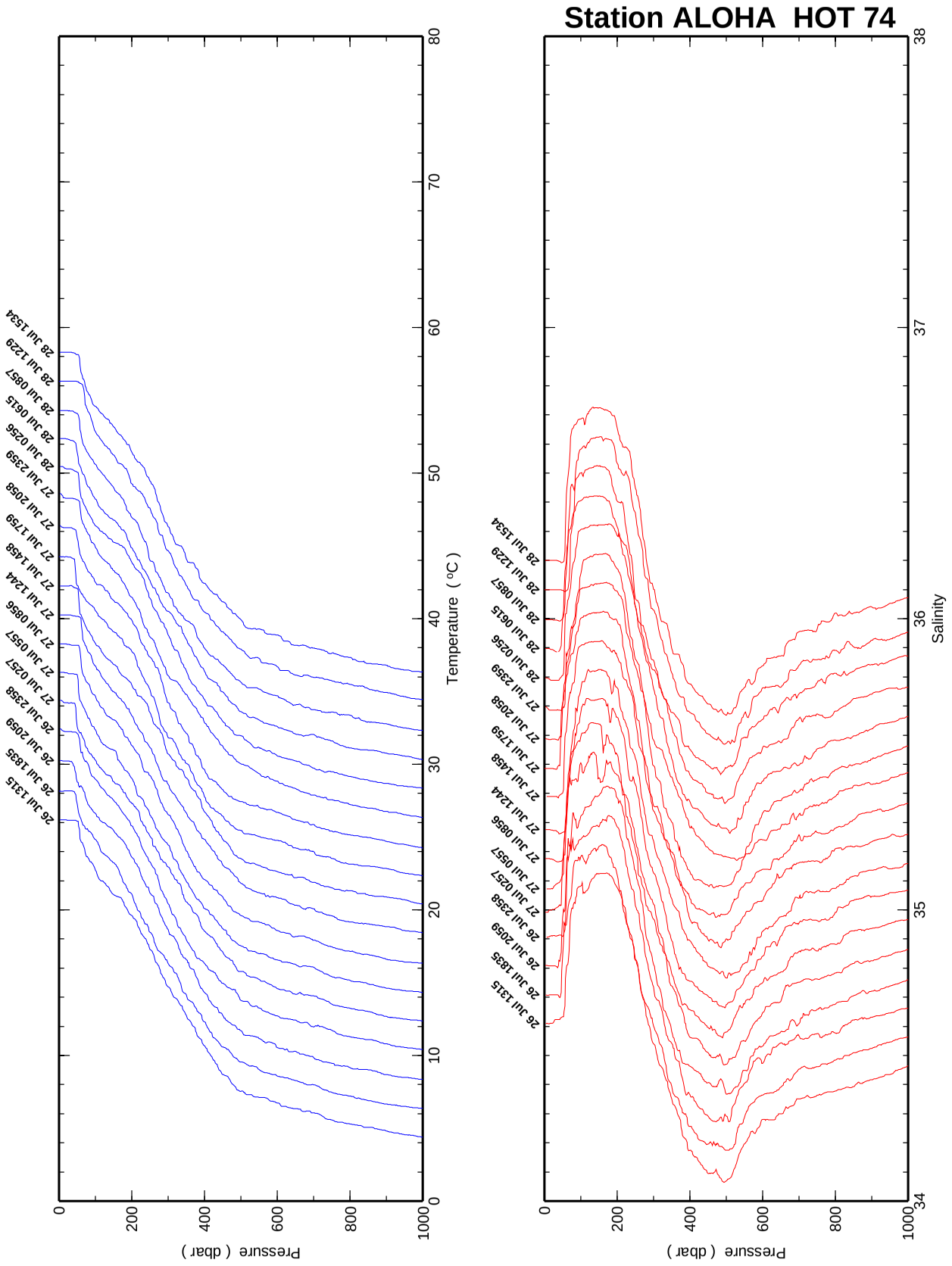
Station ALOHA HOT 74
Temperature (°C)
Salinity
Pressure (dbar)
Pressure (dbar)
0
10
20
30
40
50
60
70
80
34
35
36
37
38
0
200
400
600
800
1000
28 Jul 1534
28 Jul 1229
28 Jul 0857
28 Jul 0615
28 Jul 0256
27 Jul 2359
27 Jul 2058
27 Jul 1759
27 Jul 1458
27 Jul 1244
27 Jul 0856
27 Jul 0557
27 Jul 0257
26 Jul 2358
26 Jul 2059
26 Jul 1835
26 Jul 1315

Figure 6.1.2f

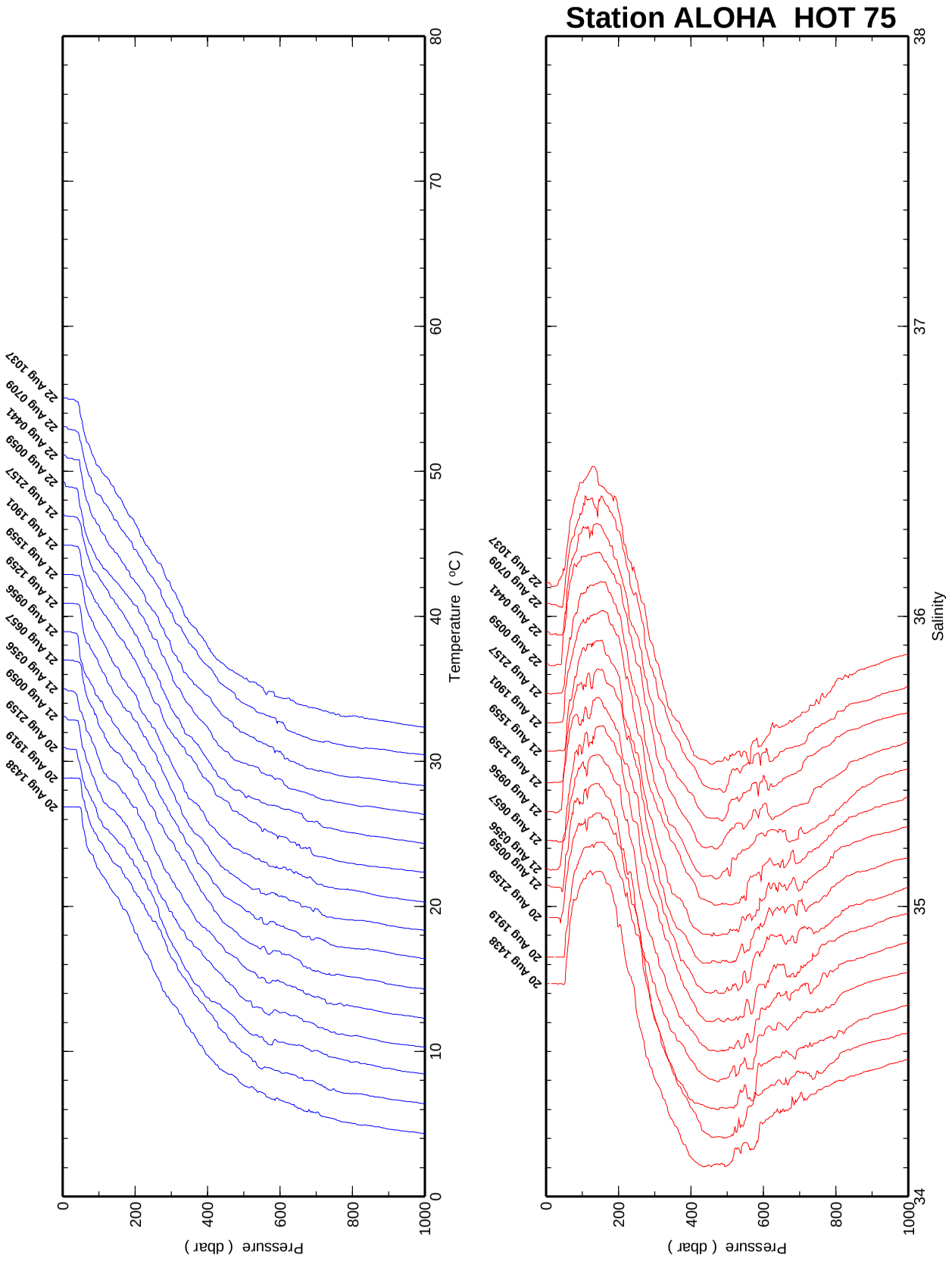
Station ALOHA HOT 75
Pressure (dbar)
Temperature (°C)
Salinity
20 Aug 1438
20 Aug 1919
20 Aug 2159
21 Aug 0059
21 Aug 0356
21 Aug 0657
21 Aug 0956
21 Aug 1259
21 Aug 1559
21 Aug 1901
21 Aug 2157
22 Aug 0059
22 Aug 0441
22 Aug 0709
22 Aug 1037

Figure 6.1.2g

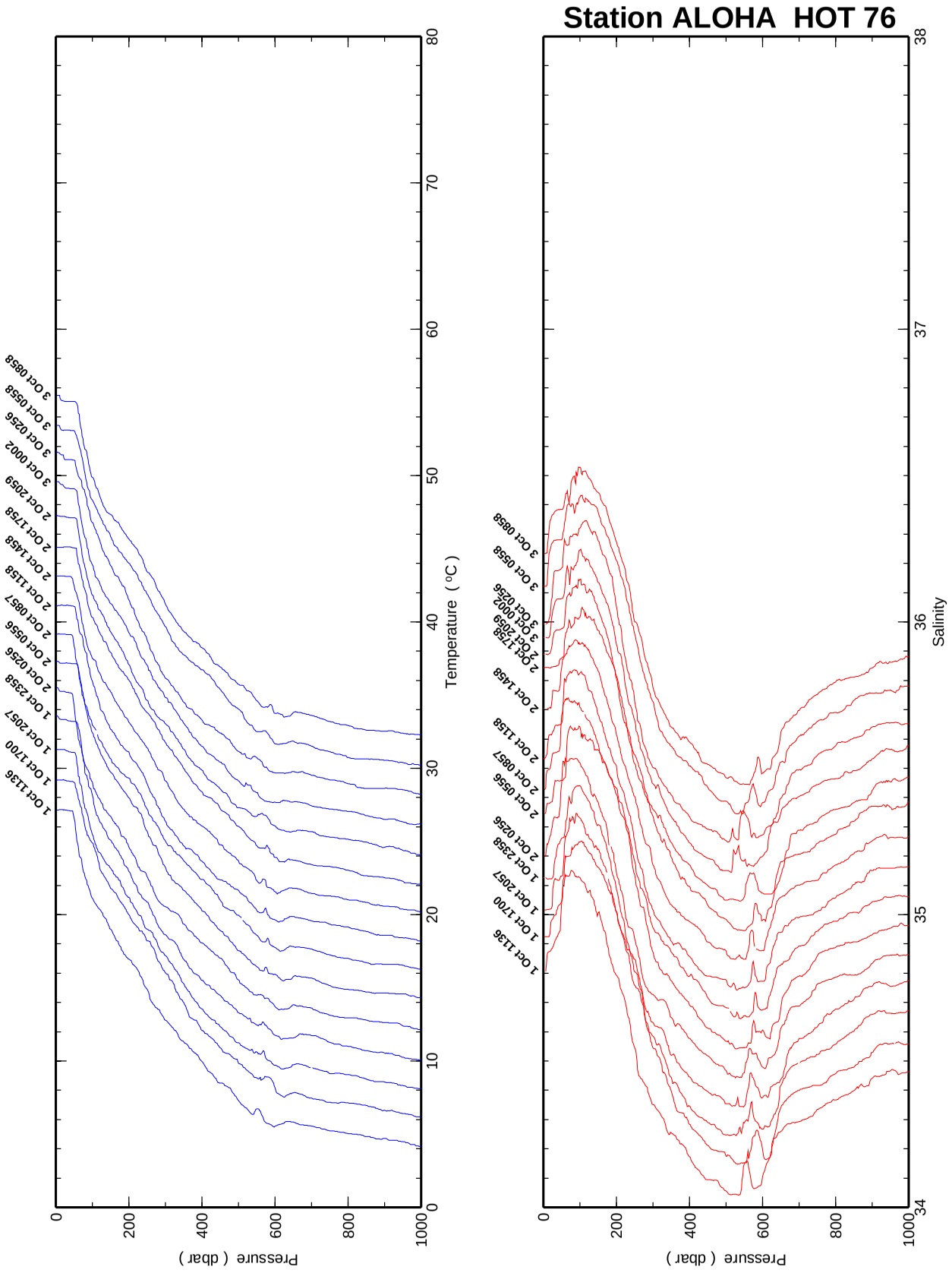
Station ALOHA HOT 76
Temperature (°C)
Salinity
Pressure (dbar)
Pressure (dbar)
3 Oct 0858
3 Oct 0558
3 Oct 0256
3 Oct 0002
2 Oct 2059
2 Oct 1758
2 Oct 1458
2 Oct 1158
2 Oct 0857
2 Oct 0556
2 Oct 0256
2 Oct 2358
1 Oct 2057
1 Oct 1700
1 Oct 1136

Figure 6.1.2h

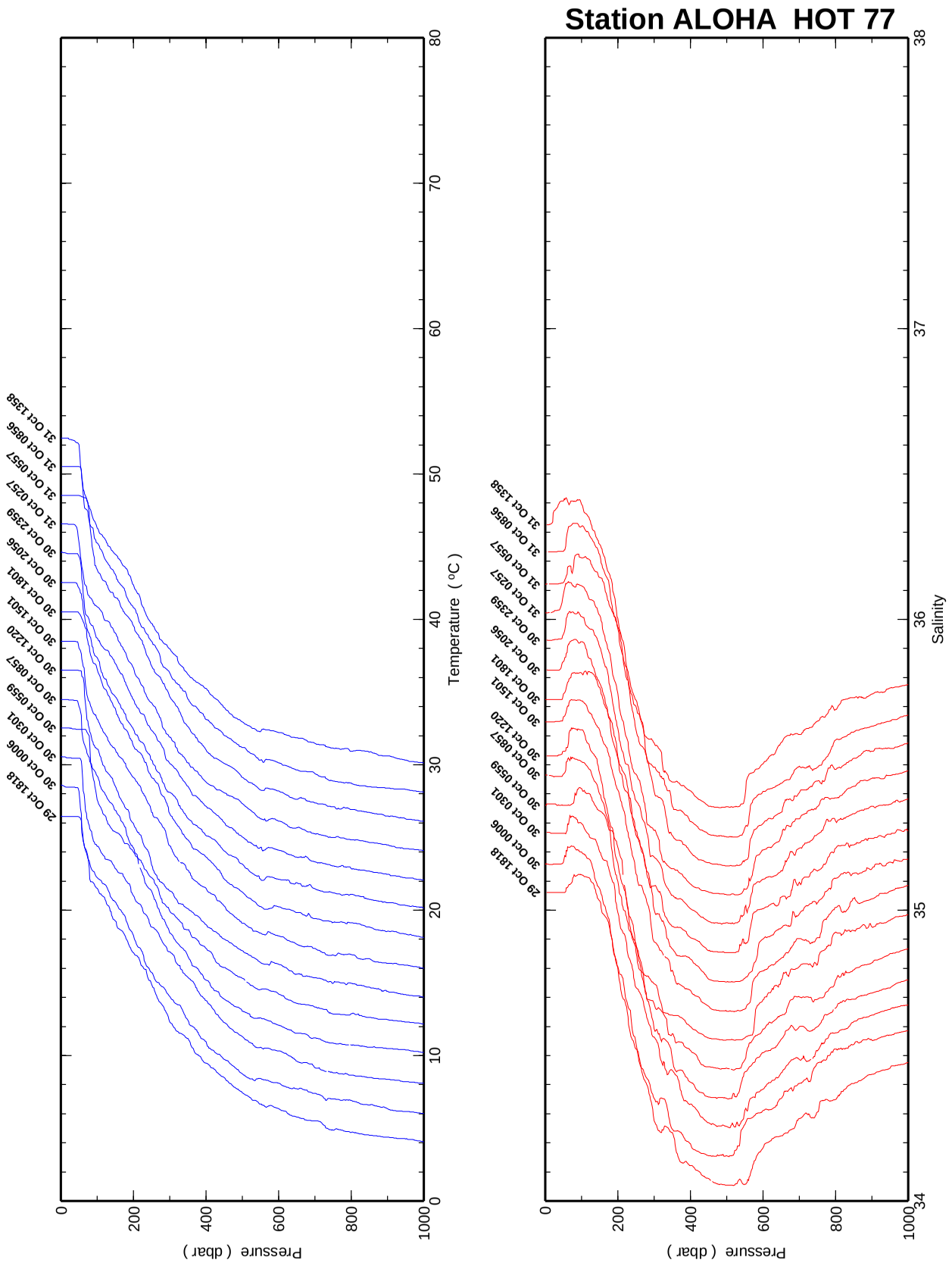
Station ALOHA HOT 77
Temperature (°C)
Salinity
Pressure (dbar)
Pressure (dbar)
31 Oct 1358
31 Oct 0856
31 Oct 0557
31 Oct 0257
31 Oct 2359
30 Oct 2056
30 Oct 1801
30 Oct 1501
30 Oct 1220
30 Oct 0857
30 Oct 0559
30 Oct 0301
30 Oct 0006
29 Oct 1818

Figure 6.1.2i

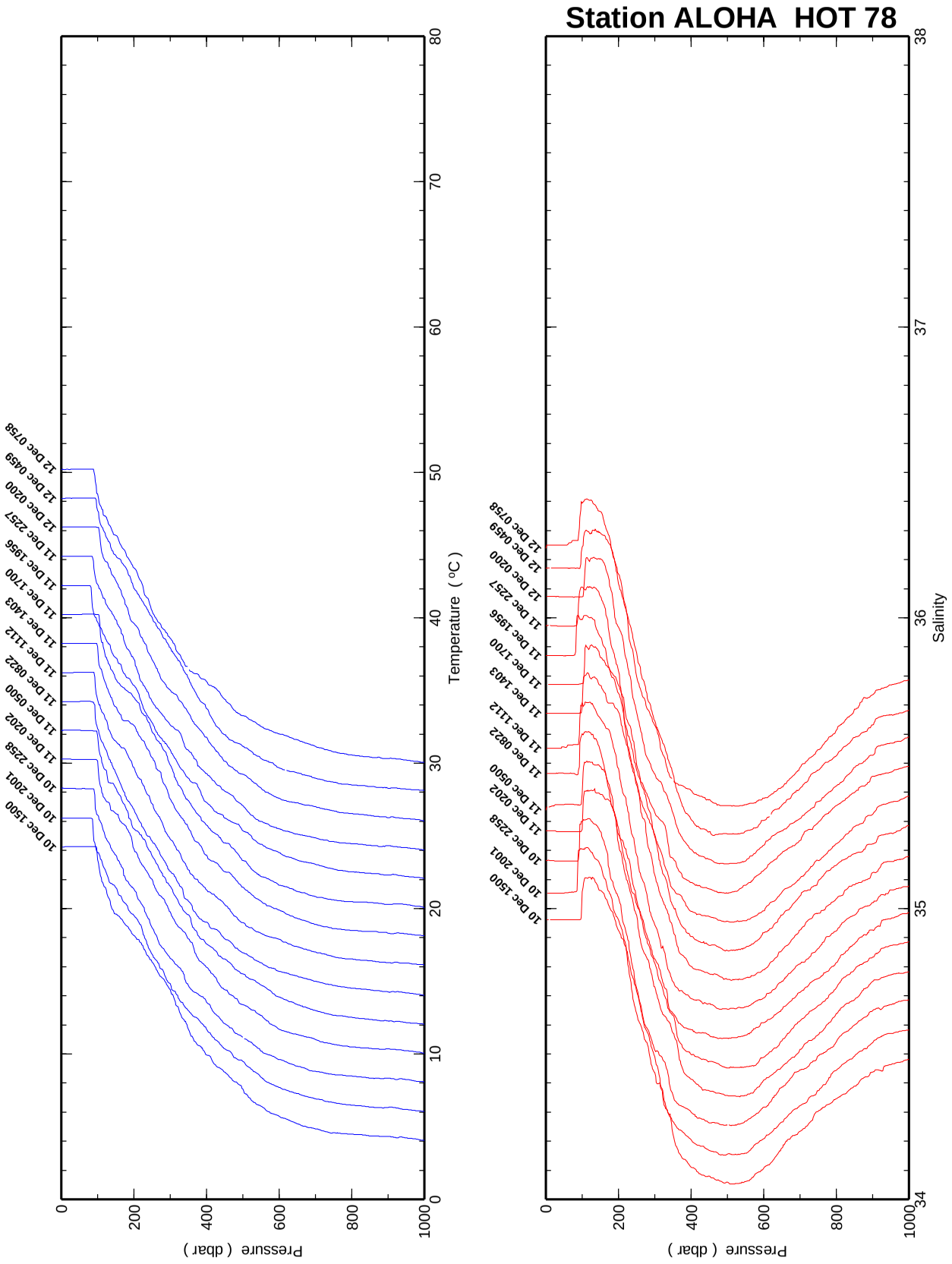
Station ALOHA HOT 78
Temperature (°C)
Salinity
Pressure (dbar)
Pressure (dbar)
10 Dec 1500
10 Dec 2001
10 Dec 2258
11 Dec 0202
11 Dec 0500
11 Dec 0822
11 Dec 1112
11 Dec 1403
11 Dec 1700
11 Dec 1956
11 Dec 2257
12 Dec 0200
12 Dec 0459
12 Dec 0758

Figure 6.1.2j

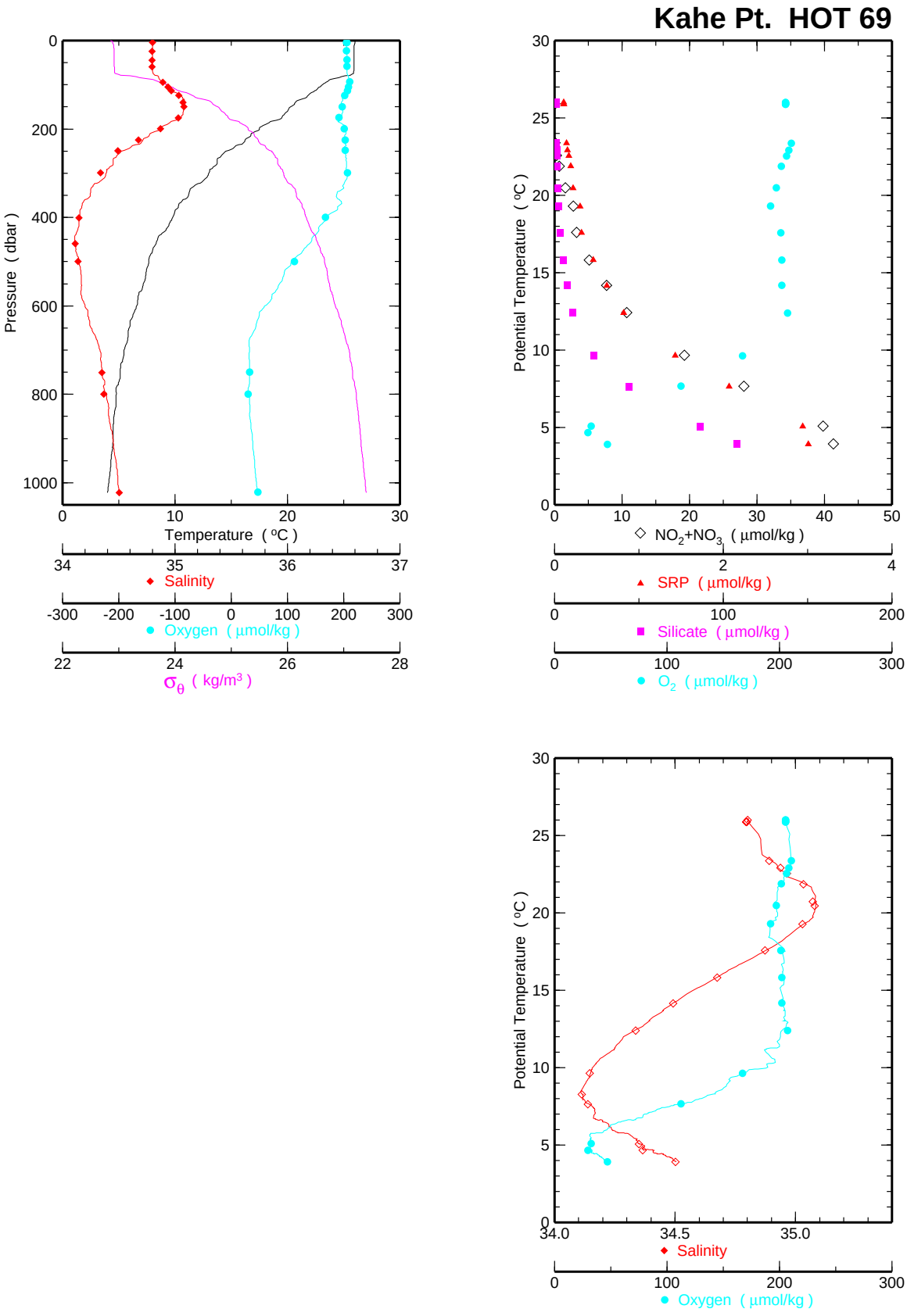
Kahe Pt. HOT 69
Pressure (dbar)
Temperature (ºC)
Salinity
Oxygen (µmol/kg)
σθ (kg/m³)
Potential Temperature (ºC)
NO2+NO3 (µmol/kg)
SRP (µmol/kg)
Silicate (µmol/kg)
O2 (µmol/kg)
Potential Temperature (ºC)
Salinity
Oxygen (µmol/kg)

Figure 6.1.3a

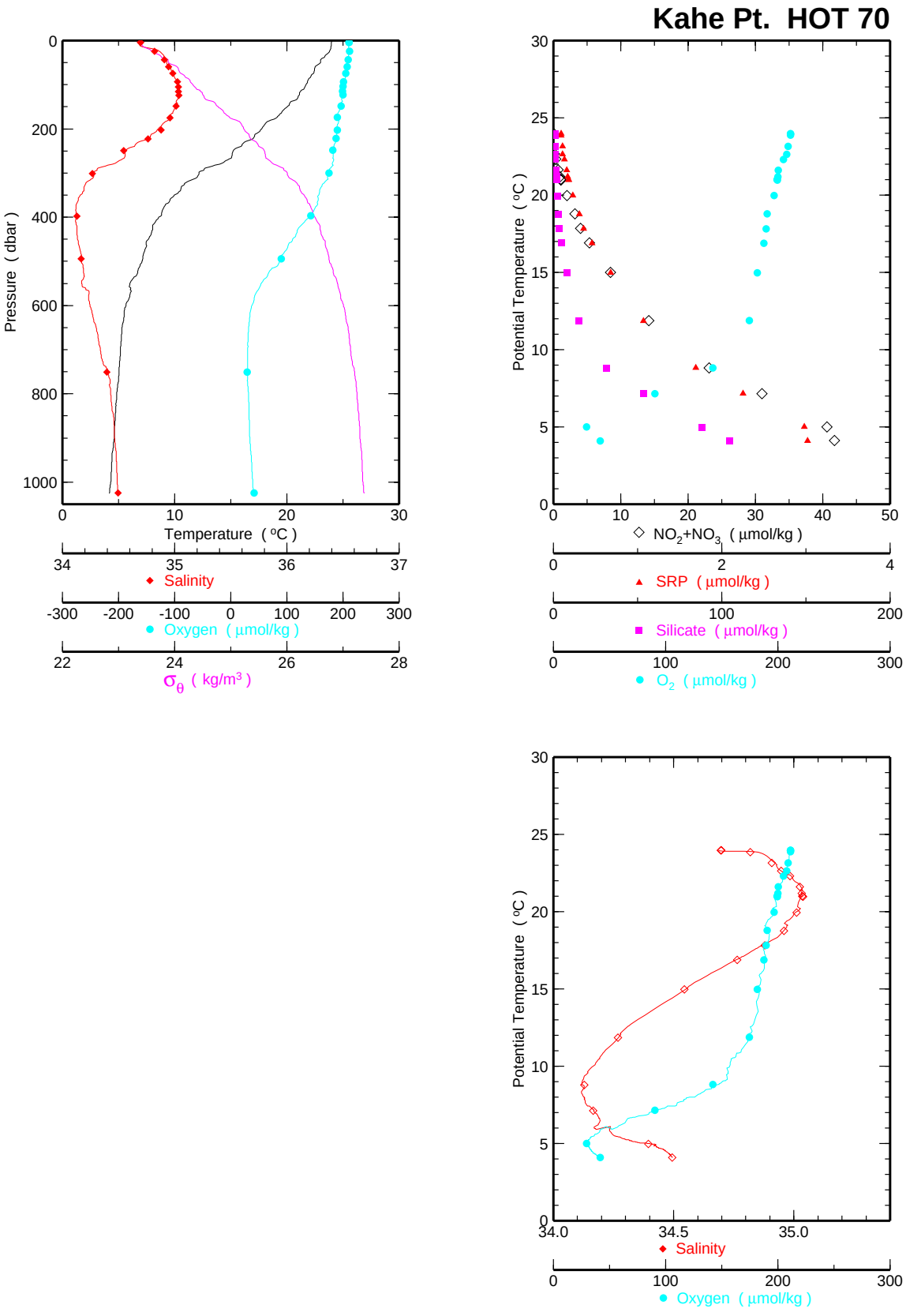
Kahe Pt. HOT 70
Pressure (dbar)
Temperature (°C)
Salinity
Oxygen (µmol/kg)
σθ (kg/m3)
Potential Temperature (°C)
NO2+NO3 (µmol/kg)
SRP (µmol/kg)
Silicate (µmol/kg)
O2 (µmol/kg)
Potential Temperature (°C)
Salinity
Oxygen (µmol/kg)

Figure 6.1.3b

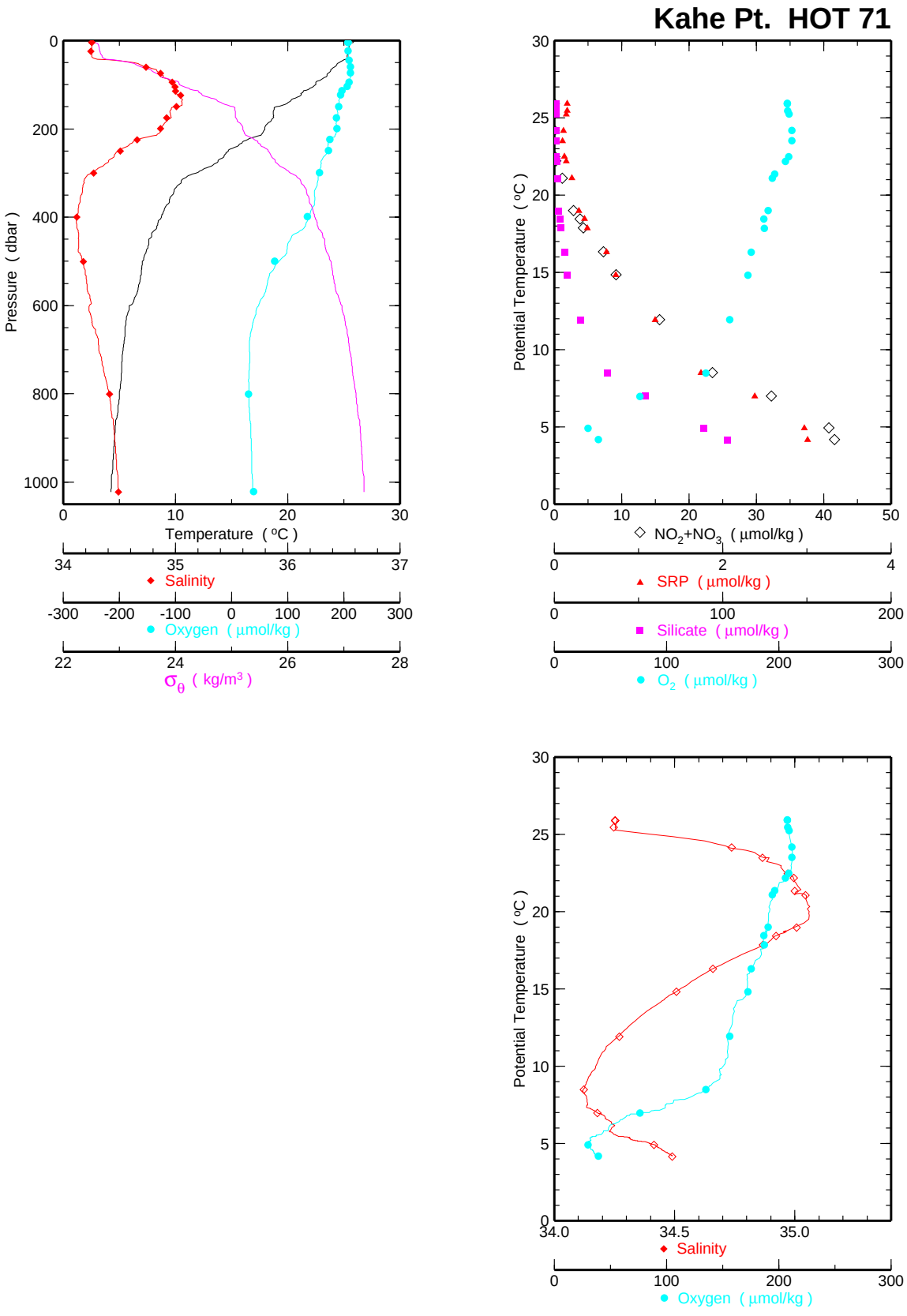
Kahe Pt. HOT 71
Pressure (dbar)
Temperature (ºC)
Salinity
Oxygen (µmol/kg)
σθ (kg/m3)
Potential Temperature (ºC)
NO2+NO3 (µmol/kg)
SRP (µmol/kg)
Silicate (µmol/kg)
O2 (µmol/kg)
Potential Temperature (ºC)
Salinity
Oxygen (µmol/kg)

Figure 6.1.3c

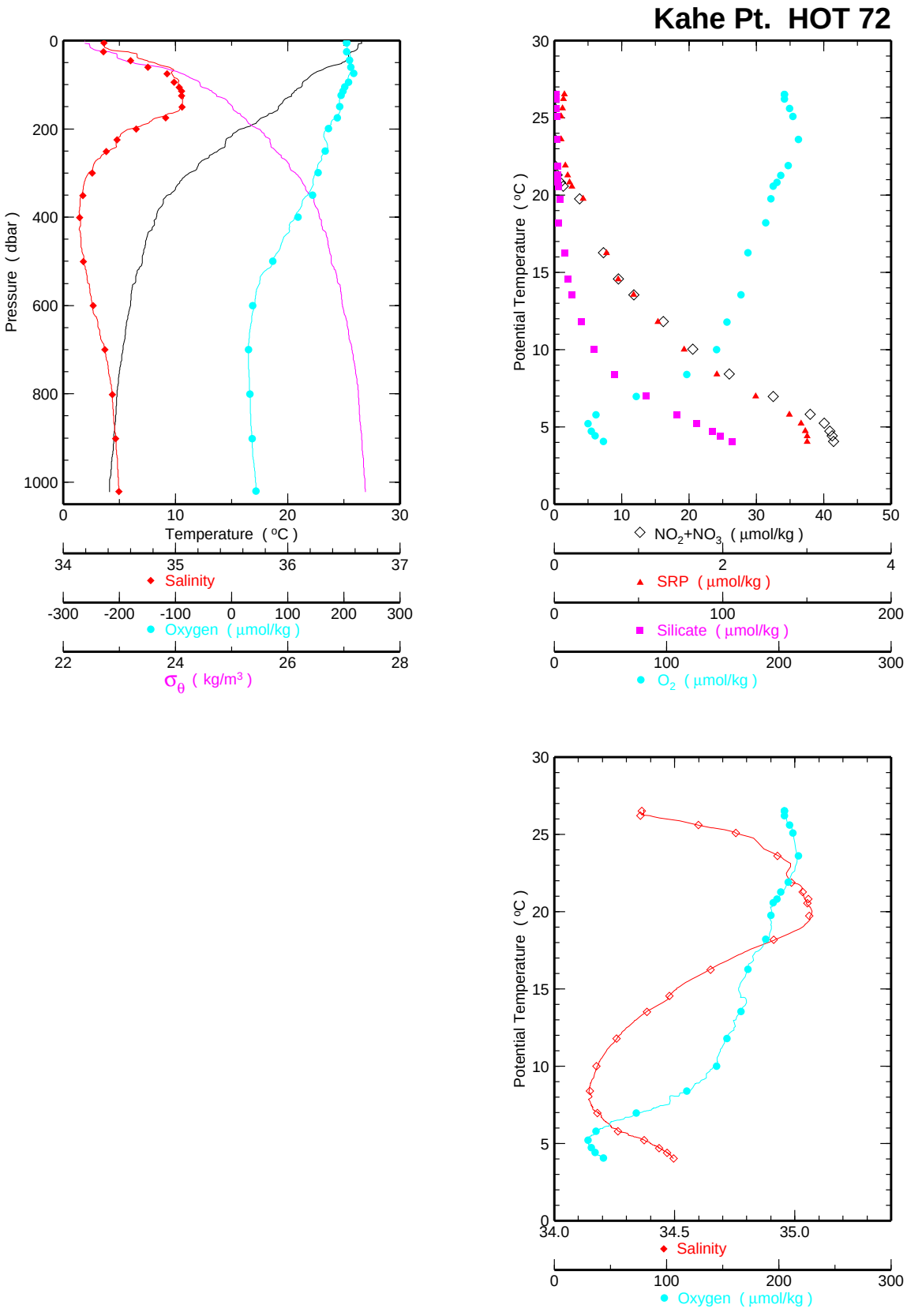
Kahe Pt. HOT 72
Pressure (dbar)
Temperature (°C)
Salinity
Oxygen (µmol/kg)
σθ (kg/m3)
Potential Temperature (°C)
NO2+NO3 (µmol/kg)
SRP (µmol/kg)
Silicate (µmol/kg)
O2 (µmol/kg)
Potential Temperature (°C)
Salinity
Oxygen (µmol/kg)

Figure 6.1.3d

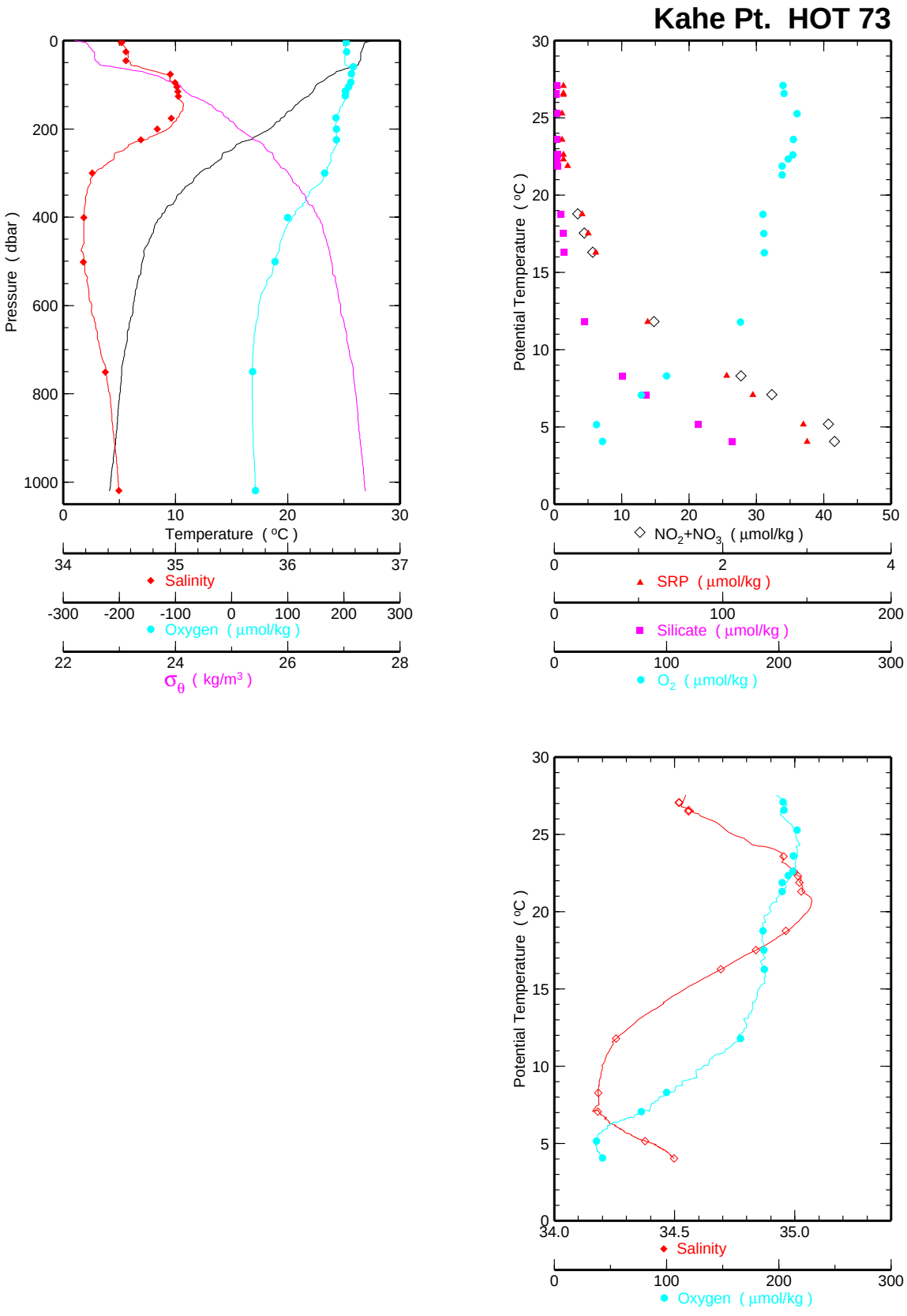
Kahe Pt. HOT 73
Pressure (dbar)
Temperature (°C)
Salinity
Oxygen (µmol/kg)
σθ (kg/m3)
Potential Temperature (°C)
NO2+NO3 (µmol/kg)
SRP (µmol/kg)
Silicate (µmol/kg)
O2 (µmol/kg)
Potential Temperature (°C)
Salinity
Oxygen (µmol/kg)

Figure 6.1.3e

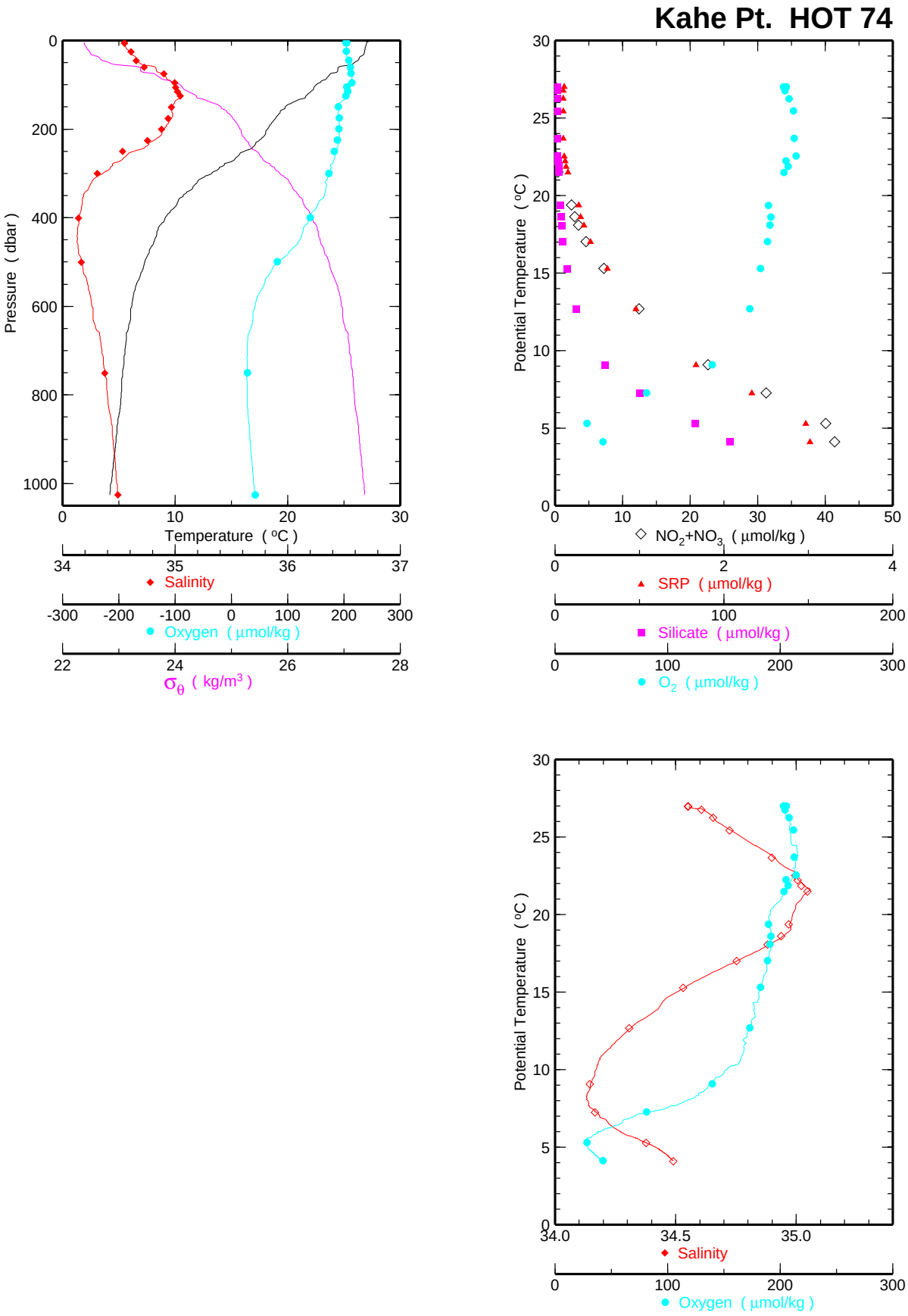
Kahe Pt. HOT 74
Pressure (dbar)
Temperature (°C)
Salinity
Oxygen (µmol/kg)
σθ (kg/m3)
Potential Temperature (°C)
NO2+NO3 (µmol/kg)
SRP (µmol/kg)
Silicate (µmol/kg)
O2 (µmol/kg)
Potential Temperature (°C)
Salinity
Oxygen (µmol/kg)

Figure 6.1.3f

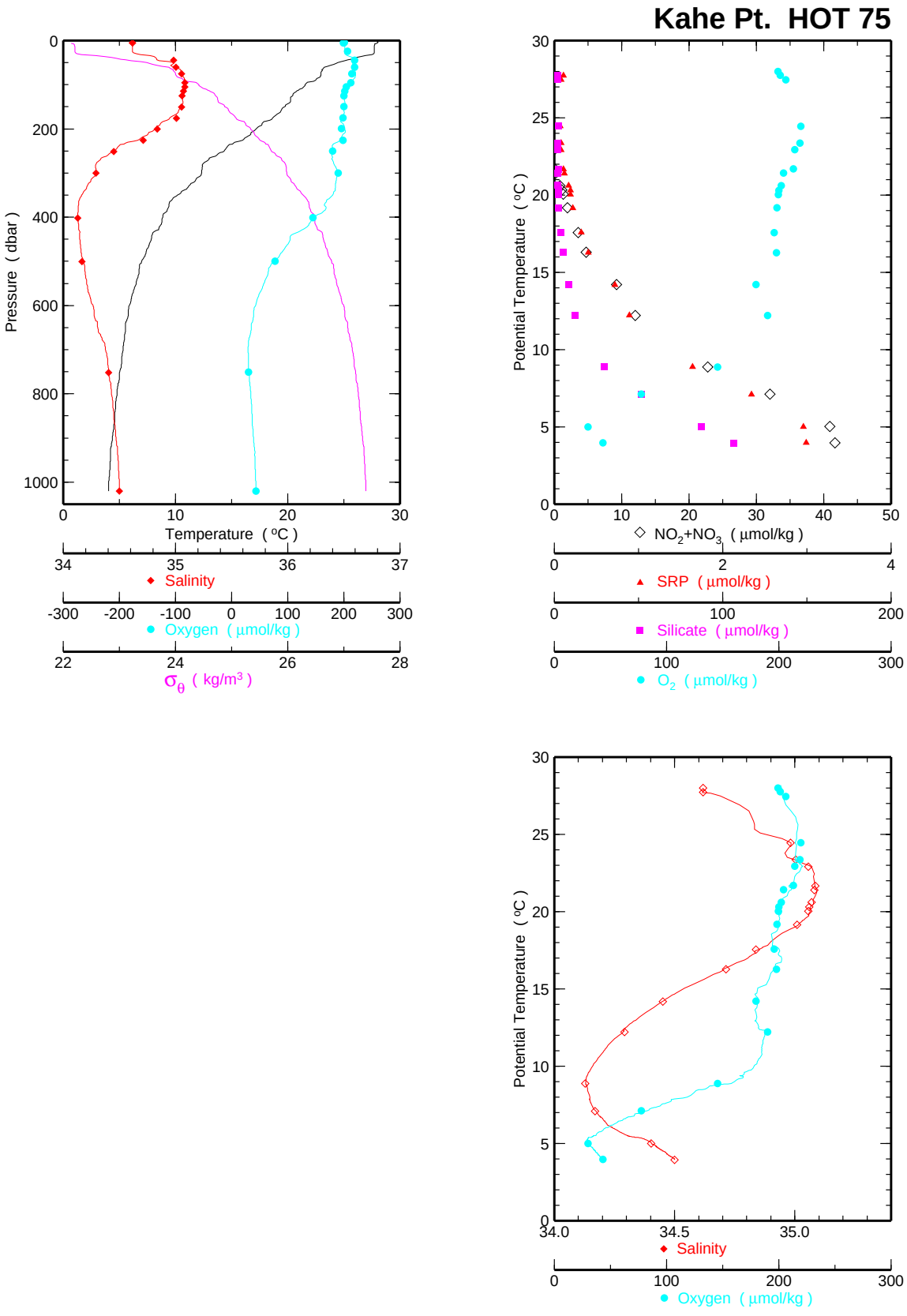
Kahe Pt. HOT 75
Pressure (dbar)
Temperature (ºC)
Salinity
Oxygen (µmol/kg)
σθ (kg/m3)
Potential Temperature (ºC)
NO2+NO3 (µmol/kg)
SRP (µmol/kg)
Silicate (µmol/kg)
O2 (µmol/kg)
Potential Temperature (ºC)
Salinity
Oxygen (µmol/kg)

Figure 6.1.3g

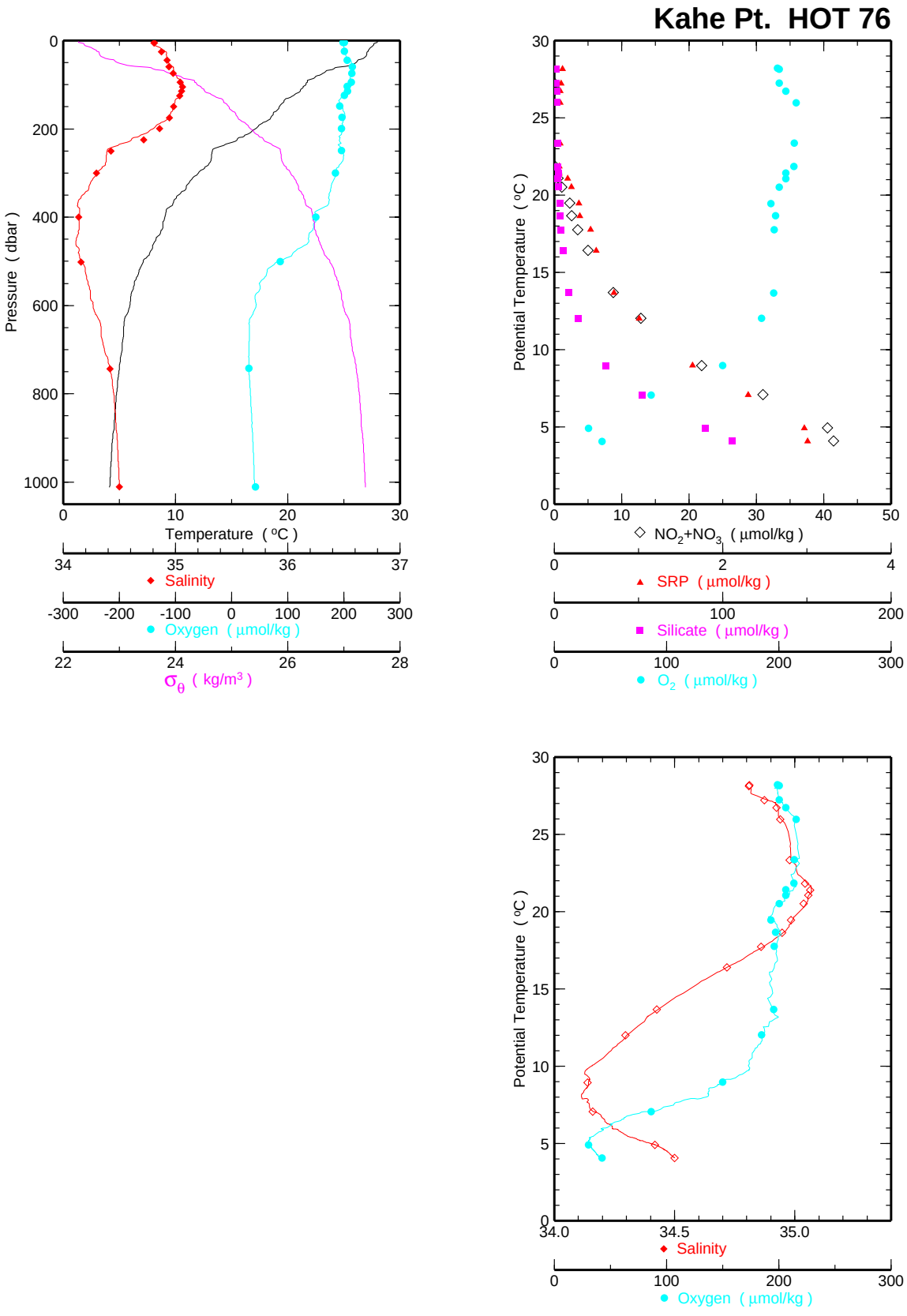
Kahe Pt. HOT 76
Pressure (dbar)
Temperature (°C)
Salinity
Oxygen (µmol/kg)
σθ (kg/m3)
Potential Temperature (°C)
NO2+NO3 (µmol/kg)
SRP (µmol/kg)
Silicate (µmol/kg)
O2 (µmol/kg)
Potential Temperature (°C)
Salinity
Oxygen (µmol/kg)

Figure 6.1.3h

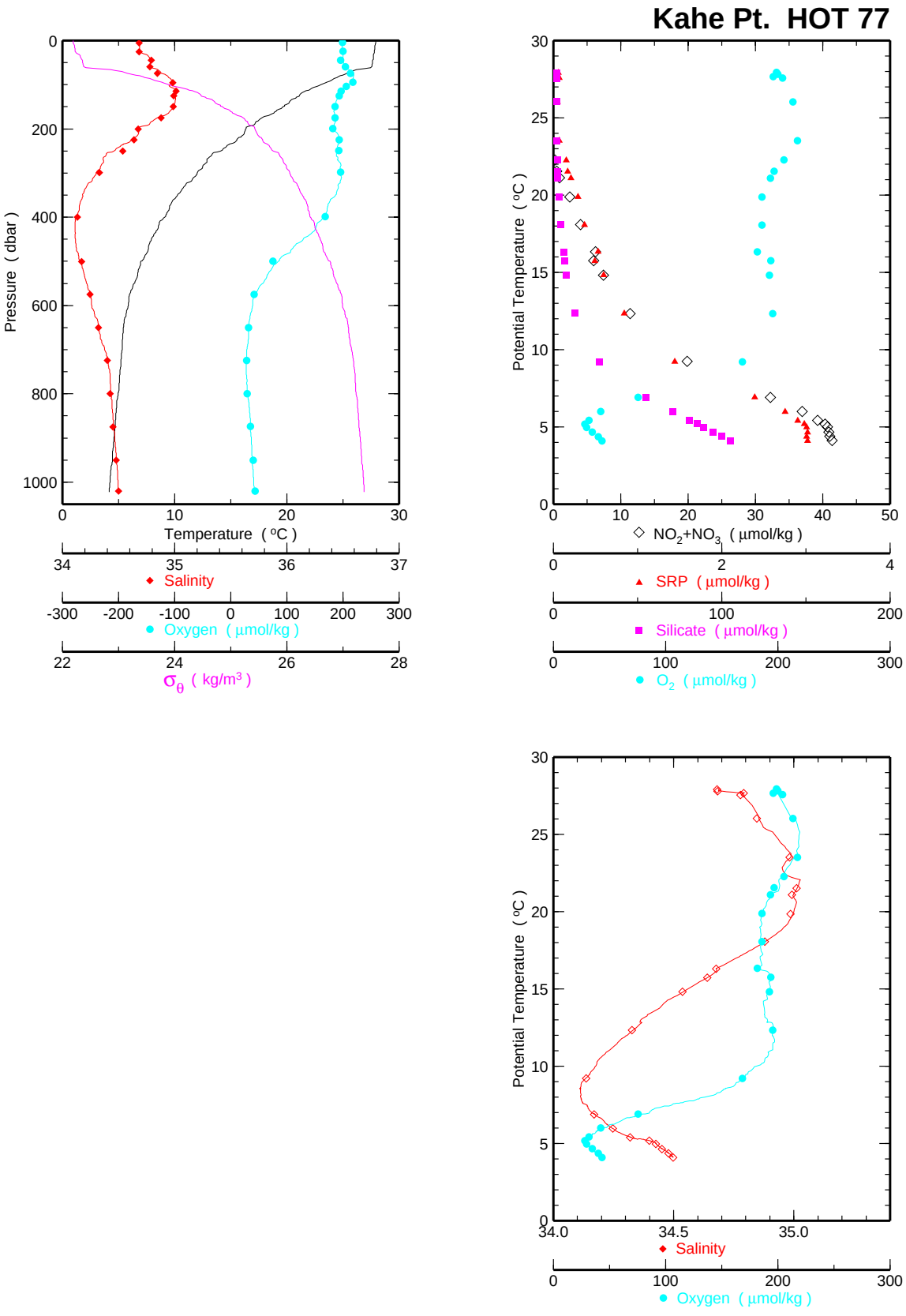
Kahe Pt. HOT 77
Pressure (dbar)
Temperature (°C)
Salinity
Oxygen (µmol/kg)
σθ (kg/m3)
Potential Temperature (°C)
NO2+NO3 (µmol/kg)
SRP (µmol/kg)
Silicate (µmol/kg)
O2 (µmol/kg)

Figure 6.1.3i

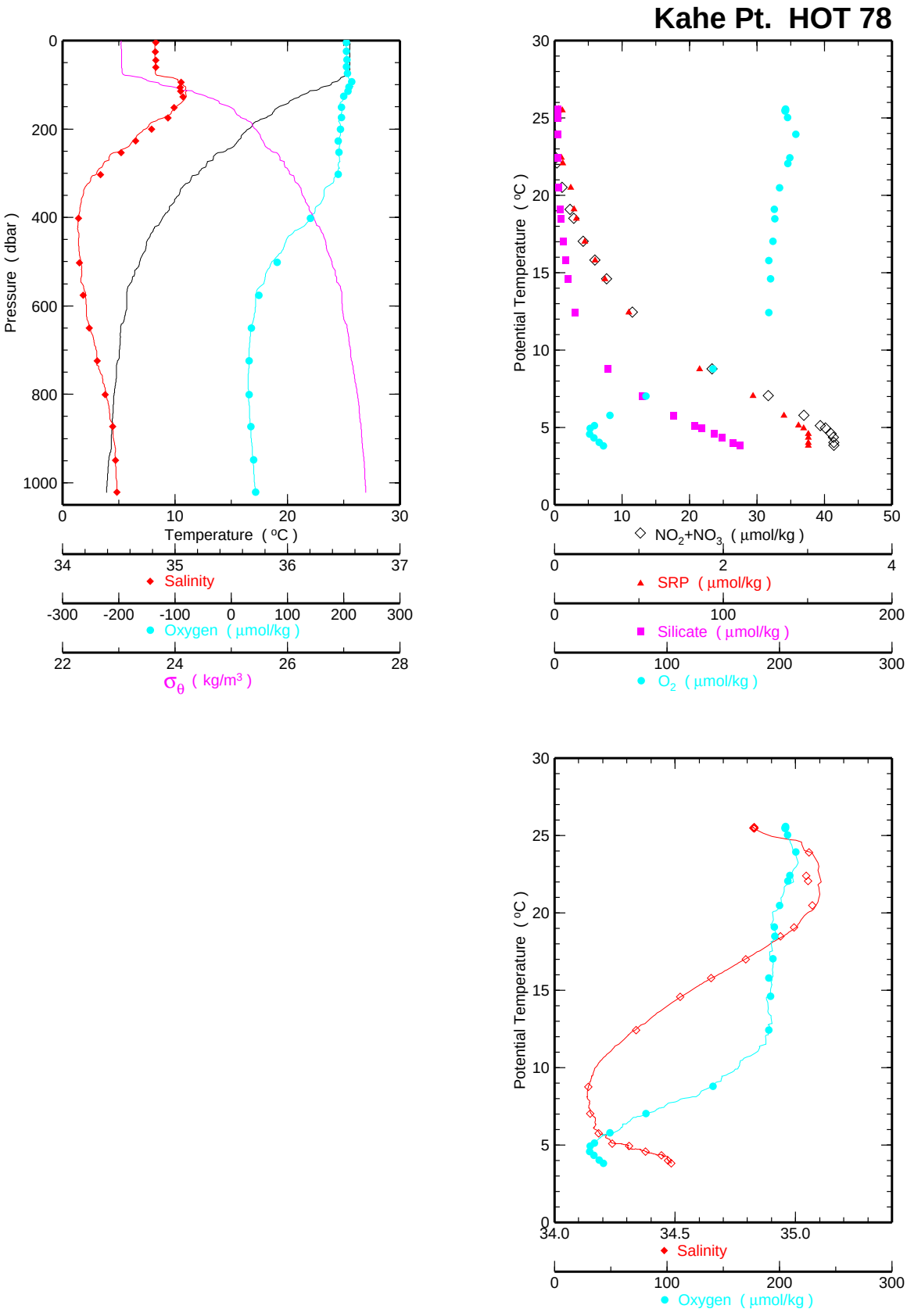
Kahe Pt. HOT 78
Pressure (dbar)
Temperature (ºC)
Salinity
Oxygen (µmol/kg)
σθ (kg/m³)
Potential Temperature (ºC)
NO2+NO3 (µmol/kg)
SRP (µmol/kg)
Silicate (µmol/kg)
O2 (µmol/kg)
Potential Temperature (ºC)
Salinity
Oxygen (µmol/kg)

Figure 6.1.3j

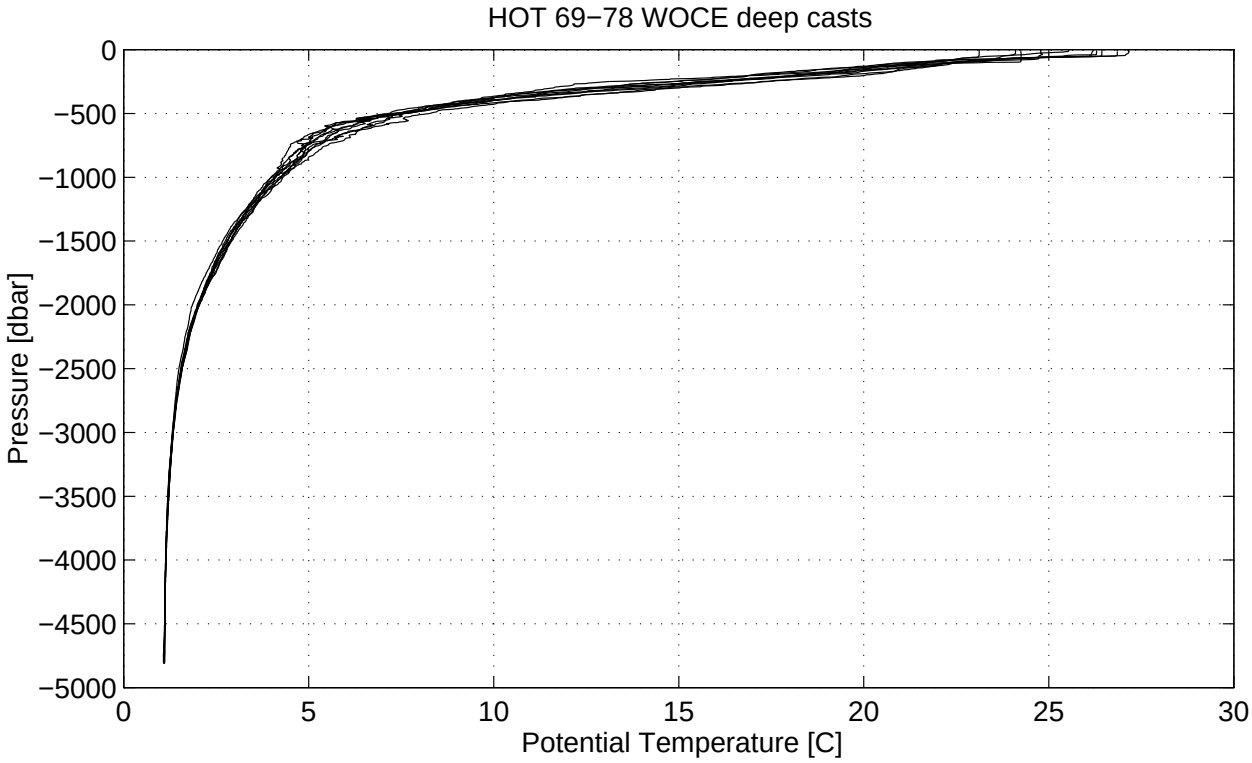
HOT 69−78 WOCE deep casts
Pressure [dbar]
Potential Temperature [C]
0
−500
−1000
−1500
−2000
−2500
−3000
−3500
−4000
−4500
−5000
0
5
10
15
20
25
30

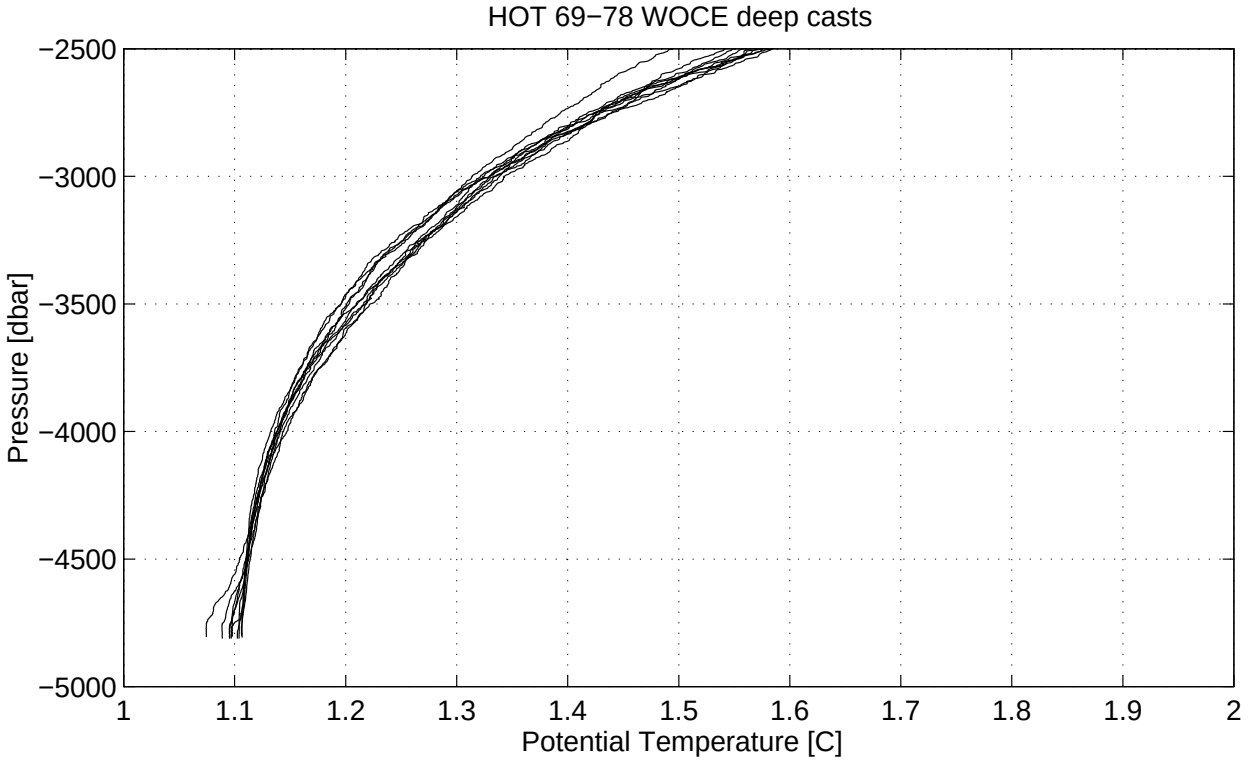
HOT 69−78 WOCE deep casts
Pressure [dbar]
Potential Temperature [C]
−2500
−3000
−3500
−4000
−4500
−5000
1
1.1
1.2
1.3
1.4
1.5
1.6
1.7
1.8
1.9
2

Figure 6.1.4

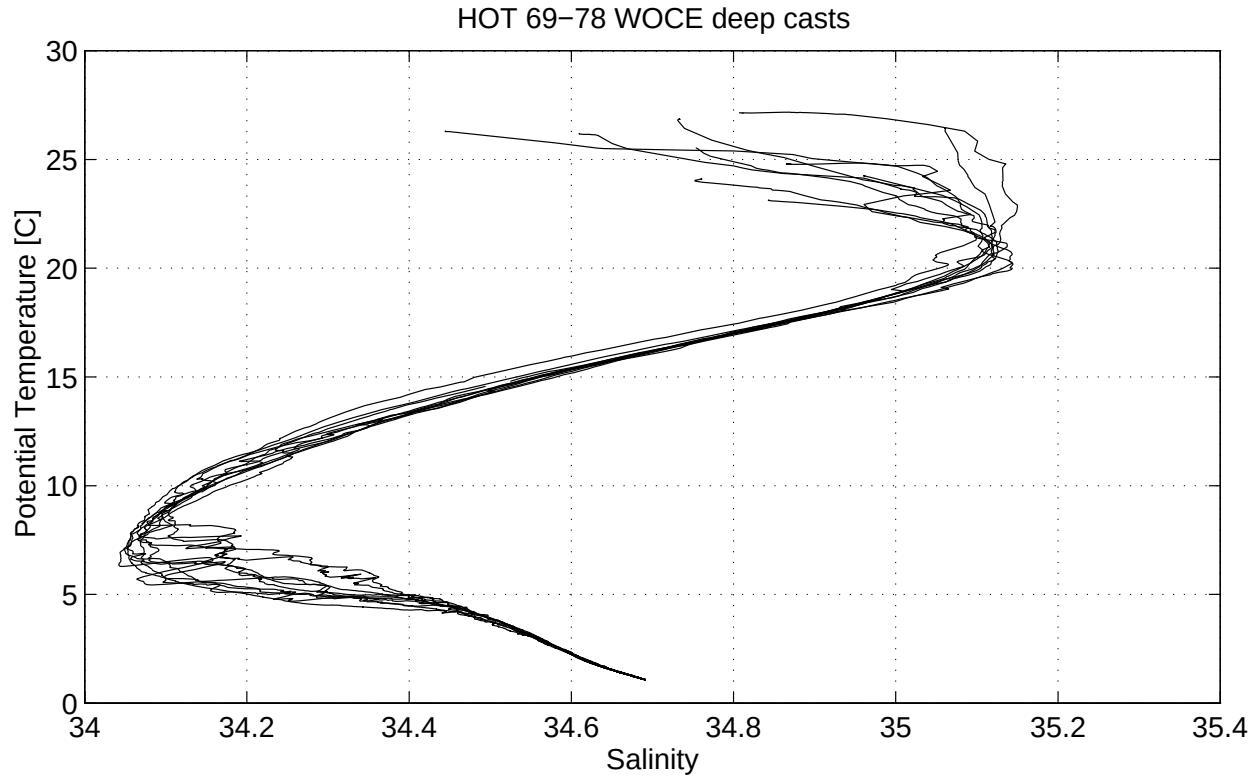
HOT 69−78 WOCE deep casts
Potential Temperature [C]
Salinity
30
25
20
15
10
5
0
34
34.2
34.4
34.6
34.8
35
35.2
35.4

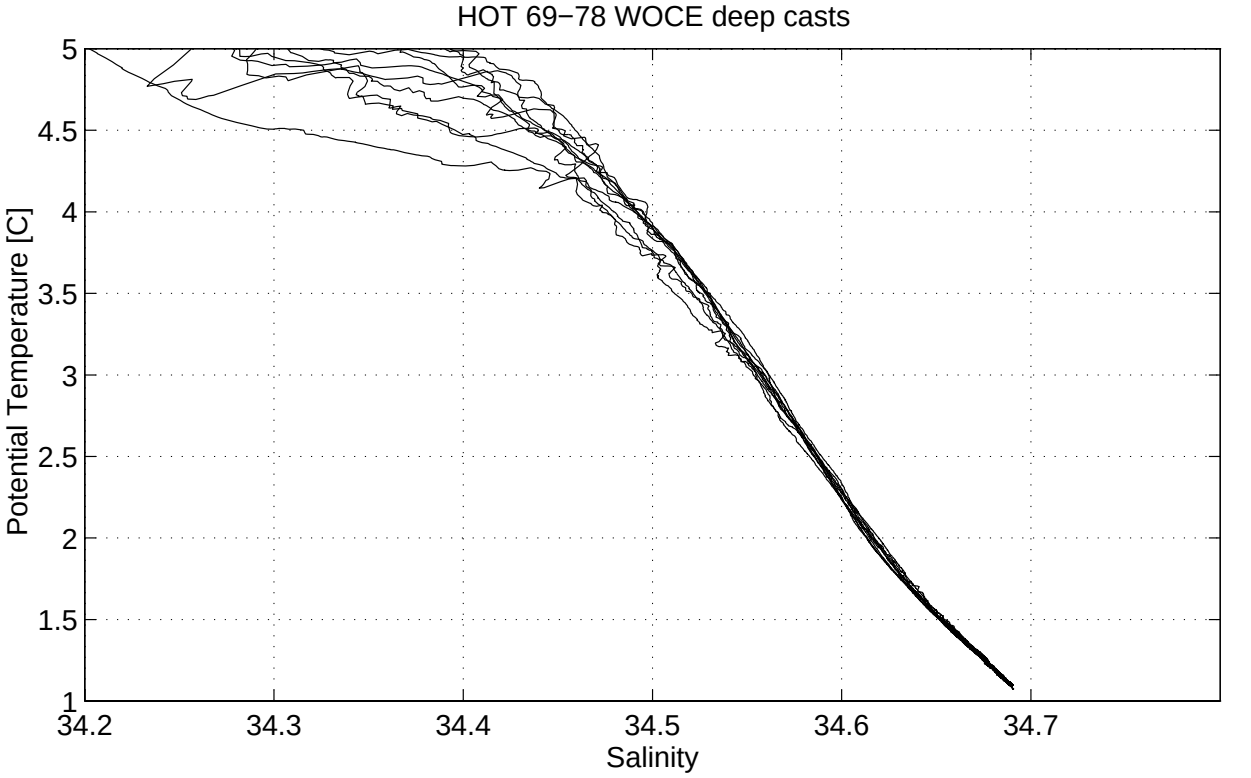
HOT 69−78 WOCE deep casts
Potential Temperature [C]
Salinity
5
4.5
4
3.5
3
2.5
2
1.5
1
34.2
34.3
34.4
34.5
34.6
34.7

Figure 6.1.5

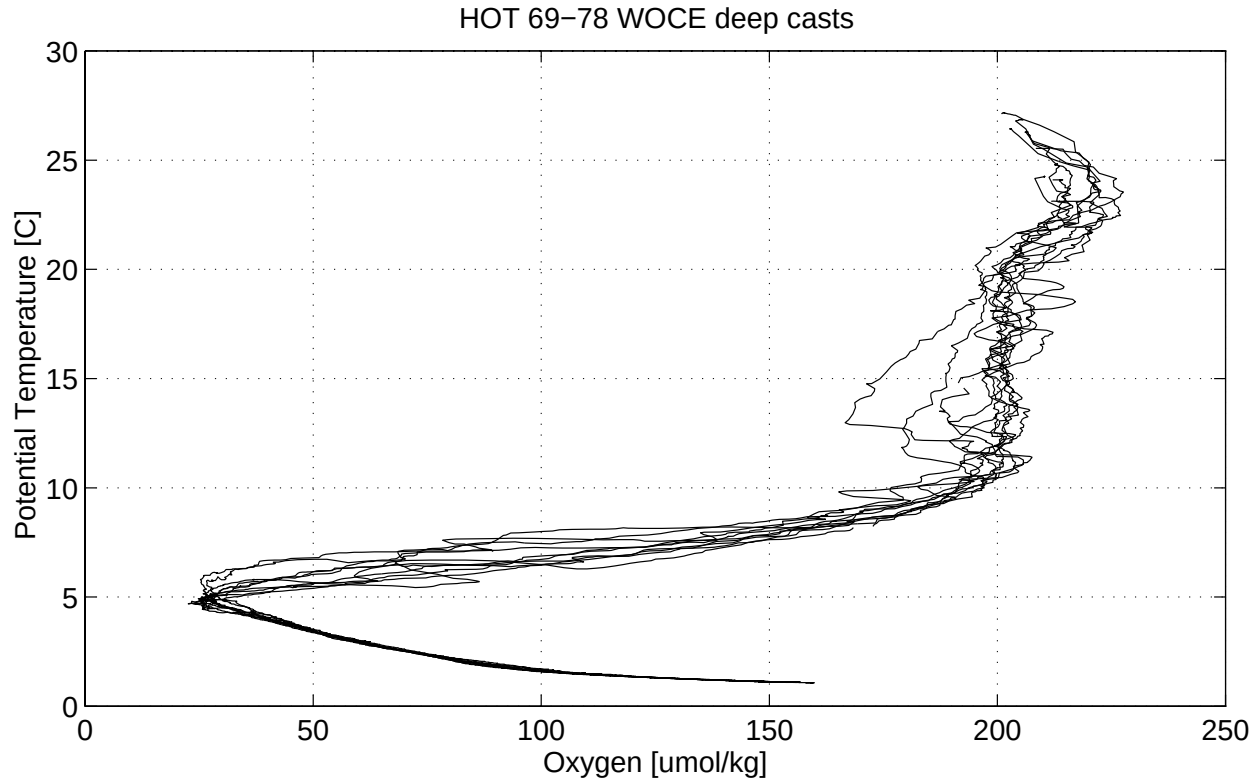
HOT 69−78 WOCE deep casts
Potential Temperature [C]
Oxygen [umol/kg]
0
5
10
15
20
25
30
0
50
100
150
200
250

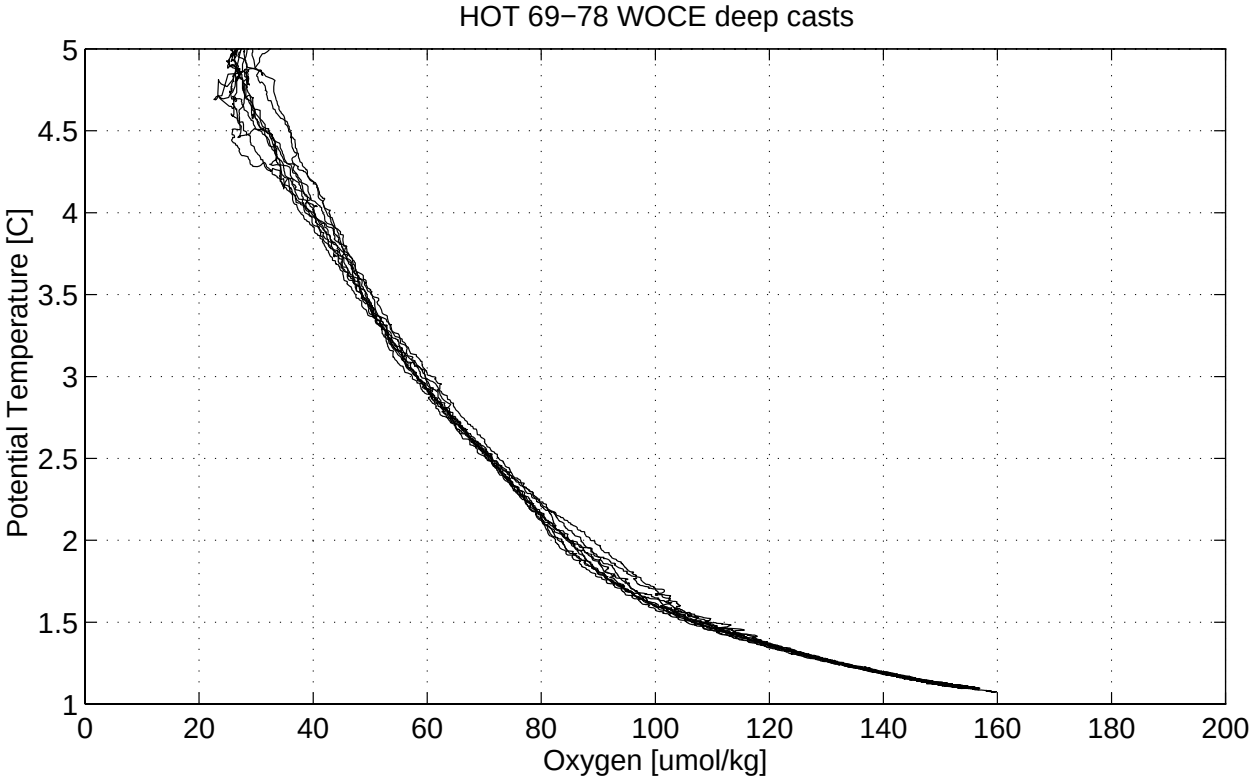
HOT 69−78 WOCE deep casts
Potential Temperature [C]
Oxygen [umol/kg]
1
1.5
2
2.5
3
3.5
4
4.5
5
0
20
40
60
80
100
120
140
160
180
200

Figure 6.1.6

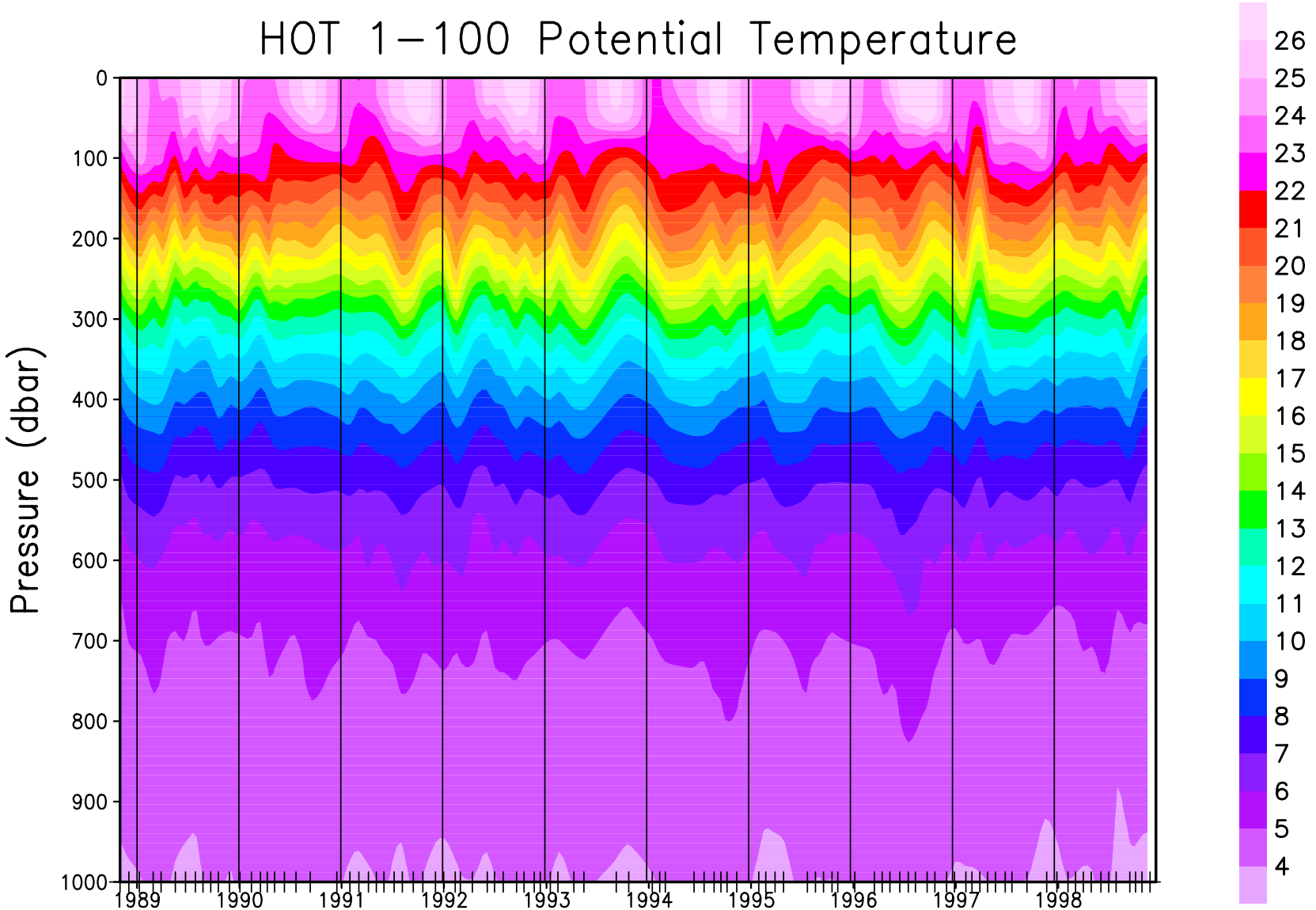

Figure 6.1.7: Contour plot of CTD potential temperature versus pressure for HOT cruises 1-100.

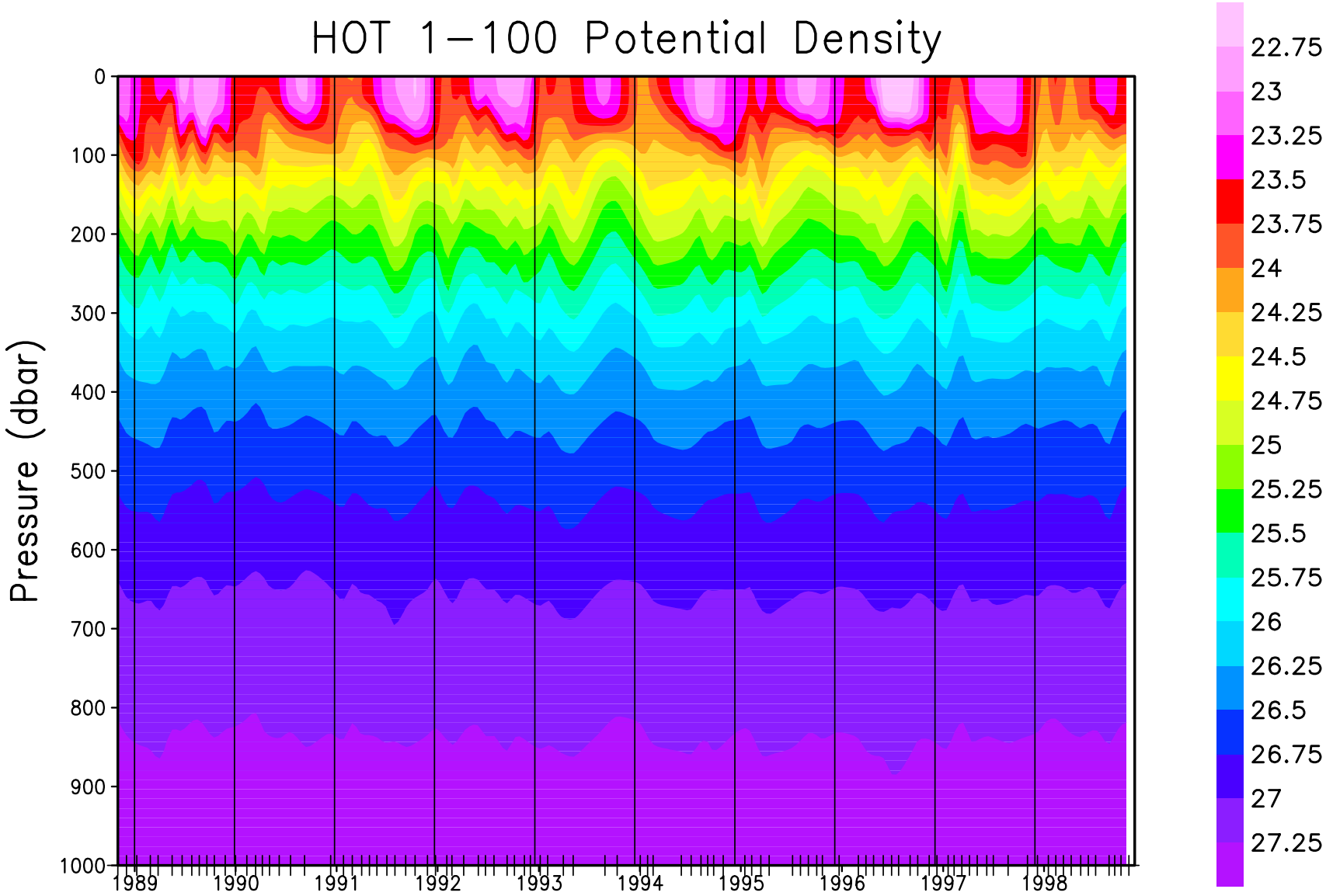

Figure 6.1.8: Contour plot of potential density (σ_θ), calculated from CTD pressure, temperature and salinity, versus pressure for HOT cruises 1-100.

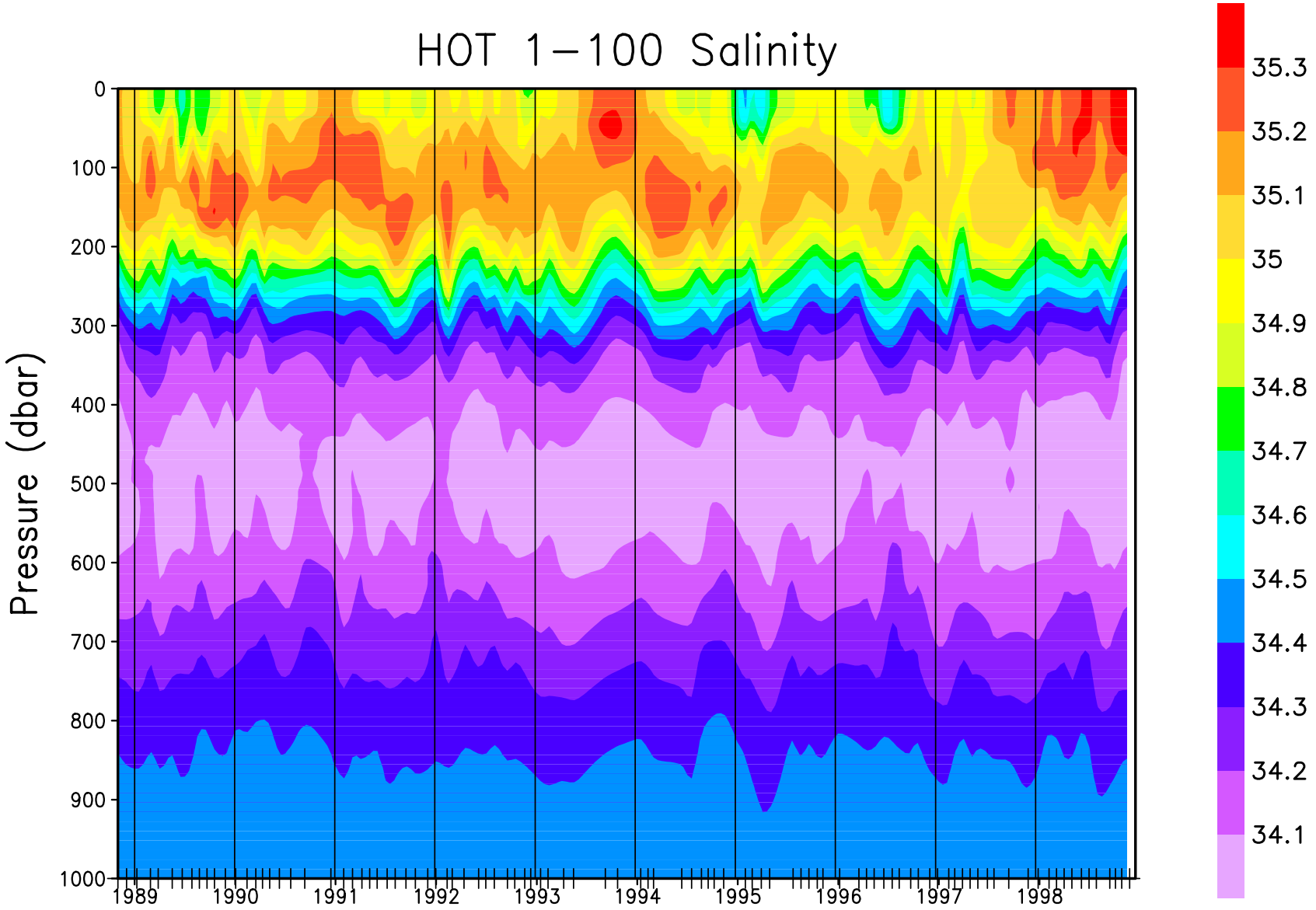

Figure 6.1.9: Contour plot of CTD salinity versus pressure for HOT cruises 1-

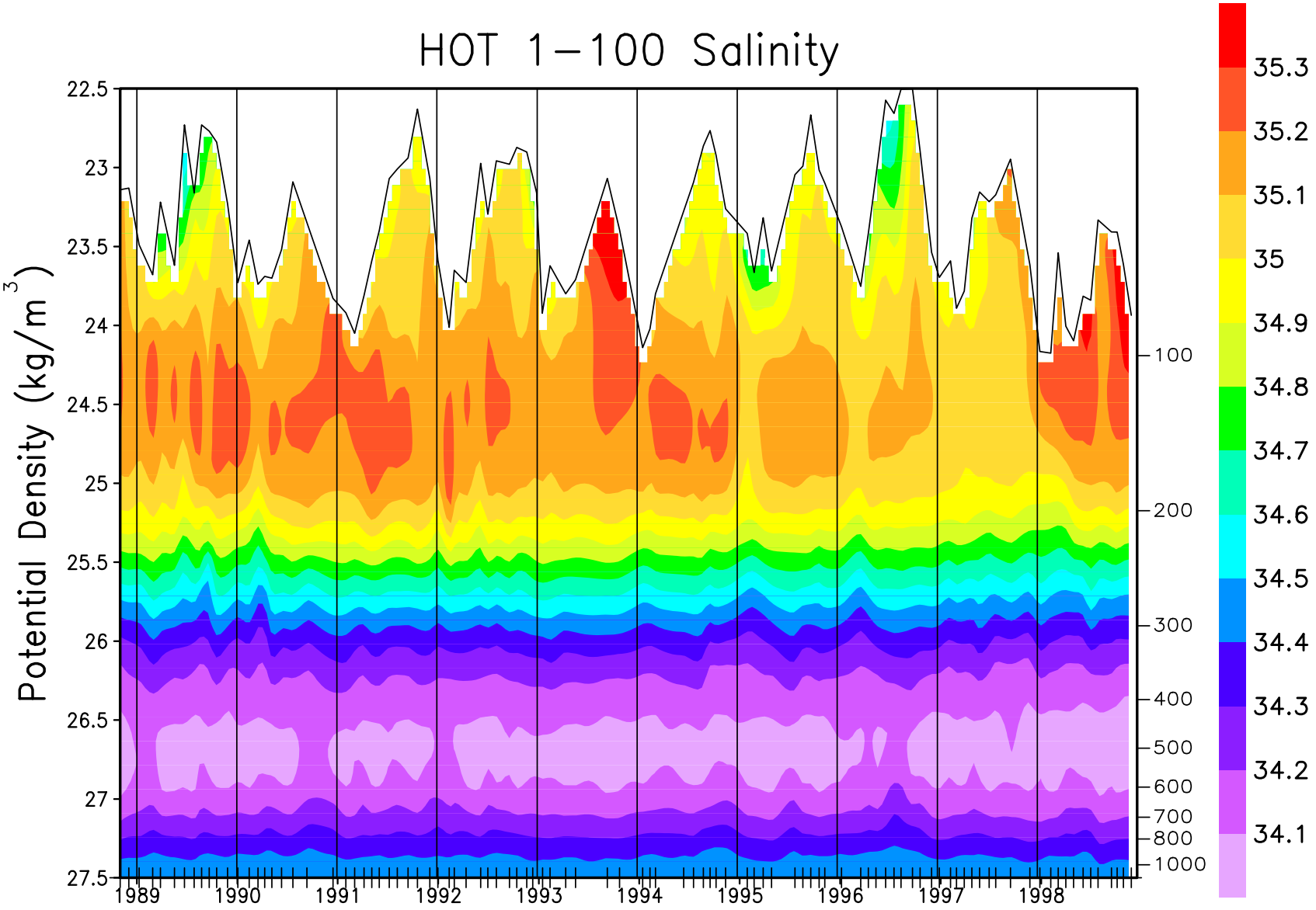

Figure 6.1.10: Contour plot of CTD salinity versus potential density (σ_θ) to 27.5 kg m^{-3} for HOT cruises 1-100. The average density of the sea surface is connected by the heavy line.

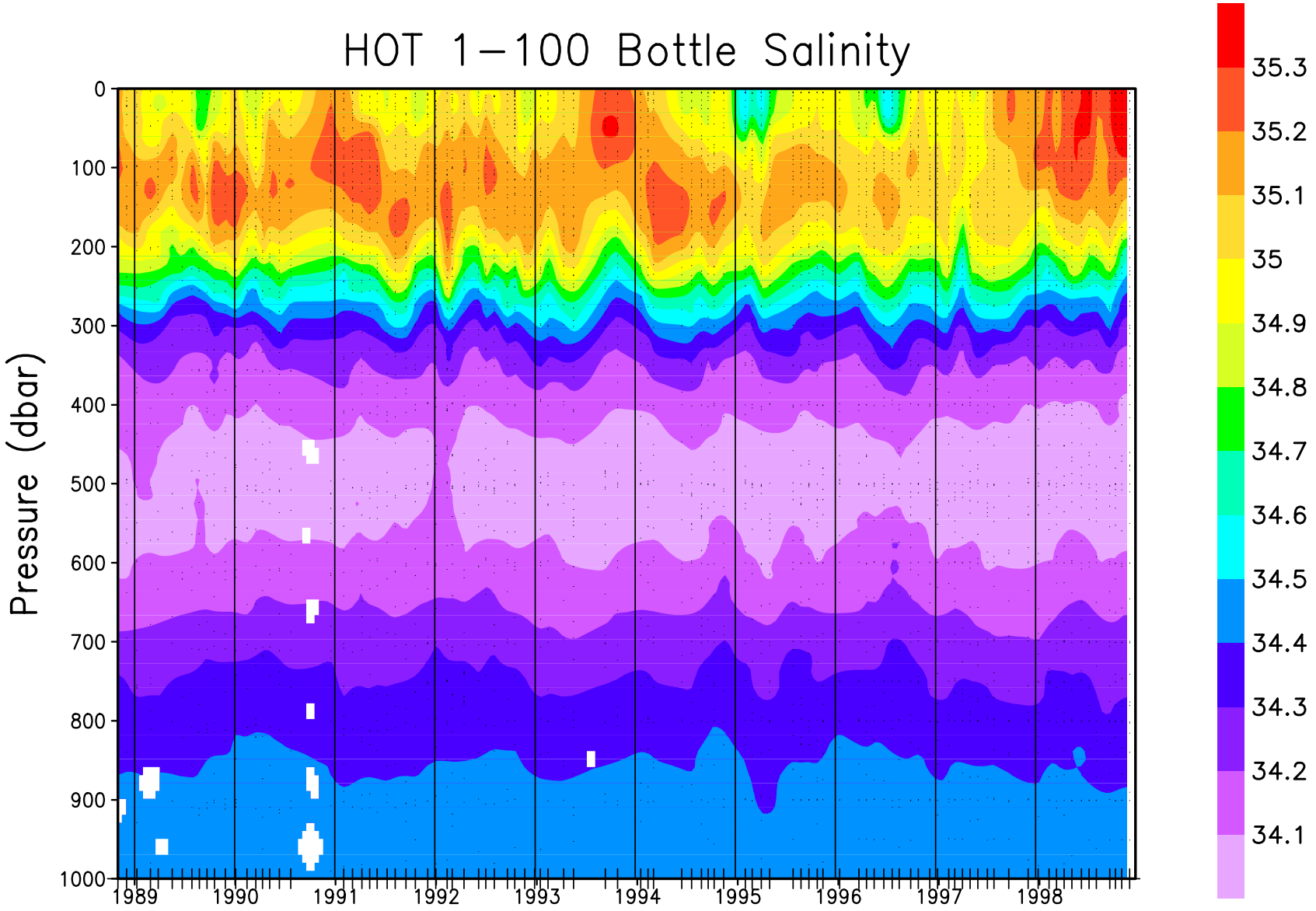

Figure 6.1.11: Contour plot of bottle salinity versus pressure for HOT cruises 1-100. Location of samples in the water column are indicated by the solid circles.

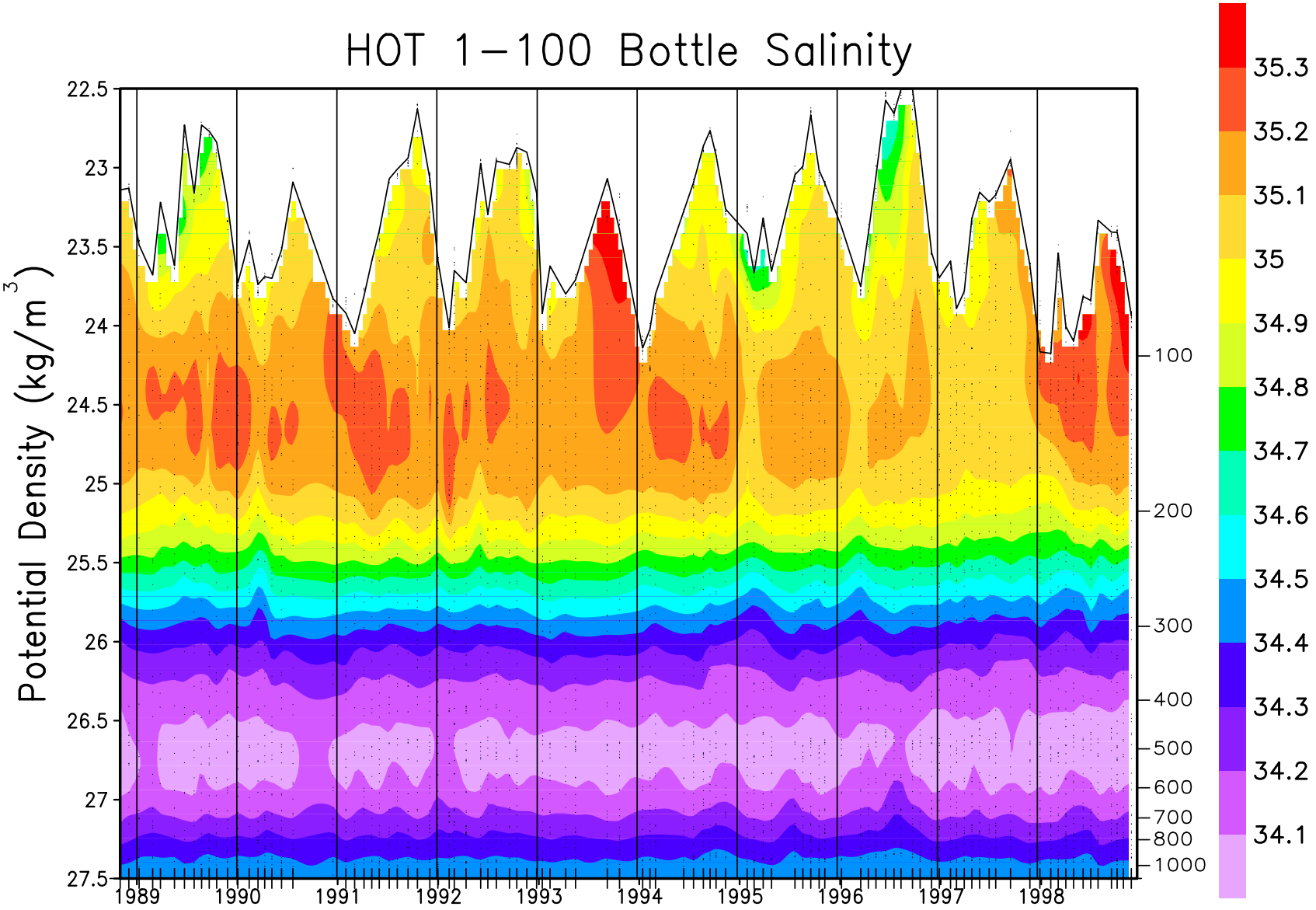

Figure 6.1.12: Contour plot of bottle salinity versus potential density (σ_θ)to 27.5 kg m^{-3} for HOT cruises 1-100. The average density of the sea surface is connected by the heavy line.

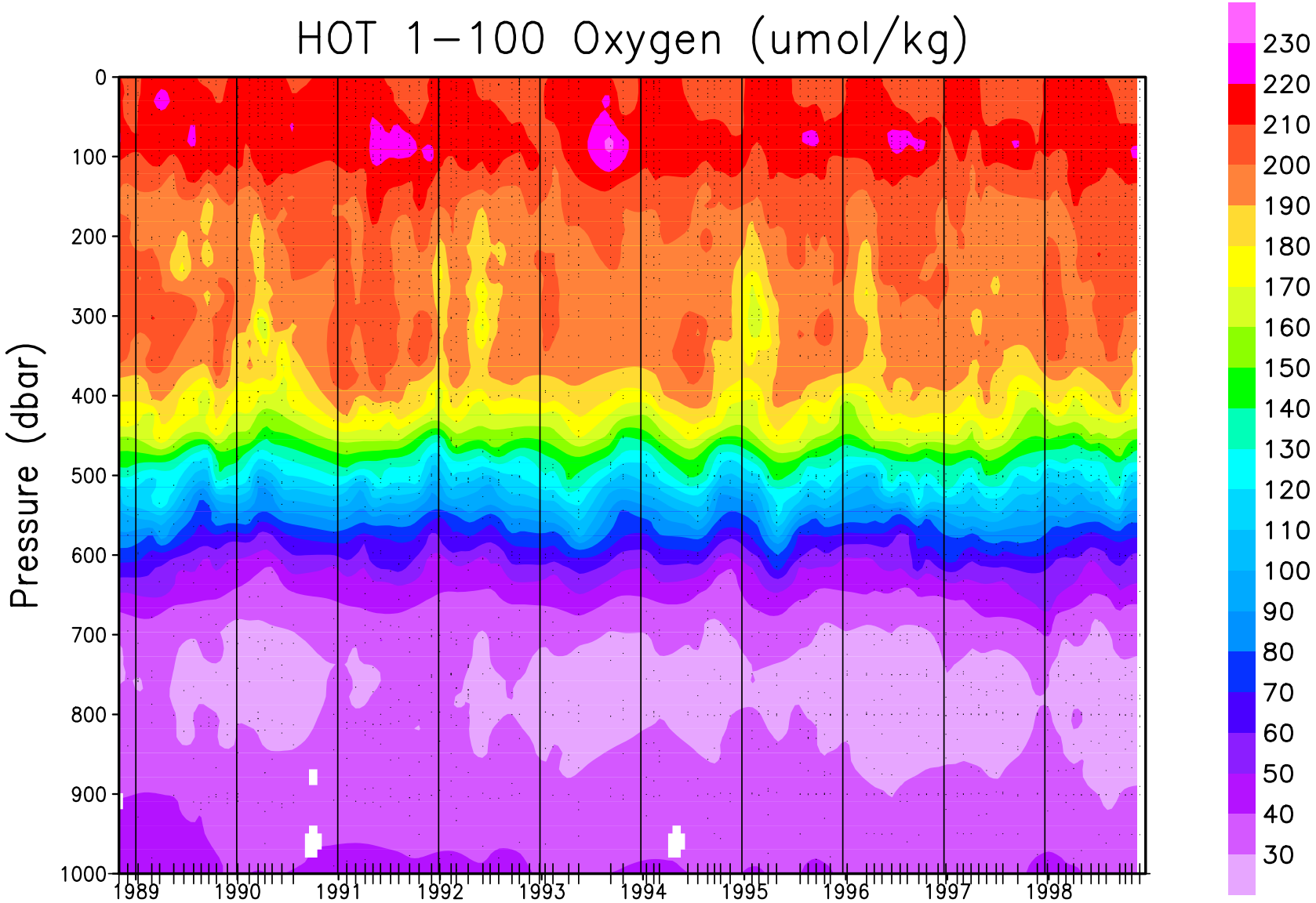

Figure 6.1.13: Contour plot of bottle oxygen versus pressure for HOT cruises 1-100. Location of samples in the water column are indicated by the solid circles.

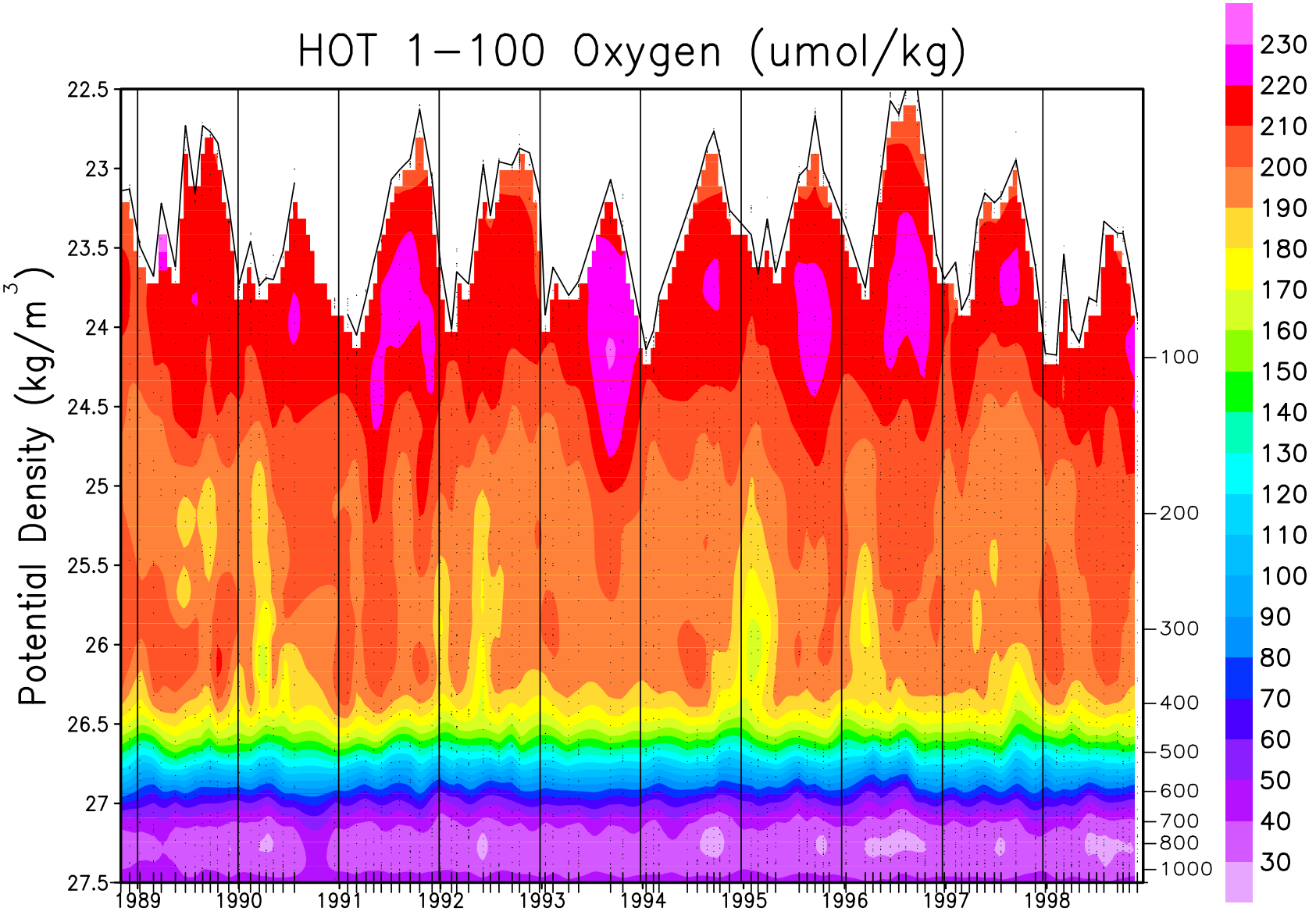

Figure 6.1.14: Contour plot of bottle oxygen versus potential density (σ_θ) to 27.5 kg m^{-3} for HOT cruises 1-100. The average density of the sea surface is connected by the heavy line.

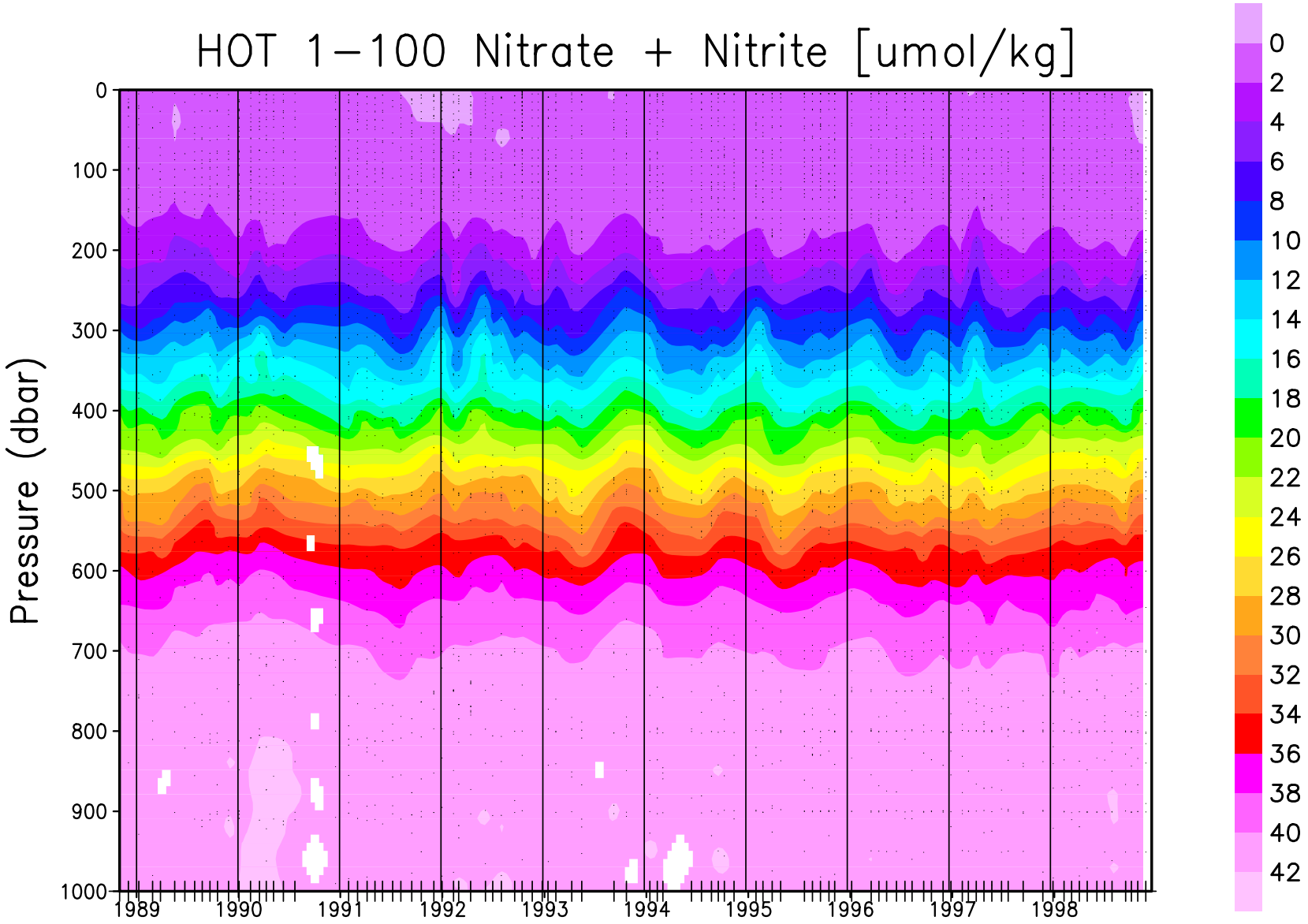

Figure 6.1.15: Contour plot of [nitrate + nitrite] versus pressure for HOT cruises 1-100. Location of samples in the water column are indicated by the solid circles.

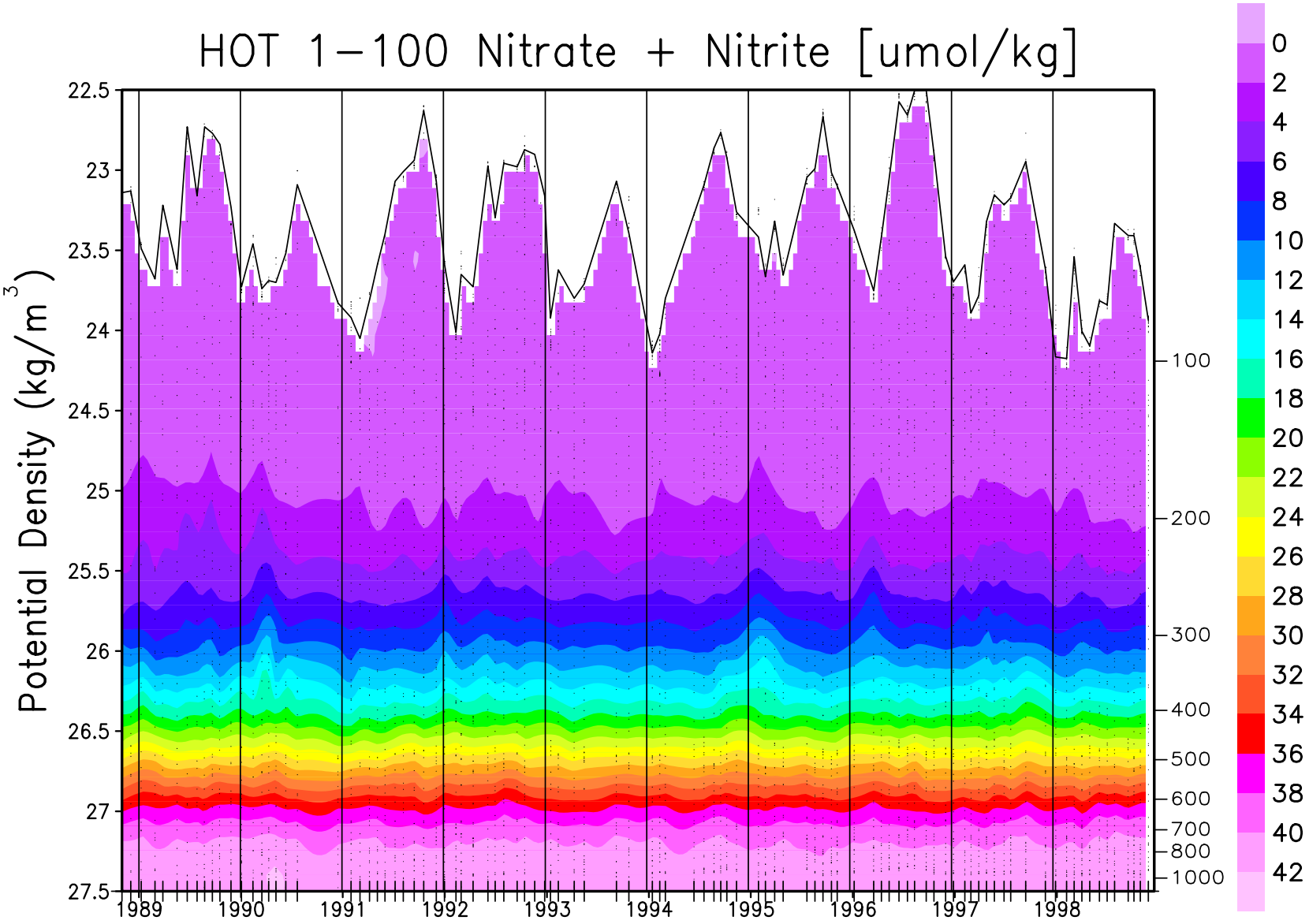

Figure 6.1.16: Contour plot of [nitrate + nitrite] versus potential density (σ_θ) to 27.5 kg m^{-3} for HOT cruises 1-100. The average density of the sea surface is connected by the heavy line.

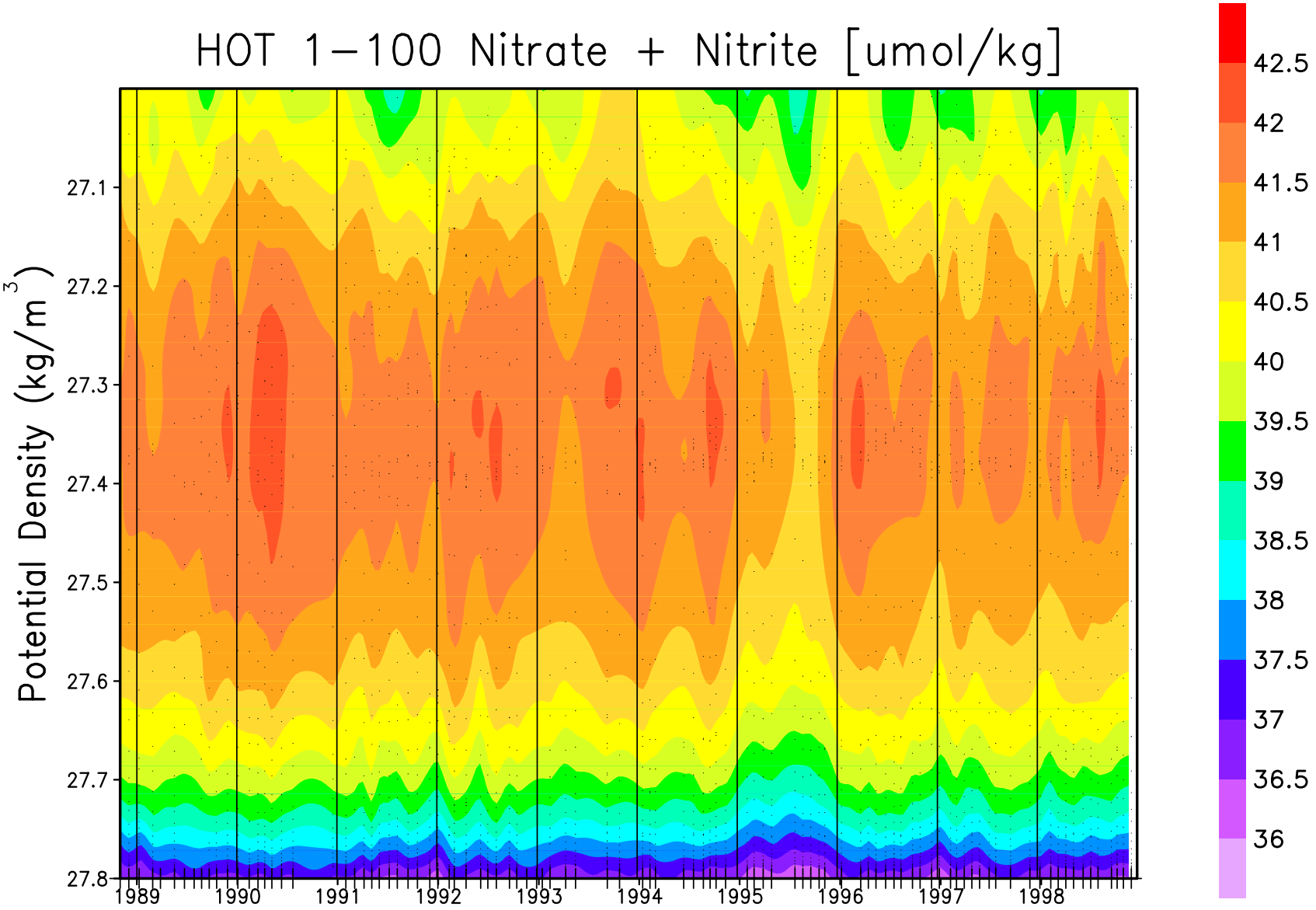

Figure 6.1.17: Contour plot of [nitrate + nitrite] versus potential density (σ_θ) from 27.0 to 27.8 kg m^{-3} for HOT cruises 1-100

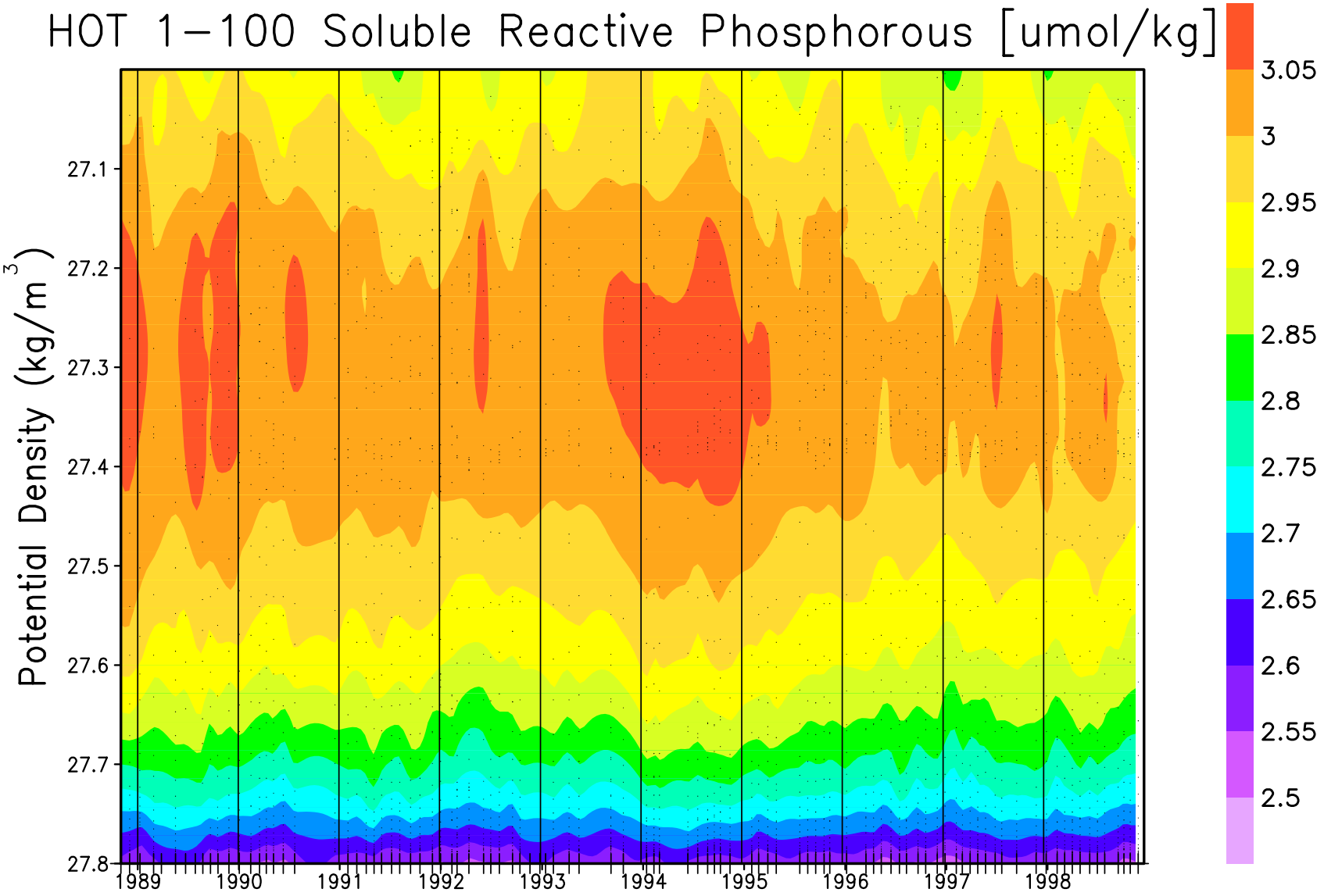

Figure 6.1.18: Contour plot of soluble reactive phosphate versus pressure for HOT cruises 1-100. Location of samples in the water column are indicated by the solid circles.

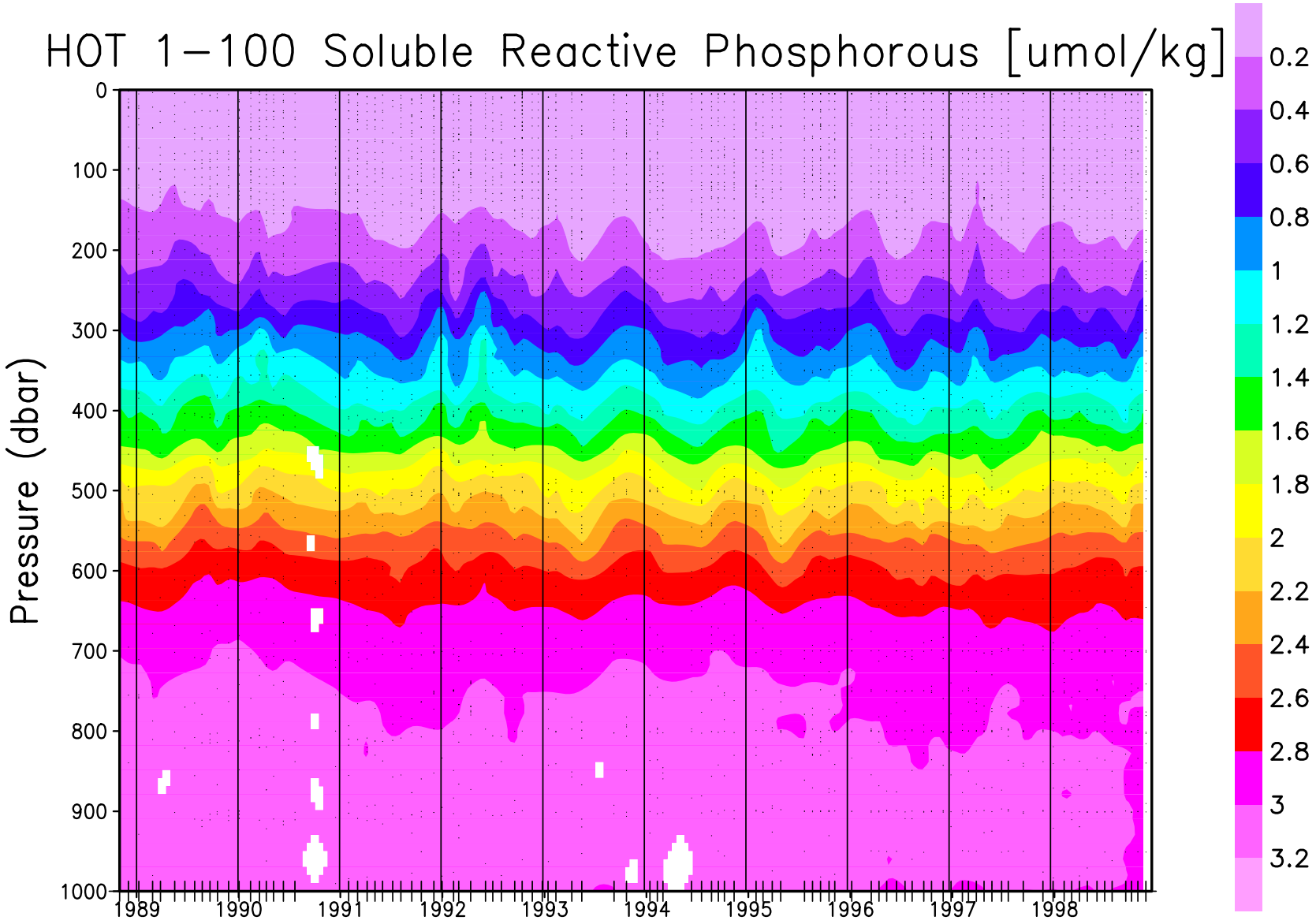

Figure 6.1.19: Contour plot of soluble reactive phosphate versus potential density (σ_θ) to 27.5 kg m^{-3} for HOT cruises 1-100. The average density of the sea surface is connected by the heavy

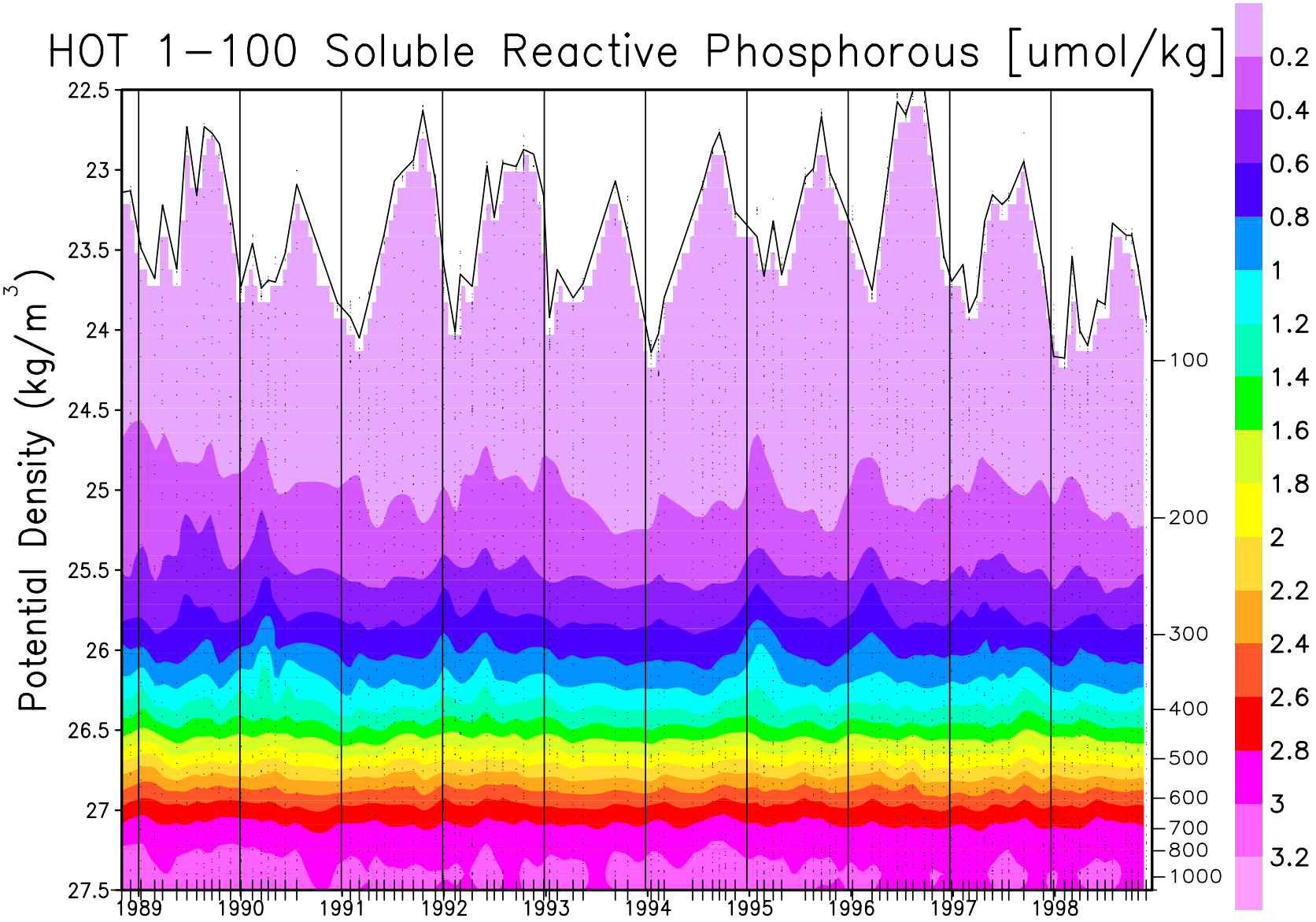

Figure 6.1.20: Contour plot of soluble reactive phosphate versus potential density (σ_θ) from 27.0 to 27.8 kg m^{-3} for HOT cruises 1-100.

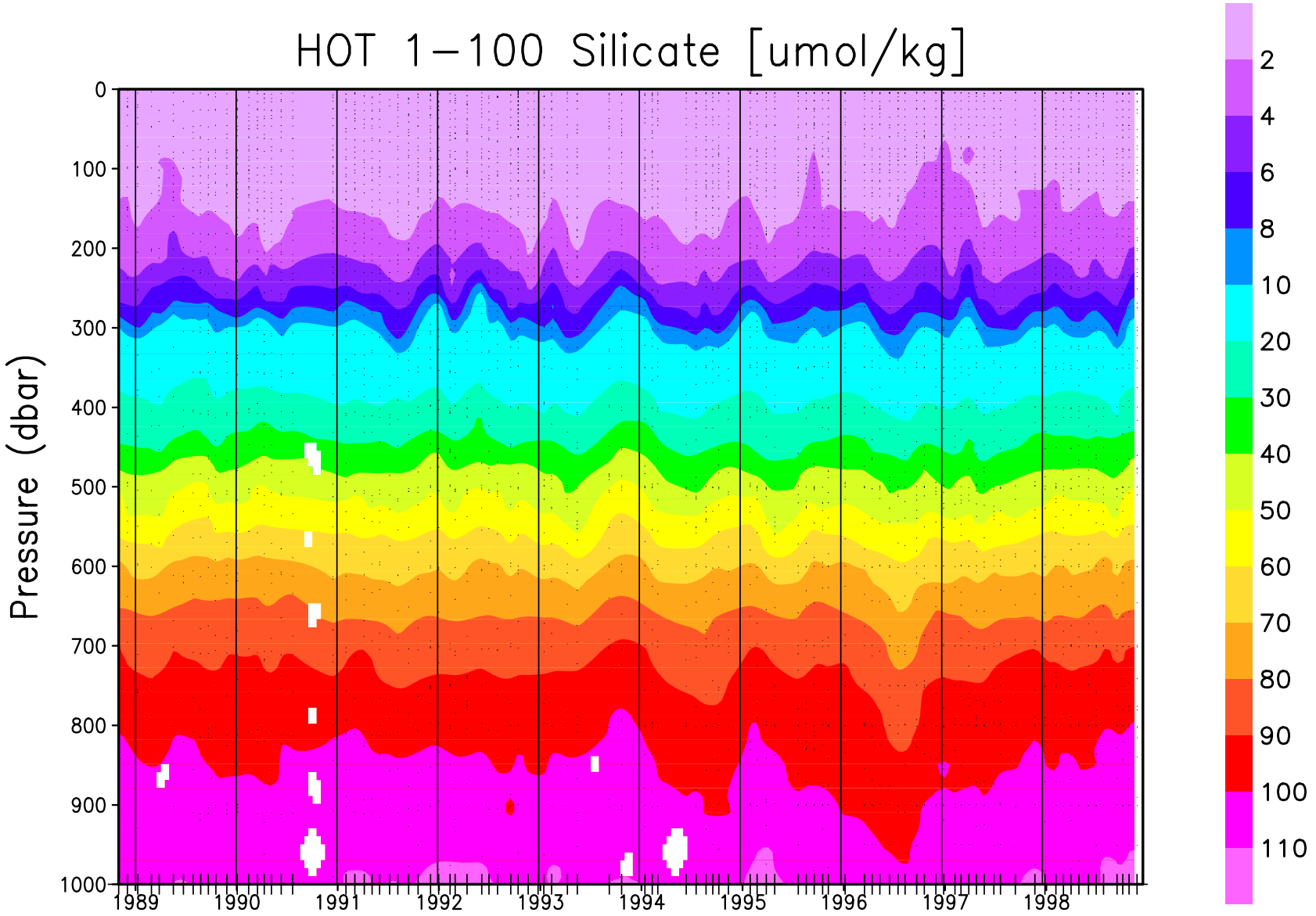

Figure 6.1.21: Contour plot of silicate versus pressure for HOT cruises 1-100. Location of samples in the water column are indicated by the solid circles.

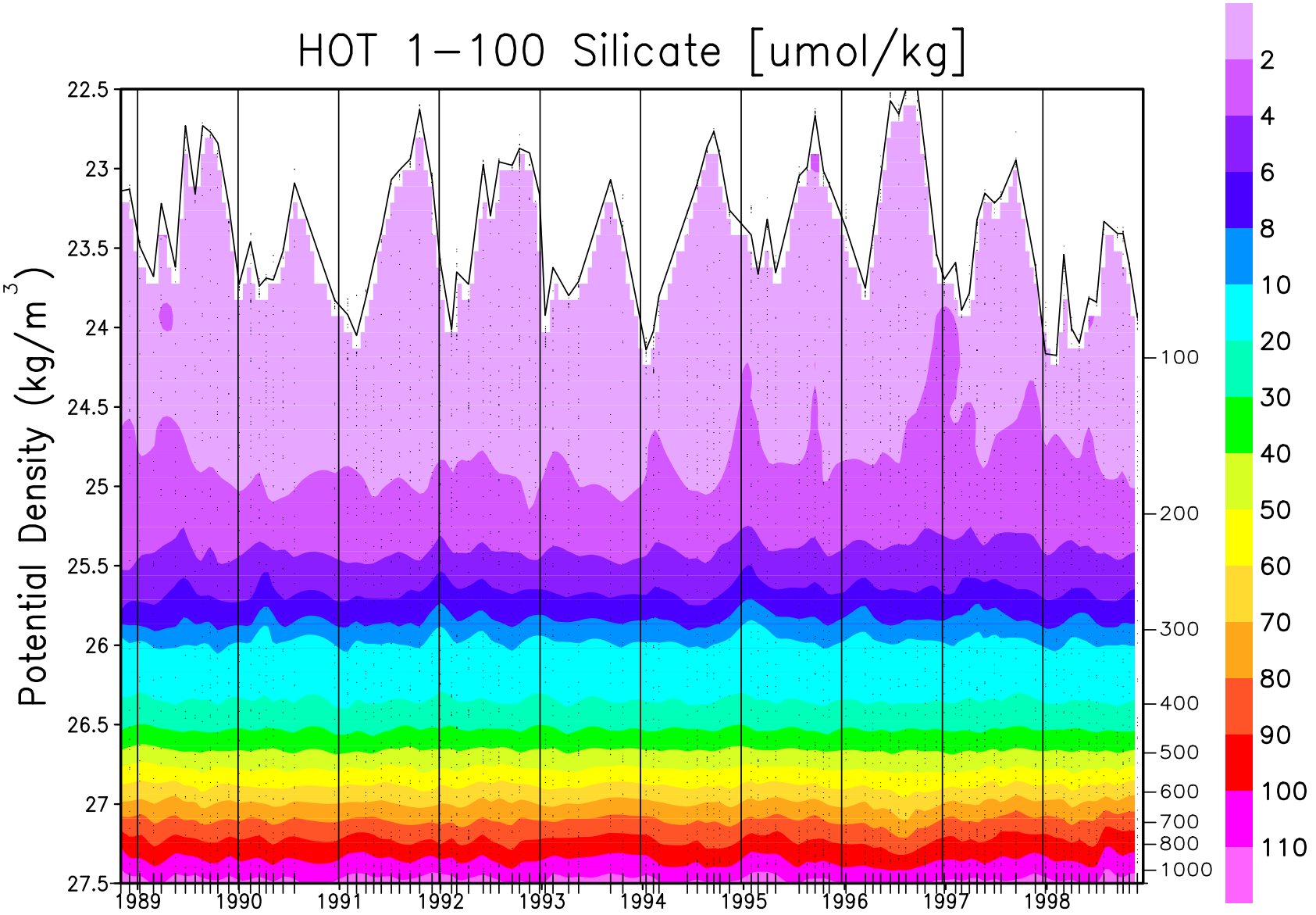

Figure 6.1.22: Contour plot of silicate versus potential density (σ_θ) to 27.5 kg m^{-3} for HOT cruises 1-100. The average density of the sea surface is connected by the heavy line.

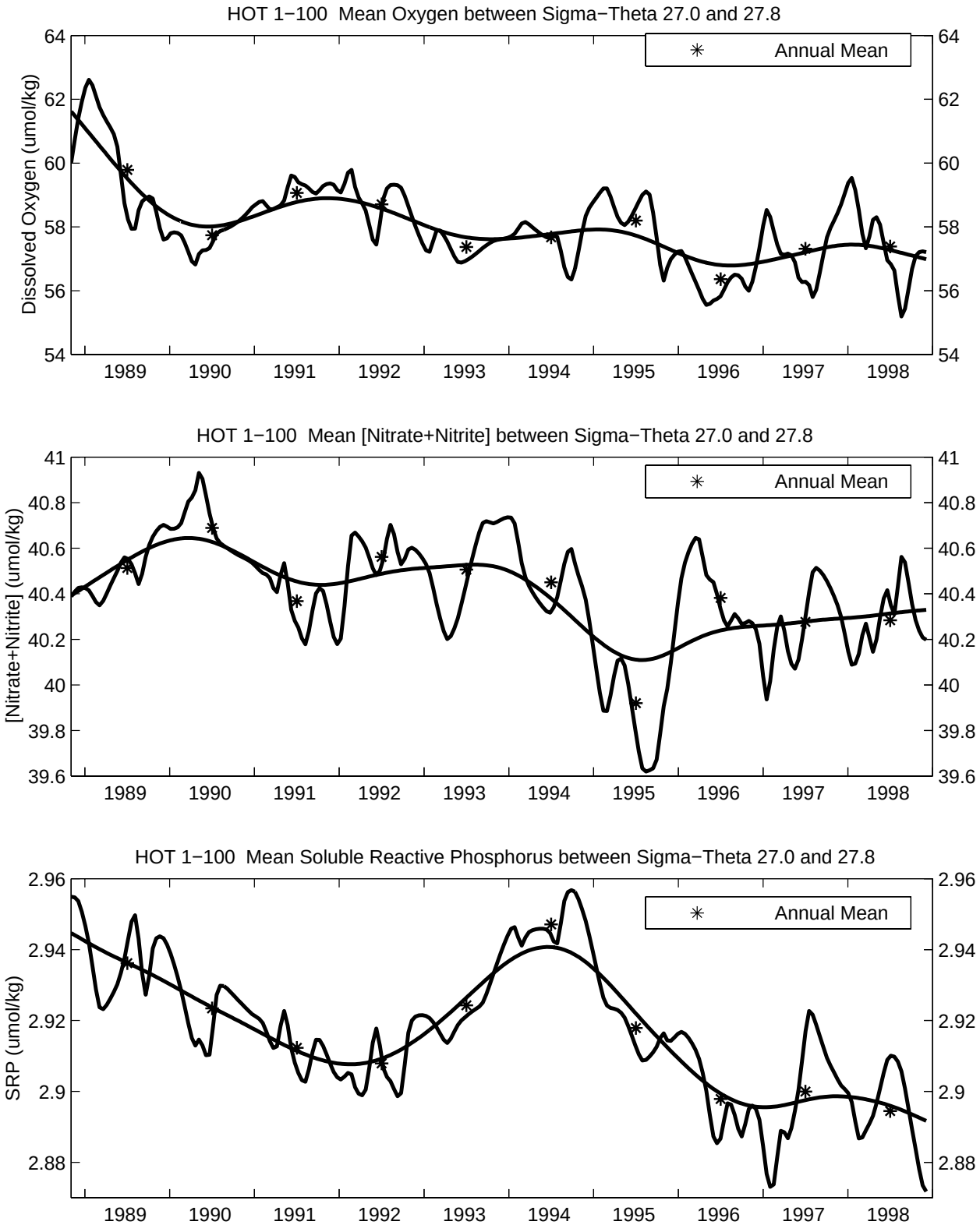
HOT 1−100 Mean Oxygen between Sigma−Theta 27.0 and 27.8
Dissolved Oxygen (umol/kg)
Annual Mean
64
62
60
58
56
54
1989
1990
1991
1992
1993
1994
1995
1996
1997
1998
HOT 1−100 Mean [Nitrate+Nitrite] between Sigma−Theta 27.0 and 27.8
[Nitrate+Nitrite] (umol/kg)
Annual Mean
41
40.8
40.6
40.4
40.2
40
39.8
39.6
HOT 1−100 Mean Soluble Reactive Phosphorus between Sigma−Theta 27.0 and 27.8
SRP (umol/kg)
Annual Mean
2.96
2.94
2.92
2.9
2.88

Figure 6.1.23

6.2. BIOGEOCHEMISTRY

Figure 6.2.1: Contour plot of bottle dissolved oxygen versus pressure for HOT cruises 1-78 from 0-200 m. Location of samples in the water column are indicated by the solid circles.

Figure 6.2.2: Contour plot of dissolved inorganic carbon versus pressure for HOT cruises 1-78 from 0-200 m. Location of samples in the water column are indicated by the solid circles.

Figure 6.2.3: Contour plot of alkalinity versus pressure for HOT cruises 1-78 from 0-200 m. Location of samples in the water column are indicated by the solid circles.

Figure 6.2.4: Time series of mean titration alkalinity (upper panel) and dissolved inorganic carbon (lower panel) for HOT cruises 1-78. Error bars represent standard deviation of pooled samples collected between 0 and 50 dbar.

Figure 6.2.5: Contour plot of pH versus pressure for HOT cruises 35-78 from 0-200 m. Location of samples in the water column are indicated by the solid circles.

Figure 6.2.6: Depth profile from 0-250 m of [nitrate + nitrite] at Station ALOHA for 1996 HOT cruises by the chemiluminescence method.

Figure 6.2.7: Depth profile from 0-250 m of soluble reactive phosphorus at Station ALOHA for 1996 HOT cruises by the magnesium induced coprecipitation (MAGIC) method.

Figure 6.2.8: Contour plot from 0-250 m of [nitrate + nitrite] at Station ALOHA for HOT cruises 1-78 by the chemiluminescence method.

Figure 6.2.9: Contour plot from 0-250 m of soluble reactive phosphorus at Station ALOHA for HOT cruises 1-78 by the magnesium induced coprecipitation (MAGIC) method.

Figure 6.2.10: Depth integrated (0-100 m) [nitrate + nitrite] concentrations at Station ALOHA from HOT cruises 1-78 by the chemiluminescence method.

Figure 6.2.11: Depth integrated (0-100 m) soluble reactive phosphorus concentrations at Station ALOHA from HOT cruises 1-78 by the autoanalyzer (solid line) and the MAGIC method (dashed line). The heavy solid line is a model I regression fit to the MAGIC data set.

Figure 6.2.12: Contour plot from 0-1000 m of dissolved organic carbon at Station ALOHA for HOT cruises 49-78.

Figure 6.2.13: Contour plot from 0-1000 m of dissolved organic nitrogen at Station ALOHA for HOT cruises 1-78.

Figure 6.2.14: Contour plot from 0-1000 m of dissolved organic phosphorus at Station ALOHA for HOT cruises 1-78.

Figure 6.2.15: Mean concentrations of particulate carbon at Station ALOHA for HOT cruises 1-78 from 0-50 dbar (upper panel) and 50-100 dbar (lower panel). Error bars represent standard deviation of pooled samples collected between 0 and 50 dbar.

Figure 6.2.16: Mean concentrations of particulate nitrogen at Station ALOHA for HOT cruises 1-78 from 0-50 dbar (upper panel) and 50-100 dbar (lower panel). Error bars represent standard deviation of pooled samples collected between 0 and 50 dbar.

Figure 6.2.17: Mean concentrations of particulate phosphorus at Station ALOHA for HOT cruises 1-78 from 0-50 dbar (upper panel) and 50-100 dbar (lower panel). Error bars represent standard deviation of pooled samples collected between 0 and 50 dbar.

Figure 6.2.18: Contour plot from 0-200 m of fluorometric chlorophyll a concentrations at Station ALOHA for HOT cruises 1-78.

Figure 6.2.19: Contour plot from 0-500 m of adenosine 5’ triphosphate concentrations at Station ALOHA for HOT cruises 1-78.

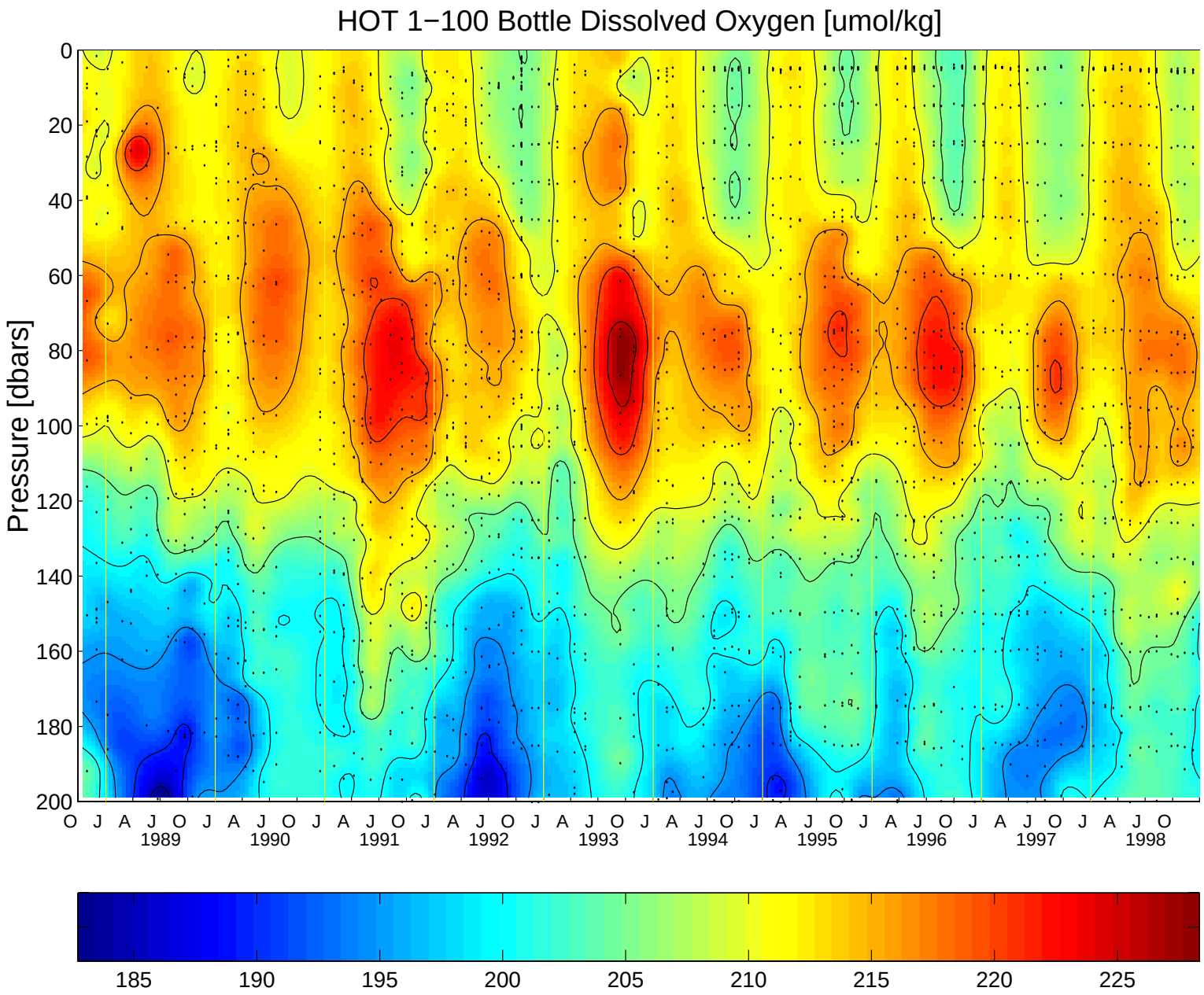
HOT 1−100 Bottle Dissolved Oxygen [umol/kg]
Pressure [dbars]
0
20
40
60
80
100
120
140
160
180
200
O J A J O J A J O J A J O J A J O J A J O J A J O J A J O J A J O J A J O J A J O J A J O J A J O J A J O
1989
1990
1991
1992
1993
1994
1995
1996
1997
1998
185
190
195
200
205
210
215
220
225

Figure 6.2.1

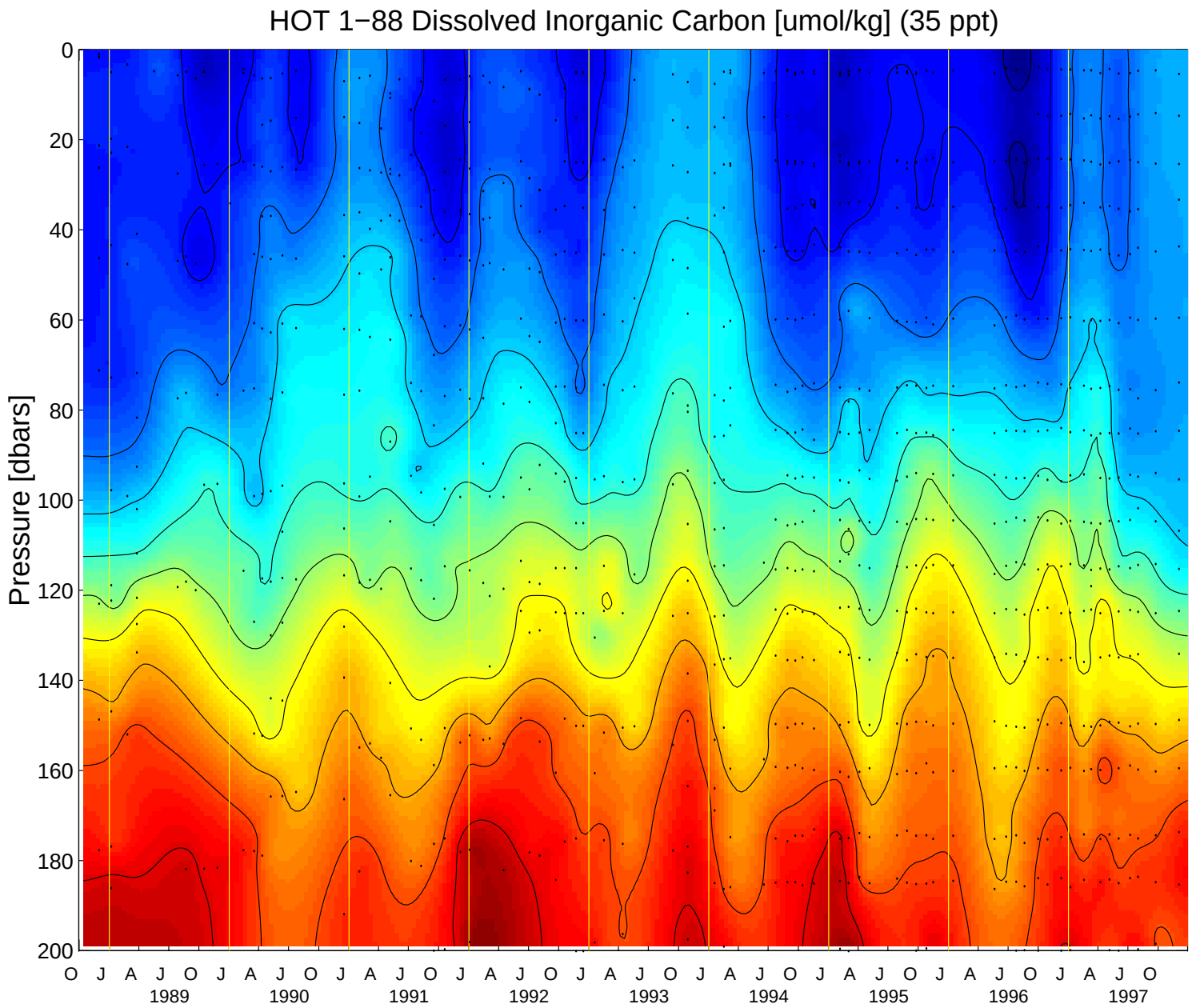
HOT 1−88 Dissolved Inorganic Carbon [umol/kg] (35 ppt)
Pressure [dbars]
0
20
40
60
80
100
120
140
160
180
200
O J A J O J A J O J A J O J A J O J A J O J A J O J A J O J A J O J A J O J A J O
1989
1990
1991
1992
1993
1994
1995
1996
1997

Figure 6.2.2

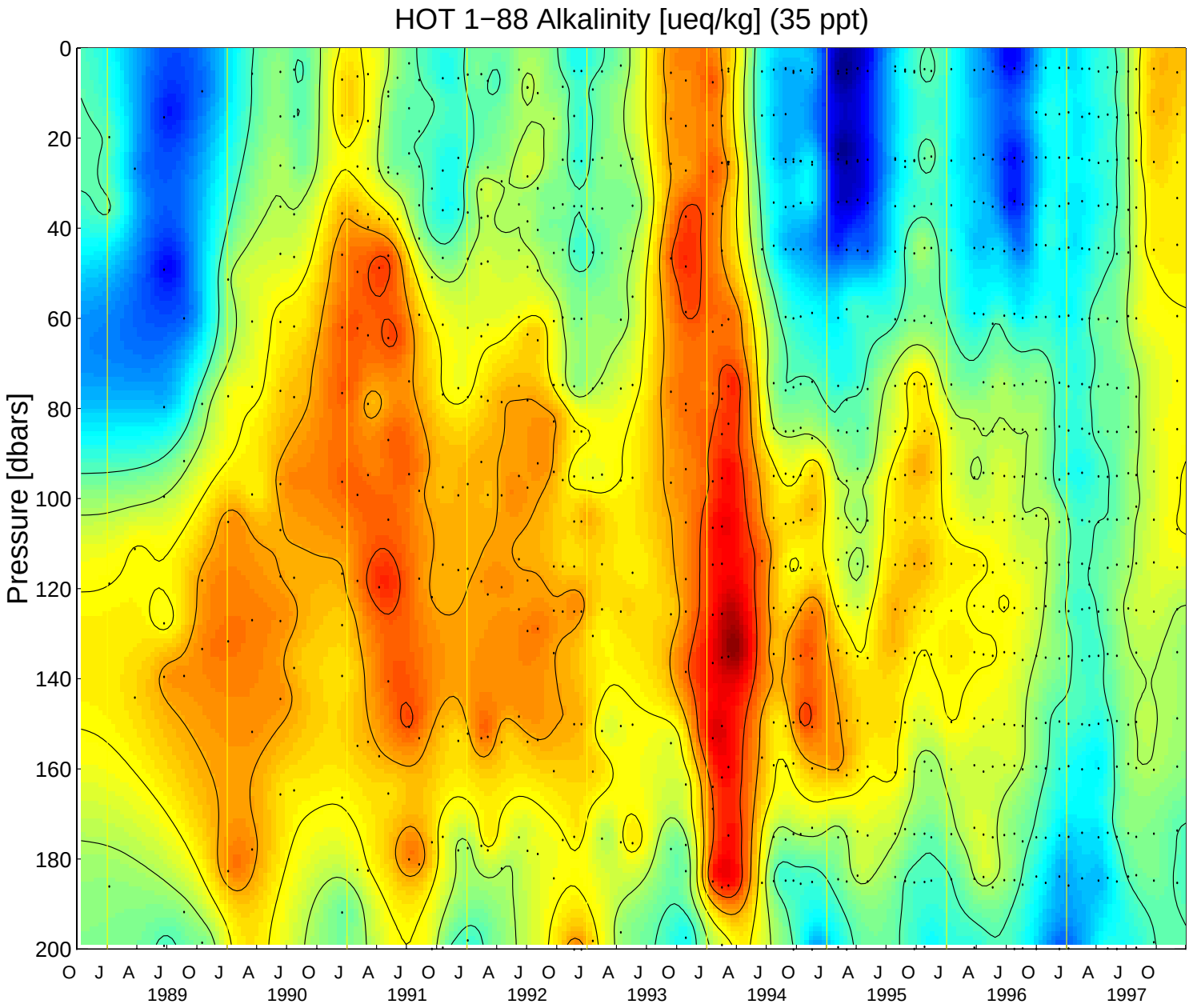
HOT 1−88 Alkalinity [ueq/kg] (35 ppt)
Pressure [dbars]
0
20
40
60
80
100
120
140
160
180
200
O J A J O J A J O J A J O J A J O J A J O J A J O J A J O J A J O J A J O J A J O
1989
1990
1991
1992
1993
1994
1995
1996
1997

Figure 6.2.3

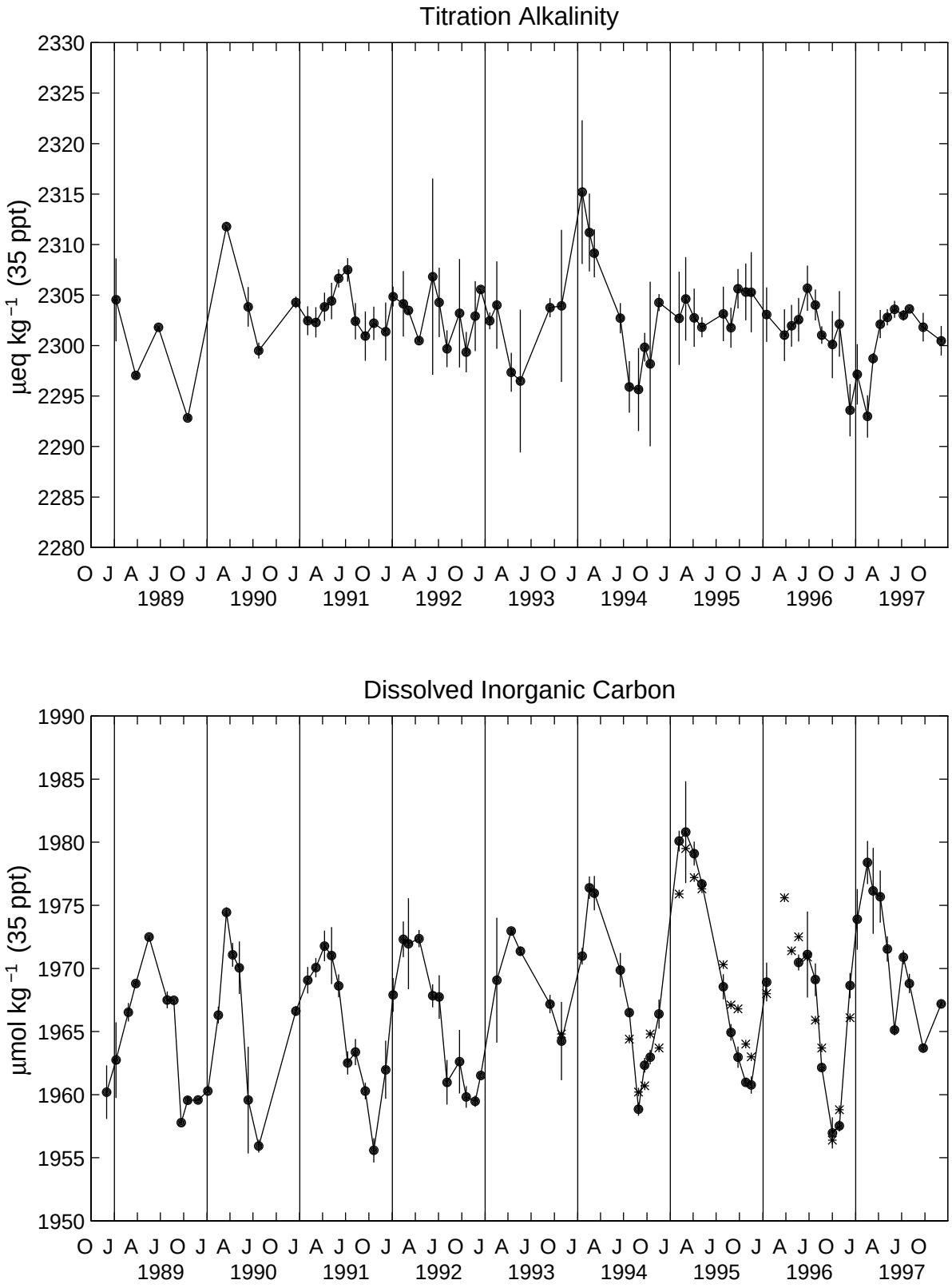
Titration Alkalinity
µeq kg⁻¹ (35 ppt)
2330
2325
2320
2315
2310
2305
2300
2295
2290
2285
2280
O J A J O J A J O J A J O J A J O J A J O J A J O J A J O J A J O J A J O J A J O
1989
1990
1991
1992
1993
1994
1995
1996
1997

Dissolved Inorganic Carbon
µmol kg⁻¹ (35 ppt)
1990
1985
1980
1975
1970
1965
1960
1955
1950
O J A J O J A J O J A J O J A J O J A J O J A J O J A J O J A J O J A J O J A J O
1989
1990
1991
1992
1993
1994
1995
1996
1997

Figure 6.2.4

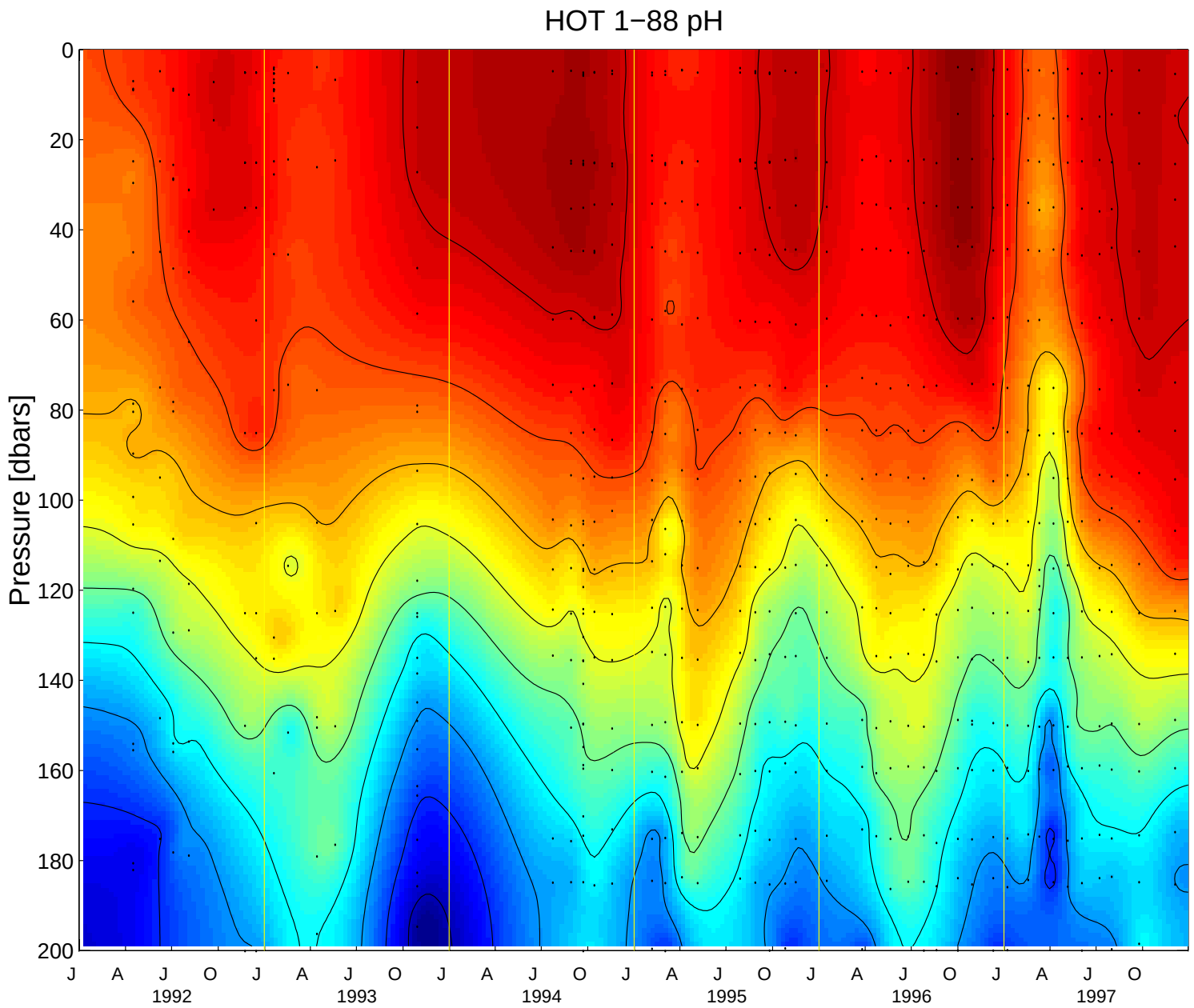
HOT 1−88 pH
Pressure [dbars]
0
20
40
60
80
100
120
140
160
180
200
J A J O J A J O J A J O J A J O J A J O J A J O J A J O
1992
1993
1994
1995
1996
1997

Figure 6.2.5

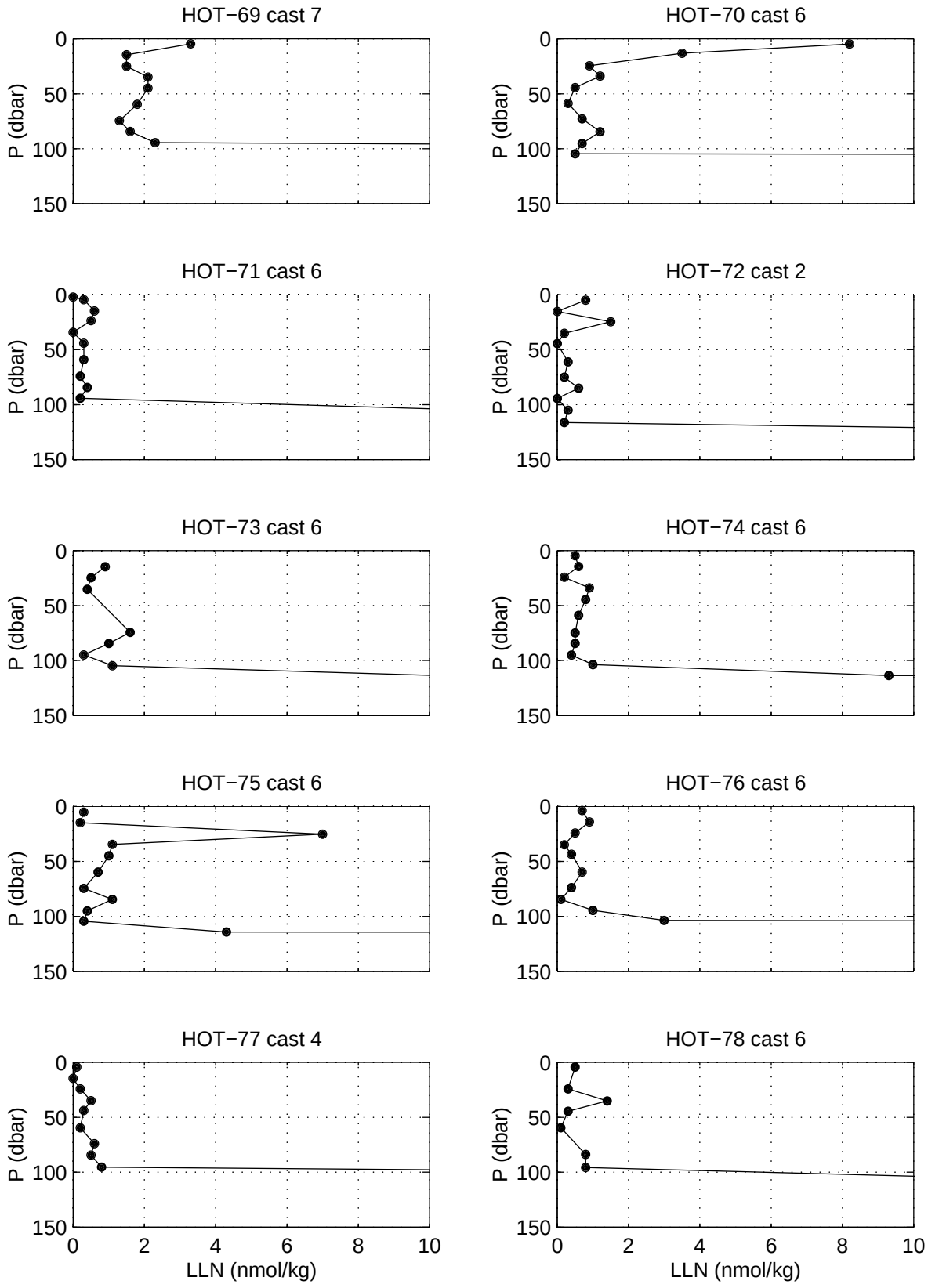
HOT−69 cast 7
HOT−70 cast 6
HOT−71 cast 6
HOT−72 cast 2
HOT−73 cast 6
HOT−74 cast 6
HOT−75 cast 6
HOT−76 cast 6
HOT−77 cast 4
HOT−78 cast 6
P (dbar)
0
50
100
150
0
2
4
6
8
10
LLN (nmol/kg)

Figure 6.2.6

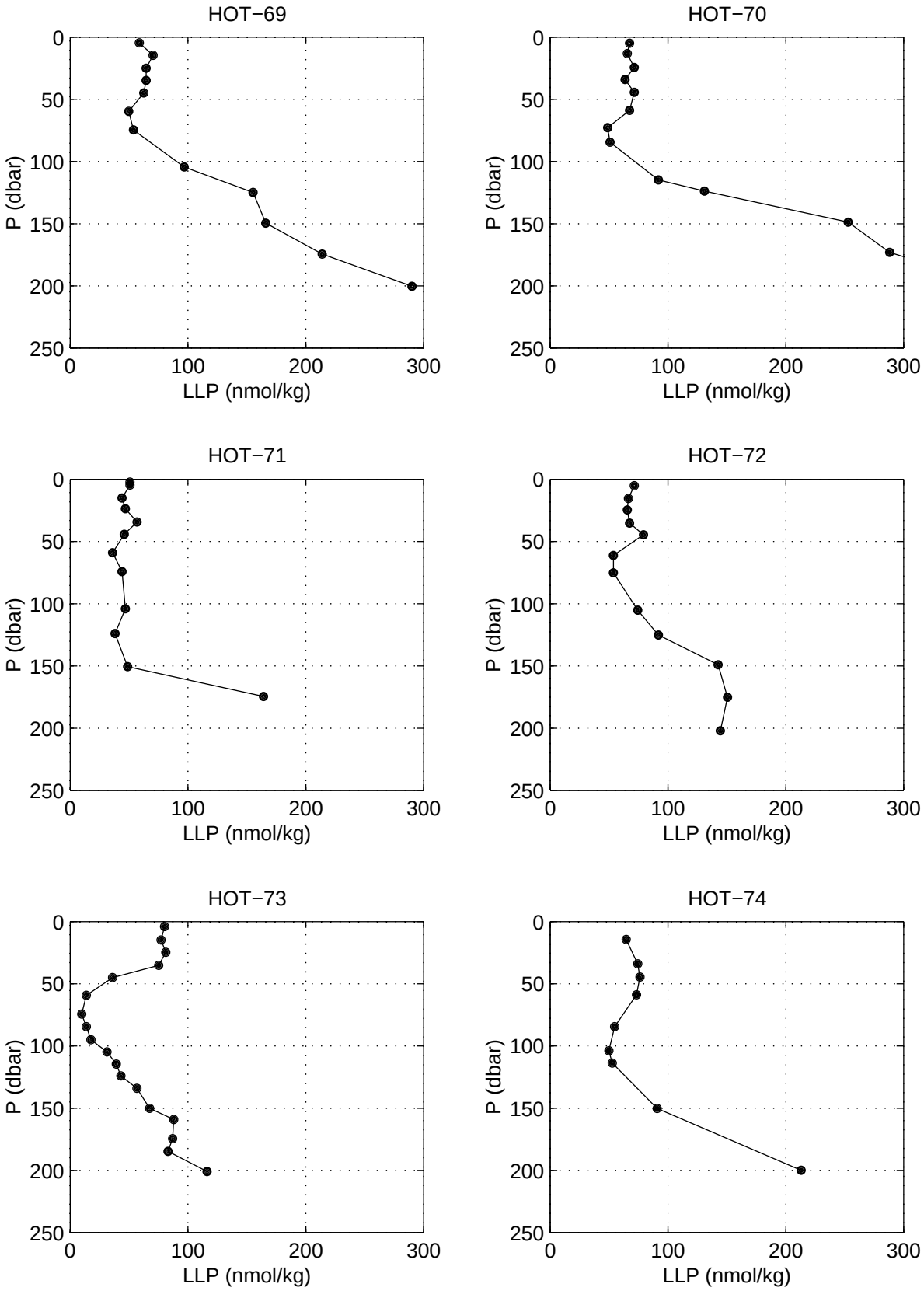
HOT−69
HOT−70
HOT−71
HOT−72
HOT−73
HOT−74
P (dbar)
LLP (nmol/kg)
0
50
100
150
200
250
0
100
200
300

Figure 6.2.7

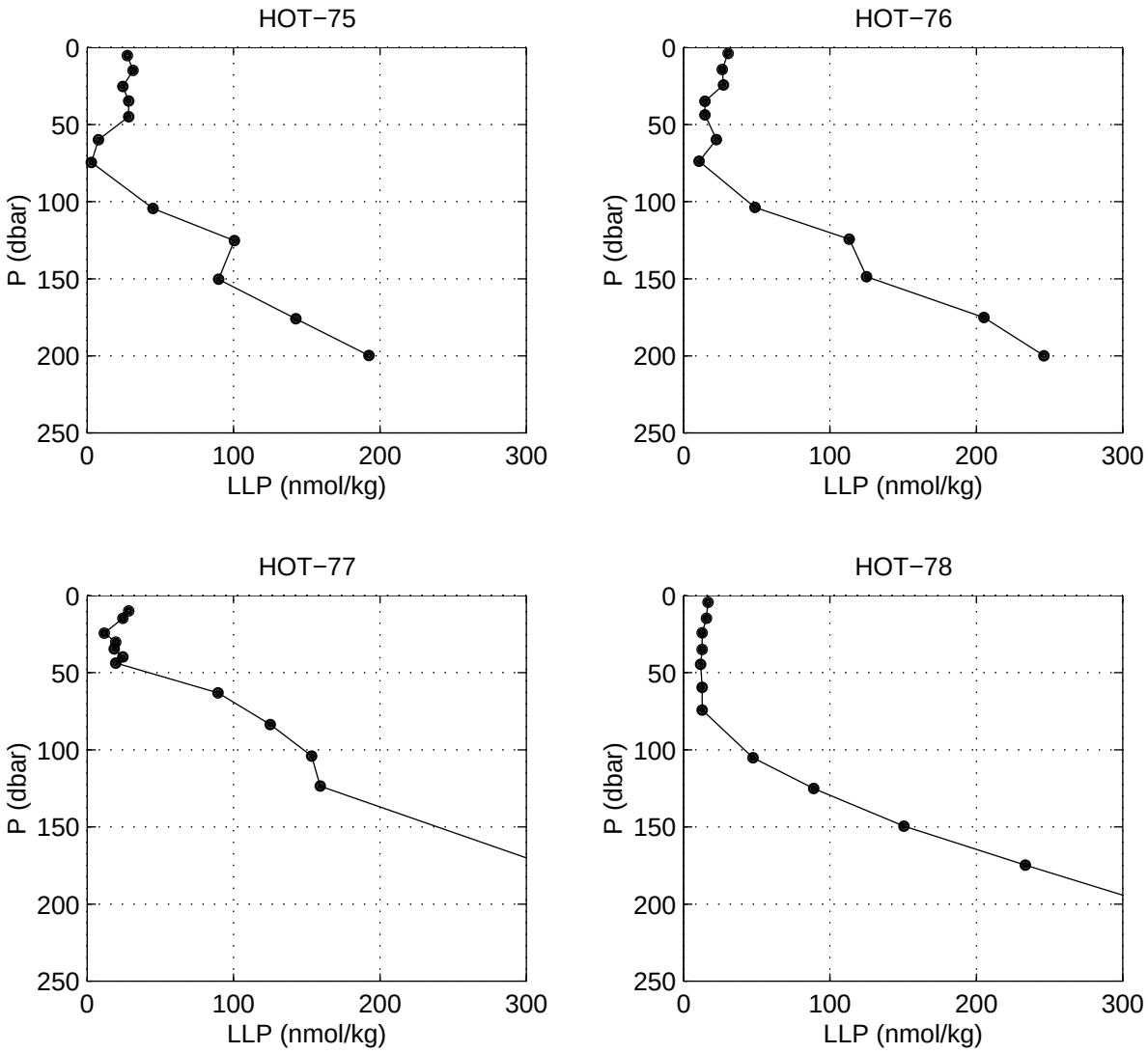

Figure 6.2.7 continued

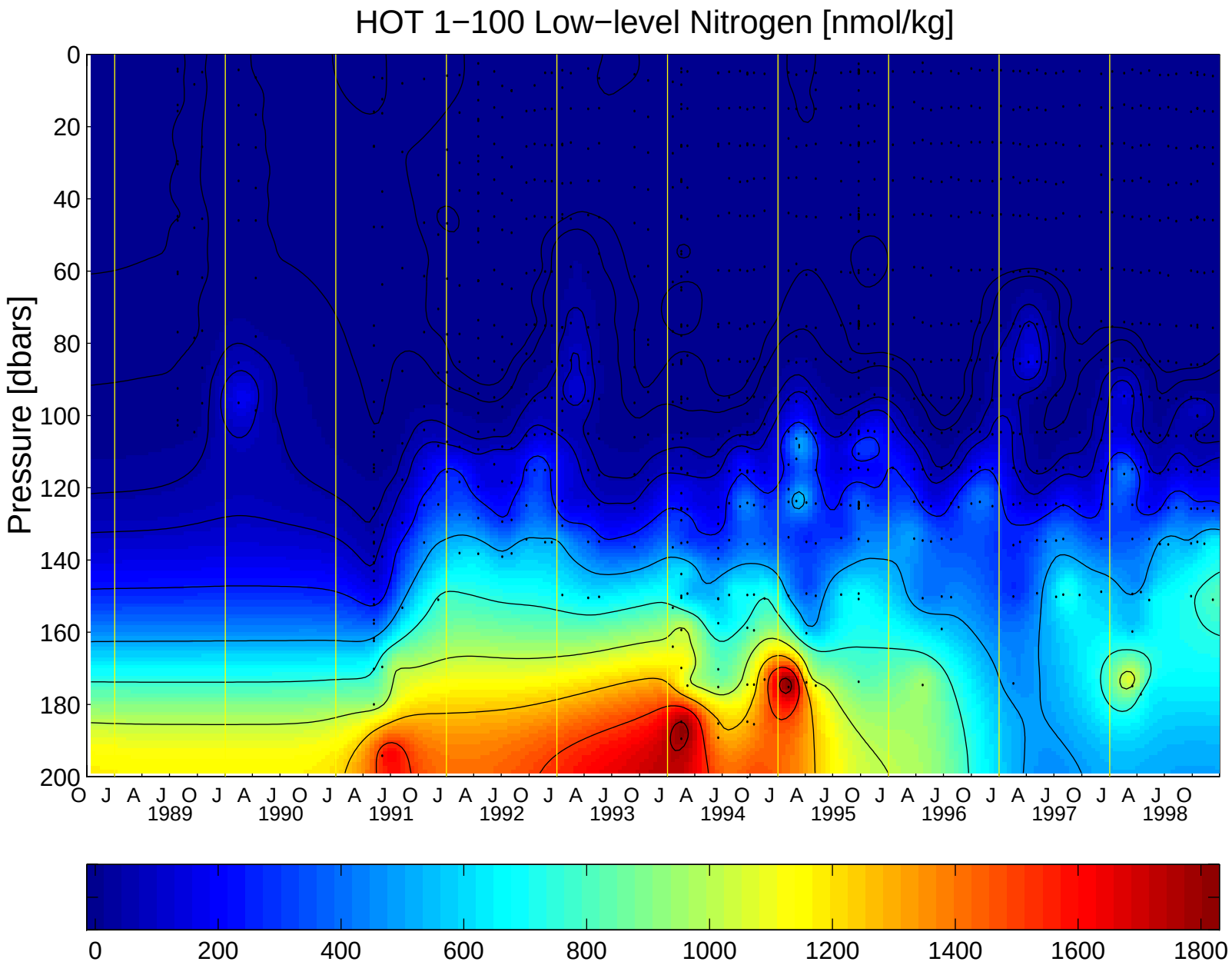
HOT 1−100 Low−level Nitrogen [nmol/kg]
Pressure [dbars]
0
20
40
60
80
100
120
140
160
180
200
O J A J O J A J O J A J O J A J O J A J O J A J O J A J O J A J O J A J O J A J O J A J O J A J O
1989
1990
1991
1992
1993
1994
1995
1996
1997
1998
0
200
400
600
800
1000
1200
1400
1600
1800

Figure 6.2.8

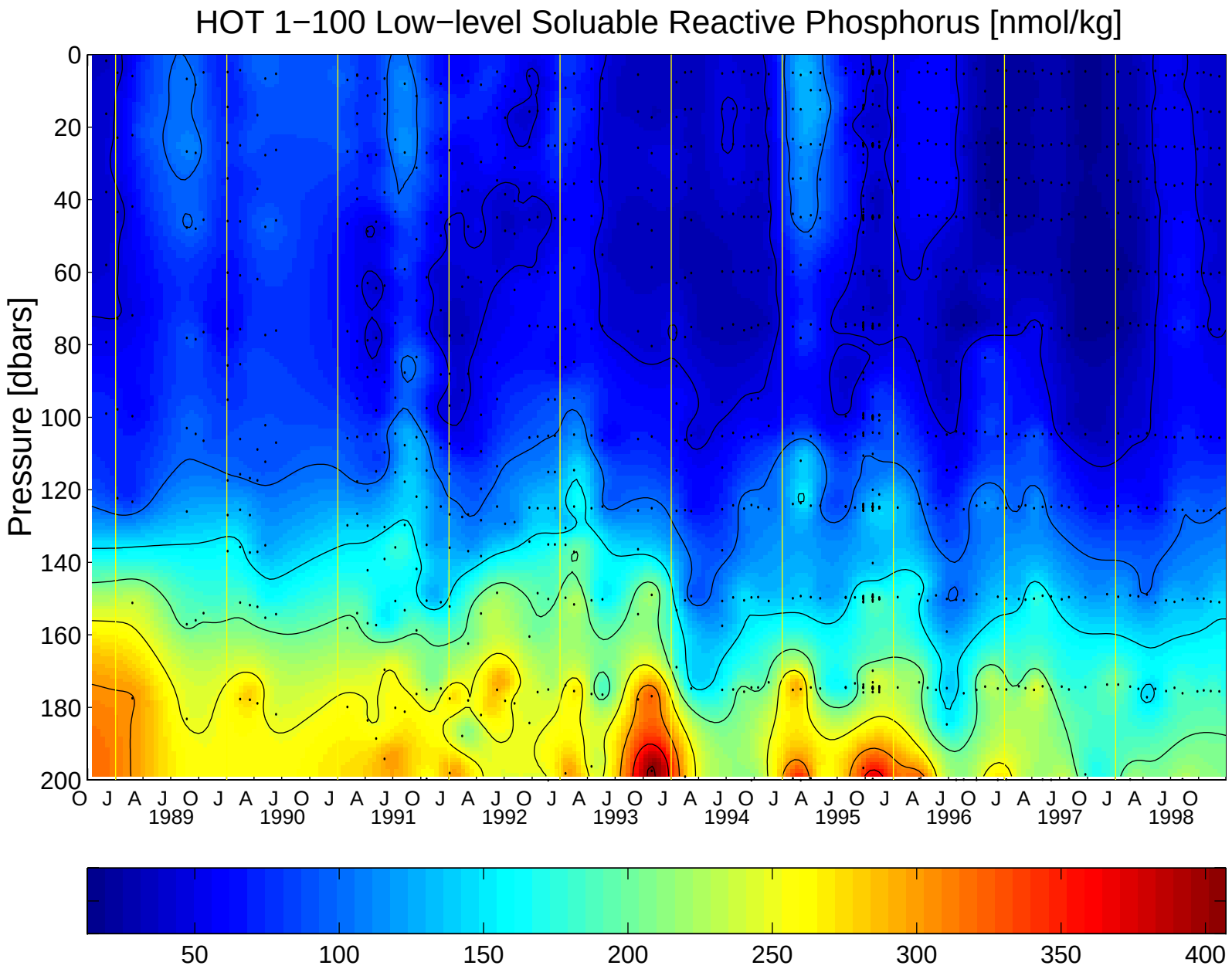
HOT 1−100 Low−level Soluable Reactive Phosphorus [nmol/kg]
Pressure [dbars]
0
20
40
60
80
100
120
140
160
180
200
O J A J O J A J O J A J O J A J O J A J O J A J O J A J O J A J O J A J O J A J O J A J O
1989
1990
1991
1992
1993
1994
1995
1996
1997
1998
50
100
150
200
250
300
350
400

Figure 6.2.9

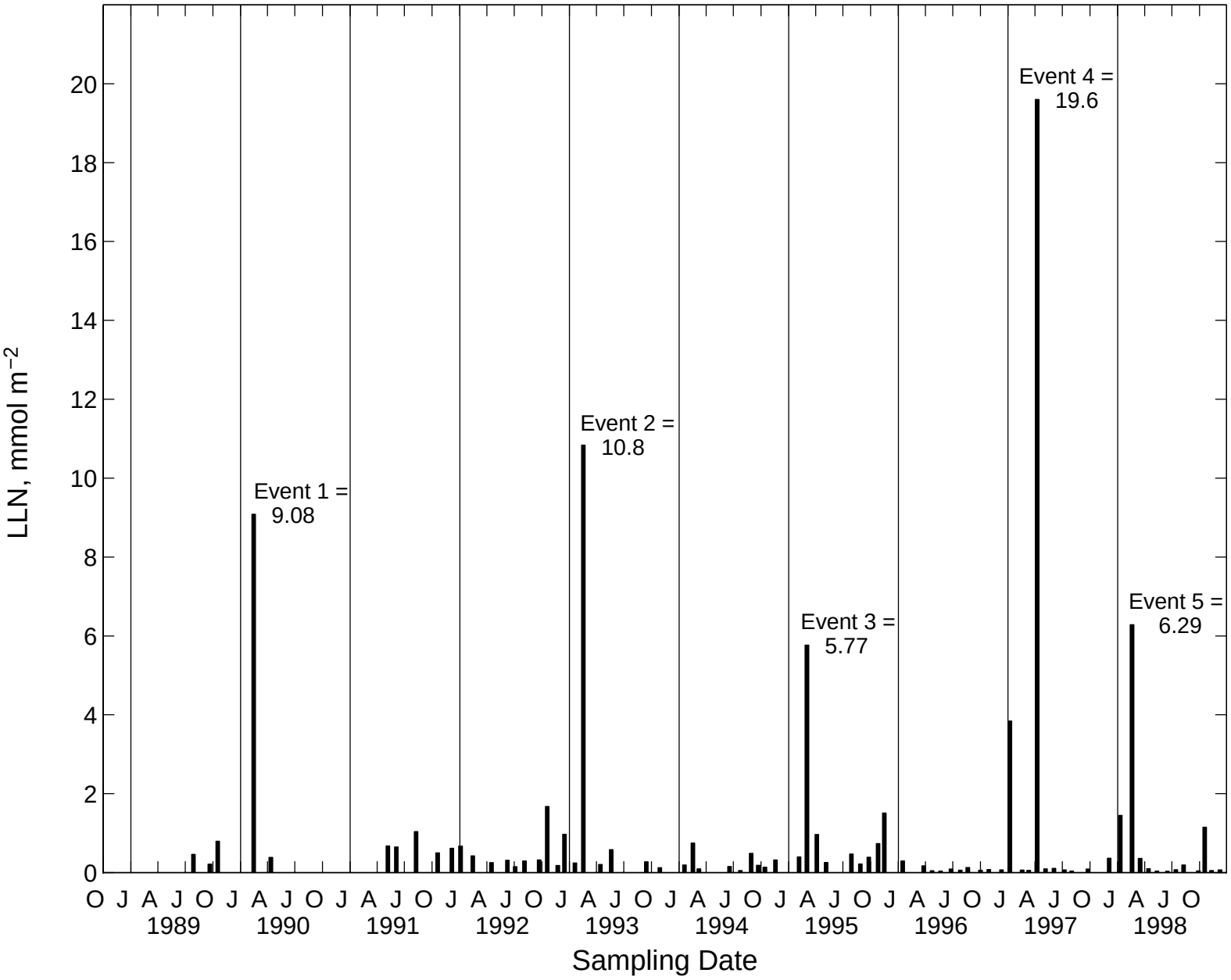
LLN, mmol m^{-2}
Event 1 = 9.08
Event 2 = 10.8
Event 3 = 5.77
Event 4 = 19.6
Event 5 = 6.29
0
2
4
6
8
10
12
14
16
18
20
O J A J O J A J O J A J O J A J O J A J O J A J O J A J O J A J O
1989
1990
1991
1992
1993
1994
1995
1996
1997
1998
Sampling Date

Figure 6.2.10

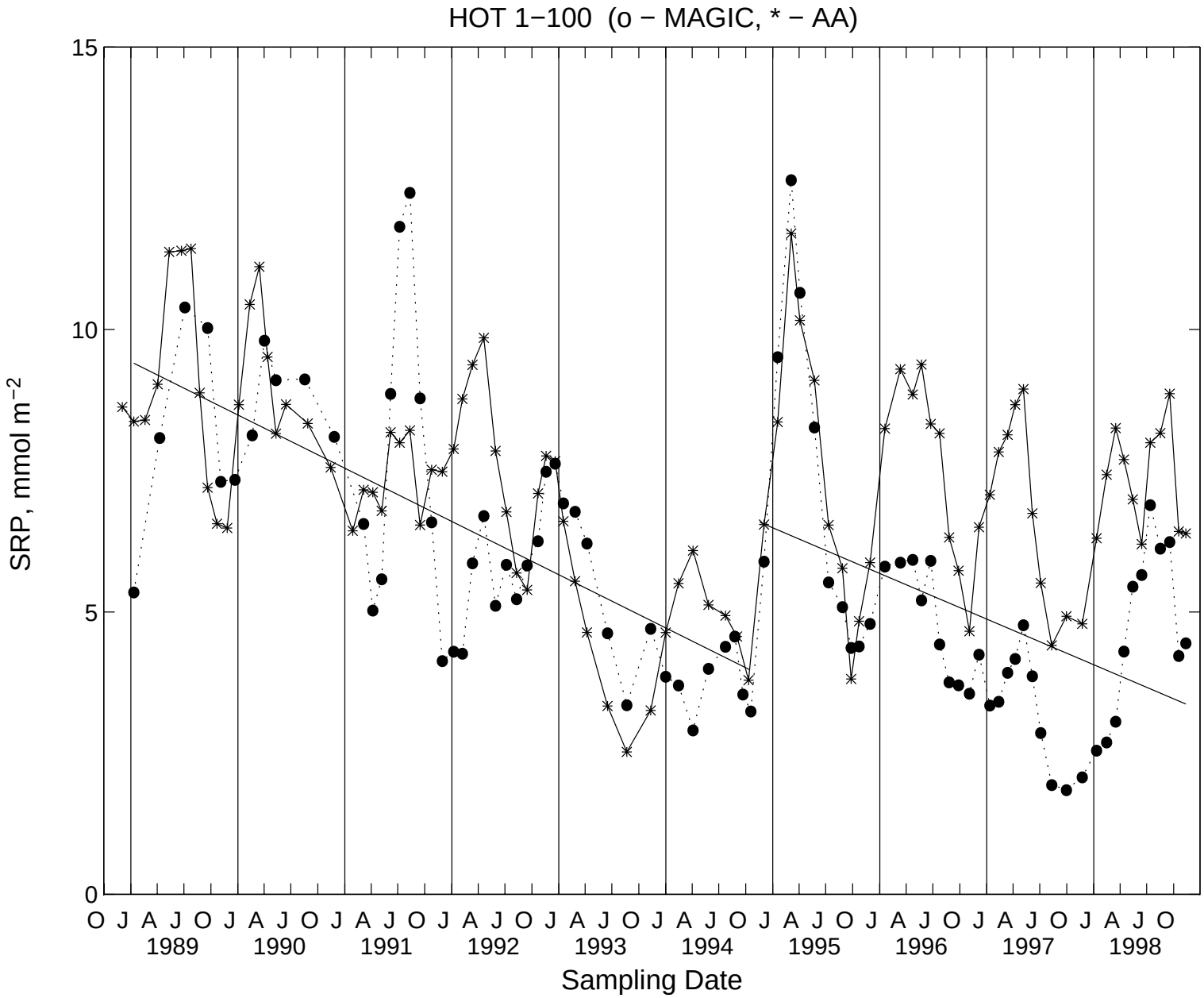
HOT 1−100 (o − MAGIC, * − AA)
SRP, mmol m^{-2}
15
10
5
0
O J A J O J A J O J A J O J A J O J A J O J A J O J A J O J A J O J A J O J A J O
1989
1990
1991
1992
1993
1994
1995
1996
1997
1998
Sampling Date

Figure 6.2.11

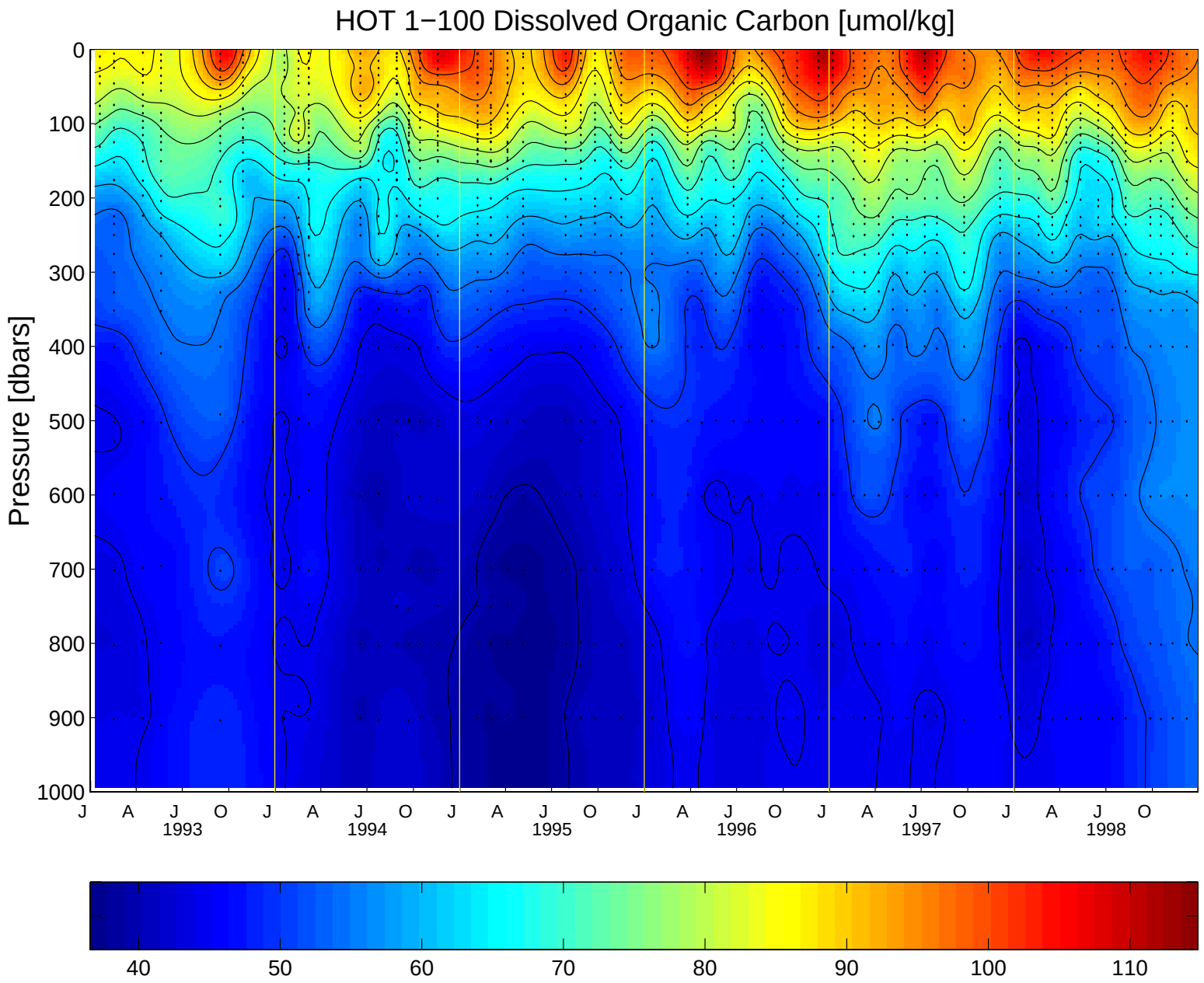
HOT 1−100 Dissolved Organic Carbon [umol/kg]
Pressure [dbars]
0
100
200
300
400
500
600
700
800
900
1000
J A J O J A J O J A J O J A J O J A J O J A J O J A J O
1993
1994
1995
1996
1997
1998
40
50
60
70
80
90
100
110

Figure 6.2.12

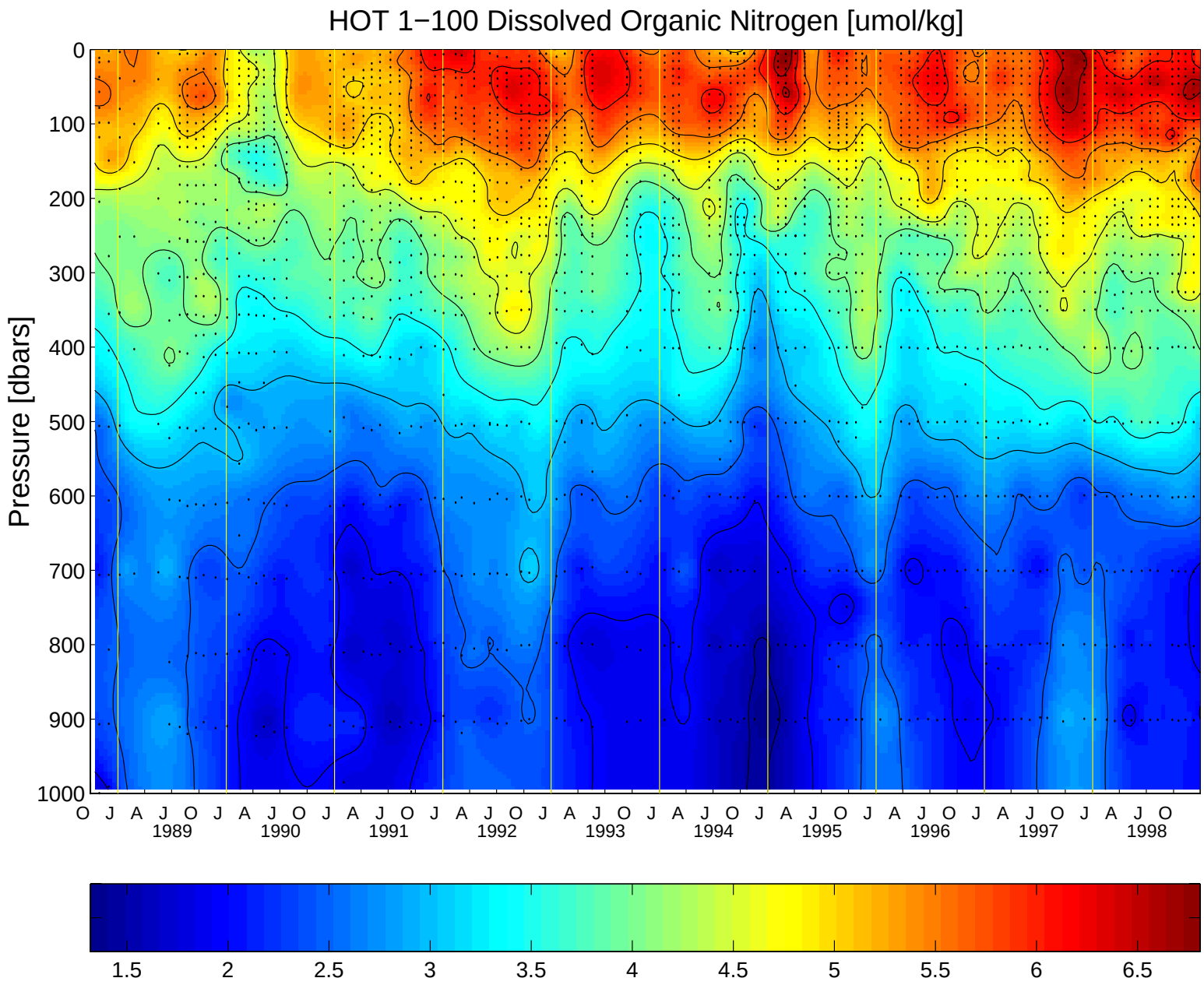
HOT 1−100 Dissolved Organic Nitrogen [umol/kg]
Pressure [dbars]
0
100
200
300
400
500
600
700
800
900
1000
O J A J O J A J O J A J O J A J O J A J O J A J O J A J O J A J O J A J O J A J O J A J O J A J O J A J O J A J O
1989
1990
1991
1992
1993
1994
1995
1996
1997
1998
1.5
2
2.5
3
3.5
4
4.5
5
5.5
6
6.5

Figure 6.2.13

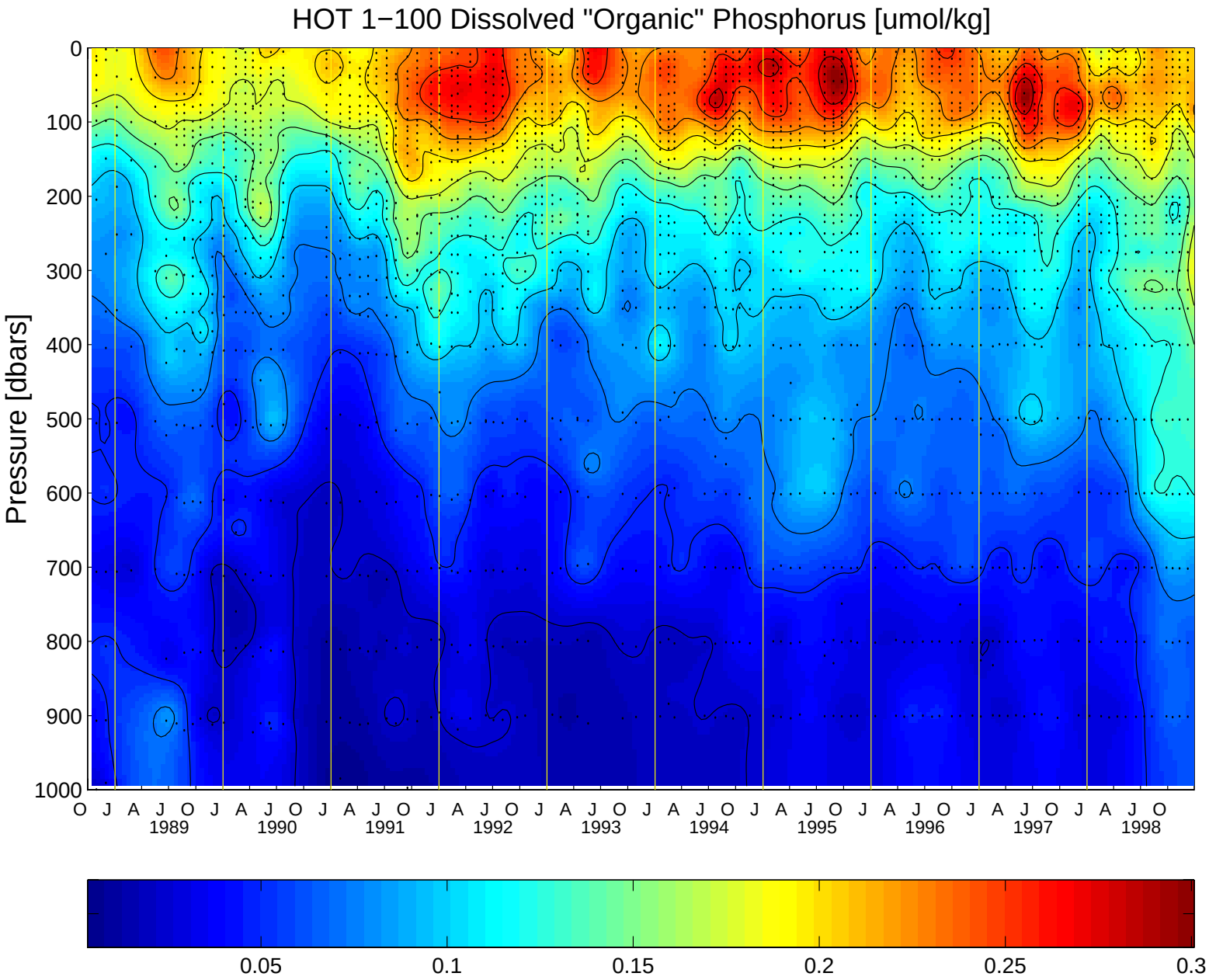
HOT 1−100 Dissolved "Organic" Phosphorus [umol/kg]
Pressure [dbars]
0
100
200
300
400
500
600
700
800
900
1000
O J A J O J A J O J A J O J A J O J A J O J A J O J A J O J A J O J A J O J A J O J A J O J A J O
1989
1990
1991
1992
1993
1994
1995
1996
1997
1998
0.05
0.1
0.15
0.2
0.25
0.3

Figure 6.2.14

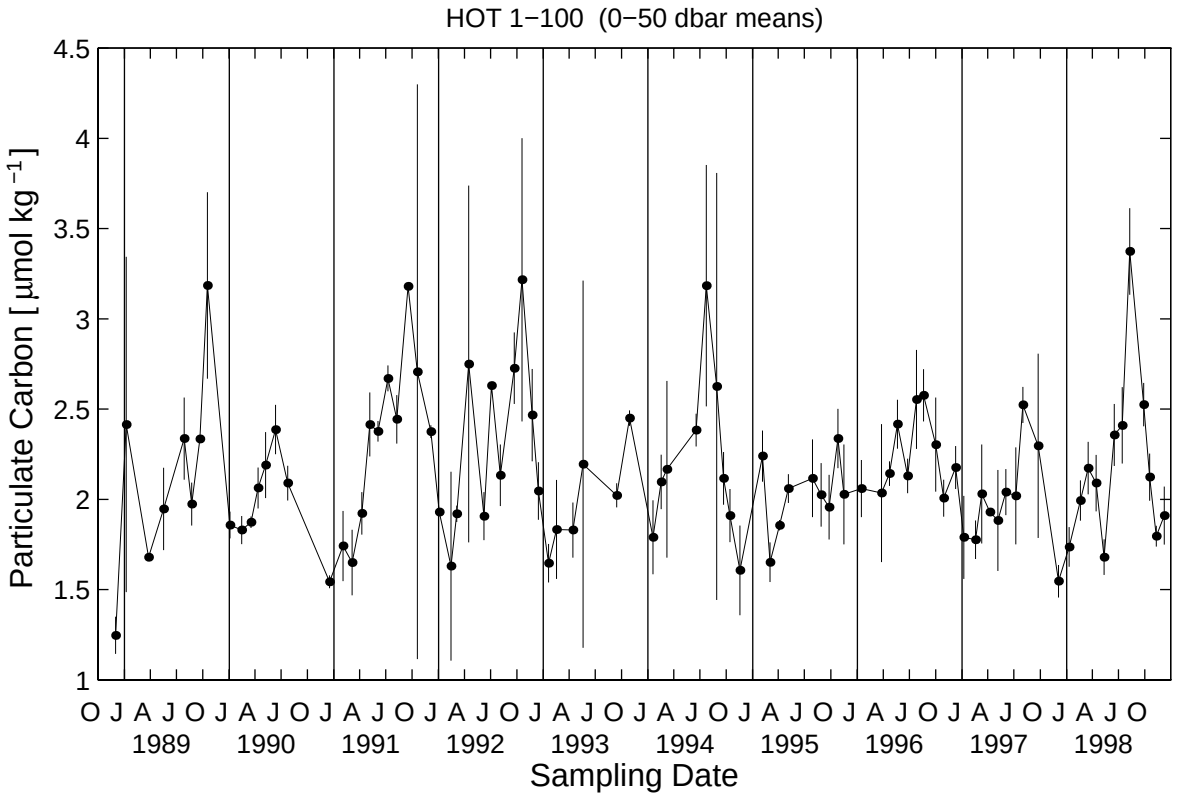
HOT 1−100 (0−50 dbar means)
Particulate Carbon [µmol kg −1]
4.5
4
3.5
3
2.5
2
1.5
1
O J A J O J A J O J A J O J A J O J A J O J A J O J A J O J A J O J A J O J A J O J A J O
1989
1990
1991
1992
1993
1994
1995
1996
1997
1998
Sampling Date

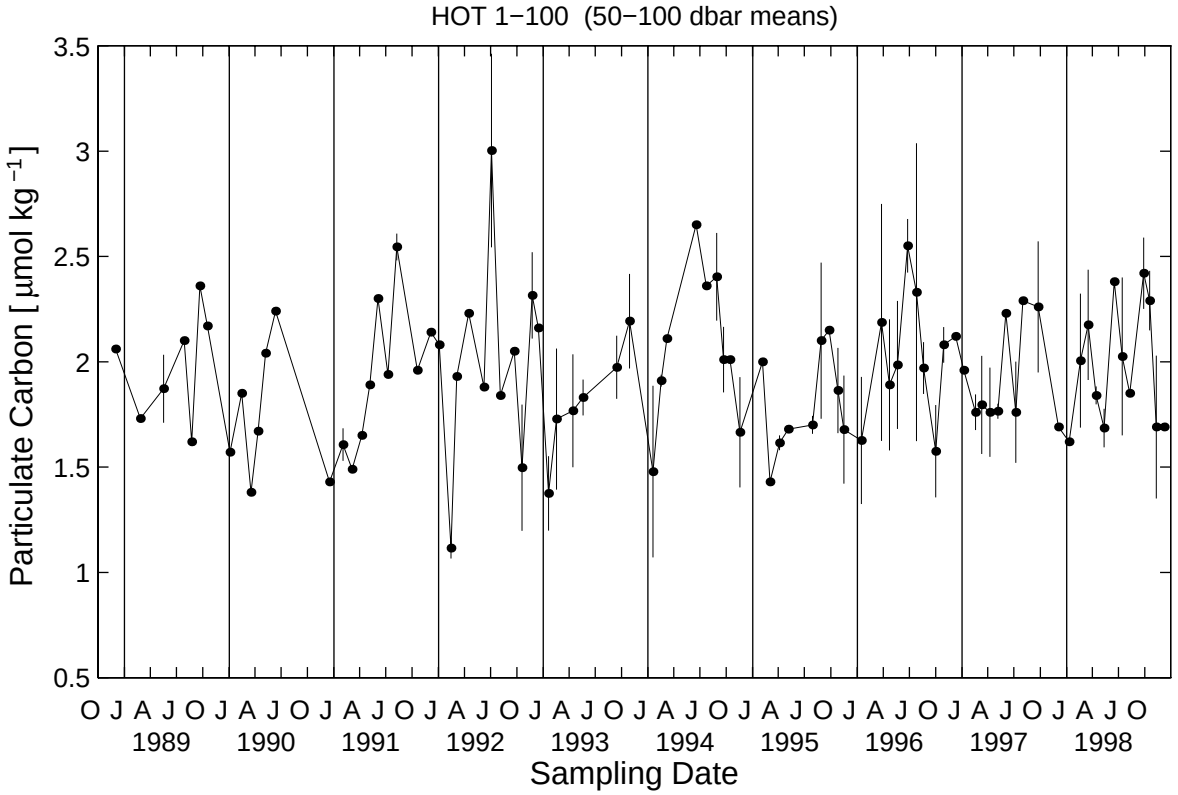
HOT 1−100 (50−100 dbar means)
Particulate Carbon [µmol kg −1]
3.5
3
2.5
2
1.5
1
0.5
O J A J O J A J O J A J O J A J O J A J O J A J O J A J O J A J O J A J O J A J O J A J O
1989
1990
1991
1992
1993
1994
1995
1996
1997
1998
Sampling Date

Figure 6.2.15

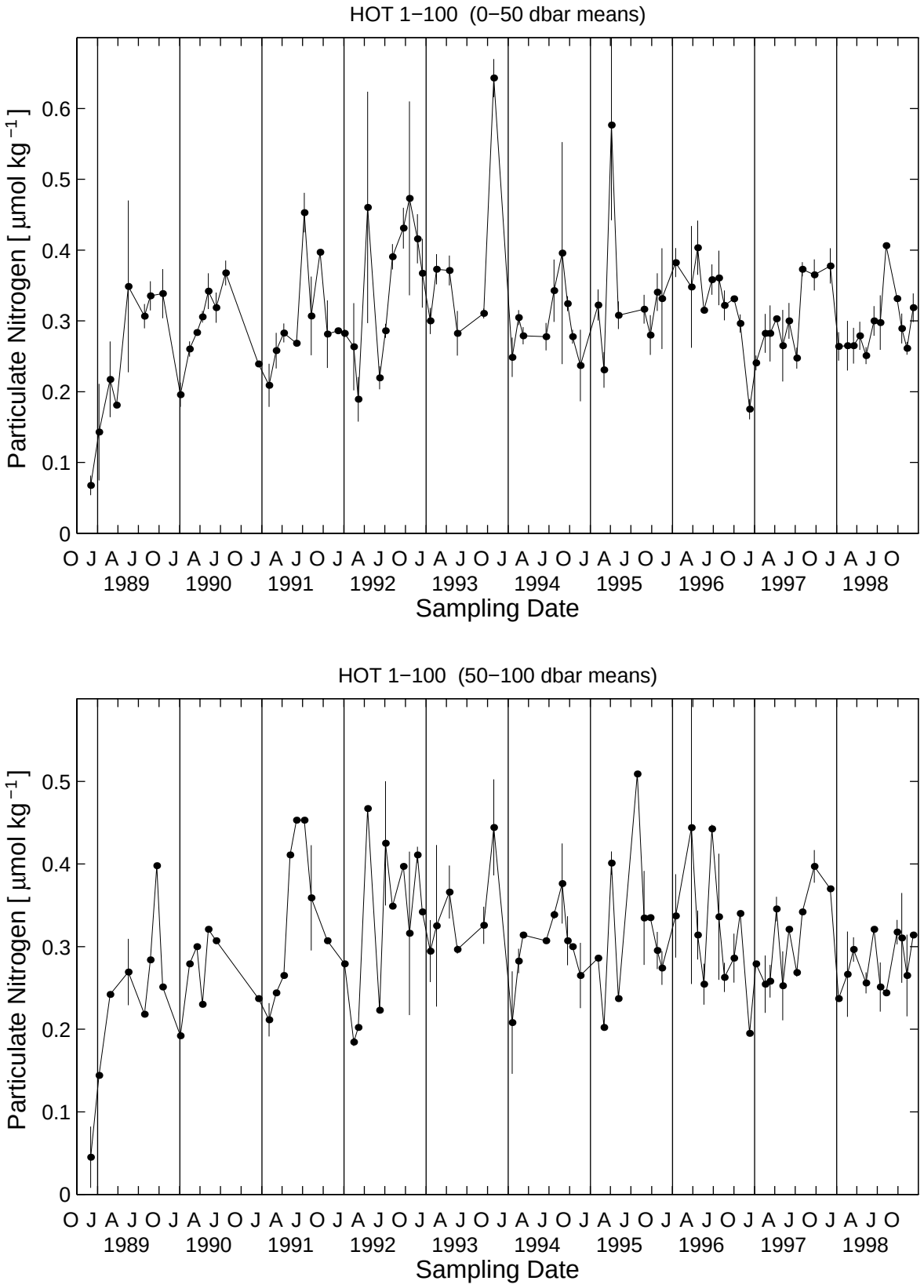
HOT 1−100 (0−50 dbar means)
Particulate Nitrogen [µmol kg −1]
0
0.1
0.2
0.3
0.4
0.5
0.6
O J A J O J A J O J A J O J A J O J A J O J A J O J A J O J A J O J A J O J A J O J A J O
1989
1990
1991
1992
1993
1994
1995
1996
1997
1998
Sampling Date
HOT 1−100 (50−100 dbar means)
Particulate Nitrogen [µmol kg −1]
0
0.1
0.2
0.3
0.4
0.5
O J A J O J A J O J A J O J A J O J A J O J A J O J A J O J A J O J A J O J A J O J A J O
1989
1990
1991
1992
1993
1994
1995
1996
1997
1998
Sampling Date

Figure 6.2.16

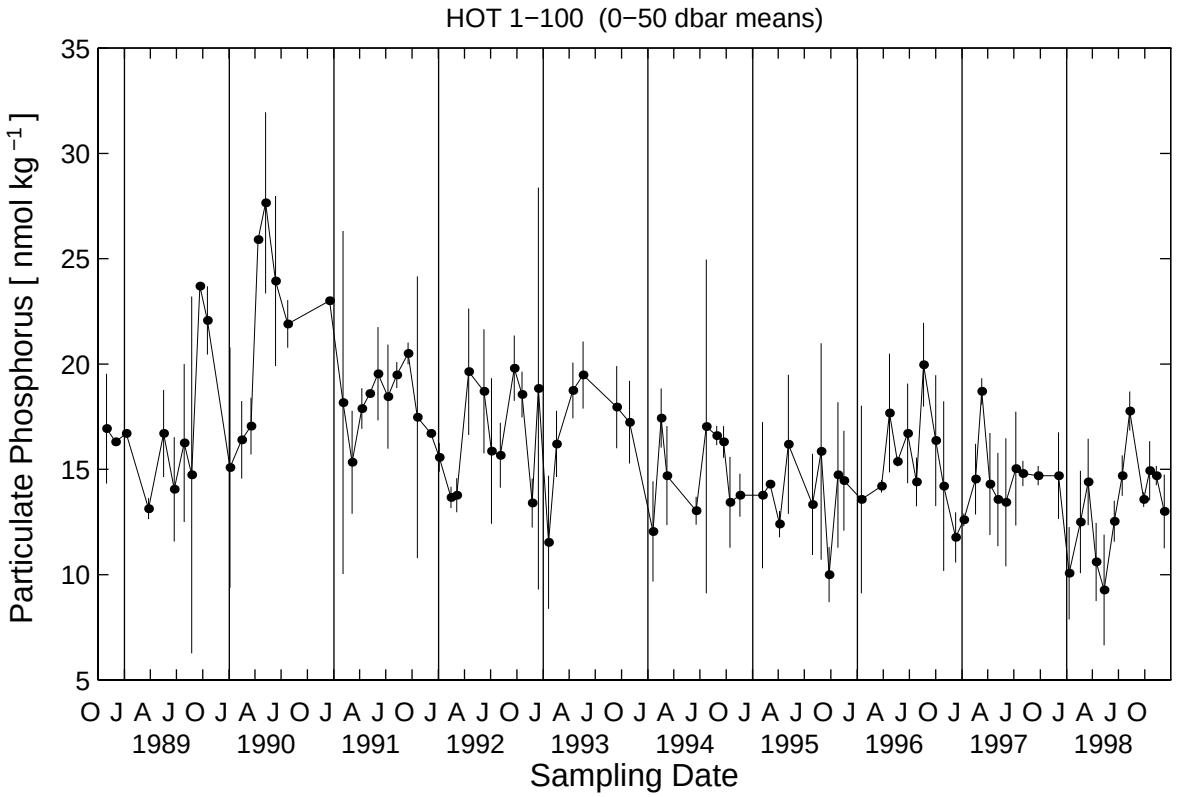
HOT 1−100 (0−50 dbar means)
Particulate Phosphorus [nmol kg −1]
35
30
25
20
15
10
5
O J A J O J A J O J A J O J A J O J A J O J A J O J A J O J A J O J A J O
1989
1990
1991
1992
1993
1994
1995
1996
1997
1998
Sampling Date

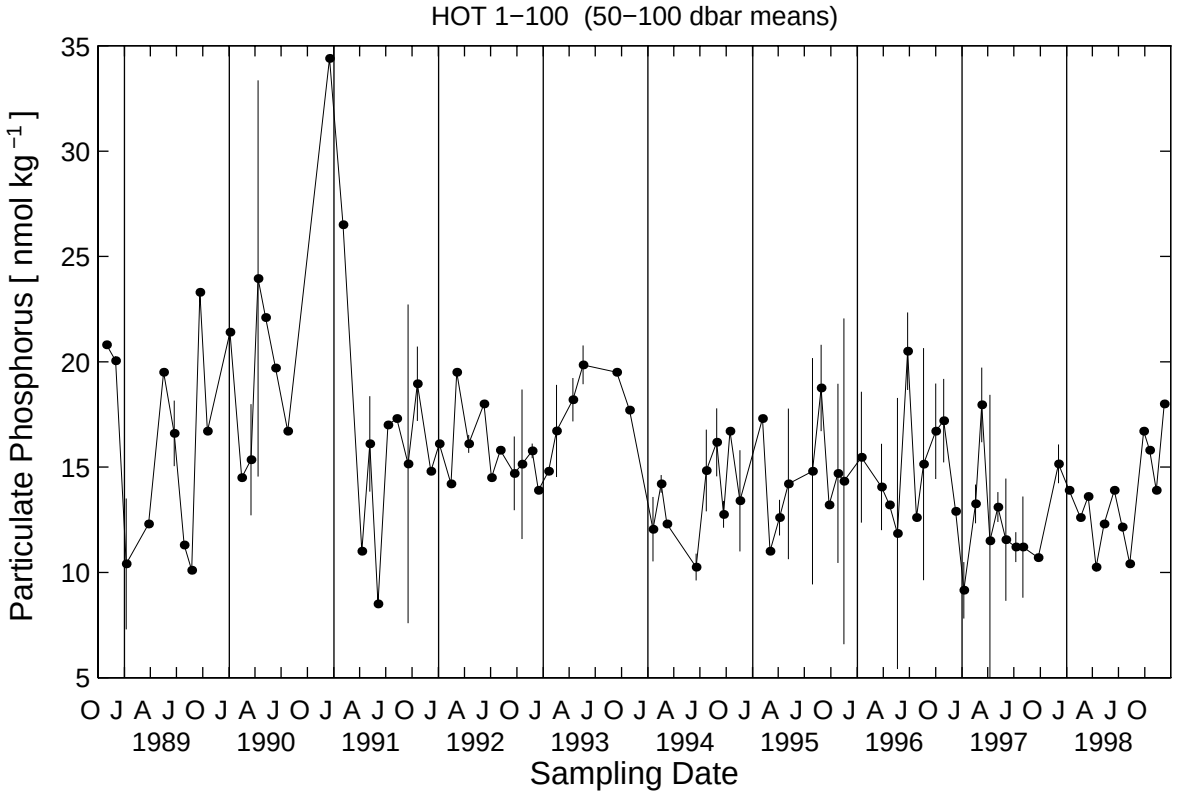
HOT 1−100 (50−100 dbar means)
Particulate Phosphorus [nmol kg −1]
35
30
25
20
15
10
5
O J A J O J A J O J A J O J A J O J A J O J A J O J A J O J A J O J A J O
1989
1990
1991
1992
1993
1994
1995
1996
1997
1998
Sampling Date

Figure 6.2.17

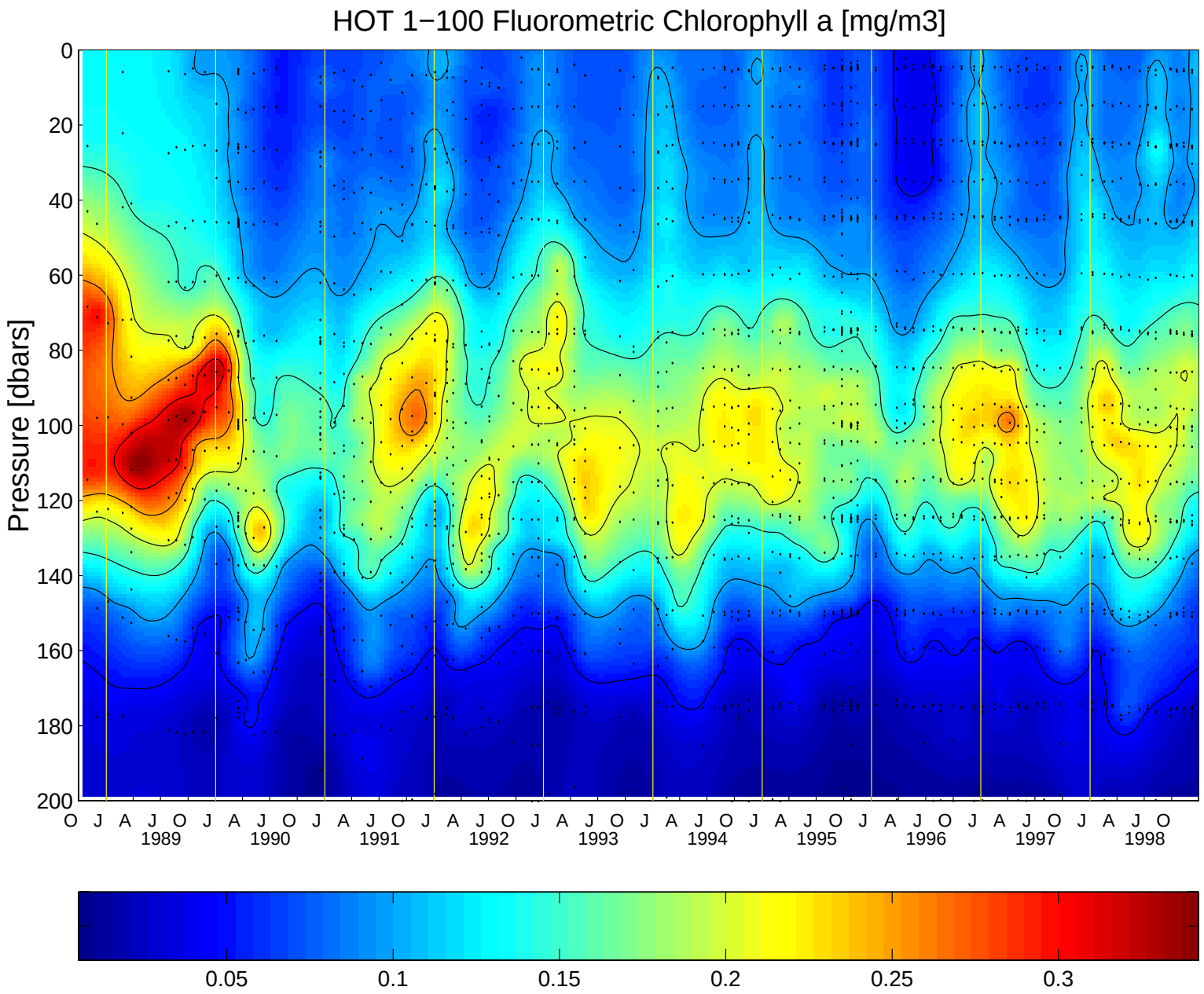
HOT 1−100 Fluorometric Chlorophyll a [mg/m3]
Pressure [dbars]
0
20
40
60
80
100
120
140
160
180
200
O J A J O J A J O J A J O J A J O J A J O J A J O J A J O J A J O J A J O J A J O J A J O J A J O J A J O
1989
1990
1991
1992
1993
1994
1995
1996
1997
1998
0.05
0.1
0.15
0.2
0.25
0.3

Figure 6.2.18

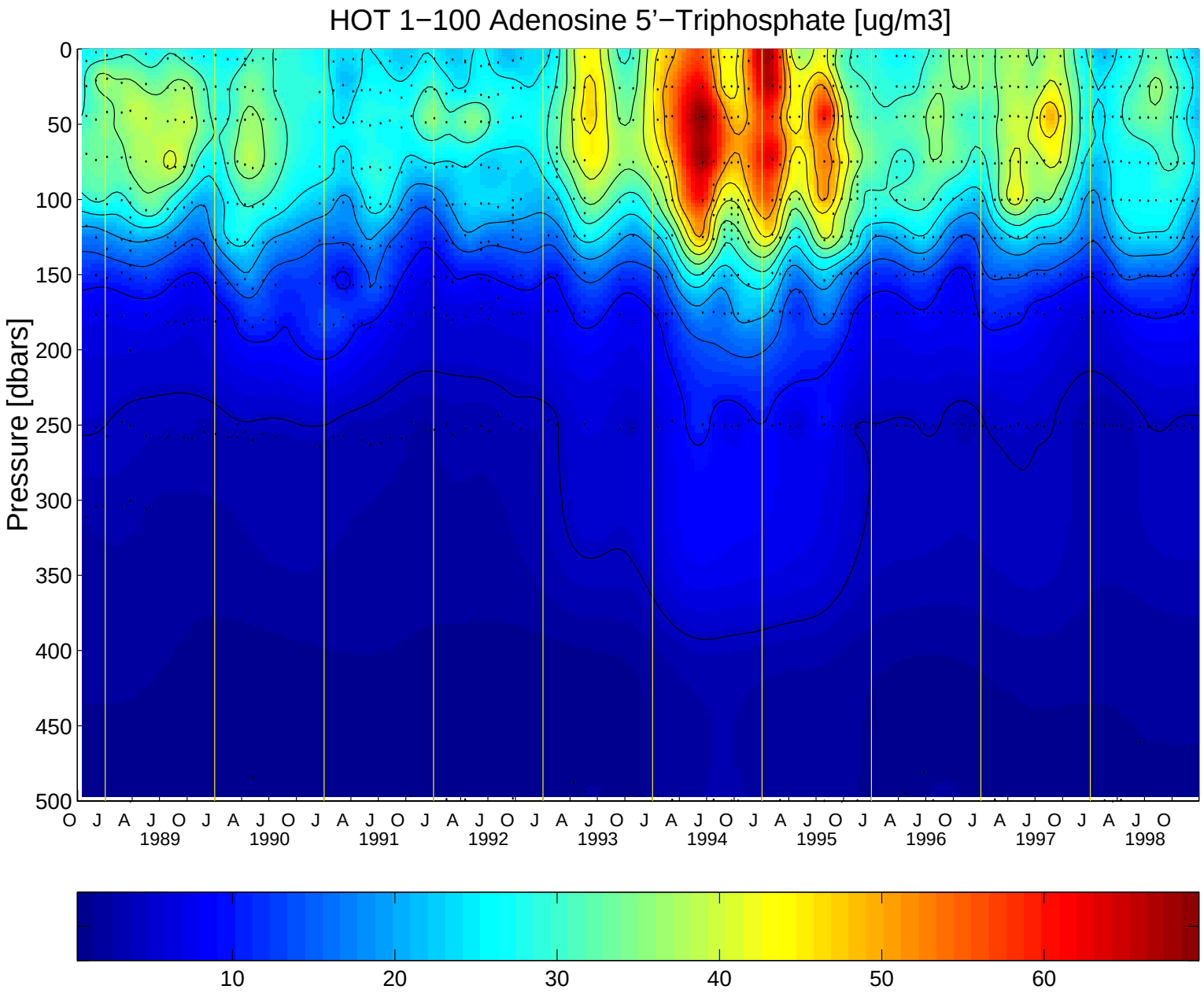
HOT 1−100 Adenosine 5'−Triphosphate [ug/m3]
Pressure [dbars]
0
50
100
150
200
250
300
350
400
450
500
O J A J O J A J O J A J O J A J O J A J O J A J O J A J O J A J O J A J O J A J O J A J O
1989
1990
1991
1992
1993
1994
1995
1996
1997
1998
10
20
30
40
50
60

Figure 6.2.19

6.3. ADCP MEASUREMENTS

Figures 6.3.1a to l: Velocity fields at Station ALOHA. Top panel shows hourly averages at 20-m depth intervals while the ship was on station. The orientation of each stick gives the direction of the current: up is northward and to the right is eastward. The bottom panel shows the results of a least-squares fit of hourly averages to a mean, trend, semi-diurnal and diurnal tides; the on-station time-series were not long enough to fit an inertial cycle. In the first column the arrow shows the mean current and the headless stick shows the sum of the mean plus the trend at the end of the station. For each harmonic the current ellipse is shown in the first column. The orientation of the stick in the second column shows the direction of the harmonic component of the current at the beginning of the station and the arrowhead at the end of the stick shows the direction of rotation of the current vector around the ellipse. The gap in the station data of HOT-71 is due to excursions to retrieve the primary productivity array and the floating sediment traps.

Figures 6.3.2a to m: Velocity fields on the transits to and from Station ALOHA and Station 3. Velocity is shown as a function of latitude averaged in 10-minute intervals. HOT-72 Leg I has 2 north and south transits to and from Station ALOHA due to a medical evacuation which was made shortly after the ship reached Station ALOHA. The transit was made to Heeia Kea boat harbor, Oahu with a return to ALOHA.

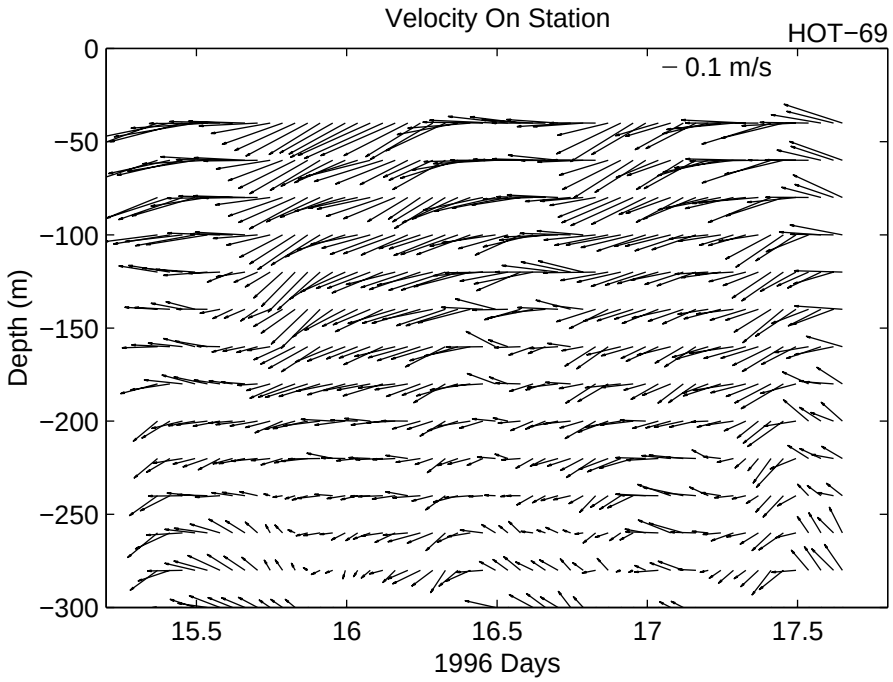
Velocity On Station
HOT−69
− 0.1 m/s
0
−50
−100
−150
−200
−250
−300
Depth (m)
15.5
16
16.5
17
17.5
1996 Days

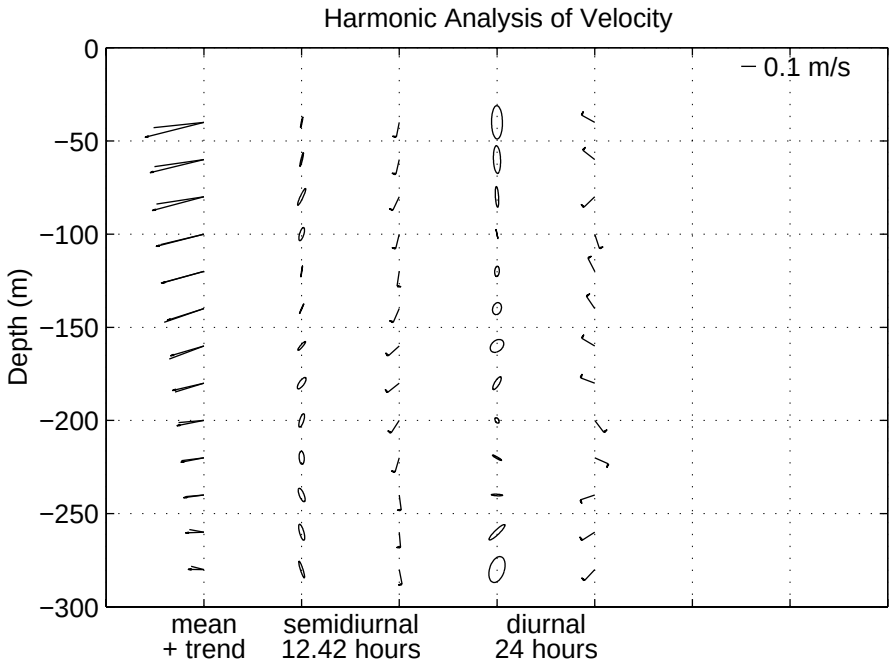
Harmonic Analysis of Velocity
− 0.1 m/s
0
−50
−100
−150
−200
−250
−300
Depth (m)
mean
+ trend
semidiurnal
12.42 hours
diurnal
24 hours

Figure 6.3.1a

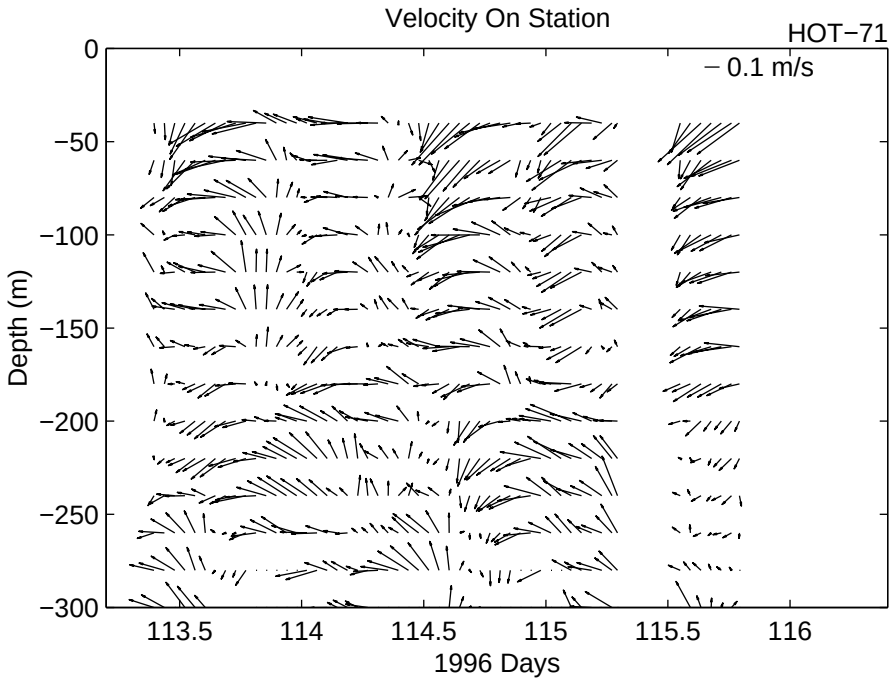
Velocity On Station
HOT−71
− 0.1 m/s
0
−50
−100
−150
−200
−250
−300
Depth (m)
113.5
114
114.5
115
115.5
116
1996 Days

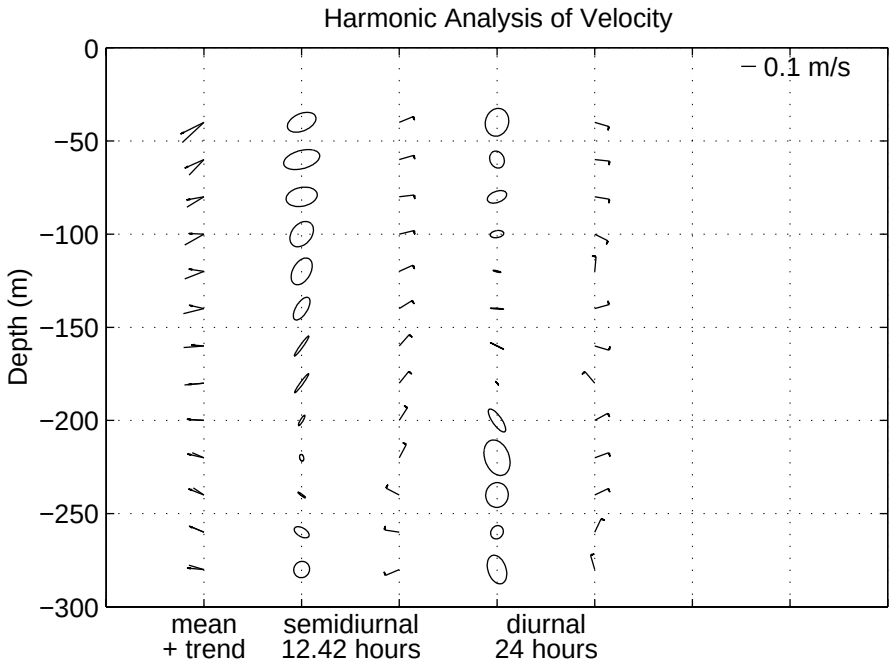
Harmonic Analysis of Velocity
− 0.1 m/s
0
−50
−100
−150
−200
−250
−300
Depth (m)
mean
+ trend
semidiurnal
12.42 hours
diurnal
24 hours

Figure 6.3.1b

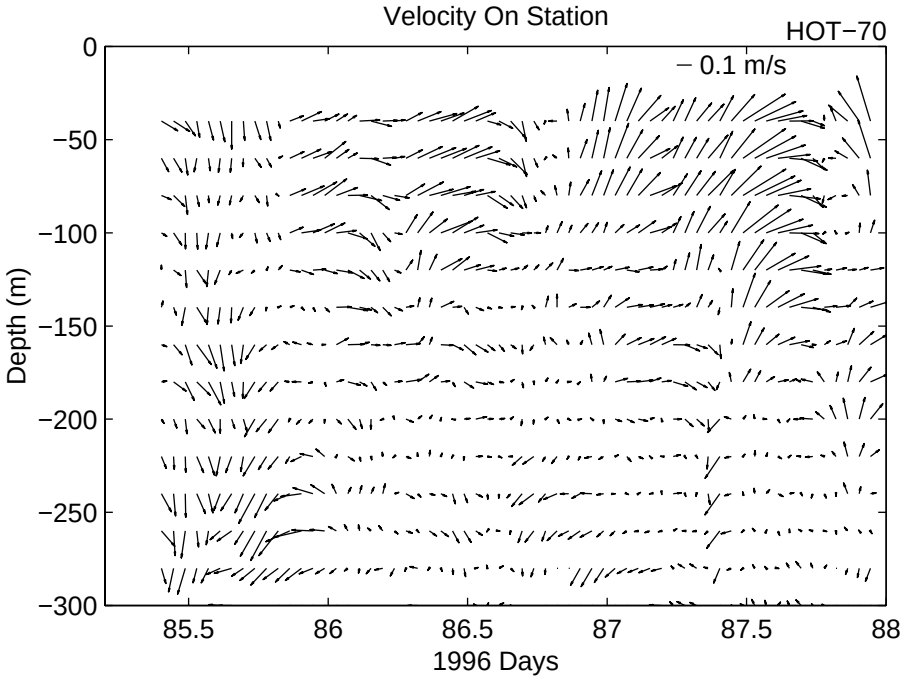
Velocity On Station
HOT−70
− 0.1 m/s
0
−50
−100
−150
−200
−250
−300
Depth (m)
85.5
86
86.5
87
87.5
88
1996 Days

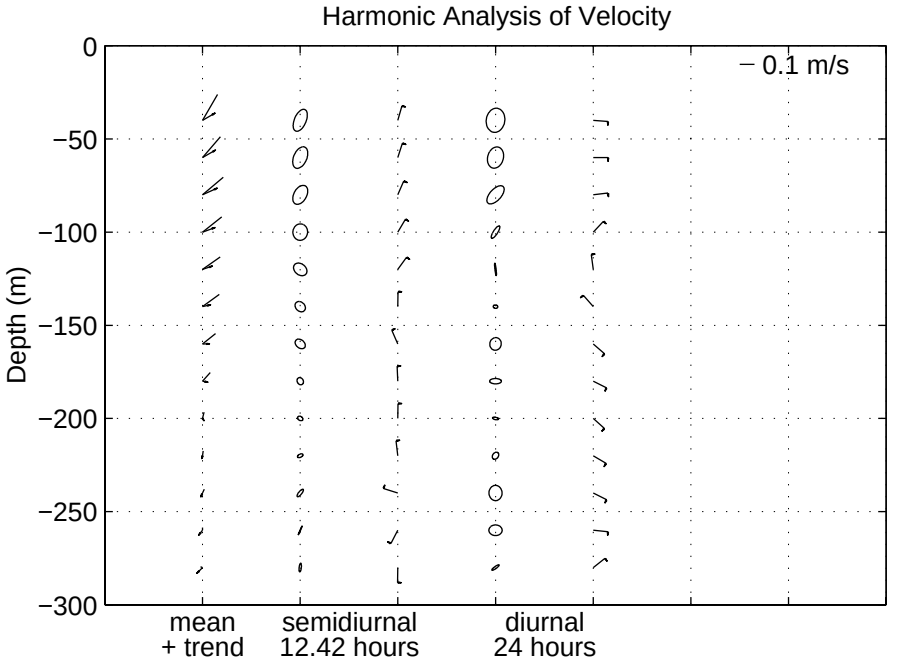
Harmonic Analysis of Velocity
− 0.1 m/s
0
−50
−100
−150
−200
−250
−300
Depth (m)
mean
+ trend
semidiurnal
12.42 hours
diurnal
24 hours

Figure 6.3.1c

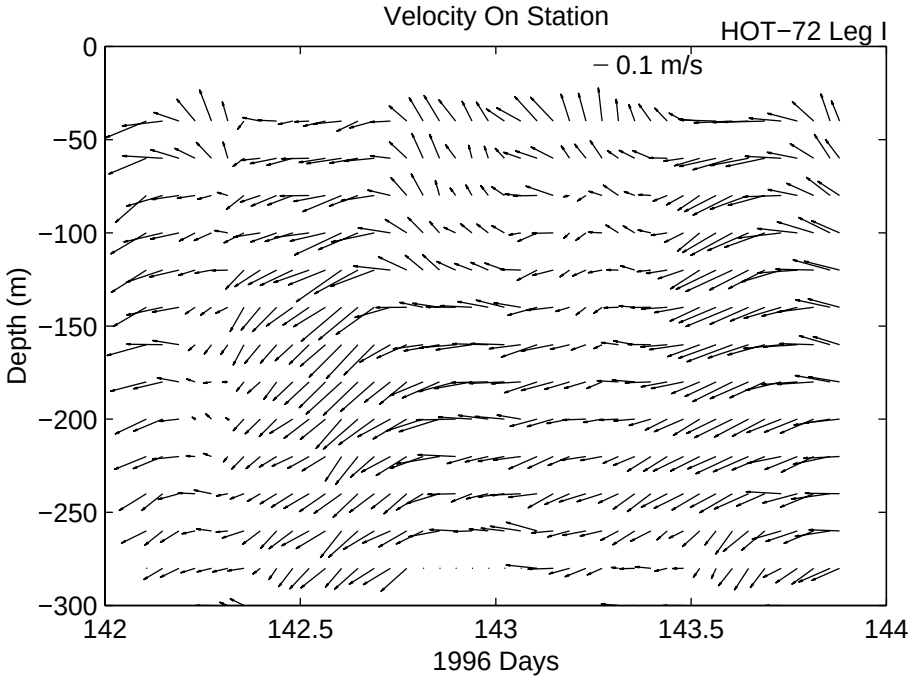
Velocity On Station
HOT−72 Leg I
− 0.1 m/s
0
−50
−100
−150
−200
−250
−300
Depth (m)
142
142.5
143
143.5
144
1996 Days

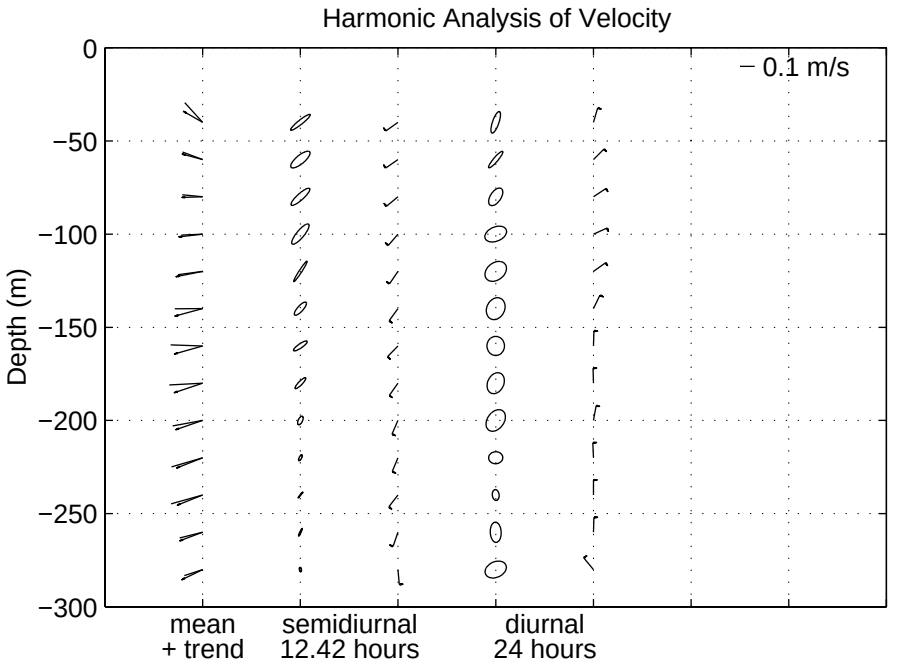
Harmonic Analysis of Velocity
− 0.1 m/s
0
−50
−100
−150
−200
−250
−300
Depth (m)
mean
+ trend
semidiurnal
12.42 hours
diurnal
24 hours

Figure 6.3.1d

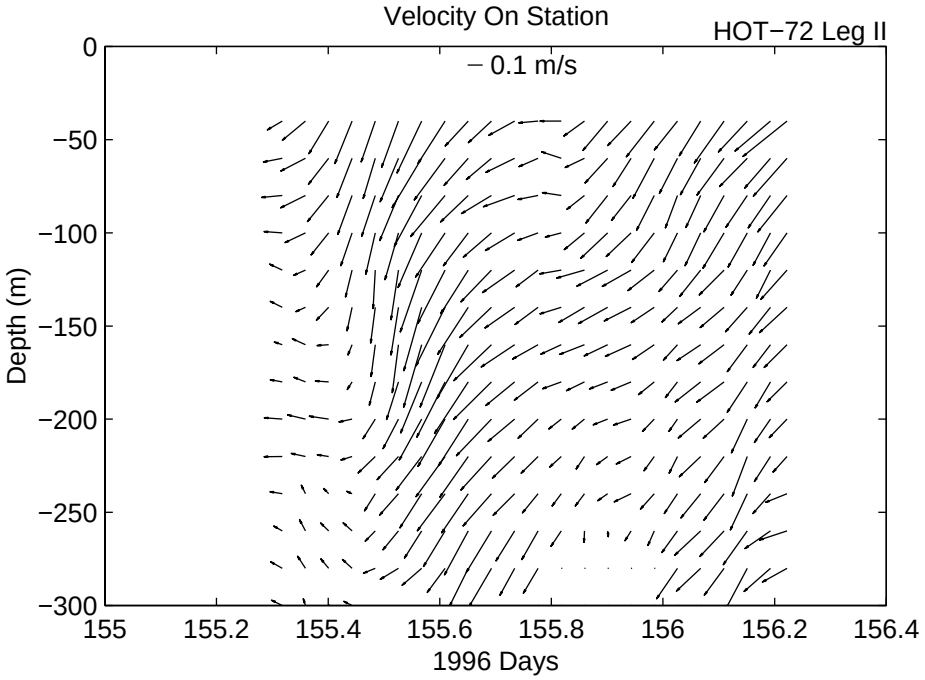
Velocity On Station
HOT−72 Leg II
− 0.1 m/s
0
−50
−100
−150
−200
−250
−300
Depth (m)
155
155.2
155.4
155.6
155.8
156
156.2
156.4
1996 Days

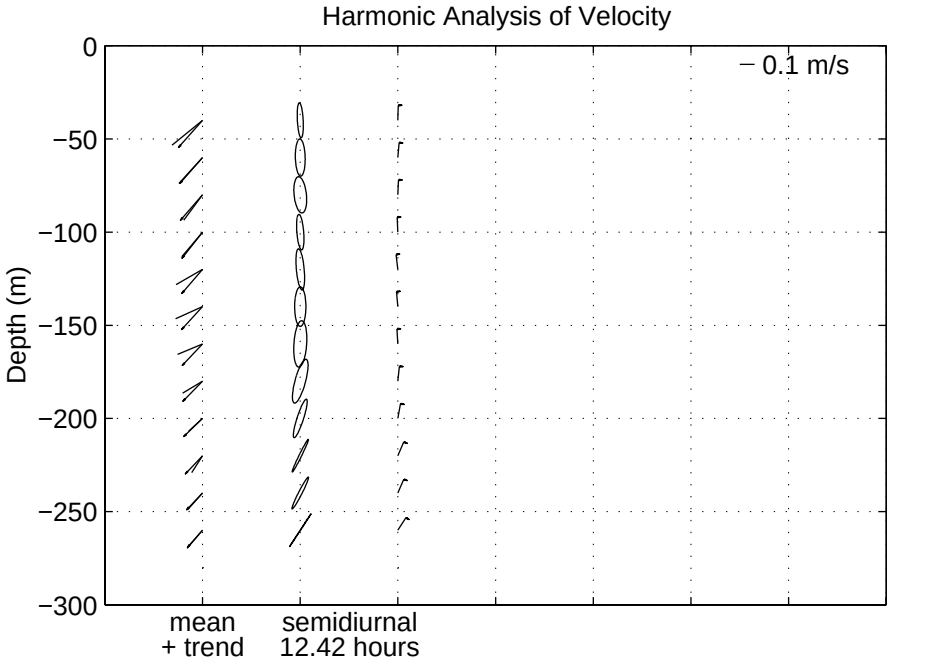
Harmonic Analysis of Velocity
− 0.1 m/s
0
−50
−100
−150
−200
−250
−300
Depth (m)
mean
+ trend
semidiurnal
12.42 hours

Figure 6.3.1e

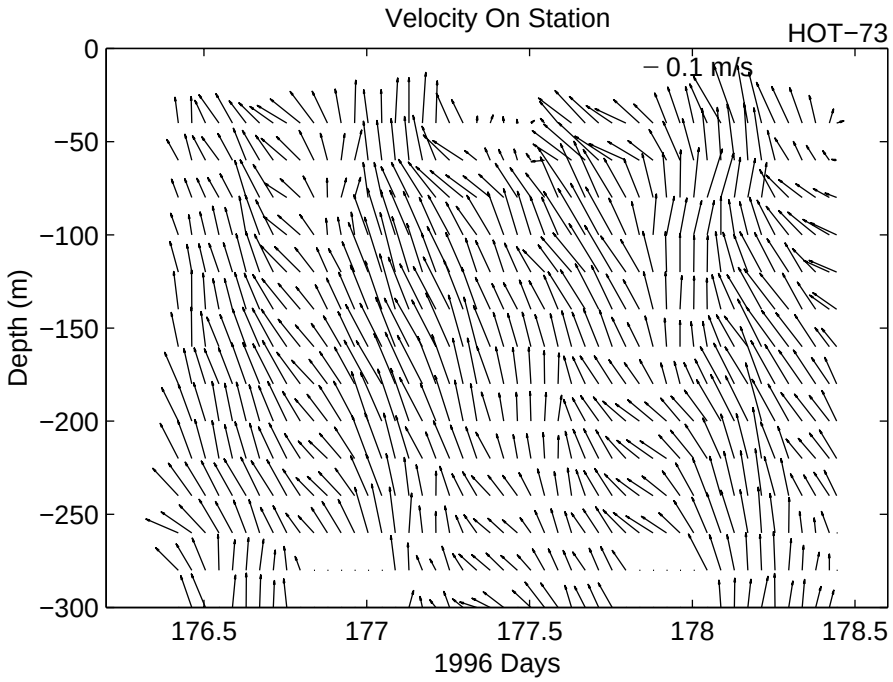
Velocity On Station
HOT−73
− 0.1 m/s
0
−50
−100
−150
−200
−250
−300
Depth (m)
176.5
177
177.5
178
178.5
1996 Days

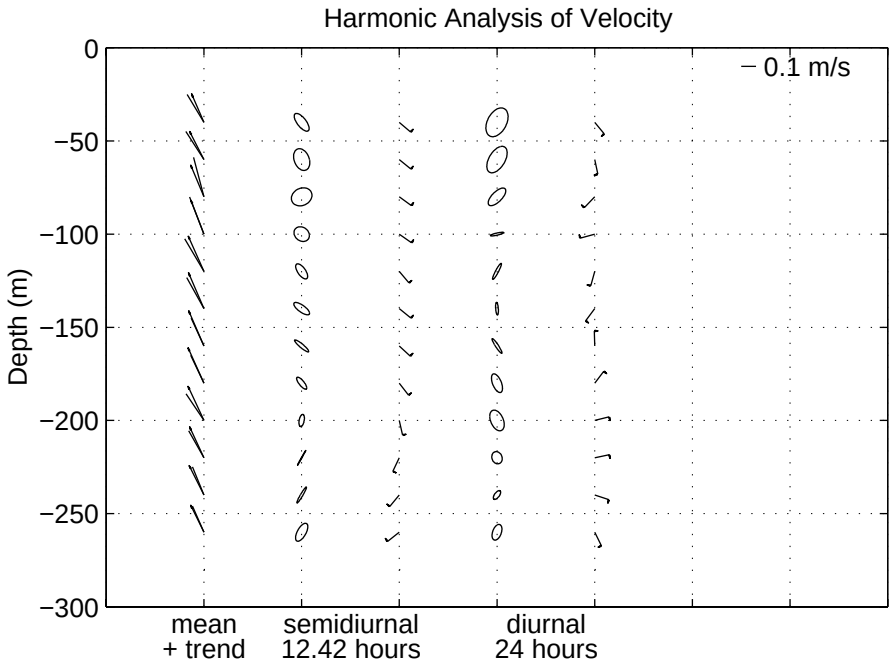
Harmonic Analysis of Velocity
− 0.1 m/s
0
−50
−100
−150
−200
−250
−300
Depth (m)
mean
+ trend
semidiurnal
12.42 hours
diurnal
24 hours

Figure 6.3.1f

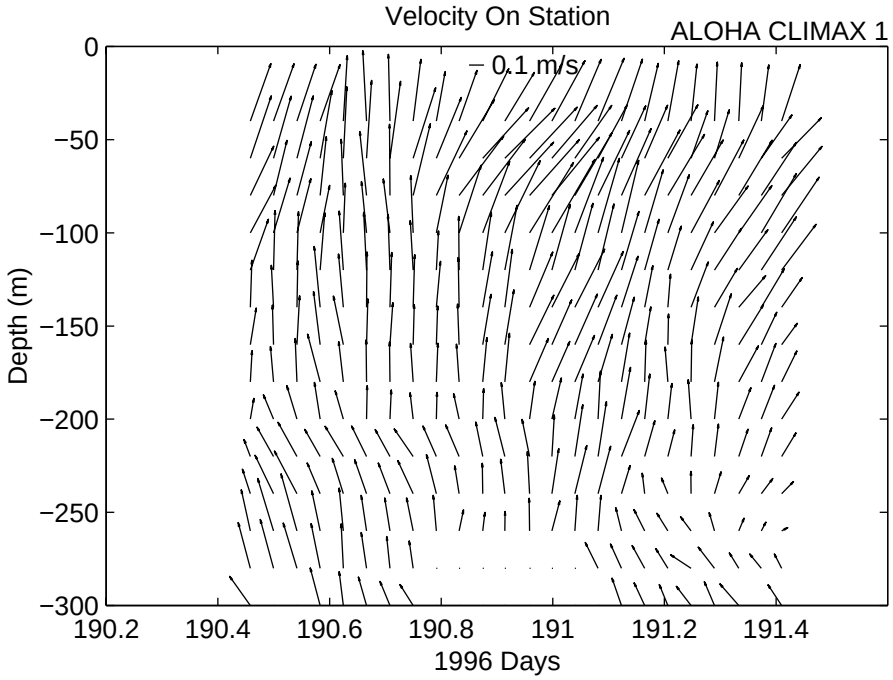
Velocity On Station
ALOHA CLIMAX 1
0.1 m/s
Depth (m)
0
−50
−100
−150
−200
−250
−300
190.2
190.4
190.6
190.8
191
191.2
191.4
1996 Days

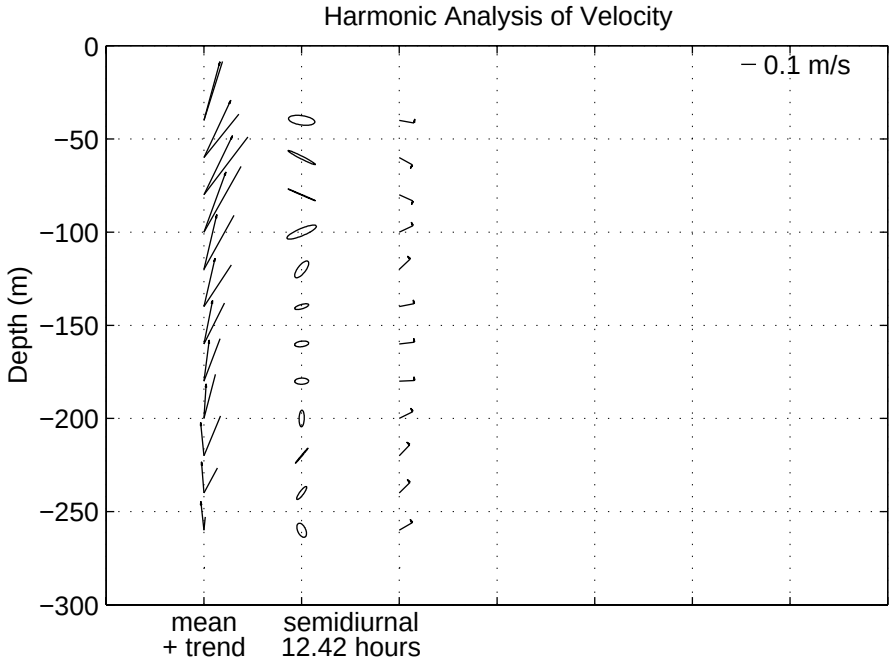
Harmonic Analysis of Velocity
0.1 m/s
Depth (m)
0
−50
−100
−150
−200
−250
−300
mean
+ trend
semidiurnal
12.42 hours

Figure 6.3.1g

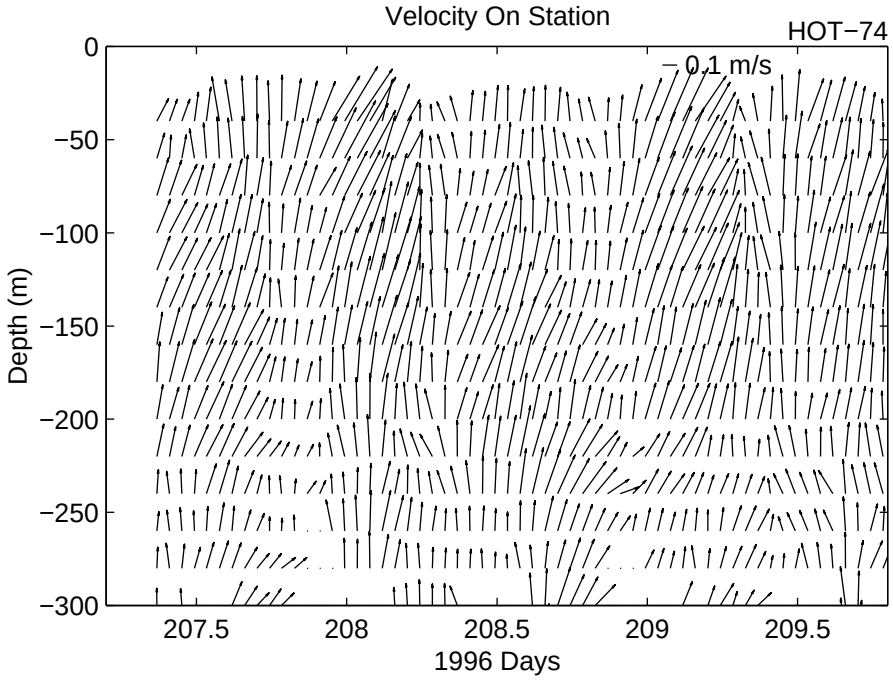
Velocity On Station
HOT−74
− 0.1 m/s
0
−50
−100
−150
−200
−250
−300
Depth (m)
207.5
208
208.5
209
209.5
1996 Days

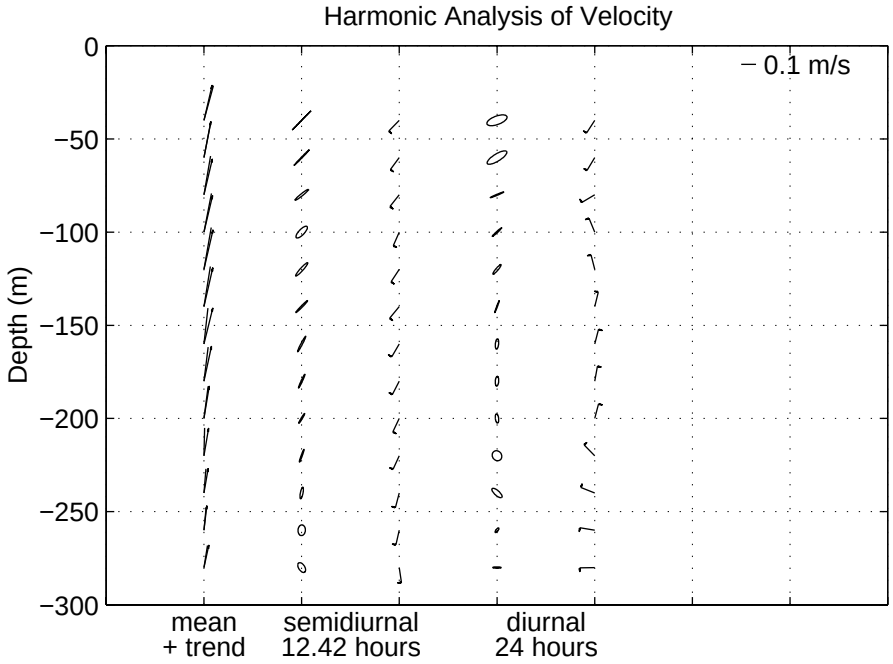
Harmonic Analysis of Velocity
− 0.1 m/s
0
−50
−100
−150
−200
−250
−300
Depth (m)
mean
+ trend
semidiurnal
12.42 hours
diurnal
24 hours

Figure 6.3.1h

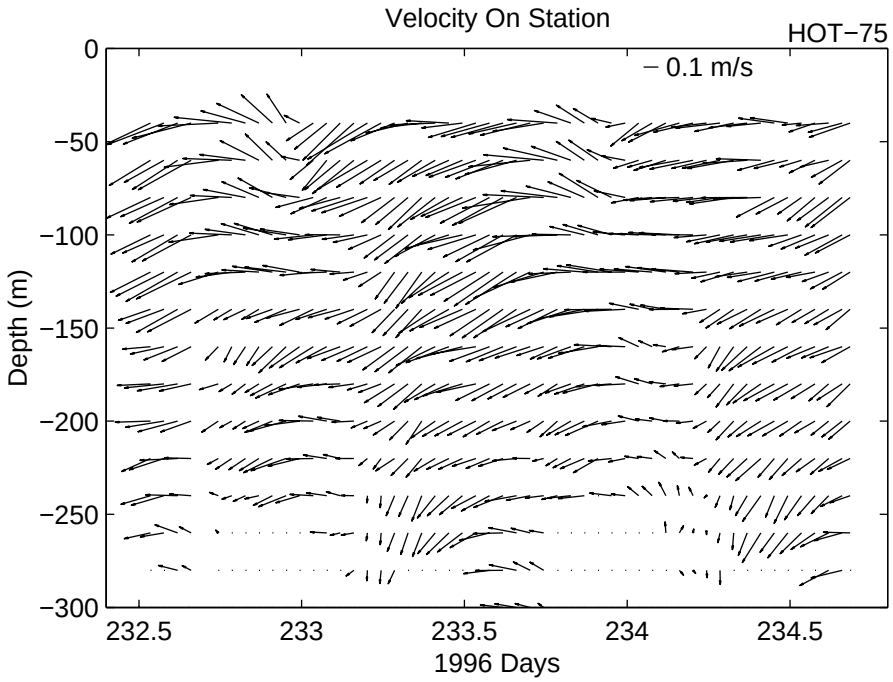
Velocity On Station
HOT−75
− 0.1 m/s
0
−50
−100
−150
−200
−250
−300
Depth (m)
232.5
233
233.5
234
234.5
1996 Days

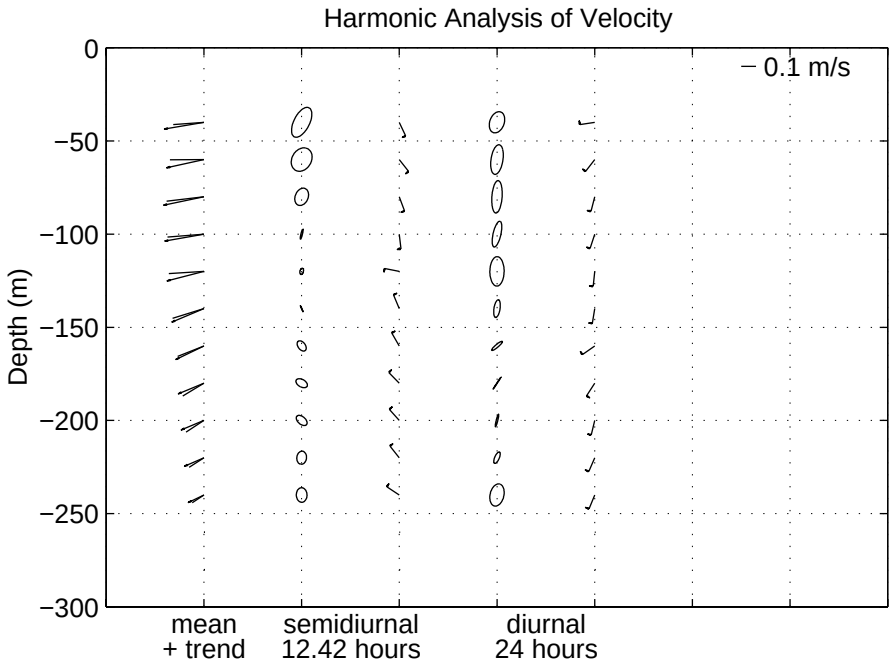
Harmonic Analysis of Velocity
− 0.1 m/s
0
−50
−100
−150
−200
−250
−300
Depth (m)
mean
+ trend
semidiurnal
12.42 hours
diurnal
24 hours

Figure 6.3.1i

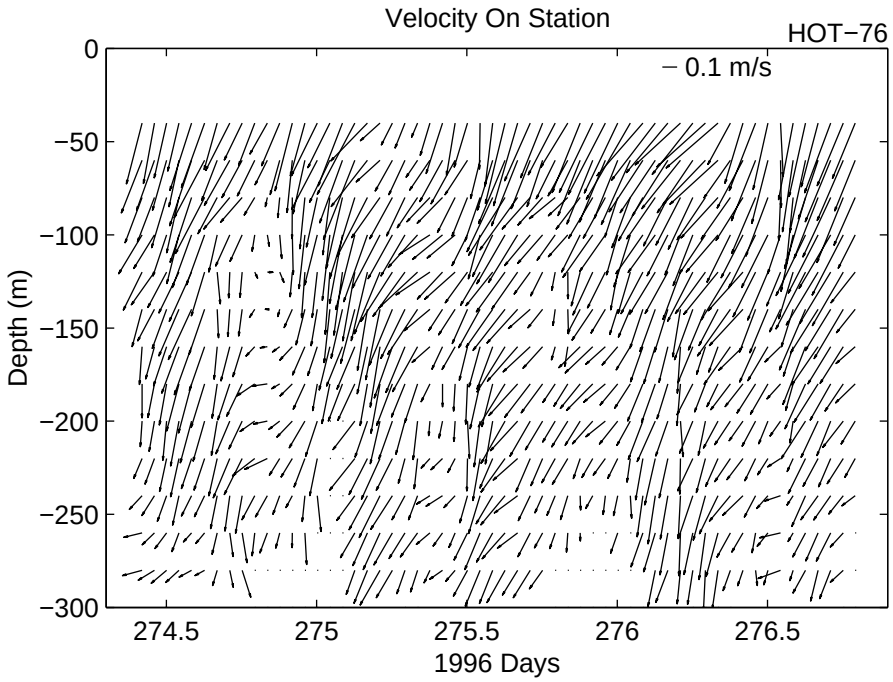
Velocity On Station
HOT−76
− 0.1 m/s
0
−50
−100
−150
−200
−250
−300
Depth (m)
274.5
275
275.5
276
276.5
1996 Days

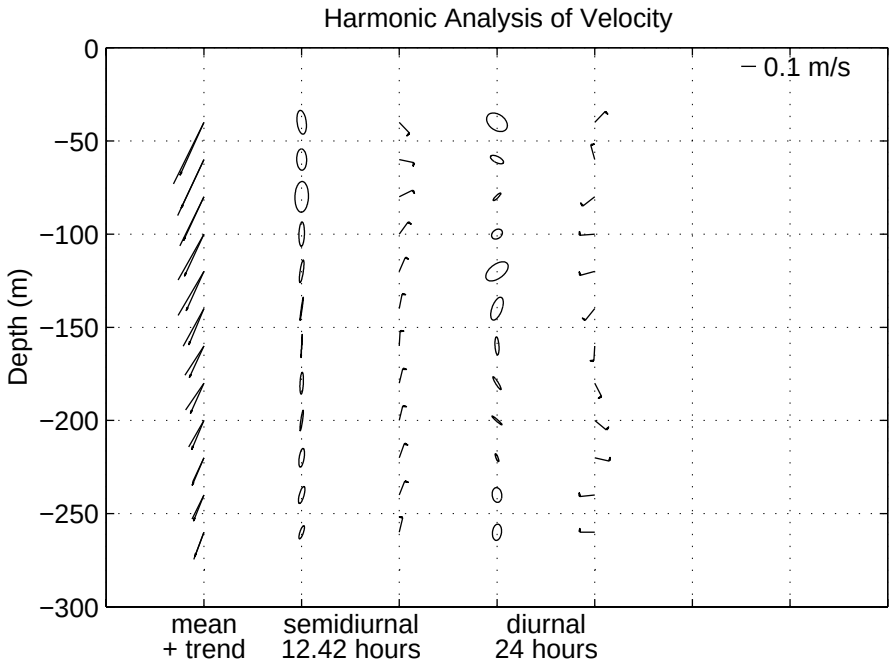
Harmonic Analysis of Velocity
− 0.1 m/s
0
−50
−100
−150
−200
−250
−300
Depth (m)
mean
+ trend
semidiurnal
12.42 hours
diurnal
24 hours

Figure 6.3.1j

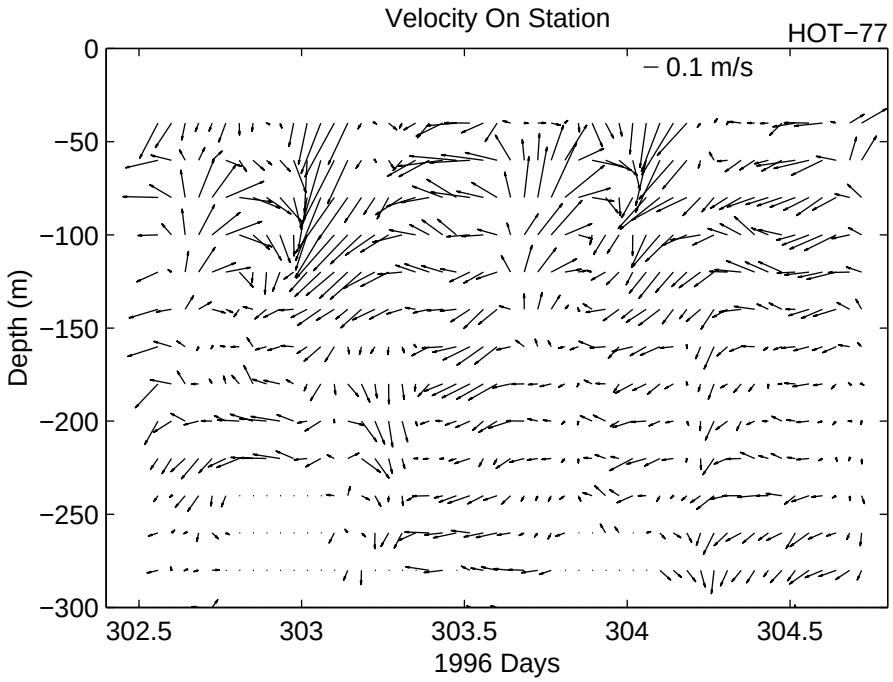
Velocity On Station
HOT−77
− 0.1 m/s
0
−50
−100
−150
−200
−250
−300
Depth (m)
302.5
303
303.5
304
304.5
1996 Days

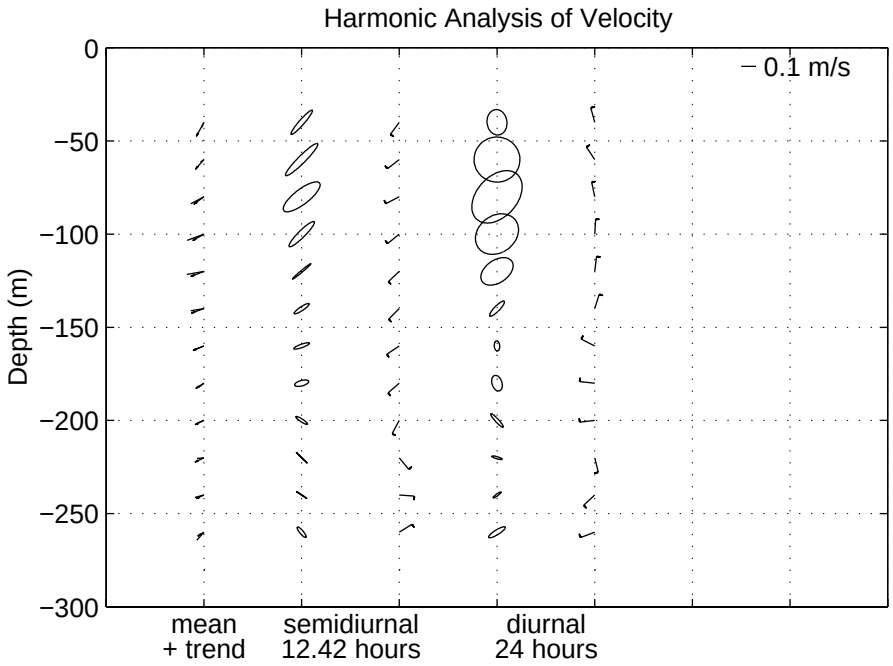
Harmonic Analysis of Velocity
− 0.1 m/s
0
−50
−100
−150
−200
−250
−300
Depth (m)
mean
+ trend
semidiurnal
12.42 hours
diurnal
24 hours

Figure 6.3.1k

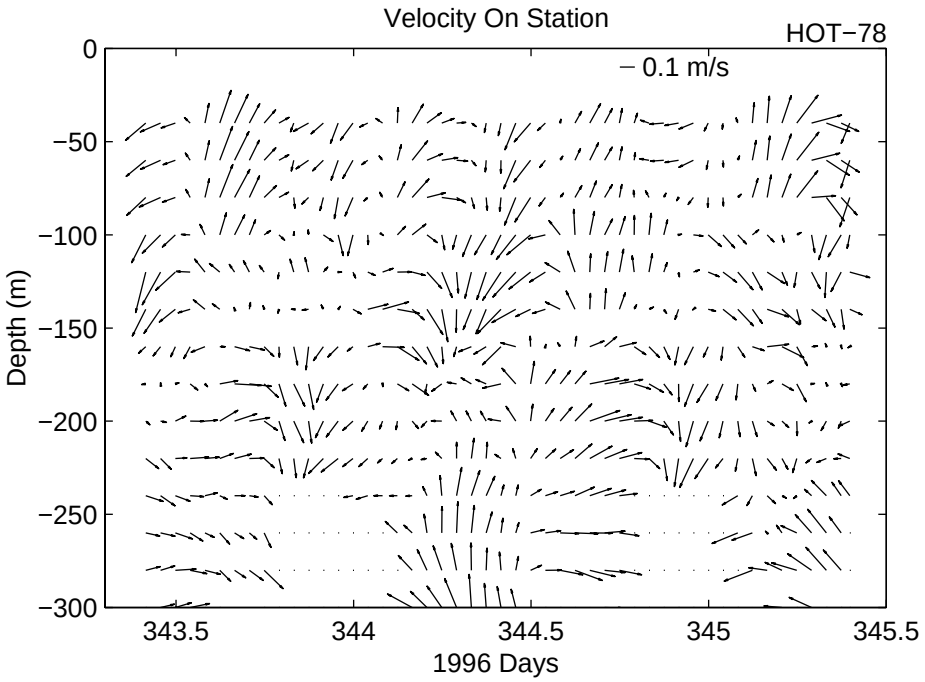
Velocity On Station
HOT−78
− 0.1 m/s
0
−50
−100
−150
−200
−250
−300
Depth (m)
343.5
344
344.5
345
345.5
1996 Days

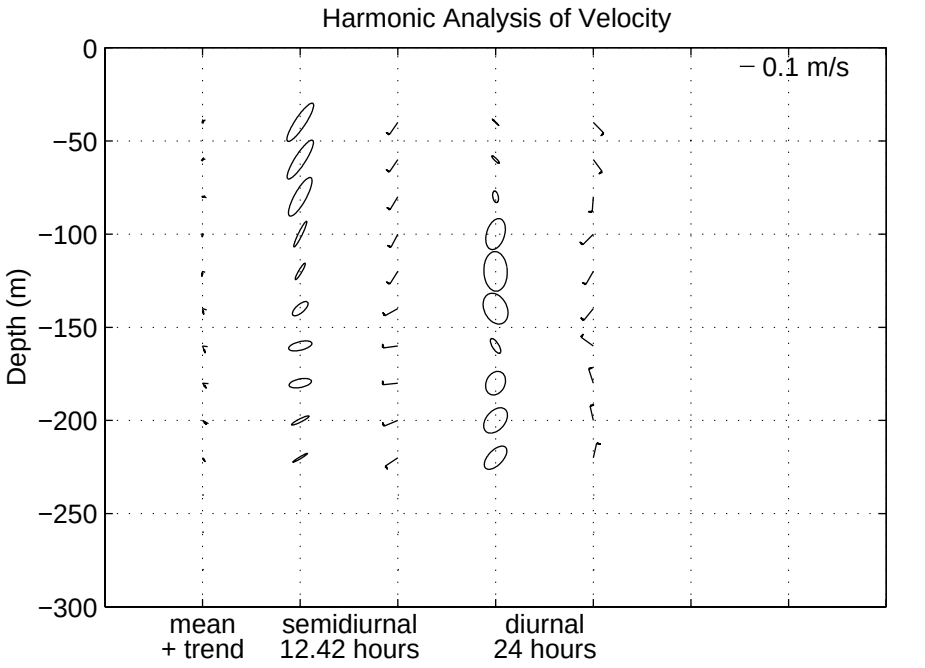
Harmonic Analysis of Velocity
− 0.1 m/s
0
−50
−100
−150
−200
−250
−300
Depth (m)
mean
+ trend
semidiurnal
12.42 hours
diurnal
24 hours

Figure 6.3.1l

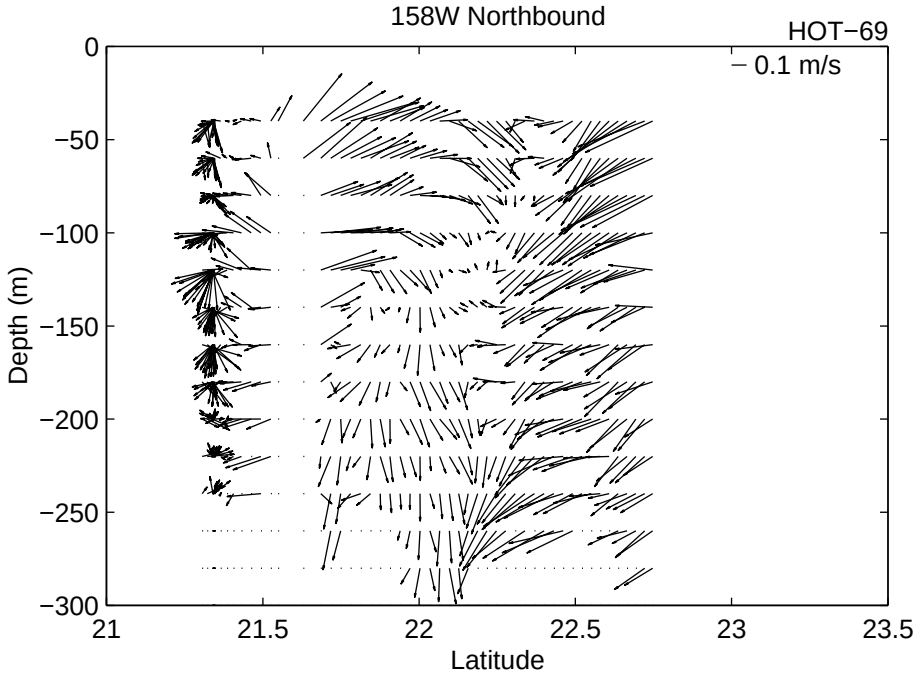
158W Northbound
HOT−69
− 0.1 m/s
0
−50
−100
−150
−200
−250
−300
Depth (m)
21
21.5
22
22.5
23
23.5
Latitude

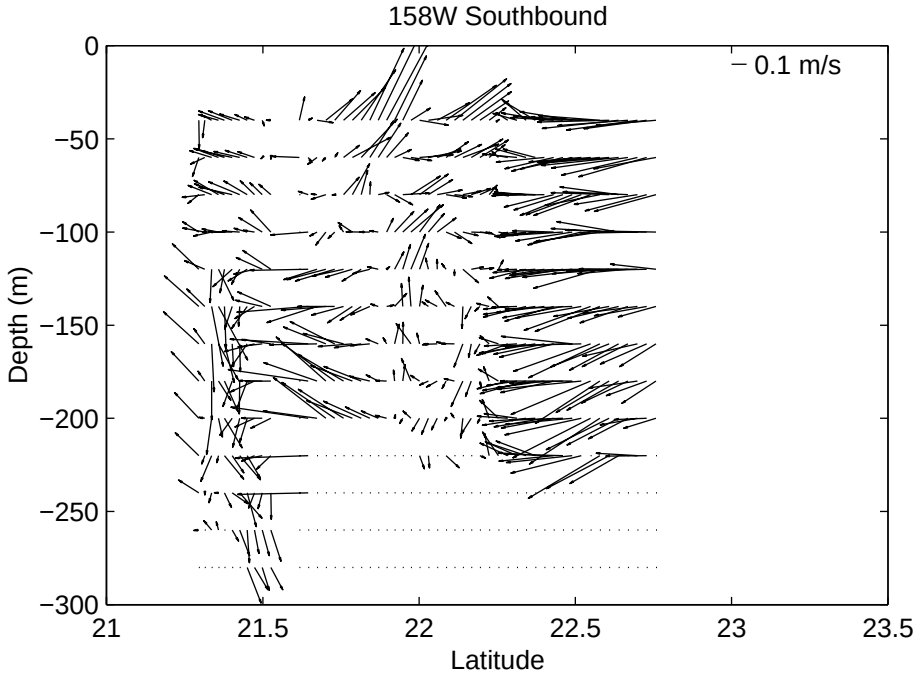
158W Southbound
− 0.1 m/s
0
−50
−100
−150
−200
−250
−300
Depth (m)
21
21.5
22
22.5
23
23.5
Latitude

Figure 6.3.2a

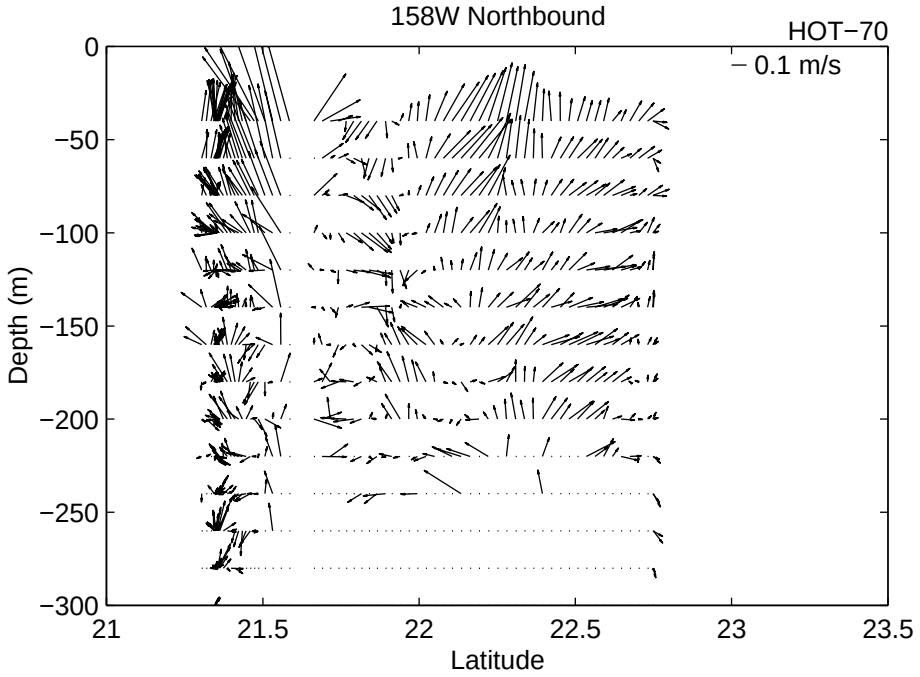
158W Northbound
HOT−70
− 0.1 m/s
0
−50
−100
−150
−200
−250
−300
Depth (m)
21
21.5
22
22.5
23
23.5
Latitude

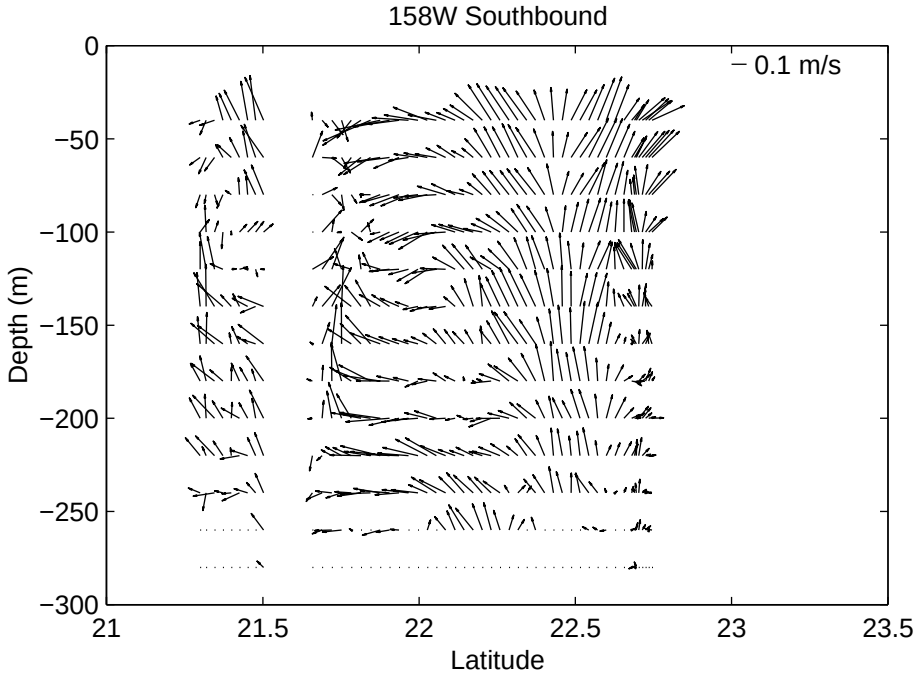
158W Southbound
− 0.1 m/s
0
−50
−100
−150
−200
−250
−300
Depth (m)
21
21.5
22
22.5
23
23.5
Latitude

Figure 6.3.2b

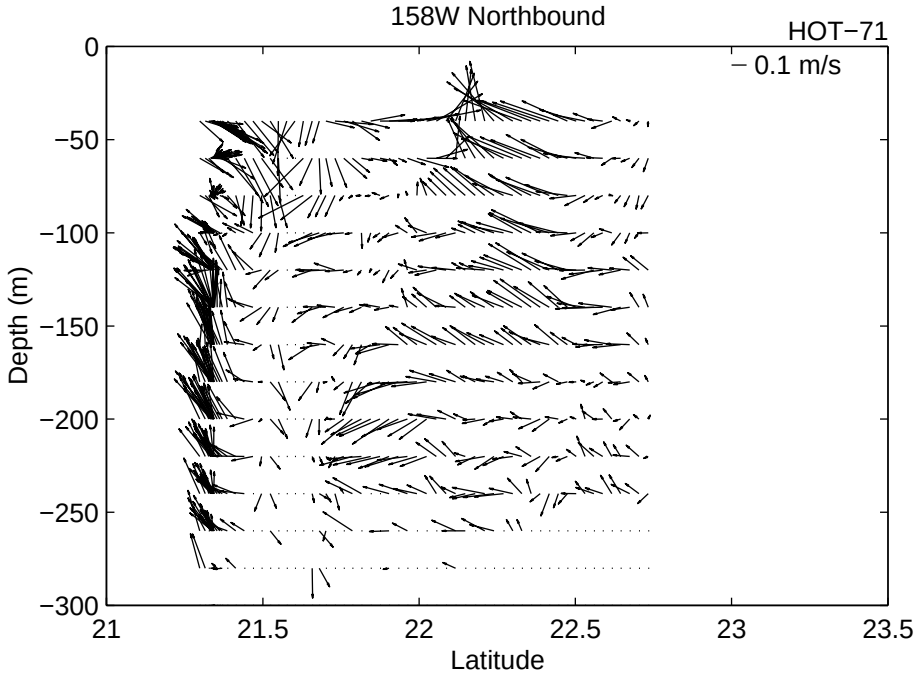
158W Northbound
HOT−71
0.1 m/s
0
−50
−100
−150
−200
−250
−300
Depth (m)
21
21.5
22
22.5
23
23.5
Latitude

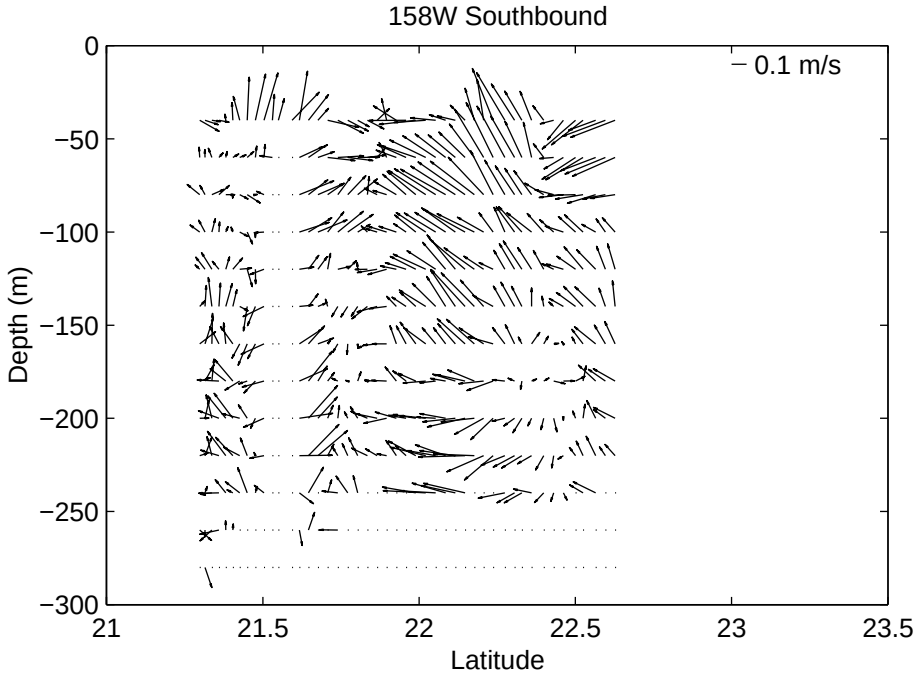
158W Southbound
0.1 m/s
0
−50
−100
−150
−200
−250
−300
Depth (m)
21
21.5
22
22.5
23
23.5
Latitude

Figure 6.3.2c

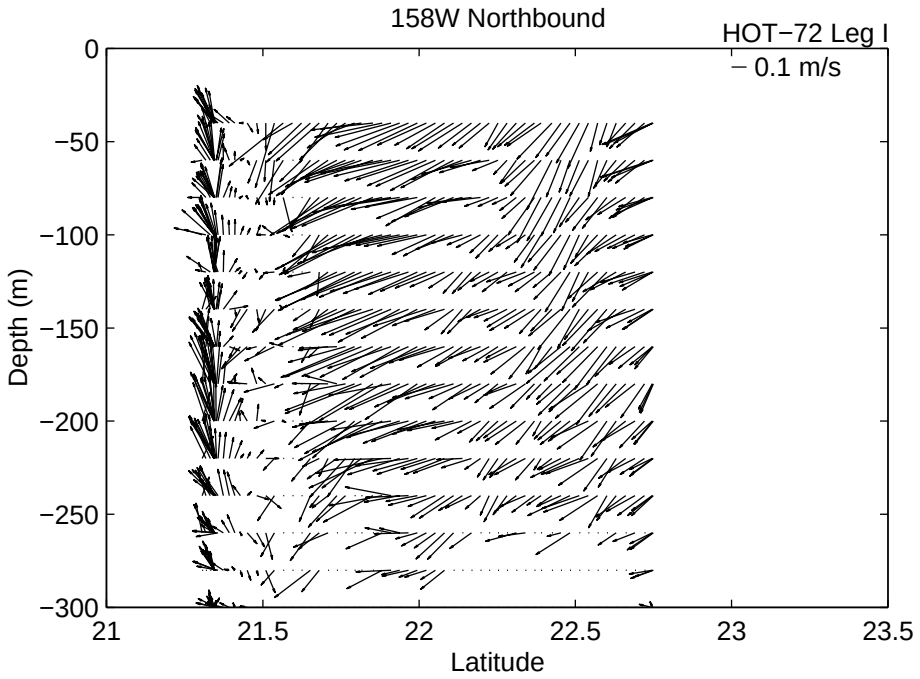
158W Northbound
HOT−72 Leg I
− 0.1 m/s
0
−50
−100
−150
−200
−250
−300
Depth (m)
21
21.5
22
22.5
23
23.5
Latitude

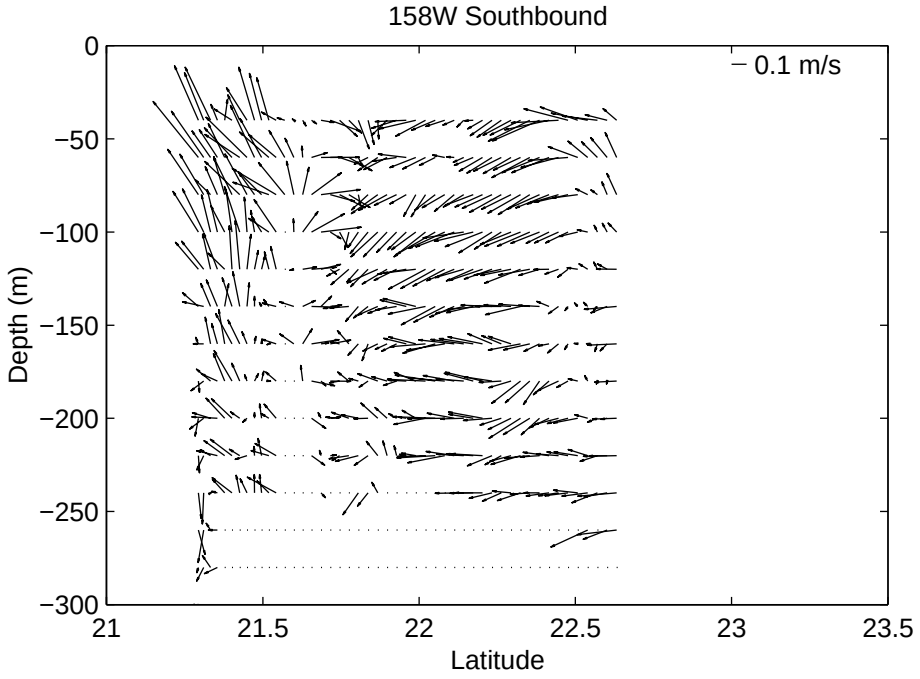
158W Southbound
− 0.1 m/s
0
−50
−100
−150
−200
−250
−300
Depth (m)
21
21.5
22
22.5
23
23.5
Latitude

Figure 6.3.2d

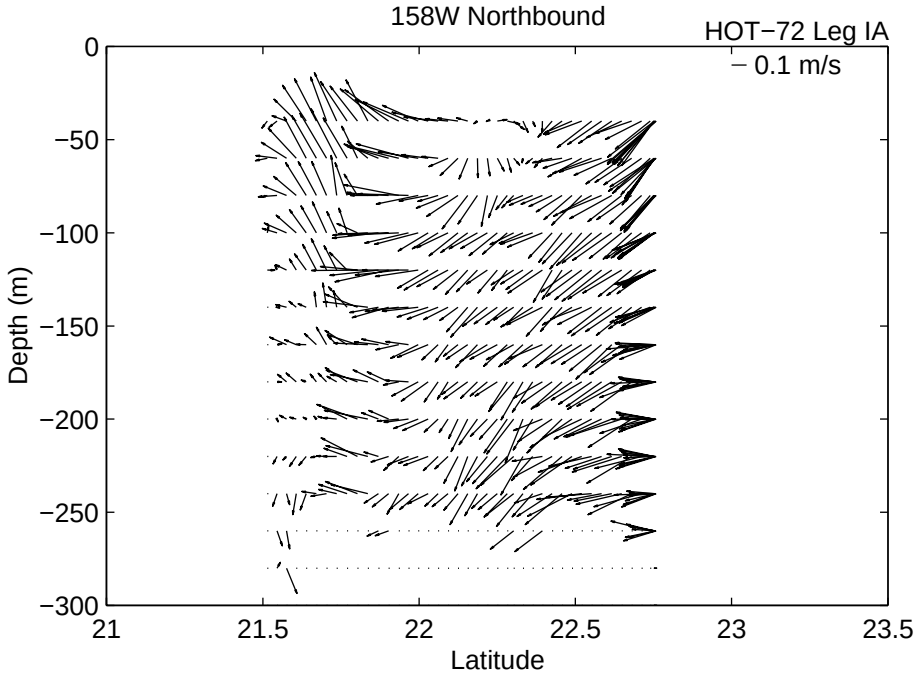
158W Northbound
HOT−72 Leg IA
0.1 m/s
Depth (m)
0
−50
−100
−150
−200
−250
−300
21
21.5
22
22.5
23
23.5
Latitude

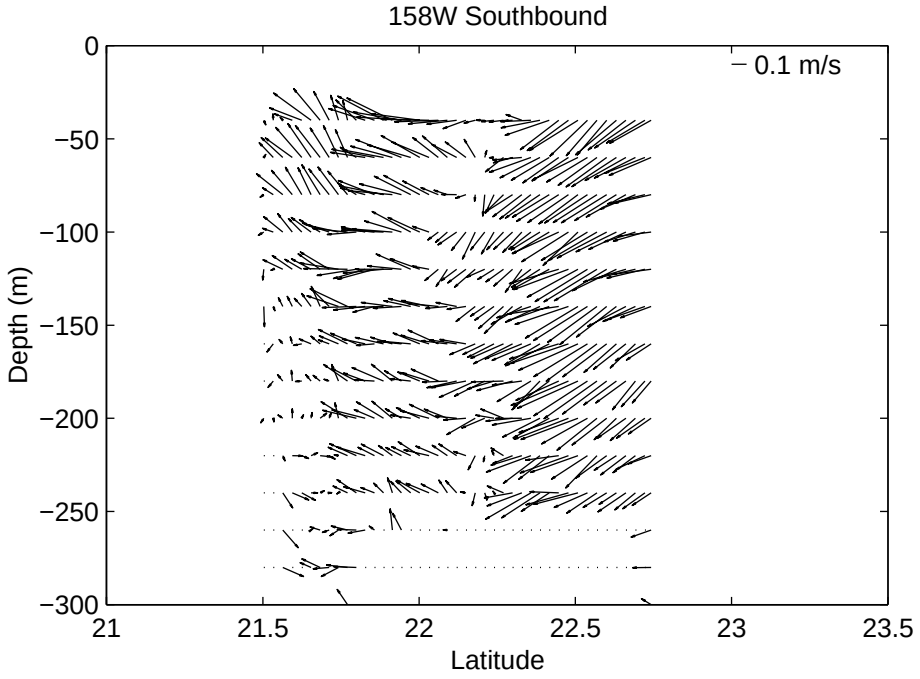
158W Southbound
0.1 m/s
Depth (m)
0
−50
−100
−150
−200
−250
−300
21
21.5
22
22.5
23
23.5
Latitude

Figure 6.3.2e

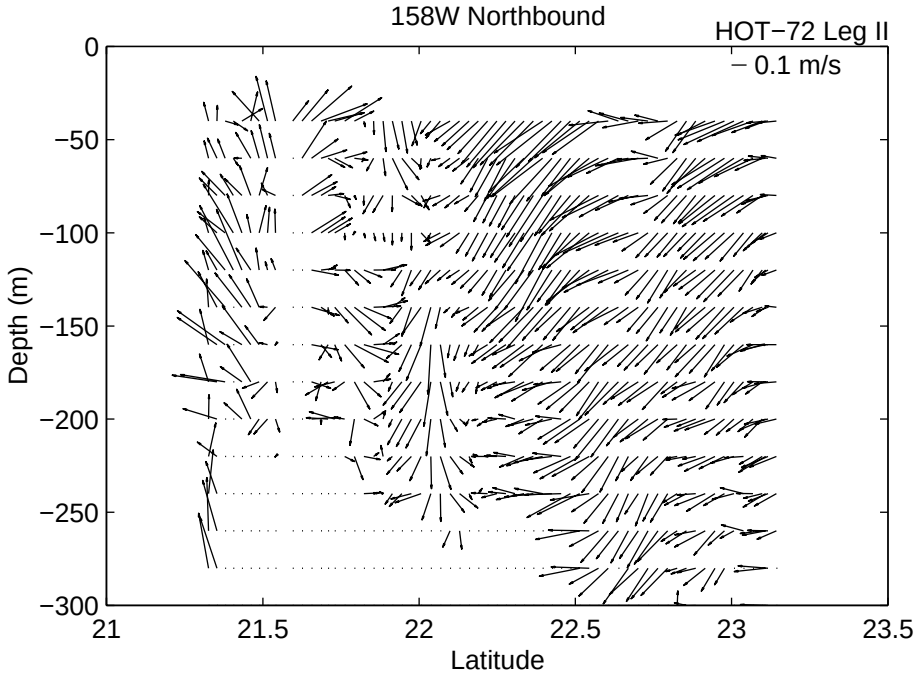
158W Northbound
HOT−72 Leg II
0.1 m/s
0
−50
−100
−150
−200
−250
−300
Depth (m)
21
21.5
22
22.5
23
23.5
Latitude

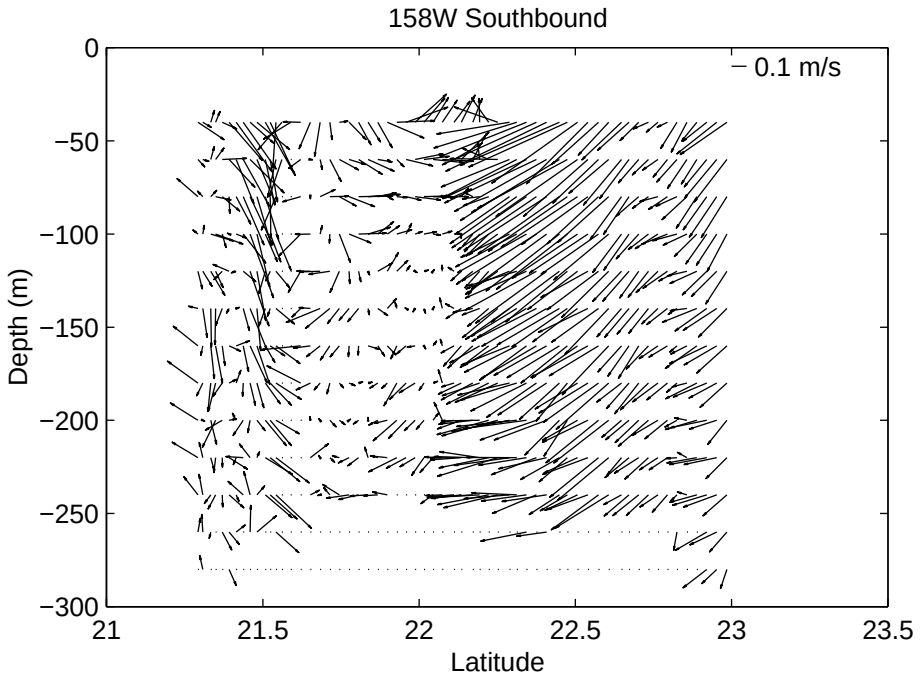
158W Southbound
0.1 m/s
0
−50
−100
−150
−200
−250
−300
Depth (m)
21
21.5
22
22.5
23
23.5
Latitude

Figure 6.3.2f

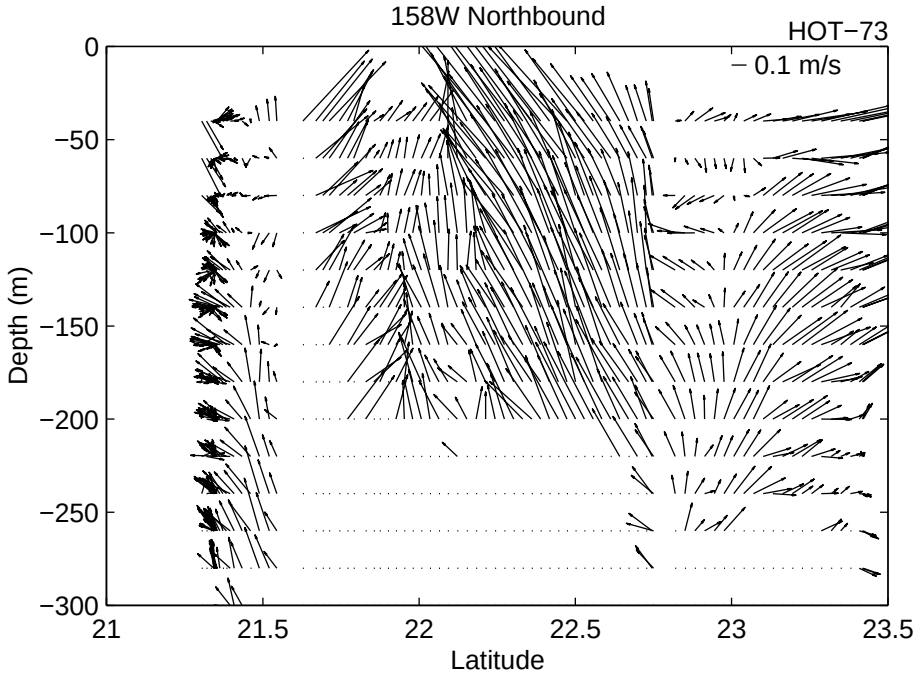
158W Northbound
HOT−73
− 0.1 m/s
0
−50
−100
−150
−200
−250
−300
Depth (m)
21
21.5
22
22.5
23
23.5
Latitude

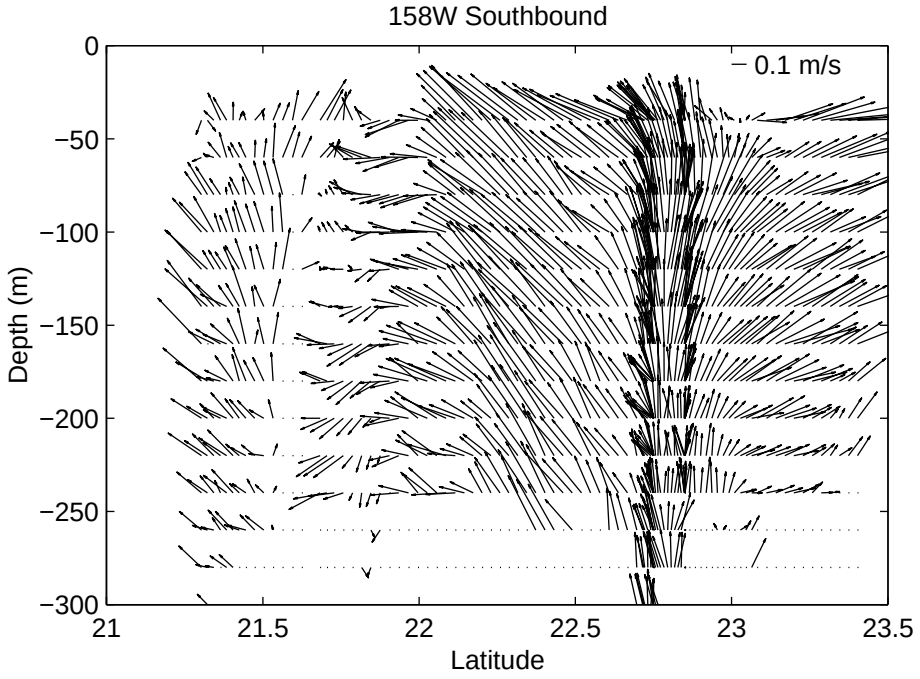
158W Southbound
− 0.1 m/s
0
−50
−100
−150
−200
−250
−300
Depth (m)
21
21.5
22
22.5
23
23.5
Latitude

Figure 6.3.2g

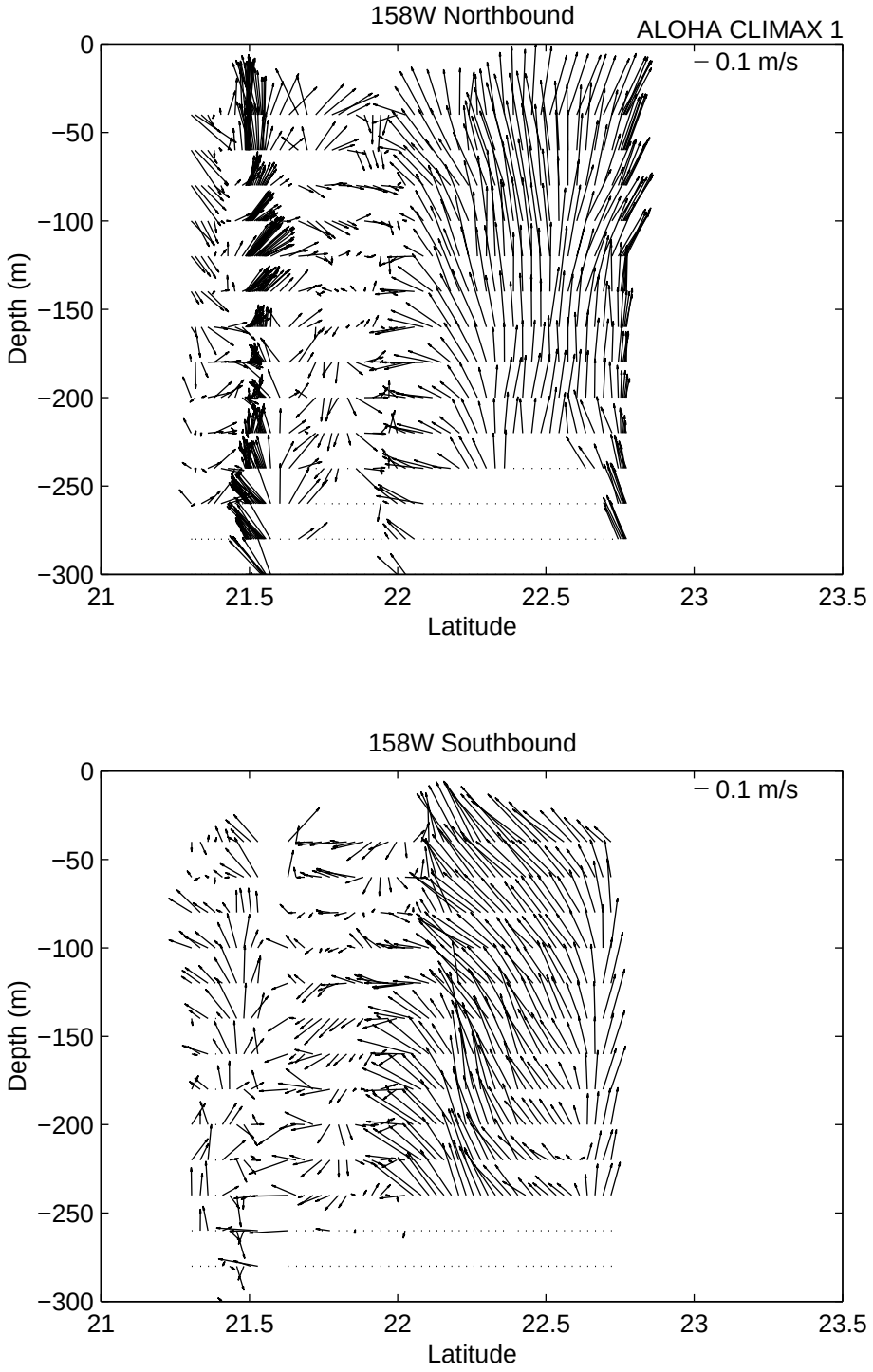
158W Northbound
ALOHA CLIMAX 1
0.1 m/s
Depth (m)
0
−50
−100
−150
−200
−250
−300
21
21.5
22
22.5
23
23.5
Latitude
158W Southbound
0.1 m/s
Depth (m)
Latitude

Figure 6.3.2h

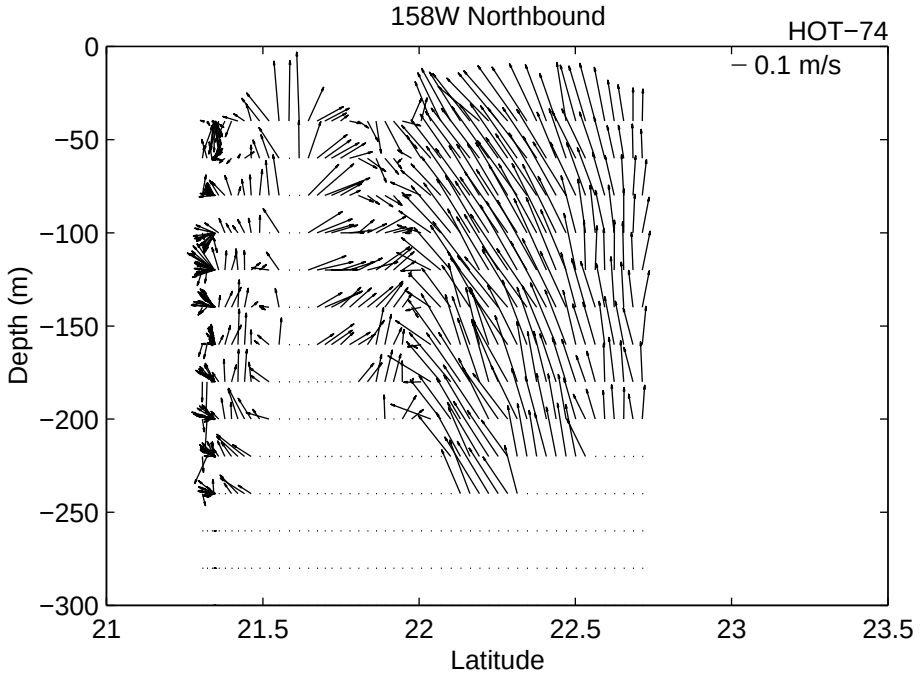
158W Northbound
HOT−74
0.1 m/s
0
−50
−100
−150
−200
−250
−300
Depth (m)
21
21.5
22
22.5
23
23.5
Latitude

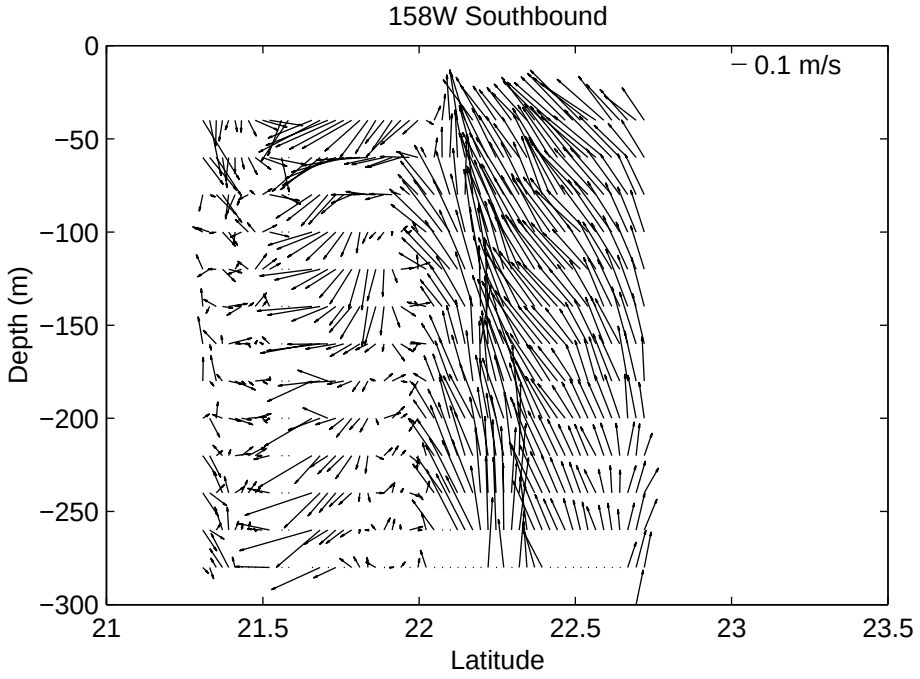
158W Southbound
0.1 m/s
0
−50
−100
−150
−200
−250
−300
Depth (m)
21
21.5
22
22.5
23
23.5
Latitude

Figure 6.3.2i

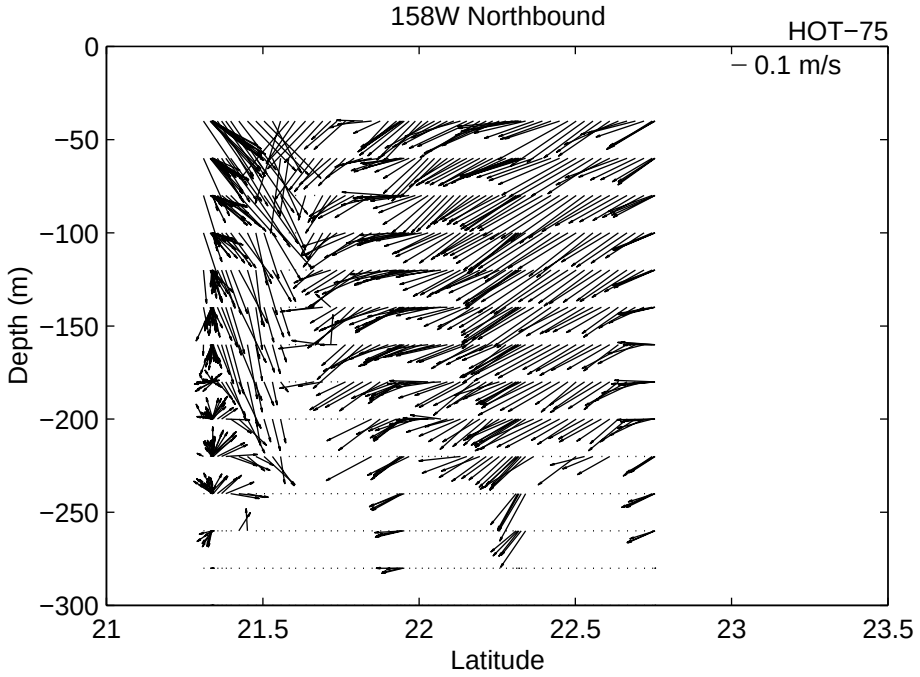
158W Northbound
HOT−75
− 0.1 m/s
0
−50
−100
−150
−200
−250
−300
Depth (m)
21
21.5
22
22.5
23
23.5
Latitude

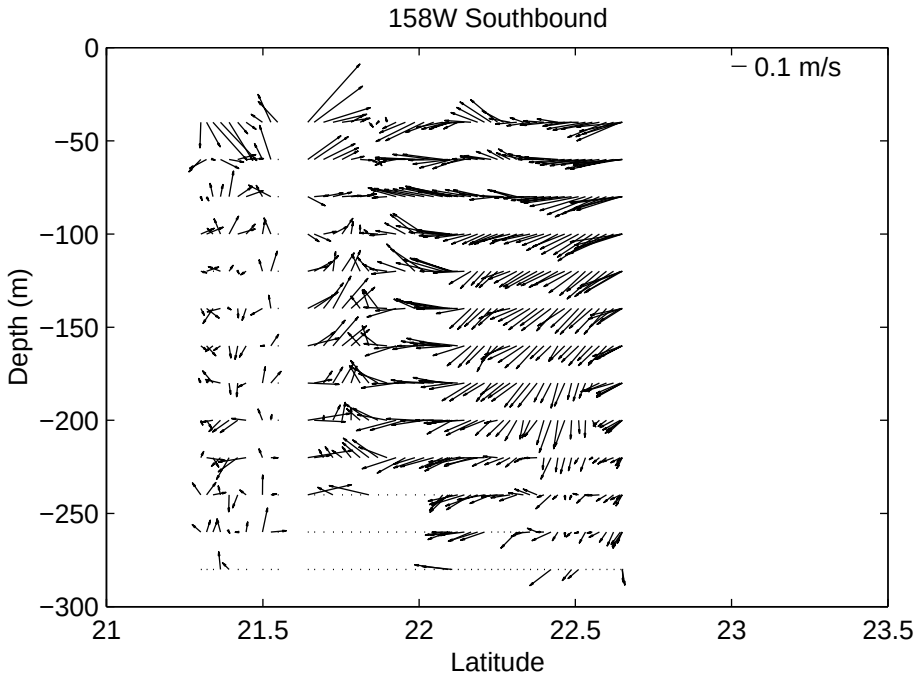
158W Southbound
− 0.1 m/s
0
−50
−100
−150
−200
−250
−300
Depth (m)
21
21.5
22
22.5
23
23.5
Latitude

Figure 6.3.2j

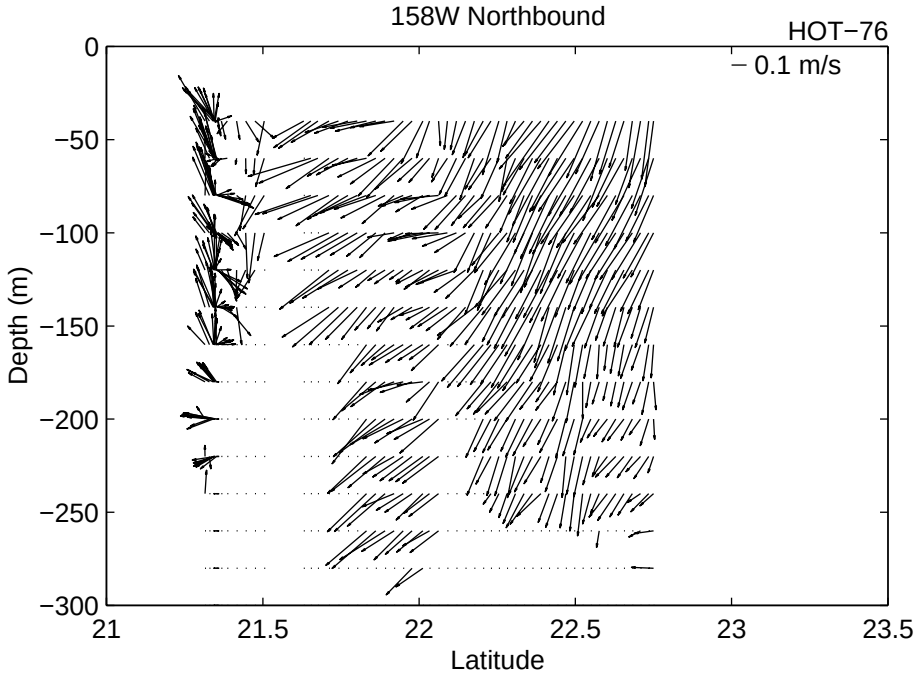
158W Northbound
HOT−76
− 0.1 m/s
0
−50
−100
−150
−200
−250
−300
Depth (m)
21
21.5
22
22.5
23
23.5
Latitude

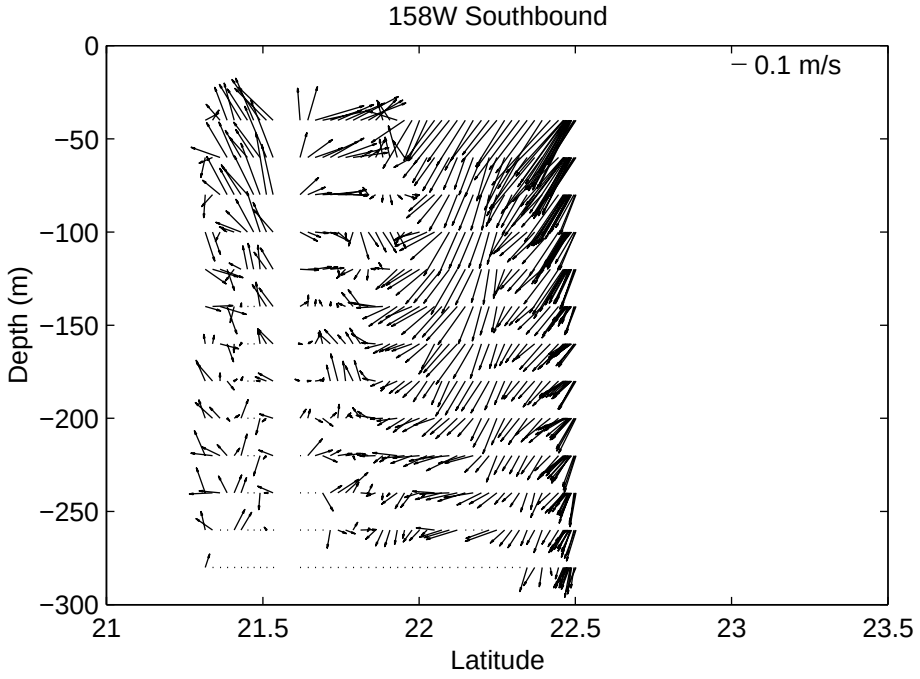
158W Southbound
− 0.1 m/s
0
−50
−100
−150
−200
−250
−300
Depth (m)
21
21.5
22
22.5
23
23.5
Latitude

Figure 6.3.2k

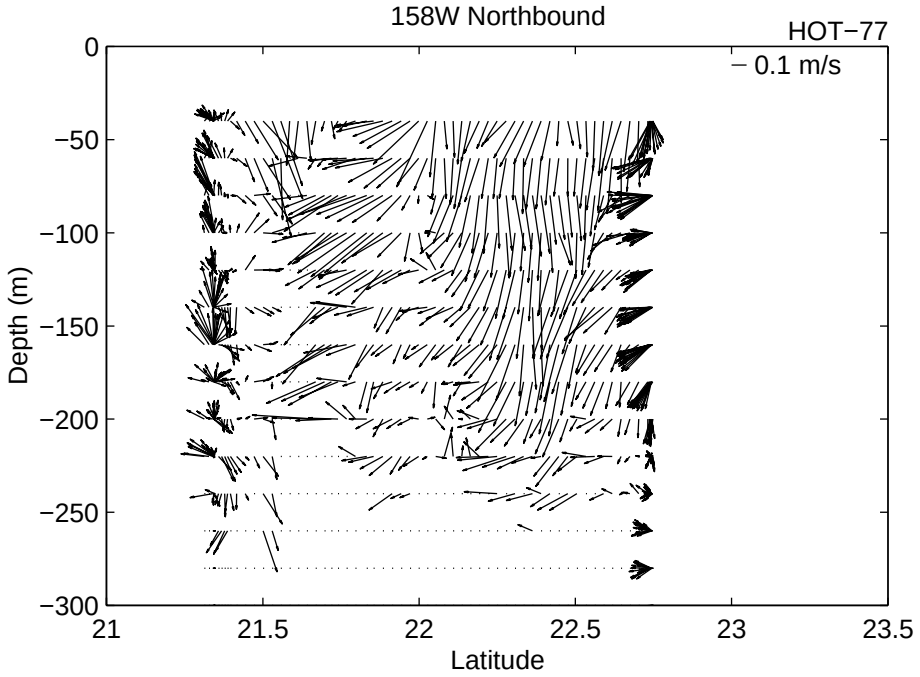
158W Northbound
HOT−77
− 0.1 m/s
0
−50
−100
−150
−200
−250
−300
Depth (m)
21
21.5
22
22.5
23
23.5
Latitude

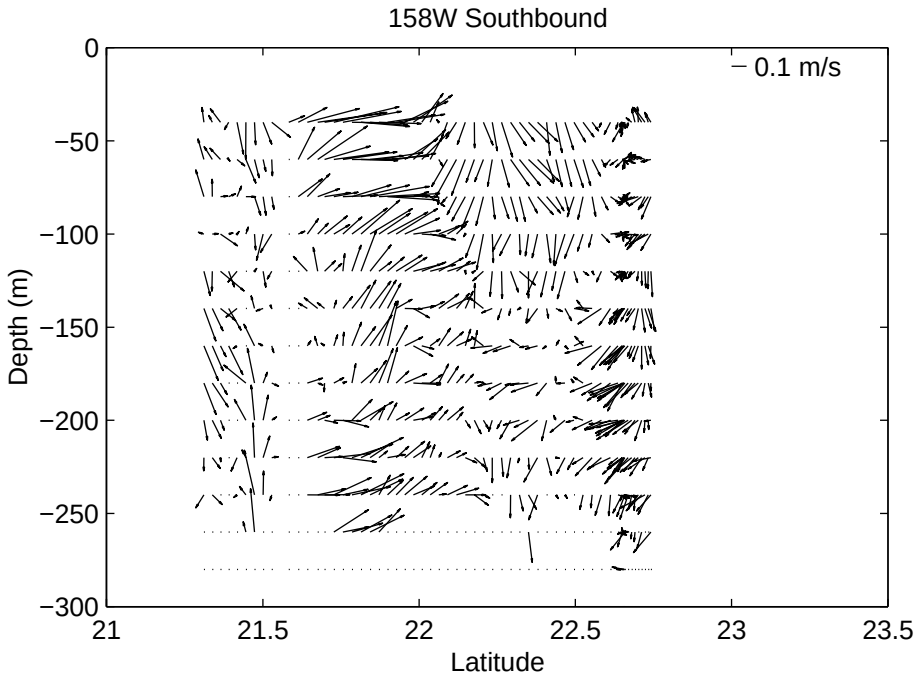
158W Southbound
− 0.1 m/s
0
−50
−100
−150
−200
−250
−300
Depth (m)
21
21.5
22
22.5
23
23.5
Latitude

Figure 6.3.2l

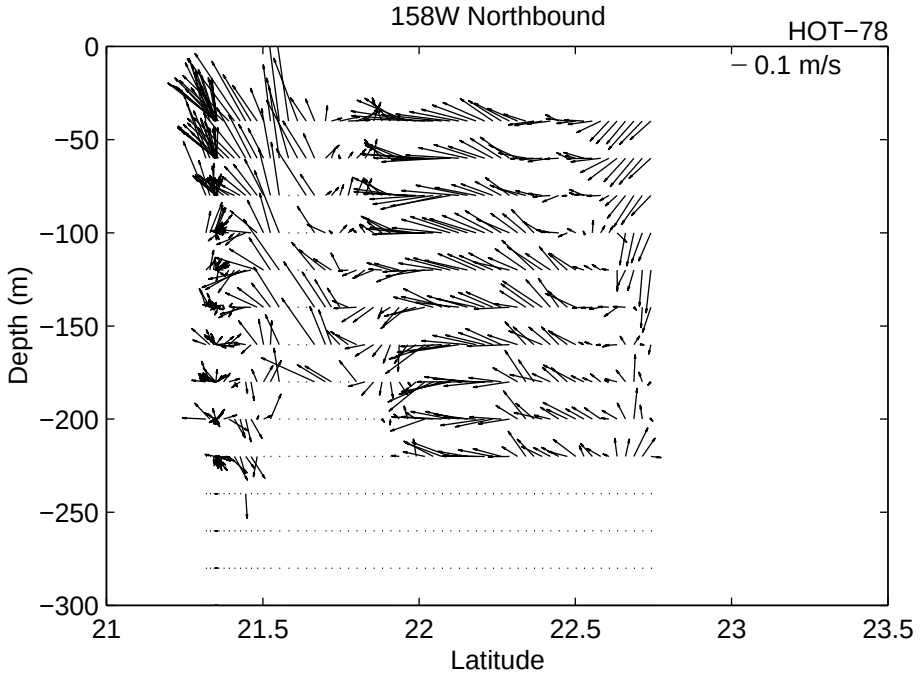
158W Northbound
HOT−78
− 0.1 m/s
0
−50
−100
−150
−200
−250
−300
Depth (m)
21
21.5
22
22.5
23
23.5
Latitude

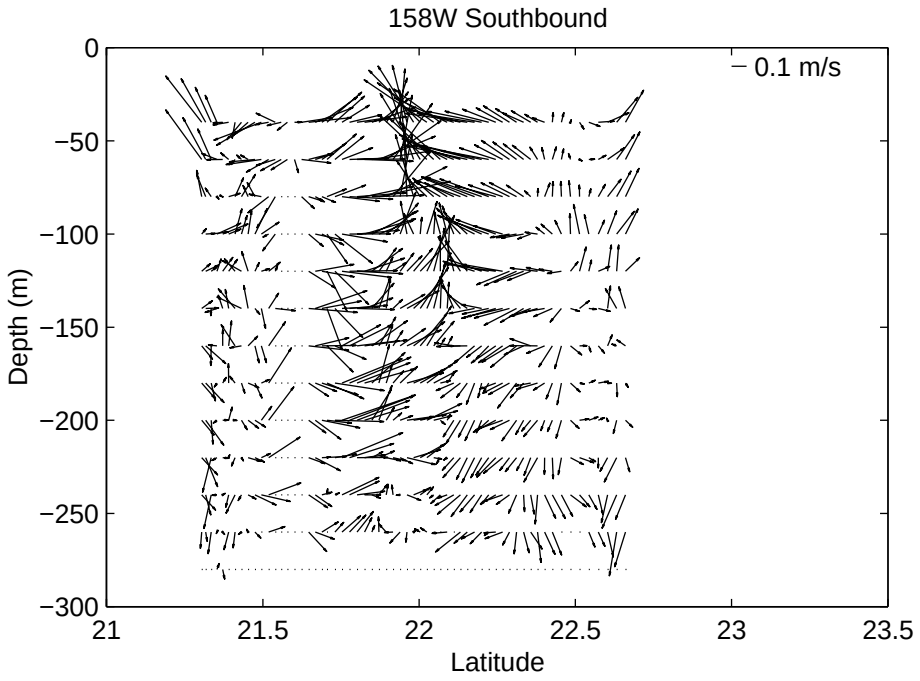
158W Southbound
− 0.1 m/s
0
−50
−100
−150
−200
−250
−300
Depth (m)
21
21.5
22
22.5
23
23.5
Latitude

Figure 6.3.2m

6.4. OPTICAL MEASUREMENTS

Figure 6.4.1a to j: Stack plots of flash fluorescence from all casts made at Station ALOHA for all 1996 HOT cruises. The first figure is plotted versus pressure to 250 dbar, the second figure is plotted versus potential density to 26 kg m^{-3}.

Figure 6.4.2: Stack plots of averaged night-time fluorescence plotted versus pressure to 250 dbar for all HOT cruises from 1988-1996. The HOT cruise number is shown on the upper x-axis.

Figure 6.4.3: Stack plots of averaged night-time fluorescence plotted versus potential density to 26 kg m^{-3} for all HOT cruises from 1988-1996. The HOT cruise number is shown on the upper x-axis.

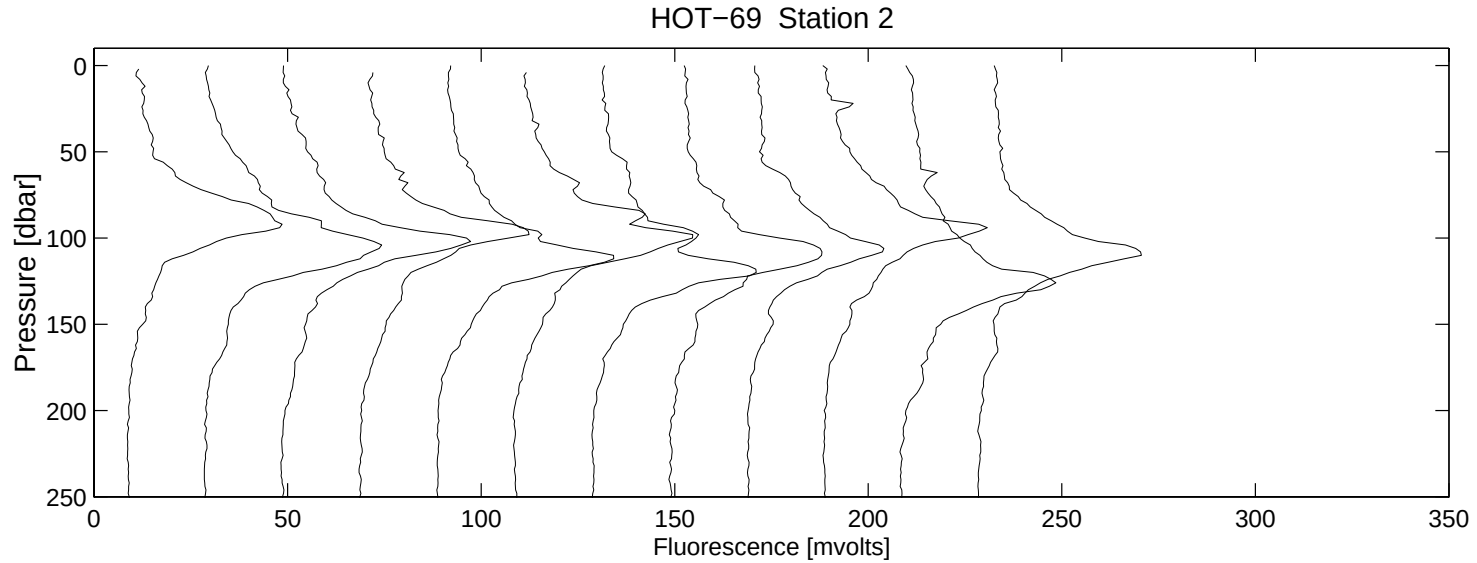
HOT−69 Station 2
Pressure [dbar]
0
50
100
150
200
250
0
50
100
150
200
250
300
350
Fluorescence [mvolts]

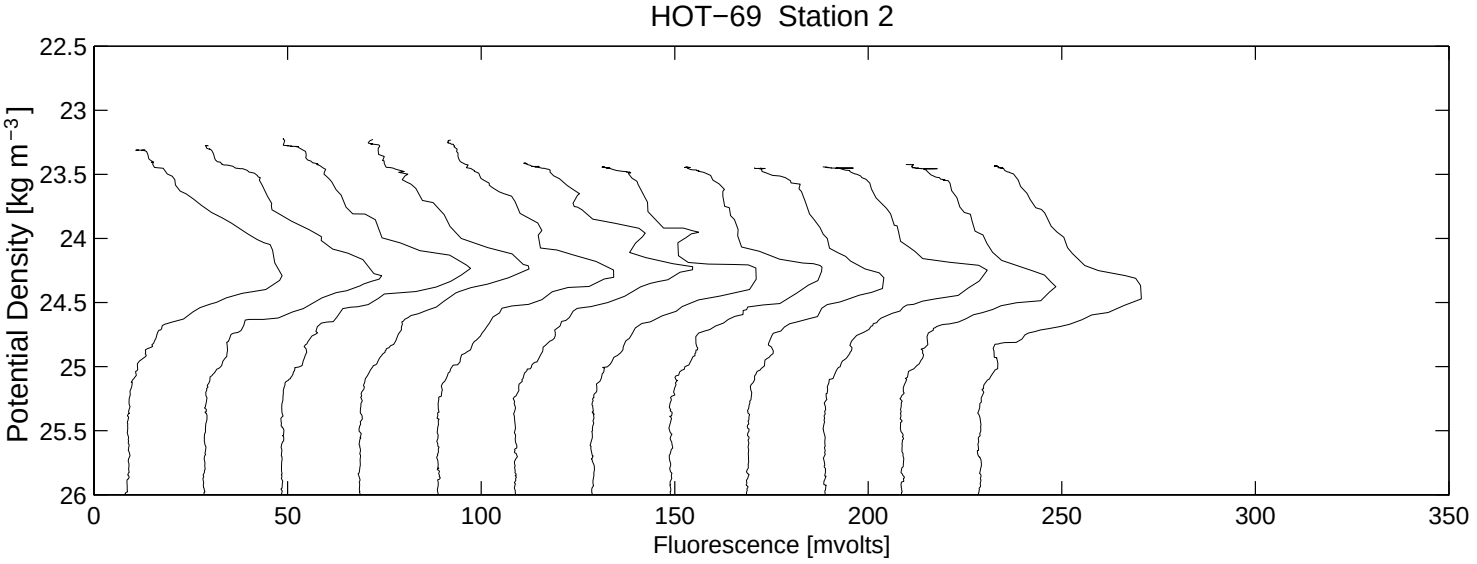
HOT−69 Station 2
Potential Density [kg m^{-3}]
22.5
23
23.5
24
24.5
25
25.5
26
0
50
100
150
200
250
300
350
Fluorescence [mvolts]

Figure 6.4.1a

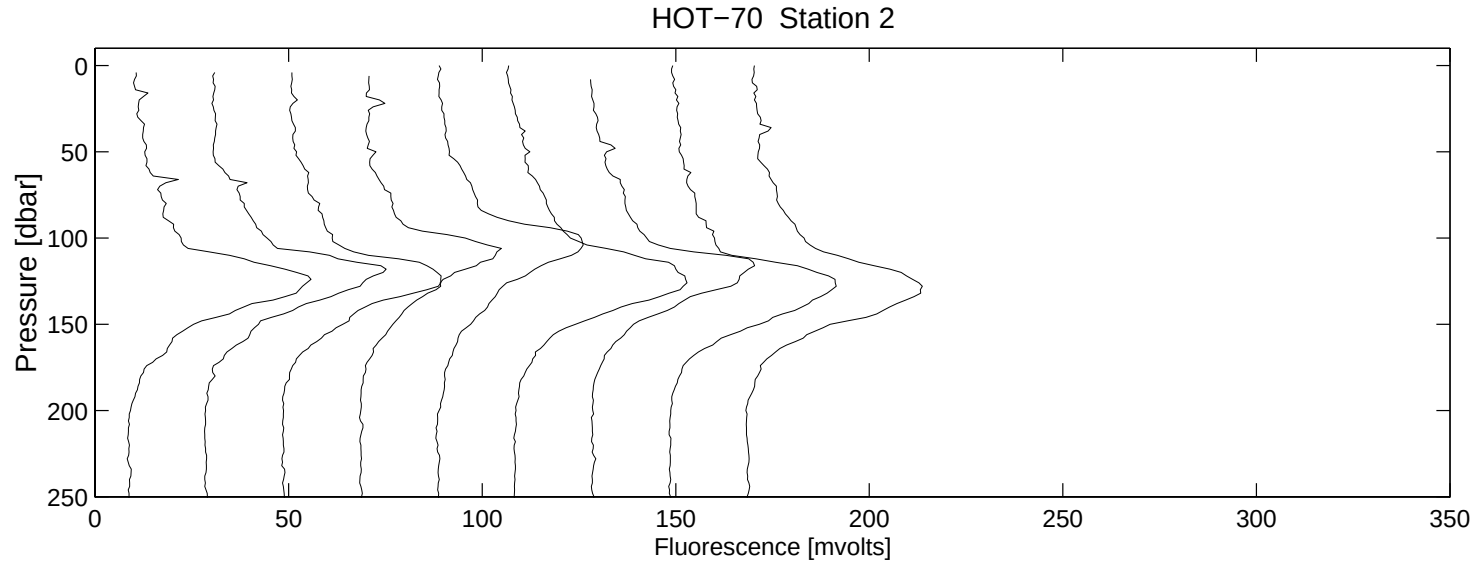
HOT−70 Station 2
Pressure [dbar]
0
50
100
150
200
250
0
50
100
150
200
250
300
350
Fluorescence [mvolts]

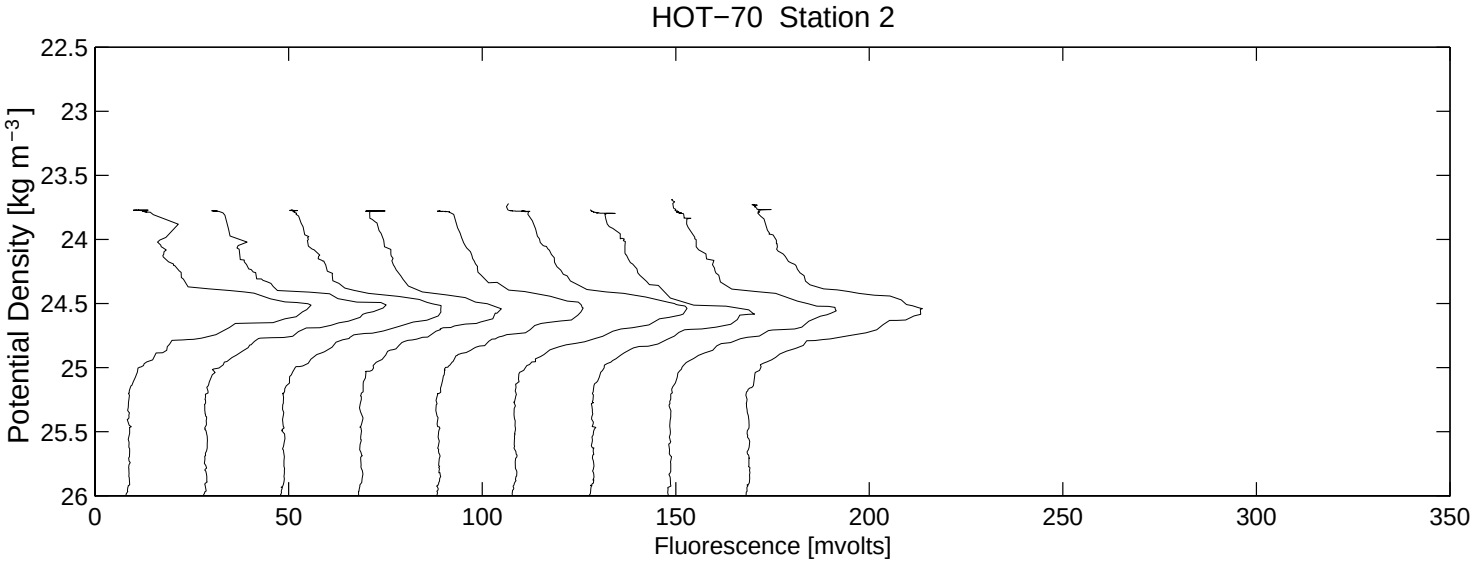
HOT−70 Station 2
Potential Density [kg m^{-3}]
22.5
23
23.5
24
24.5
25
25.5
26
0
50
100
150
200
250
300
350
Fluorescence [mvolts]

Figure 6.4.1b

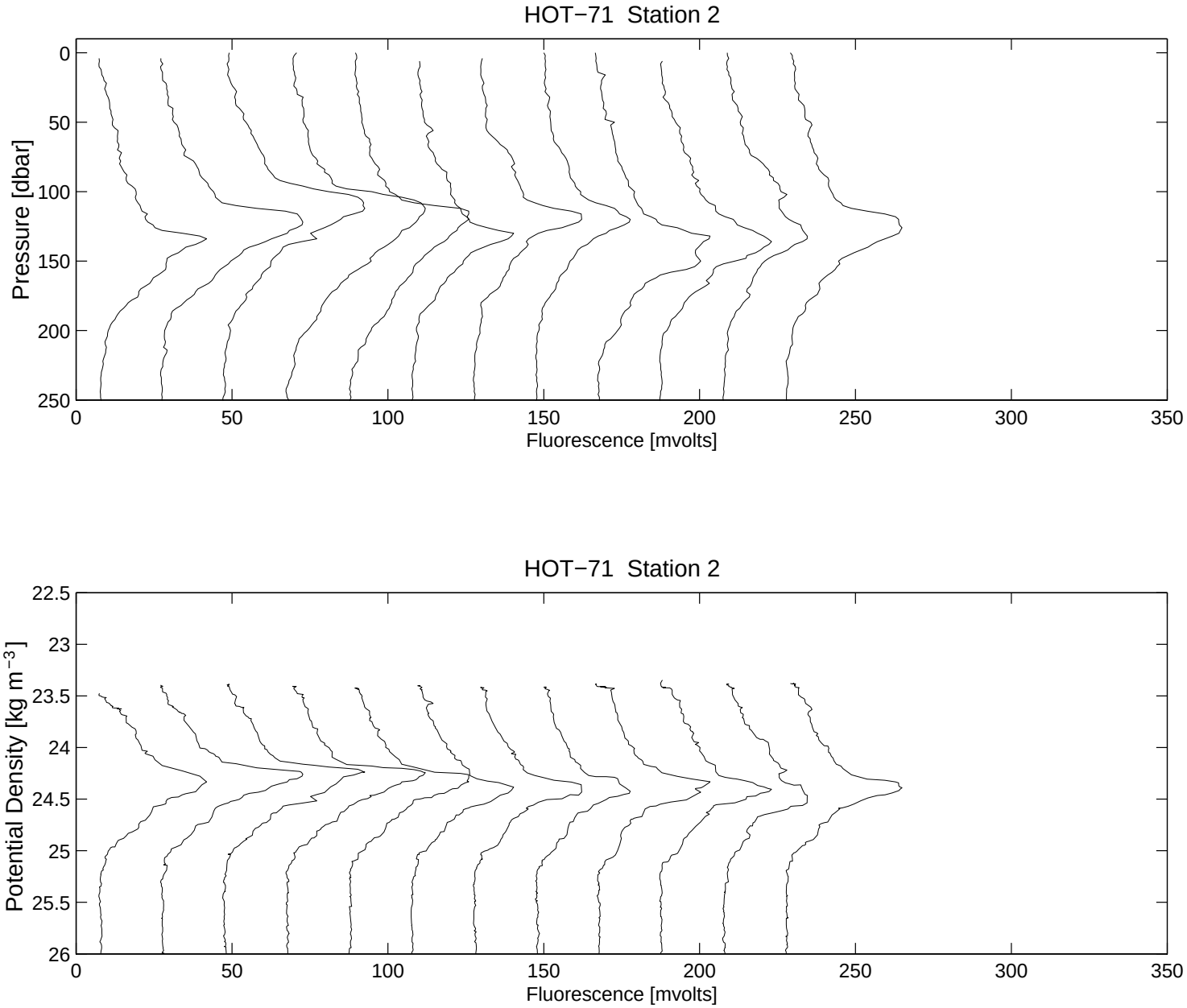
HOT−71 Station 2
Pressure [dbar]
0
50
100
150
200
250
Fluorescence [mvolts]
0
50
100
150
200
250
300
350
HOT−71 Station 2
Potential Density [kg m^{-3}]
22.5
23
23.5
24
24.5
25
25.5
26
Fluorescence [mvolts]
0
50
100
150
200
250
300
350

Figure 6.4.1c

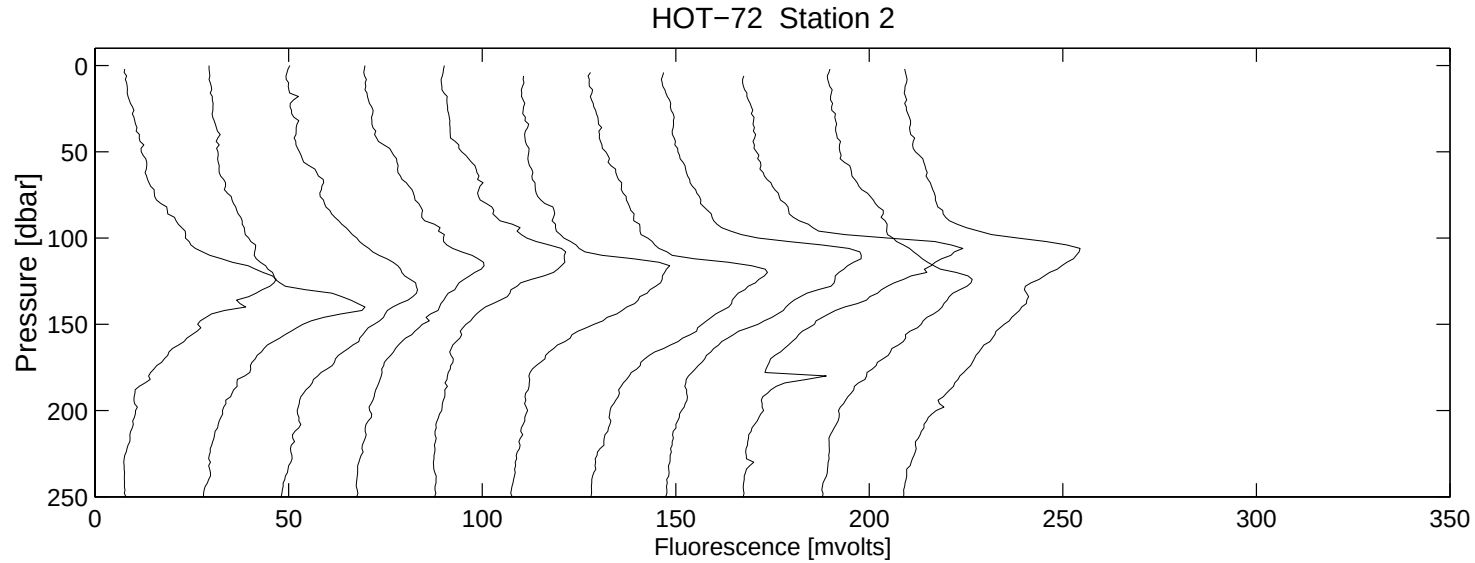
HOT−72 Station 2
Pressure [dbar]
0
50
100
150
200
250
0
50
100
150
200
250
300
350
Fluorescence [mvolts]

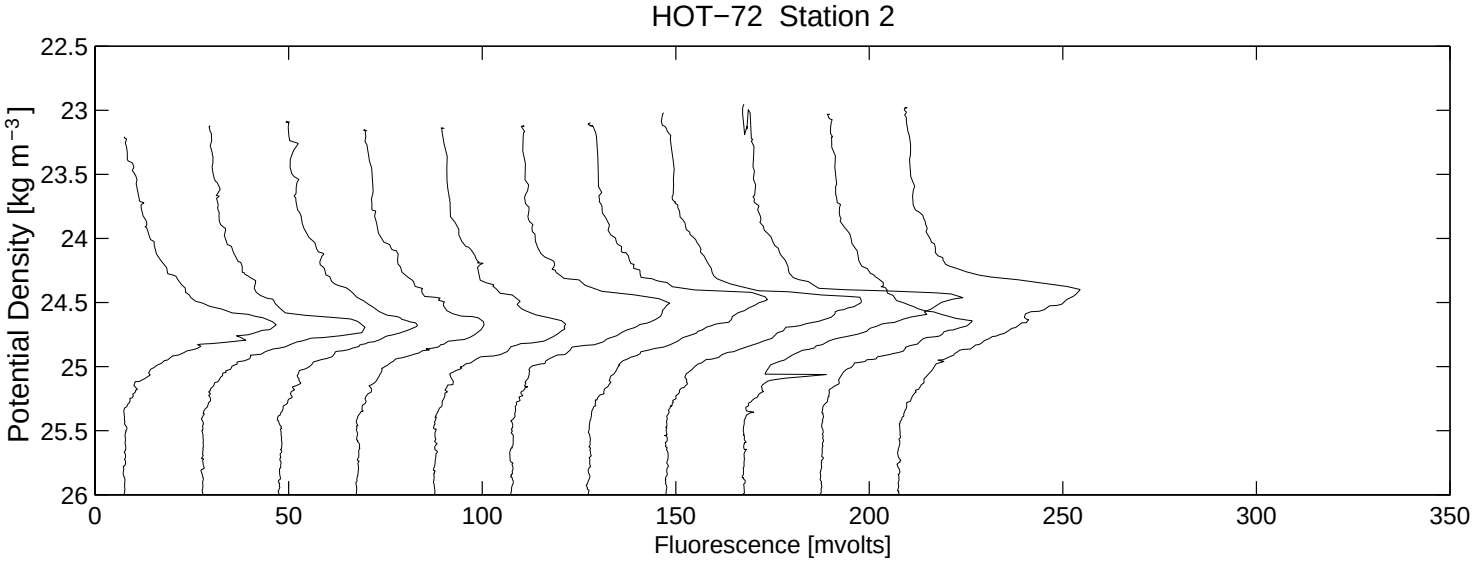
HOT−72 Station 2
Potential Density [kg m^{-3}]
22.5
23
23.5
24
24.5
25
25.5
26
0
50
100
150
200
250
300
350
Fluorescence [mvolts]

Figure 6.4.1d

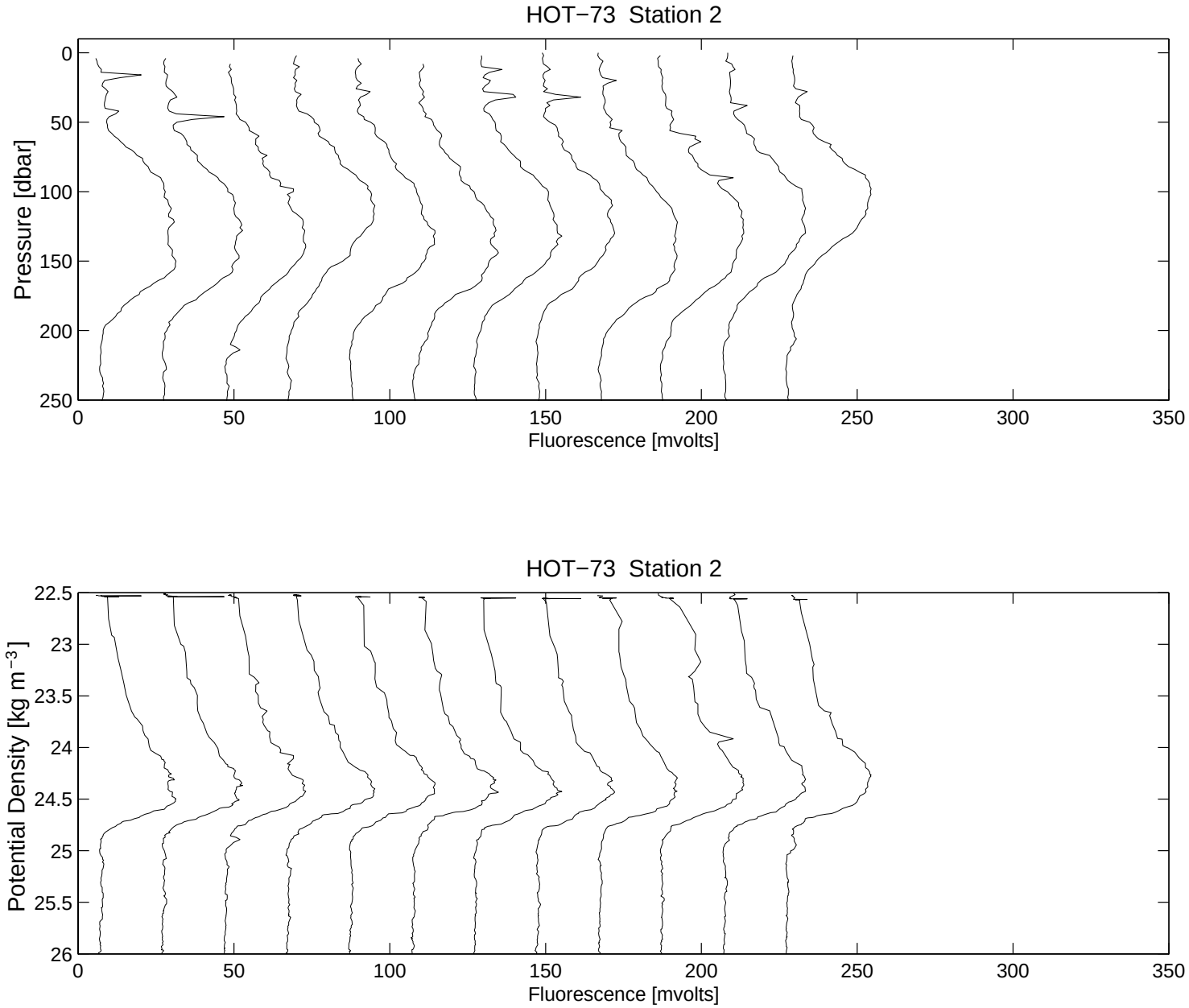
HOT−73 Station 2
Pressure [dbar]
0
50
100
150
200
250
0
50
100
150
200
250
300
350
Fluorescence [mvolts]
HOT−73 Station 2
Potential Density [kg m^{-3}]
22.5
23
23.5
24
24.5
25
25.5
26
0
50
100
150
200
250
300
350
Fluorescence [mvolts]

Figure 6.4.1e

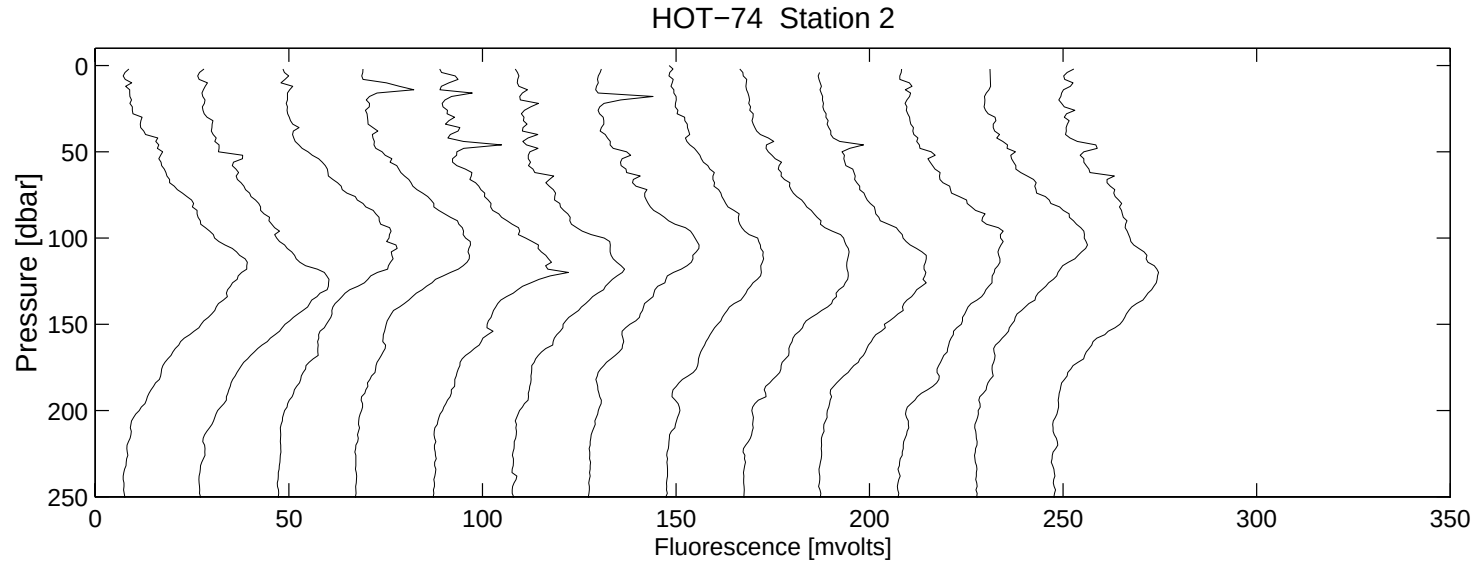
HOT−74 Station 2
Pressure [dbar]
0
50
100
150
200
250
0
50
100
150
200
250
300
350
Fluorescence [mvolts]

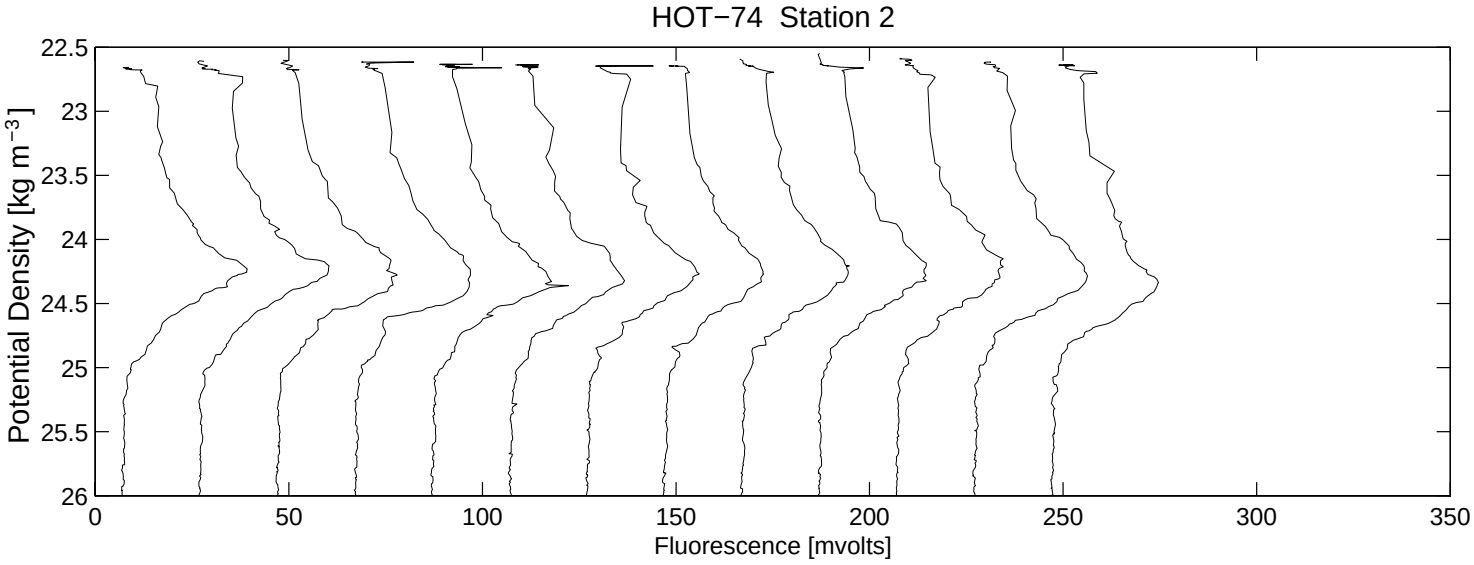
HOT−74 Station 2
Potential Density [kg m^{-3}]
22.5
23
23.5
24
24.5
25
25.5
26
0
50
100
150
200
250
300
350
Fluorescence [mvolts]

Figure 6.4.1f

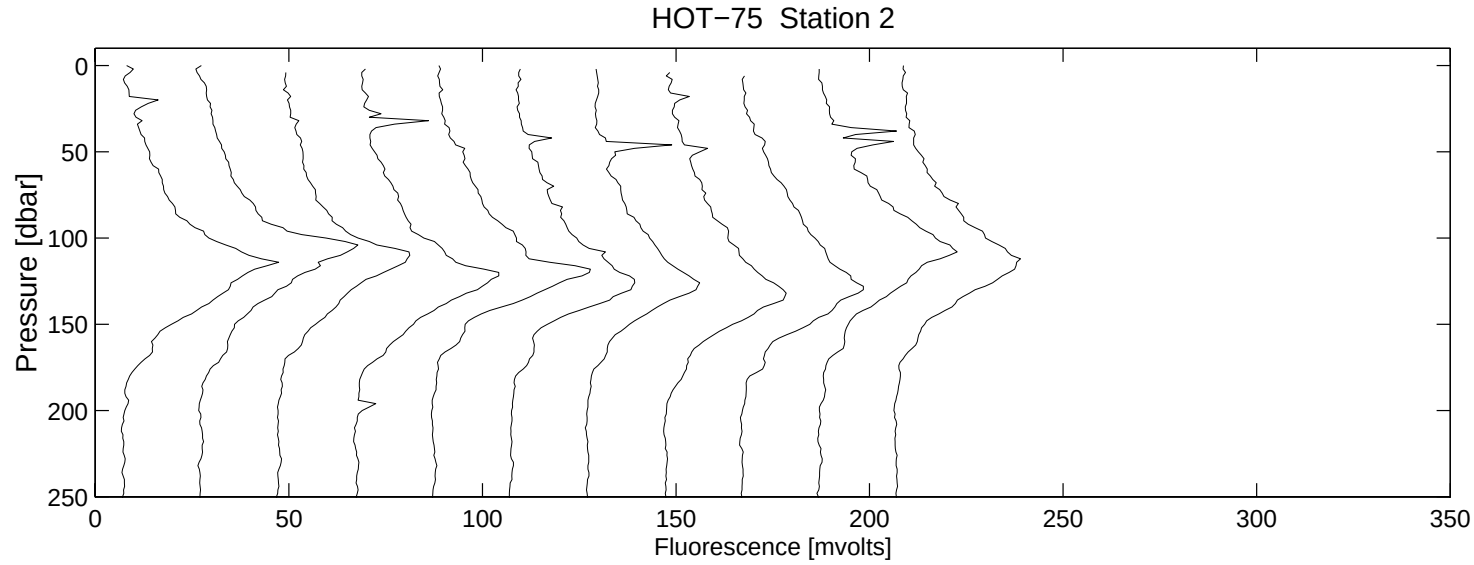
HOT−75 Station 2
Pressure [dbar]
0
50
100
150
200
250
0
50
100
150
200
250
300
350
Fluorescence [mvolts]

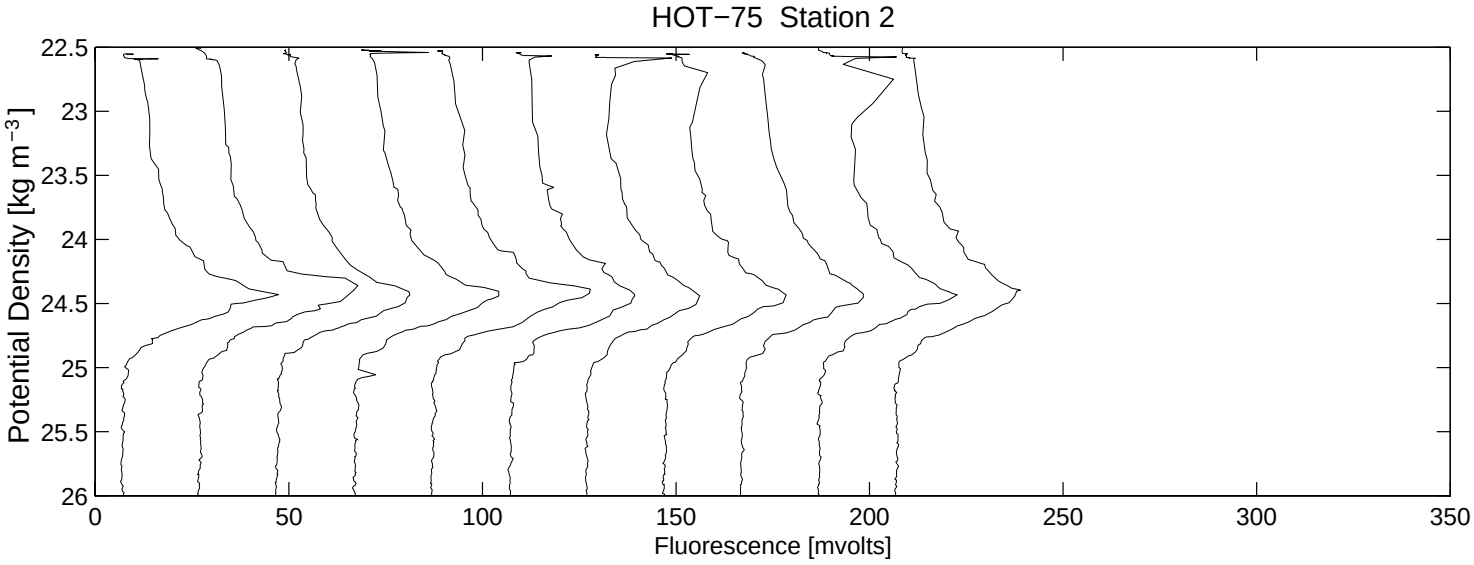
HOT−75 Station 2
Potential Density [kg m^{-3}]
22.5
23
23.5
24
24.5
25
25.5
26
0
50
100
150
200
250
300
350
Fluorescence [mvolts]

Figure 6.4.1g

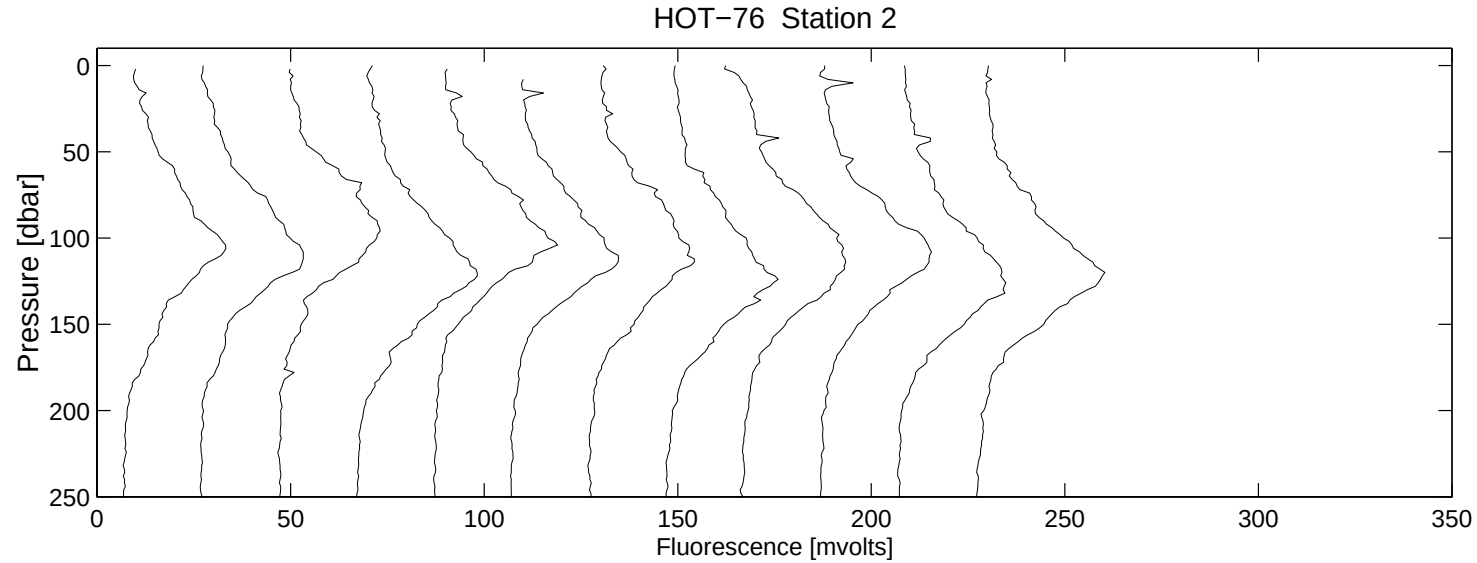
HOT−76 Station 2
Pressure [dbar]
0
50
100
150
200
250
0
50
100
150
200
250
300
350
Fluorescence [mvolts]

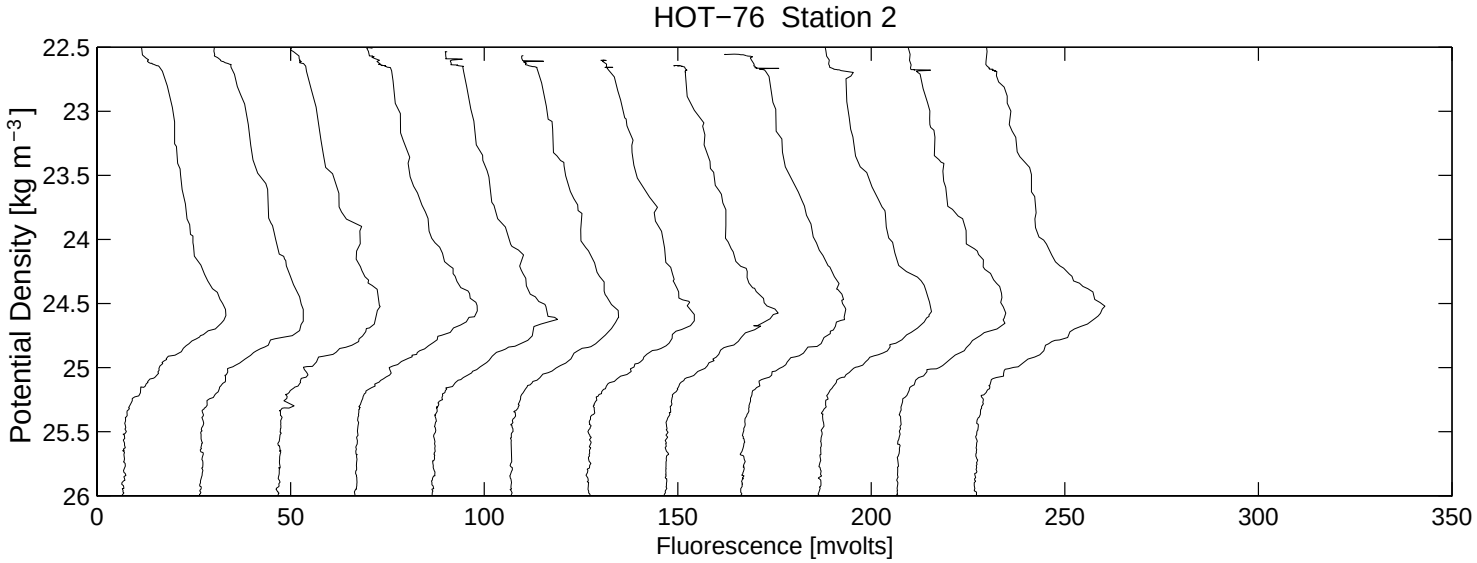
HOT−76 Station 2
Potential Density [kg m^{-3}]
22.5
23
23.5
24
24.5
25
25.5
26
0
50
100
150
200
250
300
350
Fluorescence [mvolts]

Figure 6.4.1h

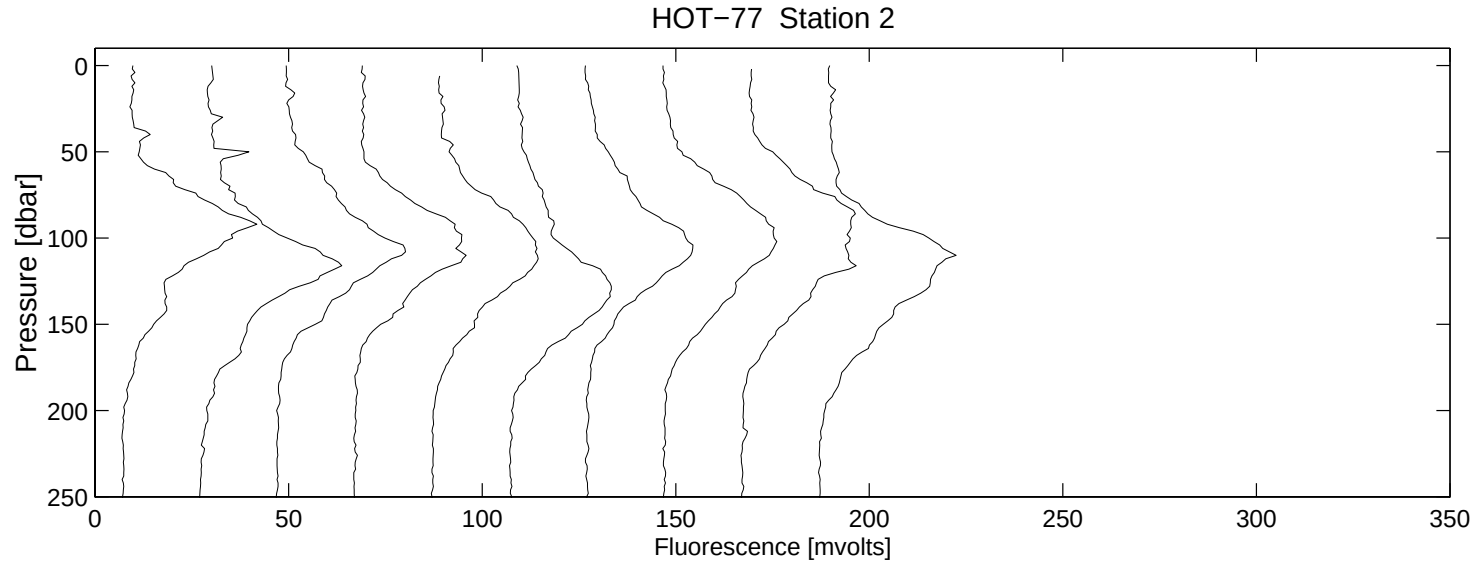
HOT−77 Station 2
Pressure [dbar]
0
50
100
150
200
250
0
50
100
150
200
250
300
350
Fluorescence [mvolts]

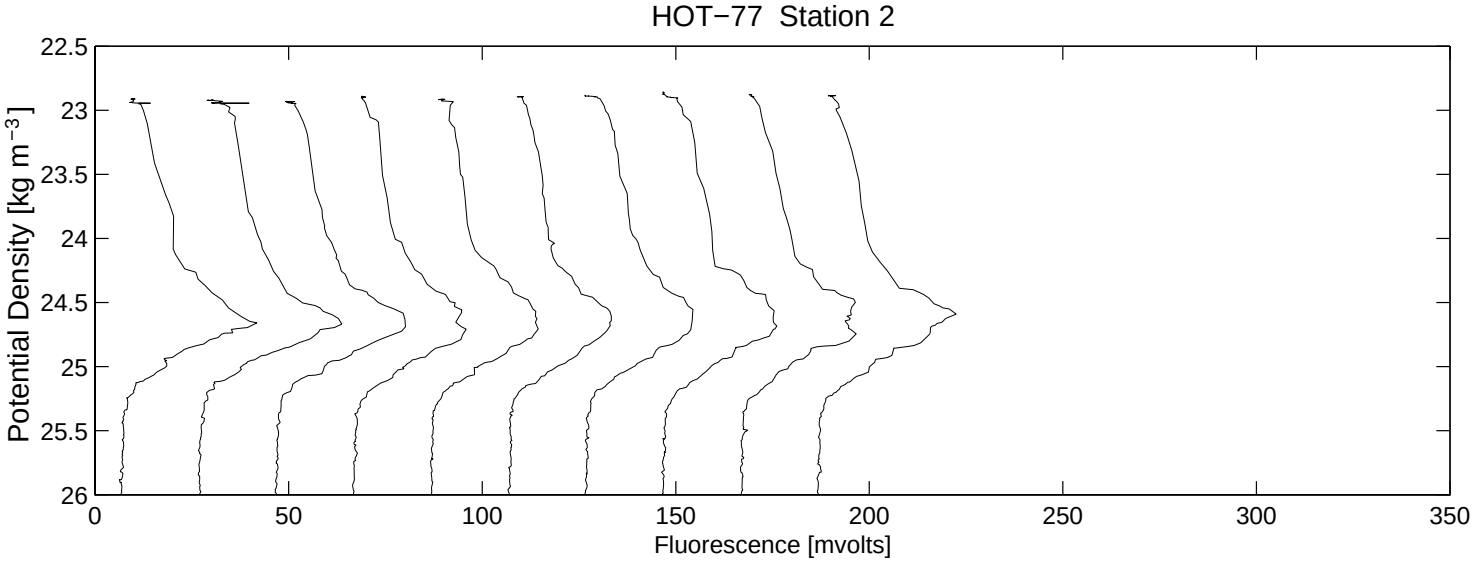
HOT−77 Station 2
Potential Density [kg m^{-3}]
22.5
23
23.5
24
24.5
25
25.5
26
0
50
100
150
200
250
300
350
Fluorescence [mvolts]

Figure 6.4.1i

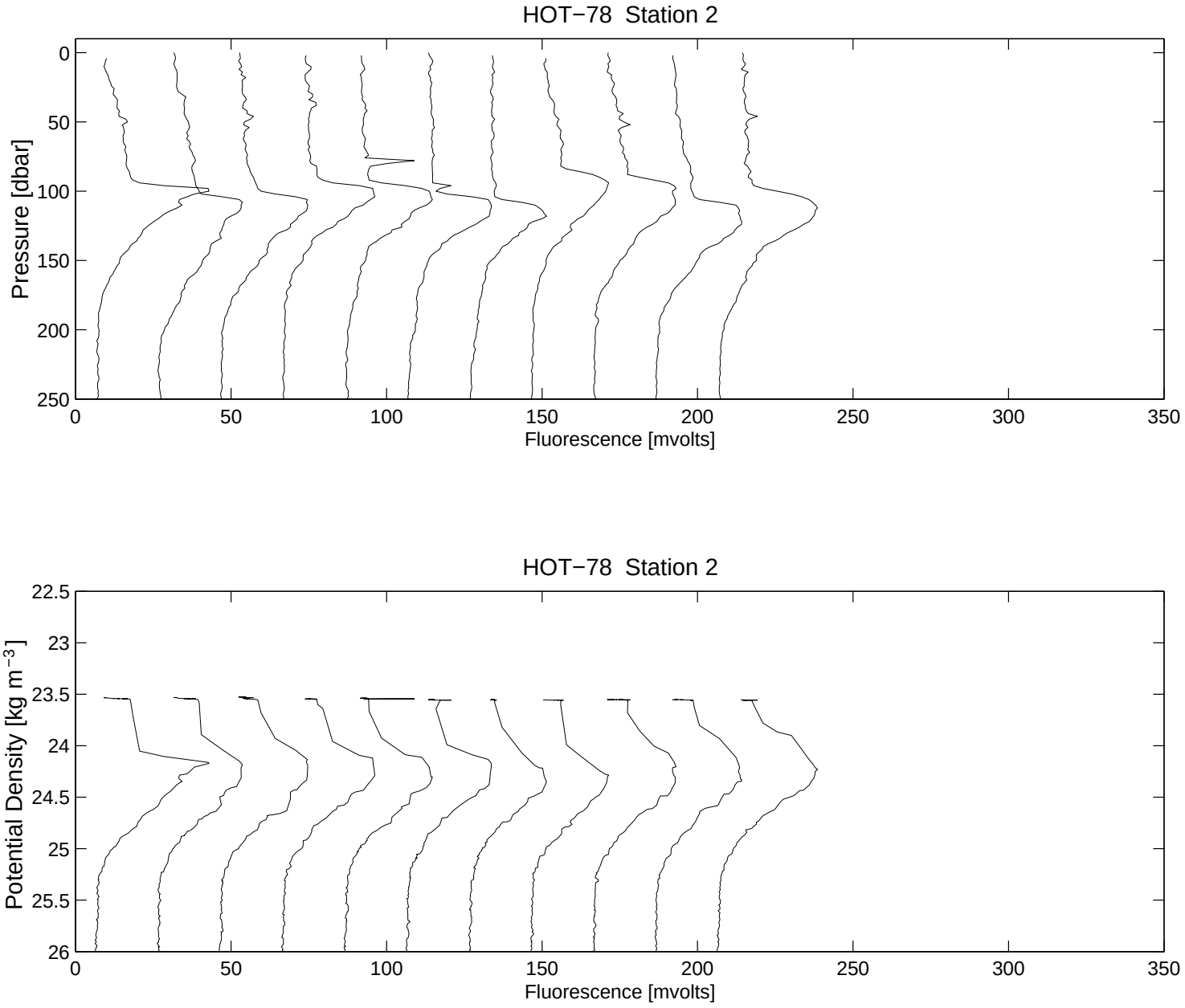
HOT−78 Station 2
Pressure [dbar]
0
50
100
150
200
250
Fluorescence [mvolts]
0
50
100
150
200
250
300
350
HOT−78 Station 2
Potential Density [kg m^{-3}]
22.5
23
23.5
24
24.5
25
25.5
26
Fluorescence [mvolts]
0
50
100
150
200
250
300
350

Figure 6.4.1j

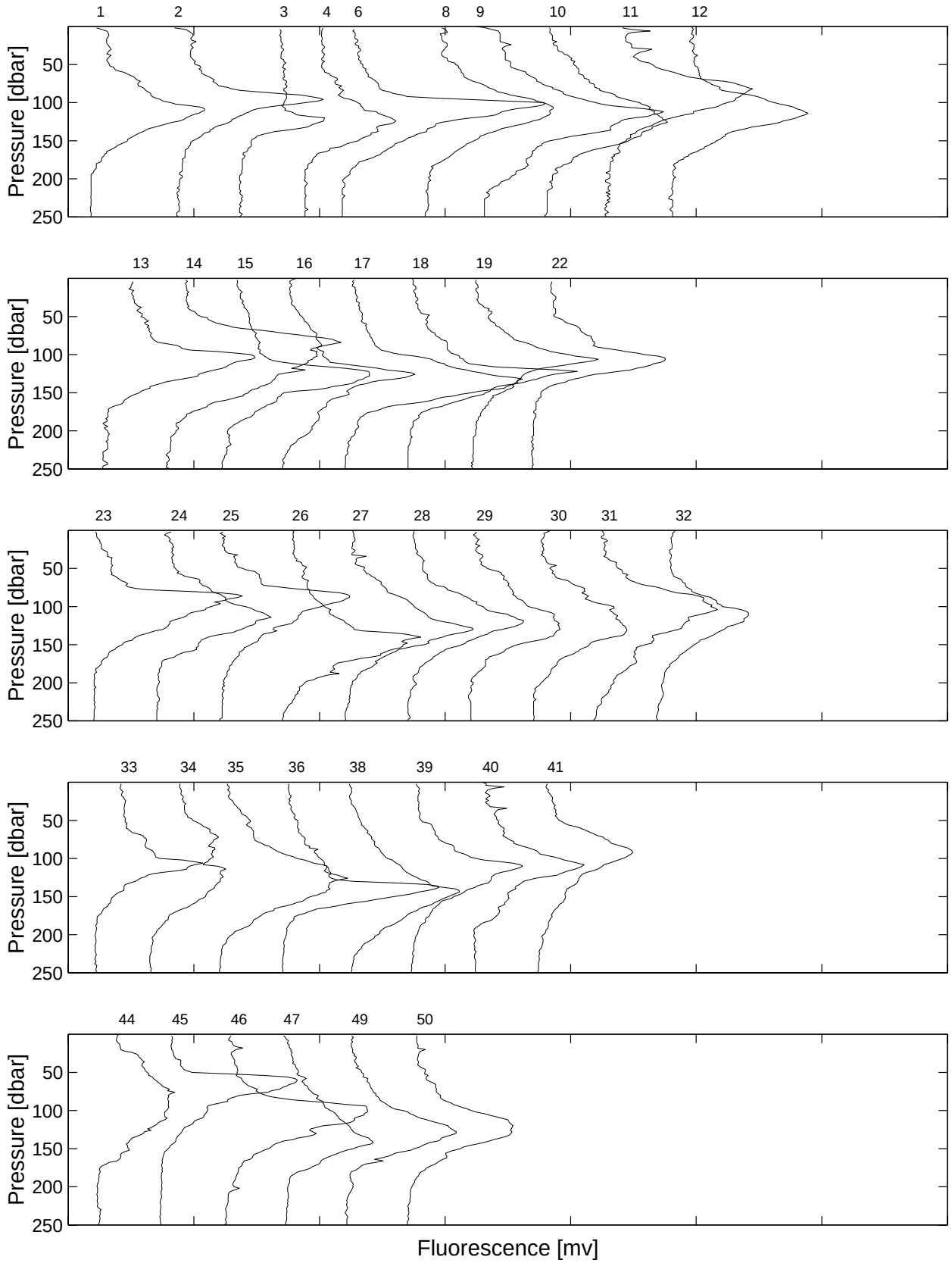
1 2 3 4 6 8 9 10 11 12
13 14 15 16 17 18 19 22
23 24 25 26 27 28 29 30 31 32
33 34 35 36 38 39 40 41
44 45 46 47 49 50
Pressure [dbar]
50
100
150
200
250
Fluorescence [mv]

Figure 6.4.2

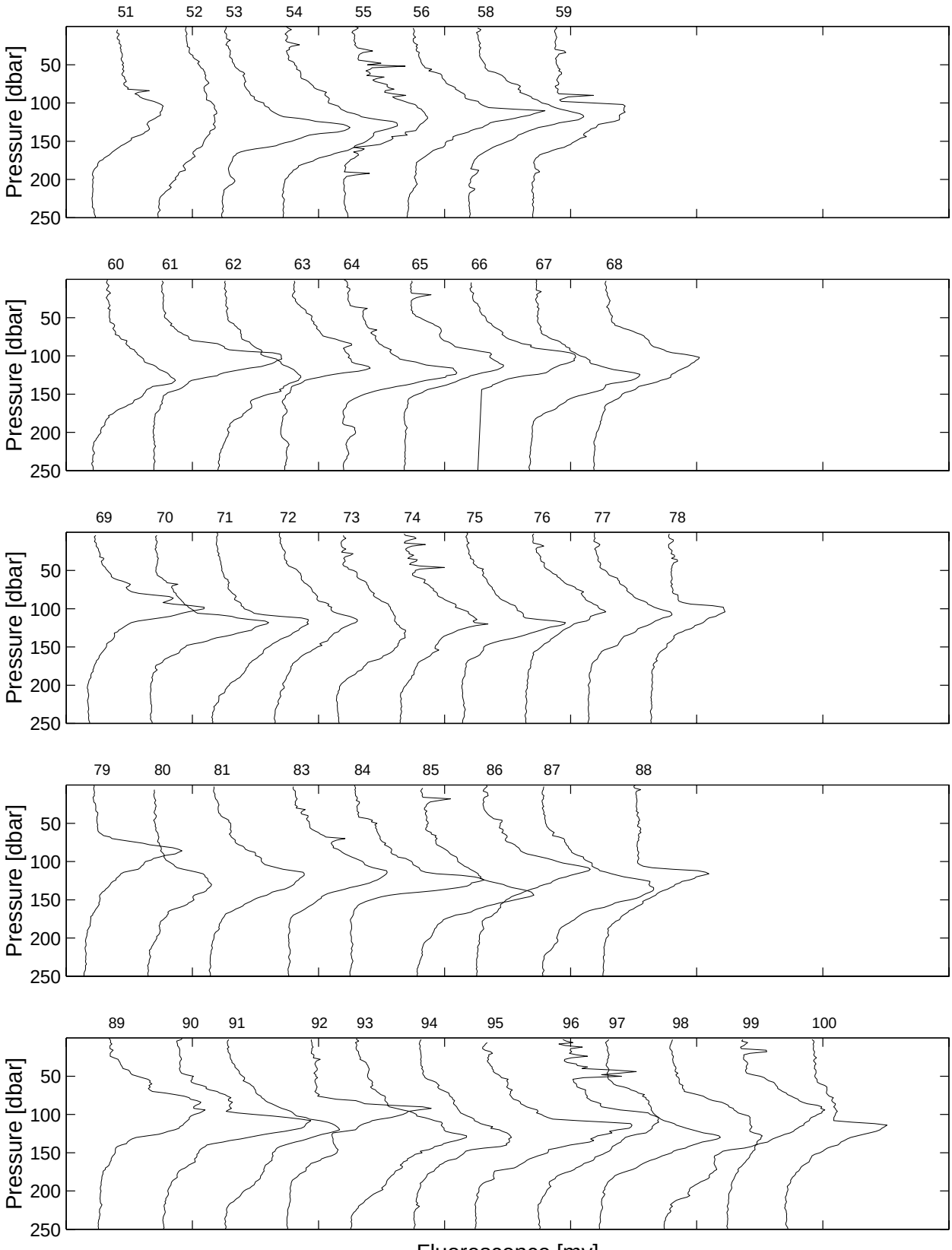

Figure 6.4.2 continued

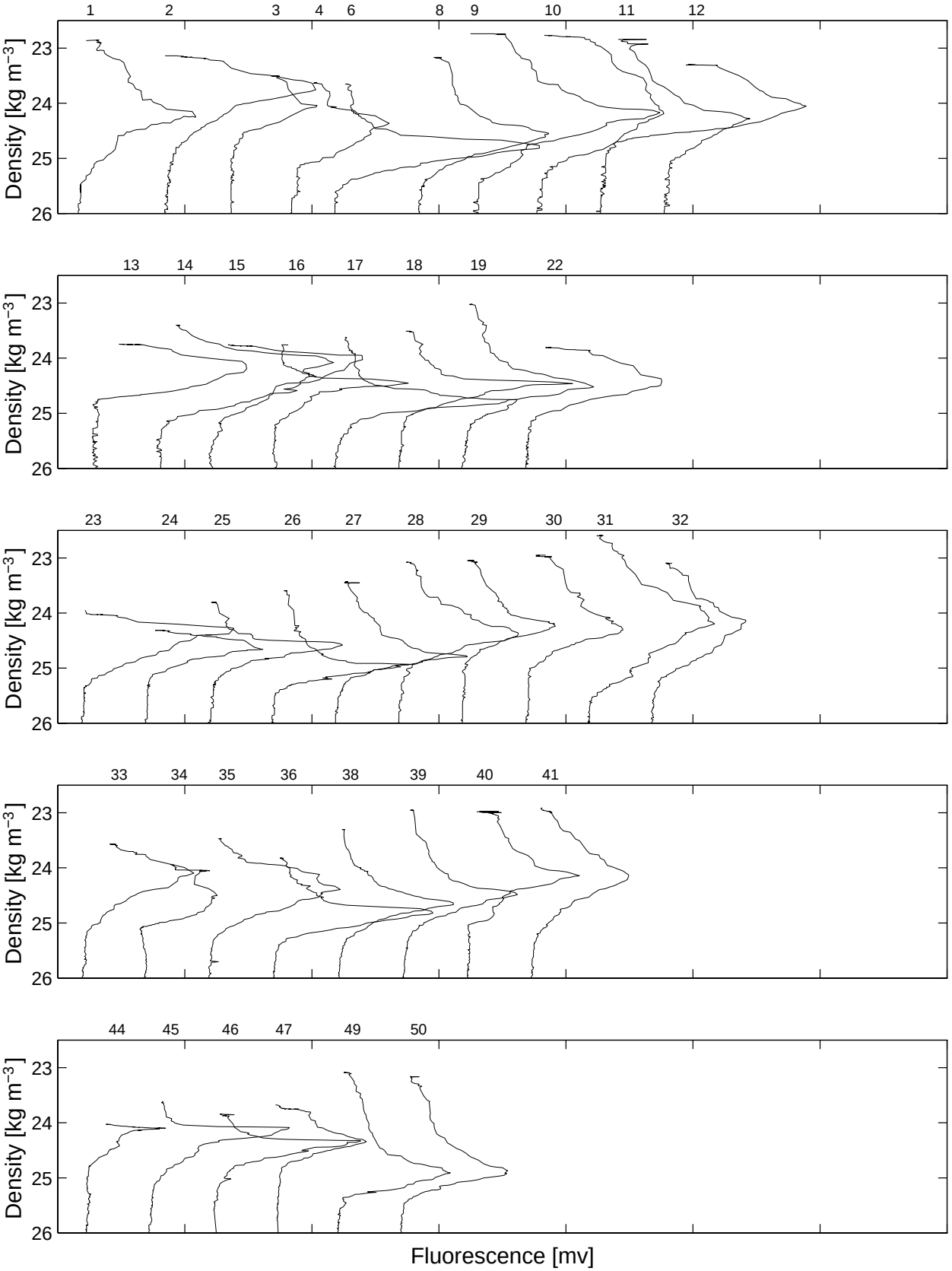
1 2 3 4 6 8 9 10 11 12
13 14 15 16 17 18 19 22
23 24 25 26 27 28 29 30 31 32
33 34 35 36 38 39 40 41
44 45 46 47 49 50
Density [kg m−3]
23
24
25
26
Fluorescence [mv]

Figure 6.4.3

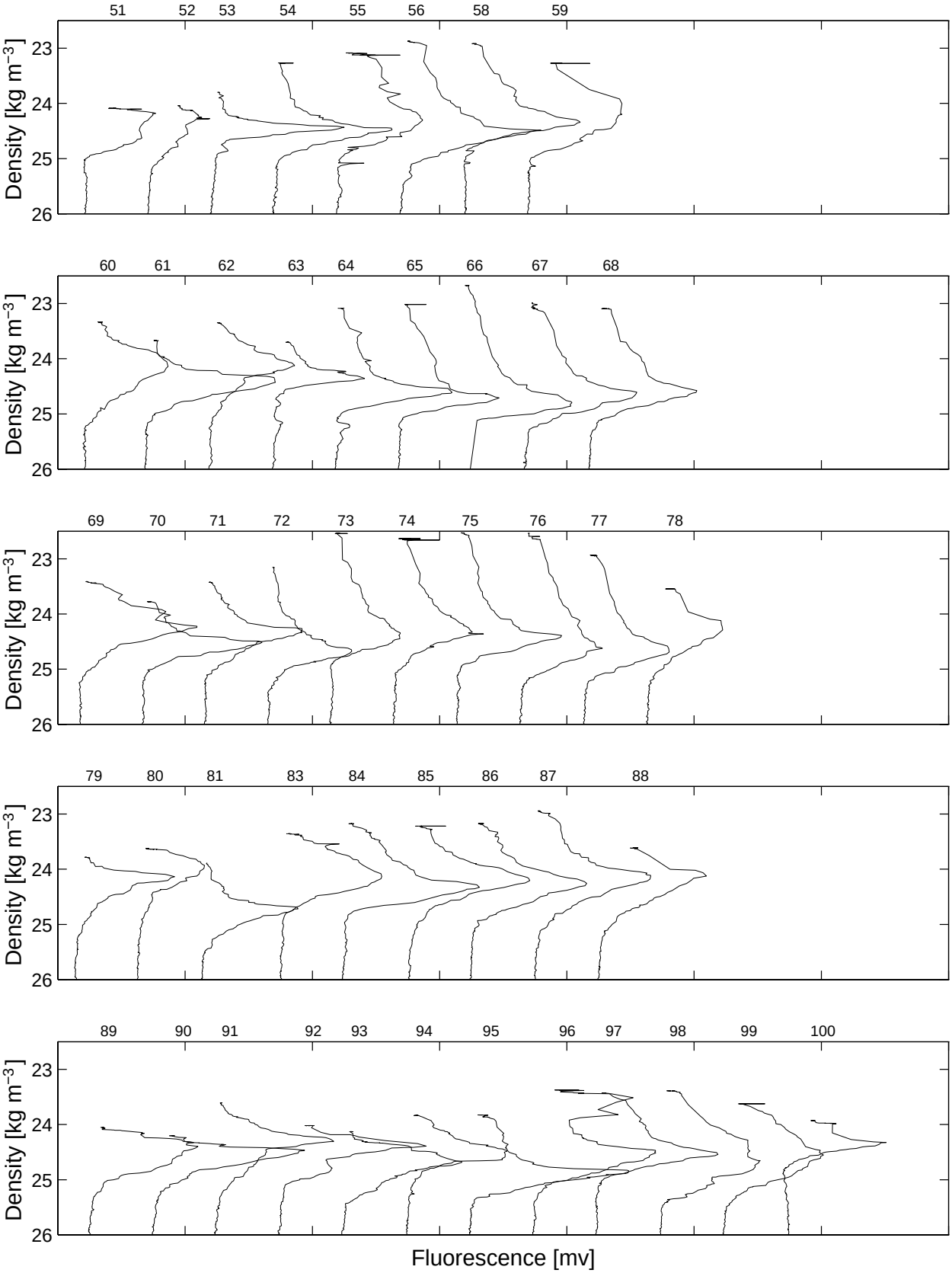

Figure 6.4.3 continued

Figure 6.5.1: [Upper panel] Atmospheric pressure while at Station ALOHA for 1996 HOT cruises. Open circles are individual measurements. [Lower panel] Sea surface temperature measured from a bucket sample while at Station ALOHA for 1996 HOT cruises.

Figure 6.5.2: [Upper panel] Dry bulb air temperature while at Station ALOHA for 1996 HOT cruises. [Lower panel] Wet bulb air temperature while at Station ALOHA for 1996 HOT cruises.

Figure 6.5.3: [Upper panel] Sea surface temperature minus dry air temperature while at Station ALOHA for 1996 HOT cruises. [Lower panel] Dry minus wet air temperature while at Station ALOHA for 1996 HOT cruises.

Figure 6.5.4: True winds measured at Station ALOHA (upper panel) and collected by NDBC buoy #51001 (lower panel) during HOT-69. The orientation of the arrows indicate the wind direction; up is northward, right is eastward.

Figure 6.5.5: True winds measured at Station ALOHA during HOT-70. The orientation of the arrows indicate the wind direction; up is northward, right is eastward.

Figure 6.5.6: True winds measured at Station ALOHA during HOT-71. The orientation of the arrows indicate the wind direction; up is northward, right is eastward.

Figure 6.5.7: True winds measured at Station ALOHA during HOT-72. The orientation of the arrows indicate the wind direction; up is northward, right is eastward.

Figure 6.5.8: True winds measured at Station ALOHA (upper panel) and collected by NDBC buoy #51001 (lower panel) during HOT-73. The orientation of the arrows indicate the wind direction; up is northward, right is eastward.

Figure 6.5.9: True winds measured at Station ALOHA (upper panel) and collected by NDBC buoy #51001 (lower panel) during HOT-74. The orientation of the arrows indicate the wind direction; up is northward, right is eastward.

Figure 6.5.10: True winds measured at Station ALOHA (upper panel) and collected by NDBC buoy #51001 (lower panel) during HOT-75. The orientation of the arrows indicate the wind direction; up is northward, right is eastward.

Figure 6.5.11: True winds measured at Station ALOHA (upper panel) and collected by NDBC buoy #51001 (lower panel) during HOT-76. The orientation of the arrows indicate the wind direction; up is northward, right is eastward.

Figure 6.5.12: True winds measured at Station ALOHA (upper panel) and collected by NDBC buoy #51001 (lower panel) during HOT-77. The orientation of the arrows indicate the wind direction; up is northward, right is eastward.

Figure 6.5.13: True winds measured at Station ALOHA (upper panel) and collected by NDBC buoy #51001 (lower panel) during HOT-78. The orientation of the arrows indicate the wind direction; up is northward, right is eastward.

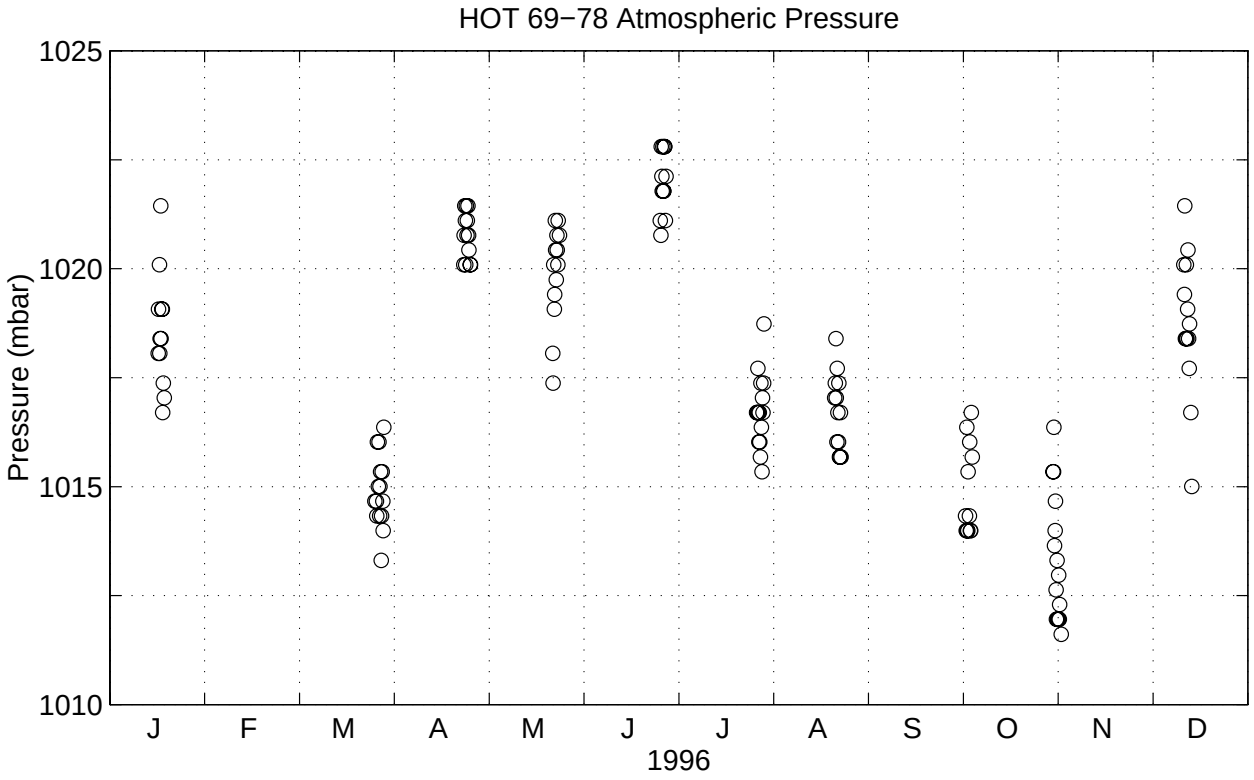
HOT 69−78 Atmospheric Pressure
Pressure (mbar)
1025
1020
1015
1010
J
F
M
A
M
J
J
A
S
O
N
D
1996

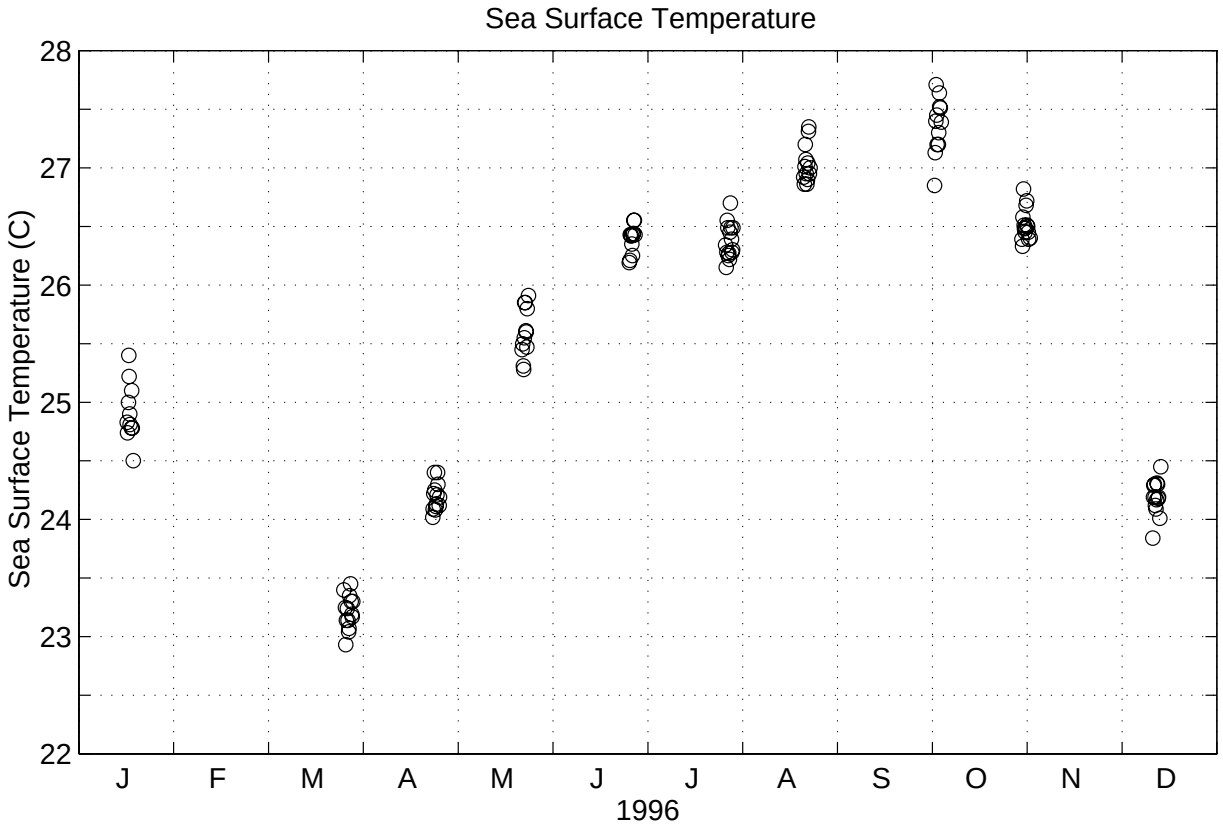
Sea Surface Temperature
Sea Surface Temperature (C)
28
27
26
25
24
23
22
J
F
M
A
M
J
J
A
S
O
N
D
1996

Figure 6.5.1

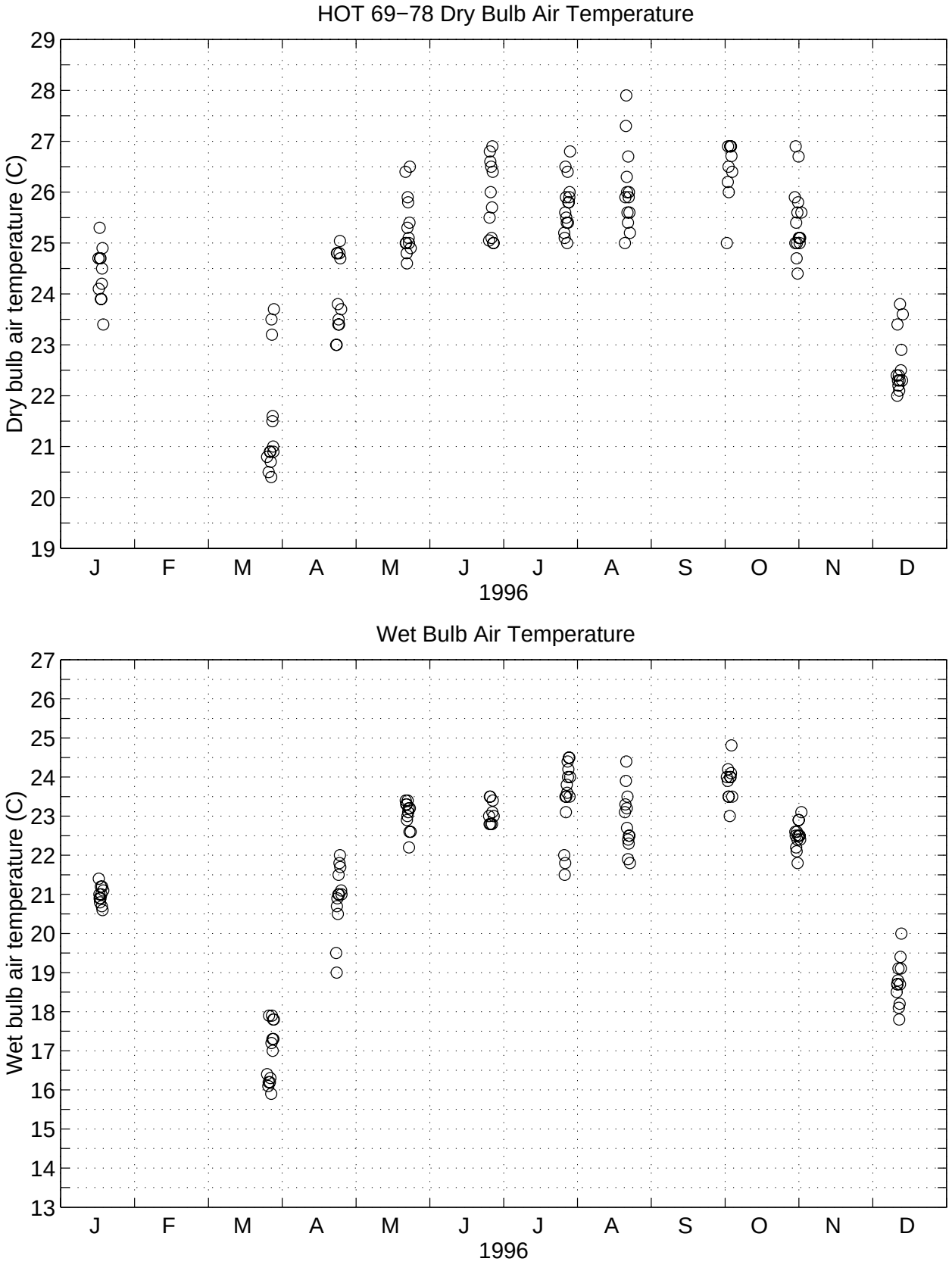
HOT 69−78 Dry Bulb Air Temperature
Dry bulb air temperature (C)
29
28
27
26
25
24
23
22
21
20
19
J F M A M J J A S O N D
1996
Wet Bulb Air Temperature
Wet bulb air temperature (C)
27
26
25
24
23
22
21
20
19
18
17
16
15
14
13
J F M A M J J A S O N D
1996

Figure 6.5.2

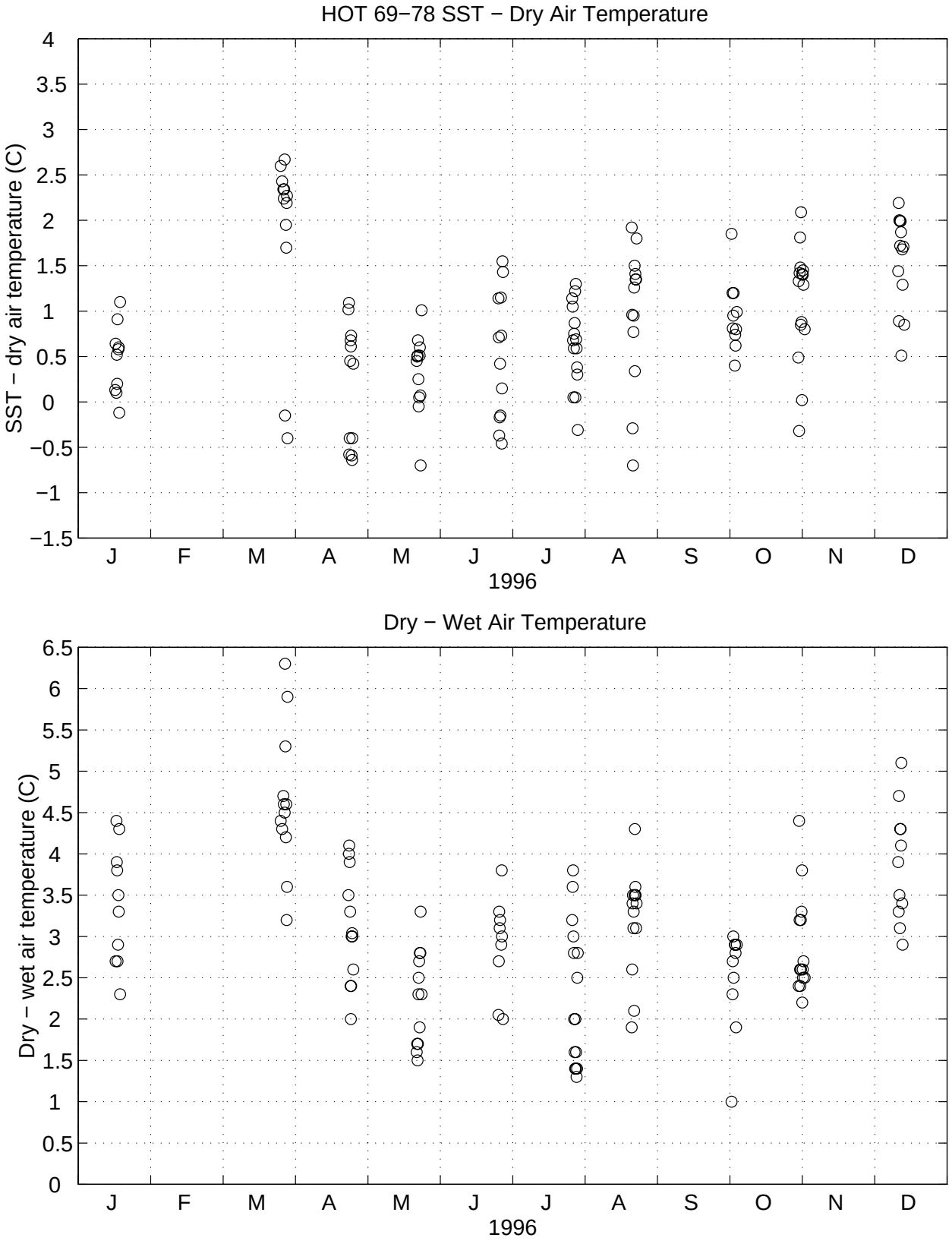
HOT 69−78 SST − Dry Air Temperature
SST − dry air temperature (C)
4
3.5
3
2.5
2
1.5
1
0.5
0
−0.5
−1
−1.5
J F M A M J J A S O N D
1996
Dry − Wet Air Temperature
Dry − wet air temperature (C)
6.5
6
5.5
5
4.5
4
3.5
3
2.5
2
1.5
1
0.5
0
J F M A M J J A S O N D
1996

Figure 6.5.3

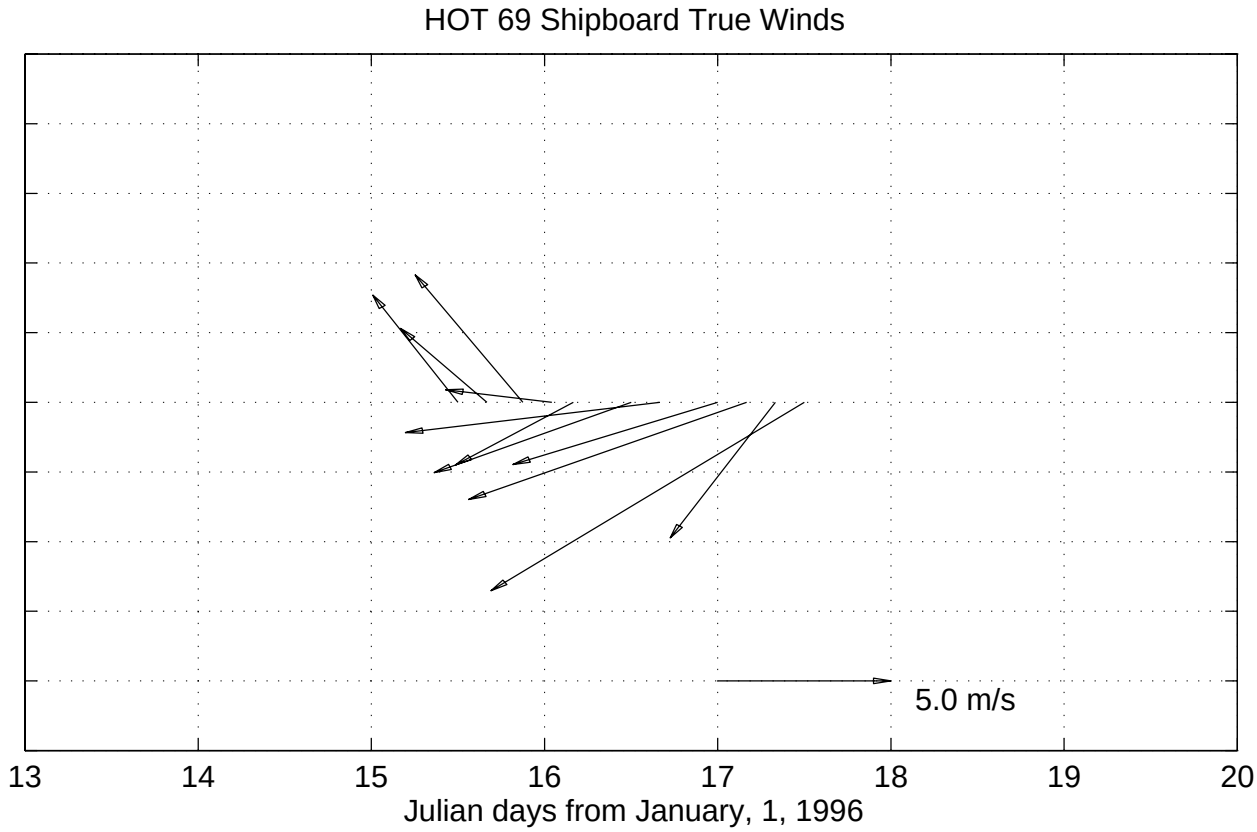
HOT 69 Shipboard True Winds
5.0 m/s
13
14
15
16
17
18
19
20
Julian days from January, 1, 1996

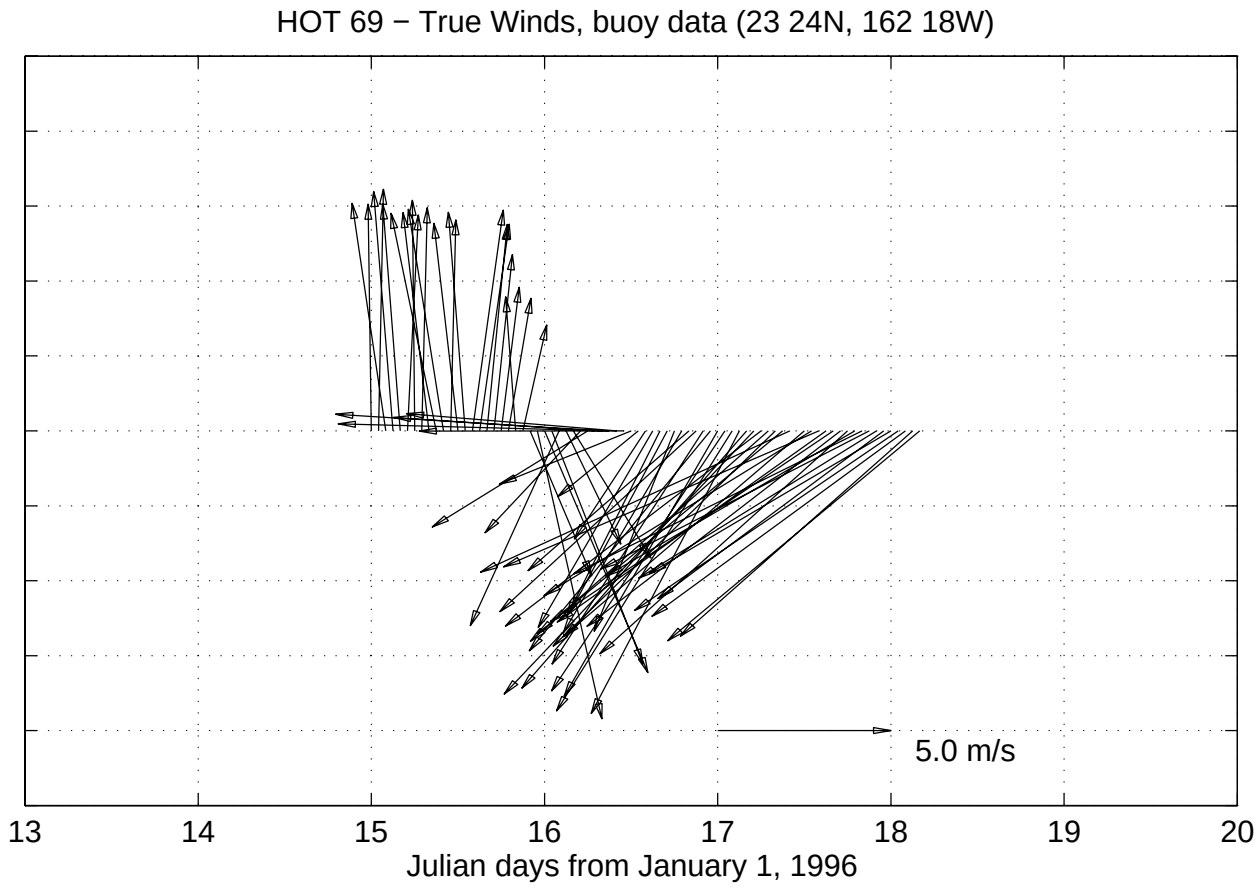
HOT 69 − True Winds, buoy data (23 24N, 162 18W)
5.0 m/s
13
14
15
16
17
18
19
20
Julian days from January 1, 1996

Figure 6.5.4

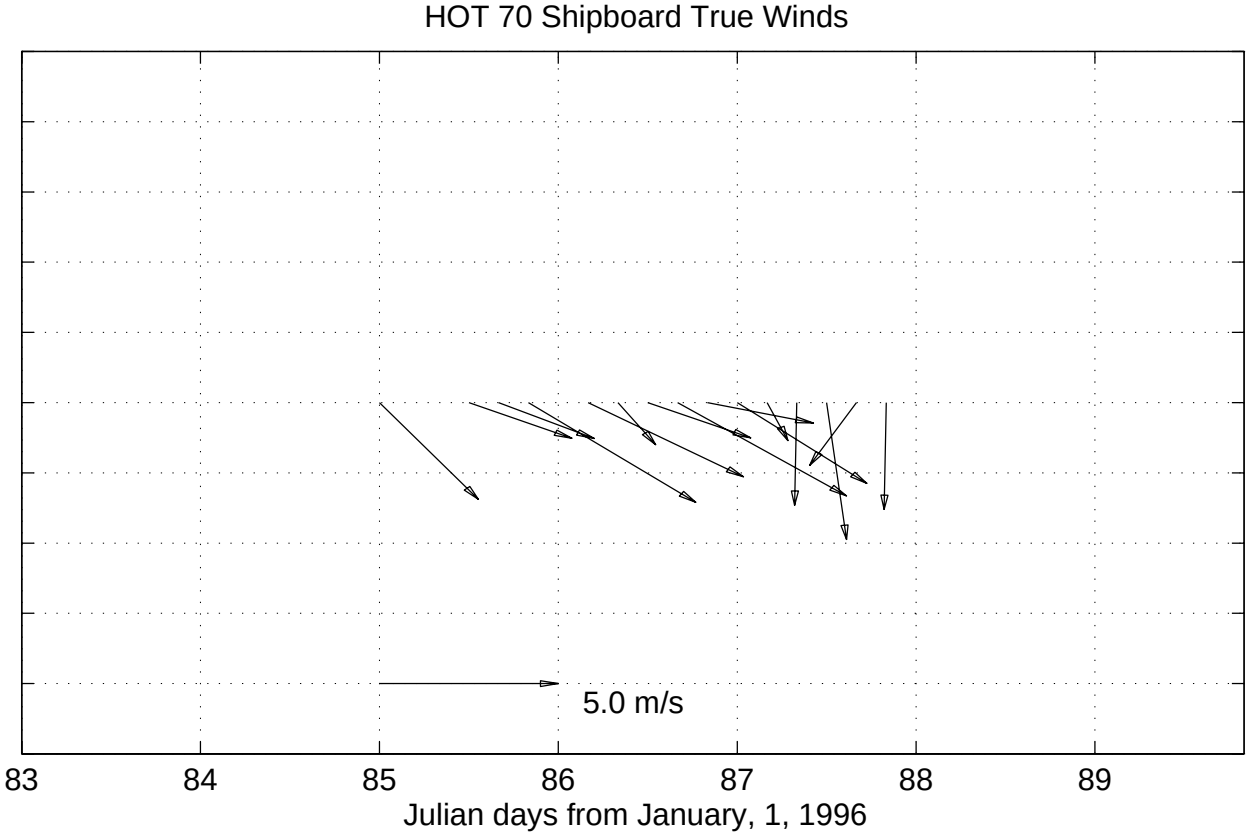
HOT 70 Shipboard True Winds
5.0 m/s
83
84
85
86
87
88
89
Julian days from January, 1, 1996

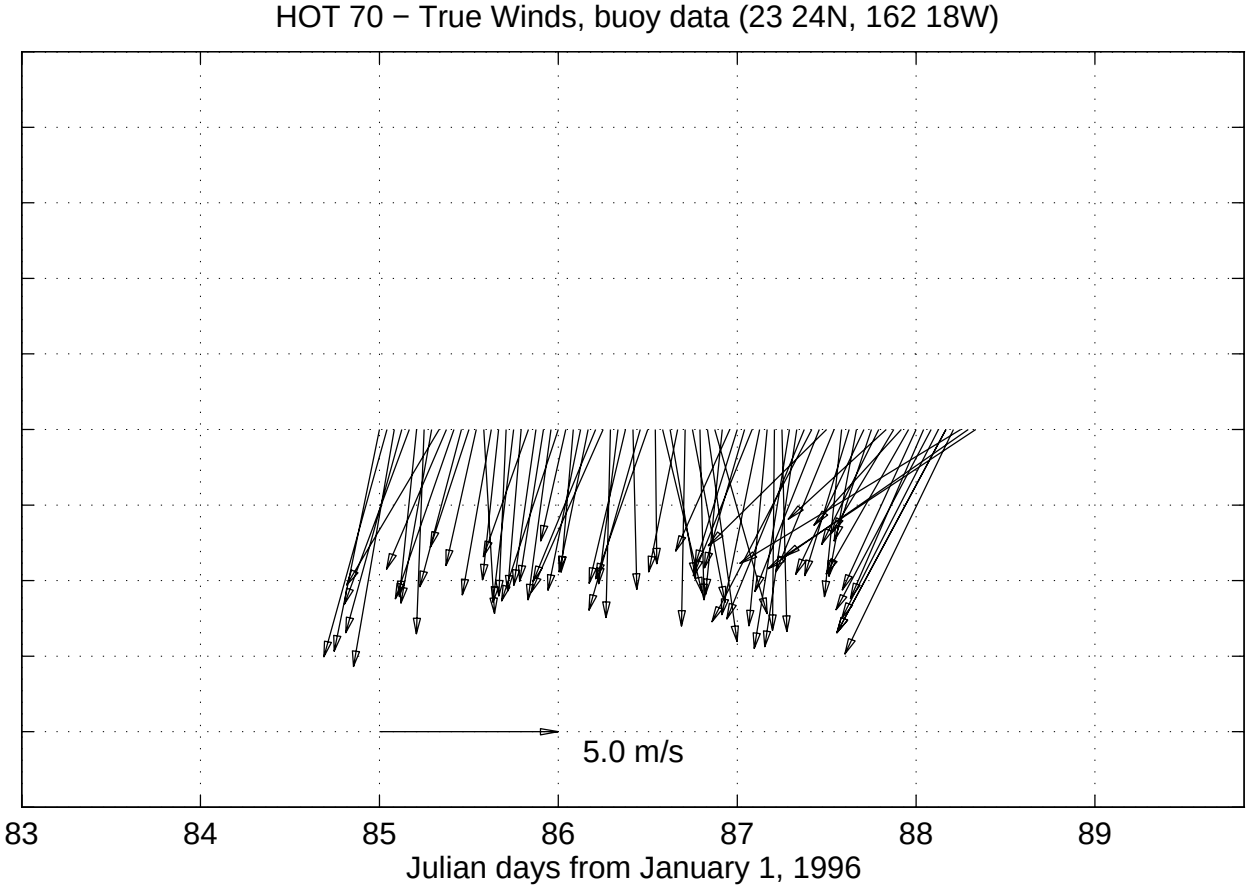
HOT 70 − True Winds, buoy data (23 24N, 162 18W)
5.0 m/s
83
84
85
86
87
88
89
Julian days from January 1, 1996

Figure 6.5.5

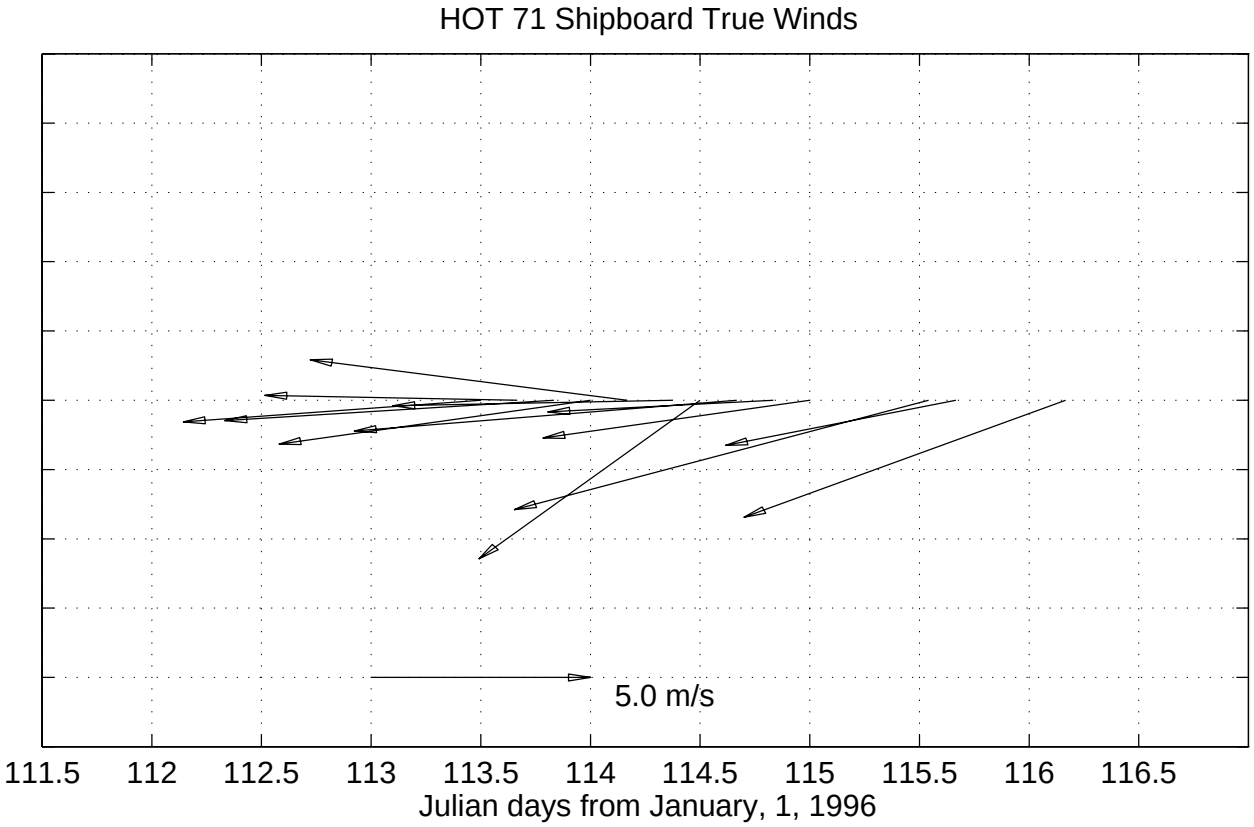
HOT 71 Shipboard True Winds
5.0 m/s
111.5
112
112.5
113
113.5
114
114.5
115
115.5
116
116.5
Julian days from January, 1, 1996

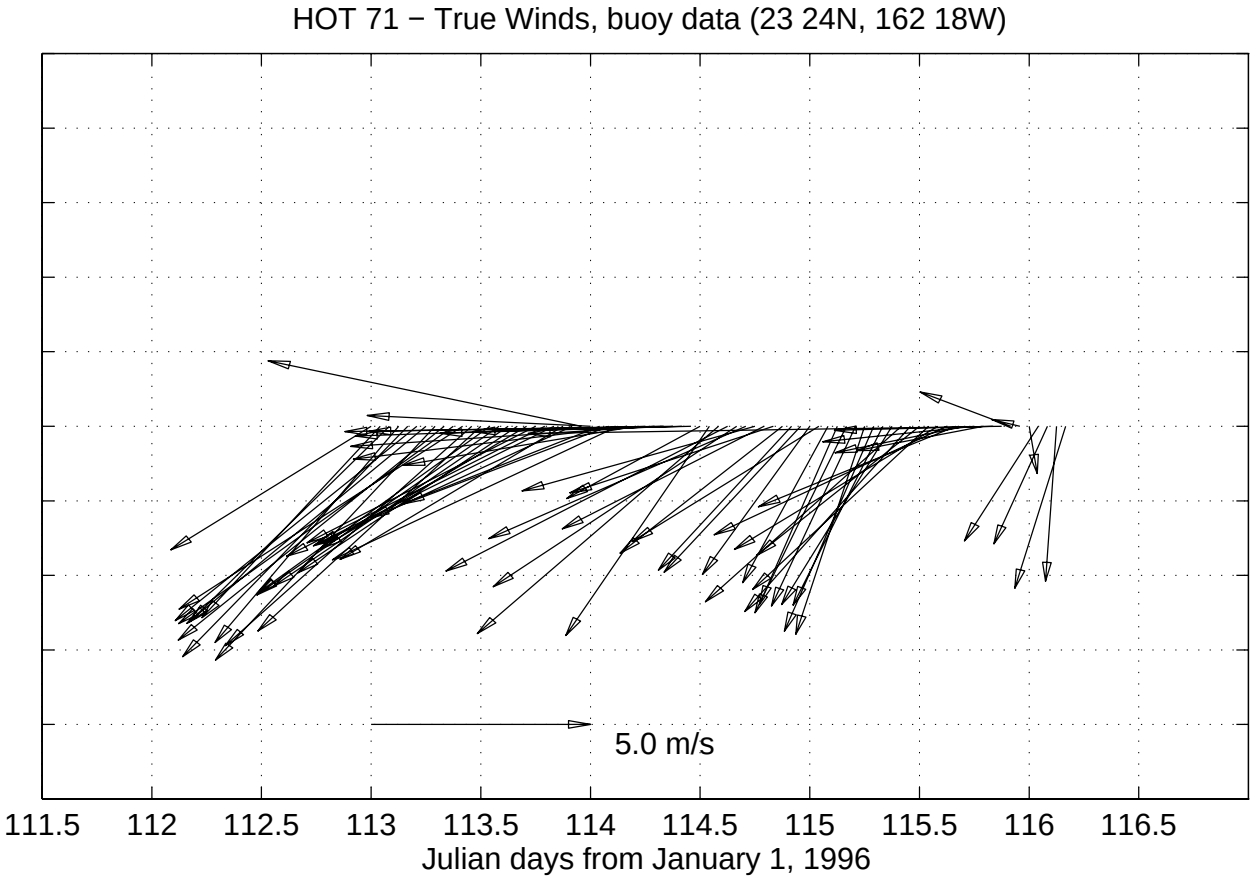
HOT 71 − True Winds, buoy data (23 24N, 162 18W)
5.0 m/s
111.5
112
112.5
113
113.5
114
114.5
115
115.5
116
116.5
Julian days from January 1, 1996

Figure 6.5.6

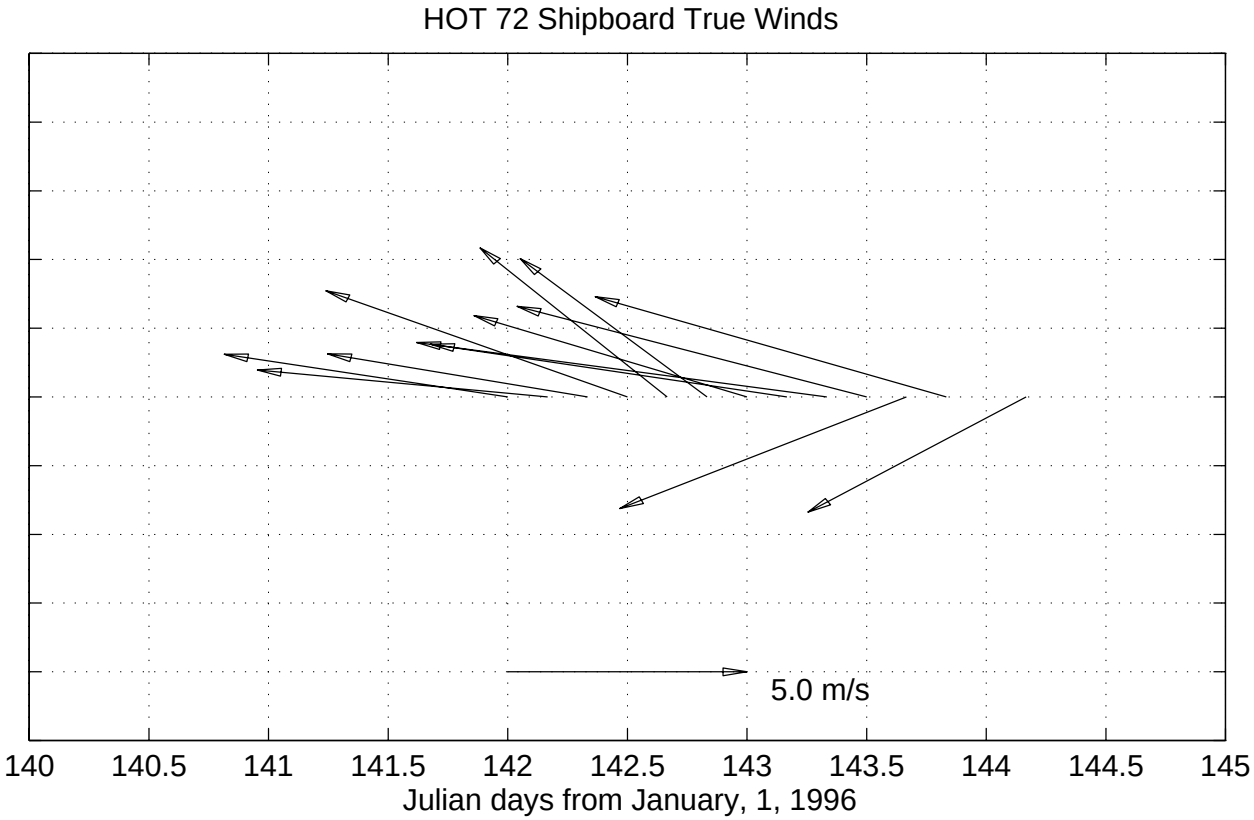
HOT 72 Shipboard True Winds
5.0 m/s
140
140.5
141
141.5
142
142.5
143
143.5
144
144.5
145
Julian days from January, 1, 1996

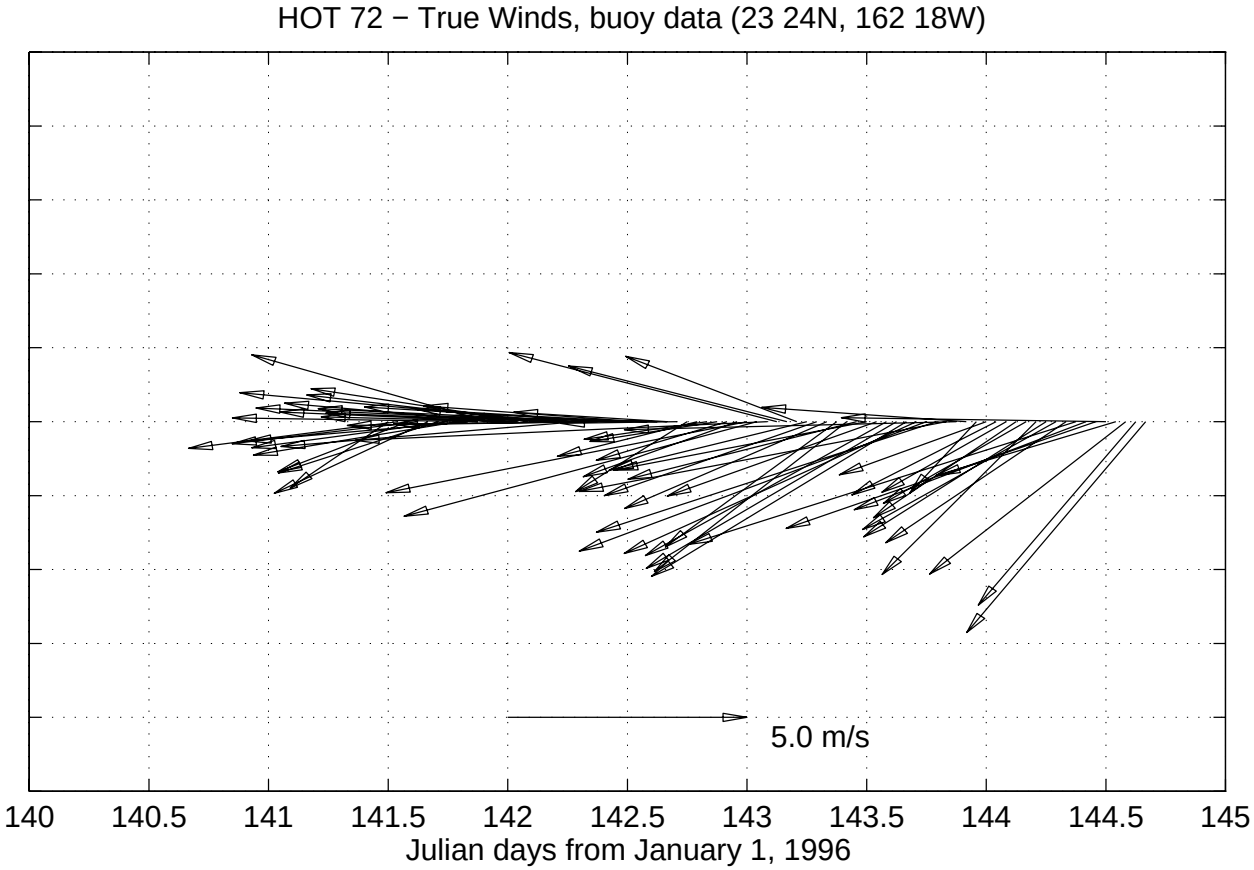
HOT 72 − True Winds, buoy data (23 24N, 162 18W)
5.0 m/s
140
140.5
141
141.5
142
142.5
143
143.5
144
144.5
145
Julian days from January 1, 1996

Figure 6.5.7

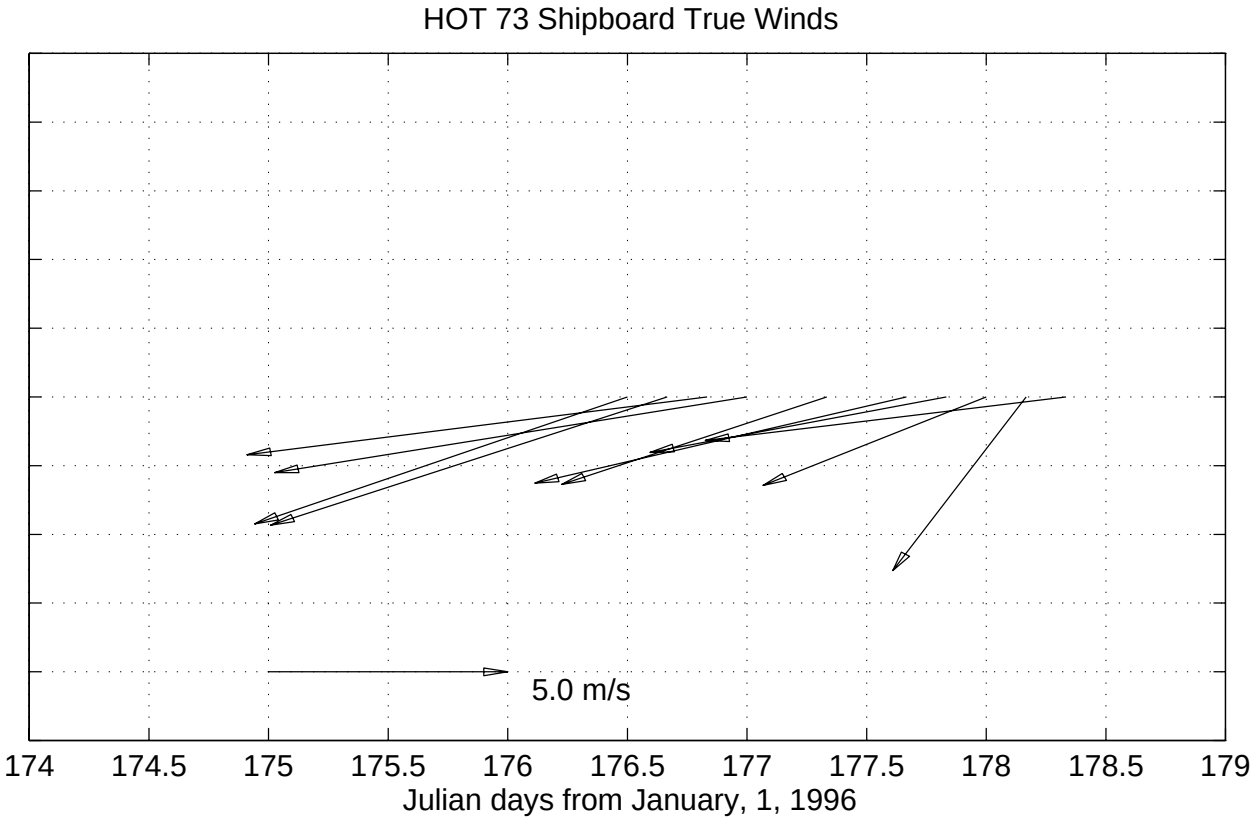
HOT 73 Shipboard True Winds
5.0 m/s
174
174.5
175
175.5
176
176.5
177
177.5
178
178.5
179
Julian days from January, 1, 1996

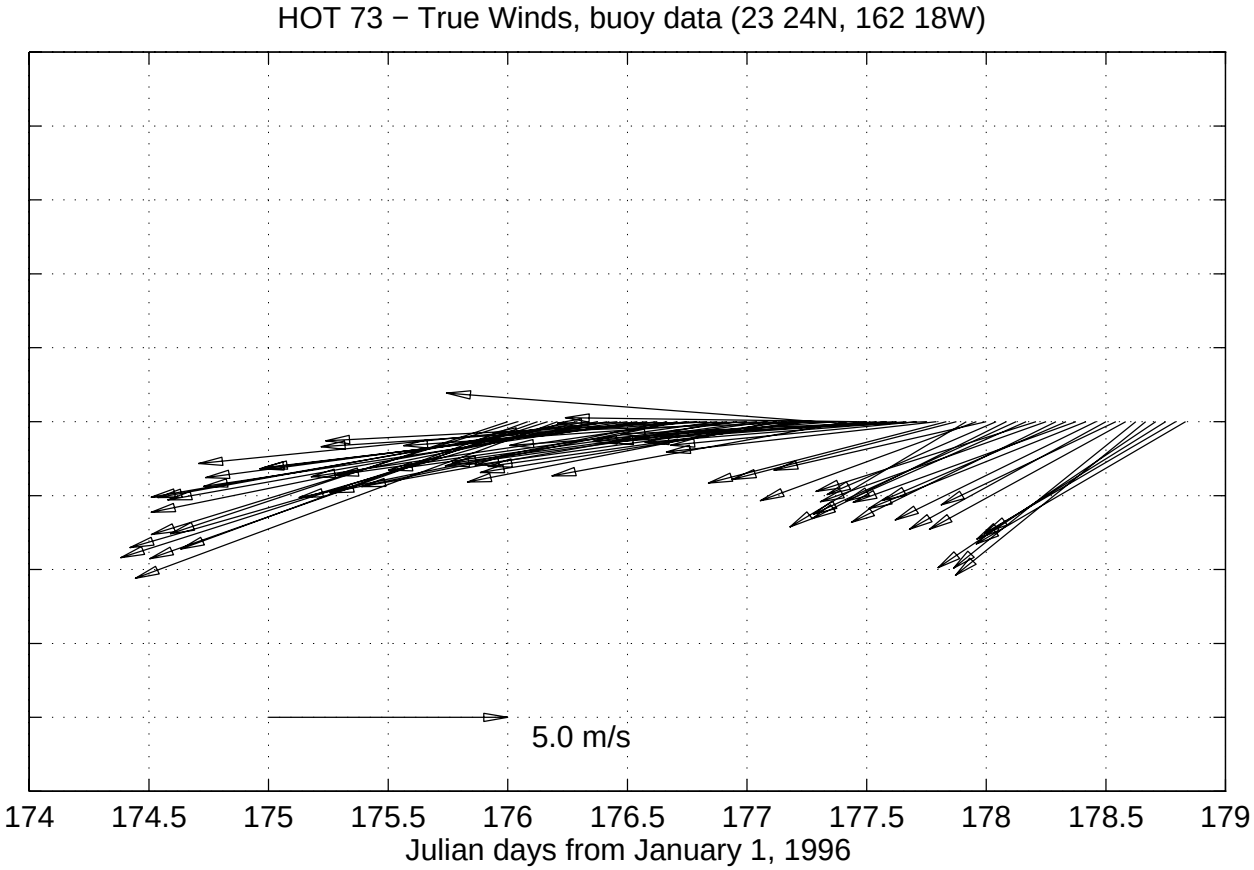
HOT 73 − True Winds, buoy data (23 24N, 162 18W)
5.0 m/s
174
174.5
175
175.5
176
176.5
177
177.5
178
178.5
179
Julian days from January 1, 1996

Figure 6.5.8

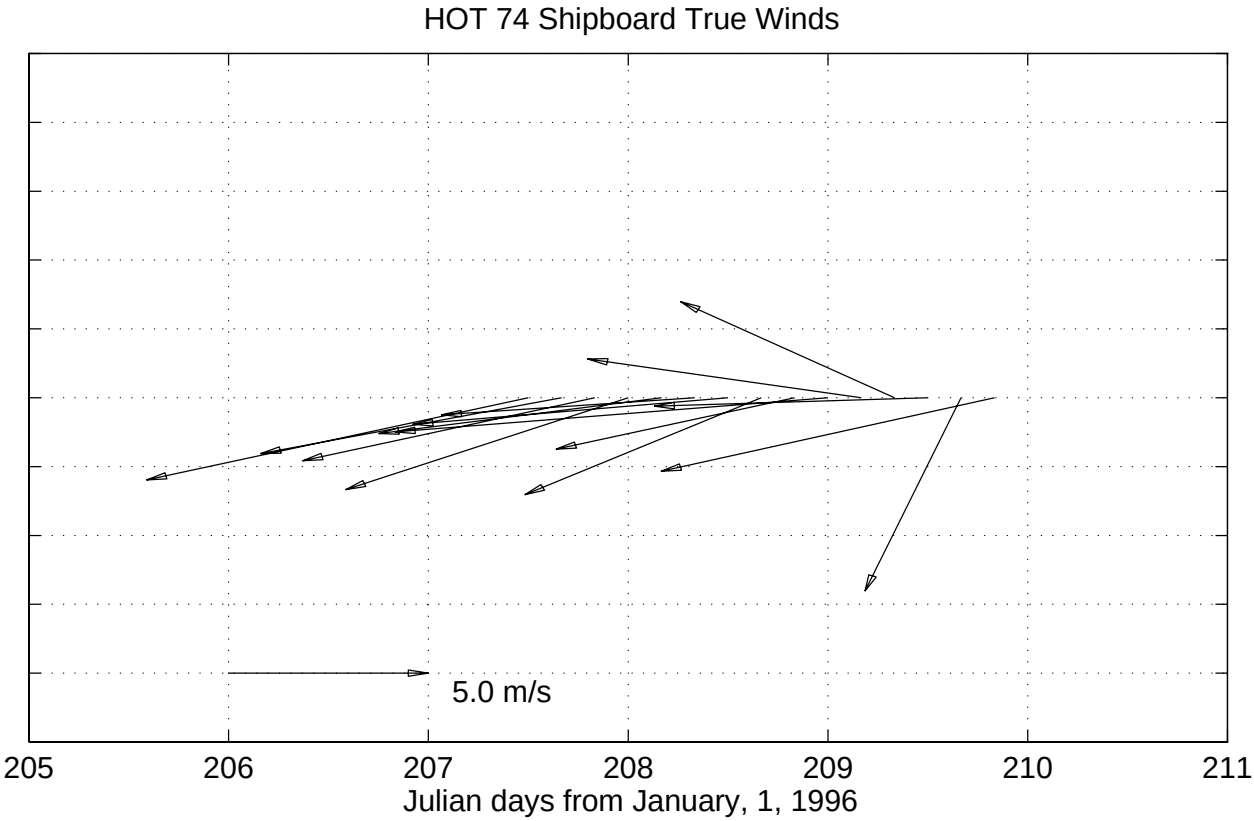
HOT 74 Shipboard True Winds
5.0 m/s
205
206
207
208
209
210
211
Julian days from January, 1, 1996

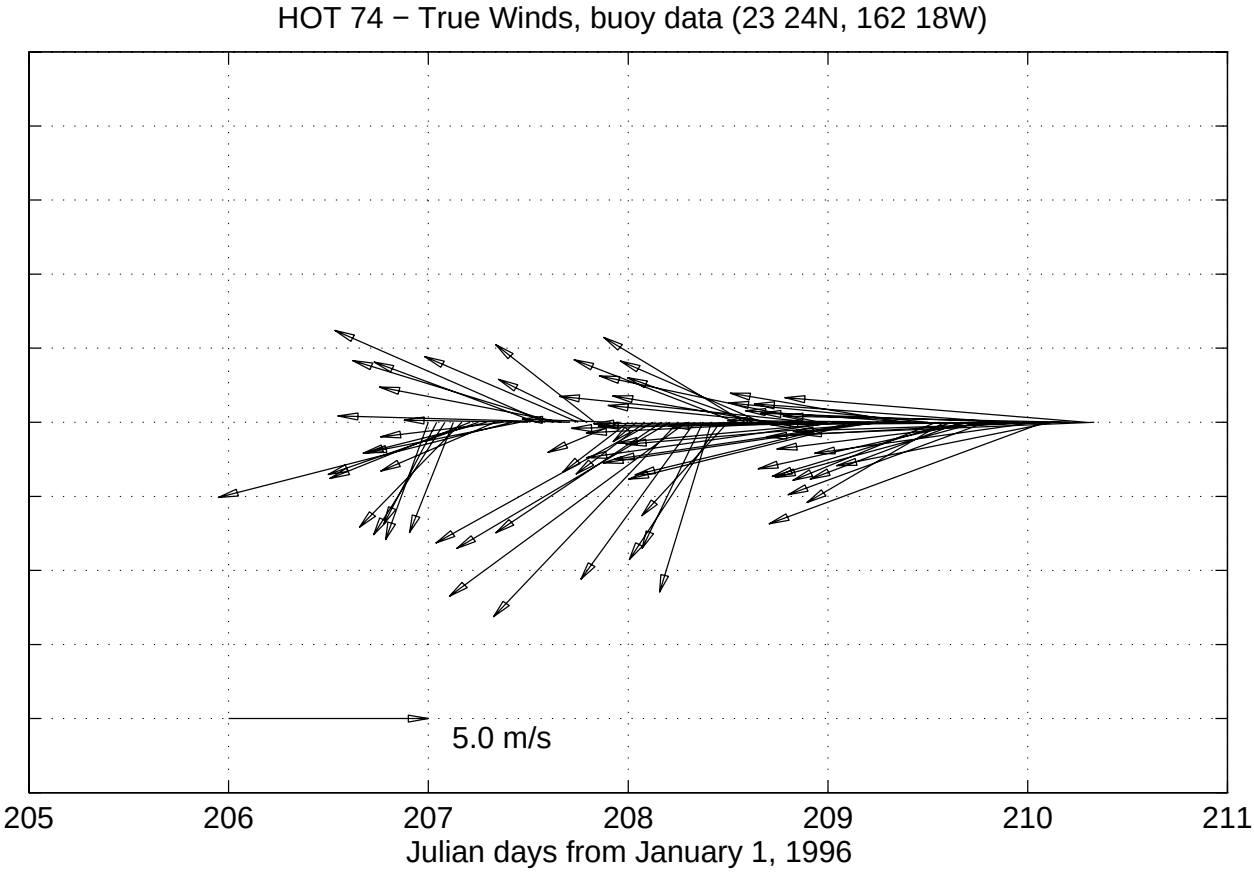
HOT 74 − True Winds, buoy data (23 24N, 162 18W)
5.0 m/s
205
206
207
208
209
210
211
Julian days from January 1, 1996

Figure 6.5.9

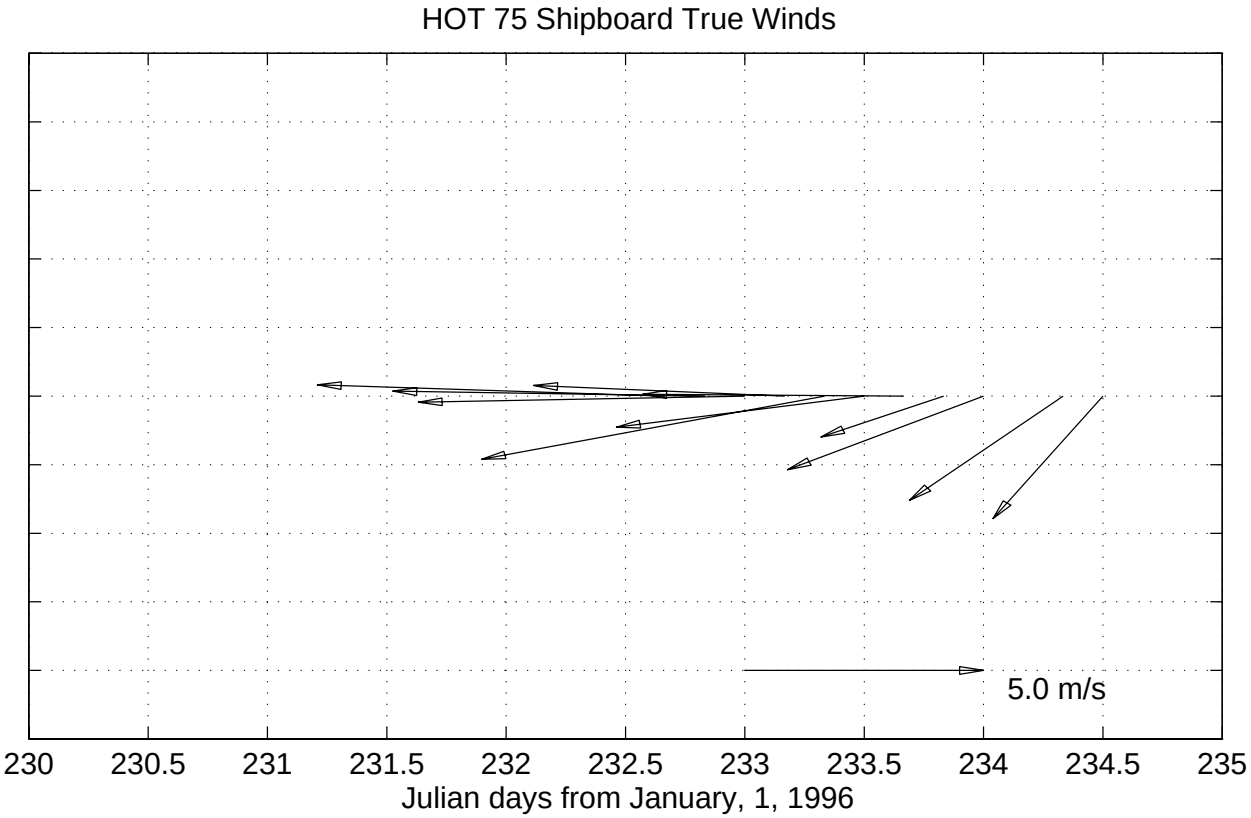
HOT 75 Shipboard True Winds
5.0 m/s
230
230.5
231
231.5
232
232.5
233
233.5
234
234.5
235
Julian days from January, 1, 1996

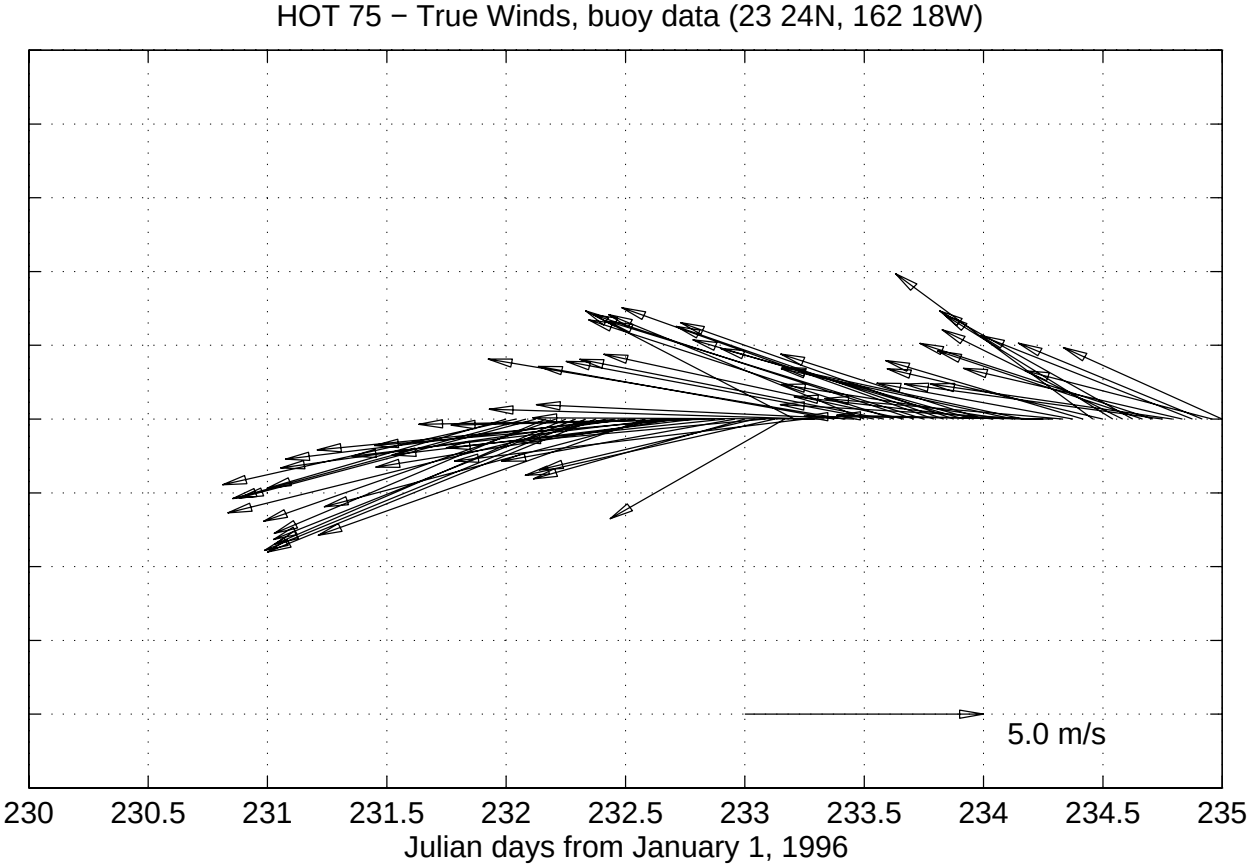
HOT 75 − True Winds, buoy data (23 24N, 162 18W)
5.0 m/s
230
230.5
231
231.5
232
232.5
233
233.5
234
234.5
235
Julian days from January 1, 1996

Figure 6.5.10

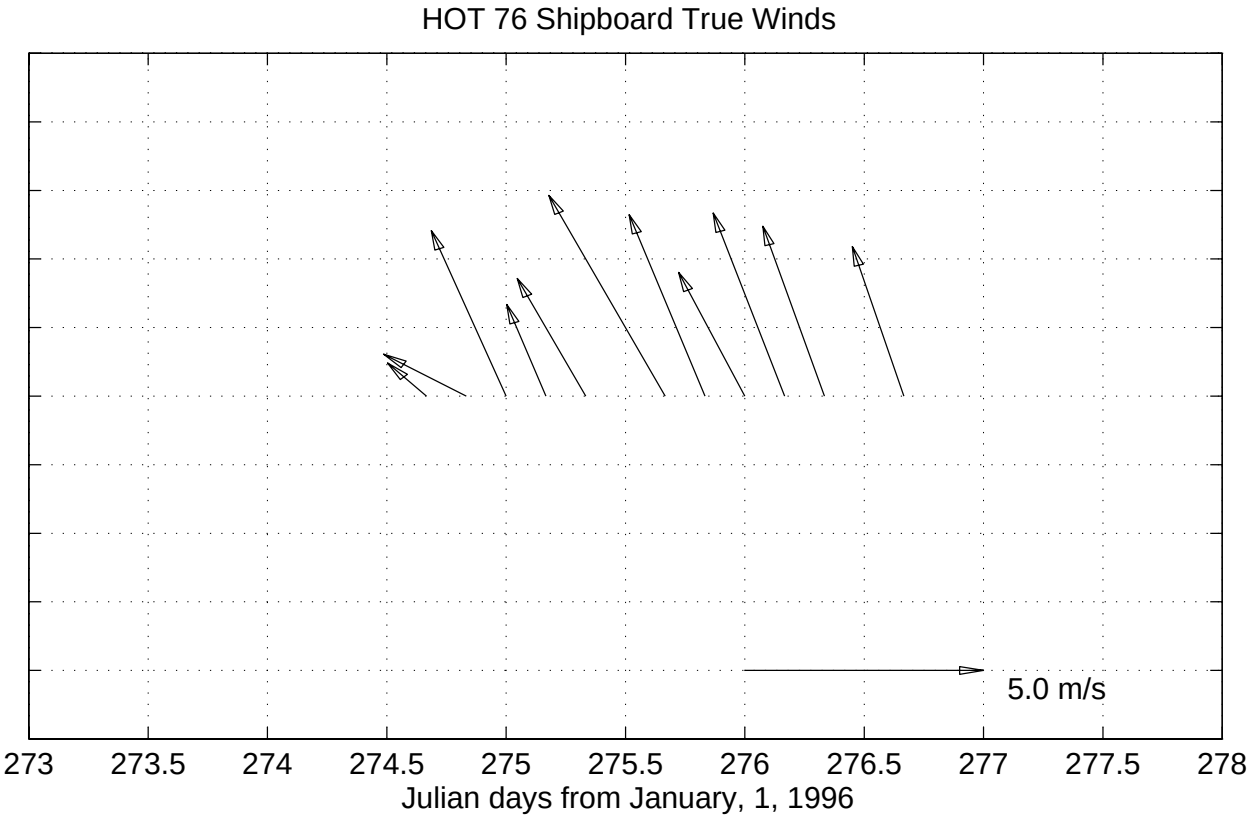
HOT 76 Shipboard True Winds
5.0 m/s
273
273.5
274
274.5
275
275.5
276
276.5
277
277.5
278
Julian days from January, 1, 1996

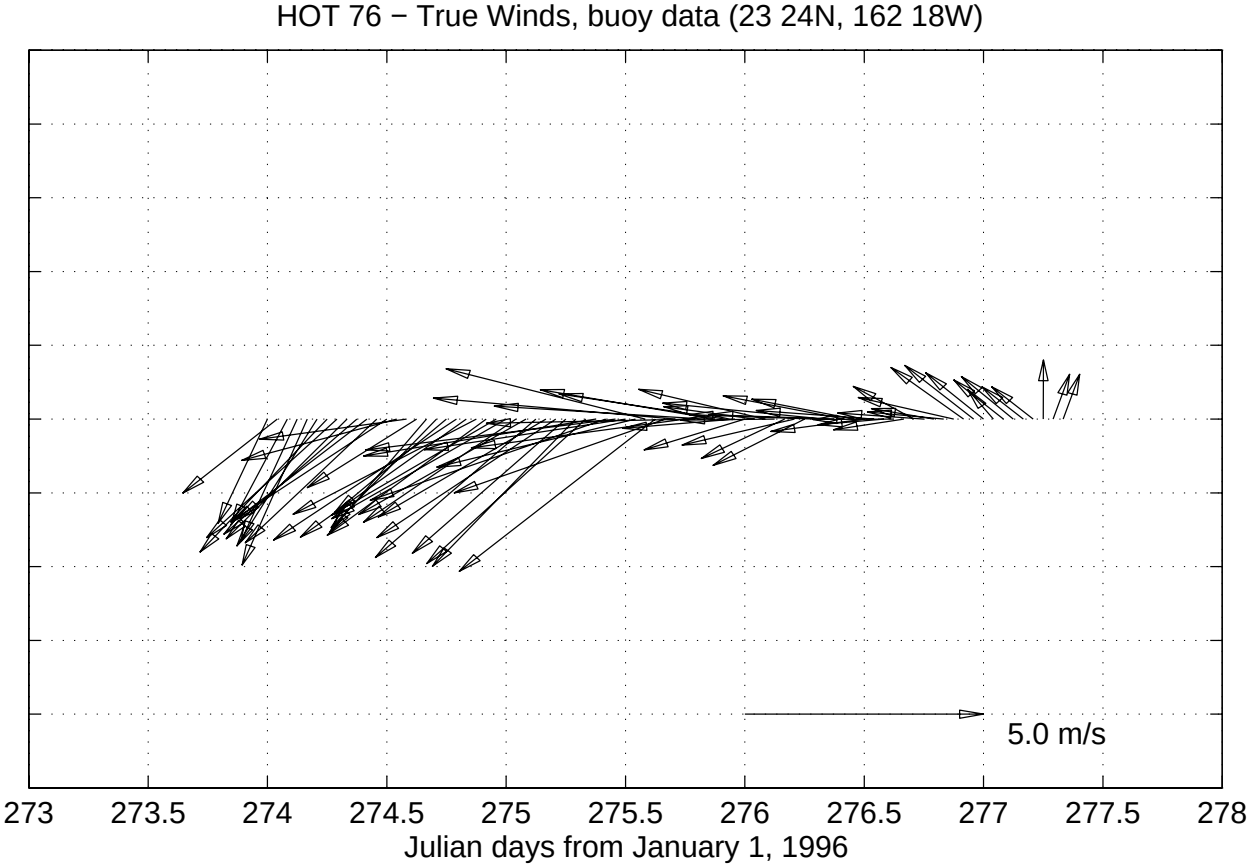
HOT 76 − True Winds, buoy data (23 24N, 162 18W)
5.0 m/s
273
273.5
274
274.5
275
275.5
276
276.5
277
277.5
278
Julian days from January 1, 1996

Figure 6.5.11

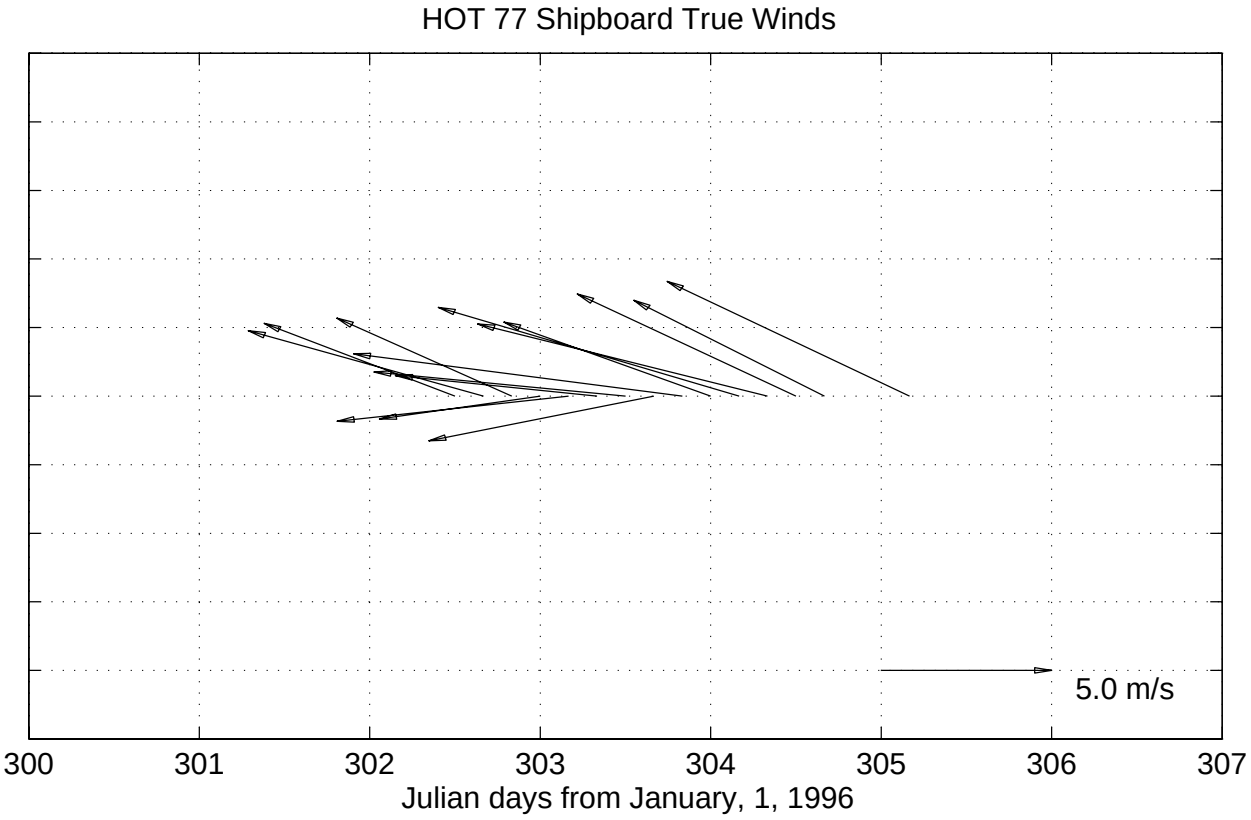
HOT 77 Shipboard True Winds
5.0 m/s
300
301
302
303
304
305
306
307
Julian days from January, 1, 1996

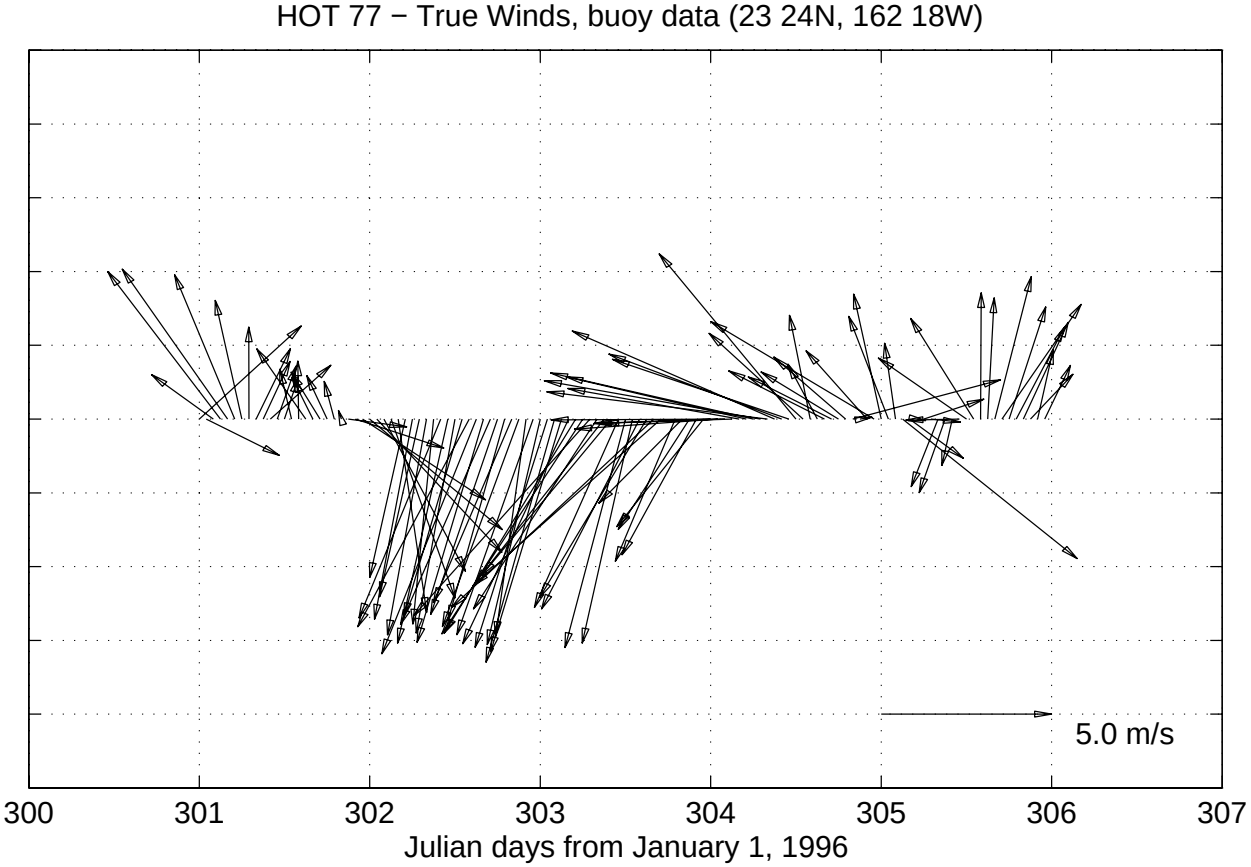
HOT 77 − True Winds, buoy data (23 24N, 162 18W)
5.0 m/s
300
301
302
303
304
305
306
307
Julian days from January 1, 1996

Figure 6.5.12

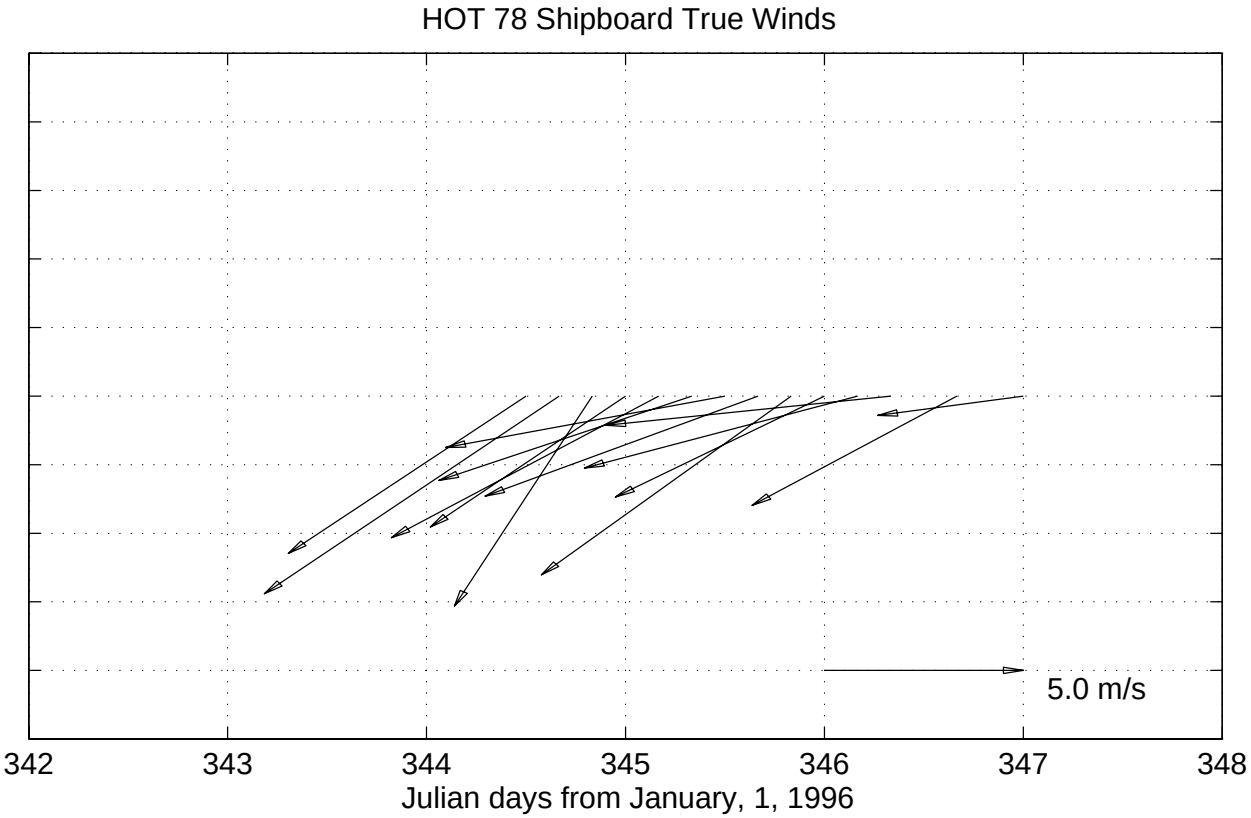
HOT 78 Shipboard True Winds
5.0 m/s
342
343
344
345
346
347
348
Julian days from January, 1, 1996

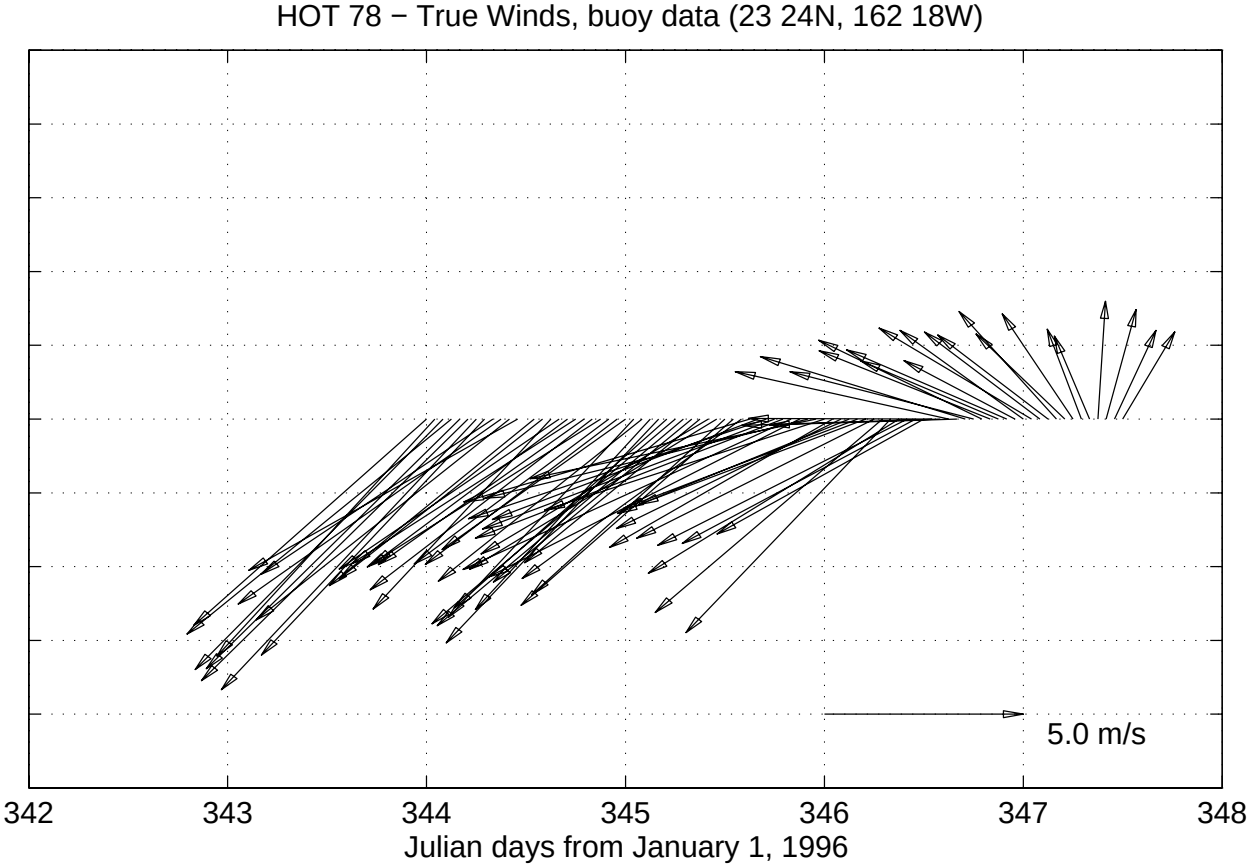
HOT 78 − True Winds, buoy data (23 24N, 162 18W)
5.0 m/s
342
343
344
345
346
347
348
Julian days from January 1, 1996

Figure 6.5.13

6.6. THERMOSALINOGRAPH

Figure 6.6a to i: For each HOT cruise in 1996, the first three panels show a time-series of near surface temperature (NST; upper panel), near surface salinity (NSS; middle panel) and potential density (lower panel) measured by the thermosalinograph. Only NST is shown for HOT-72. Circles indicate CTD data at 4 dbar and x's indicate the salinity from bottle samples collected from the thermosalinograph outlet. The next three panels show the navigation and ship speed during the cruise.

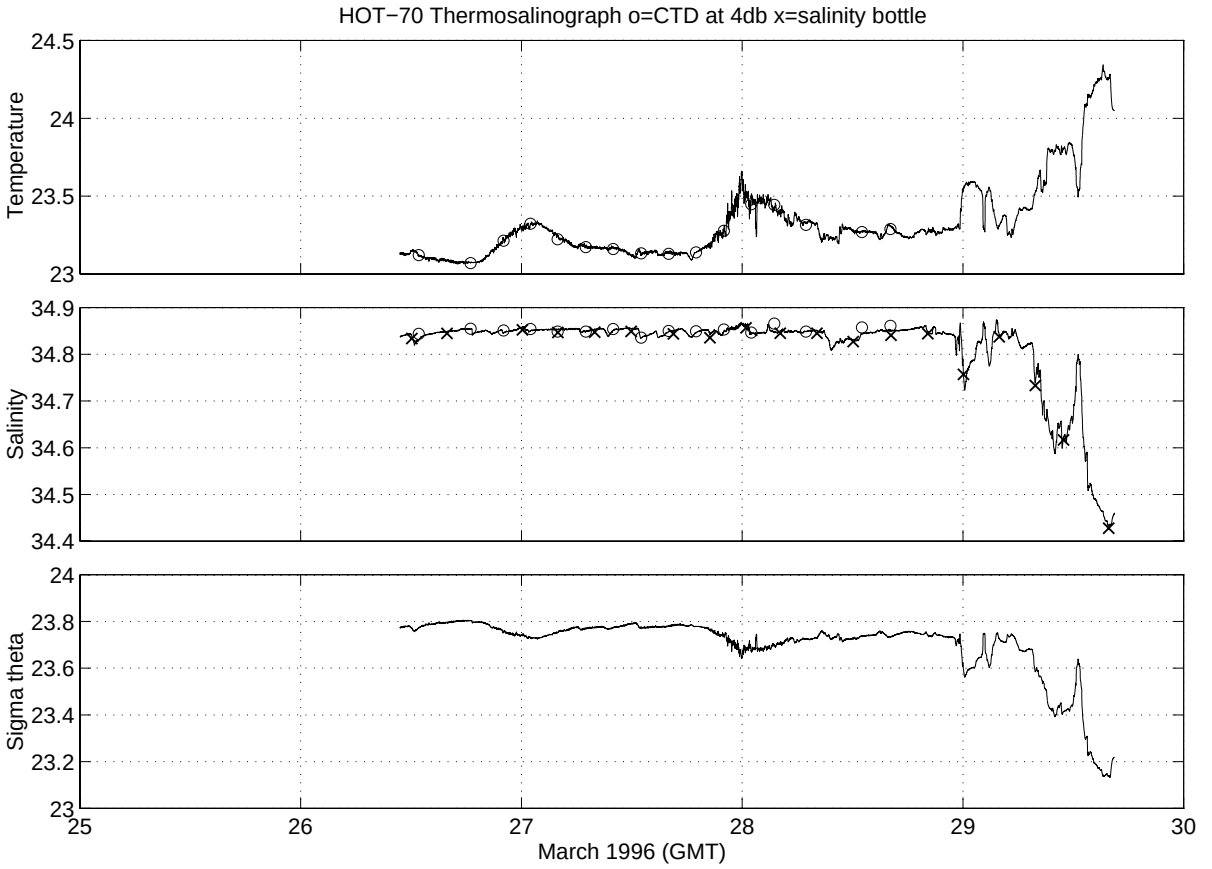
HOT−70 Thermosalinograph o=CTD at 4db x=salinity bottle
Temperature
Salinity
Sigma theta
March 1996 (GMT)

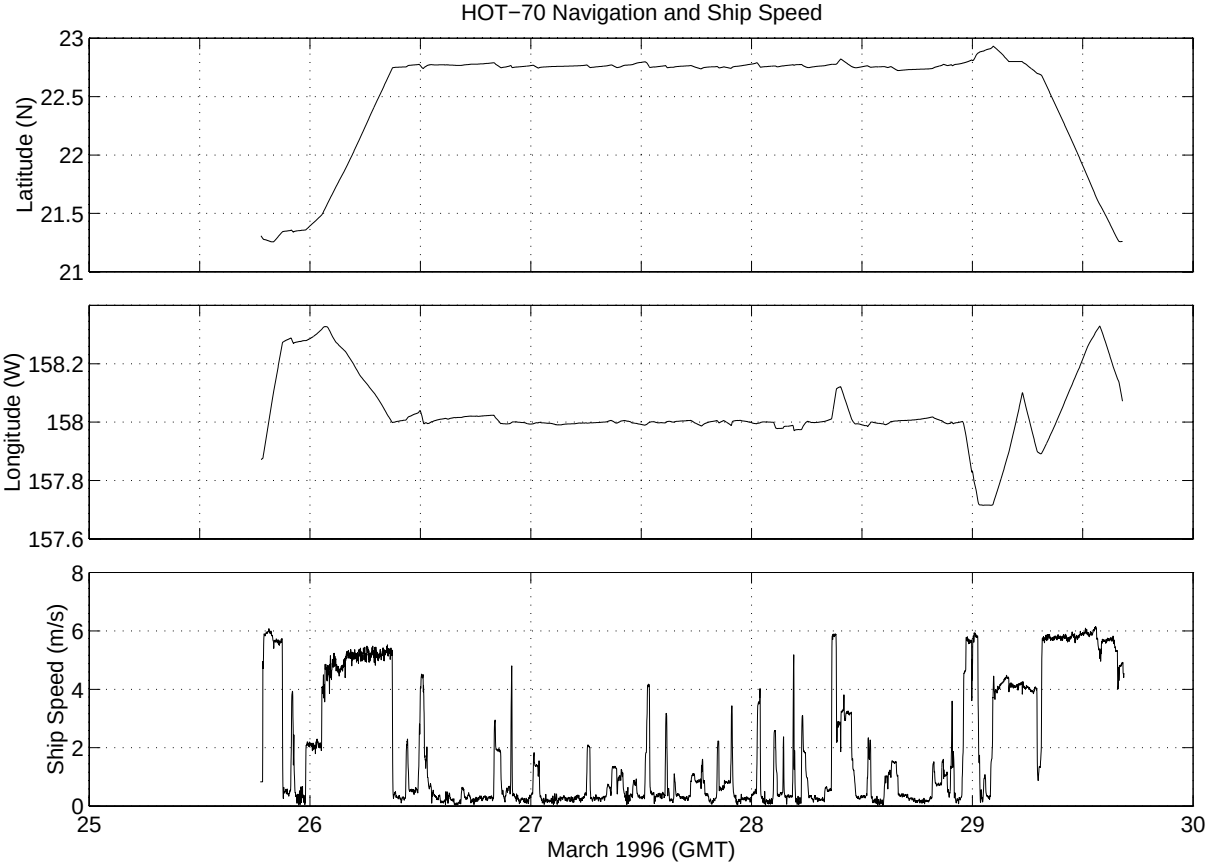
HOT−70 Navigation and Ship Speed
Latitude (N)
Longitude (W)
Ship Speed (m/s)
March 1996 (GMT)

Figure 6.6a

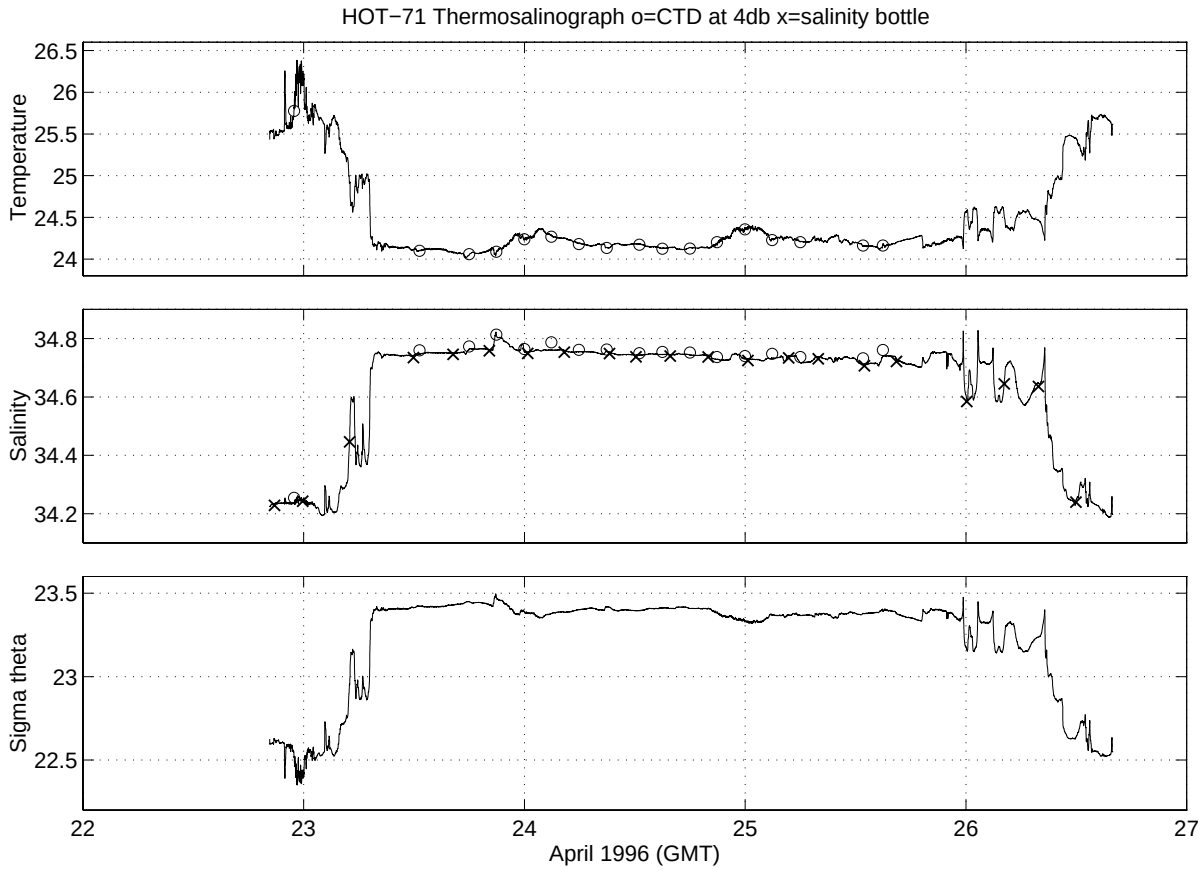
HOT−71 Thermosalinograph o=CTD at 4db x=salinity bottle
Temperature
26.5
26
25.5
25
24.5
24
Salinity
34.8
34.6
34.4
34.2
Sigma theta
23.5
23
22.5
22
23
24
25
26
27
April 1996 (GMT)

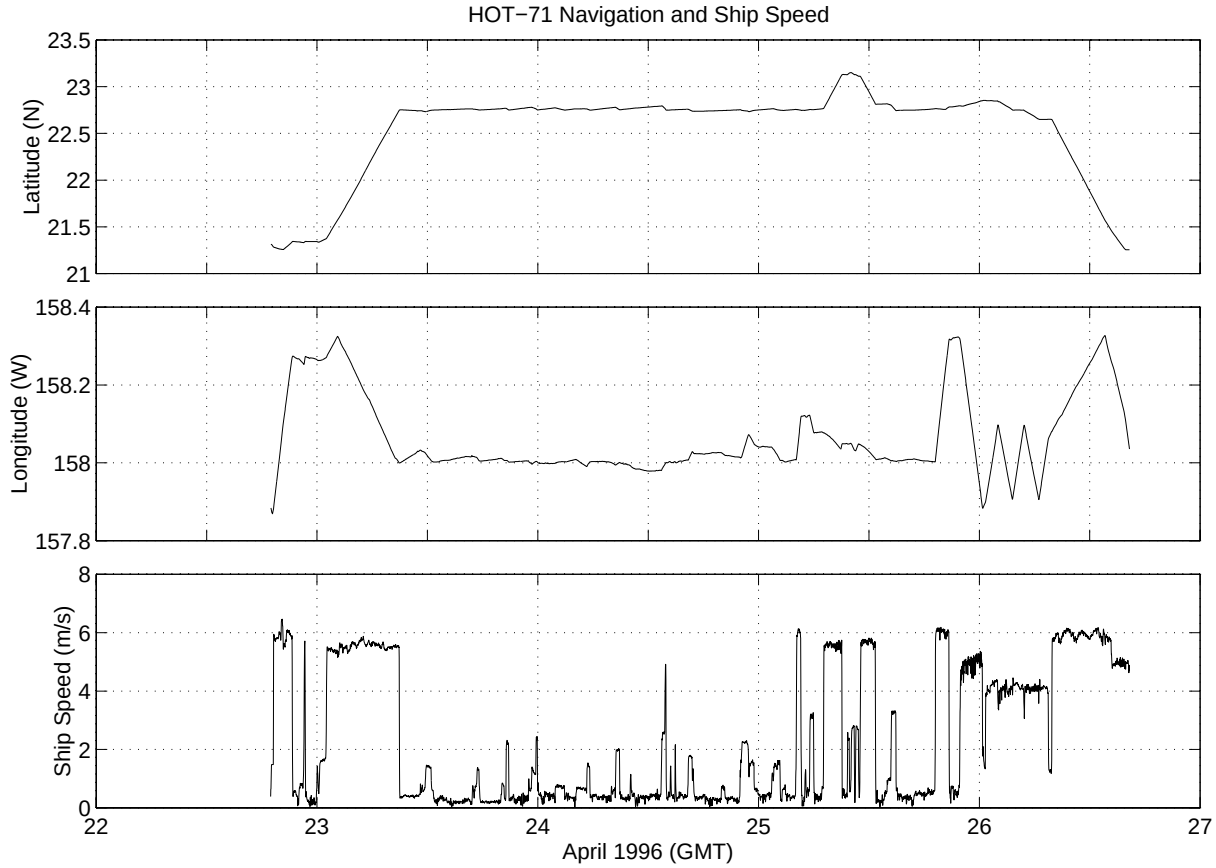
HOT−71 Navigation and Ship Speed
Latitude (N)
23.5
23
22.5
22
21.5
21
Longitude (W)
158.4
158.2
158
157.8
Ship Speed (m/s)
8
6
4
2
0
22
23
24
25
26
27
April 1996 (GMT)

Figure 6.6b

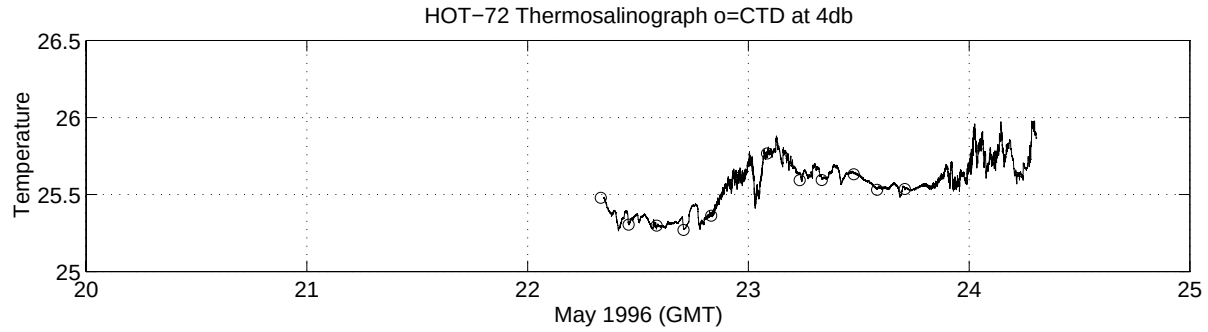
HOT−72 Thermosalinograph o=CTD at 4db
Temperature
26.5
26
25.5
25
20
21
22
23
24
25
May 1996 (GMT)

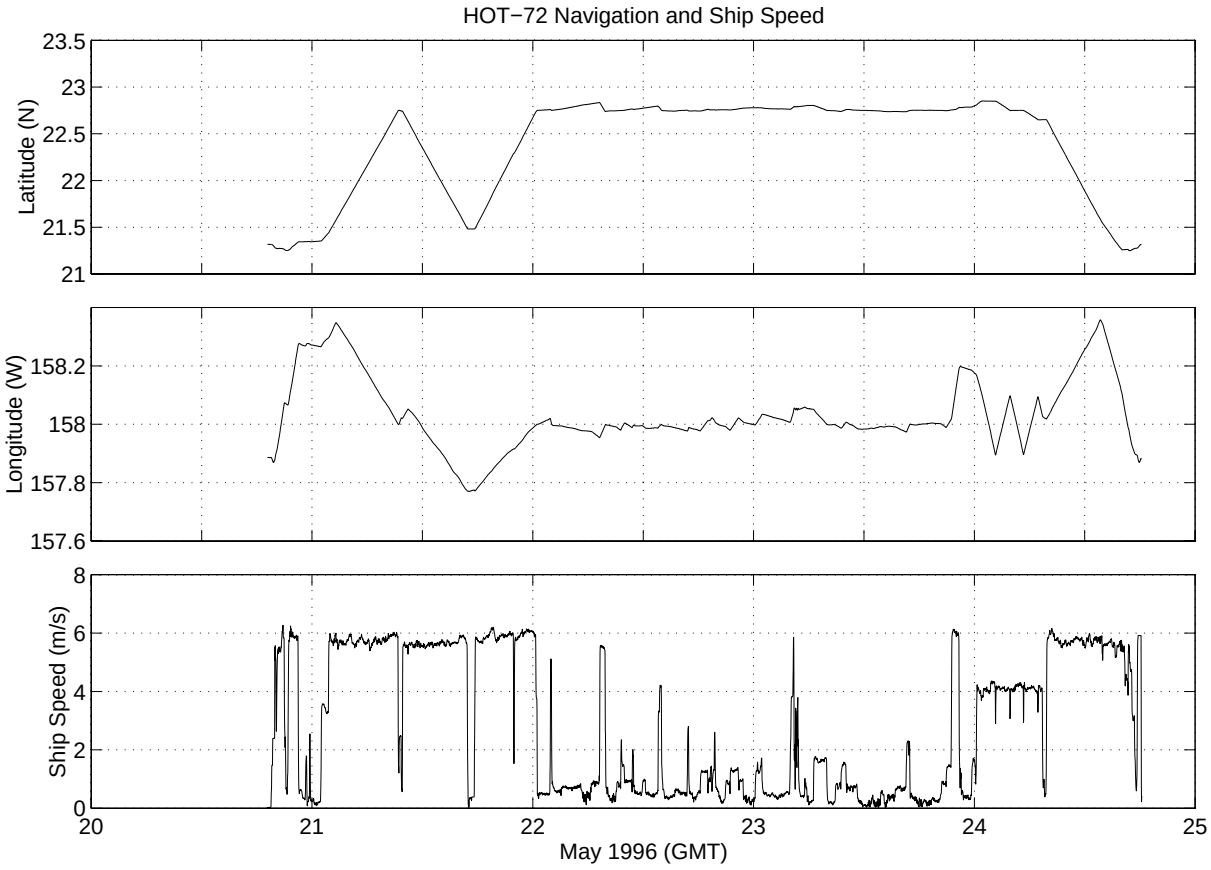
HOT−72 Navigation and Ship Speed
Latitude (N)
23.5
23
22.5
22
21.5
21
Longitude (W)
158.2
158
157.8
157.6
Ship Speed (m/s)
8
6
4
2
0
20
21
22
23
24
25
May 1996 (GMT)

Figure 6.6c

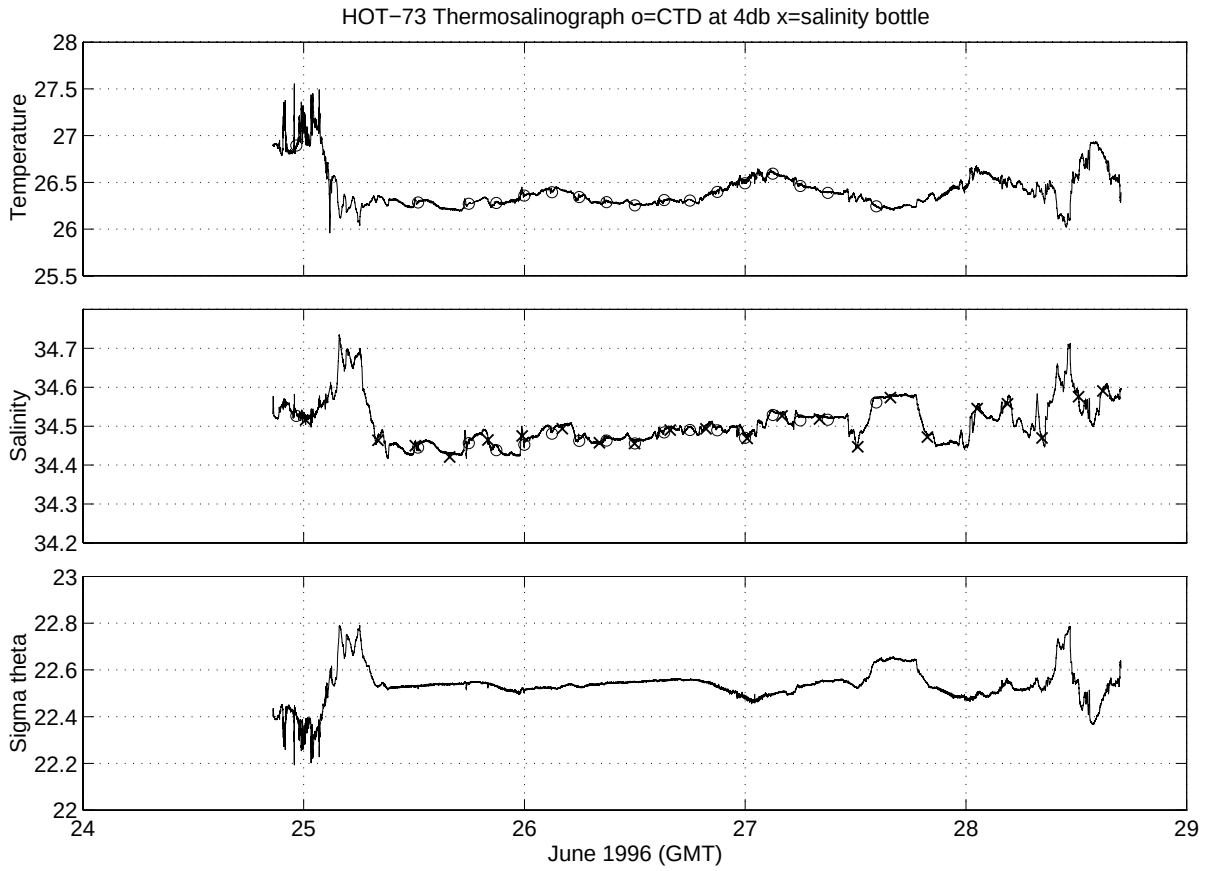
HOT−73 Thermosalinograph o=CTD at 4db x=salinity bottle
Temperature
Salinity
Sigma theta
June 1996 (GMT)

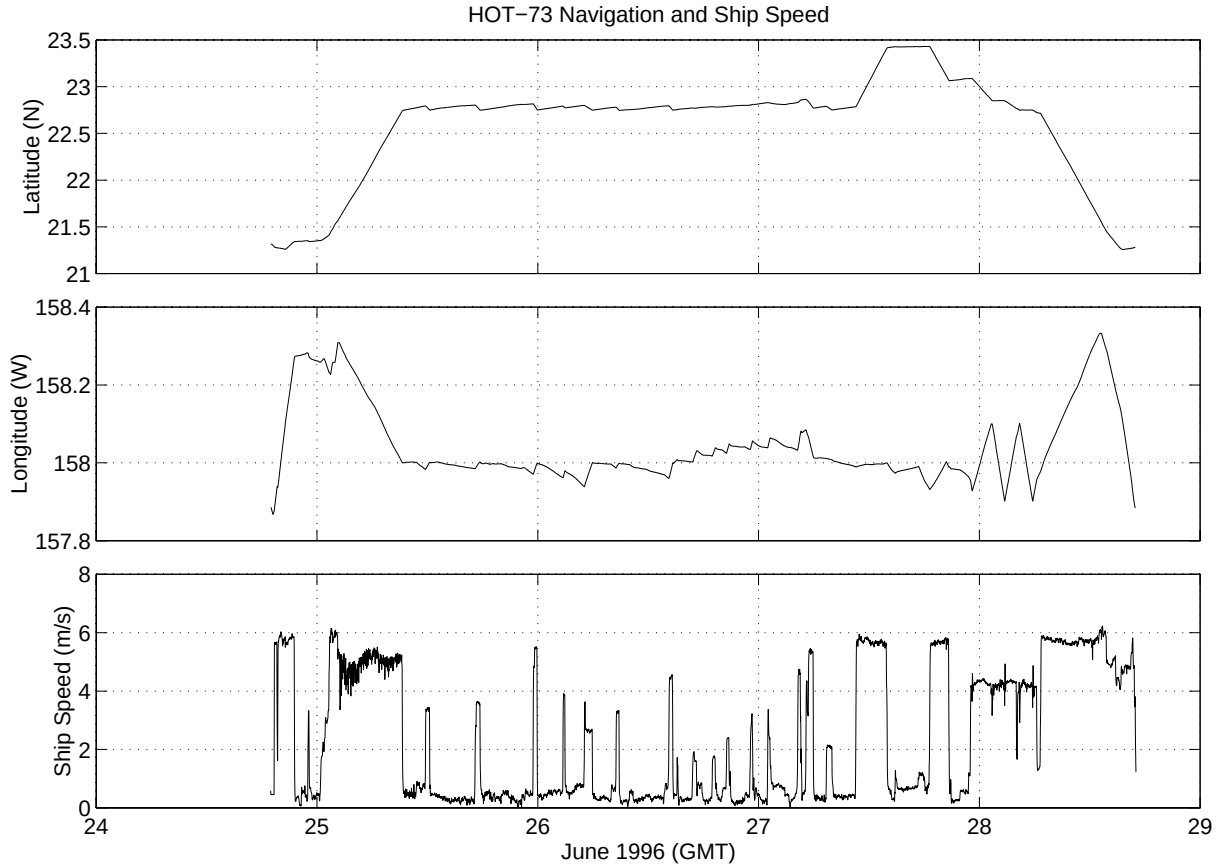
HOT−73 Navigation and Ship Speed
Latitude (N)
Longitude (W)
Ship Speed (m/s)
June 1996 (GMT)

Figure 6.6d

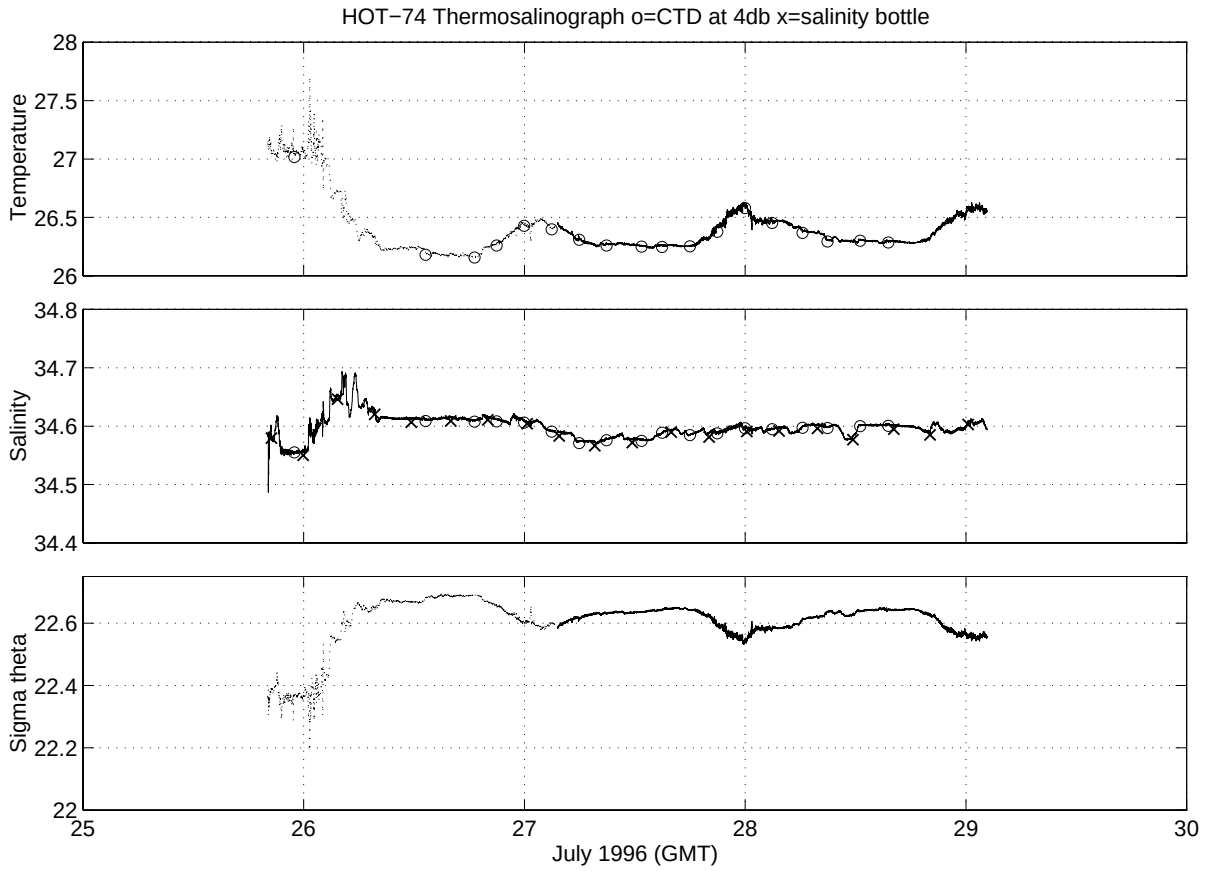
HOT−74 Thermosalinograph o=CTD at 4db x=salinity bottle
Temperature
Salinity
Sigma theta
July 1996 (GMT)

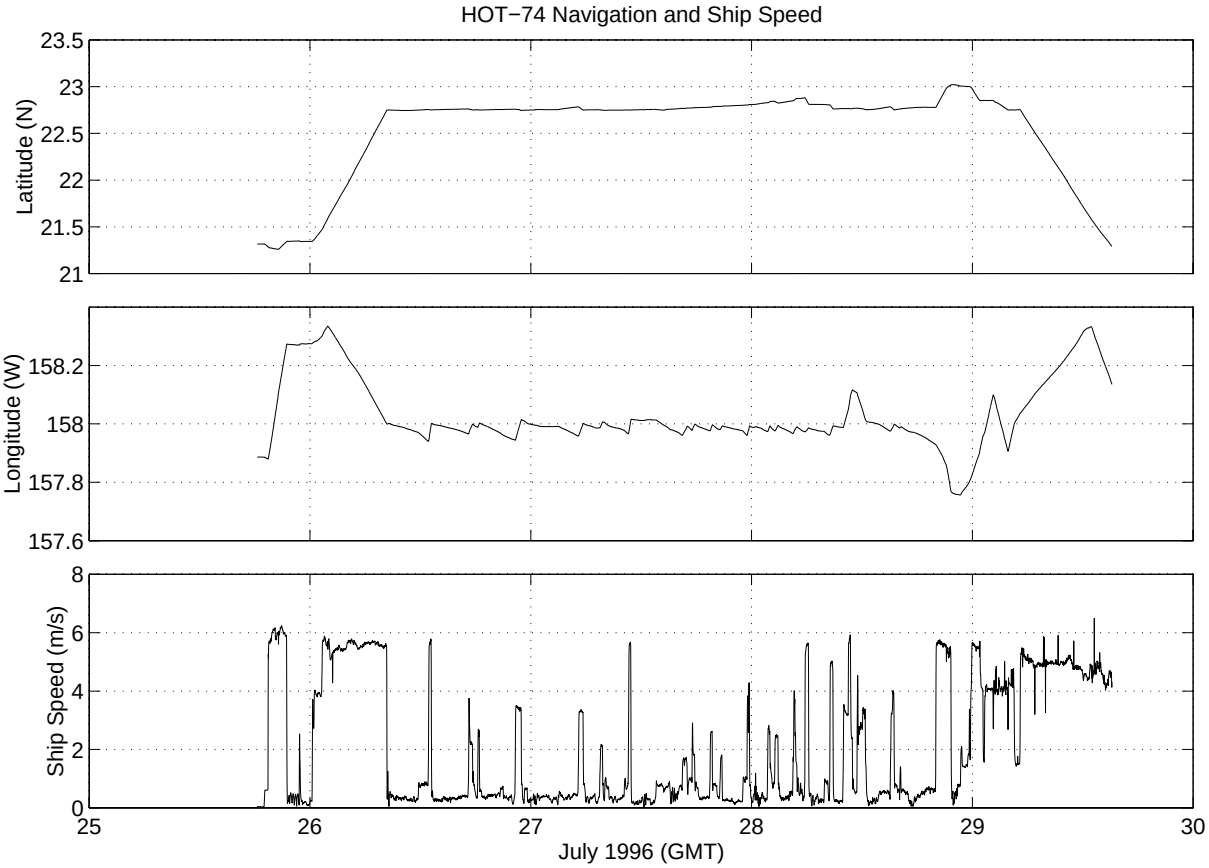
HOT−74 Navigation and Ship Speed
Latitude (N)
Longitude (W)
Ship Speed (m/s)
July 1996 (GMT)

Figure 6.6e

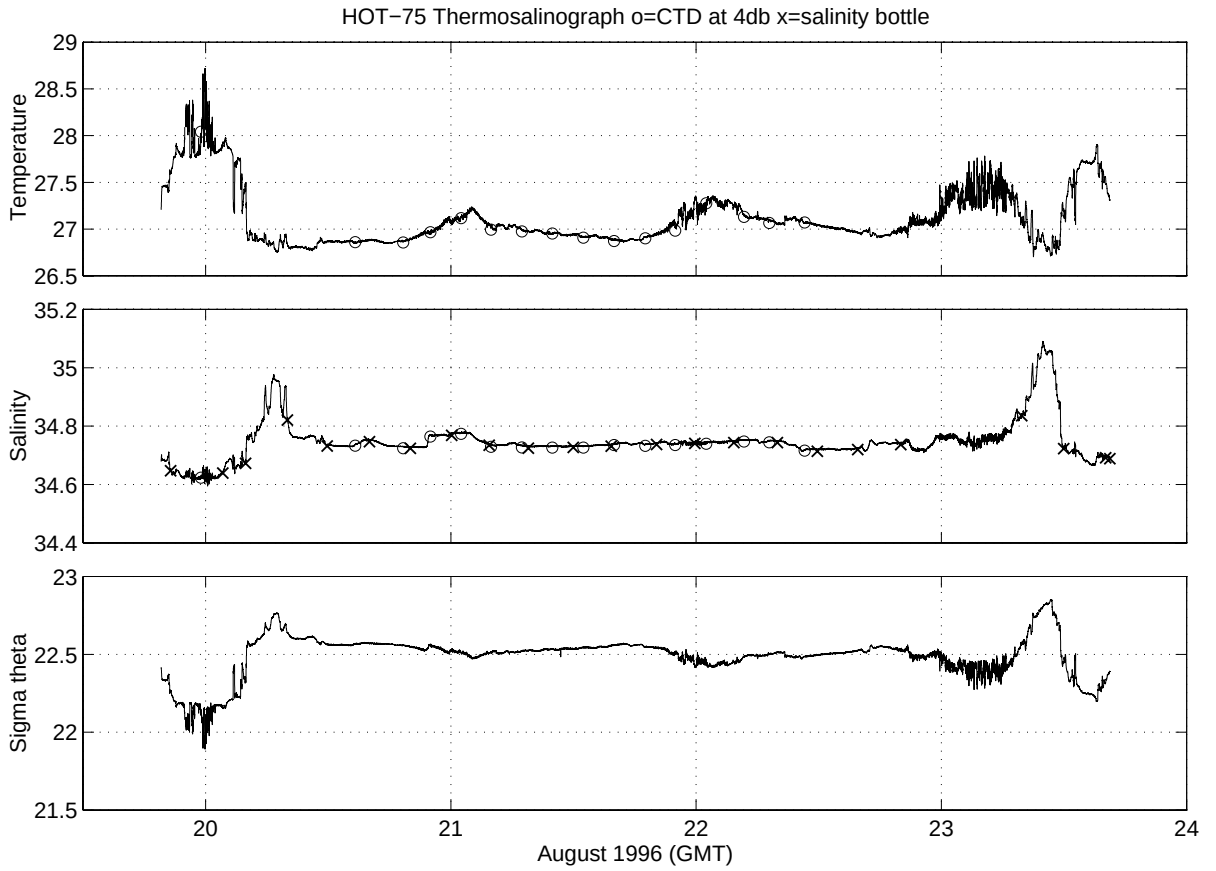
HOT−75 Thermosalinograph o=CTD at 4db x=salinity bottle
Temperature
29
28.5
28
27.5
27
26.5
Salinity
35.2
35
34.8
34.6
34.4
Sigma theta
23
22.5
22
21.5
20
21
22
23
24
August 1996 (GMT)

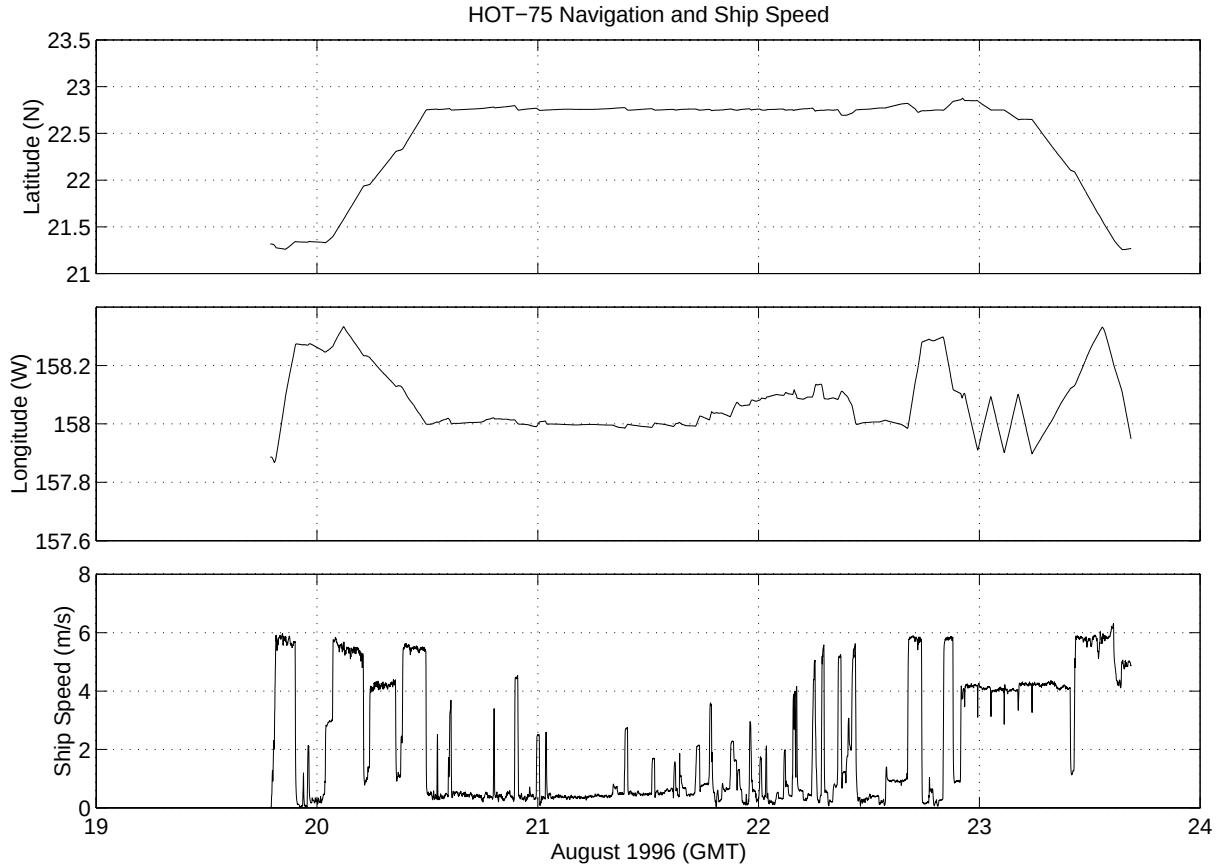
HOT−75 Navigation and Ship Speed
Latitude (N)
23.5
23
22.5
22
21.5
21
Longitude (W)
158.2
158
157.8
157.6
Ship Speed (m/s)
8
6
4
2
0
19
20
21
22
23
24
August 1996 (GMT)

Figure 6.6f

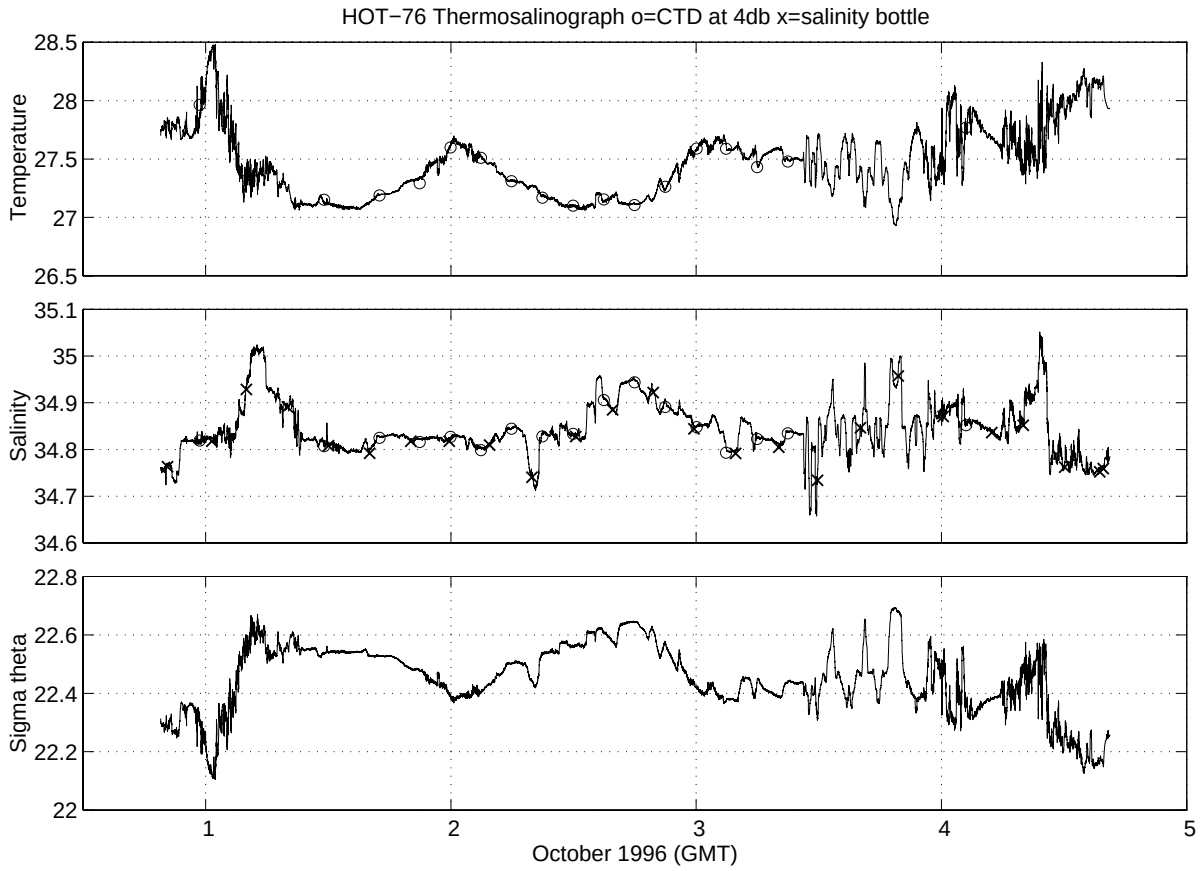
HOT−76 Thermosalinograph o=CTD at 4db x=salinity bottle
Temperature
28.5
28
27.5
27
26.5
Salinity
35.1
35
34.9
34.8
34.7
34.6
Sigma theta
22.8
22.6
22.4
22.2
22
1
2
3
4
5
October 1996 (GMT)

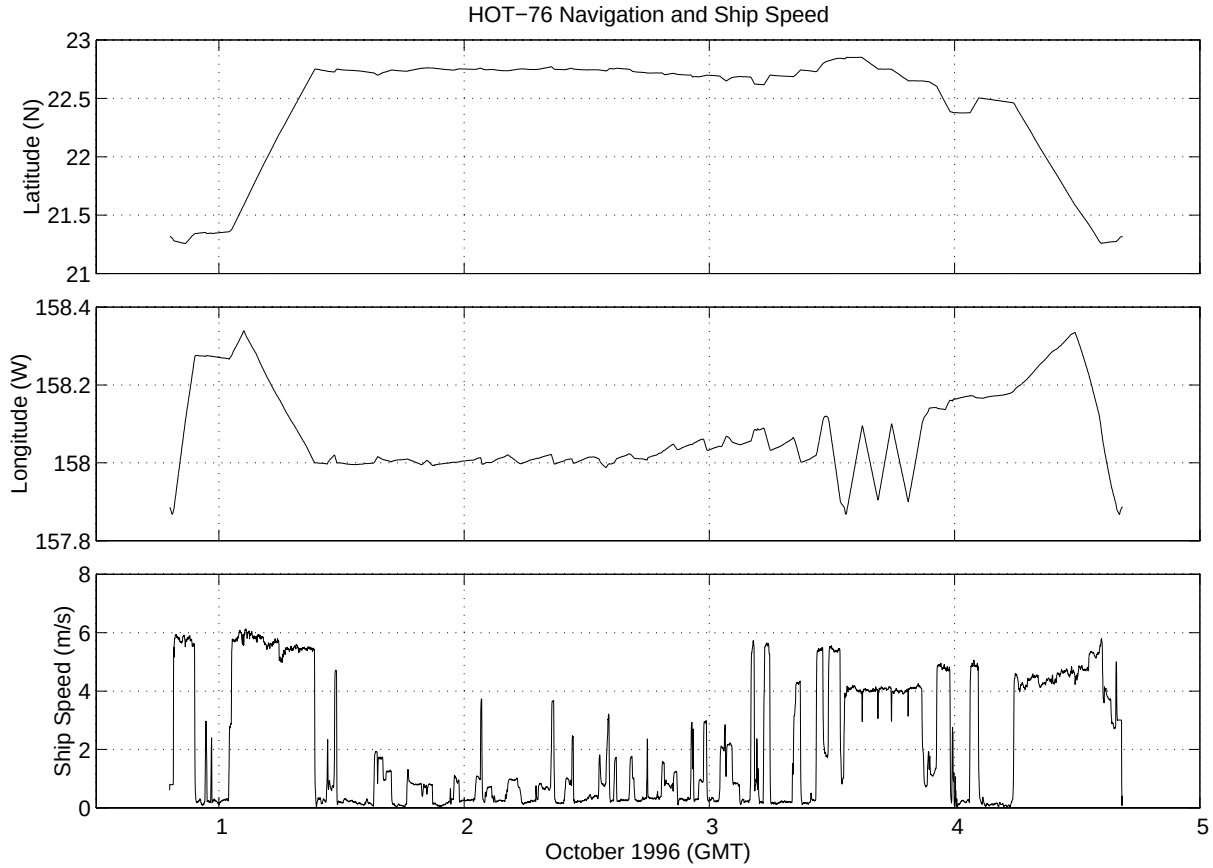
HOT−76 Navigation and Ship Speed
Latitude (N)
23
22.5
22
21.5
21
Longitude (W)
158.4
158.2
158
157.8
Ship Speed (m/s)
8
6
4
2
0
1
2
3
4
5
October 1996 (GMT)

Figure 6.6g

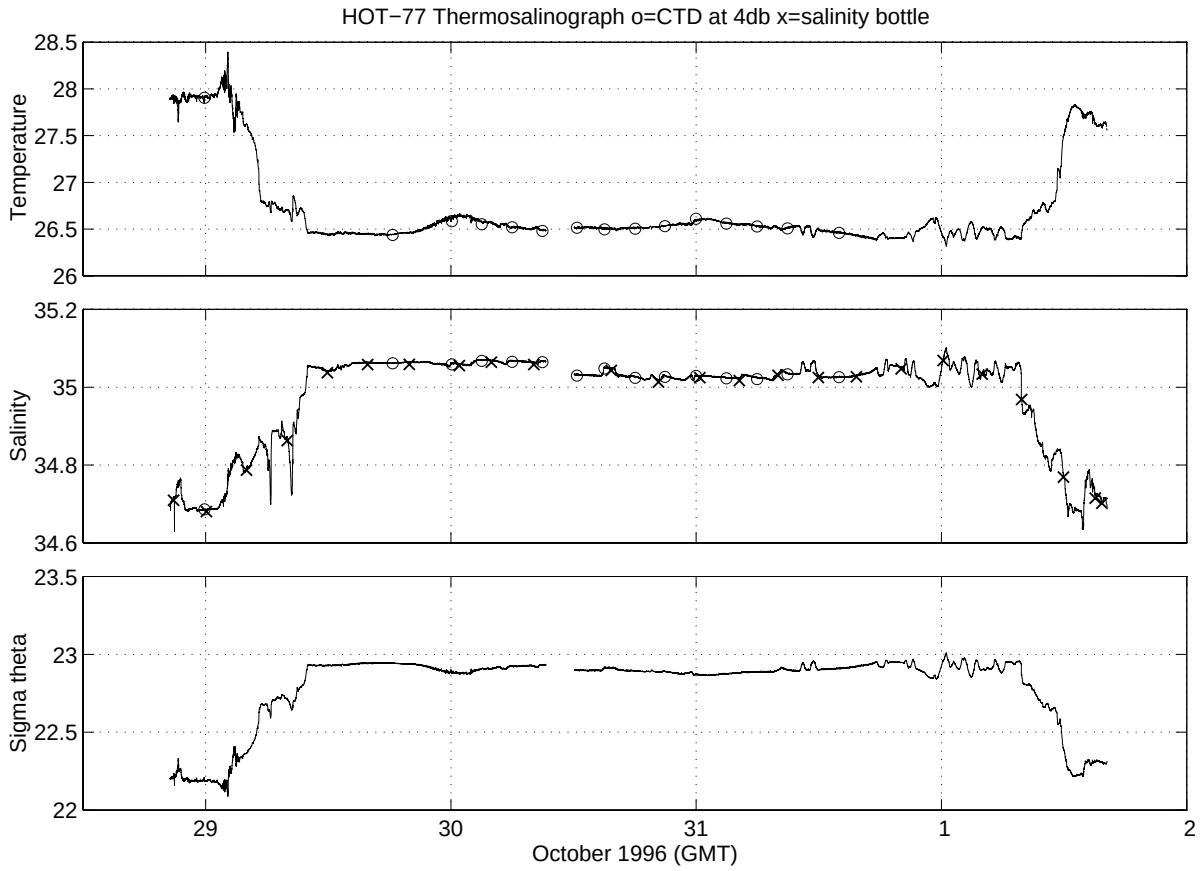
HOT−77 Thermosalinograph o=CTD at 4db x=salinity bottle
Temperature
28.5
28
27.5
27
26.5
26
Salinity
35.2
35
34.8
34.6
Sigma theta
23.5
23
22.5
22
29
30
31
1
2
October 1996 (GMT)

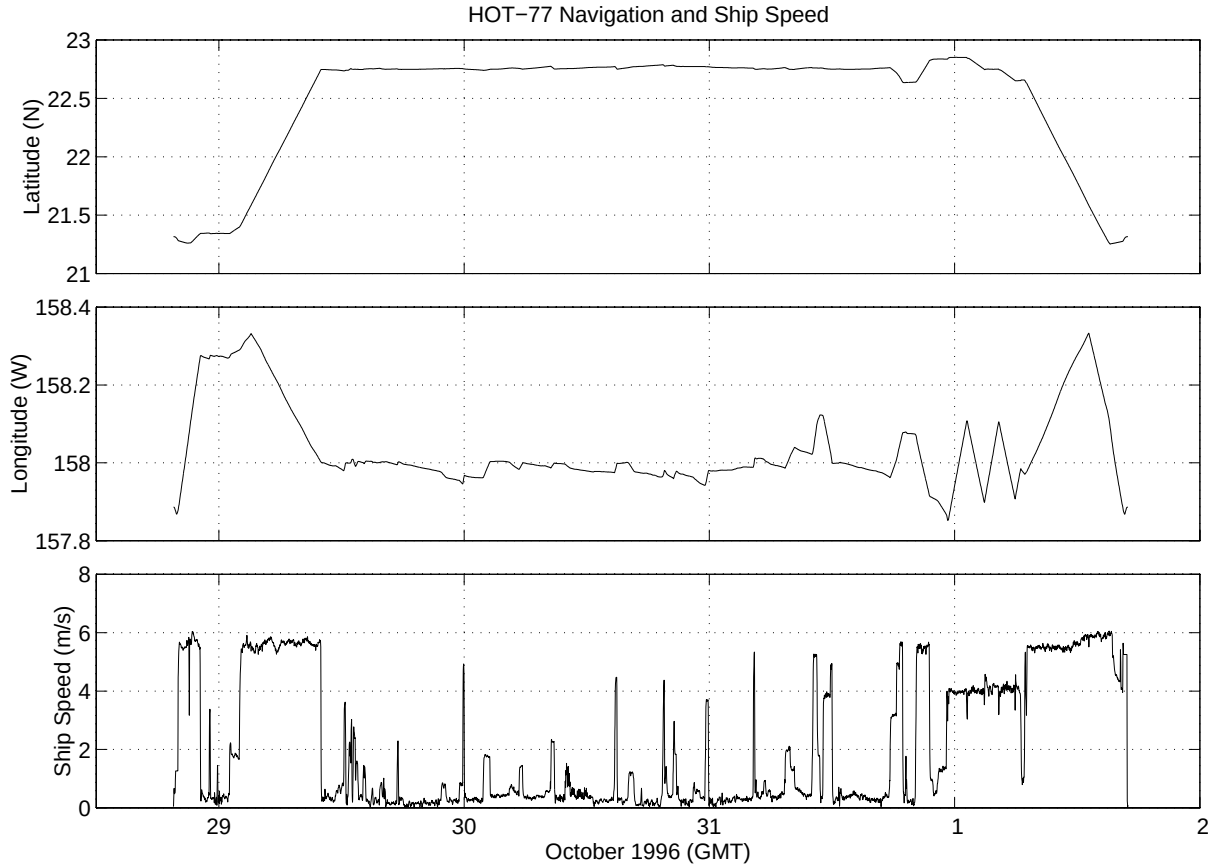
HOT−77 Navigation and Ship Speed
Latitude (N)
23
22.5
22
21.5
21
Longitude (W)
158.4
158.2
158
157.8
Ship Speed (m/s)
8
6
4
2
0
29
30
31
1
2
October 1996 (GMT)

Figure 6.6h

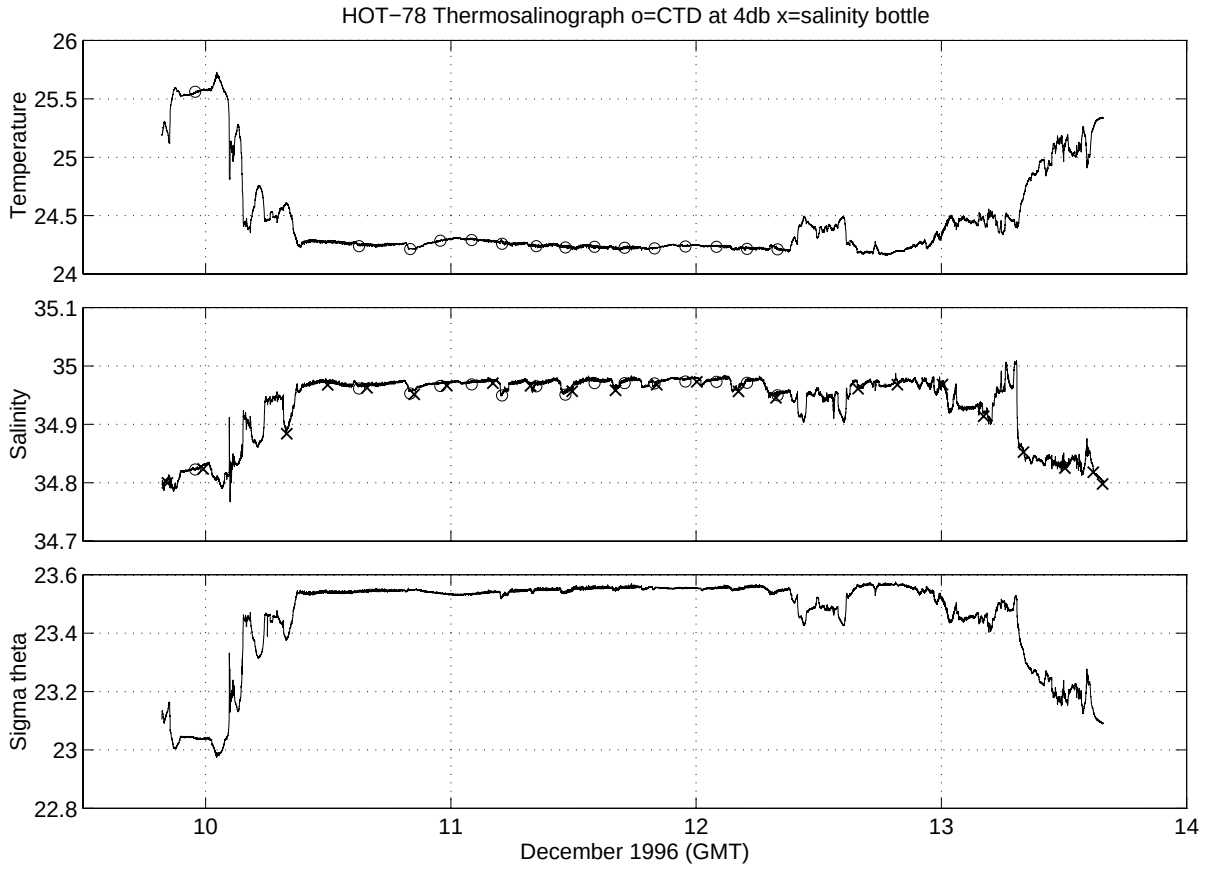
HOT−78 Thermosalinograph o=CTD at 4db x=salinity bottle
Temperature
26
25.5
25
24.5
24
Salinity
35.1
35
34.9
34.8
34.7
Sigma theta
23.6
23.4
23.2
23
22.8
10
11
12
13
14
December 1996 (GMT)

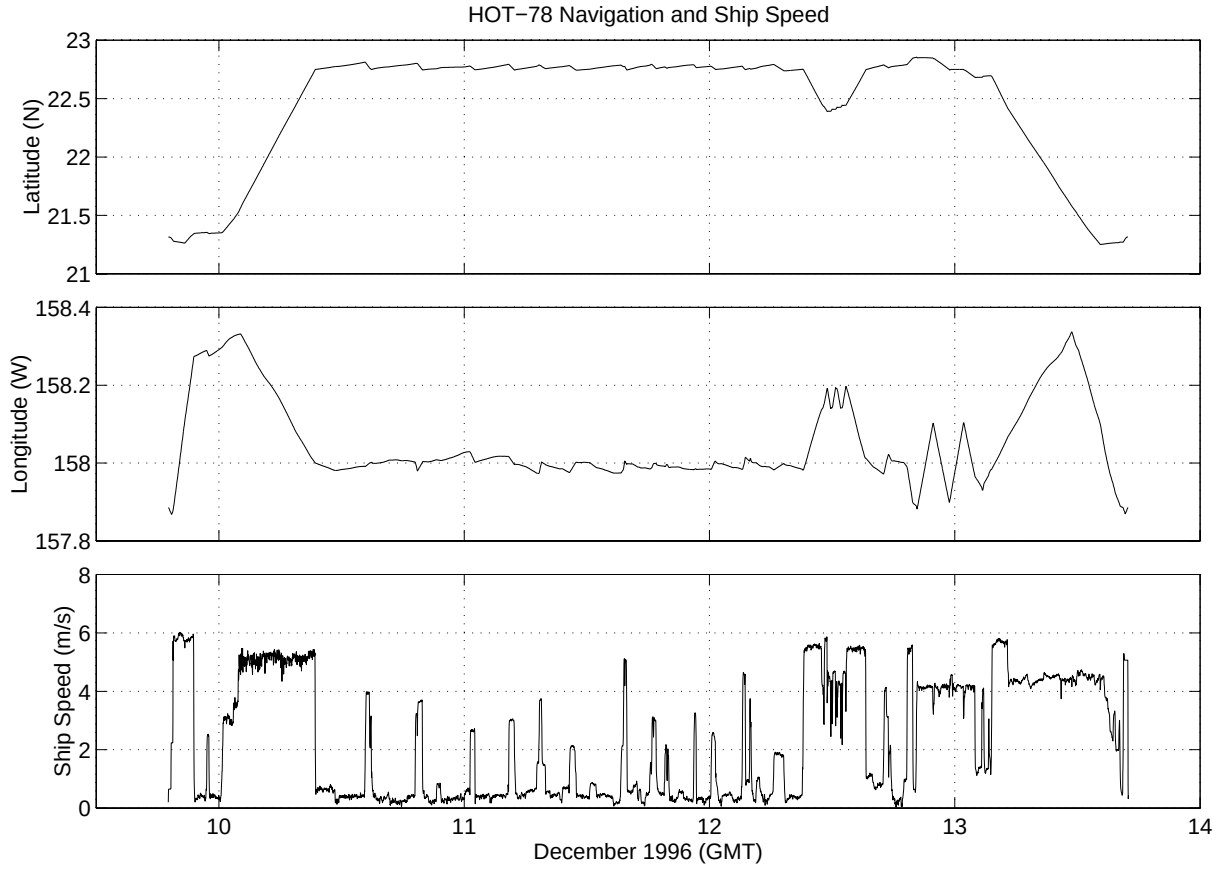
HOT−78 Navigation and Ship Speed
Latitude (N)
23
22.5
22
21.5
21
Longitude (W)
158.4
158.2
158
157.8
Ship Speed (m/s)
8
6
4
2
0
10
11
12
13
14
December 1996 (GMT)

Figure 6.6i

6.7. ALOHA-Climax Cruise I

Figure 6.7.1: The first three panels show a time-series of near surface temperature (NST), near surface salinity (NSS) and potential density measured by the thermosalinograph during the AC-1 cruise. Circles indicate CTD data at 4 dbar and x's indicate the salinity from bottle samples collected from the thermosalinograph outlet. The next three panels show the navigation and ship speed during the cruise.

Figure 6.7.2: Depth profiles of chlorophyll a concentrations collected at Station 1-5 during the AC-1 cruise.

Figure 6.7.3: Fluorescence at 45 meters measured by the WetStar fluorometer attached to the towed instrument during the transit from Station 5 to Station 8 on the AC-1 cruise.

Figure 6.7.4: Depth profile of carbon assimilation rate from experiments done at Station ALOHA using GF/F glass fiber filters following the HOT (in-situ incubation for 12 hours) and Hayward (on-deck incubation for 6 hours) protocols.

Figure 6.7.5: Depth profile of carbon assimilation rate from experiments done at Station ALOHA following Hayward protocol and using GF/F glass fiber and Millipore HA filters.

Figure 6.7.6: Depth profile of carbon assimilation rate from experiments done at Station Climax using GF/F glass fiber filters following the HOT (in-situ incubation for 12 hours) and Hayward (on-deck incubation for 6 hours) protocols.

Figure 6.7.7: Depth profile of carbon assimilation rate from experiments done at Station Climax following Hayward protocol and using GF/F glass fiber, Millipore 0.45 μm HA and Nuclepore 0.2 μm filters.

Figure 6.7.8: Time-series of meteorological observations during the AC-1 cruise as follows a) atmospheric pressure, b) sea surface temperature (SST), c) air temperature, d) wet bulb temperature, e) SST minus air temperature, f) dry minus wet bulb temperature, g) wind velocity vector collected by NDBC buoy # 51001 and h) shipboard wind velocity vector. The orientation of the arrow in panels g and h indicate the wind direction, up is northward, right is eastward.

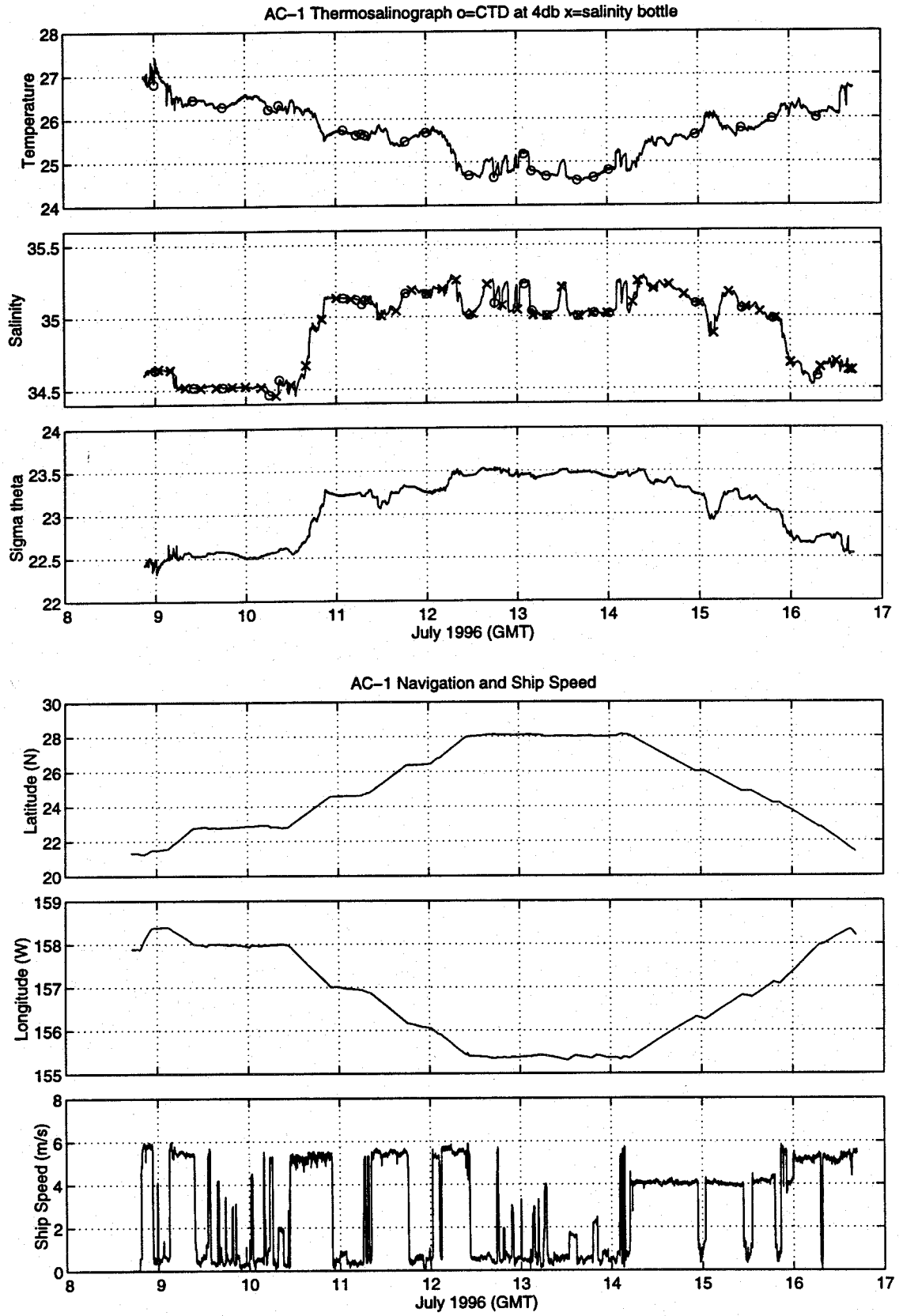
AC–1 Thermosalinograph o=CTD at 4db x=salinity bottle
Temperature
Salinity
Sigma theta
July 1996 (GMT)
AC–1 Navigation and Ship Speed
Latitude (N)
Longitude (W)
Ship Speed (m/s)
July 1996 (GMT)

Figure 6.7.1

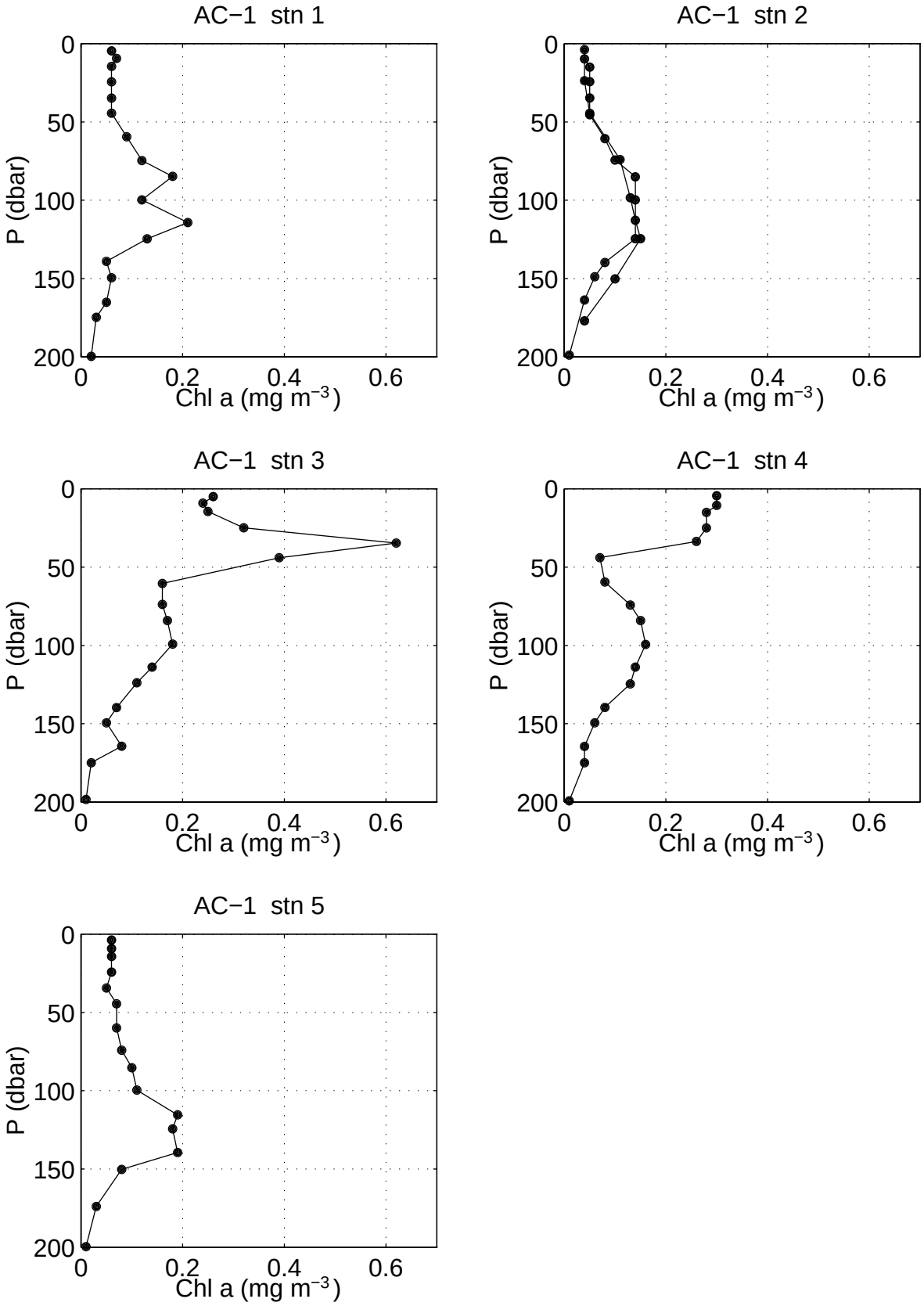
AC−1 stn 1
AC−1 stn 2
AC−1 stn 3
AC−1 stn 4
AC−1 stn 5
P (dbar)
Chl a (mg m−3)
0
50
100
150
200
0.2
0.4
0.6

Figure 6.7.2

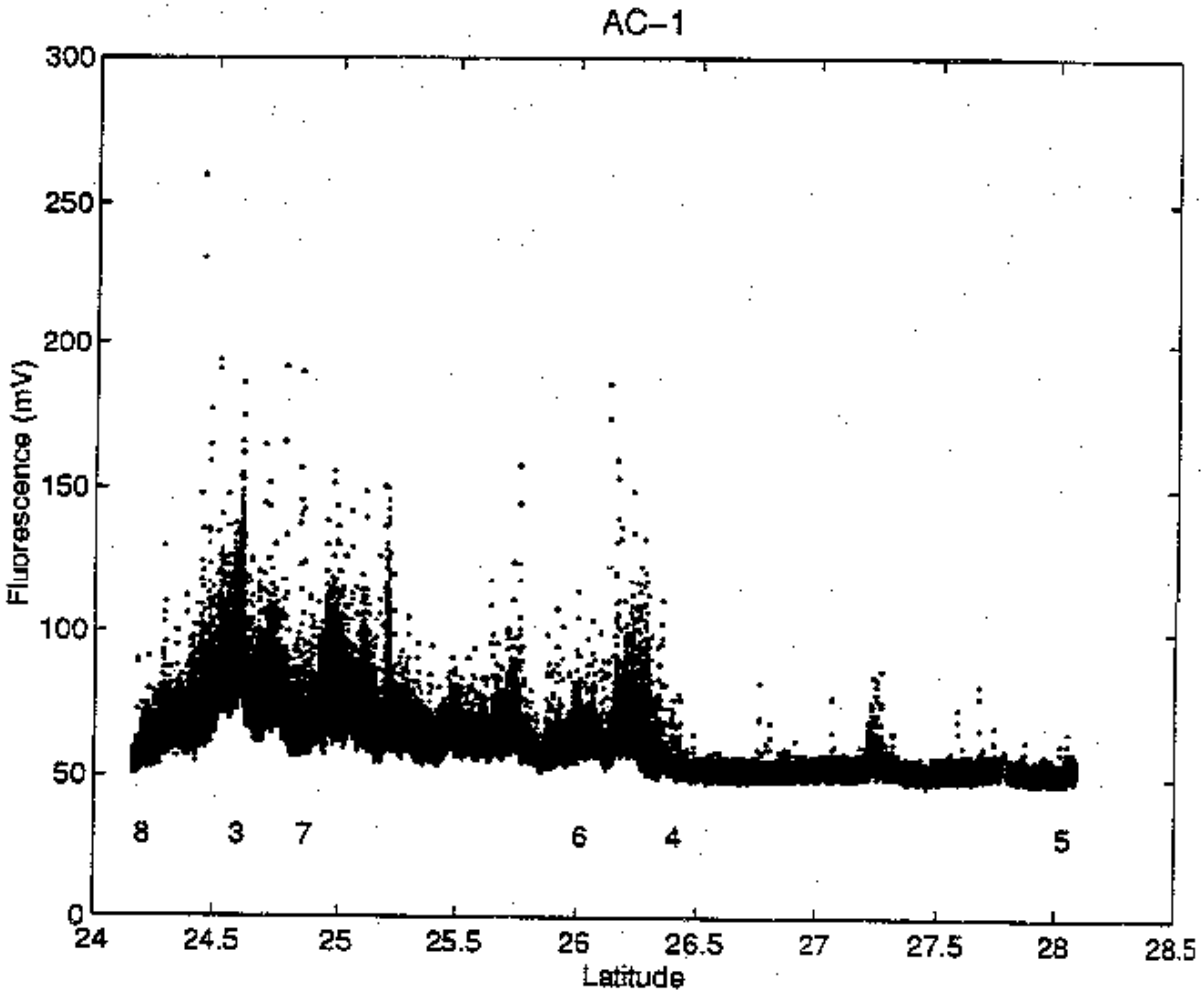
AC–1
Fluorescence (mV)
300
250
200
150
100
50
0
24
24.5
25
25.5
26
26.5
27
27.5
28
28.5
Latitude
8
3
7
6
4
5

Figure 6.7.3

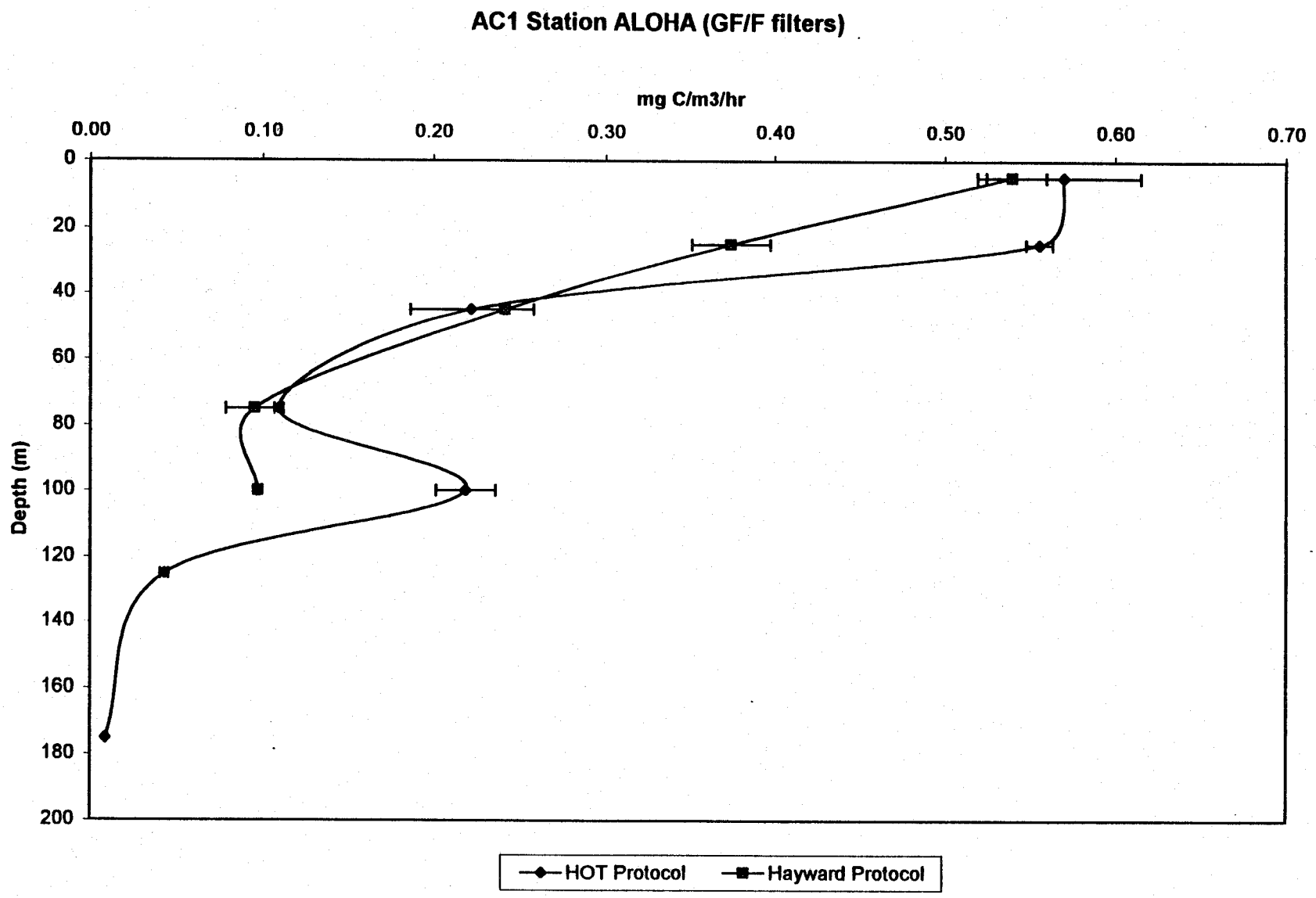
AC1 Station ALOHA (GF/F filters)
mg C/m3/hr
0.00
0.10
0.20
0.30
0.40
0.50
0.60
0.70
Depth (m)
0
20
40
60
80
100
120
140
160
180
200
HOT Protocol
Hayward Protocol

Figure 6.7.4

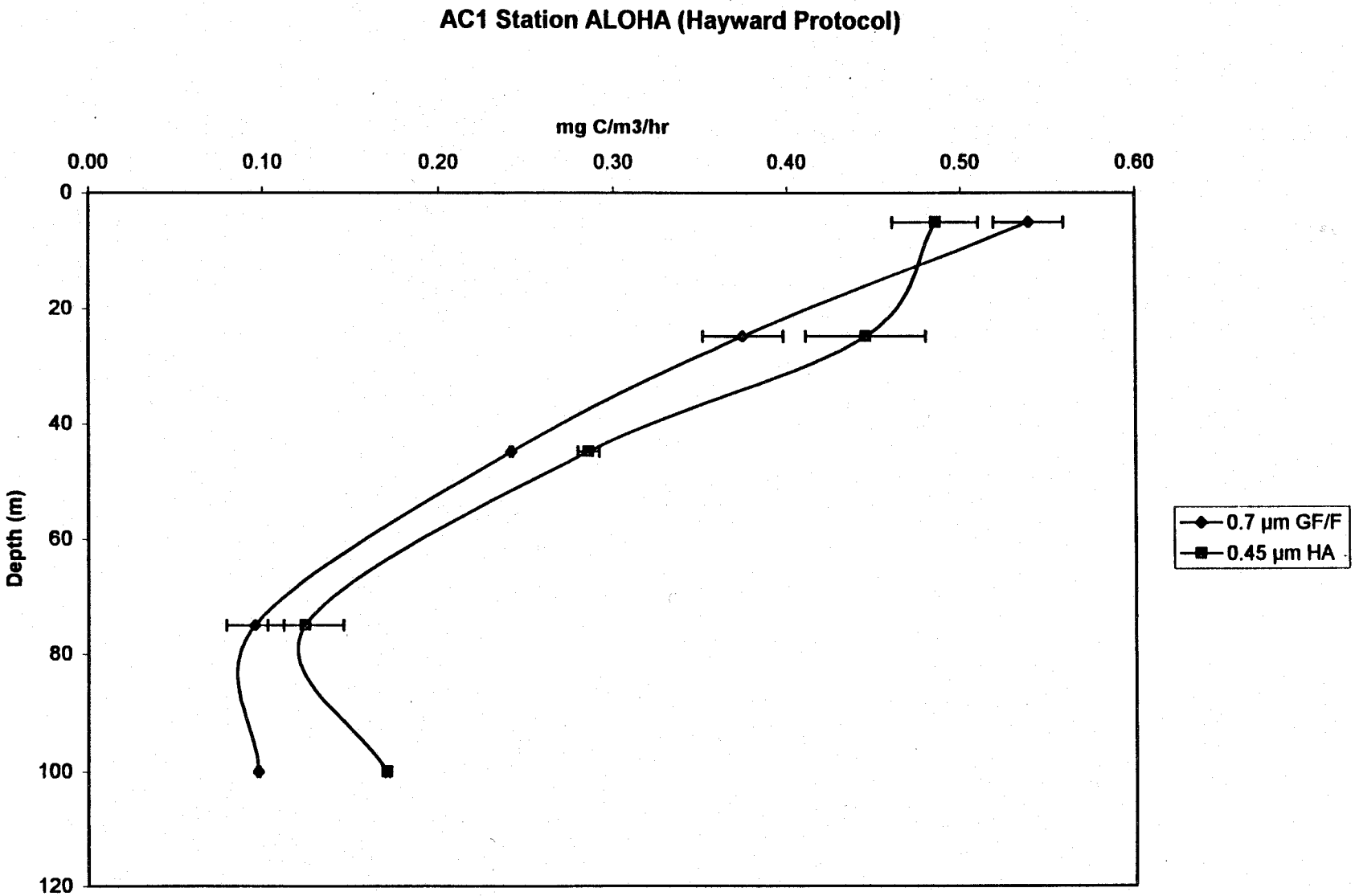
AC1 Station ALOHA (Hayward Protocol)
mg C/m3/hr
0.00
0.10
0.20
0.30
0.40
0.50
0.60
Depth (m)
0
20
40
60
80
100
120
0.7 µm GF/F
0.45 µm HA

Figure 6.7.5

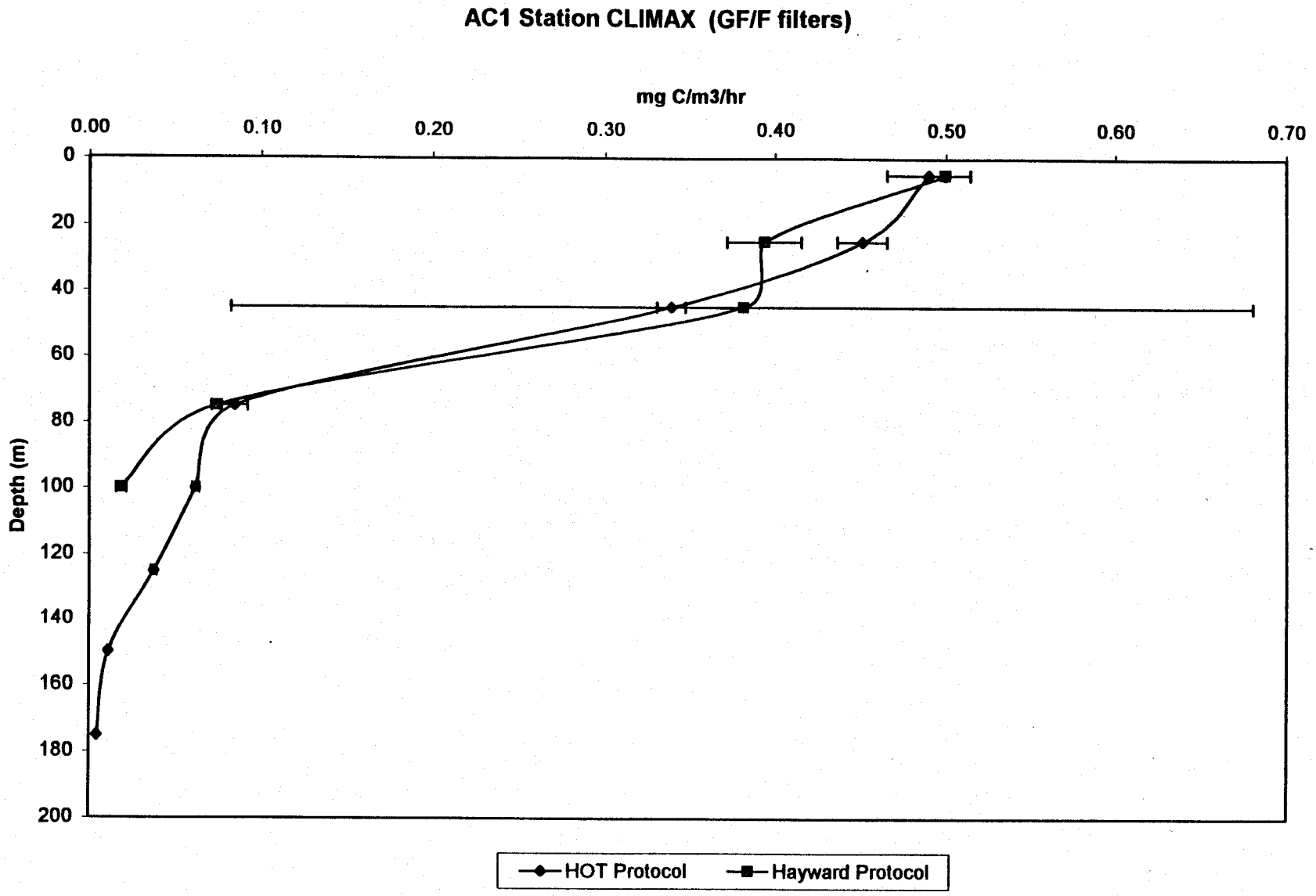
AC1 Station CLIMAX (GF/F filters)
mg C/m3/hr
0.00
0.10
0.20
0.30
0.40
0.50
0.60
0.70
Depth (m)
0
20
40
60
80
100
120
140
160
180
200
HOT Protocol
Hayward Protocol

Figure 6.7.6

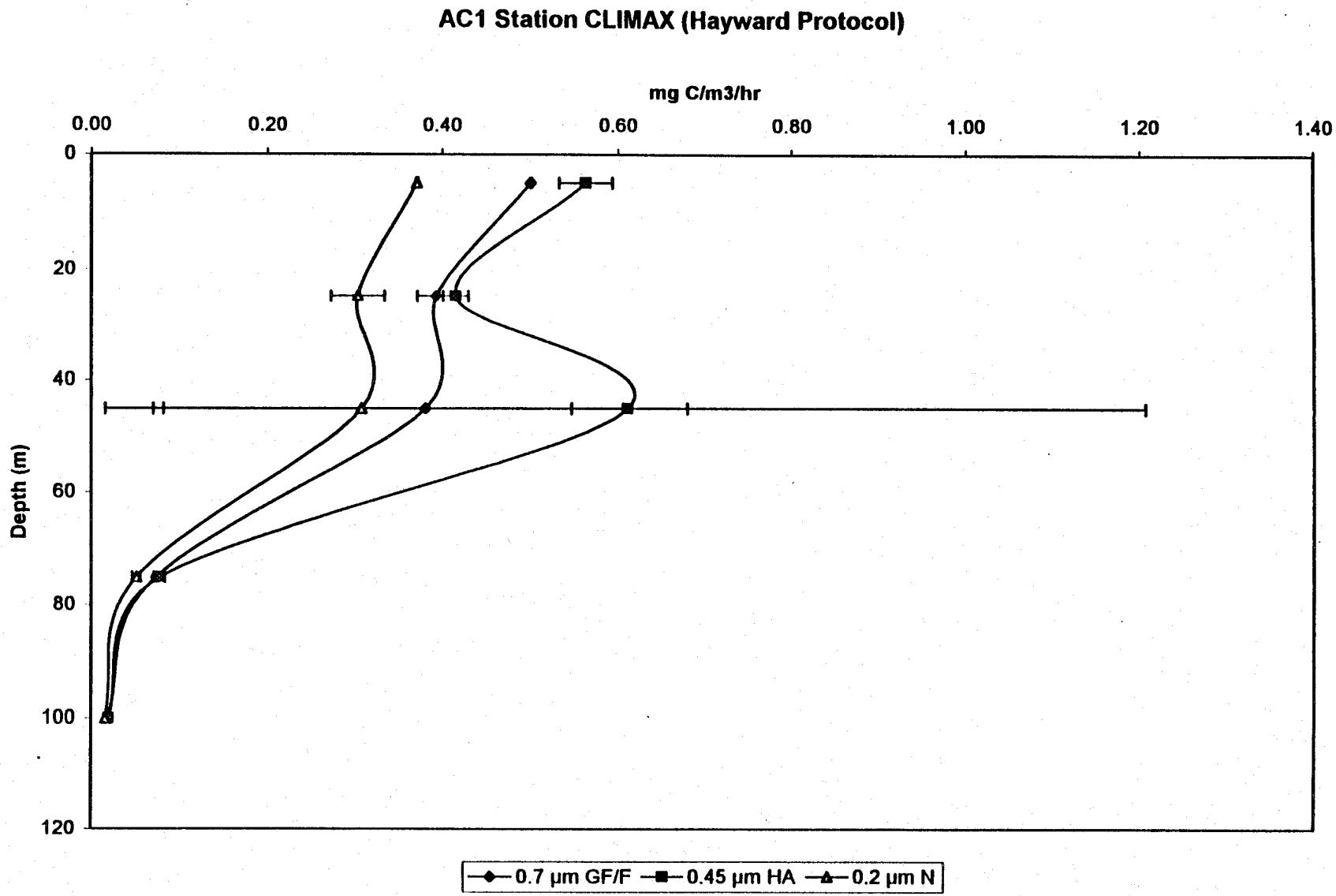
AC1 Station CLIMAX (Hayward Protocol)
mg C/m3/hr
0.00
0.20
0.40
0.60
0.80
1.00
1.20
1.40
Depth (m)
0
20
40
60
80
100
120
0.7 µm GF/F
0.45 µm HA
0.2 µm N

Figure 6.7.7

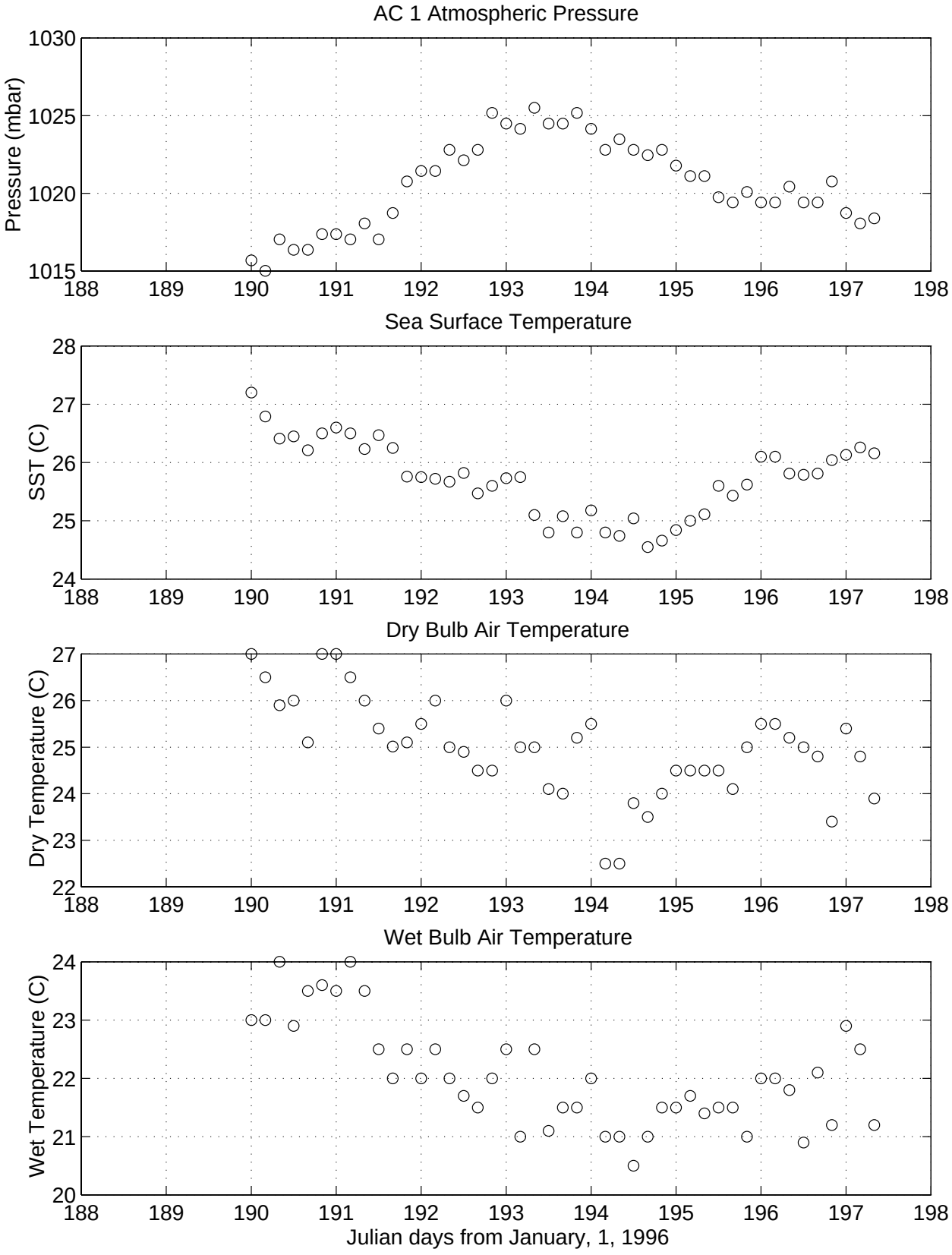
AC 1 Atmospheric Pressure
Pressure (mbar)
1030
1025
1020
1015
188
189
190
191
192
193
194
195
196
197
198
Sea Surface Temperature
SST (C)
28
27
26
25
24
Dry Bulb Air Temperature
Dry Temperature (C)
27
26
25
24
23
22
Wet Bulb Air Temperature
Wet Temperature (C)
24
23
22
21
20
Julian days from January, 1, 1996

Figure 6.7.8

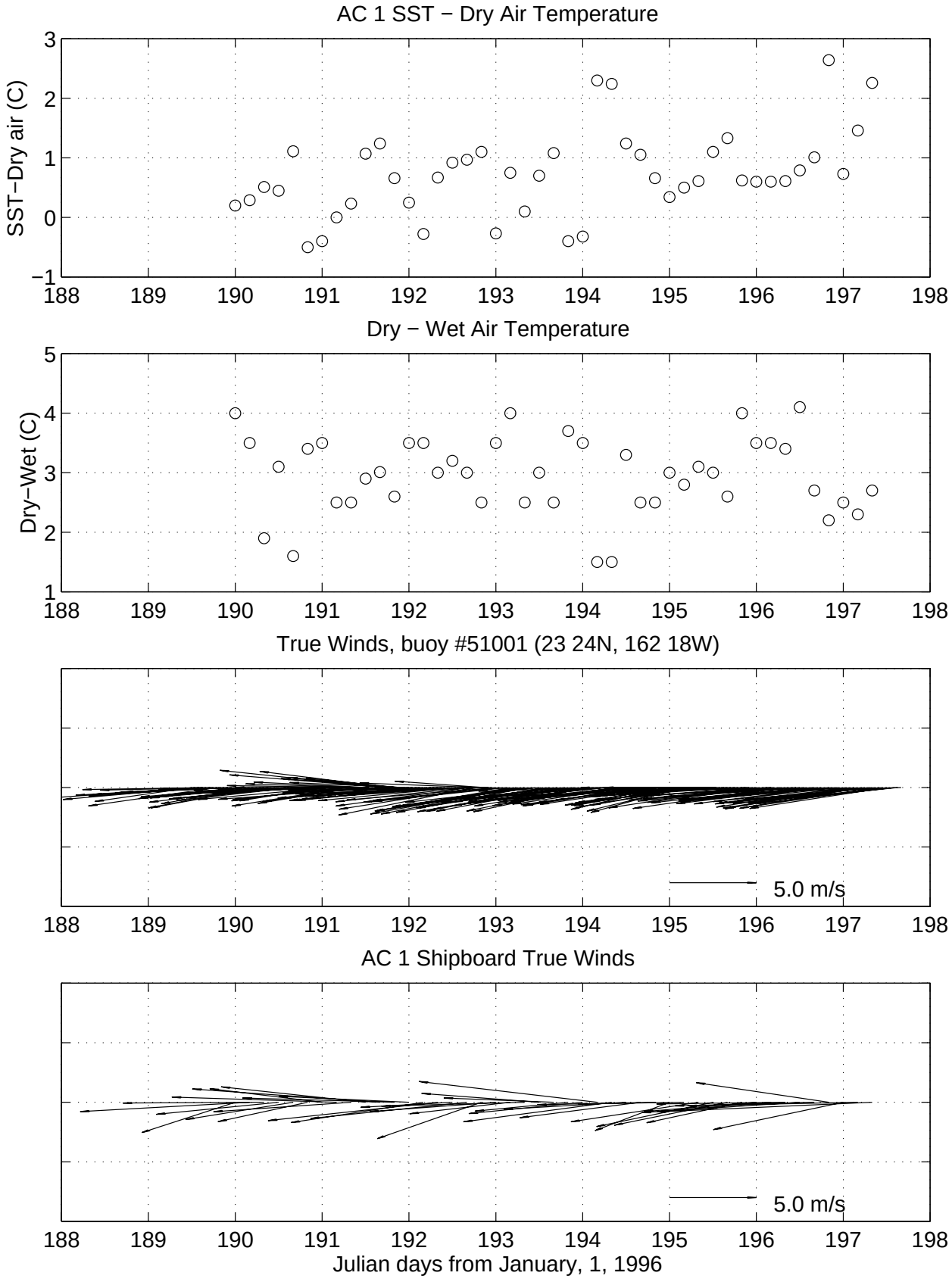

Figure 6.7.8 continued

7.0. HOT PROGRAM PRESENTATIONS AND PUBLICATIONS

I. Invited Presentations and Published Abstracts

I.1. 1988 Karl, D. NSF-sponsored symposium on Dissertations in Chemical Oceanography, "Research opportunities in Hawaiian waters", Honolulu, Hawaii, November 1988.

I.2. 1988 Karl, D. NSF/GOFS-sponsored workshop on sediment traps, "Determination of total C, N, P flux" and "Screens: A potential solution to the problem of swimmers", Gulf Coast Research Laboratory, Mississippi, November 1988.

I.3. 1989 Winn, C. D., S. Chiswell, D. M. Karl and R. Lukas. Long time-series research in the Central Pacific Ocean. The Oceanography Society 1st Annual Meeting, Monterey, California.

I.4. 1990 Karl, D., R. Letelier, D. Bird, D. Hebel, C. Sabine and C. Winn. An *Oscillatoria* bloom in the oligotrophic North Pacific Ocean near the GOFS station ALOHA. *EOS, Transactions of the American Geophysical Union* 71, 177-178.

I.5. 1990 Winn, C. D., D. Hebel, R. Letelier, D. Bird and D. Karl. Variability in biogeochemical fluxes in the oligotrophic central Pacific: Results of the Hawaii Ocean Time- Series Program. *EOS, Transactions of the American Geophysical Union* 71, 190.

I.6. 1990 Chiswell, S. M. and R. Lukas. The Hawaii Ocean Time-series (HOT). *EOS, Transactions of the American Geophysical Union* 71, 1397.

I.7. 1990 Karl, D. "JGOFS time-series programs," San Francisco, California, December 1990.

I.8. 1991 Winn, C., C. Sabine, D. Hebel, F. Mackenzie and D. M. Karl. Inorganic carbon system dynamics in the central Pacific Ocean: Results of the Hawaii Ocean Time-series program. *EOS, Transactions of the American Geophysical Union* 72, 70.

I.9. 1991 Lukas, R. Water mass variability observed in the Hawaii Ocean Time Series. *EOS, Transactions of the American Geophysical Union* 72, 70.

I.10. 1991 Letelier, R., D. Karl, R. Bidigare, J. Christian, J. Dore, D. Hebel and C. Winn. Temporal variability of phytoplankton pigments at the U.S.-JGOFS station ALOHA (22°45'N, 158°W). *EOS, Transactions of the American Geophysical Union* 72, 74.

I.11. 1991 Karl, D. "The Hawaii Ocean Time-series program: Carbon production and particle flux", The Oceanography Society 2nd Annual Meeting, St. Petersburg, Florida, March 1991.

I.12. 1991 Karl, D. NATO symposium on Biology and Ecology of Diazotrophic Marine Organisms, "*Trichodesmium* blooms and new nitrogen in the North Pacific gyre", Bamberg, Germany, May 1991.

I.13. 1992 Anbar, A. D. Rhenium in seawater: Confirmation of generally conservative behavior. *EOS, Transactions of the American Geophysical Union* 73, 278.

I.14. 1992 Schudlich, R. and S. R. Emerson. Modeling dissolved gases in the subtropical upper ocean: JGOFS/WOCE Hawaiian Ocean Time-series. *EOS, Transactions of the American Geophysical Union* 73, 287.

I.15. 1992 Tupas, L. M., B. N. Popp and D. M. Karl. Dissolved organic carbon in oligotrophic waters: experiments on sample preservation, storage and analysis. *EOS, Transactions of the American Geophysical Union* 73, 287.

I.16. 1992 Karl, D., C. Winn, D. Hebel, R. Letelier, J. Dore and J. Christian. The U.S.-JGOFS Hawaii Ocean Time-Series (HOT) program. American Society for Limnology and Oceanography Aquatic Sciences Meeting, Santa Fe, NM, February 1992.

I.17. 1992 Campbell, L., R. R. Bidigare, R. Letelier, M. Ondrusek, S. Hall, B. Tsai and C. Winn. Phytoplankton population structure at the Hawaii Ocean Time-series station. American Society for Limnology and Oceanography Aquatic Sciences Meeting, Santa Fe, NM, February 1992.

I.18. 1992 Karl, D. NSF-sponsored GLOBEC scientific steering committee meeting, "Hawaii Ocean Time-series (HOT) program: A GLOBEC 'Blue Water' initiative", Honolulu, Hawaii, March 1992.

I.19. 1992 Karl, D. IGBP International Symposium on Global Change, "Oceanic ecosystem variability: Initial results from the JGOFS Hawaii Ocean Time-series (HOT) experiment", Tokyo, Japan, March 1992.

I.20. 1992 Karl, D. Conoco HOT Topics Seminar Series, "The U.S.-JGOFS Hawaii Ocean Time- Series (HOT) Program: Biogeochemical Vignettes from the Oligotrophic North Pacific Ocean" and "Temporal Variability in Bioelement Flux at Station ALOHA (22°45'N, 158°W)", Woods Hole, Massachusetts, May 1992

I.21. 1992 Bidigare, R. R., L. Campbell, M. Ondrusek, R. Letelier and D. Vaulot. Characterization of picophytoplankton at Station ALOHA (22°45'N, 158°W) using HPLC, flow cytometry and immunofluorescence techniques. PACON 1992 Meeting, June 1992.

I.22. 1992 Winn, C. D., D. Hebel, R. Letelier, J. Christian, J. Dore, R. Lukas and D. M. Karl. Long time-series measurements in the central North Pacific: Results of the Hawaii Ocean Time-series program. PACON conference, Kona, Hawaii, June 1992.

I.23. 1993 Atkinson, M. J. A potentiometric solid state sensor for oceanic CTDs, Abstract of The Oceanography Society Annual Meeting, Seattle, Washington, April 1993.

I.24. 1993 Campbell, L., H. A. Nolla and D. Vaulot. Microbial biomass in the subtropical central North Pacific Ocean (Station ALOHA): The importance of *Prochlorococcus*, Abstract of The Oceanography Society Annual Meeting, Seattle, Washington, April 1993.

I.25. 1993 Emerson, S., P. Quay, C. Stump, D. Wilbur and R. Schudlich. Oxygen cycles and productivity in the oligotrophic subtropical Pacific Ocean. Abstract of The Oceanography Society Annual Meeting, Seattle, Washington, April 1993.

I.26. 1993 Sharp, J. H., R. Benner, L. Bennett, C. A. Carlson, S. E. Fitzwater, E. T. Peltzer, and L. Tupas. Dissolved organic carbon: Intercalibration of analyses with equatorial Pacific samples. Abstract of The Oceanography Society Annual Meeting, Seattle, Washington, April 1993.

I.27. 1993 Winn, C. D., C. J. Carrillo, F. T. Mackenzie and D. M. Karl. Variability in the inorganic carbon system parameters in the North Pacific subtropical gyre. Abstract of The Oceanography Society Annual Meeting, Seattle, Washington, April 1993.

I.28. 1993 Yanagi, K. and D. M. Karl. Note on the fractional determination of TDP in seawater by an UV-irradiation method combined with the MAGIC procedure. Abstract of the Oceanography Society of Japan annual meeting, Tokyo, Japan, April 1993.

I.29. 1993 Campbell, L., H. Liu, R. R. Bidigare and D. Vaulot. Immunochemical characterization of *Prochlorococcus*. Abstract of the American Society of Limnology and Oceanography 1993 Annual Meeting, Edmonton, Alberta, Canada, May 1993.

I.30. 1993 Christian, J. R. and D. M. Karl. Bacterial exoenzymes in marine waters: Implications for global biogeochemical cycles. Abstract of the American Society of Limnology and Oceanography 1993 Annual Meeting, Edmonton, Alberta, Canada, May 1993.

I.31. 1993 Moyer, C. L., L. Campbell, D. M. Karl and J. Wilcox. Restriction fragment length polymorphism (RFLP) and DNA sequence analysis of PCR-generated clones to assess diversity of picoeukaryotic algae in the subtropical central North Pacific Ocean (Station ALOHA). Abstract of the American Society of Limnology and Oceanography 1993 Annual Meeting, Edmonton, Alberta, Canada, May 1993.

I.32. 1993 Sharp, J. H., R. Benner, L. Bennett, C. A. Carlson, S. E. Fitzwater and L. Tupas. The equatorial Pacific intercalibration analyses of dissolved organic carbon in seawater. Abstract of the American Society of Limnology and Oceanography 1993 Annual Meeting, Edmonton, Alberta, Canada, May 1993.

I.33. 1994 Yuan, J., C. I. Measures and J. A. Resing. Rapid determination of iron in seawater: In-line preconcentration flow injection analysis with spectrophotometric detection. *EOS, Transactions of the American Geophysical Union* 75, 25.

I.34. 1994 Smith, C. R., S. Garner, D. Hoover and R. Pope. Macrobenthos, mechanisms of bioturbation and carbon flux proxies at the abyssal seafloor along the JGOFS Equatorial Pacific Transect. *EOS, Transactions of the American Geophysical Union* 75, 70.

I.35. 1994 Farrenkopf, A. M., G. W. Luther, III and C. H. Van Der Weijden. Vertical distribution of dissolved iodine species in the northwest Indian Ocean. *EOS, Transactions of the American Geophysical Union* 75, 78.

I.36. 1994 Campbell, L., C. D. Winn, R. Letelier, D. Hebel and D. M. Karl. Temporal variability in phytoplankton fluorescence at Station ALOHA. *EOS, Transactions of the American Geophysical Union* 75, 100.

I.37. 1994 Winn, C., F. T. Mackenzie, C. Carrillo, T. Westby and D. M. Karl. Air-sea carbon dioxide exchange at Station ALOHA. *EOS, Transactions of the American Geophysical Union* 75, 112.

I.38. 1994 Lukas, R., F. Bingham and A. Mantyla. An anomalous cold event in the bottom water observed north of Oahu. *EOS, Transactions of the American Geophysical Union* 75, 205.

I.39. 1994 Tupas, L. M., B. N. Popp and D. M. Karl. Dissolved organic carbon in oligotrophic waters; experiments on sample preservation, storage and analysis. *EOS, Transactions of the American Geophysical Union* 75, 287.

I.40. 1994 Bingham, F. M. Drifter observations of the North Hawaiian Ridge Current. *EOS, Transactions of the American Geophysical Union* 75, 307.

I.41. 1994 HOT Program P.I.s, staff and students. The Hawaii Ocean Time-series (HOT) program: The first five years, p. 59. Abstract of The Oceanography Society Pacific Basin Meeting, Honolulu, Hawaii, July 1994.

I.42. 1994 HOT Program P.I.s, staff and students. HOT: a time-series study of carbon cycling in the oligotrophic North Pacific, p. 24. Abstract of The Oceanography Society Pacific Basin Meeting, Honolulu, Hawaii, July 1994.

I.43. 1994 Bidigare, R. R., L. Campbell, M. E. Ondrusek, R. Letelier, D. Vaulot and D. M. Karl. Phytoplankton community structure at station ALOHA (22°45'N, 158°W) during fall 1991, p. 58. Abstract of The Oceanography Society Pacific Basin Meeting, Honolulu, Hawaii, July 1994.

I.44. 1994 Bingham, F. M. and B. Qiu. Interannual variability of surface and mixed layer properties observed in the Hawaii Ocean Time-series, p. 89. Abstract of The Oceanography Society Pacific Basin Meeting, Honolulu, Hawaii, July 1994.

I.45. 1994 Bingham, F. M. and R. Lukas. Seasonal cycles of temperature, salinity and dissolved oxygen observed in the Hawaii Ocean Time-series, p. 90. Abstract of The Oceanography Society Pacific Basin Meeting, Honolulu, Hawaii, July 1994.

I.46. 1994 Christian, J. Vertical fluxes of carbon and nitrogen at Station ALOHA, p. 61. Abstract of The Oceanography Society Pacific Basin Meeting, Honolulu, Hawaii, July 1994.

I.47. 1994 Dore, J. E. and D. M. Karl. Nitrite distributions and dynamics at Station ALOHA, p. 60. Abstract of The Oceanography Society Pacific Basin Meeting, Honolulu, Hawaii, July 1994.

I.48. 1994 Firing, E. Currents observed north of Oahu during the first five years of HOT, p. 90. Abstract of The Oceanography Society Pacific Basin Meeting, Honolulu, Hawaii, July 1994.

I.49. 1994 Fujieki, L. A., D. V. Hebel, L. M. Tupas and D. M. Karl. Hawaii Ocean Time-series Data Organization and Graphical System (HOT-DOGS), p. 61. Abstract of The Oceanography Society Pacific Basin Meeting, Honolulu, Hawaii, July 1994.

I.50. 1994 Hebel, D. V., F. P. Chavez, K. R. Buck, R. R. Bidigare, D. M. Karl, M. Latasa, M. E. Ondrusek, L. Campbell and J. Newton. Do GF/F filters underestimate particulate chlorophyll *a* and primary production in the oligotrophic ocean?, p. 62. Abstract of The Oceanography Society Pacific Basin Meeting, Honolulu, Hawaii, July 1994.

I.51. 1994 Houlihan, T., J. E. Dore, L. Tupas, D. V. Hebel, G. Tien and D. M. Karl. Freezing as a method of preservation for seawater dissolved nutrient and organic carbon samples, p. 62. Abstract of The Oceanography Society Pacific Basin Meeting, Honolulu, Hawaii, July 1994.

I.52. 1994 Kennan, S. C. and R. Lukas. Saline intrusions in the intermediate waters north of Oahu, p. 91. Abstract of The Oceanography Society Pacific Basin Meeting, Honolulu, Hawaii, July 1994.

I.53. 1994 Letelier, R. M., J. Dore, C. D. Winn and D. M. Karl. Temporal variations in photosynthetic carbon assimilation efficiencies at Station ALOHA (22°45'N; 158°00'W), p. 60. Abstract of The Oceanography Society Pacific Basin Meeting, Honolulu, Hawaii, July 1994.

I.54. 1994 Liu, H. and L. Campbell. Growth and grazing rates of *Prochlorococcus* and *Synechococcus* at Station ALOHA measured by the selective inhibitor technique, p. 59. Abstract of The Oceanography Society Pacific Basin Meeting, Honolulu, Hawaii, July 1994.

I.55. 1994 Lukas, R. Interannual variability of Pacific deep and bottom waters observed in the Hawaii Ocean Time-series, p. 91. Abstract of The Oceanography Society Pacific Basin Meeting, Honolulu, Hawaii, July 1994.

I.56. 1994 Lukas, R., F. Bingham and E. Firing. Seasonal-to-interannual variability observed in the Hawaii Ocean Time-series, p. 28. Abstract of The Oceanography Society Pacific Basin Meeting, Honolulu, Hawaii, July 1994.

I.57. 1994 Tupas, L. M., B. N. Popp, D. V. Hebel, G. Tien and D. M. Karl. Dissolved organic carbon measurements at Station ALOHA measured by high temperature catalytic

oxidation: Characteristics and variation in the water column, p. 63. Abstract of The Oceanography Society Pacific Basin Meeting, Honolulu, Hawaii, July 1994.

I.58. 1994 Winn, C. D., F. T. Mackenzie, C. Carrillo and D. M. Karl. Air-sea carbon dioxide exchange at Station ALOHA, p. 58. Abstract of The Oceanography Society Pacific Basin Meeting, Honolulu, Hawaii, July 1994.

I.59. 1994 Liu, H. and L. Campbell. Measurement of growth and mortality rate of *Prochloroccus* and *Synechococcus* at Station ALOHA using a new selective inhibitor technique. Fifth International Phycological Congress, Qingdao, China, July 1994.

I.60. 1994 Winn, C., F. T. Mackenzie, C. Carrillo, T. Westby and D. M. Karl. Air-sea carbon dioxide exchange at Station ALOHA, p. 112. Abstract of the American Society of Limnology and Oceanography 1994 Ocean Sciences Meeting, San Diego, California.

I.61. 1994 Measures, C. I., J. Yuan and J. A. Resing. The rapid determination of iron in seawater at sub-nanomolar concentrations using in-line preconcentration and spectrophotometric detection. Sixth Winter Conference on Flow Injection Analysis, San Diego, CA.

I.62. 1994 Measures, C. I., J. Yuan and J. A. Resing. Determination of iron in seawater using in-line preconcentration and spectrophotometric detection. Workshop on Iron Speciation and its Biological Activity, Bermuda Biological Station for Research, Bermuda.

I.63. 1995 Cortés, M. Y. and H. R. Thierstein. Coccolithophore dynamics during 1994 at the JGOFS time series Station ALOHA, Hawaii. 5th International Conference on Paleoceanography, Halifax, Canada, Abstract, p. 121.

I.64. 1995 Campos, M. L. A. M., T. D. Jickells, A. M. Farrenkopf and G. W. Luther, III. A comparison of dissolved iodine cycling at the Bermuda Atlantic Time Series station and Hawaii Ocean Time-series station. *EOS, Transactions of the American Geophysical Union* 76, S175.

I.65. 1995 Yuan, J. Collecting iron samples from well mounted on CTD rosette. *EOS, Transactions of the American Geophysical Union* 76, S175.

I.66. 1995 Michaels, A. F., D. Karl and A. H. Knap. Insights on ocean variability from the JGOFS time-series stations. Invited plenary lecture, The Oceanography Society Biennial Meeting, April 1995.

I.67. 1995 Emerson, S., P. Quay, L. Tupas and D. Karl. Chemical tracers of productivity and respiration in the upper ocean at US JGOFS station ALOHA, 10th Anniversary JGOFS Science Conference, Villefranche, France, May 1995.

I.68. 1995 Michaels, A. F., D. Karl and A. H. Knap. Insights on ocean variability from the JGOFS time-series stations. Invited lecture, 10th Anniversary JGOFS Science Conference, Villefranche, France, May 1995.

I.69. 1995 Karl, D. M. Oceanic carbon cycle and global environmental change: A microbiological perspective. Invited plenary talk, 7th International Symposium on Microbial Ecology, Santos, Brazil, August 1995.

I.70. 1995 Winn, C., D. Sadler and D. M. Karl. Carbon dioxide dynamics at the Hawaii JGOFS/WOCE time-series station. International Association for the Physical Sciences of the Oceans, Honolulu, Hawaii, August 1995.

I.71. 1996 Campbell, L., H. Liu and H. A. Nolla. Picophytoplankton population dynamics at Station ALOHA, p. OS65. AGU-ASLO Ocean Sciences Meeting, San Diego, CA, February 1996.

I.72. 1996 Christian, J. R., J. E. Dore and D. M. Karl. Mixing and nutrient fluxes at the US-JGOFS Station ALOHA ((22°45'N, 158°00'W), p. OS65. AGU-ASLO Ocean Sciences Meeting, San Diego, CA, February 1996.

I.73. 1996 Dulaney, T. S. and L. R. Sautter. Sedimentation of planktonic foraminifera: Seasonal changes in shell flux north of Oahu, Hawaii, p. OS85. AGU-ASLO Ocean Sciences Meeting, San Diego, CA, February 1996.

I.74. 1996 Emerson, S. Chemical tracers of biological processes: O_2, Ar and N_2 mass balance in the subtropical Pacific at the HOT station, p. OS85. AGU-ASLO Ocean Sciences Meeting, San Diego, CA, February 1996.

I.75. 1996 Hebel, D. V., D. M. Karl, J. R. Christian, J. E. Dore, R. M. Letelier, L. M. Tupas and C. D. Winn. Seasonal and interannual variability in primary production and particle flux at Station ALOHA, p. OS85. AGU-ASLO Ocean Sciences Meeting, San Diego, CA, February 1996.

I.76. 1996 Karl, D. M.. Alternation of N and P control of new and export production in the North Pacific gyre: A hypothesis based on the HOT program data set, p. OS86. AGU-ASLO Ocean Sciences Meeting, San Diego, CA, February 1996.

I.77. 1996 Lawson, L. M. and E. E. Hofmann. Time series sampling and data assimilation in a simple marine ecosystem model, p. OS86. AGU-ASLO Ocean Sciences Meeting, San Diego, CA, February 1996.

I.78. 1996 Lopez, M. D. G., Y. Zhu and M. E. Huntley. Space-time variability of zooplankton-sized particle concentrations at the Hawaii Ocean Time-series station (Station ALOHA), p. OS85. AGU-ASLO Ocean Sciences Meeting, San Diego, CA, February 1996.

I.79. 1996 Quay, P. D. and H. Anderson. Organic carbon export rates in the subtropical N. Pacific, p. OS85. AGU-ASLO Ocean Sciences Meeting, San Diego, CA, February 1996.

I.80. 1996 Richman, J. G., R. M. Letelier, M. R. Abbott and D. Pillsbury. Expandable optical mooring test at Station ALOHA (22°45'N; 158°00'W), p. OS64. AGU-ASLO Ocean Sciences Meeting, San Diego, CA, February 1996.

I.81. 1996 Scharek, R., M. Latasa, D. M. Karl and R. R. Bidigare Diatom abundance and vertical flux at the US-JGOFS/WOCE Station "ALOHA" in the oligotrophic North Pacific gyre, p. OS85. AGU-ASLO Ocean Sciences Meeting, San Diego, CA, February 1996.

I.82. 1996 Selph, K. E., M. R. Landry, R. J. Miller and H. A. Al-Mutairi. Temporal variability in the mesozooplankton community at ocean Station ALOHA, p. OS85. AGU-ASLO Ocean Sciences Meeting, San Diego, CA, February 1996.

I.83. 1996 Tersol, V., S. Vink, J. Yuan and C. I. Measures. Variations in iron, aluminum and berylium concentrations in surface waters at Station ALOHA, p. OS65. AGU-ASLO Ocean Sciences Meeting, San Diego, CA, February 1996.

I.84. 1996 Tupas, L. M., M P. Sampson and D. M. Karl. Stable nitrogen isotopic analysis of sinking particulate matter at the Hawaii Ocean Time-series site, p. OS86. AGU-ASLO Ocean Sciences Meeting, San Diego, CA, February 1996.

I.85. 1996 Venrick, E. L. A comparison between the phytoplankton species from Station ALOHA and from the Climax region, p. OS65. AGU-ASLO Ocean Sciences Meeting, San Diego, CA, February 1996.

I.86. 1996 Winn, C. D. Carbon dioxide dynamics at the Hawaii JGOFS/WOCE time-series station: Annual and interannual variability, p. OS64. AGU-ASLO Ocean Sciences Meeting, San Diego, CA, February 1996.

I.87. 1996 Lukas, R. Low-frequency climate signals emerge in the Hawaii Ocean Time-series. WOCE Pacific Workshop. Hyatt Newporter, Newport Beach, CA, 19-23 August 1996.

I.88. 1996 Santiago-Mandujano, F. Cold bottom water events observed in the Hawaii Ocean Time-series. WOCE Pacific Workshop. Hyatt Newporter, Newport Beach, CA, 19-23 August 1996.

I.89. 1997 Lukas, R. Physical studies at the Hawaii Ocean Time-series (HOT) Station. Ocean Climate Time-Series Workshop. Johns Hopkins University, Baltimore, MD, 18-20 March 1997.

II. Invited/Contributed Book Chapters and Refereed Publications

II.1. 1990 Firing, E. and R. L. Gordon. Deep ocean acoustic Doppler current profiling. In: G. F. Appell and T. B. Curtin (eds.), *Proceedings of the Fourth IEEE Working Conference on Current Measurements*, pp. 192-201. IEEE, New York.

II.2. 1990 Giovannoni, S. J., E. F. DeLong, T. M. Schmidt and N. R. Pace. Tangential flow filtration and preliminary phylogenetic analysis of marine picoplankton. *Applied and Environmental Microbiology* 56, 2572-2575.

II.3. 1991 Chiswell, S. M. Dynamic response of CTD pressure sensors to temperature. *Journal of Atmospheric and Oceanic Technology* 8, 659-668.

II.4 1991 Karl, D. M., J. E. Dore, D. V. Hebel and C. Winn. Procedures for particulate carbon, nitrogen, phosphorus and total mass analyses used in the US-JGOFS Hawaii Ocean Time- Series Program. In: D. Spencer and D. Hurd (eds.), *Marine Particles: Analysis and Characterization*, pp. 71-77. American Geophysical Union, Geophysical Monograph 63.

II.5. 1991 Karl, D. M., W. G. Harrison, J. Dore et al. Chapter 3. Major bioelements workshop report. In: D. C. Hurd and D. W. Spencer (eds.), *Marine Particles: Analysis and Characterization*, pp. 33-42. American Geophysical Union, Geophysical Monograph 63.

II.6. 1991 Karl, D. M. and C. D. Winn. A sea of change: Monitoring the oceans' carbon cycle. *Environmental Science & Technology* 25, 1976-1981.

II.7. 1991 Laws, E. A. Photosynthetic quotients, new production and net community production in the open ocean. *Deep-Sea Research* 38, 143-167.

II.8. 1991 Sabine, C. L. and F. T. Mackenzie. Oceanic sinks for anthropogenic CO_2. *International Journal of Energy, Environment, Economics* 1, 119-127.

II.9. 1991 Schmidt, T. M., E. F. DeLong and N. R. Pace. Analysis of a marine picoplankton community by 16S rRNA gene cloning and sequencing. *Journal of Bacteriology* 173, 4371- 4378.

II.10. 1992 Benner, R., J. D. Pakulski, M. McCarthy, J. I. Hedges and P. G. Hatcher. Bulk chemical characteristics of dissolved organic matter in the ocean. *Science* 255, 1561-1564.

II.11. 1992 Chen, R. F. and J. L. Bada. The fluorescence of dissolved organic matter in seawater. *Marine Chemistry* 37, 191-221.

II.12. 1992 Karl, D. M. The oceanic carbon cycle: Primary production and carbon flux in the oligotrophic North Pacific Ocean. In: Y. Oshima (ed.), *Proceedings of the IGBP Symposium on Global Change*, pp. 203-219. Japan National Committee for the IGBP, Waseda University, Tokyo, Japan.

II.13. 1992 Karl, D. M., R. Letelier, D. V. Hebel, D. F. Bird and C. D. Winn. *Trichodesmium* blooms and new nitrogen in the North Pacific gyre. In: E. J. Carpenter et al. (eds.), *Marine Pelagic Cyanobacteria: Trichodesmium and Other Diazotrophs*, pp. 219-237. Kluwer Academic Publishers, Netherlands.

II.14. 1992 Karl, D. M. and G. Tien. MAGIC: A sensitive and precise method for measuring dissolved phosphorus in aquatic environments. *Limnology and Oceanography* 37, 105-116.

II.15. 1992 Quay, P. D., B. Tilbrook and C. S. Wong. Oceanic uptake of fossil fuel CO_2: Carbon- 13 evidence. *Science* 256, 74-78.

II.16. 1993 Anbar, A. D., R. A. Creaser, D. A. Papanastassiou and G. J. Wasserburg. Rhenium in seawater: Confirmation of generally conservative behavior. *Geochimica et Cosmochimica Acta* 56, 4099-4103.

II.17. 1993 Campbell, L. and D. Vaulot. Photosynthetic picoplankton community structure in the subtropical North Pacific Ocean near Hawaii (station ALOHA). *Deep-Sea Research* 40, 2043- 2060.

II.18. 1993 Coble, P. G., C. A. Schultz and K. Mopper. Fluorescence contouring analysis of DOC intercalibration experiment samples: a comparison of techniques. *Marine Chemistry* 41, 173-178.

II.19. 1993 Emerson, S., P. Quay, C. Stump, D. Wilbur and R. Schudlich. Determining primary production from the mesoscale oxygen field. *ICES Marine Science Symposium* 197, 196-206.

II.20. 1993 Hedges, J. I., B. A. Bergamaschi and R. Benner. Comparative analyses of DOC and DON in natural waters. *Marine Chemistry* 41, 121-134.

II.21. 1993 Karl, D. M. Total microbial biomass estimation derived from the measurement of particulate adenosine-5'-triphosphate. In: P. F. Kemp, B. F. Sherr, E. B. Sherr and J. J. Cole (eds.), *Current Methods in Aquatic Microbial Ecology*, pp. 359-368. Lewis Publishers, Boca Raton.

II.22. 1993 Karl, D. M., G. Tien, J. Dore and C. D. Winn. Total dissolved nitrogen and phosphorus concentrations at US-JGOFS Station ALOHA: Redfield reconciliation. *Marine Chemistry* 41, 203-208.

II.23. 1993 Keeling, C. D. Lecture 2: Surface ocean CO_2. *NATO ASI Series* I(15), 413-429.

II.24. 1993 Letelier, R. M., R. R. Bidigare, D. V. Hebel, C. D. Winn and D. M. Karl. Temporal variability study of the phytoplankton community structure at the US-JGOFS Time-series Station ALOHA (22°45'N, 158°00'W) based on pigment analyses. *Limnology and Oceanography* 38, 1420-1437.

II.25. 1993 Mopper, K. and C. A. Schultz. Fluorescence as a possible tool for studying the nature and water column distribution of DOC components. *Marine Chemistry* 41, 229-238.

II.26. 1993 Selph, K. E., D. M. Karl and M. R. Landry. Quantification of chemiluminescent DNA probes using liquid scintillation counting. *Analytical Biochemistry* 210, 394-401.

II.27. 1993 Sharp, J. H., E. T. Peltzer, M. J. Alperin, G. Cauwet, J. W. Farrington, B. Fry, D. M. Karl, J. H. Martin, A. Spitzy, S. Tugrul and C. A. Carlson. Procedures subgroup report. *Marine Chemistry* 41, 37-49.

II.28. 1993 Winn, C. D., R. Lukas, D. Hebel, C. Carrillo, R. Letelier and D. M. Karl. The Hawaii Ocean Time-series program: Resolving variability in the North Pacific. In: N. Saxena (ed.), *Recent Advances in Marine Science and Technology*, pp. 139-150. Proceedings of the Pacific Ocean Congress (PACON).

II.29. 1994 Baines, S. B., M. L. Pace and D. M. Karl. Why does the relationship between sinking flux and planktonic primary production differ between lakes and ocean? *Limnology and Oceanography* 39, 213-226.

II.30. 1994 Björkman, K. and D. M. Karl. Bioavailability of inorganic and organic phosphorus compounds to natural assemblages of microorganisms in Hawaiian coastal waters. *Marine Ecology Progress Series* 111, 265-273.

II.31. 1994 Campbell, L., H. A. Nolla and D. Vaulot. The importance of photosynthetic prokaryote biomass in the subtropical central North Pacific Ocean (Station ALOHA). *Limnology and Oceanography* 39, 954-961.

II.32. 1994 Campbell, L., L. P.Shapiro and E. M. Haugen. Immunochemical characterization of the eukaryotic ultraplankton in the Atlantic and Pacific Oceans. *Journal of Plankton Research* 16, 35-51.

II.33. 1994 Christian, J. R. and D. M. Karl. Microbial community structure at the U.S.-Joint Global Ocean Flux Study Station ALOHA: Inverse methods for estimating biochemical indicator ratios. *Journal of Geophysical Research* 99, 14,269-14,276.

II.34. 1994 Karl, D. M. Accurate estimation of microbial loop processes and rates. *Microbial Ecology* 28, 147-150.

II.35. 1994 Karl, D. M. and B. D. Tilbrook. Production and transport of methane in oceanic particulate organic matter. *Nature* 368, 732-734.

II.36. 1994 Tupas, L. M., B. N. Popp and D. M. Karl. Dissolved organic carbon in oligotrophic waters: experiments on sample preservation, storage and analysis. *Marine Chemistry* 45, 207- 216.

II.37. 1994 Winn, C. D., F. T. Mackenzie, C. J. Carrillo, C. L. Sabine and D. M. Karl. Air-sea carbon dioxide exchange in the North Pacific subtropical gyre: Implications for the global carbon budget. *Global Biogeochemical Cycles* 8, 157-163.

II.60. 1994 Chiswell, S. Using an array of inverted echo sounders to measure dynamic height and geostrophic current in the North Pacific subtropical gyre. *Journal of Atmospheric and Oceanic Technology* 11, 1420-1430.

II.38. 1995 Atkinson, M. A., F. I. M. Thomas, N. Larson, E. Terrill, K. Morita and C. Liu. A micro-hole potentiostatic oxygen sensor for oceanic CTDs. *Deep-Sea Research* 42, 761-771.

II.39. 1995 Chavez, F. P., K. R. Buck, R. R. Bidigare, D. M. Karl, D. Hebel, M. Latasa, M. E. Ondrusek, L. Campbell and J. Newton. On the chlorophyll *a* retention properties of glass- fiber GF/F filters. *Limnology and Oceanography* 40, 428-433.

II.40. 1995 Christian, J. R. and D. M. Karl. Bacterial exocellular enzymes in marine waters: activity ratios and temperature kinetics in three oceanographic provinces. *Limnology and Oceanography* 40, 1042-1049.

II.41. 1995 Christian, J. R. and D. M. Karl. Measuring bacterial ectoenzyme activities in marine waters using mercuric chloride as a preservative and a control. *Marine Ecology Progress Series* 123, 217-224.

II.42. 1995 Emerson, S., P. D. Quay, C. Stump, D. Wilbur and R. Schudlich. Chemical tracers of productivity and respiration in the subtropical Pacific Ocean. *Journal of Geophysical Research* 100, 15,873-15,887.

II.43. 1995 Jones, D. R., D. M. Karl and E. A. Laws. DNA:ATP ratios in marine microalgae and bacteria: Implications for growth rate estimates based on rates of DNA synthesis. *Journal of Phycology* 31, 215-223.

II.44. 1995 Karl, D. M. A reply to a comment by J. A. McGowan "HOT and the North Pacific gyre." *Nature* 378, 21-22.

II.45. 1995 Karl, D. M., R. Letelier, D. Hebel, L. Tupas, J. Dore, J. Christian and C. Winn. Ecosystem changes in the North Pacific subtropical gyre attributed to the 1991-92 El Niño. *Nature* 373, 230-234.

II.46. 1995 Liu, H., L. Campbell and M. R. Landry. Growth and mortality rates of *Prochlorococcus* and *Synechococcus* measured with a selective inhibitor technique. *Marine Ecology Progress Series* 116, 277-287.

II.47. 1995 Maranger, R. and D. F. Bird. Viral abundance in aquatic systems: a comparison between marine and fresh waters. *Marine Ecology Progress Series* 121, 217-226.

II.48. 1995 Sabine, C. L. and F. T. Mackenzie. Bank-derived carbonate sediment transport and dissolution in the Hawaiian Archipelago. *Aquatic Geochemistry* 1, 189-230.

II.49. 1995 Sabine, C. L., F. T. Mackenzie, C. Winn and D. M. Karl. Geochemistry of particulate and dissolved inorganic carbon at the Hawaii Ocean Time-series station, ALOHA. *Journal of Biogeochemical Cycles* 9, 637-651.

II.50. 1995 Sharp, J. H., R. Benner, L. Bennett, C. A. Carlson, S. E. Fitzwater, E. T. Peltzer and L. M. Tupas. Analyses of dissolved organic carbon in seawater: the JGOFS EqPac methods comparison. *Marine Chemistry* 48, 91-108.

II.51. 1995 Thomas, F. I. M. and M. J. Atkinson. Field calibration of a microhole potentiostatic oxygen sensor for oceanic CTDs. *Journal of Atmospheric and Oceanic Technology* 12, 390-394.

II.52. 1995 Thomas, F. I. M., S. A. McCarthy, J. Bower, S. Krothapalli, M. J. Atkinson and P. Flament. Response characteristics of two oxygen sensors for oceanic CTDs. *Journal of Atmospheric and Oceanic Technology* 12, 687-690.

II.53. 1995 Tilbrook, B. D. and D. M. Karl. Methane sources, distributions and sinks from California coastal waters to the oligotrophic North Pacific gyre. *Marine Chemistry* 49, 51-64.

II.54. 1995 Winn, C. D., L. Campbell, R. Letelier, D. Hebel, L. Fujieki and D. M. Karl. Seasonal variability in chlorophyll concentrations in the North Pacific subtropical gyre. *Global Biogeochemical Cycles* 9, 605-620.

II.55. 1996 Andersen, R., R. Bidigare, M. Keller and M. Latasa. A comparison of HPLC pigment signatures and electron microscopic observations for oligotrophic waters of the North Atlantic and Pacific Oceans. *Deep-Sea Research* 43, 517-537.

II.56. 1996 Atkinson, M., F. Thomas and N. Larson. Effects of pressure on oxygen sensors. *Journal of Atmospheric and Oceanic Technology* 13, 1267-1277.

II.57. 1996 Bingham, F. and R. Lukas Seasonal cycles of temperature, salinity and dissolved oxygen observed in the Hawaii Ocean Time-series. *Deep-Sea Research* 43, 199-213.

II.58. 1996 Campos, M. L., A. Farrenkopf, T. Jickells and G. Luther. A comparison of dissolved iodine cycling at the Bermuda Atlantic Time-series Study station and Hawaii Ocean Time-series station. *Deep-Sea Research* 43, 455-466.

II.59. 1996 Chiswell, S. Intraseasonal oscillations at Station ALOHA, north of Oahu, Hawaii. *Deep-Sea Research* 43, 305-319.

II.61. 1996 Dore, J. E., T. Houlihan, D. V. Hebel, G. Tien, L. M. Tupas and D. M. Karl. Freezing as a method of seawater preservation for the analysis of dissolved inorganic nutrients in seawater. *Marine Chemistry* 53, 173-185.

II.62. 1996 Dore, J. E. and D. M. Karl. Nitrification in the euphotic zone as a source for nitrite, nitrate and nitrous oxide at Station ALOHA. *Limnology and Oceanography* 41, 1619-1628.

II.63. 1996 Dore, J. E. and D. M. Karl. Nitrite distributions and dynamics at Station ALOHA. *Deep-Sea Research* 43, 385-402.

II.64. 1996 Feller, R. J. and D. M. Karl. The National Association of Marine Laboratories: A connected web for studying long-term changes in US coastal and marine waters. *Biological Bulletin* 190, 269-277.

II.65. 1996 Firing, E. Currents observed north of Oahu during the first 5 years of HOT. *Deep-Sea Research* 43, 281-303.

II.66. 1996 Jones, D. R., D. M. Karl and E. A. Laws. Growth rates and production of heterotrophic bacteria and phytoplankton in the North Pacific subtropical gyre. *Deep-Sea Research* 43, 1567-1580.

II.68. 1996 Karl, D. M., J. R. Christian, J. E. Dore, D. V. Hebel, R. M Letelier, L. M. Tupas and C. D. Winn. Seasonal and interannual variability in primary production and particle flux at Station ALOHA. *Deep-Sea Research* 43, 539-568.

II.69. 1996 Karl, D. M. and A. F. Michaels. Preface: The Hawaiian Ocean Time-series (HOT) and the Bermuda Atlantic Time-series study (BATS). *Deep-Sea Research* 43, 127-128..

II.70. 1996 Karl, D. M. and R. Lukas. The Hawaii Ocean Time-series (HOT) program: Background, rationale and field implementation. *Deep-Sea Research* 43, 129-156.

II.71. 1996 Karl, D. M. and G. Tien. Temporal variability in dissolved phosphorus concentrations at Station ALOHA (22°45'N, 158°W). *Marine Chemistry* 56, 77-96.

II.72. 1996 Kennan, S. C. and R. Lukas. Saline intrusions in the intermediate waters north of Oahu, Hawaii. *Deep-Sea Research* 43, 215-241.

II.73. 1996 Latasa, M., R. R. Bidigare, M. E. Ondrusek and M. C. Kennicutt II. HPLC analysis of algal pigments: a comparison exercise among laboratories and recommendations for improved analytical performance. *Marine Chemistry* 51, 315-324.

II.74. 1996 Lawson, L., Y. Spitz and E. Hofmann. Time series sampling and data assimilation in a simple marine ecosystem model. *Deep-Sea Research* 43, 625-651.

II.75. 1996 Letelier, R. M., J. E. Dore, C. D. Winn and D. M. Karl. Temporal variations in photosynthetic carbon assimilation efficiencies at Station ALOHA. *Deep-Sea Research* 43, 467-490.

II.76. 1996 Letelier, R. M. and D. M. Karl. The role of *Trichodesmium* spp. in the productivity of the subtropical North Pacific Ocean. *Marine Ecology Progress Series* 133, 263-273.

II.77. 1996 Lukas, R. and F. Santiago-Mandujano. Interannual variability of Pacific deep and bottom waters observed in the Hawaii Ocean Time-series. *Deep-Sea Research* 43, 243-255.

II.78. 1996 Mitchum, G. On using satellite altimetric heights to provide a spatial context for the Hawaii Ocean Time-series measurements. *Deep-Sea Research* 43, 257-280.

II.79. 1996 Moyer, C. L., J. M. Tiedje, F. C. Dobbs and D. M. Karl. A computer-simulated restriction fragment length polymorphism analysis of bacterial small-subunit rRNA genes: Efficacy of selected tetrameric restriction enzymes for studies of microbial diversity in nature. *Applied and Environmental Microbiology* 62, 2501-2507.

II.80 1996 Roy-Barman, M., J. H. Chen and G. J. Wasserburg. ^{230}Th-^{232}Th systematics in the central Pacific Ocean: The sources and the fates of thorium. *Earth and Planetary Science Letters* 139, 351-363.

II.81. 1996 Schudlich, R. and S. Emerson. Gas saturation in the surface ocean: The roles of heat flux, gas exchange and bubbles. *Deep-Sea Research* 43, 569-589.

II.82. 1997 Campbell, L., H. Liu, H. A. Nolla and d. Vaulot. Annual variability of phytoplankton and bacteria in the subtropical North Pacific Ocean at Station ALOHA during the 1991-1994 ENSO event. *Deep-Sea Research* 44, 167-192.

II.83. 1997 Liu, H., L. Campbell and H. A. Nolla. *Prochlorococcus* growth rate and contribution to primary production in the equatorial and subtropical North Pacific Ocean. *Aquatic Microbial Ecology* 12, 39-42.

II.84. 1997 Sansone, F. J., B. N. Popp and T. M. Rust. Stable carbon isotopic analysis of low-level methane in water and gas. *Analytical Chemistry* 69, 40-44.

II.85 1997 Troy, P. J., Y. H. Li and F. T. Mackenzie. Changes in surface morphology of calcite exposed to the oceanic water column. *Aquatic Geochemistry* 3, 1-20.

II.86. 1997 Christian, J. R., M. R. Lewis and D. M. Karl. Vertical fluxes of carbon, nitrogen and phosphorus in the North Pacific subtropical gyre. *Journal of Geophysical Research* 102, 15,667-15,677.

II.87. 1997 Karl, D. M., R. Letelier, L. Tupas, J. Dore, J. Christian and D. Hebel. The role of nitrogen fixation in biogeochemical cycling in the subtropical North Pacific Ocean. *Nature* 388, 533-538.

II.88. 1997 Emerson, S., P. Quay, D. Karl, C. Winn, L. Tupas and M. Landry. The marine carbon pump: Flux accuracy and implications for the global carbon cycle. *Nature*, 389, 951-954.

II.89. 1997 Winn, C. D., Y. H. Li, F. T. Mackenzie and D. M. Karl. Rising surface ocean total dissolved inorganic carbon at the Hawaii Ocean Time-series site. *Marine Chemistry*, in press.

II.90. 1997 Karl, D. M. and K. Yanagi. Partial characterization of the dissolved organic phosphorus pool in the oligotrophic North Pacific Ocean. *Limnology and Oceanography*, in press.

II.91. 1997 Karl, D. M. and F. C. Dobbs. Molecular approaches to microbial biomass estimation in the sea. *Molecular Approaches to the Study of the Ocean (K. E. Cooksey, Ed.)*, in press.

II.92. 1997 Karl, D. M. Oceanic carbon cycle and global environmental change: A microbiological perspective. In: M. T. Martins (ed.), *Global Aspects of Microbial Ecology*, in press.

II.93. 1997 Letelier, R. M. and D. M. Karl. *Trichodesmium* spp. sustained physiology and nutrient fluxes in the North Pacific subtropical gyre. Submitted to *Aquatic Microbial Ecology*, in press.

III.Submitted Papers

III.1. Li, Y. H., C. Winn, D. Karl, F. Mackenzie and K. Gans. Refield ratios and the preformed nutrients at Station ALOHA. Submitted to *Marine Chemistry*.

III.2. Karl, D. M., D. V. Hebel, K. Bjorkman and R. M. Letelier. The role of dissolved organic matter fluxes in the productivity of the oligotrophic North pacific Ocean. Submitted to *Limnology and Oceanography*.

III.3. Nosse, C. Cross calibration of standard seawater batches P114, P115, P118, P121, P123, P128 and P130 through the Hawaii Ocean Time-series. Submitted to *Deep Sea Research*.

IV. Theses and Dissertations

IV.1. 1992 Sabine, C. L. Geochemistry of particulate and dissolved inorganic carbon in the central North Pacific. Ph.D. Dissertation, May 1992

IV.2. 1993 Kennan, S. Variability of the intermediate water north of Oahu. M.S. Thesis, December 1993.

IV.3. 1994 Letelier, R. M. Studies on the ecology of *Trichodesmium* spp. (*Cyanophyceae*) in the central North Pacific gyre. Ph.D. Dissertation, April 1994.

IV.4. 1994 Liu, H. B. Growth and mortality rates of *Prochlorococcus* and *Synechococcus* measured by a selective inhibitor technique. M.S. Thesis, May 1994.

IV.5. 1995 Dore, J. E. Microbial nitrification in the marine euphotic zone: Rates and relationships with nitrite distributions, recycled production and nitrous oxide generation. Ph.D. Dissertation, May 1995.

IV.6. 1995 Christian, J. R. Biochemical mechanisms of bacterial utilization of dissolved and particulate organic matter in the upper ocean. Ph.D. Dissertation, December 1995.

V. Data Reports and Manuals

V.1. 1990 Karl, D. M., C. D. Winn, D. V. W. Hebel and R. Letelier. Hawaii Ocean Time-series Program Field and Laboratory Protocols, September 1990. School of Ocean and Earth Science and Technology, Univ. of Hawaii, Honolulu, HI, 72 pp.

V.2. 1990 Collins, D. J., W. J. Rhea and A. Van Tran. Bio-optical profile data report: HOT-3. National Aeronautics and Space Administration JPL Publ. #90-36.

V.3. 1990 Chiswell, S., E. Firing, D. Karl, R. Lukas and C. Winn. Hawaii Ocean Time-series Program Data Report 1: 1988-1989. SOEST Tech. Rept. #1, School of Ocean and Earth Science and Technology, Univ. of Hawaii, Honolulu, HI, 269 pp.

V.4. 1992 Winn, C., S. Chiswell, E. Firing, D. Karl and R. Lukas. Hawaii Ocean Time-series Program Data Report 2: 1990. SOEST Tech. Rept. 92-1, School of Ocean and Earth Science and Technology, Univ. of Hawaii, Honolulu, HI, 175 pp.

V.5. 1993 Winn, C., R. Lukas, D. Karl and E. Firing. Hawaii Ocean Time-series Program Data Report 3: 1991. SOEST Tech. Report 93-3, School of Ocean and Earth Science and Technology, Univ. of Hawaii, Honolulu, HI, 228 pp.

V.6. 1993 Tupas, L., F. Santiago-Mandujano, D. Hebel, R. Lukas, D. Karl and E. Firing. Hawaii Ocean Time-series Program Data Report 4: 1992. SOEST Tech. Report 93-14, School of Ocean and Earth Science and Technology, Univ. of Hawaii, Honolulu, HI, 248 pp.

V.7. 1994 Tupas, L., F. Santiago-Mandujano, D. Hebel, E. Firing, F. Bingham, R. Lukas and D. Karl. Hawaii Ocean Time-series Program Data Report 5: 1993. SOEST Tech. Report 94-5, School of Ocean and Earth Science and Technology, Univ. of Hawaii, Honolulu, HI, 156 pp.

V.8. 1994 Voss, C. I. and W. W. Wood Synthesis of geochemical, isotopic and groundwater modeling analysis to explain regional flow in a coastal aquifer of Southern Oahu, Hawaii. In: *Mathematical Models and Their Applications to Isotope Studies in Groundwater Hydrology,* pp. 147-178, International Atomic Energy Agency, Vienna, Austria.

V.9. 1995 Tupas, L., F. Santiago-Mandujano, D. Hebel, E. Firing, R. Lukas and D. Karl. Hawaii Ocean Time-series Program Data Report 6: 1994. SOEST Tech. Report 95-6, School of Ocean and Earth Science and Technology, Univ. of Hawaii, Honolulu, HI, 199 pp.

V.10. 1996 Karl, D., L. Tupas, F. Santiago-Mandujano, C. Nosse, D. Hebel, E. Firing and R. Lukas. Hawaii Ocean Time-series Program Data Report 7: 1995. SOEST Tech. Report 99-9, School of Ocean and Earth Science and Technology, Univ. of Hawaii, Honolulu, HI, 228 pp.

VI. Newsletters

VI.1. 1989 Karl, D. M. Hawaiian Ocean Time-series program: It's HOT. *GOFS Newsletter* 1(2), 1-3.

VI.2. 1990 Karl, D. M. HOT Stuff: An update on the Hawaiian Ocean Time-series program. *US JGOFS Newsletter* 2(1), 6,9.

VI.3. 1990 Karl, David M. HOT Stuff: Rescue at sea. *US JGOFS Newsletter* 2(2), 8.

VI.4. 1991 Karl, D. M. HOT Stuff: Retrospect and prospect. *US JGOFS Newsletter* 2(3), 10.

VI.5. 1991 Karl, D. M. HOT Stuff: Hectic spring schedule keeps HOT team hustling. *US JGOFS Newsletter* 2(4), 9-10.

VI.6. 1991 Lukas, R. and S. Chiswell. Submesoscale water mass variations in the salinity minimum of the North Pacific. *WOCE Notes*, 3(1), 6-8.

VI.7. 1992 Karl, D. M. Hawaii Time-series program: Progress and prospects. *US JGOFS Newsletter* 3(4), 1,15.

VI.8. 1992 Michaels, A. F. Time-series programs compare results, methods and plans for future. *US JGOFS Newsletter* 4(1), 7,9.

VI.9. 1992 Winn, C. W. HOT program builds time-series set of carbon measurements for central Pacific. *US JGOFS Newsletter* 4(2), 7.

VI.10. 1992 Dickey, T. D. Oversight committee reviews time-series programs, issues recommendations. *US JGOFS Newsletter* 4(2), 14-15.

VI.11. 1992 Firing, E. and P. Hacker. ADCP results from WHP P16/P17. *WOCE Notes*, 4(3), 6- 12.

VI.12. 1992 Chiswell, S. Inverted echo sounders at the WOCE deep-water station. *WOCE Notes*, 4(4), 1, 3-6.

VI.13. 1993 Karl, D. M. HOT Stuff: The five-year perspective. *US JGOFS Newsletter* 5(1), 6,15.

VI.14. 1994 Karl, D. M. HOT Stuff: Surprises emerging from five years' worth of data. *US JGOFS Newsletter* 5(4), 9-10.

VI.15. 1994 Tupas, L. M. Euphotic zone nitrate variability in the central North Pacific gyre at the Hawaii Ocean Time-series Station ALOHA. *International WOCE Newsletter* 17, 21-23.

VI.16. 1994 Lukas, R. HOT results show interannual variability of Pacific Deep and Bottom waters. *WOCE Notes* 6(2), 1, 3, 14-15.

VI.17. 1995 Karl, D. M. HOT and COLD: A trapper's tale of two oceans. *US JGOFS Newsletter* 6(2): 7, 15.

VI.18. 1995 Karl, D. M. HOT Stuff: New hypotheses and projects evolve from growing data set. *US JGOFS Newsletter* 7(1): 11.

VI.19. 1996 Winn, C.D. and P. G. Driscoll. Hawaii Time-series data reveal rising ocean CO_2 levels. *US JGOFS Newsletter* 7(4): 7-8.

VI.20. 1996 Karl, D. M. The Hawaii Ocean Time-series study: Still HOT at 75. *US JGOFS Newsletter* 7(4): 8-9.

V!.21. 1997 Karl, D. M. Ocean time-series meetings explore new collaboration for future. *JGOFS Newsletter* 8(3): 15

VII. HOT symposiums

VII.1. Presentations from the "HOT Program: Progress and Prospectus" symposium, 3-4 June 1992, East-West Center, Honolulu, HI

Campbell, L. Bacterial numbers by flow cytometry: A new approach
Chiswell, S. Results from the inverted echo sounder network
Christian, J. Biomass closure in the epipelagic zone
Christian, J. Exoenzymatic hydrolysis of high molecular weight organic matter
Dore, J. Annual and short-term variability in the distribution of nitrite at the US-JGOFS time-series station ALOHA
Dore, J. and D. Hebel. Low-level nitrate and nitrite above the nutricline at Station ALOHA
Firing, E. Ocean currents near ALOHA
Hebel, D., R. Letelier and J. Dore. Evaluation of the depth dependence and temporal variability of primary production at Station ALOHA
Hebel, D., R. Letelier and J. Dore. Past and present dissolved oxygen trends, methodology, and quality control during the Hawaii Ocean Time series
Hebel, D. and U. Magaard. Structure and temporal variability in biomass estimates at Station ALOHA
Houlihan, T. and D. Hebel. Organic and inorganic nutrients: Water column structure and usefulness in time-series analysis
Karl, D. Carbon utilization in the mesopelagic zone: AOU-DOC relationships
Karl, D. HOT/JGOFS program objectives: A brief overview
Karl, D. P-control of N_2 fixation: An ecosystem model
Karl, D. Primary production and particle flux
Karl, D. et al. Review and re-assessment of core measurements: Suggestions for refinement and improvement
Karl, D. and G. Tien. Low-level SRP above the nutricline at Station ALOHA
Karl, D., L. Tupas, G. Tien and B. Popp. "High-temperature" DOC: Pools and implications
Karl, D., K. Yanagi and K. Bjorkman. Composition and turnover of oceanic DOP
Letelier, R. Temporal variability of algal accessory pigments at Station ALOHA: What does it tell about the phytoplankton community structure at the DCML?

Letelier, R. and D. Hebel. Evaluation of fluorometric and HPLC chlorophyll *a* measurements at Station ALOHA

Letelier, R. and F. Santiago-Mandujano. Wind, sea surface temperature and significant wave height records from NDBC buoy #51001 compared to ship observations at Station ALOHA

Lukas, R. Water mass variability observed in the Hawaii Ocean Time-series

Sadler, D., C. Winn and C. Carrillo. Time-series measurements of pH: A new approach for HOT

Schudlich, R. Upper ocean gas modeling at Station ALOHA

Winn, C. DIC variability

Winn, C. and C. Carrillo. DIC and alkalinity profiles and elemental ratios

VII.2. Presentations from the "HOT Golden Anniversary Science Symposium," 16 November 1993, East-West Center, Honolulu, HI

Bingham, F. M. The oceanographic context of HOT

Campbell, L., H. Nolla, H. Liu and D. Vaulot. Phytoplankton population dynamics at the Hawaii Ocean Time series Station ALOHA

Campbell, L., H. Nolla and D. Vaulot. The importance of *Prochlorococcus* to community structure in the central North Pacific Ocean

Christian, J. Vertical fluxes of carbon and nitrogen at Station ALOHA

Dore, J. Nitrate diffusive flux cannot support new production during quiescent periods at Station ALOHA

Dore, J. Nitrification in lower euphotic zone at Station ALOHA: Patterns and significance

Firing, E. The north Hawaiian ridge current and other flows near ALOHA

Hebel, D. Temporal distribution, abundance and variability of suspended particulate matter (particulate carbon, nitrogen and phosphorus) at Station ALOHA -- Observations of a seasonal cycle

Karl, D., D. Hebel, L. Tupas, J. Dore and C. Winn. Station ALOHA particle fluxes and estimates of export production

Karl, D. M., R. Letelier, L. Tupas, J. Dore, D. Hebel and C. Winn. N_2 fixation as a contributor to new production at Station ALOHA

Karl, D. M., G. Tien and K. Yanagi. Phosphorus dynamics at Station ALOHA

Kennan, S. C. Possibilities for stirring along the Hawaiian ridge

Krothapalli, S., Y. H. Li and F. T. Mackenzie. What controls the temporal variability of carbon flux at Station ALOHA?

Letelier, R. M. Inorganic carbon assimilation at Station ALOHA: Possible evidence of a change in carbon fluxes

Letelier, R. M. Spatial and temporal distribution of *Trichodesmium* sp. at Station ALOHA: How important are they?

Liu, H. and L. Campbell. Measurement of growth and mortality rates of *Prochlorococcus* and *Synechococcus* at Station ALOHA using a new selective inhibitor technique

Lukas, R. and F. Bingham. Annual and interannual variations of hydrographic properties observed in the Hawaii Ocean Time-series (HOT)

Lukas, R., F. M. Bingham and A. Mantyla An anomalous cold event in the bottom water observed at Station ALOHA

Moyer, C. L., L. Campbell, D. M. Karl and J. Wilcox. Restriction fragment length polymorphism (RFLP) and DNA sequence analysis of PCR-generated clones to assess diversity of picoeukaryotic algae in the subtropical central North Pacific Ocean (Station ALOHA)

Polovina, J. J. and D. R. Kobayashi. HOT and Hawaii's fisheries landings: Complementary or independent time-series?

Sadler, D. Time series measurement of pH at Station ALOHA

Smith, C. R., D. J. DeMaster, R. H. Pope, S. P. Garner, D. J. Hoover and S. E. Doan. Seabed radionuclides, bioturbation and benthic community structure at the Hawaii Ocean Time-series Station ALOHA

Tupas, L. M., B. N. Popp and D. M. Karl. Dissolved organic carbon in oligotrophic waters: Experiments on sample preservation, storage and analysis

Winn, C. D. Air-sea carbon dioxide exchange at Station ALOHA

Yuan, J. and C. I. Measures. Sampling and analysis of dissolved iron

VII.3. Presentations from the "HOT-75 Commemorative Science Symposium," 9 September 1996, East-West Center, Honolulu, HI

Atkinson, M. A Potentiostatic, Solid-state Oxygen Sensor for Oceanic CTDs

Bidigare, R., M. Latasa, R. Andersen and M. Keller. A Comparison of HPLC Pigment Signatures and Electron Microscopic Observations for Oligotrophic Waters of the North Atlantic and North Pacific Oceans

Campbell, L., H. Liu, H. Nolla and D. Vaulot. Annual Variability of Phytoplankton and Bacteria in the Subtropical North Pacific Ocean at Station ALOHA during the 1991-1994 ENSO Event

Christian, J., M. Lewis and D. Karl. Vertical Fluxes of Carbon, Nitrogen and Phosphorus at the US-JGOFS Time-Series Station ALOHA

Dore, J. and D. Karl. Nitrification, New Production and Nitrous Oxide at Station ALOHA

Ducklow, H. Joint Global Ocean Flux Study -- Vision and Progress

Emerson, S., C. Stump and D. Wilber. Inert Gases as Tracers of Diapycnal Mixing in the Upper Ocean

Firing, E. Currents in the Vicinity of Station ALOHA: An Update

Fujieki, L. HOTDOGS: A New Tool for HOT Program Data Base Analysis and Presentation

Hebel, D., L. Tupas and D. Karl. The Importance of Organic Exudates in the Measurement of Oligotrophic Ocean Primary Productivity

Karl, D., D. Hebel and L. Tupas. Regionalization of Station ALOHA

Karl, D., G. Tien, K. Björkman, K. Yanagi, R. Letelier, A. Colman and A. Thomson. The "Forgotten" Open Ocean P-Cycle

Karl, D., L. Tupas, D. Hebel, R. Letelier, J. Christian and J. Dore. Station ALOHA N-Cycle: The Case for N2 Fixation

Landry, M., K. Selph and H. Al-Mutairi. Seasonal and Diurnal Variability of the Mesozooplankton Community at Ocean Station ALOHA

Letelier, R. and M. Abbott. Effects of a Subsurface *Trichodesmium* spp. Bloom on the Optical Reflectance Measured in the Upper 150 m of the Water Column in the North Pacific Subtropical Gyre

Liu, H., L. Campbell and H. Nolla. *Prochlorococcus* Growth Rate and Daily Variability at Station ALOHA

Lopez, M. and M. Huntley. Particle Concentrations at the Hawaii Ocean Time-series Station (Station ALOHA) Measured with an Optical Plankton Counter

Michaels, A. and A. Knap. The Bermuda Atlantic Time-Series Study (BATS): A View from the "Other" Ocean

Nolla, H., J. Kirshtein, M. Landry, D. Karl, L. Campbell and D. Pence. Flow Cytometry Correction Factors for Enumeration of Heterotrophic Bacteria and Phytoplankton

Quay, P. and H. Anderson. A Dissolved Inorganic Carbon Budget at Station ALOHA

Santiago-Mandujano, F. and R. Lukas. Cold Bottom Water Events Observed in the Hawaii Ocean Time-Series: Modelling and Implications for Vertical Mixing

Scharek, R., M. Latasa, D. Karl and R. Bidigare. Vertical Flux of Diatoms at the JGOFS/WOCE Station ALOHA

Smith, C., R. Miller, R. Pope and D. DeMaster. Seafloor Inventories of Pb-210, Th-234 and Benthic Biomass as Proxies for Deep POC Flux: Placing Export Production at the HOT Station in a General Oceanic Context

Tien, G., D. Pence and D. Karl. Hydrogen Peroxide Measurements at Station ALOHA

Tupas, L., G. Tien, D. Hebel and D. Karl. Dissolved Organic Carbon Dynamics in the Upper Water Column at Station ALOHA

Vink, S., K. Falkner, V. Tersol, J. Yuan and C. Measures. Variations in Iron, Aluminum, Beryllium and Barium Concentrations in Surface Waters at Station ALOHA

Winn, C. Secular Changes in Inorganic Carbon Parameters at HOT and BATS

8.0. DATA AVAILABILITY AND DISTRIBUTION

8.1. Hard Copies

Data collected by HOT program scientists are made available to the oceanographic community in various ways as soon after processing as possible. The complete data set, containing data collected since year 1 of the HOT program (1988), as well as 2 dbar averaged CTD data, are available from two sources. The first is through the National Oceanographic Data Center. The second source is from the HOT data base residing in a workstation at the University of Hawaii, and may be accessed using anonymous ftp on the Internet or the World Wide Web (www). Access via ftp or through the web is described in more detail below. Details of each web page are described in the section 8.3.

8.2. File Transfer Protocol

In order to maximize ease of access, the data are in ASCII files. File names are chosen so that they may be copied to DOS machines without ambiguity. (DOS users should be aware that Unix is case-sensitive, and Unix extensions may be longer than 3 characters.)

The data are in a subdirectory called ***/pub/hot***. More information about the data base is given in several files called ***Readme.**** at this level. The file ***Readme.first*** gives general information on the data base; we encourage users to read it first.

The following is an example of how to use ftp to obtain HOT data. The user's command are denoted by bold italicized text. The workstation's Internet address is ***mana.soest.hawaii.edu***, or ***128.171.154.9*** (either address should work). All information, except optical data, reside at this address. Optical data are stored at ***hahana.soest.hawaii.edu***, or ***128. 171. 154. 13***.

1. At the Prompt >, type ***ftp 128.171.154.9*** or ***ftp mana.soest.hawaii.edu.***

2. When asked for your login name, type ***anonymous***.

3. When asked for a password, type ***your email address***.

4. To change to the HOT database, type ***cd /pub/hot***. To view files type **ls**. A directory of files and subdirectories will appear.

5a. To obtain information about the database type ***get Readme.first***. This will transfer an ASCII file to your system. Use any text editor to view it.

5b. To obtain a list of publications, type ***cd publication-list*** then ***get hotpub.lis***.

5c. To obtain the HOT Field and Laboratory Protocols manual, type ***cd protocols*** then ***get 1142.asc***.

5d. To obtain CTD data, type ***cd ctd/hot-#***, where # is the HOT cruise of interest, then type ***mget *.ctd*** to transfer all the cruise CTD files to your system.

5e. To obtain water column data, type ***cd water***, then ***get <filename>*** where the filename is hot#.gof (JGOFS data) or hot#.sea (WOCE data) and # is the HOT cruise of interest.

6. To exit type ***bye***.

7. Data on optical parameters are located on another server. To obtain light data, at the prompt type ***ftp 128.171.154.13*** or ***ftp hahana.soest.hawaii.edu*** then follow steps 2 to 4.

8.3. World Wide Web

The Hawaii Ocean Time-series Program maintains a site on the world wide web where data and information about the program and its activities can easily be accessed over the Internet. The address is http://hahana.soest.hawaii.edu/hot/hot.html. This web page is the springboard from which the homepages of the WOCE and JGOFS components are accessible. Regardless of which site is accessed, there is only one common data base which is referred to by both components. The first half of the most recent year's data is usually available by July and the second half by January the following year with certain quality control caveats. All data are quality controlled by around April of the following year. Down loading of data is through ftp but the web pages provide a more detailed means of access.

8.3.1. HOT-WOCE Homepage

The World Ocean Circulation Experiment component of the HOT program maintains a web page at http://www.soest.hawaii.edu/HOT_WOCE. This web page includes (underlined items provide access to the specified section):

- Introduction:
  - HOT objectives
  - Site location
  - Observations description
  - HOT-WOCE Hydrographic sampling Procedures Manual
- Cruise Dates and Summaries:
  - Summaries of cruise's CTD station and cast
  - Chief Scientist's Reports
- Data description and Transfer:
  - Current status of HOT database
  - Data format information
  - Data transfer (FTP)
- WOCE Highlights:
  - Color contour of HOT time-series
  - Abstracts and figures of published papers from current research
  - Poster: Ocean Climate Variations in HOT
- Personnel:
  - The people that make the WOCE component of HOT possible

Accessing data files from the HOT-WOCE site can be accomplished by going to the Data description and transfer section. This section includes 1) data format and transfer information and 2) ftp data guides to (underlined items provide access to the specified section or operation):

- Current data status
- CTD data
- Bottle data
- Cruise summary
- ADCP data
- XBT data
- Meteorological observations
- Inverted Echo Sounder

8.3.2. HOT-JGOFS Homepage

The Joint Global Ocean Flux Study component of the HOT program maintains a web page at http://hahana.soest.hawaii.edu/hot/hot_jgofs.html. This web page includes (underlined items provide access to the specified section):

What's new (and updated)

Overview

- Introduction
  - Ancillary Projects Supported by HOT
  - Location of the HOT Water Column and Bottom Stations
  - Parameters Measured
- Cruise Schedules and Reports
- Principal Investigators and Staff
  - Past Cruise Participants
- HALE ALOHA - physical/biogeochemical mooring
  - Pictures of the Deployment
  - Mooring Positions
  - Bottom Topography
  - Results
- Special Topics and Events
  - Deep-Sea Research Special Volume
  - HOT-75 Commemorative Science Symposium

Data Links

- Interactive Access to HOT Data (HOT-DOGS)
- Request sample acquisition &/or Cruise Participation
- Analytical Methods and Results
- Current Data Trends
- References
  - Field and Laboratory Protocols
  - Publications

8.3.2.1. Data Access

Accessing of data through the HOT-JGOFS can be accomplished by going to the Analytical Methods and Results section. This section includes:

- Status & Summaries
  - Current Status of the HOT data base
  - Corrections
  - Cruise summaries
- Methods and Results
  - Hydrography
    (includes pressue, temperature, conductivity, oxygen, fluorescence and beam transmission)
  - Biogeochemistry
    (includes salinity, oxygen, dissolved inorganic carbon, titration alkalinity, pH, dissolved inorganic nutrients, dissolved organic nutrients, low-level nutrients, particulate matter, pigments, ATP)
  - Primary Production
  - Particle Flux
  - ADCP Measurements
  - Meteorology
  - Light Measurements
  - XBT
  - Buoy and shipboard Observations
  - Inverted Echo Sounder Observations
  - Bottom Moored Sediment Traps
  - Macrozooplankton
  - Thermosalinograph

- Endeco Towfish

8.3.2.1. HOT-DOGS©

HOT-DOGS© is the acronym for HOT Data Organizational and Graphical System. HOT-DOGS is a Matlab© based program that displays HOT data in a graphical format, as depth profiles or contour plots, or the numerical data for each parameter measured. All figures can be printed as hard copies or files. In addition to its graphical capabilities, HOT-DOGS provides a means of downloading data of selected parameters during specific years of the program. The program allows the user to perform the following:

- Data Extraction
  - Bottle
  - Particle Flux
  - Primary Production
- Display (vertical water column)
  - Bottle
  - CTD
  - HPLC Pigments
  - Particle Flux
  - Primary Production
- Standard depths (vertical water column)
  - Bottle
  - HPLC Pigments
  - Primary Production
- Time-series
  - Bottle
  - HPLC
  - Particle Flux
  - Primary Production

An advanced version of HOT-DOGS is available but at present only operable in the HOT-JGOFS workstation. This version can do more sophisticated graphical presentations such as contour plots. This software can also do graphical presentations of other JGOFS data bases such as the Bermuda Atlantic Time-series and the JGOFS process studies data bases. Development is underway to make the advanced version available through the world-wide web.